

Lecture Notes in Mechanical Engineering

B. B. V. L. Deepak

D. R. K. Parhi

B. B. Biswal

Pankaj C. Jena *Editors*


Applications of Computational Methods in Manufacturing and Product Design

Select Proceedings of IPDIMS 2020

 Springer


Lecture Notes in Mechanical Engineering

Series Editors

Francisco Cavas-Martínez , Departamento de Estructuras, Construcción y Expresión Gráfica Universidad Politécnica de Cartagena, Cartagena, Murcia, Spain

Fakher Chaari, National School of Engineers, University of Sfax, Sfax, Tunisia

Francesca di Mare, Institute of Energy Technology, Ruhr-Universität Bochum, Bochum, Nordrhein-Westfalen, Germany

Francesco Gherardini , Dipartimento di Ingegneria “Enzo Ferrari”, Università di Modena e Reggio Emilia, Modena, Italy

Mohamed Haddar, National School of Engineers of Sfax (ENIS), Sfax, Tunisia

Vitalii Ivanov, Department of Manufacturing Engineering, Machines and Tools, Sumy State University, Sumy, Ukraine

Young W. Kwon, Department of Manufacturing Engineering and Aerospace Engineering, Graduate School of Engineering and Applied Science, Monterey, CA, USA

Justyna Trojanowska, Poznan University of Technology, Poznan, Poland

Lecture Notes in Mechanical Engineering (LNME) publishes the latest developments in Mechanical Engineering—quickly, informally and with high quality. Original research reported in proceedings and post-proceedings represents the core of LNME. Volumes published in LNME embrace all aspects, subfields and new challenges of mechanical engineering. Topics in the series include:

- Engineering Design
- Machinery and Machine Elements
- Mechanical Structures and Stress Analysis
- Automotive Engineering
- Engine Technology
- Aerospace Technology and Astronautics
- Nanotechnology and Microengineering
- Control, Robotics, Mechatronics
- MEMS
- Theoretical and Applied Mechanics
- Dynamical Systems, Control
- Fluid Mechanics
- Engineering Thermodynamics, Heat and Mass Transfer
- Manufacturing
- Precision Engineering, Instrumentation, Measurement
- Materials Engineering
- Tribology and Surface Technology

To submit a proposal or request further information, please contact the Springer Editor of your location:

China: Ms. Ella Zhang at ella.zhang@springer.com

India: Priya Vyas at priya.vyas@springer.com

Rest of Asia, Australia, New Zealand: Swati Meherishi at swati.meherishi@springer.com

All other countries: Dr. Leontina Di Cecco at Leontina.dicecco@springer.com

To submit a proposal for a monograph, please check our Springer Tracts in Mechanical Engineering at <https://link.springer.com/bookseries/11693> or contact Leontina.dicecco@springer.com

Indexed by SCOPUS. All books published in the series are submitted for consideration in Web of Science.

More information about this series at <https://link.springer.com/bookseries/11236>

B. B. V. L. Deepak · D. R. K. Parhi · B. B. Biswal ·
Pankaj C. Jena
Editors

Applications of Computational Methods in Manufacturing and Product Design

Select Proceedings of IPDIMS 2020

 Springer

Editors

B. B. V. L. Deepak
Department of Industrial Design
National Institute of Technology Rourkela
Rourkela, Odisha, India

D. R. K. Parhi
Department of Mechanical Engineering
National Institute of Technology Rourkela
Rourkela, Odisha, India

B. B. Biswal
National Institute of Technology Rourkela
Rourkela, Odisha, India

Pankaj C. Jena
Department of Production Engineering
VSS University of Technology
Burla, Odisha, India

ISSN 2195-4356

ISSN 2195-4364 (electronic)

Lecture Notes in Mechanical Engineering

ISBN 978-981-19-0295-6

ISBN 978-981-19-0296-3 (eBook)

<https://doi.org/10.1007/978-981-19-0296-3>

© The Editor(s) (if applicable) and The Author(s), under exclusive license to Springer Nature Singapore Pte Ltd. 2022

This work is subject to copyright. All rights are solely and exclusively licensed by the Publisher, whether the whole or part of the material is concerned, specifically the rights of translation, reprinting, reuse of illustrations, recitation, broadcasting, reproduction on microfilms or in any other physical way, and transmission or information storage and retrieval, electronic adaptation, computer software, or by similar or dissimilar methodology now known or hereafter developed.

The use of general descriptive names, registered names, trademarks, service marks, etc. in this publication does not imply, even in the absence of a specific statement, that such names are exempt from the relevant protective laws and regulations and therefore free for general use.

The publisher, the authors and the editors are safe to assume that the advice and information in this book are believed to be true and accurate at the date of publication. Neither the publisher nor the authors or the editors give a warranty, expressed or implied, with respect to the material contained herein or for any errors or omissions that may have been made. The publisher remains neutral with regard to jurisdictional claims in published maps and institutional affiliations.

This Springer imprint is published by the registered company Springer Nature Singapore Pte Ltd. The registered company address is: 152 Beach Road, #21-01/04 Gateway East, Singapore 189721, Singapore

Preface

This book gathers cutting-edge research articles from 2nd Innovative Product Design and Intelligent Manufacturing System (IPDIMS), which will be held at National Institute of Technology Rourkela during 12–13 February 2021. It covers the methods and tools from all research fields of design and manufacturing for the enhancement of the innovation process. This book discusses the current technology issues like design methodologies, Industry 4.0, smart manufacturing, advances in robotics, etc. The contents of this volume are useful to the academicians and professionals working in the research areas—industrial design, mechatronics, robotics, soft computing and automation.

Rourkela, India
Rourkela, India
Rourkela, India
Burla, India

B. B. V. L. Deepak
D. R. K. Parhi
B. B. Biswal
Pankaj C. Jena

Contents

Aesthetical Design of a Bio-inspired Futuristic Vehicle for Smart Transportation	1
Gurmeet Singh and Krishnaraj Ramakrishnan	
Detection and Counting of Nuts and Bolts with Image Processing Using MATLAB	13
Gunji Bala Murali, Gaikwad Tejas Vasant, Dhananjay D. Kupwade, and Deshmukh Atharva Girish	
Evaluation of EDM Die-Sinking Electrode Wear Rate of COOH-MWCNT/Al Nanocomposite	21
Md. Zakir Hussain, Sabah Khan, and Pranjal Sarmah	
Agribots Concepts and Operations—A Review	31
Ramu Eeram, B. B. V. L. Deepak, Umamaheswar Rao Mogili, and P. Syam Sundar	
Over View of Sensors for Measuring Soil Parameters, Supporting Agricultural Practices	41
P. Syam Sundar, B. B. V. L. Deepak, Ramu Eeram, and Umamaheswara Rao Mogili	
Design of Pin on Disk Tribometer Under International Standards	49
Byron Dario Analuiza Hidalgo, Vanessa C. Erazo-Chamorro, Diana Belén Peralta Zurita, Edilberto Antonio Llanes Cedeño, Gustavo Adolfo Moreno Jimenez, Ricardo P. Arciniega-Rocha, Paul D. Rosero-Montalvo, Alejandro Toapanta Lema, and José A. Pijal-Rojas	
Optimal Design Optimization of a Hybrid Rigid–Soft Robotic Hand Using an Evolutionary Multi-objective Algorithm	63
Golak Bihari Mahanta, B. B. V. L. Deepak, Amruta Rout, and B. B. Biswal	

A Simplified Fifth Order Shear Deformation Theory Applied to Study the Dynamic Behavior of Moderately Thick Composite Plate	73
Sarada Prasad Parida and Pankaj C. Jena	
Referring Expressions in Discourse Structure: A Study of Local and Global Focus	87
Harjit Singh	
Developing Products for the Elderly: PUIA Design Taxonomy	101
Neha Yaragatti and Ravi Kumar Gupta	
A GWO Tuned Probabilistic Roadmap Approach for Coarse Mapping of Humanoid Robot in Inclined Terrain	111
Abhishek Kumar Kashyap, D. R. K. Parhi, Saroj Kumar, and Anish Pandey	
Path Optimization and Control of Mobile Robot Using Modified Cuckoo Search Algorithm	125
Saroj Kumar, D. R. K. Parhi, Abhishek K. Kashyap, and Vikas	
A Braitenberg Path Planning Strategy for E-puck Mobile Robot in Simulation and Real-Time Environments	135
Bhaskar Jyoti Gogoi and Prases K. Mohanty	
Experimental Investigation on the Performance of the Novel 3D-Printed Micro-Cross Axis Wind Turbine	153
V. S. Surya Prakash, P. S. V. V. Srihari, P. S. V. V. S. Narayana, G. Udaysai, P. S. S. Rajesh, and K. Venu	
Novel Application of Electrolysis on Vehicle: Hydrogen Fuel Cell	165
Pavan Kumar Rejeti, Subrat Kumar Barik, and S. Balakrishna	
Influence of Process Parameters on Microstructural and Mechanical Properties of Friction Stir Processed AA6063/Zn Composite	179
Pavan Kumar Rejeti and Sandhyarani Biswas	
Self-sustainable Toilet System	189
Adithya Kameswara Rao, S. Karthi, K. Vedhanarayan, A. Ssmrithi, P. Niranjan Kumar, Kevin Mathew Thomas, and Mayank Kapur	
Novel Water-Conserving Faucet Attachment	201
Adithya Kameswara Rao, R. Jayendran, P. Niranjan Kumar, J. Sudarsana Jayandan, and K. Harikrishna	
Novel Design of Selective Action Knee Assistive Device	211
Kulkarni Atharva Kumar, S. M. Deepsikha, Kevin Mathew Thomas, Kunal Yadav, Navneeth Rajiv, K. Rohit Surya, and K. Vedhanarayan	

‘Saarathi’—Novel Design and Prototype of Single Person Operated Casualty Evacuation Stretcher 221
 Karthi Saran, Kunal Yadav, Yash Prakash, Nithin Subhash, Amritha Suresh, and Siddharth Mahesh

Review on the Application of CGP to Improve AZ31 Mg Alloy Properties 237
 A. Muni Tanuja, Anoop Kumar, and B. Nageswara Rao

T-Ceres—An Automated Machine for Any T-Shirt to Bag Conversion 247
 S. Premkumar, Yash Prakash, Burhanuddin Shirose, K. M. Dhivakar, Mayank Kapur, L. N. Puthiyavan, and Ssmrithi Arul

Automatic Attendance Monitoring System (AAMS) 259
 Abhinav Santosh Pandey, Kumar Mayank Verma, Tanya Verma, and Abhay Kumar

Coronavirus Visual Dashboard and Data Repository: COVID-19 269
 M. Arvindhan, Mohit Bhatia, Nishant Sinha, and Tarun Kumar

Influence of Drop Weight Low-Velocity Impact on Thin Panels Study by Numerical Simulation and Experimental Approach 281
 I. Ramu, K. V. G. R. Seshu, P. Srinivas, and P. SenthilKumar

Analysis of Segmental Vibration Transmissibility of Seated Human 289
 Veeresalingam Guruguntla and Mohit Lal

Early Detection of Sepsis Using LSTM and Reinforcement Learning ... 297
 R. Dhanalakshmi, T. Sudalaimuthu, and K. R. Radhakrishnan

Design of Cost-Effective Bamboo Reinforced Manhole Cover; A Step Toward Sustainable Development 307
 Shilpa Kewate, Manisha Jamgade, and Madhulika Sinha

Design and Development of a Trolley for the Finishing Department of Garment Industry to Enhance Feeding Helper Productivity 317
 M. Rajesh and N. V. R. Naidu

Optimization of Dynamic Capacity of Deep Groove Ball Bearing by Using Genetic Algorithm 329
 Krapa Bhanuteja, Mummina Vinod, and Duvvuri Vamsee Krishna

Suitability of Hybrid Aluminium Metal Matrix Composite Material to Replace Cast Iron in Automobile Components 339
 Mohammad Habibullah, N. V. V. Manikanta, A. Varun, and M. Praveen

Design and Analysis Studies in Pellet Extrusion Additive Manufacturing Processes 351
 Abhishek Patel, Krishnanand, and Mohammad Taufik

Intelligent Flooring Systems in Interiors-Exploring the Impact on Well-Being	361
Zeba Shaikh, Tamanna Naaz, and Banafsha Rajput	
Impacts of Integrating High-Tech and IoT Developments for Workplace Performance	377
Zehra Hafizji, Banafsha Rajput, and Amna Rafi Chaudhry	
Recognition of Dubious Tissue by Using Supervised Machine Learning Strategy	395
G. S. Pradeep Ghantasala, D. Nageswara Rao, and Rizwan Patan	
Performance Prediction of Students Using Machine Learning Algorithms	405
Sai Sudha Gadde, Dama Anand, N. Sasidhar Babu, B. V. Pujitha, M. Sai Reethi, and G. S. Pradeep Ghantasala	
Pedal Operated Weeder for Eco-Friendly Management of Aquatic Weeds	413
R. B. Choudary, B. Ajayaram, A. Ravi Kant, K. D. A. N. V. S. Prakash, and K. S. Manikanta	
Ergonomic Evaluation of the Three Implements of the Manual Weeder for Farmers	421
R. B. Choudary, A. Ravi Kant, B. Ajayaram, and B. Madhuri	
Blockchain in Smart Healthcare Application	431
Avnish Vishwakarma, Maniket Kumar, and M. Arvindhan	
Investigation of Diesel Engine's Performance Using Nano Additives in Biodiesel Blends (B20, B30 and B40)	441
Bandaru Bangarraju, P. Srinivas, G. Narasinga Rao, and Ch. Bhanuprakash	
Cloud Serverless Security and Services: A Survey	453
A. Arul Prakash and K. Sampath Kumar	
Early Prediction of Credit Card Transaction Using Local Outlier Factor and Isolation Forest Tree Machine Learning Algorithms	463
K. P. Arjun, Godlin Atlas, N. M. Sreenarayanan, S. Janarthanan, and M. Arvindhan	
Heat Transfer Characteristics of Spherical Finned Rectangular Microchannel	473
S. Venkata Sai Sudheer, C. H. Naveen Kumar, G. Mahesh, and C. H. Bhanu Prakesh	
Design and Fabrication of Automatic Vehicle for Railway Track Monitoring by Using ESP8266 Module	483
L. Daloji, I. Ramu, Narasinga Rao, and P. Manikanta	

Design and Evaluation of Manual Weeder for Dryland Crops 491
 P. D. V. N. Krishna, V. Mahesh Chakravarthi, Mummina Vinod,
 and Srinivas Pothala

Computational Analysis of a Convergent Divergent Nozzle 503
 Srinivas Pothala, M. V. Jagannadha Raju, B. Bangarraju,
 and V. Lakshmi Narayana

**Implementation of Autonomous Maintenance and Its Effect
 on MTBF, MTTR, and Reliability of a Critical Machine in a Beer
 Processing Plant** 511
 Aezeden Mohamed, Jacob Ben, and Kamalakanta Muduli

**An Assessment on Bone Cancer Detection Using Various
 Techniques in Image Processing** 523
 Dama Anand, G. Arulselvi, and G. N. Balaji

**Small-Scale Hydropower Generation from the Otherwise-Wasted
 Kinetic Energy in MultiStory Building** 531
 Srikanth Allamsetty, Animesh Shukla, and Rishav Bhagat

A Model for Identifying Fake News in Social Media 539
 Ishita Singh, Joy Gupta, Ravikant Kumar, Srinivasan Sriramulu,
 A. Daniel, and N. Partheeban

**Driver Drowsiness Detection Using Machine Learning to Prevent
 Accidents** 549
 Srinivasan Sriramulu, A. Daniel, N. Partheeban, Vaibhav Singh,
 Asad Ali Khan, and Shivam Sharma

**Comparative Study of Various Authentication Schemes in Tele
 Medical Information System** 557
 Charul Dewan, T. Ganesh Kumar, and Sunil Gupta

**Analysis of Load Balancing Detection Methods Using Hidden
 Markov Model for Secured Cloud Computing Environment** 565
 M. Arvindhan and D. Rajesh Kumar

Banking Management System—The Web Application Way 581
 Prathmesh Rai, Aryan Singh, Tushar Sharma, and N. M. Sreenarayanan

**A Novel of Survey: In Healthcare System for Wireless Body-Area
 Network** 591
 C. Rameshkumar and T. Ganeshkumar

Facial Expression Recognition System and Play Customized Ad 611
 Shivalik Sharma, Arnab Ajey, Nishant Singh, and N. M. Sreenarayanan

Application of Taguchi Technique to Study the Influence of Process Parameters of Ultrasonicator-Assisted Stir Casting on Tensile Strength of Al6061/Nano Rice Husk Ash Composites 621
Subrahmanyam Vasamsetti, Lingaraju Dumpala, and V. V. Subbarao

Effects of UAV Flight Parameters Over Droplet Distribution in Pesticide Spraying 633
Umamaheswara Rao Mogili, B. B. V. L. Deepak, P. Syam Sundar, and Ramu Eeram

A Review of Human Activity Recognition (HAV) Techniques 643
T Venkateswara Rao and Dhananjay Singh Bisht

Pothole Detection on Roads Using Canny Edge Detection Algorithm . . . 653
Gunji Bala Murali, V. Santosh Kumar, Dibya Narayan Behera, Kapil Kumar Mohanta, Omkar Tulankar, and Sanketh S. Salimath

Survey on Optimization of Resource Scheduling in Cloud Platforms 663
Bhaskararao Kasireddi and Raju Anitha

About the Editors

Dr. B. B. V. L. Deepak is currently working at National Institute of Technology, Rourkela as head of the Department of Industrial Design. He received his Master's and Ph.D. degrees from the National Institute of Technology Rourkela in 2010 and 2015, respectively. He has 11 years of research and teaching experience in Manufacturing and Product Design fields. He produced four Ph.D. theses and is currently supervising three Ph.D. scholars. He has published more than 100 papers in various peer-reviewed journals and conferences along with 1 patent. He is also currently handling two sponsored research projects in the field of robotics. He received several national and international awards such as Ganesh Mishra Memorial Award-2019, IEI Young Engineer Award-2018, Early Career Research Award-2017, etc.

Prof. D. R. K. Parhi is working in NIT Rourkela as a Professor (HAG). He is currently heading the Department of Mechanical Engineering. He has received his Ph.D. in Mobile Robotics field from Cardiff School of Engineering, UK. He has 27 years of research and teaching experience in robotics and artificial intelligence fields. He has guided more than 20 Ph.D. theses and published more than 300 papers in various journals and conferences along with three patents. He has completed and currently handling several sponsored research projects in the field of robotics.

Prof. B. B. Biswal is currently acting as Director of National Institute of Technology Meghalaya. He is also a Professor (HAG) in the Department of Industrial Design of NIT Rourkela. He has 33 years of research and teaching experience in FMS, CAD/CAM, robotics fields. He has guided more than 15 Ph.D. theses and published more than 200 papers in various journals and conferences along with 3-patents/copyrights. He has international collaboration with Loughborough University and Slovak University of Technology in Bratislava. He has also completed and currently handling several sponsored research projects in his research field.

Dr. Pankaj C. Jena is currently an Associate Professor at the Department of Production Engineering, Veer Sirendra Sai University of Technology, Burla, Odisha, India. He obtained his B.E. (Mechanical Engineering) and M.Tech. (Mechanical System

Design) from Biju Patnaik University of Technology, Odisha, and Ph.D. (Engineering) from the Jadavpur University, Kolkata. His major areas of research interests include composite material structures, fault diagnosis, fuzzy technique, vibration engineering and use of waste materials in engineering applications. He has published 19 papers in reputed international journals, 15 papers in international conferences, six book chapters and one book. Currently, he is an editorial board member of the *International Journal of Materials Manufacturing Technology*.

Aesthetical Design of a Bio-inspired Futuristic Vehicle for Smart Transportation



Gurmeet Singh  and Krishnaraj Ramakrishnan

Abstract Designers need to cultivate storylines and strategies inciting discussions over the key issues of smart and sustainable futuristic transportation. The automotive exterior aesthetics will be of prime importance in the future's individualistic social scenario. With its form and overall personality, vehicle aesthetics needs to respond to the emotional state of the user. Bio-inspiration has been of prime interest in automotive design to meet automobile makers' need to associate their machines with the appeal and capabilities of naturally optimized creatures. The proposed futuristic vehicle's aesthetics has been conceptualized using the technology pull approach of bio-inspiration and the analogy transfer was considered to mimic the biological features and mechanisms of a whale into the aesthetical form of the proposed futuristic vehicle. Blue whales have unique skin pleats that act like human fingerprints to distinguish one creature from the other. This vehicle uses a similar mechanism for its identification and replaces the chassis number system of present-day vehicles. The geometric-organic infused aesthetics of the proposed concept come with a unibody to support the safety and materials needs of future transit. The overall form is cohesive and appeals to users with clean geometric lines blended into the organic body. Upwards-outwards opening doors add to the statement of the user. These doors overlap with the semantics of wings ready to fly.

Keywords Bio-inspiration · Biomimicry · Futuristic vehicle · Automotive styling · Smart transportation

1 Introduction

The aesthetic appeal connects a prospective consumer to a product and leads to the possible purchase of that product. Designers are appreciating the significance

G. Singh (✉)
World University of Design (WUD), Sonapat, India

K. Ramakrishnan
Studio 34, Gurugram, India

of inducing emotions and communicating product personality to hold users' attention and craft delightful experiences but designing for emotions is not easy as all individuals have their own set of personal experiences and cultured connotations.

People like to show off their sense of style and good taste with their houses, interiors, clothes, and other possessions. Personal vehicles are also a style statement nowadays. Concept cars are dream machines for people as they are stylish, unique, and thrilling to prospective buyers. The appearance is the most significant requirement for a concept car. It must be aesthetically attractive to catch the public's attention. The same aesthetics elicits a sense of pleasure and makes a statement to the users [1]. A study of users' responses toward product newness including trendiness, complexity, and emotion as the product semantics found that the trendiness governs the novelty whereas it has a linear relationship with the preferred aesthetics of the product. The study found that the emotional aspect was largely associated with the curves and wholeness of the product body [2]. Usefulness and usability aspects of a product are heightened with desirable features and aesthetics is the most prominent emotion and desirable feature as a starting touchpoint for purchase of the product. Emotion is the experience that dominates decision-making by commanding attention and creating memory [1].

In the coming decades, the world will see a greater emphasis on resource conservation, energy conservation, town planning, as well as public transport. Congestion and roadblocks are getting complicated, wasting time and business, and adding to the drivers' frustration. The current cities' infrastructure was planned and built years ago and needs reconstruction which is not an easy task [3]. The HIRIKO design team found that private automobiles are the major source of pollution and CO₂ emissions, congesting roads and streets. According to their research, public transport does not cover the entire cities having inconvenient running schedules and thus the first mile and the last mile issue of the transit is getting complicated [4]. The HIRIKO is a compact, folding, two-seat urban electric car which was launched globally in January 2012.

Future transportation is going to be more challenging than ever and bio-inspiration may hold the key to solve its issues. The bio-inspired design establishes nature in the form of inspiration and a guide. It is an iterative methodology applied to many diverse fields. It involves abstraction, search, analysis, comparison, and the transfer of bio-inspired analogies as the core activities of the process [5]. Bio-inspiration is known as biomimicry, biomimetics, biofabrication, and bionics also. Leonardo da Vinci used bio-inspiration as his creativity source and made drawings of many technical machines. The invention of hook-and-loop fastener, Velcro®, is also an example of this phenomenon. "Form follows function" is an industrial design principle and the natural optimization of plants and animals clearly exhibits this. A study showed that the bio-inspired design is efficient in protective structures also. Scholars matched the protection function of the vehicle with fruit peels to introduce the crash-resistant and lightweight design of protective structures [6]. Other research provided an overview of the sharkskin mechanism for drag reduction to enhance the design understanding for efficient surface fabrication with reduced drag force. Fluid engineering finds many applications of sharkskin surface fabrication including swimsuits, golf balls, and

airplanes [7]. The authors proposed a whale optimization algorithm grounded on the bubble-net hunting tactic inspired by the community practice of humpback whales. They found the whale optimization algorithm highly competitive as compared with conventional meta-heuristic algorithms [8].

One more study created analogy categories of architecture, form, function, materials, process, surface, and systems for bio-inspired design with definitions and examples. The form category included visual features such as shape, geometry, and aesthetics [9]. The research into bio-inspired design presents the technology pull and biology push as two main methods of this phenomenon. The technology pull is known as “problem-driven” or “top-down” approach also whereas the biology push is called “solution-driven” or “bottom-up” approach [5].

This research paper presents a new bio-inspired approach using the technology pull method to address the sustainability and last mile issues of futuristic transportation. This work and the methodology can be used to develop a fully functional futuristic vehicle in future studies.

1.1 Bio-inspiration in Automobile Sector

Animals are naturally and efficiently optimized having functional superiority and aesthetical appeal with curves, distinctive forms, and overall cohesiveness. Researchers have studied a boxfish to design an energy-efficient car body and found that the boxfish-inspired car’s drag coefficient was much lower than that of a typical passenger car. But the boxfish is not very good looking which limits the bio-inspiration to the hydrodynamics of the body only [10].

Many scholars have studied the use of animal features in car appearance and styling design also. They categorized some of the commercial cars like Peugeot 206, Toyota Previa, Citroën Xsara, Ford Cougar, VW Golf, Renault Megane, Ford Focus, Mazda MX-5, Ford Puma, and Toyota Celica based on their front face design inspired from various shapes of animal eyes [11]. Most of the famous car brands and car models have been named after animals, birds, and even insects as presented in Table 1 [11]. This shows the automobile makers’ desire and needs to attract customers by associating their machines with the appeal and capabilities of these creatures.

1.2 Bio-inspired Designs in Other Sectors

The most classical example of bio-inspired design is that of Japan’s bullet train inspired by a kingfisher’s beak [12]. Another invention is the loop-hook fastener-Velcro® inspired by burrs. A biomechanic by profession, Frank Fish, has developed wind turbines inspired by humpback whales [13]. Climbing gloves from geckos [12], well-ventilated buildings from termite mounds, hydrophobic surfaces from lotus leaves, and responsive facades from plants are other examples of bio-inspired

Table 1 Some of the car brands and models named after animals, birds, and insects

S. No.	Car model	Named after	S. No.	Car model	Named after
1.	Jeep Eagle	Eagle (Bird)	11.	Dodge Viper	Viper (Snake)
2.	Ford Mustang	Horse (Animal)	12.	Buick Skylark	Skylark (Bird)
3.	Ford Puma	Puma (Animal)	13.	Hudson Wasp	Wasp (Insect)
4.	Ford Cougar	Puma (Animal)	14.	Ford Thunderbird	Thunderbird (Mythological Bird)
5.	Ford Falcon	Falcon (Bird)	15.	Lancia Hyena	Hyena (Animal)
6.	Jaguar	Jaguar (Animal)	16.	AC Cobra	Cobra (Snake)
7.	Chevrolet Impala	Impala (Animal)	17.	Triumph Stag	Stag (Animal)
8.	Corvette Stingray	Stingray (Fish)	18.	Volkswagens Beetle	Beetle (Insect)
9.	Sunbeam Tiger	Tiger (Animal)	19.	Peugeot Lion	Lion (Animal)
10.	Renault Spider	Spider (Insect)	20.	Mercury Lynx	Lynx (Animal)

designs [14]. The facades of Esplanade Theater are bio-inspired from the semi-rigid skin of the durian plant. This building's exterior modifies during the day to let sunlight in without overheating the interiors.

2 Futuristic Smart Transportation

We are all naturally interested in the future, including how our own lifestyles may pan out, and how the world might develop over time. Studies showed the scope of “personal mobility” and “co-operative driving” as the new concepts in a rapidly evolving new society. As the living organisms interact with each other in nature, futuristic vehicles will interact with other vehicles, their surroundings, and humans [15].

In the future, we will manage more complex scenarios as road safety, CO₂ emissions, fuel usage, and sustainable public and personal mobility need to be addressed [16]. Futuristic technology will keep the driver out of the loop going beyond the emerging driverless trend. Manually driven vehicles are prone to fatal accidents and this may be the biggest reason for keeping the driver out of the loop. In contrast to this, other researchers have recommended a shared control of technology between the vehicle and the user [17]. An overall system will be developed in future cities to accommodate these smart vehicles to make the human-machine interactions easy, safe, and engaging.

The designers of HIRIKO found that the evolving concept of smart cities will attract 90% of the total population growth. Such cities will be occupied by 60% of the population having a total of 80% share of wealth. The global urban population increased to 47% in 2000 as compared to that of the 13% in 1990. This became 50%

in 2007 with 3.3 billion people being “urban” and will cross the 60% mark in 2030 and 70% mark in 2050 with 9 billion people being urban. This will change the urban settings with a more young and active population [3]. In such a scenario, technology will be everywhere and anywhere with all the devices and even the smart homes connected to the internet. Residents of these cities will seek personal user experience from the products they will be using [4].

2.1 Futuristic Concept Cars and Their Aesthetics

All the recent concept cars of 2019 are electric, showing the commitment toward zero emissions transport of the future. Most of these are built around sustainable, autonomous, and engaging user experience approaches of future transit. These cars are shown in Fig. 1 [18, 19]. The Bentley “EXP 100 GT” envisions a sustainable, autonomous, and electric grand touring by the year 2035. It has options of driving by the user and being driverless. The Mercedes-Benz vision EQS also sticks to green and luxury mobility with the sustainable, elegant, two-toned design and sculptural exterior. Hyundai unveiled the “45 EV” with clean lines and a minimalistic structure having 45° angled exterior in front and back. The AUDI AI: TRAIL Quattro has the ability for automatic driving with excellent outdoor experiences.

DS automobiles developed the DS X E-tense concept supercar with an electric drive embedded in an asymmetric body. Its asymmetric shape is the most user-appealing design feature that keeps the driver out in the wind and the passenger enclosed. Launched in March 2020, the Hyundai Prophecy has a sensuous sporty

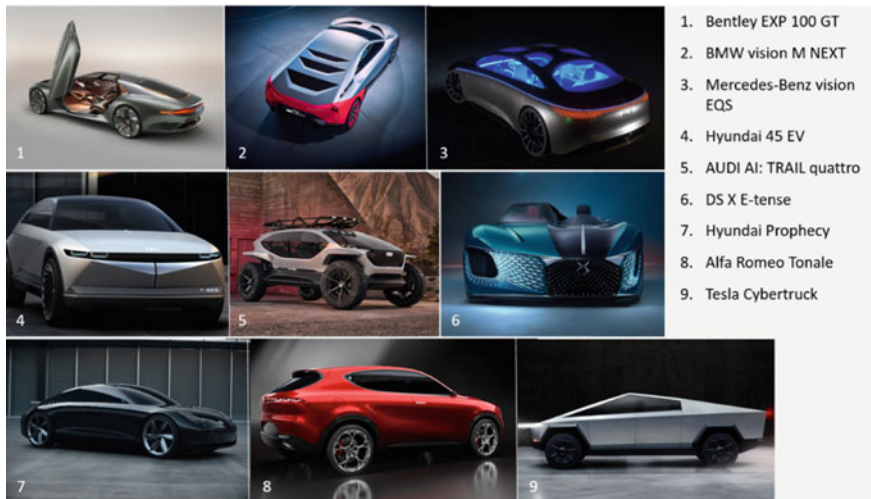


Fig. 1 The most recent futuristic concept cars of 2019–20

design with a voluptuous side section possibly inspired by a perfectly weathered stone. The clean and simple one curve streamline cut ranges from front to rear with a minimalist restriction. The active and sophisticated boat-tail line generated by the rear quarter panels seems to propel the form forward even when it is standing still [18]. The Alfa Romeo Tonale concept presented the electrification feature with the Italian label's exceptional, distinguishing and celebrated styling. Its bold and elegant exterior is enhanced with clean lines and the sculptural front and rear lights. Tesla also launched its Cybertruck, which got a lot of publicity. The design was partially inspired by the lotus esprit sports car that transformed into a submarine in one of the James Bond movies.

Round headlights overlap the grille in the style of their "bower", and the rear is reminiscently sloped in the Bentley EXP 100 GT. Its illuminated matrix grille dominates the view, pairing with the headlamps and flying B mascot to create dramatic and dynamic lighting. The sleek, taut body surfaces are coated in a special silver finish made from a pigment that is a by-product of the rice industry. The design looks complete with spectacular two-meter wide doors that pivot outwards and upwards.

The BMW vision M NEXT has typical sports car proportions inspired by the styling of both classic and contemporary BMWs, such as the "turbo" and "i8". Its low-slung front with strikingly thin headlamps is sharply cut into a wedge-shaped silhouette at the rear. Along the side, the car is defined by smoothly sculpted surfaces as well as gullwing doors. The extended, sophisticated, intense, and dominant one-bow styling of the Mercedes-Benz vision EQS is immediately notable by its two-tone color scheme of silver and dark blue. Its extremely sculptural form comes with a shoulder line—"lightbelt" that encircles the whole car [19]. The most recent futuristic cars of 2019–20 and their main styling features are presented in Table 2.

Table 2 Major exterior styling features of some of the most recent futuristic concept cars

S. No.	Concept car	Major exterior design features
1.	Bentley EXP 100 GT	Outwards-upwards opening doors
2.	BMW vision M NEXT	Gullwing doors
3.	Mercedes-Benz vision EQS	Shoulder line (lightbelt) around the full body
4.	Hyundai 45 EV	Sharp, clean lines with 45° angle cut on front panel
5.	AUDI Futuristic Buggy	Outside view with robust and super-sporty body exteriors
6.	DS X E-tense	Asymmetric compelling body
7.	Hyundai Prophecy	Smooth one cut body exteriors
8.	Alfa Romeo Tonale	Sculptural exterior inspired by human muscular body
9.	Tesla's Cybertruck	Bulletproof geometric minimalistic body

2.2 The Futuristic Scenario and the User Persona

It is wicked to find what kind of mobility and transit should or will be in 2030 or 2050 but designers need to cultivate storylines and strategies inciting discussions over the key issues regarding smart and sustainable futuristic transportation [3]. Machines will be men's friends and he will fall in love with them in the future. Human homes, shopping malls, hospitals, and vehicles will be interconnected with the help of the Internet. Driverless cars may totally disrupt the way they look and feel. The traditional vehicle designs may be objects of the past. The big question is—what will futuristic vehicles look like? Will they be able to fly?

The literature confirms that futuristic smart transport will be based on environmental and economic sustainability to reduce CO₂ emissions and enhance user experience with customized journey experiences. As the roads are congested, the current infrastructure is difficult to rebuild and users are becoming experience-centric; futuristic vehicles' aesthetics and in-journey experiences will be at the core of designers' considerations along with other functional necessities. The smart transportation of the future may have flying cars with highly customizable interiors and exteriors. People will be living alone or with long-distance relationships, with time constraints and internet-connected devices. They will need a companion which they may find in a machine—their personal vehicle. These vehicles may be able to understand the emotional and cognitive state of the user and take the journey accordingly to delight the user. The device interfaces will change drastically and may become completely voice commanded. In this time of full automation and AI, the vehicle aesthetics should be able to convey trust, friendliness, and freshness to the user.

The ideal user persona for future transportation is derived from all the literature reviewed in alignment with the current industry trends synthesized from the careful study of the mentioned concept cars and their exteriors. The user is an individual, working in a private company and living away from family and friends. He wants to go to his job conveniently, avoiding all the road-jam chaos and in a relaxed state of mind. In the evening, he wants to pick up his friend for a coffee. While they are enjoying their coffee, the vehicle should get charged. For all this, he needs a dynamic, fast, friendly, and trustworthy vehicle. The bio-inspired vehicle from whales is an attempt to design such aesthetically pleasing vehicle.

3 Design Process for the Aesthetics of Whale-Inspired Futuristic Vehicle

The technology pull method starts with an identified technical problem and results in a biological inspiration. Whereas the biology push method starts with a known biological solution to be applied in a technical product or problem [5]. The proposed futuristic vehicle's aesthetics has been conceptualized using the technology pull approach of bio-inspiration as presented in Fig. 2.

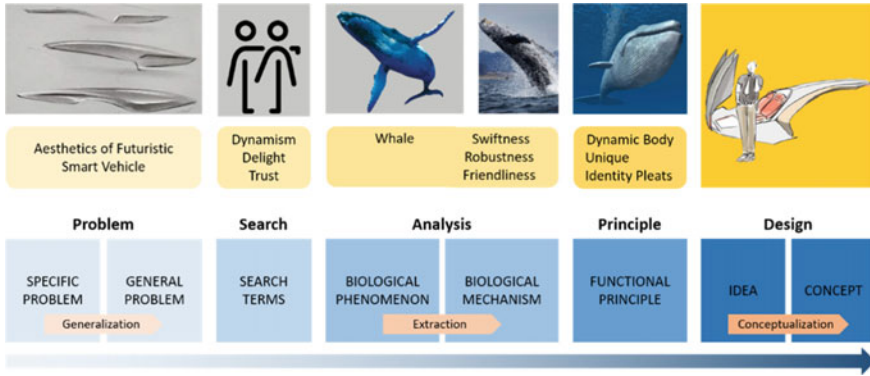


Fig. 2 Design process of a whale-inspired futuristic vehicle aesthetics by the technology pull approach of bio-inspiration framework

3.1 Requirement Analysis and Analogy Transformation for Bio-inspiration

The requirement generation for this futuristic vehicle styling is grounded in three aspects of the future-people and their relationships, cities and their environment along with technology and industries. The users will need an emotional bond, unique identity, and style statement with energy-efficient systems, friendly machines, and appealing aesthetics of the same. The form of the vehicles may be governed by the technologies and materials of that time. The form and body of the solution should support the future manufacturing materials in terms of safety, endurance, and speed as this aspect was the main factor in Tesla's bulletproof Cybertruck. The Cybertruck was designed with an impassable exoskeleton and ultra-hard 30X cold-rolled stainless steel body along with Tesla armor glass [19].

Analogy transfer is considered for mimicking the biological features and mechanisms into the designed solution. In the technology pull method of the bio-inspiration framework, the particular problem is generalized to look for bio-inspiration. In this case, the problem is aesthetics design for futuristic vehicles and the whale is the source of bio-inspiration. Whales have a naturally optimized streamlined fusiform and strong body having limbs modified into flippers to steer. They can conserve the oxygen by reducing their heart rates when staying underwater for long and communicate with melodic sounds even by mimicking human speech. They use various means of communication including fin flapping, tail flapping, breaching, blowing, and ticks. Blue whales have unique skin pleats that act like human fingerprints to distinguish one creature from the other [20]. These pleats expand to accommodate the huge amount of nutrients and food in the water when needed. Despite being such a large body, it is amazing to see the whales moving so easily and swiftly. In some parts of the world, whale watching has emerged as a prominent leisure-cum-adventure activity.



Fig. 3 The whale-inspired futuristic vehicle design phases

3.2 Conceptualization and Modeling

Various forms were drawn based on the analogy transfer from a whale's biological aspects as shown in Table 2. The concept sketch lines illustrated the speed, dynamism, playfulness, and wholeness.

The final result was a new body design inspired by the shape of the whale in considerations with materials, user's emotional bond, and vehicle personality needs of the future transportation system [3, 15, 17]. In spite of being such a large creature, it is impossible to see other creatures that befriend themselves at the first meeting with the man. Whales, like humans, are able to use language, express emotions, and socialize easily. This vehicle has some parts similar to the throat pleats on the bottom of the blue whale's body [20]. These work like its identity and may be considered as an alternate to the present chassis number mechanism for vehicle identification. This vehicle will be able to communicate with the outside world by displaying many colors through these pleats. Further, this mechanism can be utilized to make extra space for the luggage and legs of the passengers.

The overall form is cohesive and appeals to users to induce an emotional bond with the product personality [1] and clean geometric lines blended in an organic body. This form may be manufactured as unibody as per the materials and future transit safety needs. Upwards-outwards opening doors add to the statement of the user. These doors overlap with the semantics of wings to fly. The side view of this vehicle looks ready to fly. This adds the connotation of being on toes the moment you need it. The final 3D modeling and renderings were done using the Autodesk Alias AutoStudio 2016 and Autodesk VRED Design 2016 (Figs. 3 and 4).

4 Discussion and Future Scopes

Futuristic transportation holds many challenges as the roads are getting congested, pollution is rising, transit safety is vulnerable and technology is disrupting the industry [3, 4]. Bio-inspiration may provide reliable solutions for both functional and aesthetical aspects of the futuristic smart transportation system [5]. This futuristic transit concept vehicle is designed for aesthetical aspects and overall exterior form to excite users' emotions for a bond. This form and aesthetics have been conceptualized with an understanding of the futuristic smart transportation scenario [4, 15–17]. For

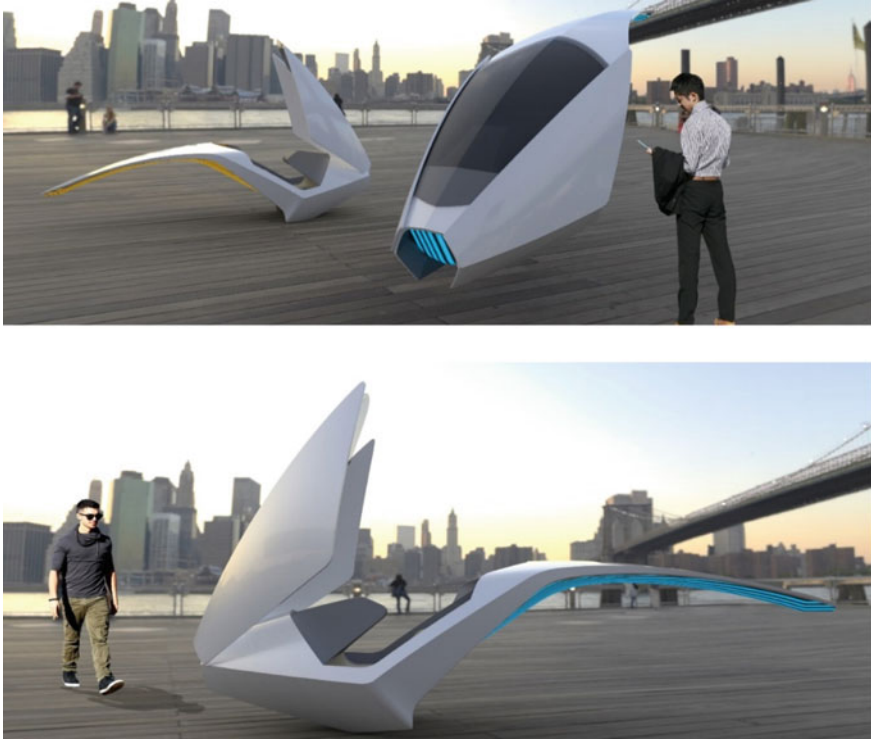


Fig. 4 Final renderings of the whale-inspired futuristic vehicle

the development of functional mechanisms, it needs further research and strategies for a better vision and understanding of technological advancements.

The unibody form with clean geometric lines blended into the organic body is appealing and a style statement for the prospective users of personal vehicles in the future. This vehicle body can be formed using highly reliable and strong cold-rolled stainless steel as that of Tesla Cybertruck [19]. The outwards-upwards opening doors inspired by the whale fins are a delight for anybody looking for style. Whales offer a great source of naturally optimized biological features to use as an inspiration for both functional and aesthetical designs [20]. The same bio-inspiration analogy transfer, as presented in Table 3, can be taken to design the interior and functional elements of this vehicle in future studies.

Previous studies have used the Ask Nature and function-based biologically inspired design methods to design protective structures [6], direct bio-replication, synthetic fabrication, and micro-rolling methods to create a drag reduction surface from sharkskin [7], mathematical modeling of bubble-net feeding behavior of humpback whales for algorithm optimization [8], bio-inspired analogy establishment [9], computational and experimental methods to design a boxfish-inspired energy-efficient car which lacks the user appeal [10] and the application of animal forms in

Table 3 Analogy transfer for the whale-inspired futuristic vehicle aesthetics

S. No.	Biological aspect of a whale	Vehicle aesthetics design aspect
1.	Streamlined fusiform body	Sporty and playful exterior lines
2.	Limbs modified into flippers	Transformable features for turbulent rides
3.	Log out of the water to travel faster	May automatically switch to performance mode for speed increase
4.	Conserves oxygen by slowing down heart rate	Refuel-sense and smart energy saver mode transit
5.	Communicate using melodic sounds and can mimic human speech	Voice operated instructions
6.	Good with teaching, learning and co-operating	AI-powered automated response and behavior
7.	Unique pleats act like fingerprints and expand to accommodate water and food	Vehicle identification provision and expansion for extra space
8.	Naturally optimized for strength and endurance	Efficient and aerodynamic form

automotive styling without any novel contribution in terms of the design of a new form or vehicle [11]. Whereas, the present paper used the technology pull methodology of the bio-inspiration approach along with the analogy transfer methodology for the aesthetical design of a smart futuristic vehicle. These methodologies work better as compared to those used in the previous studies [6–11] to devise a whale-inspired systematic and comprehensive solution for smart futuristic transportation.

5 Conclusion

The challenges of futuristic smart transportation may be met with bio-inspiration as animals and plants have been optimized naturally for performance and sustainability. Concept vehicles also may find many biological features and mechanisms to mimic for appeal and emotional connection with the user. As the prospective personal vehicle owners are projected to be living alone with long-distance relationships, they might find their machines as friends [15]. Their vehicles need to be well developed for their emotional and mobility needs. Thus, the aesthetics and overall personality of such vehicles are very important.

This study has proposed one such vehicle concept with its aesthetics inspired by a whale. As whales are creatures of performance, friendly and trustworthy nature, quest to learn, and a unique personality with their throat pleats, they can help to develop many systems for personal use in the future. The geometric-organic infused aesthetics of this vehicle come with a unibody to support future transit safety needs and materials of endurance. This concept can be further detailed using the same

technology pull method as presented in Table 3 to transfer more of the biological features and mechanisms of whales to enhance the solution.

References

1. Van Gorp T, Adams E (2012) Design for emotion. Elsevier, Amsterdam
2. Hung WK, Chen LL (2012) Effects of novelty and its dimensions on aesthetic preference in product design. *Int J Des* 6(2):81–90
3. Hickman R, Banister D (2014) Transport, climate change and the city. Routledge, New York
4. HIRIKO. Driving mobility. https://www.un.org/esa/dsd/susdevtopics/sdt_pdfs/meetings2012/statements/espiau.pdf. Accessed 14 May 2020
5. Farzaneh HH, Lindemann U (2018) A practical guide to bio-inspired design. Springer, Berlin
6. Mehta PS, Ocampo JS, Tovar A, Chaudhari P (2016) Bio-inspired design of lightweight and protective structures. SAE technical paper no. 2016-01-0396
7. Chen D, Liu Y, Chen H, Zhang D (2018) Bio-inspired drag reduction surface from sharkskin. *Biosurf Biotribol* 4(2):39–45
8. Mirjalili S, Lewis A (2016) The whale optimization algorithm. *Adv Eng Softw* 95:51–67
9. Nagel JK, Schmidt L, Born W (2018) Establishing analogy categories for bio-inspired design. *Designs* 2(4):47
10. Chowdhury H, Islam R, Hussein M, Zaid M, Loganathan B, Alam F (2019) Design of an energy efficient car by biomimicry of a boxfish. *Energy Procedia* 160:40–44
11. Burgess SC, King AM (2004) The application of animal forms in automotive styling. *Des J* 7(3):41–52
12. Fisch M (2017) The nature of biomimicry: toward a novel technological culture. *Sci Technol Hum Values* 42(5):795–821
13. Goel AK (2015) Biologically inspired design: a new paradigm for AI research on computational sustainability? In: Workshops at the twenty-ninth AAAI conference on artificial intelligence
14. Cohen YH, Reich Y (2016) Biomimetic design method for innovation and sustainability. Springer, Berlin
15. Norman D (2009) The design of future things, Reprint. Basic Books, New York
16. Damiani S, Deregibus E, Andreone L (2009) Driver-vehicle interfaces and interaction: where are they going? *Eur Transp Res Rev* 1(2):87–96
17. Terken J, Pflöging B (2020) Toward shared control between automated vehicles and users. *Automot Innov* 3(1):53–61
18. CISION PR Newswire. <https://www.prnewswire.com/news-releases/hyundai-motor-unveils-prophecy-concept-ev-301014938.html>. Accessed 15 May 2020
19. Designboom. <https://www.designboom.com/technology/top-10-concept-cars-of-2019-12-13-2019/>. Accessed 14 May 2020
20. Whale. <https://en.wikipedia.org/wiki/Whale>. Accessed 20 May 2020

Detection and Counting of Nuts and Bolts with Image Processing Using MATLAB



Gunji Bala Murali, Gaikwad Tejas Vasant, Dhananjay D. Kupwade,
and Deshmukh Atharva Girish

Abstract Machine vision system plays vital roles in the industrial application in order to maintain quality and control the process. Machine vision technology has numerous applications in various industries like automotive industry, pharmaceutical industries, food and beverage, electronics, packages, and process control. The purpose behind this work is the awareness of machine vision technology and the identification of mechanical components particularly nuts and bolts. An automotive uses nuts and bolts and are assembled at different stages of assembly. The count of these nuts and bolts becomes vital in order to avoid shortage at any stage of assembly. Thus, sorting of the nuts and bolts and their counting is necessary in order to save time. The system can be designed using different algorithms, and all algorithms can be integrated using MATLAB software.

Keywords Machine vision · MATLAB · Nuts bolts counting · Image processing technique

1 Introduction

Image processing techniques play crucial role in extraction of information from the image. The image processing technique can be applied almost all the fields like surveillance, face tracking, defect identification, counting size sorting, and many more. The applications of image processing techniques are enormously increased in

G. B. Murali (✉) · G. T. Vasant · D. D. Kupwade · D. A. Girish
Vellore Institute of Technology, Vellore, Tamil Nadu 632014, India
e-mail: balamurali.g@vit.ac.in

G. T. Vasant
e-mail: gaikwadtejas.vasant2019@vitstudent.ac.in

D. D. Kupwade
e-mail: dhananjay.dattatray2019@vitstudent.ac.in

D. A. Girish
e-mail: atharvagirish.deshmuh2019@vitstudent.ac.in

the field mechanical engineering. Sathiyamoorthy has explained various software's like Lab VIEW, MV Impact, OpenCV, and MATLAB in applying digital image processing technique for obtaining required information from an acquired image [1].

Jian et al. apply machine vision system to identify the shaft diameter is within the permissible range. In the algorithm, the authors classify the components as OK, Not OK, over size, and under size based on the measured diameter [2]. Zhang et al. have done the similar work using edge detection algorithm. The images are processed by the Lab VIEW software, and the output is displayed on the monitor. The algorithm works on counting the number of pixels along the edge of the shaft; by counting the number of pixels, the pixel range is calculated and compared with the acceptance range of pixels value to qualify the shaft [3].

Cheng and Jafari proposed vision-based system to control the damage of the top die for punch press machine. In this system, a camera is placed in such a way to see the upper die weather component is attached in the top die or not. If the component is attached in the top die, pneumatic actuator is used to lock the pedal [4]. Fernandes et al. suggested vision-based method for blister pack inspection for identifying the tablets in the packets. From the proposed system, the patient can identify whether the blister pack consist of tablet or not, which will be helpful to the patients in emergency conditions [5]. Hsu et al. worked on development of vision system to identify the level of the liquid in the bottle and the presence of cap for the bottle. From the designed system, the algorithm can easily identify the presence of cap and level of liquid in the bottle [6]. Amit et al. implemented image processing technique to identify the size of nuts and bolts. In the developed system, artificial neural network is used to train the dataset for identifying the size of nut and bolts [7]. Priya et al. proposed mathematical morphology approach to identify the defects for the fabrics using image processing technique. In the research article, the authors used concept of converting the images to the bit planes, by which defect portion on the fabric can be identified [8].

Karimi and Asemani have written a review article in the area of defect identification on tiles using image processing techniques. In the review article, the authors elaborated different kinds of image processing algorithms like wavelet transform, filtering, morphology and contourlet transform, and their performance comparison on defect identification for tiles [9]. Karimi et al. have proposed vision system to identify defects on rail surfaces. The authors used spectral image differencing procedure (SIDP) to identify defects like flakes, cracks, grooves, or break-offs on rail surfaces [10].

Keeping in mind the numerous advantages with the vision system, in this research article, image processing and enhancement techniques are implemented using MATLAB to identify and count the nuts and bolts. The developed code is tested with different sort of images consisting of nuts and bolts, and the results obtained are satisfactory, and the algorithm identifies the nuts and bolts with 90% accuracy. In this research article, a simple method using MATLAB to identify the

shape of the object is proposed, which doesn't require any sort of training the algorithms like in ANN or CNN to sort the object, which is the novelty of the present work.

2 Proposed Methodology

In automotive industries, the assembly of a vehicle uses nuts and bolts in huge quantity. It is important that at the time of assembly, the pairs of nut and bolt should be available in appropriate number in order to optimize the assembly time. To detect and count the nuts and bolts, MATLAB platform is used with suitable feature extraction algorithm. Study different algorithms for detection on nuts and bolts. Optimize the assembly time. The workflow may be stated as per Fig. 1 shown. Starting from the preparatory stage, deciding the area of the work project planning is done. Several research papers were studied as of the literature review is concerned. Logical design is developed as per the application. The MATLAB code was developed for the recognition and measurement of nuts and bolts. The images of nuts and bolts ran through the code, and the results were obtained.

Fig. 1 Proposed methodology

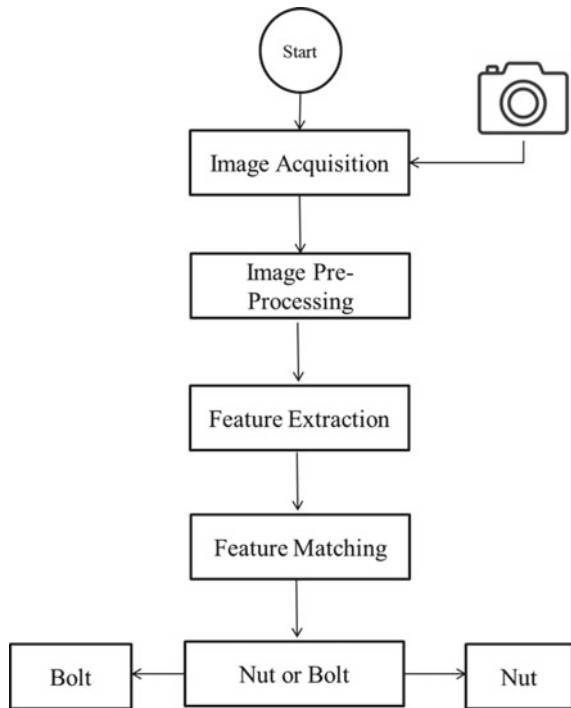


Image acquisition can be achieved by means of different cameras available in the market. For the testing purpose, mobile phone camera or laptop camera can be utilized. After the image acquisition, the image will be preprocessed in order to make it suitable and feasible for the further process. Thereafter, feature extraction is done. The feature extraction will distinguish nuts and bolts. The program detects nuts based on its circular feature; and by subtracting the number of nuts, the number of bolts is measured. The nuts and bolts are differentiated as the nut is component which is having hole, and bolt is component which is having length. The proposed methodology for identifying and counting the nuts and bolts is shown in Fig. 1.

The system proposed can be roughly demonstrated as shown in Fig. 2. The image acquisition is done by the camera installed over the conveyor. The image is the preprocessed by the preprocessor. The data are then sent to the classifier. Afterward, the decision is made, and nuts and bolts are identified and counted.

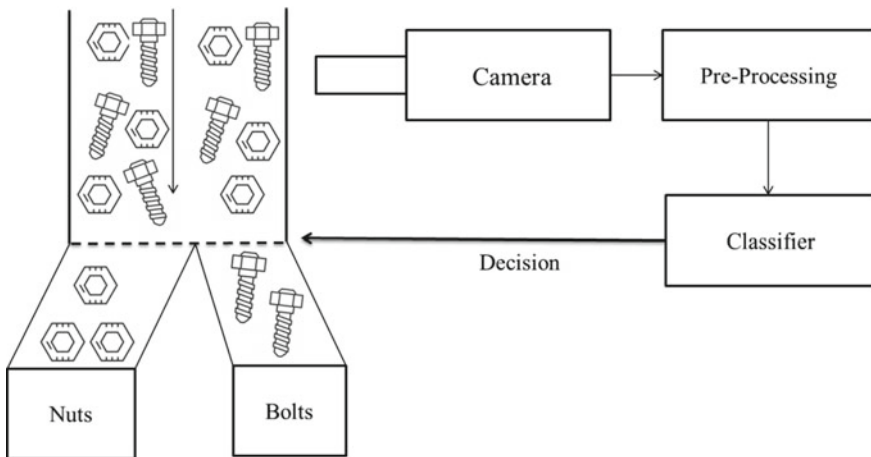


Fig. 2 Line diagram of machine vision system

3 MATLAB Code for Detection and Nut Bolt Counting

```

I = imread('NUTBOLT.jfif');
im = rgb2gray(I);
im = imadjust(im);
im = im2bw(im, 240/255);
im = medfilt2(im);
figure, imshow(im);
Rmin = 30;
Rmax = 80;
im = ~im;
[center, radius]
= imfindcircles(im, [Rmin, Rmax], 'Sensitivity', 0.9, 'ObjectPolarity', 'bright');
viscircles(center, radius);
cir = size(center);
tot_cir = cir(1);
im = imopen(im, strel('disk', 2));
im = imfill(im, 'holes')

% figure, imshow(im);
[llabel num] = bwlabel(im);
disp(num);
Iprops = regionprops(llabel);
lbox = [Iprops.BoundingBox];
lbox = reshape(lbox, [4 num]);
= bwboundaries(im);
a = size(b);
disp('Number of Bolts = ');
disp(a(1) - tot_cir);
bolt = a(1) - tot_cir;
disp('Number of Nuts = ');
disp(tot_cir);
figure, imshow(I);

%figure, imshow(im);
for cnt = 1:num
    rectangle('position', lbox(:, cnt), 'edgecolor', 'r');
end
title(sprintf('No of Bolts = %1.0f , No of Nuts = %1.0f', bolt, tot_cir));

```

4 Results and Discussion

The primary objective of the work is to identify and count the nuts and bolts using machine vision system in order to maintain the adequate supply of nuts and bolts. This helps in reducing the labor by reducing manpower required for the task which indeed saves the cost and time. The execution of algorithm in MATLAB is shown in Fig. 3.

During the execution of the algorithm, input parameters (dimensions of the nut and bolt) of the algorithm have to be defined. The proposed methodology converts the RGB image to grayscale image and stores in the form of matrix. In the next step, the algorithm calculates the dimension (length and breadth by framing the box) of the nuts and bolts image captured by the camera and compares with the predefined values to identify size of the nuts and bolts. In the further step of identifying the nut and bolt, estimate the shape of the image by the algorithm and compares with the predefined shapes of assigned nut and bolt. For example, to identify the nut shape, the outer shape of the nut image has to be appear as hexagon, and the inner side is to be circle. The obtained shapes are to be match with the predefined shapes; then, the algorithm recognizes as nut. The test results of algorithm in identifying the nut and bolts for different images are show in Fig 4. In Fig. 4, the algorithm displays the results as '0' in the absence of nuts and '-1' in the absence of blot during identifying the nuts and bolts in the image.

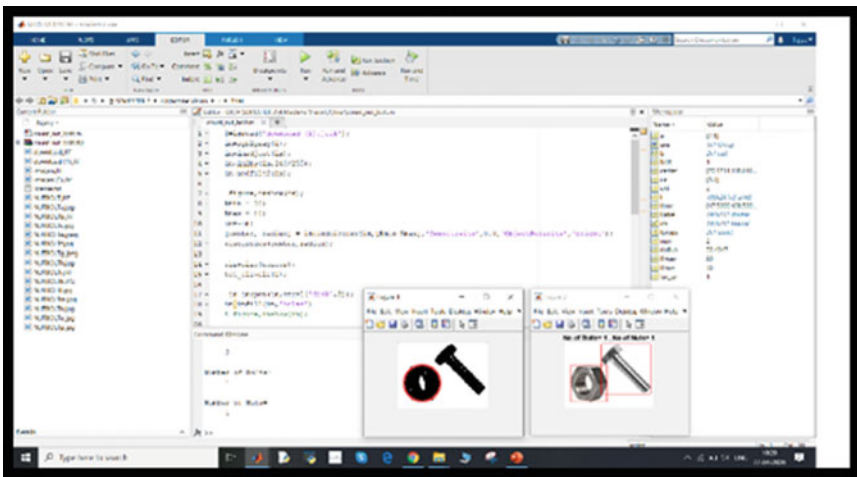


Fig. 3 Represents the MATLAB software

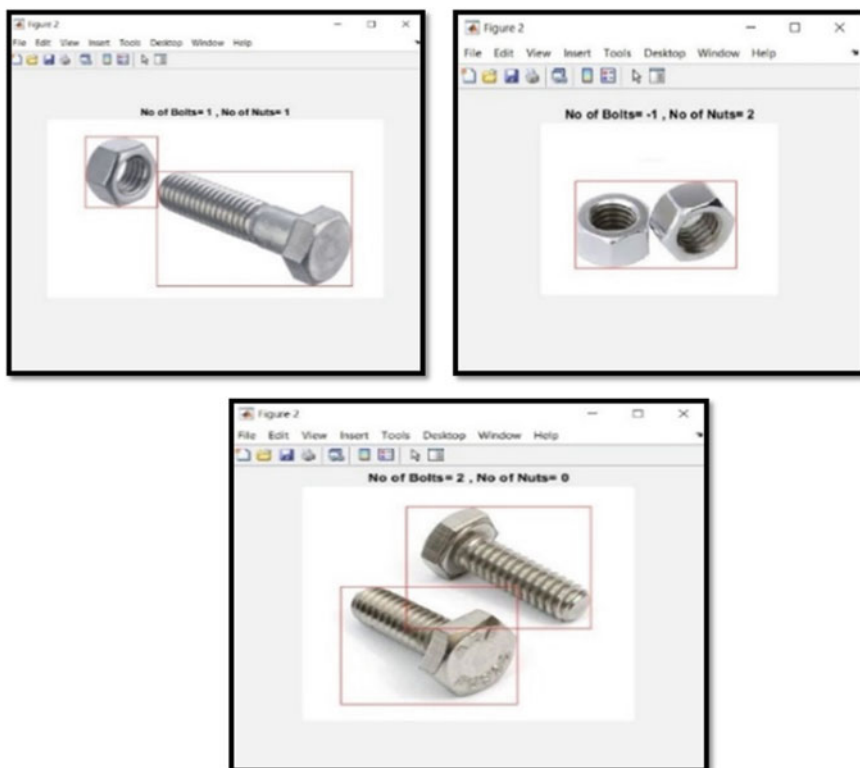


Fig. 4 Different case studies executed in MATLAB to identify the nuts and bolts

5 Conclusion

Image processing techniques are used to identify the nuts and bolts and to count the nuts and bolts using MATLAB. The algorithm shows proper results as compared to the stationary images. The success rate is more than 90%. The success rate can be improved up to 95% if we had used an additional spotlight on the object, proper camera.

As a future scope, identifying the washer instead of nut with the present algorithm can be improved to identify separately.

References

1. Sathiyamoorthy S (2014) Industrial application of machine vision. Int J Res Eng Technol (IJRET). eISSN: 2319-1163, pISSN: 2321-7308
2. Jian-hai H, Shu-shang Z, Wei S (2007) Research on sub pixel detecting on-line system based

- on machine vision for inner diameter of bearings. In: International conference on robotics and biometrics, Sanya, 15–18 Dec 2007, pp 2049–2052
3. Zhang Z, Chen Z, Shi J, Jia F, Dai M (2008) Surface roughness vision measurement in different ambient light conditions. In: 15th international conference on mechatronics and machine vision in practice, Auckland, 2–8 Dec 2008
 4. Cheng Y, Jafari M (2008) Vision-based online process control in manufacturing applications. *Trans Autom Sci Eng* 5(1):140–153
 5. Fernandes AO, Moreira LFE, Mata JM (2011) Machine vision applications and development aspects. In: 2011 9th IEEE international conference on control and automation (ICCA), 19–21 Dec 2010, pp 1274, 1278
 6. Hsu RC, Kao P-W, Lai W-J, Liu C-T (2010) An initial edge point selection and segmental contour following for object contour extraction. In: 2010 11th international conference on control automation robotics & vision
 7. Kale AA, Bhojane DS, Junghare PM (2018) An application for the separation of nuts and bolts using image processing and artificial intelligence. *Int J Latest Technol Eng Manag Appl Sci (IJLTEMAS)* VII(I). ISSN 2278-2540
 8. Priya S, Ashok Kumar T, Paul V (2011) A novel approach to fabric defect detection using digital image processing. In: 2011 international conference on signal processing, communication, computing and networking technologies. IEEE, pp 228–232
 9. Karimi MH, Asemani D (2014) Surface defect detection in tiling Industries using digital image processing methods: analysis and evaluation. *ISA Trans* 53(3):834–844
 10. Deuschl E, Gasser C, Niel A, Werschonig J (2004) Defect detection on rail surfaces by a vision based system. In: IEEE intelligent vehicles symposium, 2004. IEEE, pp 507–511

Evaluation of EDM Die-Sinking Electrode Wear Rate of COOH-MWCNT/Al Nanocomposite



Md. Zakir Hussain , Sabah Khan, and Pranjali Sarmah 

Abstract This research paper investigates the effect of different wt% of COOH-MWCNT in Al matrix on the EDM die-sinking electrode wear rate. X-ray diffraction pattern and EDX spectrum were used for phase and chemical composition analysis. Actual mass density and % of pores volume of COOH-MWCNT/Al nanocomposites show that the mass density and % of pores volume decreases with increasing wt% of COOH-MWCNT. The result shows that the wear rate of nanocomposite decreases with increasing wt% of COOH-MWCNT, and the electrode wear rate was improved with the addition of COOH-MWCNT as compared to pure Al electrode. The surface morphographs show that the mode of electrode wear was due to brittle fractured during the wear process. Therefore, COOH-MWCNT/Al nanocomposite may be used as an EDM die-sinking electrode for EDM die-sinking machining operation.

Keywords Nanocomposite · Aluminum · Carbon nanotubes · Electro-discharge die-sinking machine · Mass density · Electrode wear rate

1 Introduction

Wear is defined as progressive loss of material from contact surfaces move relative to one another [1]. Aluminum (Al) has light weight, soft, and highly ductile metal widely used in aerospace industries. Improvement of its mechanical and wear property can be achieved through reinforcement of nano-filler material. The term nanocomposite indicates composite materials having one phase dimension in nanometer range [2]. The discovery of carbon nanotubes in 1991 showed that it acts as an ideal reinforcement material for the fabrication of metal matrix nanocomposites

Md. Z. Hussain · S. Khan (✉)

Department of Mechanical Engineering, Jamia Millia Islamia, New Delhi 110025, India
e-mail: skhan2@jmi.ac.in

P. Sarmah

Mechanical Engineering Department, Dibrugarh University, Dibrugarh 786004, India
e-mail: pksnit0@7gmail.com

because it has excellent strength, high value of Young's modulus, low density, and also high aspect ratio [3, 4].

Hussain et al. prepared F-MWCNTs/Al nanocomposite and found that the hardness of the nanocomposite depended on wt% of MWCNTs [5]. Esawi et al. fabricated wt% MWCNT/Al nanocomposite through powder metallurgy technique as the technique was a promising route for the fabrication of this type of nanocomposite [6]. Sharma et al. investigated mechanical and dry sliding tribological behavior of aluminum alloy 6101-graphite composites and found that the wear rate was decreased with increasing the volume fraction of graphite. The researchers also found that the wear rate was optimum at 4 wt% graphite [7]. Xavier and Suresh fabricated wet grinder sbb tone dust particles/Al composite and found that the hardness and wear resistance of the composite was increased with increasing wt% of dust particles but reduced composite ductility [8]. Kandeve et al. fabricated different wt% of TiC/Al micro-composite and concluded that the reinforcement of aluminum alloys by TiC micro-particles significantly increased the wear resistance [9]. Rashad et al. presented the effect of multiwalled carbon nanotubes (MWCNTs) on the mechanical properties of the hypoeutectic Al-Si nanocomposite, and the composites were fabricated by using a novel processing approach called modified stir casting technique [10]. Manjunatha and Dinesh prepared MWCNT/Al6061 nanocomposite in different wt% of 0, 0.5, 1, 1.5, 2, 2.5, and 3% of MWCNT through powder metallurgy process and found that hardness and tensile strength of nanocomposites were increased as compare to Al6061 [11].

In electro-discharge machining (EDM), Cu and graphite are commonly used as tool materials. In this article, an attempt has been made to investigate electrode wear of electrode material COOH-MWCNTs/Al nanocomposite for the development of EDM die-sinking electrode material. Electrical discharge die-sinking machining is a non-conventional engineering part manufacturing process widely used for machining very hard material, making complex shape parts, and fine holes in mold and die industries where material from workpiece is removed by series of repeated spark produced in between electrode and workpiece immersed in the dielectric fluid medium [12]. A comparative study was carried out by Bhaumik and Maity by using Cu, Zn, and brass electrodes, machining on Ti grade 6 alloy based on the material removal rate and tool wear rate. They observed that the Cu electrode showed minimum tool wear and less recast layer compared to other types of electrodes [13]. Khan found that the electrode wear of Cu and brass electrodes increased with an increase in current and voltage [14]. Banker et al. found that the tool wear rate of Al was minimum compared to Cu and brass electrode. They also found that Al and Cu tools showed similar tool wear, material removal rate, and surface roughness characteristics [15]. Hussain et al. found that EDM die-sinking electrode wear of $\text{Al}_2\text{O}_3/\text{Cu}$ micro-composite depended on mass density, Rockwell hardness value, and protective carbonate layer formation [16]. Hussain et al. found that the peak current was the most effective parameter that affects electrode wear and material removal rate of $\text{Al}_2\text{O}_3/\text{Cu}$ composite [17].

In this article, pure Al, 0.1, 0.3, 0.5, 0.7, and 1.0 wt% COOH-MWCNTs/Al nanocomposites were prepared through a cost-effective powder metallurgy process [4, 5, 16]. The nanocomposite samples were compacted by using pellet press machine

(make: Nitin hydraulic and engineering) and sintered in a furnace (make: Shambhavi Impex, Model: SILMF-01, Maximum temperature limit ~ 1200 °C). The electrode wear rate has been evaluated by using EDM die-sink (Electronica Hitech).

2 Experimental Work

2.1 Materials

–COOH group functionalized multiwalled carbon nanotubes (COOH-MWCNTs) were used as filler material (Production method: chemical vapor deposition, purity >90 vol%, average diameter (outer): 20 nm, average diameter (inner): 5 nm, length: 20 μm , amorphous carbon content <1 wt%, metal particles $<5\%$, SSA: >350 m^2/g , content of –COOH: 1.8%), and base material used was Al particle (density: 2.7 g/cm^3 , particle size <75 μm , assay: $\geq 99.95\%$ trace metals basis, melting point: 660 °C).

2.2 Fabrication of COOH-MWCNTs/Al Nanocomposite

All the nanocomposites samples were fabricated by using powder metallurgy method, and the processing method was available in literature [4, 5]. In shortly, 0, 0.1, 0.3, 0.5, 0.7, and 1 wt% of COOH-MWCNTs were mechanically mixed with Al powder, and 0.789 wt% ethanol was added in the mixture to avoid oxidation of Al powder and also reduce friction during compaction process [5]. In the head stock of an automatic lathe machine (make: HMT), the ball milling flask was attached [18]. The speed of spindle was at 150 rpm. A hydraulic press machine was used to compact the mixed power at gage reading 150 MPa. The sintering process was done in Muffle furnace at a temperature of 450 °C. The 0.1 wt% COOH-MWCNTs/Al nanocomposite is shown in Fig. 1.

3 Result and Discussion

3.1 X-Ray Diffraction Pattern

X-ray diffraction pattern of 0.1 wt% COOH-MWCNT/Al nanocomposite is depicted in Fig. 2. From Fig. 2, it is observed that all major peaks are similar to peak corresponds to Al cubic F-center, Fm-3m (225) having lattice constants of $a = 0.4049$ nm, $b = 0.4049$ nm, and $c = 0.4049$ nm. The diffraction peak of COOH-MWCNTs should locate at 26.20° in (002) plane. But, due to its low wt% of COOH-MWCNTs, the

Fig. 1 COOH-MWCNT/Al nanocomposite

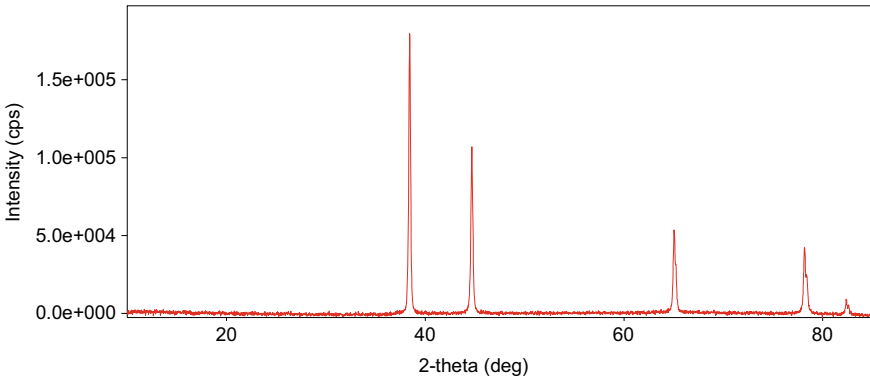


Fig. 2 XRD pattern of COOH-MWCNT/Al nanocomposite

intensity of peak is small. The confirmation of MWCNTs has been made through EDX analysis.

3.2 Energy Dispersive X-Ray (EDX) Analysis

The energy dispersive X-ray spectrum of 0.1 wt% COOH-MWCNTs/Al nanocomposite is shown in Fig. 3. The figure revealed that the presence of chemical elements Al, C, and O in the nanocomposite samples. The presence of C is due to the presence of MWCNTs. The EDX spectrum also shows the presence of O may be due to the presence of $-COOH$ group functionalized MWCNTs or surface oxidation of Al. The spectrum data region also revealed that the presence of small white particles, thus, proving the presence of MWCNTs in nanocomposite samples.

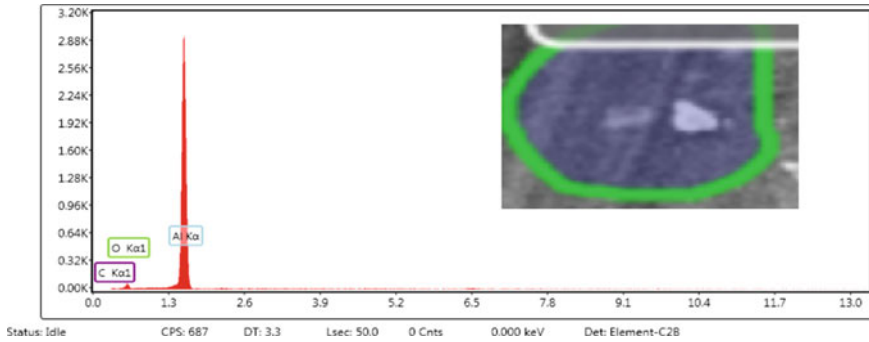


Fig. 3 Energy dispersive X-ray spectrum of 0.1 wt% COOH-MWCNTs/Al nanocomposite

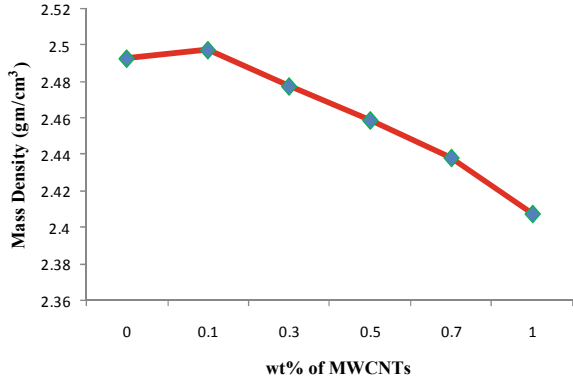
3.3 Sintered Mass Density of COOH-MWCNTs/Al Nanocomposite

Table 1 shows the mass density data nanocomposite samples. The theoretical mass density of nanocomposites was determined by using rule of mixture. The theoretical mass density data indicate that the density decreases with the addition of COOH-MWCNTs in nanocomposites. The experimental mass density of nanocomposite was determined by measurement of mass and volume of composite samples. Figure 4 shows the variation of actual mass density with respect to wt% of COOH-MWCNT. The actual mass density analysis shows that the mass density of pure Al is 2.49291 g/cm³, and it decreases with addition of COOH-MWCNT. The lowest mass density of nanocomposite was 2.407 g/cm³ achieved at 1 wt%. The % of porosity shows that the pore volume of nanocomposite samples has been decreases with addition of wt% of COOH-MWCNT.

Table 1 Mass density of COOH-MWCNT/Al nanocomposite

S. No.	wt% of COOH-MWCNTs	Theoretical mass density	Actual mass density	Porosity %
1	0	2.70	2.49291	7.67
2	0.1	2.687	2.49756	7.05
3	0.3	2.661	2.47765	6.89
4	0.5	2.635	2.458982	6.68
5	0.7	2.609	2.438371	6.54
6	1.0	2.570	2.407576	6.32

Fig. 4 Variation of mass density with wt% MWCNT



3.4 Evaluation of Electrode Wear Rate

Electrode wear of nanocomposite samples was evaluated by using electro-discharge machine die-sink type as shown on Fig. 5. The peak current and voltage and machining time were set at 10 A, 30 V, and 10 min, respectively. The nanocomposite samples were fixed in a holder and attached to the machine.

$$\text{TWR} = \frac{w_i - w_f}{\rho_w \times t}$$

where

w_i = weight of electrode material before machining.

w_f = weight of electrode material after machining.

ρ_w is density of electrode material, and t is the machining time.

Table 2 show that the experimental result of electrode wear rate of different wt% of COOH-MWCNTs. The electrode wear rate of pure Al is 0.04847 g/cm³. The

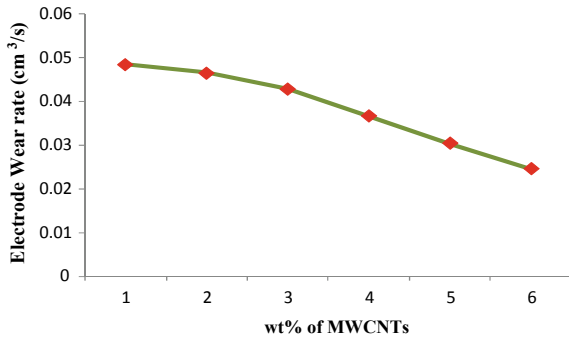
Fig. 5 Experimental setup



Table 2 Electrode wear rate of COOH-MWCNT/Al nanocomposite

S. No.	wt% of COOH-MWCNTs	Electrode wear rate (cm ³ /s)
1	0	0.04847
2	0.1	0.04651
3	0.3	0.04285
4	0.5	0.03671
5	0.7	0.03045
6	1.0	0.02459

Fig. 6 Variation of electrode wear rate with wt% MWCNTs



experimental result shows that that the addition of COOH-MWCNTs in Al matrix decreases electrode wear rate. The 1 wt% of COOH-MWCNTs shows lower electrode wear rate compared to other wt% of COOH-MWNTs. The electrode wear rate of 1 wt% of COOH-MWCNTs is 0.04847 g/cm³. The variation of electrode wear rate with respect to wt% COOH-MWCNT as shown in Fig. 6 shows the wear resistance of COOH-MWCNT/Al nanocomposite is improved with addition of COOH-MWCNT as compared to pure Al.

3.5 Microscope Images of Wear Surface of COOH-MWCNT/Al Nanocomposite

Figure 7 shows the microscope image at ×123 of fractured surface of 1 wt% COOH-MWCNT/Al nanocomposite. The figure revealed that the particles are worn out from nanocomposite surface by brittle fracture. Figure 8a–f also show that the failure mode of electrode wear is brittle in nature. The figures also revealed that pure Al shows higher wear rate compare to different wt% of COOH-MWCNTs, and the electrode wear rate decreases with wt% of COOH-MWCNTs.

Therefore, electrode wear rate is highly depending on wt% of COOH-MWCNTs and presence of pores in nanocomposites.

Fig. 7 Fractured surface of 0.2 wt% nanocomposite at $\times 12$

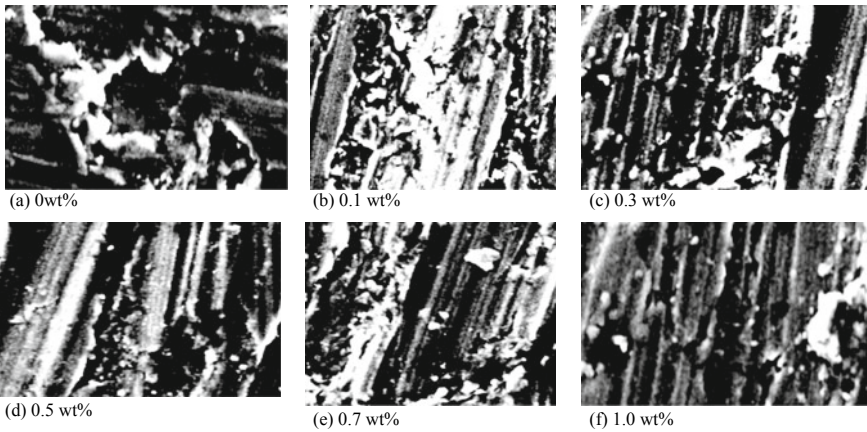
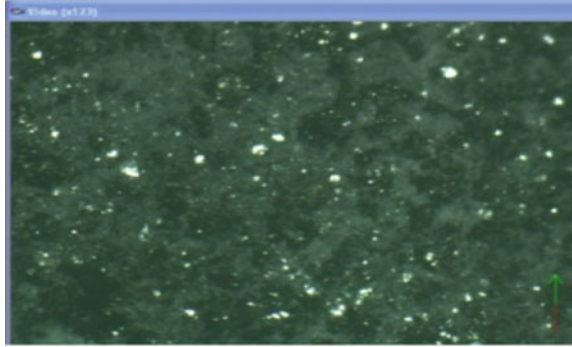


Fig. 8 Fractured surface of different wt% COOH-MWCNT/Al nanocomposite

4 Conclusion

In the present study, pure Al and 0.1, 0.3, 0.5, 0.7, and 1.0 wt% of COOH-MWCNT/Al nanocomposites were fabricated by using powder metallurgy process. Actual mass density and % of pores volume of COOH-MWCNT/Al nanocomposites show that the density decreases with addition of COOH-MWCNT. The XRD pattern shows that the presence of Al in nanocomposite sample. The EDX spectrum indicates the existence of chemical elements Al, C and O in the nanocomposite samples. The electrode wear result shows that electrode wear rate of nanocomposite decreases with increasing wt% of COOH-MWCNT. The 1.0 wt% COOH-MWCNT shows minimum electrode wear rate, and electrode wear rate of COOH-MWCNT/Al nanocomposite is improved compare to pure Al. The surface morphograph of pure Al and different wt% of COOH-MWCNT/Al nanocomposite show that the mode of electrode wear was due to brittle fractured.

It is concluded that the different wt% of COOH-MWCNT in Al matrix may be used as EDM die-sinking electrode for machining operations.

References

1. Bhushan B (2013) Introduction to tribology. Wiley. ISBN: 1119944538
2. Camargo PH, Satyanarayana KG, Wypych F (2009) Nanocomposites: synthesis, structure, properties and new application opportunities. *Mater Res* 12(1):1–39
3. Wernik JM, Meguid SA (2010) Recent developments in multifunctional nanocomposites using carbon nanotubes. *Appl Mech Rev* 63(5):050801
4. Hussain MZ, Khan S, Nagarajan R, Khan U, Vats V (2016) Fabrication and microhardness analysis of MWCNT/MnO₂ nanocomposite. *J Mater* 2016
5. Hussain MZ, Khan U, Chanda AK, Jangid R (2017) Fabrication and hardness analysis of F-MWCNTs reinforced aluminium nanocomposite. *Procedia Eng* 173:1611–1618
6. Esawi AM, Morsi K, Sayed A, Gawad AA, Borah P (2009) Fabrication and properties of dispersed carbon nanotube–aluminum composites. *Mater Sci Eng A* 508(1–2):167–173
7. Sharma P, Paliwal K, Garg RK, Sharma S, Khanduja D (2017) A study on wear behaviour of Al/6101/graphite composites. *J Asian Ceram Soc* 5(1):42–48
8. Xavier LF, Suresh P (2016) Wear behavior of aluminium metal matrix composite prepared from industrial waste. *Sci World J* 2016
9. Kandeva M, Vasileva L, Rangelov R, Simeonova S (2011) Wear-resistance of aluminum matrix microcomposite materials. *Tribol Ind* 33(2):57–62
10. Rashad RM, Awadallah OM, Wifi AS (2013) Effect of MWCNTs content on the characteristics of A356 nanocomposite. *J Achiev Mater Manuf Eng* 58(2):74–80
11. Manjunatha LH, Dinesh P (2013) Fabrication and properties of dispersed carbon nanotube–Al6061 composites. *Int J Innov Res Sci Eng Technol* 2(2):500–507
12. Khan ZA, Siddiquee AN, Khan NZ, Khan U, Quadir GA (2014) Multi response optimization of wire electrical discharge machining process parameters using Taguchi based grey relational analysis. *Procedia Mater Sci* 6:1683–1695
13. Bhaumik M, Maity K (2018) Effect of different tool materials during EDM performance of titanium grade 6 alloy. *Eng Sci Technol Int J* 21(3):507–516
14. Khan AA (2008) Electrode wear and material removal rate during EDM of aluminum and mild steel using copper and brass electrodes. *Int J Adv Manuf Technol* 39(5–6):482–487
15. Banker KS, Oza AD, Dave RB (2013) Performance capabilities of EDM machining using aluminum, brass and copper for AISI 304L material. *Int J Appl Innov Eng Manag (IJAIEEM)* 2(8):186–191
16. Hussain MZ, Khan U, Jangid R, Khan S (2018) Hardness and wear analysis of Cu/Al₂O₃ composite for application in EDM electrode. *IOP Conf Ser Mater Sci Eng* 310(1):012044. IOP Publishing
17. Hussain MZ, Khan U (2018) Evaluation of material removal rate and electrode wear rate in die sinking EDM with tool material Al₂O₃/Cu composite through Taguchi method. *Int J Mater Eng Innov* 9(2):115–139
18. Hussain MZ, Khan S, Sarmah P (2018) Evaluation of erosive wear rate of Al₂O₃/Cu composite through Taguchi method. *Adv Mater Manuf Charact* 8(2):102–108

Agribots Concepts and Operations—A Review



Ramu Eeram, B. B. V. L. Deepak, Umamaheswar Rao Mogili,
and P. Syam Sundar

Abstract This analysis explores the gaps between robots used in agricultural research, development, revolution, and related policies, predictions, errors, and field operations. Robots are very complex and have various subsystems built-in that need to be built and synchronized. Robot systems must be profitable but at the same time have inherent security, good personal safety, the necessary environment, crop, and machine protection. Data recovery systems, embedded sensors, and data surveys that are desired to adapt to the agricultural environment based on valid structured conditions. Integrating humans requires detailed research where operator steps into the system's controlling strategies to meliorate its execution and reliableness. Need to reduce overall size of the system, while improving all components and component integration.

Keywords Agribots · Robots · Agricultural operations

1 Introduction

Farmland has already applied various robots and automation for use, and the use of technology is generally proven. New exploration and development of robotics in the harvesting field operations and related approaches, assumptions, constraints, and the gap were analyzed [1]. This is an essential goal that the application of distinct technologies aims to improve crop yield and condition while reducing harvesting cost. For instance, precise sowing and increased sowing. With advent of advanced technology in agriculture, the plant growth would be optimal with optimum fertilizer application and irrigation, there by reducing the input cost and maximizing the crop produce [2]. The income generated by the fuzzy interpretation system is twice the income achieved. Use of recommended unified apps need 32% more nitrogen [2]. However, harvesting is still difficult due to a serious shortage of skilled workers, especially in the gardening area. The problem stemming from the absence of workers

R. Eeram (✉) · B. B. V. L. Deepak · U. R. Mogili · P. Syam Sundar
National Institute of Technology, Rourkela, Rourkela 769008, India

is that farms are growing in size, the decreasing trend is expanding the number of farmers and the impact on the environment is also increasing. Food production needs more effective agricultural practices [3] and the capacity of traditional agriculture, of which manual crop farming and authority.

Farmers naturally improve by using smart devices machines [4]. Even though the robot and need automation expensive professional labor with implements, they help enhancing agriculture capacity, because of needed labor, inclusive of skilful operators (of machines), dropped sufficiently in order to compensate to get a higher initial cost. The highest agricultural activity is found in unstructured environments. Time, space changes rapidly like underwater, military, or space environments [5]. Vegetation, terrain visibility, uncertain lighting, and other weather conditions are constantly changing, with the required uncertainty, and produce reliable dynamics location [5].

Visibility of a row of peppers in a greenhouse explaining the direction of the sun and the effects of lighting. When dealing with natural objects, it adds complexity. For example, fruits and leaves are textures, colors, sizes, orientations, and locations because of the large variation in shape. In this case, a priori cannot decide. The robot world can be divided into four categories. Structural attributes of objects, environment: (1) Climate, objects both are structured; (2) Climate-unstructured and object-structured; (3) Climate-structured, the object-unstructured, and (4) Both climate, objects are unstructured. Every field of robots, such as industrial, medical, health care, mining, etc. can be combined with one of the following below-mentioned (Fig. 1) [1]. The figure shows variations in complexity and difficulty between domains of the agricultural field is related to the fourth category in which nothing is structured, which



Fig. 1 Figures showcasing pepper crop rows from a green house captured through robot showing the light intensity [1, 6]

Table 1 Robotics domain associated with four groups [1]

		Atmospheric conditions	
		Unstructured	Structured
Object	Unstructured	Agriculture sector	Health sector
	Structured	Defence, space, underwater, mining	Industries

poses challenges in the following areas commercialize. Robots are programmable perceptive machines that perform precise tasks, make diagnoses, and take action in real-time [1] (Table 1).

Much research has been done in the thirty years of harvesting robots, and automation projects for inventions have not implemented in real time. Primary reason of this unsuccessfulness is the high development cost, unfitness to perform the requisite harvesting tasks, the endurance of the lower system, and system’s unsuccessful reproduction of the same work in one kind of different environment or to meet the mechanical, economic and industrial requirements. Mostly the methodologies adapted are of industrial perspective [7].

1.1 Regulations of Robotic Systems in Agriculture

For improving of requirements related to harvesting robotic systems, establish complex and intelligent sensing algorithms, and plan and control to address difficult and unorganized dynamic agricultural environments [8]. Nevertheless, automated system deployment was not successful in these areas. Some development has been adopted and resolved [9]. Introduce the human operator (HO) into the loop operation that communicates with it, an alternative to the system observation is the relatively new farm robot analysis trends, helps in improving operations apart from reducing the problems in the system as well. Few significant development was observed during past twenty years. As per [10], Cooperation Agricultural robots with human–robot system helps solve three problems; (I) Drive robots from tree to farmland Tree and/or line by line; (II) Detect and identify construction; (III) Grab and separate selected products in the analysis, we succeeded in developing the human–robot system is called “AGRIBOT” [1].

2 Assumptions and Components

2.1 Assumptions and Skills Required

The crop yield autonomous robot system that consists of many auxiliary systems and machines that enable the operation and execution of tasks. Processing path planning, exploration, or intelligence functions, maneuverability, drive control, guidance, controllers, or related functional devices, end effectors, these all occur in these subsystems and devices. Guidelines for urgent and somewhat autonomous management methods, individually or together [11]. Agribots are generally designed to perform “main functions”. This is a variety of harvesting operations including planting, weeding, cutting, harvesting, packing, and picking. To complete the “main function”, the autonomous robot system must be able to perform certain “auxiliary tasks” such as searching for, placing, locating, analyzing, or executing the actions of the object to be processed. Intelligence and instructions are linked between “auxiliary tasks” and “auxiliary” and “main function”. In Fig. 2, each “auxiliary task” controls one or more auxiliary and equipment and the auxiliary or device distributes certain “auxiliary tasks”. The “main function” requires condition monitoring, the ability of the autonomous robot system to perform its “assistive tasks” of self-localization, route planning, maneuvering and plot exploration from its exact location until recently, cooperate with HO, interact with humans and other robots and unexpectedly untrained devices, and adjust route planning as needed.

Thin lines represent the transfer of commands, data, and information. The thin line represents a conceptual connection. The notation in parentheses is an example of the “main function”, “support work”, and subsystem of the agricultural robot. Example of the “main function”, “support work”, and subsystem of the agricultural robot.

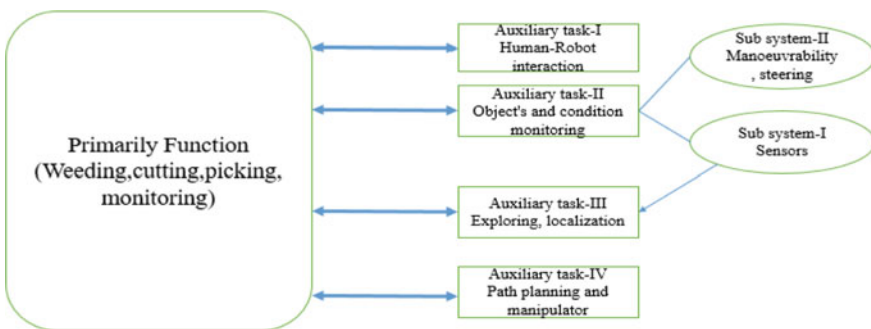


Fig. 2 Structure of task subsystem in agricultural robot [1]

2.2 Mobility and Steering

The maneuverability and drive assistance system are connected via a ground connection to guide the agribot to the required location at the proper speed [12]. Modified a four-wheel-drive agribot platform embedded work environments and precision seeding practices for agricultural needs. There are four servo motors, drive motors, and four stepper motors, regardless of wheel rotation and drive. Central controller adjustment eight motors. They used exactly four-wheel-drive components. Each component could be manipulated and moved forward. Allow the vehicle to have any desired control, modify or maneuver the vehicle direction separately, even while running the platform turning process. Better mobility and mobility: The platform allows the vehicle to move parallel to the lineup during the rotation process [1]. The platform permits the orientation drive in the whatsoever required way and modifies/adjusts the independent wheel displacement alignment, at same time corners.

2.3 Self-localization and Sensing Action

Many functions such as mapping, exploration, orientation and location identification, factory inspection, ambient variables, aerial soil and water, and weed detection are possible with aid of devices called sensors. They are used for analysis and decision making, manipulation, activation, task execution, and machine performance evaluation. Sensor possible the data generated by them is divided into the following categories: (a) Identification of limited characteristics using machine vision [13]; (b) Movement evaluation, energy, and manual indicators, laser positioning; (c) Environmental parameters that use different types of sensors like infrared (IR), acoustic, optic, X-ray, fluorescence; (d) Infinite emplacement with GPS (Global Positioning System) [14]. Sensors applications, besides may be its location else the information measurement, namely sensors of external and internal. Internal sensors can quantify many different states various parts of the system, such as joints of encoder reportings/wheels angle, an accelerometer to measure inertia or linear acceleration, and gyroscope measure angular acceleration. The above sensors are usually employed for precise computations [1] (Fig. 3).

3 Discussions

3.1 Application of Various Robotics Principles in Agriculture

With advancements in robotics research, they now occupy a predominant position in most of the fields viz., Industries, Medical, Space exploration, Education and

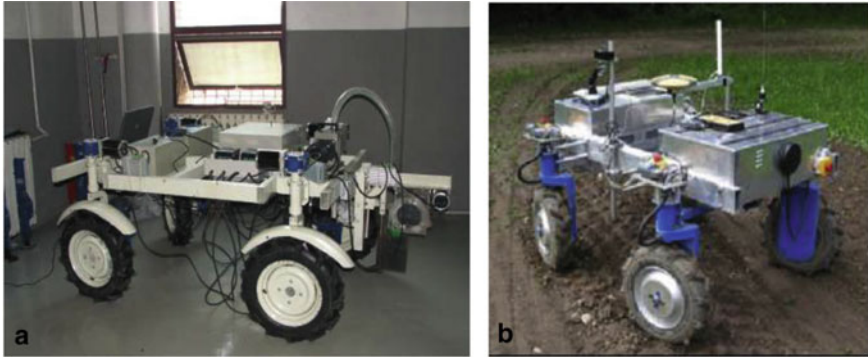


Fig. 3 The four-wheel drive agrobots platforms for **a** cereal precision seeding [12], **b** weed detection [15]

with minor applications in agriculture. Robotics in agriculture is mostly of indoor, whereas the real time and commercialization were still foreseen. Figure 4 depicts the agricultural robots available for different applications (Figs. 5 and 6).

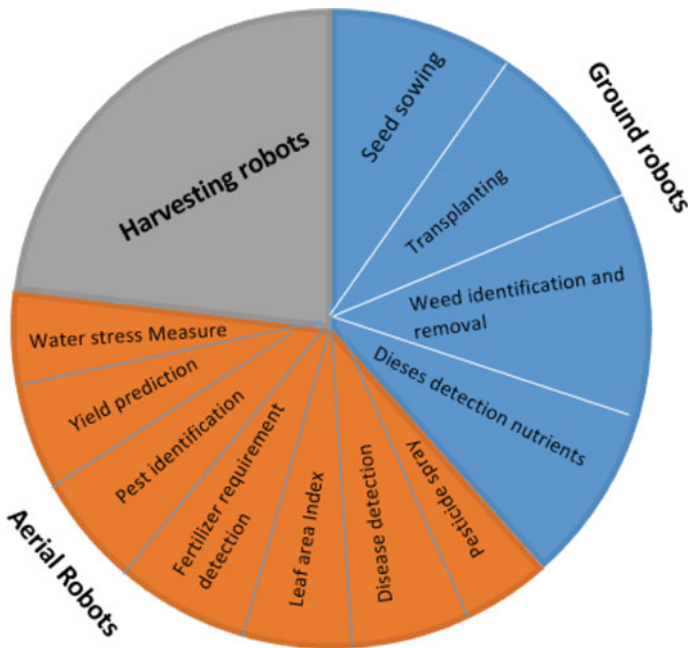


Fig. 4 Representing robots employed in various agriculture operations

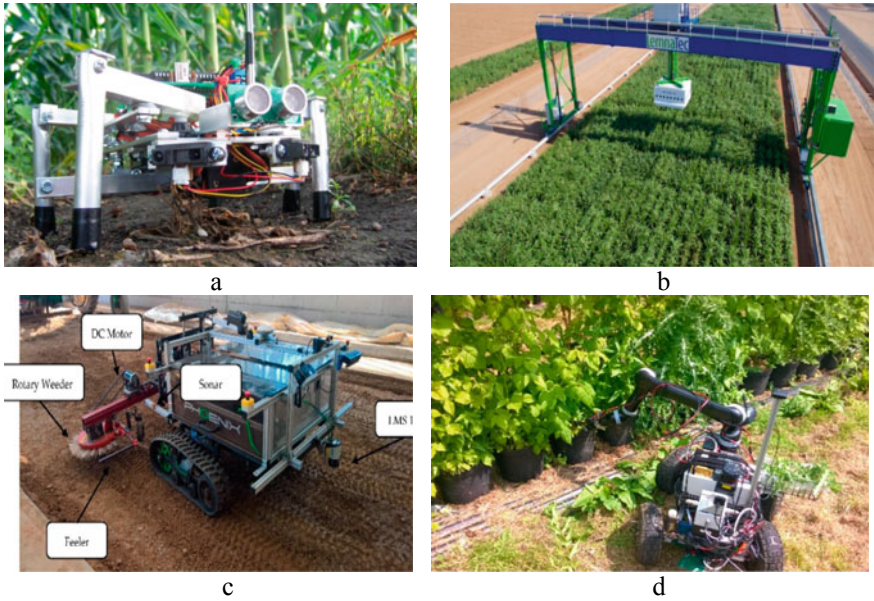


Fig. 5 Various agricultural ground robots **a** AgAnt, **b** IPK dual-arm robot, **c** RAL space agribot with robot, **d** weeding robot [16]

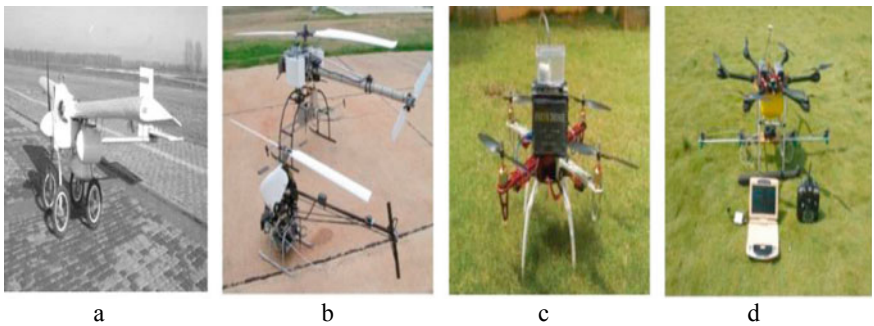


Fig. 6 Various agricultural aerial robots **a** single rotor, **b** double rotor, **c** quad copter, **d** octa copter [17]

3.2 *Predominant Factors for Design of Agriculture Robots*

Agricultural robot design for real application is definitely not an easy task. Unlike other field of robotics, the environmental conditions, plant characteristics are quite unpredictable. But efforts are made to develop automated machinery of requisite application. For example soil behavior is not constant throughout field. In addition

Table 2 Design factors w.r.t. robot construction [18]

S. No.	Robots perspective	Remarks
1	Sensing and localization	It is a required to consider this factor as sensing the parameters in the agricultural environments as this is the primary task of any manipulator
2	Path planning	This is to be considered as it is an algorithm or set points for the robot in various field operation like, seed sowing, weeding based on sensor's data
3	Mobility and steering	This factor has a considerable impact as this is actuation form of above two steps
4	End effector manipulation	Determine end effector/tool design, kinematics and dynamics application such as cutting operation in harvesting, picking of roots, spraying operations, etc.

Table 3 Design factors w.r.t crop's perspective [18]

S. No.	Design factor	Remarks
1	Row to row and plant to plant distance	It is to be considered as size (length, breadth) of the robot or machine
2	Type of crop (underground crop/above surface crops)	This factor influences the robot or machinery height and its attachment (for example digging attachments of ground nuts, cutting attachments for paddy etc.)
3	Type of soil 1. Draft requirements 2. Soil properties like: strength, moisture holding capacity, friction, etc.	Useful parasitic forces plays a prominent role in the shape of robot
4	Type of operations viz., tillage, sowing, intercultural and plant protection, harvesting, post harvesting etc.	The manipulator or mechanism depends on this factor as each operation requires uniqueness
5	Size and field capacity	This factor should be considered as optimal size robot or machinery is expected in the field, also the machinery design is expected to have high field capacity

its behavior becomes more unpredictable when after irrigation. Here are some most predominant factors identified for the agricultural robots design (Tables 2 and 3).

3.3 Sensors

Human is in complete with sense organs and sensors of the robots/automated systems are equivalent to sense organs. In the robots decision making is dependent parameter on the sensory data received. Today with advent of MEMS and other advanced

Table 4 Various sensors used in agricultural application [20]

S. No.	Sensors	Purpose
1.	Ultrasonic sensor	Obstacle detection, plant height measurements
2.	Soil moisture sensor	Indicating of soil moisture
3.	pH sensor	Indicating of soil pH
4.	Strain gauges	Measuring implement’s draft
5.	Rotary encoder, wheel stud sensor	Measuring of angular displacement
6.	Cone penetrometer	Measuring of soil pulverization
7.	Accelerometer	Measure the acceleration
8.	Gyroscopic sensor	To measure the rotational motion
9.	Magneto meter	To measure magnetic field
10.	Camera	To record visual images
11.	Multi spectral camera	Images at specific frequencies
12.	Hyper spectral cameras	Images at narrow spectral bands
13.	Thermal cameras	To record low light imaginary
14.	Altimeter	To measure altitude
15.	Anemometer	For measure wind of speed

technologies we have sensors for most of the applications which compact, reliable and cost effective. Researchers are now imbibing these sensors systems into agriculture too for better yield and productivity. Here are some of the sensors enlisted along with their application in agriculture, different type of sensors mentioned (Table 4) [19].

4 Conclusion

Automation robot systems are usually more difficult because they have different subsystems. Properly integrate and synchronize to carry the required data fully executed and successfully completed. This combination is required to allow cycle times, duration and characteristic. Intelligent by each support system Crop production robot systems are more complex because they have to run in an unstructured environment. (1) Technology development is highly essential in order to get way the challenges viz., unstable environments such as vibration, dust, moisture and over-heating. (2) Intelligent system evaluation successful operation in such an environment. (3) The cost of a robotic system should be low enough to be economically usable as it is a relatively low value processed agricultural product. (4) Agricultural robot systems can only be assimilated with other solutions (for example, as machine-less or robot-free machines or automation), their marginal utility is reduced. Agricultural robot systems can only be assimilated with other solutions such as machine-less or robot-less machines or automation, reducing its usefulness.

References

1. Bechar A, Vigneault C (2016) Agricultural robots for field operations: concepts and components. *Biosyst Eng* 149:94–111
2. Tremblay N, Fallon E, Ziadi N (2011) Sensing of crop nitrogen status: opportunities, tools, limitations, and supporting information requirements. *HortTechnology* 21(3):274–281
3. Nagasaka Y, Umeda N, Kanetai Y, Taniwaki K, Sasaki Y (2004) Autonomous guidance for rice transplanting using global positioning and gyroscopes. *Comput Electron Agric* 43(3):223–234
4. Xia C, Wang L, Chung B-K, Lee J-M (2015) In situ 3D segmentation of individual plant leaves using a RGB-D camera for agricultural automation. *Sensors* 15(8):20463–20479
5. Bechar A, Edan Y (2003) Human-robot collaboration for improved target recognition of agricultural robots. *Ind Rob Int J* 30(5):432–436
6. Dar I, Edan Y, Bechar A (2011) An adaptive path classification algorithm for a pepper greenhouse sprayer. Paper presented at the American society of agricultural and biological engineers annual international meeting 2011, Louisville, KY
7. Vidoni R, Bietresato M, Gasparetto A, Mazzetto F (2015) Evaluation and stability comparison of different vehicle configurations for robotic agricultural operations on sideslopes. *Biosyst Eng* 129:197–211
8. Edan Y, Bechar A (1998) Multi-purpose agricultural robot. Paper presented at the sixth IASTED international conference, robotics and manufacturing, Banff
9. Burks T, Villegas F, Hannan M, Flood S, Sivaraman B, Subramanian V et al (2005) Engineering and horticultural aspects of robotic fruit harvesting: opportunities and constraints. *HortTechnology* 15(1):79–87
10. Ceres R, Pons FL, Jimenez AR, Martin FM, Calderon L (1998) Design and implementation of an aided fruit harvesting robot (agribot). *Ind Rob* 25(5):337–346
11. van Henten EJ, Bac CW, Hemming J, Edan Y (2013) Robotics in protected cultivation. *IFAC Proc Vol* 46(18):170–177
12. Lin H, Dong S, Liu Z, Yi C (2015) Study and experiment on a wheat precision seeding robot. *J Robot*. Article ID: 696301
13. Hague T, Marchant JA, Tillett ND (2000) Ground based sensing systems for autonomous agricultural vehicles. *Comput Electron Agric* 25(1–2):11–28
14. Li Z, Vigneault C, Wang N (2010) Automation and robotics in fresh horticulture produce packinghouse. *Stewart Postharvest Rev* 6(3):1–7
15. Bak T, Jakobsen H (2004) Agricultural robotic platform with four wheel steering for weed detection. *Biosyst Eng* 87(2):125–136
16. Fue KG, Porter WM, Barnes EM, Rains GC (2020) An extensive review of mobile agricultural robotics for field operations: focus on cotton harvesting. *AgriEngineering* 2(1):150–174
17. Mogili UR, Deepak BBVL (2020) An intelligent drone for agriculture applications with the aid of the MAVlink protocol. In: *Innovative product design and intelligent manufacturing systems*. Springer, Singapore, pp 195–205
18. Bainer R, Kepner RA, Barger EL (1960) Principles of farm machinery. *Soil Sci* 81(2):155
19. Liljedhal JB, Turnquist PK, Smith DW, Hoki M (1996) Tractors and their power units
20. Mogili UR, Deepak BBVL (2018) Review on application of drone systems in precision agriculture. *Procedia Comput Sci* 133:502–509

Over View of Sensors for Measuring Soil Parameters, Supporting Agricultural Practices



P. Syam Sundar, B. B. V. L. Deepak, Ramu Eswam,
and Umamaheswara Rao Mogili

Abstract Agricultural practices are indigenous, accounts for considerable GDP of India, livelihood for most of the rural population either directly or indirectly and the products obtained are major energy sources of human body. In recent decades due to enormous population growth and rock-bottomed cultivable land, add on to cultivation practices are postulated, adhering to supply apropos to demand of food grains. The extensive research and development in various fields especially in sensory systems in specific Micro Electro Mechanical System (MEMS)-based sensors and automation have witnessed tremendous achievements beyond imagination due to precise sensory technology on tap economically. Withal, the commercially available technology integrated with sensory/automation systems and the research highlights in agriculture reported till date are lowest in equate to rest. Incorporating sensors with electronics and information technology, cited as precision agriculture (PA), meliorates the quality and inflated agricultural yeild. This paper throws a light on the key role of microcontrollers, assorted sensors along with fundamentals of their working, showcasing the applications of sensors for soil parameters of agriculture field for improved productivity and sensitivity. Nevertheless discussing the pros and cons of the ssensors, the paper unfolds the sensors employed for finer agricultural ontogenesis and caters a path for developmental aspects of commercialization.

Keywords MEMS · Automation · Precision agriculture · Soil parameters

1 Introduction

Instauration of technological features revolutionized the mankind [1]. The agricultural practices today are results of umpteen changes through years since inception of human via age long process of evaluation involving various other changes [2]. In addition, industrial revolution was an add on to agriculture for enhanced human

P. Syam Sundar (✉) · B. B. V. L. Deepak · R. Eswam · U. R. Mogili
National Institute of Technology, Rourkela, Rourkela 769008, India

© The Author(s), under exclusive license to Springer Nature Singapore Pte Ltd. 2022
B. B. V. L. Deepak et al. (eds.), *Applications of Computational Methods in Manufacturing and Product Design*, Lecture Notes in Mechanical Engineering,
https://doi.org/10.1007/978-981-19-0296-3_5

survival and sound lifestyle [3]. Industrial revolution, though supported a significant rise in agricultural productivity, yet technology support assets are expected to meet the demand [4]. As per United Nation’s food and agricultural organization human’s population would reach 9.2 billion by the year 2050 and the agricultural produce is to be ascended to 70% to meet the needs [5]. Farming practices of most countries essentially should experience a phase shift to encounter the needs [6]. A part from technological support, many inevitable factors namely, climatic conditions, unpredictable rainfall, global temperatures, etc. affects the productivity [7]. Smart practices viz., climate smart agriculture (CSA) in countries like Malawi [8], Micro electro mechanical system (MEMS)-based agriculture [9], conservation agriculture in Zambia, Smart phone controllable sensors in agriculture [10] and Intelligent drone assisted agriculture [11]. Covering basics and working principles of MEMS-based and other sensors used in agriculture, this paper is aimed to elucidate various challenges and limitations associated with current technology. The roots of MEMS traces back to late 1980s [12]. MEMS, due to their precision, compactness and low cost enrooted in diversified systems viz. Projection systems, smartphones, biosensors, digital cameras, optical sensors, accelerometers, gyroscopes, etc. Integration of MEMS into agriculture is very new and opens doors to advanced research fields viz., precision agriculture (PA) [13] and are also used in agricultural drones [14] for increased productivity.

2 General Working Principle of Accelerometer

MEMS work on various principles viz., capacitive, electromagnetic, piezoelectric, thermal, electrostatic, etc. [12]. Let us take an example of MEMS device, accelerometer that measures vibration. Here if a physical stimulus say force, tilt, etc. When impinged, induces mass difference in the device, giving rise to electric potential proportionate to stimulus which is processed further and calibrated (through appropriate circuits/ICs). Other MEMS devices include gyroscope, inertial sensors, etc. [15]. In this review, for simplicity capacitive and piezoelectric type accelerometers are discussed.

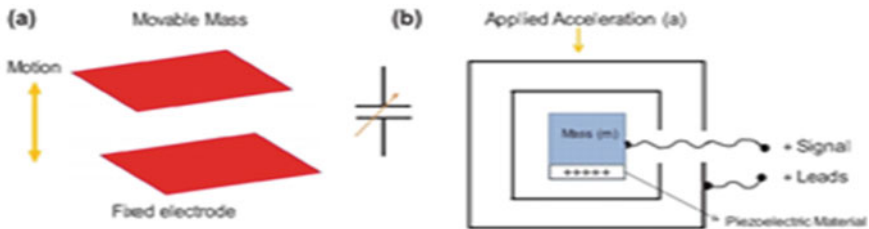


Fig. 1 Schematic of accelerometer working illustration of a capacitive, b piezoelectric [4]

Figure 1a, b is an illustration for working principle of an accelerometer based on capacitance and piezoelectric. In capacitance type, accelerometer makes up a with a fixed and mobile plate. Either or both the plates are charged with electrical potential. The gap between the plates varies and previous when stimulus (say tilt) is applied and change in gap gives to change in the output of accelerometer in terms of voltage, which is calibrated with respect to application [16]. The other type is of piezoelectric effect. In this type, if the crystal receives stimulus (say mechanical force/pressure), the charges stacked in the crystal exhibits mobility, ensuring the exchange of polarity from the other. Then, the charges piled are amplified and transposed into voltage or current by suitable circuits [17]. The resultant is then calibrated based on application. The other types of accelerate meters include Hall effect-based [18], optical [19], surface acoustic wave (SAW) [20], resonance [21], etc. and still many more.

3 Agriculture with Soil Sensors

Here, let us have a look on recent advancements/developments in sensors with respect to agricultural applications. In a glance, the predominant areas are enlisted, where successfully the sensors in the agriculture are imbibed viz., sensors for soil's moisture, water flux density, electrical conductivity and nitrogen, phosphorous, potassium levels measurement, etc.

3.1 Soil of Agricultural Field

Soil plays vital role in agriculture as the major crop parameters like yield, growth are dependents of it. Among soil's parameters, pH is the one which controls various other parameters associated with crop productivity which restrains and specifies moisture content and electrical conductivity as well. Each crop has its own requirement of pH value for its well-being. At this point, it is clear that determining moisture content and electrical conductivity can help to find out pH [22]. For time being let us look at soil moisture measurement.

3.2 Soil Moisture Content Measurement

Measurement of soil moisture content obtained with the aid of Dual Probe Heat Pulse (DPHP) [23, 24]. Some polymers which are sensible to pH are to be taken into account for soil pH measurement [25]. For effectual soil moisture measurement, DPHP (silicon-based) was used. Heat pulse, when applied for a certain time (Fig. 2a), there occurs maximum increase in the temperature that measured by placing the probe at the heat source (Fig. 2b). The applied heat pulse of short duration results in delayed

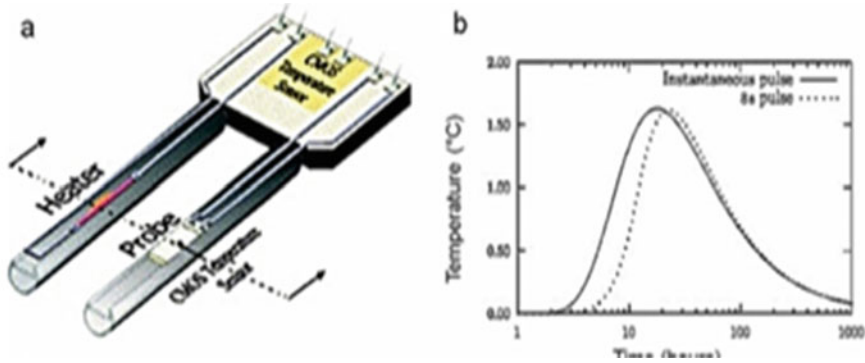


Fig. 2 Schematic showing **a** soil moisture sensor, **b** time versus temperature graph of sources of pulsed line. *Source* [12]

time, there by observing maximum changes of temperature. These changes helps to find out volumetric heat capacity, there by directing to determine soil moisture content [26]. Conductive polymer-based micro sensor [27] is also used to determine soil moisture content. There are many other methods apart from above to measure the moisture content.

3.3 Water Flux Density Measurement

Water flux density (J) is a key factor in assessing transportation properties of soil, which when measured accurately may help interpreting the soil’s capacities in a finer way. The HPP which abbreviation for Heat Pulse Probe [28] is a technique for quantifying soil’s response of thermal activity, apart from other properties too in a transient way and used for real-time and laboratory measurements. Unlike (SPHP/DPHP), HPP too has its different variants, but both converge at a point of their working science. Measuring soil’s thermal response versus heat pulse in fixed by the heat probe at a certain distance [29]. As DPHP comprising of twin terminals/sensors namely, temperature and heat probes, the outcomes are then plotted into a heat transfer model and to a data of response of temperature [30]. For the sake of simplicity [28], a mere mathematical relation of soil’s characteristics related to thermal activity and water flux density is given below.

$$(J) = (C_{bw}/C_w) * (V_{hp}) \tag{1}$$

representing C_w —volumetric heat capacity ($m^{-3} \text{ } ^\circ C^{-1}$), C_{bw} —bulk volumetric heat capacity ($m^{-3} \text{ } ^\circ C^{-1}$), V_{hp} as heat pulse velocity (ms^{-1}) and J —water flux density [4].

3.4 Soil Electrical Conductivity Measurement

Another absolutely essential parameter of soil to be considered is electrical conductivity (EC) of the soil. Apart from water flux density, soil moisture content is also a key factor for effective productivity. In this review, a special probe is depicted and capable of measuring thermal, water, and electrical conductivity as well [31]. For the time being EC measurement is discussed here. EC measured through a Werner array ring, comprising two twin pairs of parallel ring electrodes, employed to the resistivity (electrical), which in turn helps to approximate the soil's EC [32]. From basic physics, it to be noted that the EC and resistivity are inversely proportional. Werner array (Fig. 3b) here by can be used in the measurement of electrical conductivity (σ_s) and also typified mathematically as,

$$\sigma_s = (I/V_{MN})(1/2\kappa\pi) \tag{2}$$

In the above equation, I (in Amperes) being source current, $1/2K\pi$ (in m^{-1}) which is cell constant, V_{MN} is voltage potential across electrodes M, N . $1/K$ is given by

$$\{[(BM - AM)/(AM * BM)] - [(BN - AN)/(AN * BN)]\} \tag{3}$$

A part from above SPHP/DPHP can also be employed for measuring electrical conductivity [23].

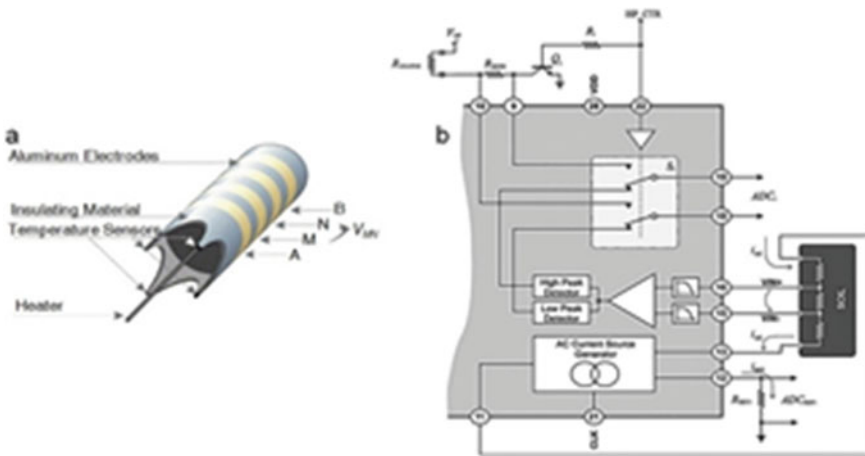


Fig. 3 Schematic of a multi functional probe, b Werner array. Source [31]

3.5 Soil Nitrogen (N), Phosphorous (P), Potassium (K) Measurement

The macro nutrients, nitrogen, phosphorous, potassium (NPK) are regarded as vital elements predominantly influencing crop's biological [33]. By measuring NPK content in the agricultural field one can easily understand the rest amount to be added, benefiting farmer and environment as well [34]. Figure 4 represents a schematic of an optical device experimental setup, works through light transmission and its detection, consisting of LED pair, which coupled to other circuits for signal enhancement. A lucid Polyethylene Terephthalate (PET) bowl is placed with a stand in which soil sample is kept. The wavelength of LED for the detection of nutrients are 470 nm, 950 nm and 660 nm for N, P and K, respectively. The LED pair and signal conditioning are interfaced with Arduino board (detection system), which also generates a square wave in order to track LED's sequence, time period of light's emanation and also for frequency control. Whole system when powered by rated DC (Direct current as per Arduino board specifications) light of LED luminosity directly interacts with soil sample and its absorbed luminosity incurred by the photo detector, converting into photocurrent. The signal conditioning circuit comprising capacitor filter, amplifier, etc., implies the received nano amperes of photo current into scaled voltage [35]. In order to obtain levels of a N, P, K, the Beer-Lambert Law can be used to obtain absorbance as shown in Eq. (3)

$$A = -\log_{10}(I_1/I_0) \quad (4)$$

where I_1 is transmitted light, I_0 is incident light, A is absorbance [36]. Another method of determining NPK by using colorimetry consisting of RGB sensor (TCS3471), Light Dependent Resistor, Arduino board and misc [37].

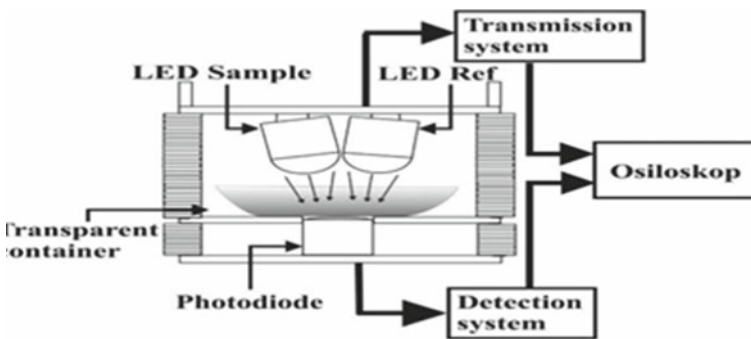


Fig. 4 An optical device setup for nitrogen, phosphorous, potassium measurement [35]

4 Conclusion

Through this paper, efforts are made to depict few MEMS-based sensors employed in soil parameters viz., moisture content, water flux density, electrical conductivity and NPK concentration. Efforts are also made to render how conventional sensors had took their shape into agricultural sensors. Consolidating the above mentioned sensors are to name just a few spanning from variety of other applications too. The point to be observed is that MEMS-based agricultural sensors are mostly restrained as laboratories models and are into the knowledge of individuals through research articles. With no surprise commercializing them would make the world's to reach less/no challenges in the real-time farm.

References

1. Singh AN, Thakre RD, More JC, Sharma PK, Agrawal YK (2015) Block copolymer nanostructures and their applications: a review. *Polym Plast Technol Eng* 54:1077–1095
2. Svizzero S, Tisdell CA (2015) The persistence of hunting and gathering economies. *Soc Evol Hist* 14:3–25
3. Zamboni I, Cecchini M, Egidi G, Saporito MG, Colantoni A (2019) Revolution 4.0: industry vs. agriculture in a future development for SMEs. *Processes* 7:36
4. Singh N, Singh AN (2020) Odysseys of agriculture sensors: current challenges and forthcoming prospects. *Comput Electron Agric* 171:105328
5. Basnet B, Bang J (2018) The state-of-the-art of knowledge-intensive agriculture: a review on applied sensing systems and data analytics. *J Sens* 2018
6. De Bon H, Parrot L, Moustier P (2010) Sustainable urban agriculture in developing countries. A review. *Agron Sustain Dev* 30:21–32
7. Lobell DB, Burke MB, Tebaldi C, Mastrandrea MD, Falcon WP, Naylor RL (2008) Prioritizing climate change adaptation needs for food security in 2030. *Science* 319:607–610
8. Sanchez PA, Denning GL, Nziguheba G (2009) The African green revolution moves forward. *Food Secur* 1:37–44
9. Dell JM, Milne JS, Antoszewski J, Keating AJ, Schuler LP, Faraone L (2009) MEMS-based Fabry-Perot microspectrometers for agriculture. *SPIE*
10. Pongnumkul S, Chaovalit P, Surasvadi N (2015) Applications of smartphone-based sensors in agriculture: a systematic review of research. *J Sens* 2015
11. Mogili UR, Deepak BBVL (2020) An intelligent drone for agriculture applications with the aid of the MAVlink protocol. In: *Innovative product design and intelligent manufacturing systems*. Springer, Singapore, pp 195–205
12. Valente A (2017) MEMS devices in agriculture. In: Zhang D, Wei B (eds) *Advanced mechatronics and MEMS devices II*. Springer International Publishing, Cham, pp 367–385
13. Barnes AP, Soto I, Eory V, Beck B, Balafoutis A, Sánchez B, Vangeyte J, Fountas S, van der Wal T, Gómez-Barbero M (2019) Exploring the adoption of precision agricultural technologies: a cross regional study of EU farmers. *Land Use Policy* 80:163–174
14. Mogili UR, Deepak BBVL (2018) Review on application of drone systems in precision agriculture. *Procedia Comput Sci* 133:502–509
15. Shakur A, Kraft J (2016) Measurement of coriolis acceleration with a smartphone. *Phys Teach* 54:288–290
16. Elwenspoek M, Wiegink R (2012) *Mechanical microsensors*. Springer Science & Business Media

17. Tahmasebipour M, Vafaie A (2020) A novel single axis capacitive MEMS accelerometer with double-sided suspension beams fabricated using μ WEDM. *Sens Actuators A Phys* 112003
18. Chen K-Y, Shah RC, Huang J, Nachman L (2017) Mago: mode of transport inference using the hall-effect magnetic sensor and accelerometer. *Proc ACM Interact Mob Wearable Ubiquitous Technol* 1:8
19. Li R-J, Lei Y-J, Chang Z-X, Zhang L-S, Fan K-C (2018) Development of a high-sensitivity optical accelerometer for low-frequency vibration measurement. *Sensors* 18:2910
20. Shevchenko S, Kukaev A, Khivrich M, Lukyanov D (2018) Surface-acoustic-wave sensor design for acceleration measurement. *Sensors* 18:2301
21. Wang S, Wei X, Zhao Y, Jiang Z, Shen Y (2018) A MEMS resonant accelerometer for low-frequency vibration detection. *Sens Actuators A Phys* 283:151–158
22. Ham J, Benson E (2004) On the construction and calibration of dual-probe heat capacity sensors. *Soil Sci Soc Am J* 68:1185–1190
23. Heitman J, Horton R, Ren T, Ochsner T (2007) An improved approach for measurement of coupled heat and water transfer in soil cells. *Soil Sci Soc Am J* 71:872–880
24. Valente A, Morais R, Couto C, Correia JH (2004) Modeling, simulation and testing of a silicon soil moisture sensor based on the dual-probe heat-pulse method. *Sens Actuators A Phys* 115:434–439
25. Palaparthi VS, Baghini MS, Singh DN (2013) Review of polymer-based sensors for agriculture-related applications. *Emerg Mater Res* 2:166–180
26. Jackson T, Mansfield K, Saafi M, Colman T, Romine P (2008) Measuring soil temperature and moisture using wireless MEMS sensors. *Measurement* 41:381–390
27. Liu J, Agarwal M, Varahramyan K, Berney ES, Hodo WD (2008) Polymer-based microsensor for soil moisture measurement. *Sens Actuators B Chem* 129:599–604
28. Ravazzani G (2017) Open hardware portable dual-probe heat-pulse sensor for measuring soil thermal properties and water content. *Comput Electron Agric* 133:9–14
29. Kamai T, Kluitenberg GJ, Hopmans JW (2015) A dual-probe heat-pulse sensor with rigid probes for improved soil water content measurement. *Soil Sci Soc Am J* 79:1059–1072
30. Basinger J, Kluitenberg G, Ham J, Frank J, Barnes P, Kirkham M (2003) Laboratory evaluation of the dual-probe heat-pulse method for measuring soil water content. *Vadose Zone J* 2:389–399
31. Valente A, Morais R, Tuli A, Hopmans JW, Kluitenberg GJ (2006) Multi-functional probe for small-scale simultaneous measurements of soil thermal properties, water content, and electrical conductivity. *Sens Actuators A Phys* 132:70–77
32. Umar EP (2018) Identification of subsurface layer with Wenner-Schlumberger arrays configuration geoelectrical method. *IOP Conf Ser Earth Environ Sci* 118:012006. IOP Publishing
33. Malvi UR (2011) Interaction of micronutrients with major nutrients with special reference to potassium. *Karnataka J Agric Sci* 24(1)
34. Kraiser T, Gras DE, Gutiérrez AG, González B, Gutiérrez RA (2011) A holistic view of nitrogen acquisition in plants. *J Exp Bot* 62(4):1455–1466
35. Masrie M, Rosli AZM, Sam R, Janin Z, Nordin MK (2018) Integrated optical sensor for NPK nutrient of soil detection. In: 2018 IEEE 5th international conference on smart instrumentation, measurement and application (ICSIMA), Nov 2018. IEEE, pp 1–4
36. Wankhede A, Giripunje S (2016) Review on determination of macronutrients from compost. In: 2016 international conference on information communication and embedded systems (ICICES). IEEE, pp 1–5
37. Regalado RG, Cruz JCD (2016) Soil pH and nutrient (nitrogen, phosphorus and potassium) analyzer using colorimetry. In: 2016 IEEE region 10 conference (TENCON), Nov 2016. IEEE, pp 2387–2391

Design of Pin on Disk Tribometer Under International Standards



Byron Dario Analuiza Hidalgo, Vanessa C. Erazo-Chamorro, Diana Belén Peralta Zurita, Edilberto Antonio Llanes Cedeño, Gustavo Adolfo Moreno Jimenez, Ricardo P. Arciniega-Rocha, Paul D. Rosero-Montalvo, Alejandro Toapanta Lema, and José A. Pijal-Rojas

Abstract The document exposes a machine built for testing the friction, lubrication and spoilage. Its test conditions have a large filed of options to execute tribology tests checking the working conditions, like movement way (reciprocating or linear), parts in contact, movement speed, self-lubrication, part geometry, temperature range, humidity, materials. To perform this test, the tribometer uses the principle of the disc revolution, the load is applied directly over the arm and do the measure according to the standard obtaining the results with accuracy. The use load cell to measure the force created during the test and at the same time get the distance of the wear track in real time. As a result, it can be calculated by software the coefficient of friction using the data got completing the purpose of the tribotester machine.

Keywords Friction · Tribometer · Wear · Lubrication

1 Introduction

The use and basic aspects of tribology are old. The term comes from “tribos” that in Greek means “rubbing”, of course, some significant tribological observations were proposed by scientists and engineers from Greek. During 400 B.C., Aristotle proposed that the friction is very low for circular objects and it is easy identifying in other geometries objects [4]. Nowadays, all enterprises are trying to save money through the study of the wear and friction field to increase the life-time in machine parts lowering the maintenance cost [2]. To determine friction coefficients everybody, think that is so simply like the normal force and the opposition produced between the object and a surface during a relative tangential motion, but is necessary to remember

B. D. A. Hidalgo (✉) · D. B. P. Zurita · E. A. L. Cedeño · G. A. M. Jimenez
International University SEK, Quito, Ecuador

V. C. Erazo-Chamorro · R. P. Arciniega-Rocha · A. T. Lema · J. A. Pijal-Rojas
Instituto Superior Tecnológico 17 de Julio, Ibarra, Ecuador

P. D. Rosero-Montalvo
University of Salamanca, Salamanca, Eapañar, Spain

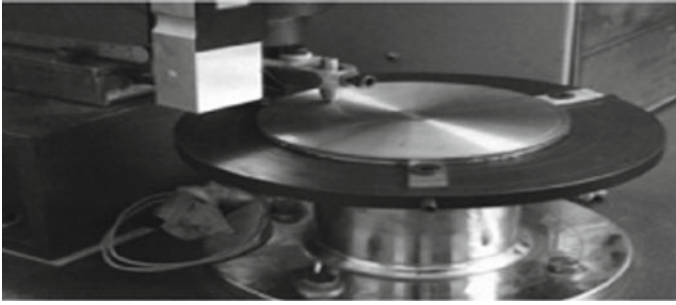


Fig. 1 Pin on disk tribometer [9]

the tribology is an entire science and its main proposal is to easy this measurement and standardize it. Since begin of the history of the science researchers have measured frictional quantities with help of different devices like pulleys, spring scales or ramps [5].

The opposition to the movement between contact surfaces is known as friction, it produces surface heat and wear of the material. Inside of an engine, it reduces the power unit. The friction depends on some characteristics of the material like surface finishing, part material, the pressure between objects and the speed movement between objects in contact [6]. Inside of machine the friction between parts cannot be optimal measured and it could be expensive; thus, currently we can get this friction data in the laboratories that obtain previously from instruments called tribometers. One simple definition for a tribometer will be a way to evaluate the friction force. Figure 1 shows the work way of the tribometer pin on disk.

Currently, there are several techniques working since occupying petty prototypes or occupy the correspondent part. Since to tribology was born several test friction standards were set forth; nevertheless, In the actuality, some world organizations that voluntary and government-sponsored have suggested practices guidelines (standards) to lead engineers to structure the data of measured friction. Non-standard methods are useful as well to make the process. In the present work we focus on the existing standards developed for the tribology study which are described by ASTM Standards in Table 1 shown.

The standards identify the variables to be controlled and which of these variables will be allowed, the way to get the data, and the way to present the results. But, it is important to know that if some parameter is not mentioned on a standard it does not mean that the affection of it could not be significant under another set of circumstances [7].

In the previous studies a mathematical semi-physical phenomenological base model of sliding pairs is developed in order to predict the wear rate [14] and a model focused in the control design with respect to the moving parts in the tribometer machine [10]. So the mechanical parametric design is a main part in the machine development in order to reduce optimizing the economical factor. Friction measuring

Table 1 Standardized methods [3]

ASTM standard	Title	Parameters measurement
G99 – 05	Wear test with a tribotester	Losses in the geometric volume
D 2981 – 94	Solid film lubricants in oscillation motion	The coefficient in case of failure by friction or wear
D913 – 03e1	Resistance to wear of traffic paint	Degree of substrate in hedge distinctive zone of wear
B611 – 85	Cemented carbide wear resistance and abrasion	Wear number and abrasion toughness
D3702 – 94	Self-lubricating materials wear rate and friction coefficient	Coefficient of friction, and wear

Table 2 Tribometer classification [7]

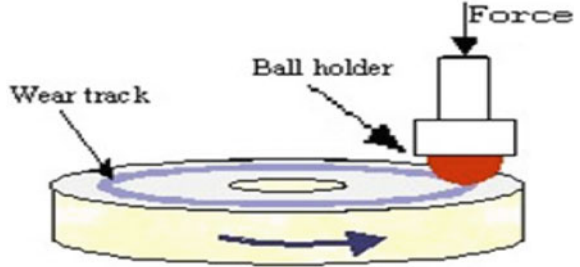
Number	Tribometer classification by purpose of development
I	For particular machine tribocontact situation simulation
II	Evaluation of candidate-bearing materials
III	Evaluation of lubricants
IV	To qualify lubricants for use on the basis of established criteria
V	To monitor part surface
VI	To acquire non-tribosystem-specific friction data as a mean to compare and develop new materials
VII	To investigate the fundamental nature of friction

laboratory techniques had been used and developed for a variety of purposes in Table 2 the purposes shall be described.

Several variables can affect friction. Some of the most important of these variables are listed like: (a) Velocity, normal force and acceleration characteristics, (b) System stiffness, (c) Motion direction related to the surface configuration, (d) Surface finishing and cleanliness, (e) Frictional heating, (f) Relative humidity, (g) Lubricant characteristics, (h) Impurity presence.

Standard ASTM G99 explains the test guidelines to calculate the material wear while the contact parts movement using a pin-on-disk tester. The process shall be made in pairs and nominally located in non-abrasive conditions. These experimental guidelines show the correct steps for the principal areas attention in using this type of apparatus to measure wear. One of the main purposes using this apparatus is to determine the coefficient of friction of the materials, during pin-on-disk method is necessary to have a pair of samples. The first will be a pin with a round end which is perpendicularly located with respect to the other sample material. The pin specimen commonly is a ball rigidly held. The test machine causes either the pin sample or the disk revolving about the center. Therefore, the sliding path (in either case) is a track with a circular shape on the disk surface as shown in Fig. 2 in blue color. This kind of test may develop putting the plane of the disk oriented either horizontally or

Fig. 2 Pin on disk function sketch [11]



vertically. And something important to remark, at time to design the tribometer is that the wear results can be different using different orientations of the apparatus [8].

The next part of this report is configured with the following sections: Sect. 2 materials and methods, Sect. 3 results. Finally, Sect. 4 conclusions and future work.

2 Materials and Methods

The given data parameters in international standards shall be considered for the design, to enhance the main machine parameters to assure a good friction test, getting optimal material junction grade in the different machine mechanisms, consequently, this work is developed in two phases (a) Conceptual design, (b) Analytical Design [2].

2.1 Conceptual Design

For develop the conceptual design it is necessary to start with a part selection and then present the different concepts to study to choose the best one. When the international standards were studied the different requirements are selected and shown in Table 3 according to the importance of each one of these.

Shall be used a popular system of notations B, S, W to classify the importance of the requirements, meaning Basic, Standard and Wished requirements, respectively—they order lowering degree of importance. The numbers preceding the letters mean a scale of importance from uttermost as 1 to least important as 10, to provide further classification. This optional extra scaling was not applied to Basic requirements since they were considered equally important, a complete must.

Table 3 List of requirements for pin on disk construction

No.	Description	Classification	Num. value	Importance
1	Stability	Structural		B
2	Minimization of action space	Structural		B
3	Comfort ability for users	Ergonomic		B
4	Does fit fire safety regulations	Safety		B
5	Must avoid cause accident by detachment of parts	Safety		S10
6	Must provide power protection in case of power shortage	Safety		B
7	Alert in case of malfunctioning (light, sound)	Ergonomic		S3
8	Long service lifetime	Ergonomic		S6
9	Emergency stop possibility	Safety		S2
10	Operating load of specimens	Specific by norm		S4
11	Operating speed rotation of the disk	Specific by norm		S3
12	Operating temperature	Specific by norm		S7
13	Operating atmosphere; humidity	Specific by norm		S8
14	Less vibration as possible of the machine to make sure high accuracy in the results	Structural		W5
15	Less noisy as possible to avoid interfere the tested results	Structural		W5
16	Wear measuring system	Specific by norm		B
17	Surface finish	Specific by norm		B
18	Dimensions of the specimens	Specific by norm		B

2.2 Parts Selection

The existing tribometer tester in being on market was investigated identifying repetitive parts of the machine to choose the best characteristics set to use in conceptual design and then check with the necessary requirements in the different standards with which our device is designed. Table 4 shows the repetitive parts.

After had analyzed the Matrix of concepts-functions of existent tribometers in the previous Table 4 where they examined the more repeated solutions concepts for each part of the tribometers existent in the market, now it is possible to develop our own designs of tribometer. The conceptions were first designed and after, its 3D models were developed using a CAD system. According to this, the three different designs are presented with its simulation results below.

Table 4 Matrix of concepts-functions of existent tribometers

Functions/features	Sub function	Concepts	1 Ducom pin on disk	2 Disc trimeter horizontal loading	3 MCR tribology cell T-PID/44	# of machine using the concept	Concept more repeated
Geometry	–	Horizontal	x		x	2	E
		Vertical		x		1	
Rotation	–	Pin rotation				1	
		Disk rotation	x	x		2	E
Pin specimen	Pin holder	Chuck pin holder		x	x	2	E
		Press pin holder	x			1	
Holder and lever arm	Disk holder	Disk holder external fit	x	x	x	3	E
		Centre holder external fit	x	x	x	3	E
Motor drive	–	Direct to the shaft				0	
		Belts	x	x		2	E
		Gears				1	
Wear measuring system	–	Load cell	x	x	x	2	E
		Torque sensor				0	
		Piezoelectric sensor				0	

2.3 Catalog Parts Selection

The main parts of the machine are selected from catalogs and web pages of the companies that are dedicated to the design and sale of the motor, motor drive and the chuck [2] to verify the correct operation of the mechanisms.

Disk Rotation The disc revolution to realize the test for use of the load applied directly over the arm and do the measure according to the standard obtaining the results with accuracy. To drive the disk of the revolution of the machine, transmit the torque of the test and the control of speed is used in different ways to transmit the torque to the shaft to move the disk. When one machine needs torque middle or low, it is necessary use belts to transmit the required force and to reduce the vibrations produced by the friction during the test. It is important to reduce these vibrations because they can affect directly the engine producing failure if the needed torque is high, is used gears to transmit the necessary force, but the vibrations could affect.

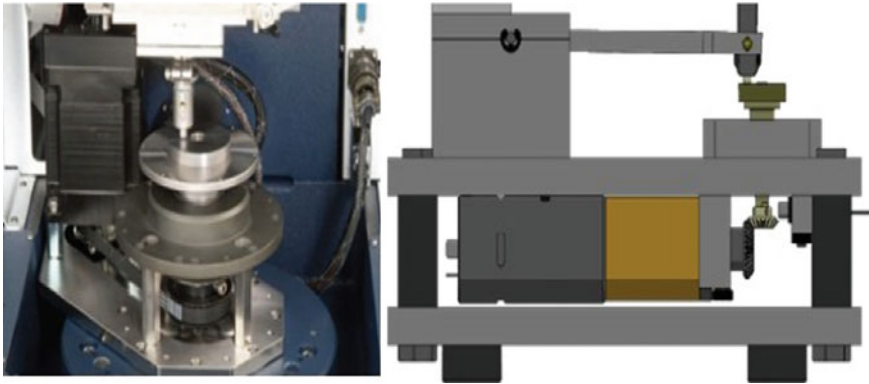


Fig. 3 Motor drive system [2]

Figure 3 motor drive system is shown, in relation with the international standards the machine will work under middle to low torque in that way a belt drive system is chosen.

Disk Holder for fit the sample disc is possible use the bolts to make sure the disk will be in the correct position. For fit it is possible use one bolt in the middle of the disk to fix the sample with the disk of the revolution of the machine. Other option for fitting the disk can be use some bolts in the perimeter of the disk to fix the sample with the revolution disk of the machine as is visible on Fig. 4.

Pin Holder The process of adjusting the sample in the arm will be done by different techniques depending on the material to be used. The chuck fits the specimen of the test to the arm and allows using different size of the pin of the materials. The other way to fit the pin is through or two metallic pieces fixed by bolts to the arm and between of that pieces is located the sample of material as is visible on Fig. 5.

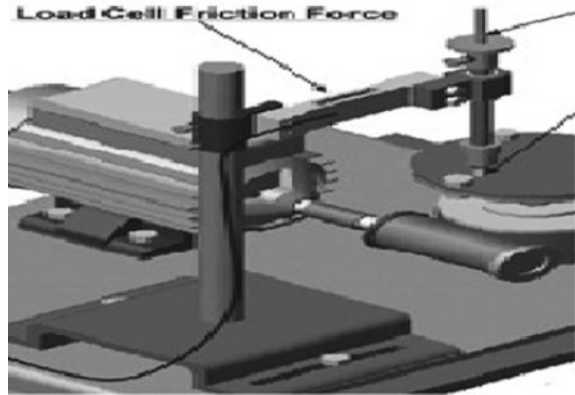


Fig. 4 Disk holder [9]



Fig. 5 Pin holder [1]

Fig. 6 Pin holder [1]



Wear Measuring Systems Figure 6 shows the used system in most of the existent tester in the market use load cell to measure the force created during the test and at the same time get the distance of the wear track in real time. It can be calculated by software the coefficient of friction using the data got completing the purpose of the tribotester machine. Some different algorithms are necessary to determine the appropriate one that can be presented to the previously acquired data set. The main task is the identification of a wear track [12, 13, 15].

2.4 Machine Concepts Designs

After had analyzed the matrix of concepts-functions of existent tribometers in Table 4 and after the selection of components, the geometry proposal of three different models

will be carried out to find the device that allows the greatest precision and repetition in the results during the process [2].

Tribometer with the load over the measurement arm. The most important characteristic in the measurement machine is the way to apply the load; in this case, the load is located directly over the measurement arm and in the load space, and so reducing the machine size as are shown in Fig. 7.

Tribometer with the load in one side the measurement arm. In the design number 2 the load is located in one side of the machine with an extension the measurement arm and in the load space as is shown in Fig. 8.

Tribometer with the horizontal load in the end the measurement arm. For this design the load is positioned in one side of the machine with an extension the measurement arm. But in the design 3 now the load space is located in horizontal position. The model of the design 3 can be appreciated in Fig. 9.

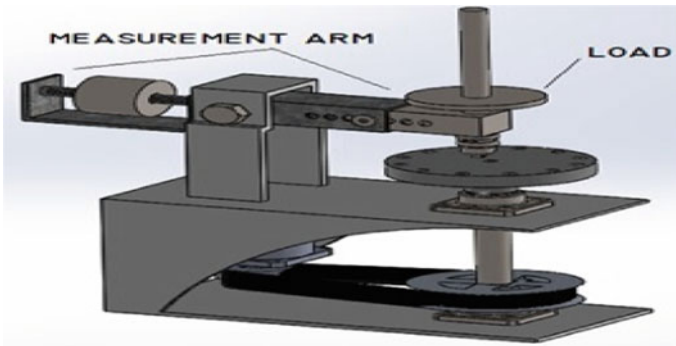


Fig. 7 Tribometer with the load over the measurement arm [7]

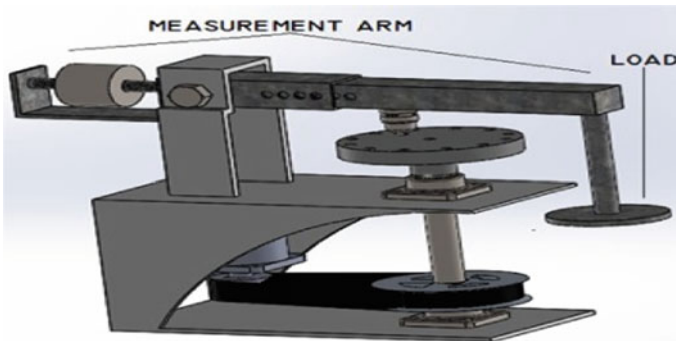


Fig. 8 Tribometer with the load in one side the measurement arm [7]

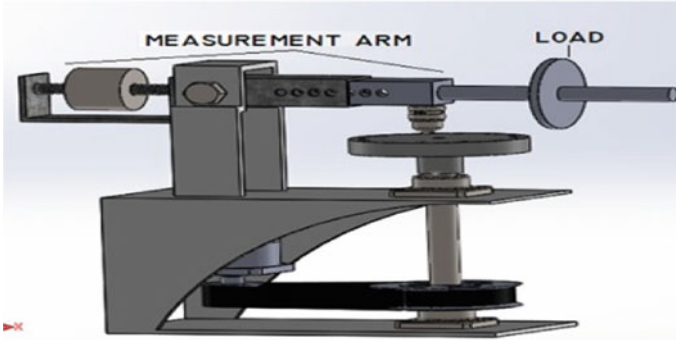


Fig. 9 Tribometer with the horizontal load in the end the measurement arm [7]

3 Results

In order to obtain a machine that works correctly, tension and stress studies should be sought for the analysis of results.

3.1 Stress Analysis

The stress analysis shows the behavior of the machine under the work forces, ensuring the minimum deformation with respect to the applied forces. The behavior of the structure of each design with respect to the working forces is shown in Fig. 10, getting as a result extremely low deformations, allowing to verify that the designed structure is adequate for this function [2].

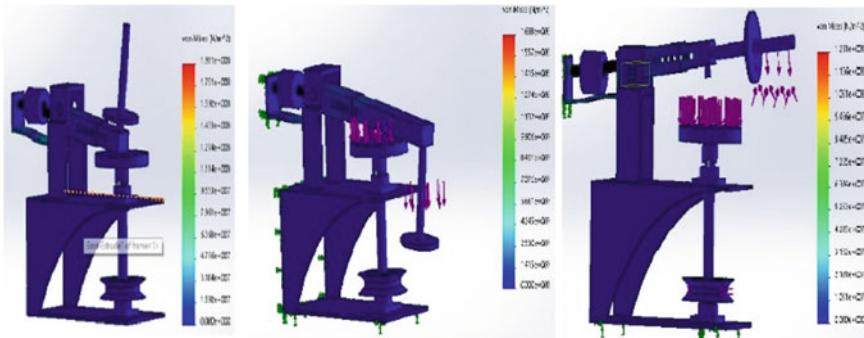


Fig. 10 Tribometer stress data analysis result [7]

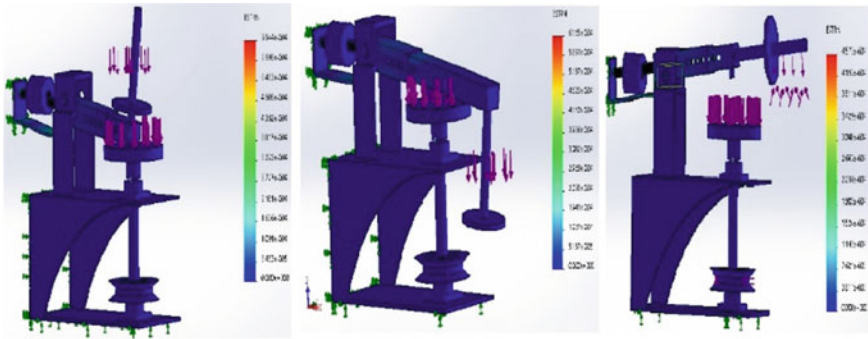


Fig. 11 Tribometer strain data analysis result [7]

3.2 Strain Analysis

As shown in Fig. 11 the analysis of deformation data in the structure allows detecting changes in the shape or size of a body due to the applied forces. It can also be seen that the designed machine is working in a safe area within the elastic zone of the behavior of the materials [2].

3.3 Displacement Analysis

After the comparison of each concept model with respect to stress and deformation aspects, the obtained behavior is very similar between it, getting a good functioning in all cases, this is the reason to select the most optimal model to make this work the most important aspects is the displacement analysis mainly in the work area that is in contact with the analysis samples and the all their components. The displacement analysis shows that the maximum displacement in the tester is low and no one displacement in the design overcomes the critical limits of functioning as is possible in Fig. 12 [2].

3.4 Model Comparison

After the result analysis is necessary to determine the stiffness of the models to select the best one, in that context the displacement and deformation are analyzed.

Stiffness Ratio: Is the ability of a structural element to withstand efforts without acquiring large deformations. And it is defined by the equation [2]:

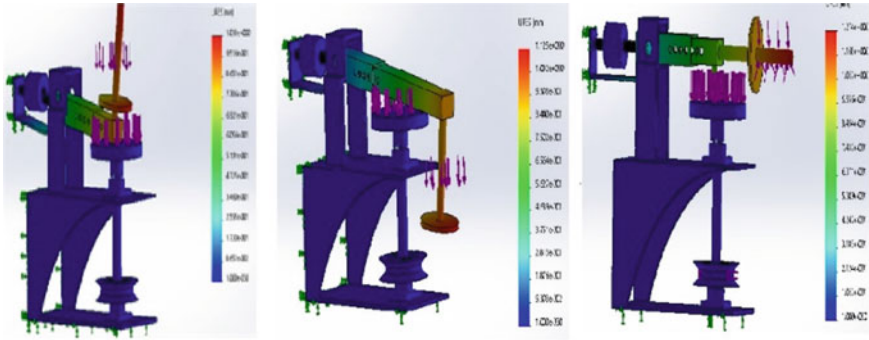


Fig. 12 Tribometer displacement data analysis result [7]

Table 5 Tribometer mechanical data analysis result [7]

Parameter	Concept 1	Concept 2	Concept 3
Mass (kg)	31.33	32.726	30.387
Maximum displacement (mm)	8.749 10 ³	4.708 10 ³	7.557 10 ³
Stiffness	45,719.51	84,961.76	52,931.057
Mass to stiffness ratio	1459.288	2596.154	1741.89

$$K_i = \frac{F_o}{\sigma_i} \tag{1}$$

where:

K_i = Stiffness modulus

F_o = Applied force

σ_i = Displacement.

Mass to Stiffness Ratio: Consists of the elastic module per unit of mass that allows us to identify the most optimal design of our models thus selecting the model with the highest index between stiffness and mass [2].

Analyzing the matrix showed in Table 5 is possible to see that the value of Mass to stiffness ratio is biggest in the design #2. Therefore, we select the second one concept like the best design.

4 Conclusions and Future Works

The adaptive method type H is applied to obtain the study of convergence of results shown in Fig. 13, the selection criterion used to define the optimal model guarantees the functioning of the concept and the correct parts selected.

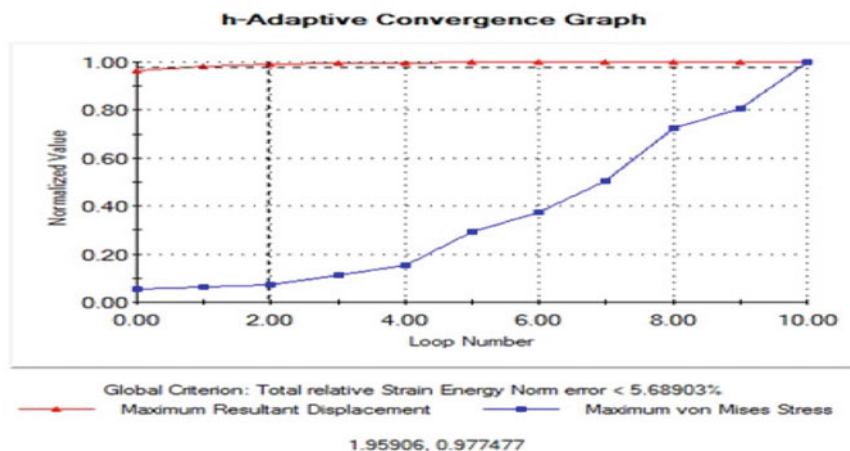


Fig. 13 Tribometer displacement data analysis result [7]

Acknowledgements This work is supported by Budapesti Műszaki és Gazdaságtudományi Egyetem <http://portal.bme.hu/>.

References

1. Abdel-Jaber GT, Mohamed MK, Ali WY (2014) Effect of magnetic field on the friction and wear of polyamide sliding against steel. *Mater Sci Appl* 05(01):46–53. <https://doi.org/10.4236/msa.2014.51007>
2. Arciniega-Rocha RP, Rosero-Montalvo PD, Erazo-Chamorro VC, Arciniega-Rocha VM, Ubidia-Vasconez RA, Aguirre-Chagna VH, Aulestia RR (2019) Gasket tester for low-pressure pipelines: design and tests. In: 2019 IEEE 4th Ecuador technical chapters meeting, ETCM 2019. Institute of Electrical and Electronics Engineers Inc. <https://doi.org/10.1109/ETCM48019.2019.9014904>
3. ASTM. ASTM International—BOS volume 03.02 corrosion of metals; wear and erosion—2013 contents. https://www.astm.org/bookstore/bos/tocs_2013/03.02.html
4. Brown RA (1951) Man the maker: a history of technology and engineering. R. J. Forbes. *Sch Rev* 59(7):437. <https://doi.org/10.1086/441839>. <https://www.iberlibro.com/primer-edicion/man-maker-history-Technology-Engineering-Forbes/14231051842/bd>
5. Charlton W (2009) A new approach in tribological characterization of high performance materials. Technical report
6. DIC Engineering Dictionary. <https://www.engineering-dictionary.com/index.php?definition=1851>
7. Erazo-Chamorro VC. Artículo científico. Máquina peladora rotatoria de maní tostado para la industria. Technical report
8. Erazo-Chamorro VC (2018) Design a pin on disk according to related standards
9. Friction: friction and wear::friction and wear: pin on disc tribometer. <http://www.frictionwear.com/products/pin-on-disc-test-mc>
10. Grau DT, Caballero SS (2018) Universitat Politècnica de València. Technical report

11. Miskolc. A case study of wear testing. http://emrtk.uni-miskolc.hu/projektek/adveng/home/kurzus/korszanyagtech/1konzultacio_elemei/casestudy.html
12. Rosero-Montalvo PD, Lopez-Batista V, Puertas VE, Maya-Olalla E, Dominguez-Limaico M, Zambrano-Vizuete M, Arciengas-Rocha RP, Erazo-Chamorro VC (2020) An intelligent system for detecting a person sitting position to prevent lumbar diseases. In: *Advances in intelligent systems and computing*, vol 1069. Springer, pp 836–843. https://doi.org/10.1007/978-3-030-32520-6_60
13. Rosero-Montalvo PD, Lopez-Batista VF, Peluffo-Ordóñez DH, Erazo-Chamorro VC, Arciniega-Rocha RP (2019) Multivariate approach to alcohol detection in drivers by sensors and artificial vision. In: *Lecture notes in computer science (including subseries lecture notes in artificial intelligence and lecture notes in bioinformatics)*. LNCS, vol 11487. Springer Verlag, pp 234–243. https://doi.org/10.1007/978-3-030-19651-6_23
14. Rudas FJS, Gomez ELM, Toro A (2014) Modelamiento del proceso de desgaste de un tribometro pin-disco: flash temperature y mecanismos de disipacion. *ITECKNE* 10(2). <https://doi.org/10.15332/iteckne.v10i2.397>. <https://dialnet.unirioja.es/servlet/articulo?codigo=4991562>
15. Toapanta-Lema A, Gallegos W, Rubio-Aguilar J, Llanes-Cedeño E, Carrascal-García J, García-Lopez L, Rosero-Montalvo PD (2020) Regression models comparison for efficiency in electricity consumption in Ecuadorian schools: a case of study. In: *Communications in computer and information science*, CCIS, vol 1194. Springer, pp 363–371. https://doi.org/10.1007/978-3-030-42520-3_29

Optimal Design Optimization of a Hybrid Rigid–Soft Robotic Hand Using an Evolutionary Multi-objective Algorithm



Golak Bihari Mahanta , B. B. V. L. Deepak, Amruta Rout, and B. B. Biswal

Abstract Conventional rigid bodied robotic gripping systems have established their presence in the industrial applications are challenged by the rapid advances in the soft material robotic systems. Soft material robotic manipulators are progressively infiltrating to the market due to their capability of safe interaction with the human operators and objects to be grasped, which leads to the economical operation of the robotic systems. In this study, we presented a geometric model of a hybrid soft–rigid robotic gripper that uses the benefits of both rigid and soft materials. A multi-objective optimal design approach for an underactuated hybrid soft–rigid three fingers with three phalanges in each finger actuated by tendon is introduced to find the optimum grasping condition using improved multi-objective antlion optimization algorithm (I-MOALO) evolutionary algorithm. A mathematical model is formulated to find the contact forces of the proposed robotic hand while grasping the object followed by the development of the two fitness functions and several geometric constraints incorporated into the proposed model. The obtained Pareto optimal fonts by solving the proposed gripper optimization model using I-MOALO are analyzed by a designer to select the optimal design parameters and also present a significant relation between the objective function and design variables. A sensitivity analysis of the system is conducted to verify the effect of the design variables with the change in the systems.

Keywords Underactuated · Gripper · Optimization · Anthropometric

1 Introduction

Early robotic automation is developed to automated hazardous and repetitive work to perform with a higher speed and accuracy. A key role is played by robotic gripper in

G. B. Mahanta (✉)

Department of Robotics Engineering, Karunya Institute of Technology and Sciences, Coimbatore, Tamil Nadu 641114, India

B. B. V. L. Deepak · A. Rout · B. B. Biswal

Department of Industrial Design, National Institute of Technology Rourkela, Rourkela 769008, India

© The Author(s), under exclusive license to Springer Nature Singapore Pte Ltd. 2022
B. B. V. L. Deepak et al. (eds.), *Applications of Computational Methods in Manufacturing and Product Design*, Lecture Notes in Mechanical Engineering,
https://doi.org/10.1007/978-981-19-0296-3_7

automatic grasping which is a complex area of robotic automation as grippers need to be designed for a unique and pre-specified work in the industrial applications for enhancing the capability of the systems considering the nature of the workpiece such as weight, size, materials, surface properties, and shape of the object. It is crucial to choose the best gripper in the industrial automation systems for ensuring economic viability. Nature of the job plays a vital role while selecting a gripper for the automation process like vacuum gripper are most efficient while doing the rapid loading or unloading whereas finger type gripper used for the automation process accuracy is more.

In the past few decades, due to the rapid technological advancement in the areas of material developments, soft fabrics, shape memory alloys, carbon fiber, and smart fluids, more robust robotic systems are introduced in the manufacturing processes. For decades, robots have been used in a restricted environment without the interference of human beings is now shifting focus toward the use of collaborative robots in human environments [1]. Collaborative robots have been used alongside the human operator, so it is necessary to provide softness to the robotic gripper to avoid injury and also provided enough rigidity for the stable grasping of the object. Advancement in fabrication methods leads to the production of less cost soft materials [2]. Nature plays a vital role while developing the soft robots by taking inspiration from the different morphologies available like fin ray inspired gripper [3], octopus's tentacle inspired soft robot arm [4], *Manduca Sexta* [5], bird's beak [6], and foot [7] and much more. Apart from the rigid and soft manipulator, there is a space for the hybrid manipulator consists of soft and rigid material similar to the human hand made up of rigid bone and soft skin. The most famous robotic gripper that developed using soft and rigid material is iRobot-Harvard-Yale (iHY) hand [8], and Yale open-source robot hand [9]. Though some of the existed robotic grippers consist of rigid and soft material, only the joints are made of soft materials. The main drawback of the existed grippers has the intricate design and high development cost due to which it is not adequately explored. Rigid actuators have the benefit of accurate motion, and superior exerted force. At the same time, soft actuator displays a higher degree of freedom, and better compliance, but lags in the exerted force.

2 Materials and Methods

In this section, we presented and discussed the design motivation considered for the development of the hybrid soft–rigid robotic gripper. The human finger is regarded as the primary source of motivation for the design of the proposed hybrid finger as it is present in the middle of the design space between soft and rigid fingers. Rigid grippers can generate higher force and do the precision work, whereas grippers developed from the soft materials have better compliance and a higher degree of freedom. By taking advantage of both the rigid and soft material, a hybrid soft–rigid robotic gripper can develop, which can generate higher force, good compliance, higher DOF, and able to do more precise work. A schematic diagram is illustrated to show the presence

of hybrid soft–rigid robotic gripper in the middle of the unexplored design space between rigid and soft gripper, as presented in Figs. 1, 2, 3 and 4. Finger-based grippers have superior ability in the in-hand manipulation, whereas soft universal gripper filled with granular materials is capable of grasping a wide range of products.

$$f_1 = F_1 + F_2 + F_3$$

$$f_2 = (\bar{F} - F_1)^2 + (\bar{F} - F_2)^2 + (\bar{F} - F_3)^2$$

$$\bar{F} = \frac{F_1 + F_2 + F_3}{3}$$

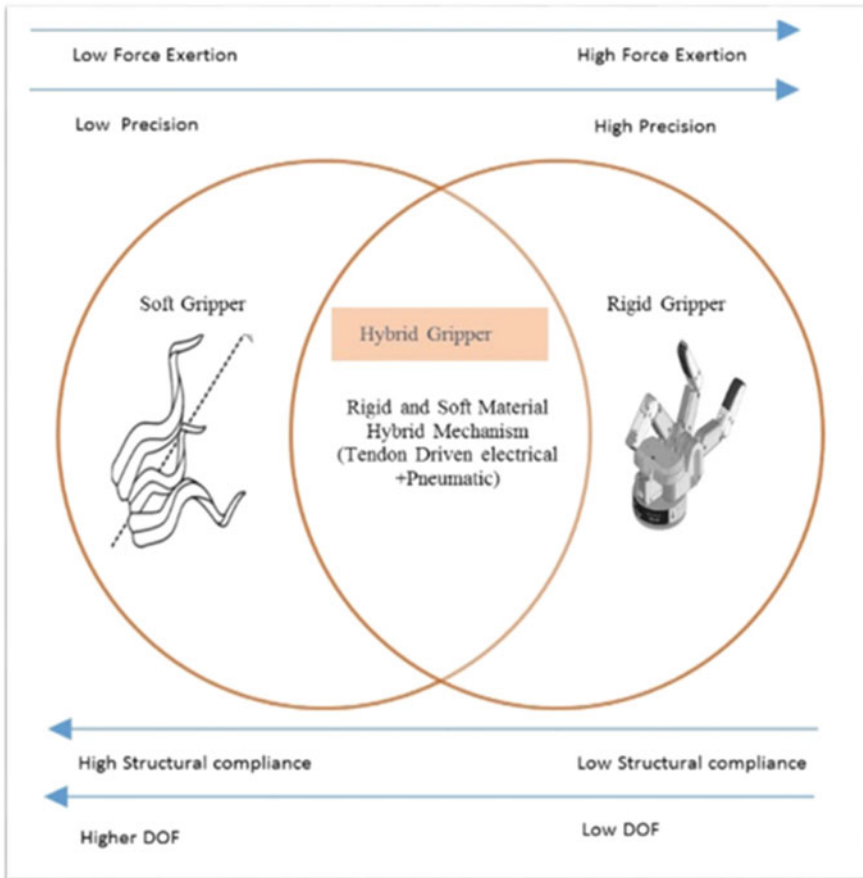


Fig. 1 Position of the hybrid soft–rigid gripper in the design space

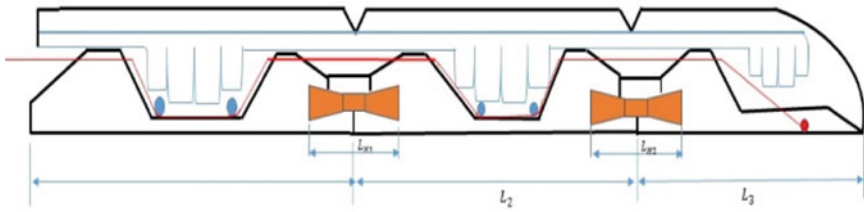


Fig. 2 Conceptual design of a single finger

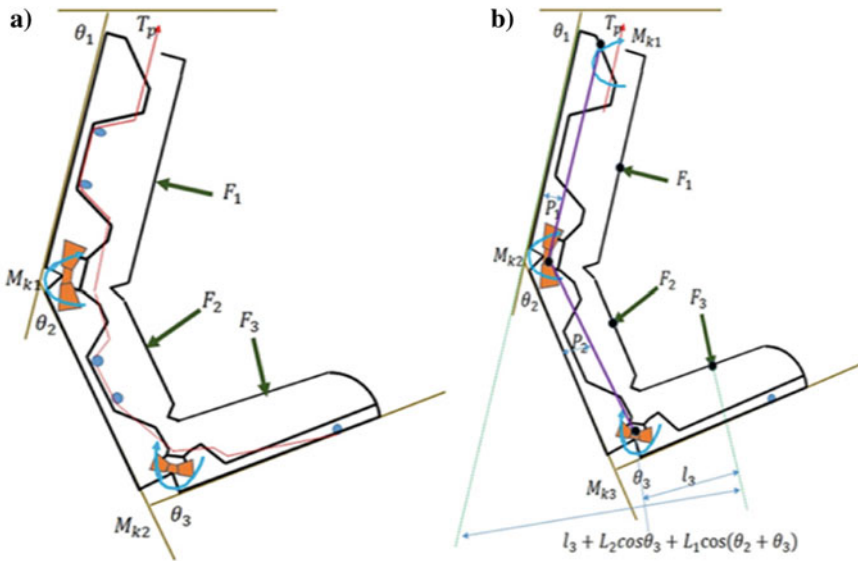


Fig. 3 a Schematic layout of the single finger with contact forces and developed tensions, b free body diagram of the proposed robotic finger concerning distal joint

3 Proposed Methodology

The hunting behavior of antlion gave the inspiration to develop the Multi-Objective Ant Lion Optimizer (MOALO) (Mirjalili et al. 2017) [10]. The strongest Antlion, which has the maximum probability of catching prey, is known as the elite Antlion. MOALO algorithm is shown superior performance compared to other evolutionary algorithms due to its higher convergence rate with properties to avoid local optima because of its excellent exploration and higher exploitation that have a greater tendency to address the multi-objective problems with constraints equations. Previously, we developed an improved version of MOALO to find the optimal dimensions [11]. So, in this article, the improved mechanism of the algorithm is not elaborately explained. The fundamental differences are to use beta distribution and modified

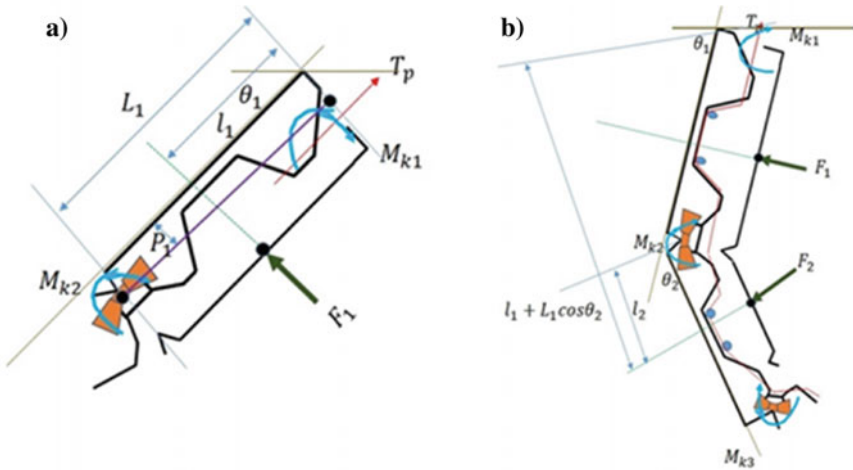


Fig. 4 **a** FBD of a single robotic finger concerning proximal joint, **b** FBD of a single robotic finger concerning middle joint

elitism approach in the improved version of the algorithm, which is explained elaborately in the article and the schematic flow of the algorithm is shown in Fig. 5. In this work, we used the I-MOALO to obtain the optimal design parameters of the proposed hybrid soft–rigid robotic hand.

4 Results and Discussion

To validate the proposed methodology to obtain the optimal geometric parameters of a hybrid soft–rigid robotic hand, a simulation study is conducted using the I-MOALO algorithm in MATLAB R2015a. The algorithm parameters for this study are presented in Table 1. A clear explanation regarding the selection of the tuning parameters can be found in the article [11], which is beyond the scope of this article.

The proposed multi-objective problem is solved using the algorithm, and the obtained result in terms of Pareto front is presented in Fig. 6. The designer’s sole responsibility to select the most appropriate design criteria according to their application from the obtained Pareto front. Here, we considered three points, as shown in Fig. 6, by considering a point at the extreme right (Point C), one point at center (Point B), and other at the extreme left (Point A). All three points of the Pareto fronts are selected, keeping in attention that consider all the area while obtaining the optimal geometric parameters of the proposed systems. All the geometric design parameters are in mm, which can be obtained from the selected points of the Pareto fonts. The limits of the predefined design variables are presented in Table 2.

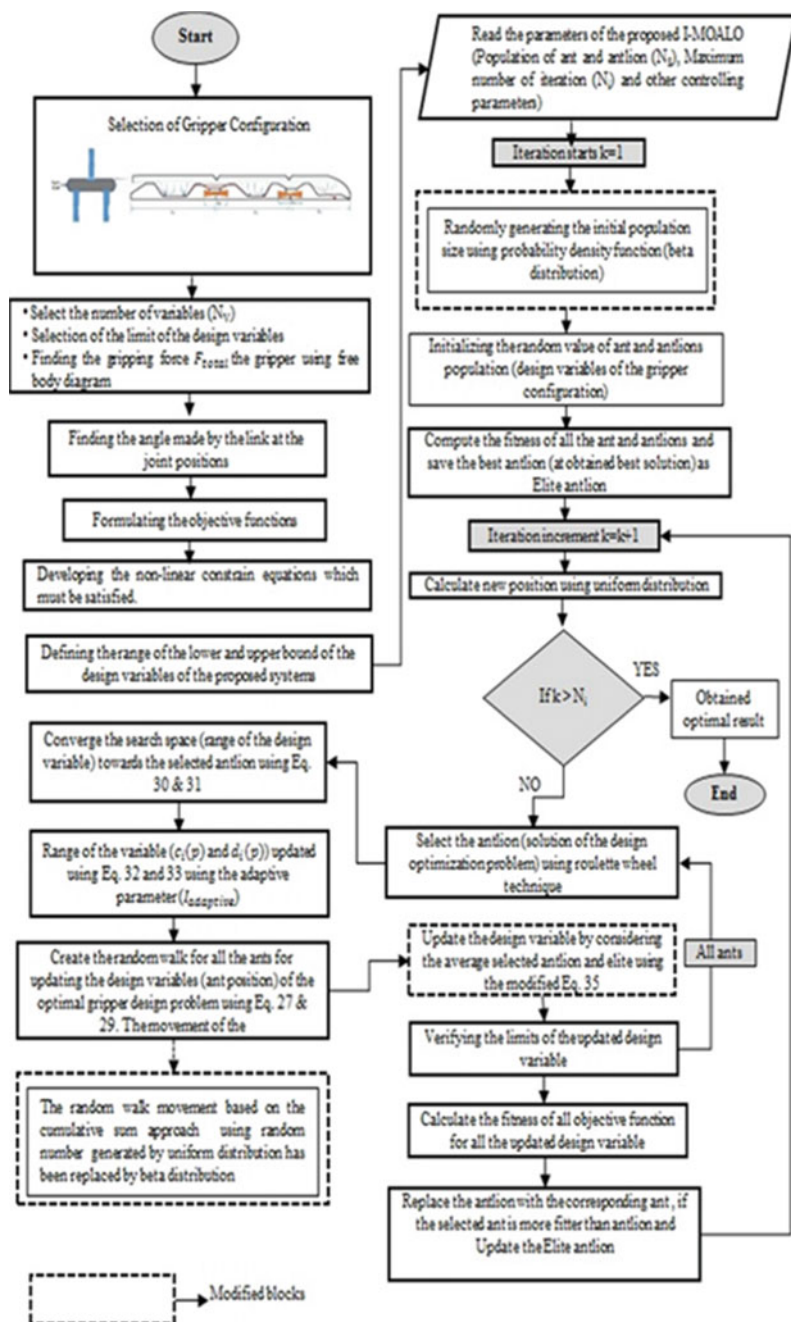


Fig. 5 Implementation procedure to find out the optimal dimensions of the hybrid soft-rigid hand

Table 1 Tuning parameters of I-MOALO

Algorithm	Pop. size	No. of iterations	Max. size of archive
I-MOALO	400	400	400

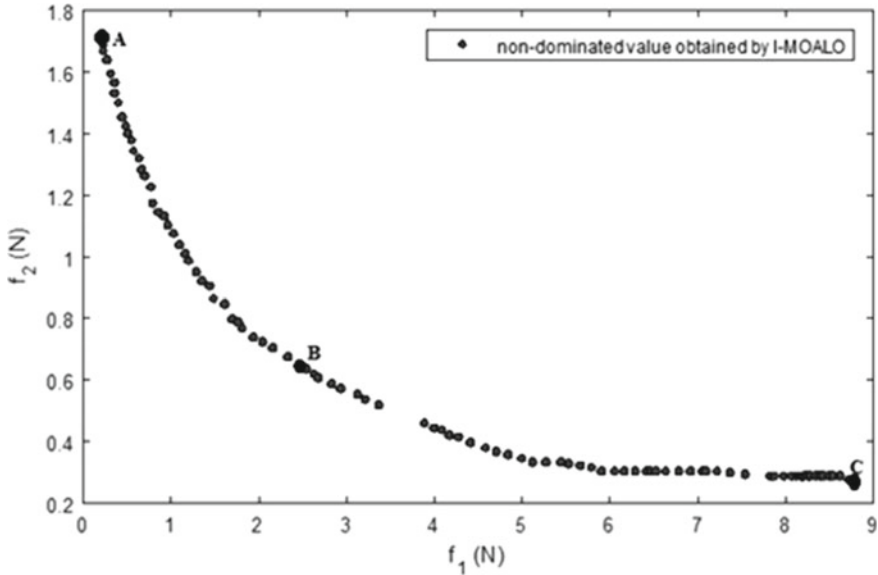


Fig. 6 Obtained non-dominated solutions using I-MOALO

Table 2 Present limits of the design variable

Design parameters (mm)	L_1	L_2	L_3	d_1	d_2	d_3	$2P_1$	$2P_2$	$2P_3$
Lower limit (mm)	35	20	10	6	6	6	12	12	12
Upper limit (mm)	55	50	30	20	20	20	22	22	22

The main responsibility in multi-objective optimization problem is to select the most suitable Pareto solution and the trade-off solution from the obtained result is selected on the designer choice. Area of application of the robotic hand plays a crucial role while the selection of the Pareto fronts. Small objects grasping required the précised gripper (Fig. 7) which have the tendency to grasp the objects with higher accuracy and with minimum force. A fuzzy membership function is employed to find the optimal points among all the solutions for this study (Tables 3, 4 and 5).

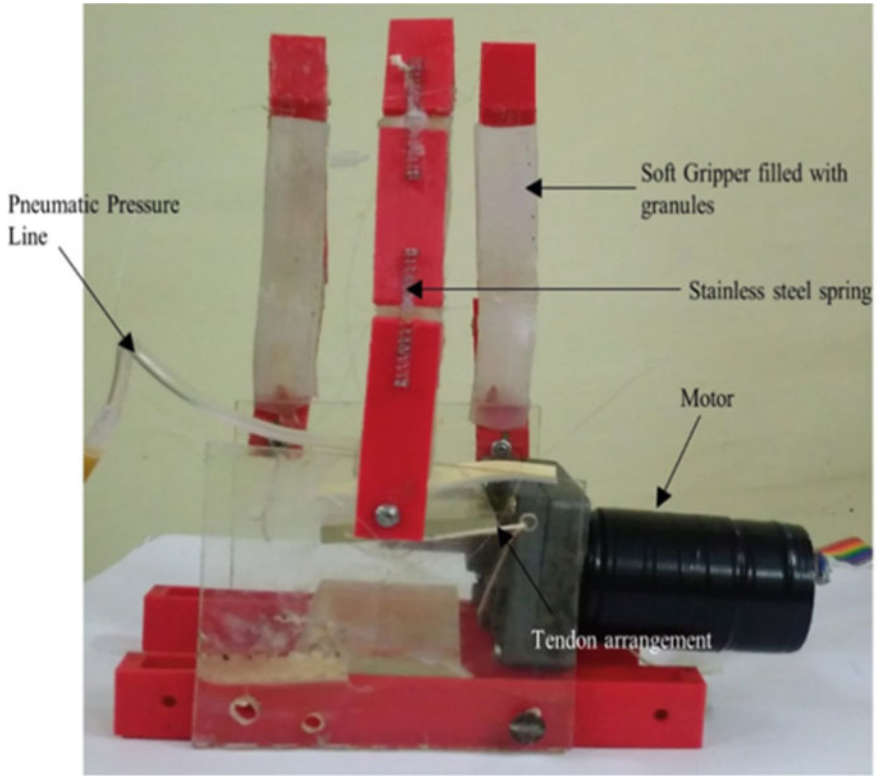


Fig. 7 Fabricated preliminary prototype considering the obtained dimensions

Table 3 Comparison with other algorithms

	$f_1(x)$	$f_2(x)$	L_1	L_2	L_3	d_1	d_2	d_3	$2P_1$	$2P_2$	$2P_3$
NSGA-II	5.2	2.4	50.2	30.5	26.2	17.4	8.9	18.9	19.6	16.6	17.8
MOALO	3.8	1.2	54.6	34.2	26	15.8	8.3	17	17.5	17.9	18
I-MOALO	2.94	0.56	53.8	33.2	25	15.5	7.7	16.8	17.2	16.8	17.9

Table 4 Computation time comparison

Algorithms	Time (s)
NSGA-II	179.45
MOALO	143.67
I-MOALO	120.5

Table 5 Obtained optimal design variable

Point	$f_1(x)$	$f_2(x)$	L_1	L_2	L_3	d_1	d_2	d_3	$2P_1$	$2P_2$	$2P_3$
A	0.195	1.714	55.2	34.1	25.7	15.4	7.9	16.9	17.6	17.1	18.4
B	2.944	0.569	53.8	33.2	25.0	15.5	7.7	16.8	17.2	16.8	17.9
C	6.788	0.268	52.9	35.4	24.2	15.3	7.1	15.8	17.5	17.2	18.0

5 Conclusion

This article presents a new and efficient approach for finding the optimal design conditions for a hybrid soft–rigid robotic gripper. The optimal design optimization problem of the hybrid soft–rigid robot gripper is formulated as a multi-objective optimization problem with two objective functions. The optimization problem is solved effectively by an improved multi-objective antlion optimizer (I-MOALO) method with beta distribution to generate an initial random number and compared with other algorithms to verify its effectiveness. Finally, a design sensitivity analysis has been investigated to find the effect of change in the design variable toward the objective functions of the proposed hybrid soft–rigid robotic hand. In future, we extended this study to investigate for the bio-inspired optimization process, topology optimization, and control methodology to handle the hybrid soft–rigid robotic hand.

Acknowledgements This research did not receive any specific grant from funding agencies in the public, commercial, or not-for-profit sectors.

References

1. Robotiq Inc, blog (one per model) (2019) <https://blog.robotiq.com/where-are-we-now-with-collaborative-robotics>. [Online]. Accessed 02 Mar 2019
2. Miriyev A, Stack K, Lipson H (2017) Soft material for soft actuators. *Nat Commun* 8(1):1–8
3. Crooks W, Vukasin G, O’Sullivan M, Messner W, Rogers C (2016) Fin ray® effect inspired soft robotic gripper: from the RoboSoft grand challenge toward optimization. *Front Robot AI* 3:1–9
4. Laschi C, Cianchetti M, Mazzolai B, Margheri L, Follador M, Dario P (2012) Soft robot arm inspired by the octopus. *Adv Robot* 26(7):709–727
5. Crooks W, Rozen-Levy S, Trimmer B, Rogers C, Messner W (2017) Passive gripper inspired by *Manduca sexta* and the fin ray® effect. *Int J Adv Robot Syst* 14(4):1–7
6. Festo, blog (2019) <https://www.festo.com/group/en/cms/10237.html>. [Online]. Accessed 02 Mar 2019
7. Makinde OA, Mpofu K, Vrabic R, Ramatsetse BI (2017) A bio-inspired approach for the design of a multifunctional robotic end-effector customized for automated maintenance of a reconfigurable vibrating screen. *Robot Biomim* 4
8. Ma RR, Odhner LU, Dollar AM (2013) A modular, open-source 3D printed underactuated hand. In: *Proceedings of IEEE international conference on robotics and automation*, pp 2737–2743
9. Ma RR, Buehler M, Kohout R, Howe RD, Dollar AM (2014) A compliant, underactuated hand for robust manipulation. *Int J Rob Res* 33(5):736–752

10. Rao RV, Waghmare G (2015) Design optimization of robot grippers using teaching-learning-based optimization algorithm. *Adv Robot* 29:431–447. <https://doi.org/10.1080/01691864.2014.986524>
11. Mahanta GB, Rout A, Deepak BBVL, Biswal BB (2019) An improved multi-objective antlion optimization algorithm for the optimal design of the robotic gripper. *J Exp Theor Artif Intell* 1–30

A Simplified Fifth Order Shear Deformation Theory Applied to Study the Dynamic Behavior of Moderately Thick Composite Plate



Sarada Prasad Parida and Pankaj C. Jena

Abstract In this work the order of the generalized higher-order-shear-deformation-theory (HSDT) is set to five and the motion field is taken as function of thickness in vertical direction also. The stress components, static deflection and natural frequencies in dynamic study are studied. The results of the theory assumed is compared with the findings of classical-plate-theories (CLT), first-order-shear-deformation theory (FSDT), HSDT without thickness function included in transverse direction and FEA. GFRP composite plates have been considered to get the dynamic responses. The effect of filler materials such as grapheme and flyash is meanwhile also tested. The fundamental frequencies of vibrations of the GFRP samples with filler are contrasted with the neat GFRP plate and the filler percentage is then optimized.

Keywords Filler · Graphene · Flyash · HSDT · GFRP · Dynamic study · Fundamental frequency

Symbols Used

u, v, w	Displacement field in x, y and z direction
u_0, v_0, w_0	Mid-plane displacement at static condition
h	Plate thickness
w_b	Displacement by bending
w_s	Displacement by twisting
$\phi(z)$	Angular displacement
$\varepsilon_x, \varepsilon_y, \varepsilon_z$	Linear strain in x, y, z direction
γ	Shear strain
V_m	Volume fraction matrix
V_f	Reinforcement volume fraction

S. P. Parida · P. C. Jena (✉)

Department of Production Engineering, Veer Surendra Sai University of Technology, Burla, Odisha 768018, India

e-mail: pcjena_pe@vssut.ac.in

ν	Poisson's ratio
E	Young's modulus
G	Shear modulus
$[Q]$	Stiffness-matrix
$[T]$	Transformation-matrix
$[\bar{Q}]$	Transformed stiffness-matrix
ρ	Density

1 Introduction

Fiber reinforced polymeric composites (FRP) are more commonly used in today's materialistic need of life. It's various design to use properties and environment readiness are more preferred than that of conventional materials. Apart from smaller uses in small house appliances, these composite parts are also used as building materials or structural materials in automobiles, ships decks, aero-components, and etc. These large structures are generally analyzed under the plate-theories for static/dynamic responses. Analyses of a plate like structure are based on certain assumption and approximations. As discussed [1] this assumption leads to set the displacement field to be linear or non-linear. Though the linear approximation of displacement is easier to set and compute, it gives unrealistic results for analysis of stress and strain components. Thus, the displacement fields are modified to higher orders. A number of plate theories such as CLT, FSDT, SSDT, TSDT and HSDT are available.

A number of works have been contributed in this regard defining the plate theories. The review works [1–15] have described the classification of plate theories, their implications, formulations, and their limitation to the real problems. The use of plate theory to any geometric structure is generally based on its dimension. While considering the shear deformation theory, it is decided wheatear to consider the bending deformation or shear deformation. Also, it is stated that the displacement field in thickness direction is either constant or a linear function of the thickness. While the displacement along length and width direction is defined by the shape function depending upon the order of the equation. Later, this displacement fields can be related to find strain components and the stiffness parameters. A number of works are available co-relating the higher order shear deformation displacement field with the modal parameters such as modal frequency and mode shapes. Sayyad and Ghugal [10] have explained the HSDTs framed a new n th order theory and conducted static/dynamic responses of the composite plate. The preliminary works have been conducted on multilayered composites are by Noor [16]. He proposed a two phase computational method first to derive the natural frequency. An n th order SDT has been formulated by Reddy and Kuppusamy [17]. Based on Reddy's HSDT, a number of works have been conducted on the modal analysis of composite plates [18–22]. A wide variety of preparation methodology of composites are available. Some of the works have been referred [23–28]. Numerical simulations is a popularly adopted

method to analyze modal study of the composite structures as described and followed by the works [29–33].

In this work, a fifth order displacement field is set and using variational approach; the linear and shear strains are determined as a function of displacement field. Glass fiber reinforced polymeric composite with graphene and flyash as filler is prepared [22], the mechanical property of the test specimens are found out and used for the numerical investigation. The modal parameters such as frequencies and mode shapes are obtained and explained in terms of their constitutional properties.

2 Theoretical Formulation

The displacements of a composite plate assuming HSDT by Reddy’s approach, in x , y and z -axis as shown in Fig. 1 is given by;

$$\begin{aligned}
 u &= u_0 - z \frac{\partial w_b}{\partial x} - \frac{1}{5} \left(\frac{2}{h} \right)^4 z^5 \left(\frac{\partial w_s}{\partial x} \right) \\
 v &= v_0 - z \frac{\partial w_b}{\partial y} - \frac{1}{5} \left(\frac{2}{h} \right)^4 z^5 \left(\frac{\partial w_s}{\partial y} \right) \\
 w &= (w_b + w_s) + z\phi(z)
 \end{aligned}
 \tag{1}$$

The strain components associated to the displacement fields are given by;

$$\epsilon_x = \frac{\partial u}{\partial x} \quad \epsilon_y = \frac{\partial v}{\partial y} \quad \epsilon_z = \frac{\partial w}{\partial z}$$

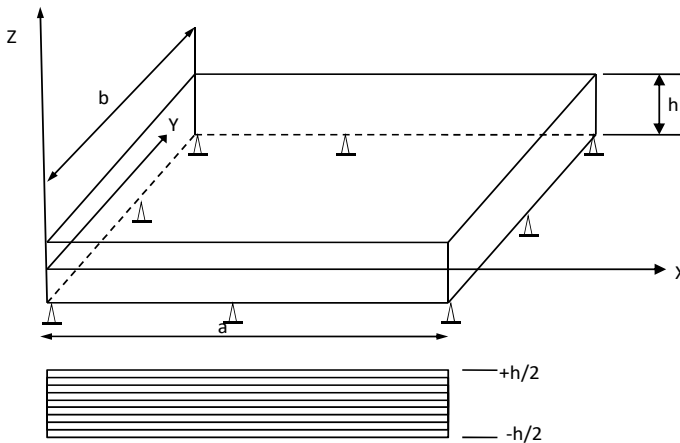


Fig. 1 Modeled composite plate with supported end condition

$$\gamma_{xy} = \frac{\partial v}{\partial x} + \frac{\partial u}{\partial y} \quad \gamma_{xz} = \frac{\partial u}{\partial z} + \frac{\partial w}{\partial x} \quad \gamma_{yz} = \frac{\partial v}{\partial z} + \frac{\partial w}{\partial y} \quad (2)$$

Stress-strain relationship for each composite lamina using micromechanical analysis is given by;

$$E_x = E_y = E_f V_f + E_m(1 - V_f) \quad (3)$$

$$\gamma_{xy} = \nu_f V_f + \nu_m(1 - V_f) \quad G_{xy} = \frac{G_m G_f}{V_m G_f + V_f G_m} \quad (4)$$

Relation of stress and strain of an orthotropic composite lamina is given by;

$$\{\sigma\} = [\overline{Q}]\{\varepsilon\} \quad (5)$$

With $[\overline{Q}] = [T][Q]$.

2.1 Dynamic Analysis of Clamped-Clamped Plate

The differential equation of motion of a rectangular isotropic plate is given by;

$$D \nabla^2 \nabla^2 w(x, y, t) + \rho h \frac{\partial^2 w(x, y, t)}{\partial t^2} \quad (6)$$

where $\nabla^2 = \frac{\partial^2}{\partial x^2} + \frac{\partial^2}{\partial y^2}$, $D = \frac{Eh^3}{12(1-\nu)}$.

For an orthotropic material D is replaced by $[D]$ and is given by;

$$[D] = \begin{bmatrix} D_{11} & D_{12} & D_{16} \\ D_{12} & D_{22} & D_{26} \\ D_{16} & D_{26} & D_{66} \end{bmatrix} \quad (7)$$

With

$$D_{i,j} = \frac{1}{3} \sum_{k=1}^N (\overline{Q}_{i,j})_k (z_k^3 - z_{k-1}^3) \quad (8)$$

The general solution to the above equation under simple supported boundary condition is given by;

$$w(\xi, \eta) = A_{m,n} \sin n\pi\eta \sin m\pi\xi \quad (9)$$

with $\xi = x/a$ and $\eta = y/b$.

The corresponding modal frequency of a square-plate and is given by[34, 35];

$$\omega^2 = \frac{\pi^4}{\rho} [D_{11}(m/a)^4 + 2(D_{12} + 2D_{66})(m/a)^2(n/b)^2 + D_{22}(n/b)^4] \quad (10)$$

Here m and n represents odd integers only for symmetric modes.

2.2 Finite Element Model

For the study an eight noded iso-parametric brick element as shown in Fig. 2 is designed using MATLAB, the global stiffness matrix and mass matrix is assembled from each nodal stiffness matrix and mass matrix.

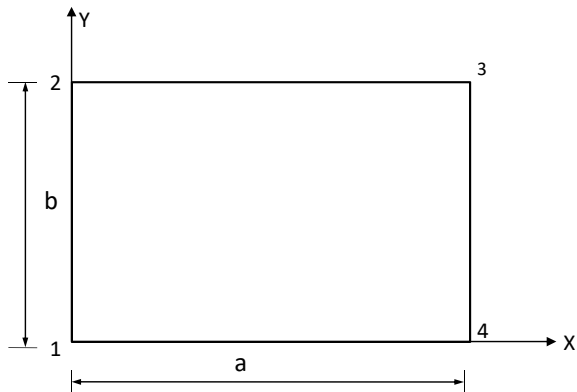
Corresponding Eigen-frequencies were obtained by constraining the boundary condition to simple support. The corresponding natural frequencies and mode shapes for the plates were obtained. A sample figure of first four mode shapes of a simple supported square isotropic plate with aspect ratio ($a/h=0.1$) is presented in Fig. 3a–d. The characteristics equation of free vibration is given by;

$$([K] - \omega^2[M]) = 0 \quad (11)$$

3 Results and Discussion

A computer program has been developed using the proposed theory and considering the micromechanical stress strain behavior of orthotropic composite material by the help of MATLAB. Glass fiber reinforced GFRP composite square plates of thickness

Fig. 2 Eight noded iso-parametric brick element



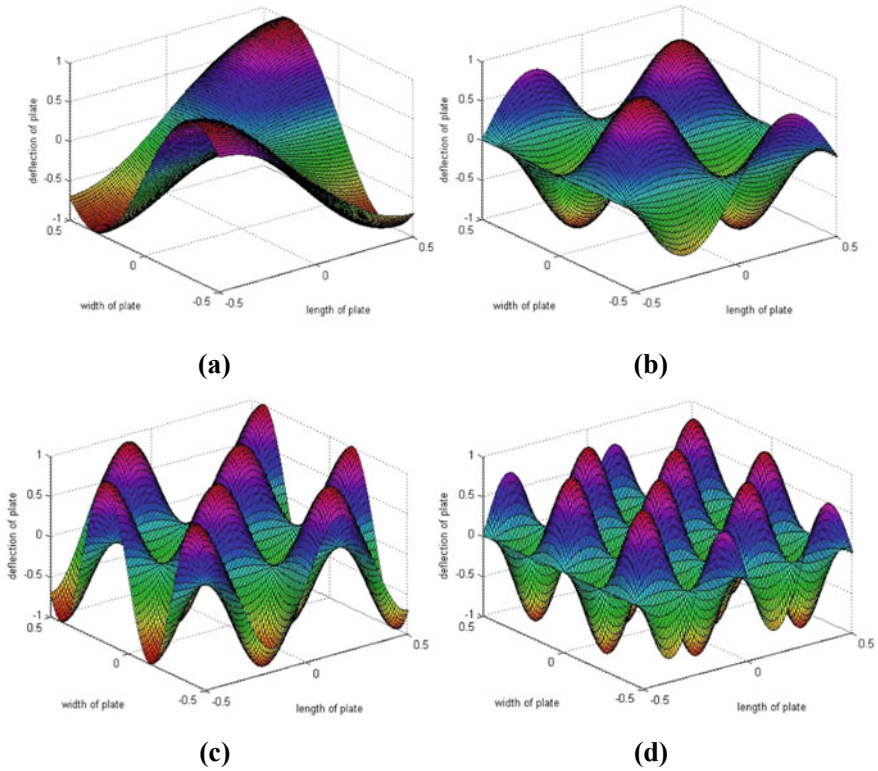


Fig. 3 Simulated mode shapes of composite plate **a** First mode shape. **b** 2nd mode shape. **c** 3rd mode shape. **d** 4th mode shape

6 mm are considered. L56 epoxy with its corresponding hardener MS91 is used as matrix. Graphene or flyash are used as reinforced filler. The mechanical properties are evaluated using the rule of mixture. The weight fraction of the matrix is fixed to 40% while the filler and the fiber content all together is regarded as reinforcement and limited to 60%. During the study, h/a ratio is varied from 0.01 to 0.5 and the percentage content of the filler is changed from 0 to 10%. The effect of this input parameters are observed in the fundamental frequency.

3.1 Validation of the Study

Before analyzing the study, the feasibility of the proposed theoretical model has been studied, the result of the model is checked by the several models available in the literature. For this purpose, a square isotropic plate with $\nu = 0.3$ and aspect ratio $a/h = 0.01$ is taken. The non-dimensional natural frequencies as described by

Eq. (10) is calculated theoretically and compared with the results of the references and the result of FEA.

Table 1 represents the non-dimensional natural frequencies of a square isotropic plate in symmetric and anti-symmetric modes of vibration. Figure 4 presents the comparison of natural frequencies for a fixed aspect ratio $a/h = 0.01$ for an isotropic plate in simple supported end condition at the four edges. It can be observed that there is a small deviation in results of the framed displacement field and hence the use of shear correction factor is not necessary. Also, from the graph it is evident that the methods applied for FEA study have the closed values of results with other theoretical models and models adopted in this work. The error percentage of the simulated result is found to be near about 2–4%. Further, h/a of the plate is changed and the effect is studied. Figure 5 represents the deviation of fundamental-frequency with h/a . It is observed that the increase in aspect ratio increases fundamental frequency.

Table 1 Non-dimensional natural frequencies $\omega_{m,n}$ for an isotropic square plate

m	n	CPT [18]	FSDT [36]	HSDT [19]	Present HSDT	FEA
1	1	0.0955	0.0930	0.093	0.091	0.093
1	2	0.2360	0.2219	0.222	0.215	0.241
1	3	0.4629	0.4149	0.341	0.392	0.445
2	3	0.5951	0.5206	0.522	0.498	0.511
3	3	0.8090	0.6834	0.686	0.683	0.687
3	4	1.0965	0.8896	0.854	0.875	0.889
1	5	1.1365	0.9174	0.923	0.837	0.961
2	5	1.2549	0.9984	1.084	0.906	1.015
4	4	1.3716	1.0764	1.013	0.973	1.014

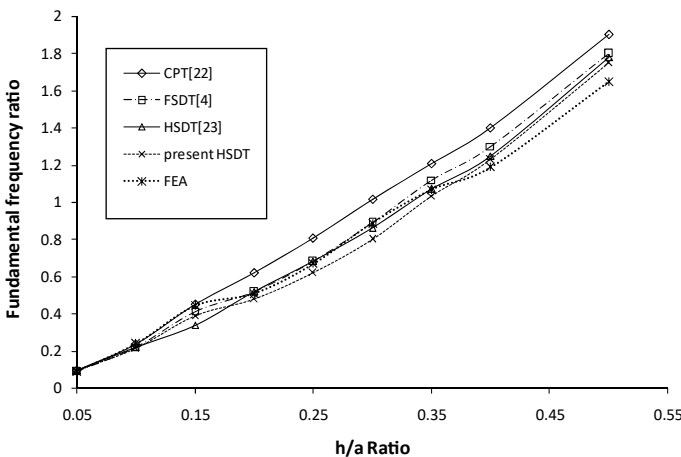


Fig. 4 Variation of non-dimensional frequencies of a square isotropic plate

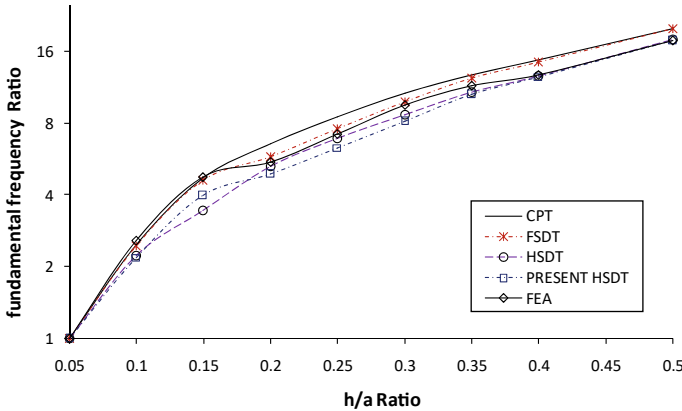


Fig. 5 Fundamental frequency versus aspect ratio

From the graph, it can be also observed that increase in h/a ; there is a remarkable difference in the fundamental frequency initially. However, when the aspect ratio reached to 0.5, the natural frequencies tends to converge. This convergence is due to the smaller dimension of the plate. The diagram exhibits good agreements of the results obtained by the different theories and the FEA.

3.2 Effect of Filler on Fundamental Frequency

The effects of addition of flyash and graphene on natural frequencies were studied. For the purpose, the filler material as a constituent is incorporated in the mixture rule and the mechanical properties are evaluated. The simplified fifth order SDT is then used to calculate the modal frequencies.

3.2.1 Effect of Addition of Graphene

The non-dimensional fundamental frequency for GFRP composite square plate with graphene content of 2.5, 5 and 10% weight fraction is compared with the plain GFRP composite and presented by Fig. 6. The change in aspect ratio value in all the specimens have been examined. It is observed that the increase in h/a increases fundamental frequency value. The increase in h/a decreases in plate dimension which stiffens the structure as a result there is increase in fundamental frequency value. From the chart, it can also be pragmatic that rise in graphene weight percentage also increases the fundamental frequency. The fundamental frequencies of GFRP plates with graphene content are expressed relative to the fundamental frequency

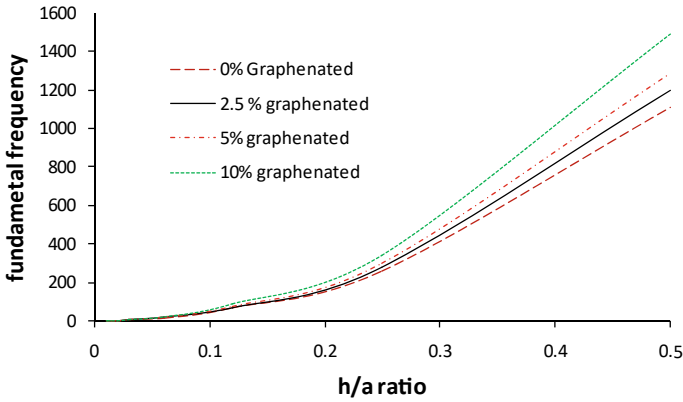


Fig. 6 Fundamental frequency versus aspect ratio of graphenated GFRP plate

of plane GFRP composite as fundamental frequency ratio and plotted against the weight fraction in Fig. 7.

$$\varpi = \frac{\omega_{gr}}{\omega_0}$$

where, ω_{gr} : fundamental frequency of Graphenated GFRP plate and ω_0 : fundamental frequency of plain or neat GFRP plate.

Figure 7 presents the variation of fundamental frequency ratio of five square plates with aspect ratio of 0.01, 0.03, 0.06, 0.12, and 0.5. The non-dimensional fundamental frequency increases linearly with increase in weight fraction of Graphene initially up to 6–8%. Further increase in graphene content causes non-linear variation of fundamental frequency. It is due to the increase in shear strength and elastic modulus with decrease in density of the composite plates. Hence, the graphene content in

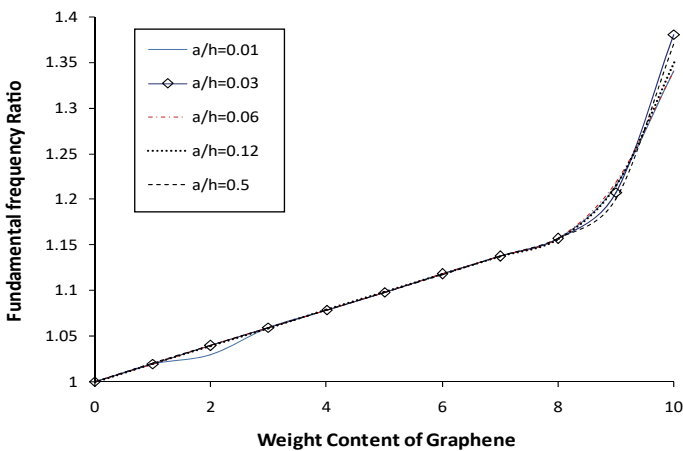


Fig. 7 Fundamental frequency ratio versus graphene content

any composite should not exceed this limit which in return reduces the flexibility of the structure. The variation of shear modulus, Young's modulus and density of the composite with increase in graphene and flyash content is presented through Fig. 8a–c.

3.2.2 Effect of Addition of Flyash

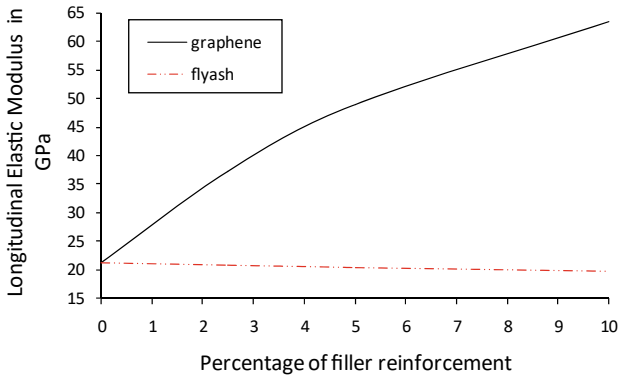
As like of graphene, flyash is added as filler and its effect on natural frequency is studied correspondingly. Figure 9 presents the deviation of non-dimensional fundamental frequency with aspect ratios of the square GFRP plate having 0, 2.5, 5, and 10% flyash filler. It is pragmatic that the increase in h/a increases the frequency however the increase in flyash content decreases the fundamental frequency. The distinction in fundamental frequency is more visible with increase in aspect ratio value. Figure 10 presents the variation of fundamental frequency ratio of GFRP composites with flyash content. In contrast to the use of graphene as filler, the increase in weight percentage of flyash decreases the natural frequency. It is due to the overall decrease of elastic modulus, shear modulus and density of the composite specimens.

3.2.3 Effect of Addition of Flyash and Graphene Altogether

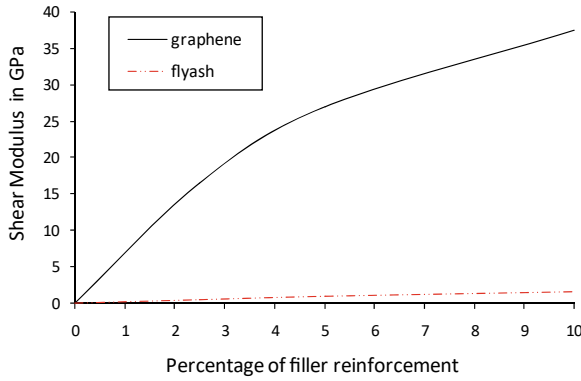
Flyash and graphene are also added altogether as filler in GFRP composite plates and their effect on the natural frequencies are studied. Figure 11 presents the variation of fundamental frequency of 4 kinds of samples with the h/a . It is studied that composite plates with graphene as filler have the highest and the flyash as filler has lower fundamental frequency as compared to the fundamental frequencies of plain GFRP composite plate. The fundamental frequencies of the test samples with 5% flyash and 5% graphene filler are also determined and compared. It is observed that the fundamental-frequencies of these kinds of samples have intermediated values of fundamental frequency of the individual samples having 10% weight fraction of graphene and flyash each.

4 Conclusion

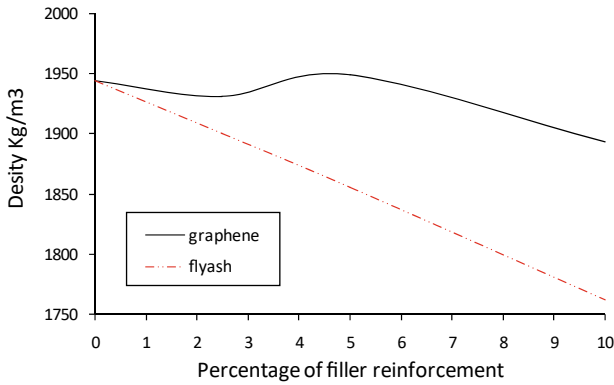
The proposed HSDT copes with the result of the other plate theories and the results of FEA model. The result shows that there is no need of shear correction factor. The increase in aspect ratios stiffens the structure which is reflected on the natural frequency. Also, it is observed that increasing the aspect ratio over 0.25; there is abrupt variation in the fundamental frequency. The material property is dependent on the constituent materials. The raise in graphene content rises the stiffness of the composite plates while increase in flyash content decreases the stiffness of the composite plates. It is reflected on the fundamental frequency ratios. Young's



(a)



(b)



(c)

Fig. 8 Variation of material property of composite; a elastic modulus. b shear modulus. c density

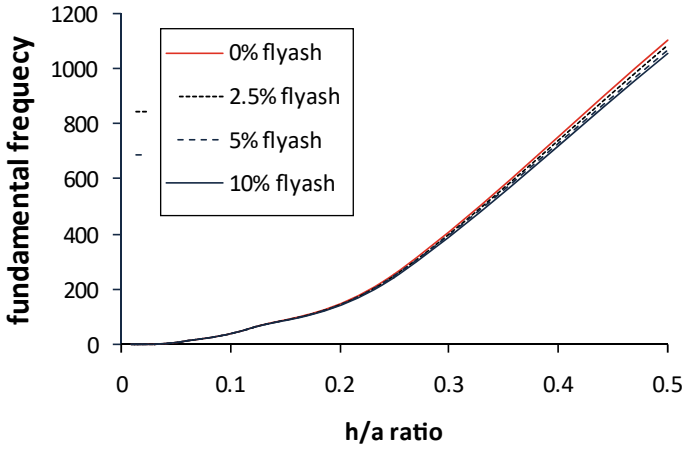


Fig. 9 Fundamental frequency versus aspect ratio of GFRP plate with flyash filler

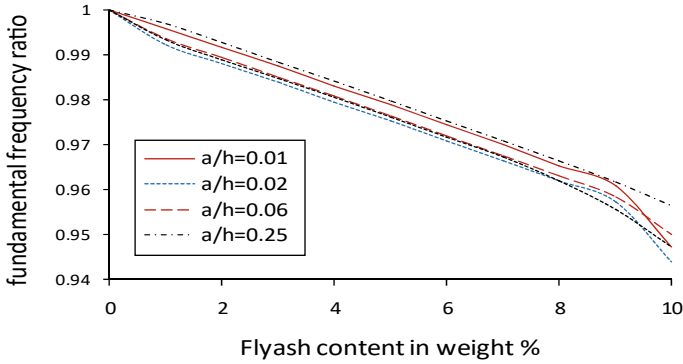


Fig. 10 Fundamental frequency ratio versus flyash content

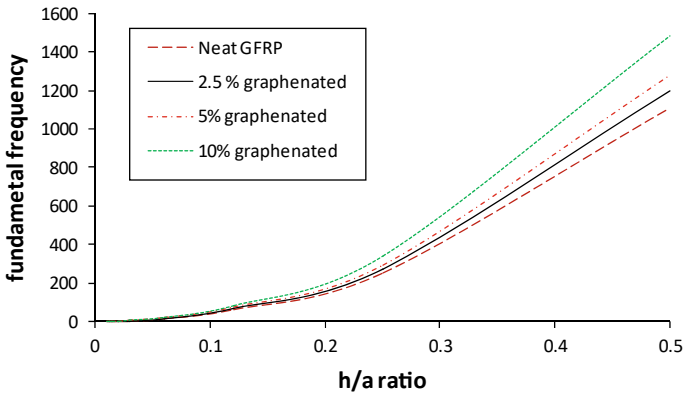


Fig. 11 Comparisons of fundamental frequency of GFRP plates with different type of fillers

and shear modulus of a composite sample increases with increase in graphene content while decreases by increasing the flyash content. However, the density of the composite specimens decreases in both the cases. The weight fraction of graphene should be less than 8% of total composite plate weight, additional increase in graphene content stiffens the structure in unusual way. The rate of change of natural frequencies is more abrupt in composite plates with graphene filler as compared to the flyash filler. This work is limited only to the theoretical approximation, further it can be validated by actual experimentations. Also, the other types of end conditions needs to be examined. The fillers added are more sensitive to water absorption and hygro-thermal behavior, the works in this direction may be extended.

References

1. Parida SP, Jena PC (2020) Advances of the shear deformation theory for analyzing the dynamics of laminated composite plates: an overview. *Mech Compos Mater* 56(4):1–40
2. Ghugal YM, Shimpi RP (2016) A review of refined shear deformation theories of isotropic and anisotropic laminated plates. *J Reinf Plast Compos* 20:255–272
3. Hu H, Belouettar S, Potier-Ferry M, Daya EIM (2008) Review and assessment of various theories for modeling sandwich composites. *Compos Struct* 84:282–292
4. Caliri Jr MF, Ferreira AJM, Tita V (2016) A review on plate and shell theories for laminated and sandwich structures highlighting the finite element method. *Compos Struct* 156(216):63–77
5. Tornabene F, Fantuzzi N, Baccocchi M, Viola E (2018) Mechanical behavior of damaged laminated composites plates and shells: higher-order shear deformation theories. *Compos Struct* 189:304–329
6. Kant T, Swaminathan K (2000) Estimation of transverse/interlaminar stresses in laminated composites—a selective review and survey of current developments. *Compos Struct* 49:65–75
7. Kapania RK, Raciti S (1989) Recent advances in analysis of laminated beams and plates, part I: shear effects and buckling. *AIAA J* 27(7)
8. Khandan R, Noroozi S, Sewell P, Vinney J (2012) The development of laminated composite plate theories: a review. *J Mater Sci* 47:5901–5910
9. Liu D, Li X (1996) An overall view of laminate theories based on displacement hypothesis. *J Compos Mater* 30(14)
10. Sayyad AS, Ghugal YM (2015) On the free vibration analysis of laminated composite and sandwich plates: a review of recent literature with some numerical results. *Compos Struct* 129:177–201
11. Swaminathan K, Naveenkumar DT, Zenkour AM, Carrera E (2014) Stress, vibration and buckling analyses of FGM plates—a state-of-the-art review. *Compos Struct*. <https://doi.org/10.1016/j.compstruct.2014.09.070>
12. Zhang YX, Yang CH (2009) Recent developments in finite element analysis for laminated composite plates. *Compos Struct* 88:147–157
13. Piskunov VG, Rasskazov AO (2002) Evolution of the theory of laminated plates and shells. *Int Appl Mech* 38:135–166
14. Vasiliev VV (2000) Modern conceptions of plate theory. *Compos Struct* 48:39–48
15. Vijayakumar K (2013) On a sequence of approximate solutions: bending of a simply supported square plate. *Int J Adv Struct Eng* 5:18. <https://doi.org/10.1186/2008-6695-5-18>
16. Noor AK (1972) Free vibrations of multilayered composite plates. *AIAA J*
17. Reddy JN, Kuppasamy T (1984) Natural vibrations of laminated anisotropic plates. *J Sound Vib* 94(1):63–69

18. Srinivas S, Rao AK (1970) Bending, vibration and buckling of simply supported thick orthotropic rectangular plates and laminates. *Int J Solids Struct* 6:1464–1481
19. Reddy JN (2007) Nonlocal theories for bending, buckling and vibration of beams. *Int J Eng Sci* 45:288–307
20. Abualnour M, Houari MSA, Tounsi A, Bedia EAA, Mahmoud SR (2018) A novel quasi-3D trigonometric plate theory for free vibration analysis of advanced composite plates. *Compos Struct* 184:688–697
21. Li D, Liu Y, Zhang X (2013) A layer wise/solid-element method of the linear static and free vibration analysis for the composite sandwich plates. *Compos Part B Eng* 52:187–198
22. Zhang LW, Selim BA (2017) Vibration analysis of CNT-reinforced thick laminated composite plates based on Reddy's higher-order shear deformation theory. *Compos Struct* 160:689–705
23. Bousahla AA, Houari MSA, Tounsi A, Adda Bedia EA (2014) A novel higher order shear and normal deformation theory based on neutral surface position for bending analysis of advanced composite plates. *Int J Comput Methods* 11(06):1350082
24. Abdelmalek A, Bouazza M, Zidour M, Benseddiq N (2019) Hygrothermal effects on the free vibration behavior of composite plate using nth-order shear deformation theory: a micromechanical approach. *Iran J Sci Technol Trans Mech Eng* 43(1):61–73
25. Parida SP, Jena PC (2020) Preparation of epoxy-glass composites with graphene and flyash filler. *Mater Today Proc* 26:2328–2332
26. Parida SP, Jena PC (2019) An overview: different manufacturing techniques used for fabricating functionally graded material. *Mater Today Proc* 18:2942–2951
27. Parida SP, Jena PC, Dash RR (2019) FGM beam analysis in dynamical and thermal surroundings using finite element method. *Mater Today Proc* 18:3676–3682
28. Saraswati PK, Sahoo S, Parida SP, Jena PC (2019) Fabrication, characterization and drilling operation of natural fiber reinforced hybrid composite with filler (fly-ash/graphene). *Int J Innov Technol Explor Eng (IJITEE)* 8(10). ISSN: 2278-3075
29. Singh S, Parida SP, Ekka P, Jena PC (2019) Characterization of fabricated FG pipe with natural fiber-flyash-epoxy using centrifugal casting. *Int J Innov Technol Explor Eng (IJITEE)* 8(11). ISSN: 2278-3075
30. Jena PC, Parhi DR, Pohit G (2014) Theoretical, numerical (FEM) and experimental analysis of composite cracked beams of different boundary conditions using vibration mode shape curvatures. *Int J Eng Technol (IJET)* 6(2). ISSN: 0975-4024
31. Jena PC, Parhi DR, Pohit G (2016) Dynamic study of composite cracked beam by changing the angle of bidirectional fibres. *Iran J Sci Technol Trans Sci*. <https://doi.org/10.1007/s40995-016-0006-y>
32. Jena PC (2018) Free vibration analysis of short bamboo fiber based polymer composite beam structure. *Mater Today Proc* 5:5870–5875
33. Jena PC (2018) Identification of crack in SiC composite polymer beam using vibration signature. *Mater Today Proc* 5:19693–19702
34. Timoshenko S, Kreiger SW. *Theory of plates and shells*
35. Gorman DJ (1930) *Free vibration analysis of rectangular plates*. Elsevier
36. Vasiliev VV, Morozov EV (2001) *Mechanics and analysis of composite materials*. Elsevier

Referring Expressions in Discourse Structure: A Study of Local and Global Focus



Harjit Singh

Abstract This paper studies local and global focus by investigating dialogue forms within the discourse structure. By and large, it has been found that a term reference or so-called referring expressions always play a significant role among interlocutors. They organize dialogue set up through intention and attention states. We also interested to study such states by observing the local and global focus here. Briefly, we start with developing a sense of discourse structure including the coherence relations. Secondly, we survey the focusing mechanism of discourse structure. Finally, we choose ‘Ek Kahani’ which is written by Sukhdeep Singh for generalizing local and global focus forms in the Punjabi dialogues. We conclude that both proper names and pronouns are actively more intended at local focus level while only a pronoun category may be seen at the global focus level in all three selected dialogue forms.

Keywords Referring expressions · Discourse structure · Local focus · Global focus · Ek kahani

1 Introduction

The paper is especially focused on referring expressions in details. They are not only dealt in philosophy, syntax, and semantics but also attracts to pragmatics and computational linguistics as well. In general, referring expressions find as a matter of “identity of reference” within a language. Related discourse structure, many studies discuss the focusing mechanism and about cognitive-pragmatic approaches for referring expressions in a natural language.

The term “referring expressions”¹ have different modes and explanations in pragmatics, discourse analysis and computational linguistics. Each and every discipline has given many cues to understand the relationship between referring expressions

H. Singh (✉)

Indira Gandhi National Tribal University, Amarkantak, M.P 484887, India

¹ An expression like noun phrase usually indicates towards person, place, object, event, etc. that is called R-expression (The Oxford Dictionary of English Grammar, 2014).

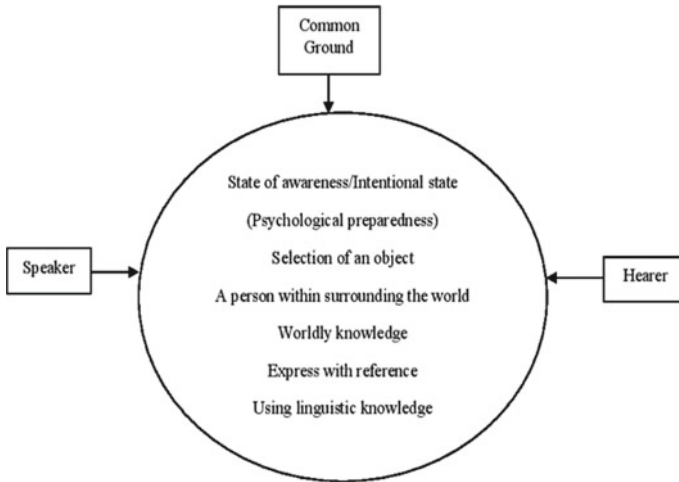


Fig. 1 Contextual Picture of Referring Expressions

and discourse structure. As pragmatics has pointed out that an intentional level of a speaker may help us to understand the conscious status of a hearer. On the other hand, when we pick up an object or entity in a discourse and give it a linguistic label that is called referring expressions only. We can see contextually the referring expressions in Fig. 1.

Figure 1 shows that both speaker and hearer involved in communication process to share the common experiences. It is said that referring expressions may be categorized into definite and indefinite forms. In English, anaphoric demonstratives pronouns (*this, that*) have also been acquired similar sense. Sometimes, they give an explicit representation when they appear with NPs/definite or indefinite articles and pronouns. While on the other hand, they become implicit and treated like ellipsis/zero anaphors in English. Referring expressions may be varied from a language to language. As we generally know that pronouns and deixis are categories which have inherent nature of pointing or referring to something in the universe of discourse. Similarly, definiteness and indefiniteness come with familiarity and uniqueness like notions those equally significant in a discourse or a text.

In this paper, we mainly study the referring expressions in the context of a discourse structure and on the other hand, we search local and global focus in Punjabi. We have total six sections in the paper. First section deals with the referring expressions from dialogue participant's point of view, Second section presents the background study of discourse structure. Third section discusses the aims and objectives. Fourth section describes the background and recent trends of local and global focus. Fifth section shows the focus choices in Punjabi and presents the results. Sixth section discusses the conclusion and future endeavors related local and global focus.

2 Related Works

Semantically, a pronoun² may go for disassociating the referents in a speech. It has been pointed out that a pronoun may be substituted with common nouns (e.g., father, mother, enemy) without affecting the semantics [1, p. 123]. Some scholars have argued that a matter of reference and referring expressions in a discourse is depended upon pronouns and a speaker who gives himself or herself reference through the first person pronoun (I) ([2, , p. 218] It is usually happened that pronouns carry various interpretations and they act like determiners and may appear before a noun. Sometimes, they may also be appeared in the plural form and followed by nouns.

This/That boy
 Det (____N)
 We people
 Pr pl (____N)

We have found that discourse units present an independent structure within semantic domain. They may be compared with a building, an apartment and a tree, etc. Thus, a discourse looks like a building or a tree whose elements and components actively participated in it [3]. From sociolinguistics point of view, it has been explored that conjunctions, interjunctions and other word classes may be assumed as boundary markers within a text or discourse. A tree structure represents both linguistic and social aspects of a discourse structure. Figure 2 shows the building blocks in linguistic discourse model [4].

Figure 2 shows that there are four blocks in a linguistic discourse model. Block (1) describes the discourse constituent units (dcu) that further consist of sequence, expansion, binary structure and interruption in block (2). While the block (3) discusses about discourse parser in terms of co-ordinated and sub-ordinated nodes. Last block (4) gives an information about higher level discourse structure like speech events in a natural language.

3 Aims and Objectives

To present a general survey about referring expressions.

To discuss referring expressions in the context of discourse structure.

To describe local and global focus in the light of referring expressions.

To analysis focus mechanism in Ek Kahani written by Sukhdeep Singh.

To discuss the results and future works.

² They can be used to show nominal categories and have not descriptive content. They seem to us like nominals and complementizers however in real sense they are different and are place holder, particularly in the case of nouns (Simon and Wiese 2002, pp. 1–2).

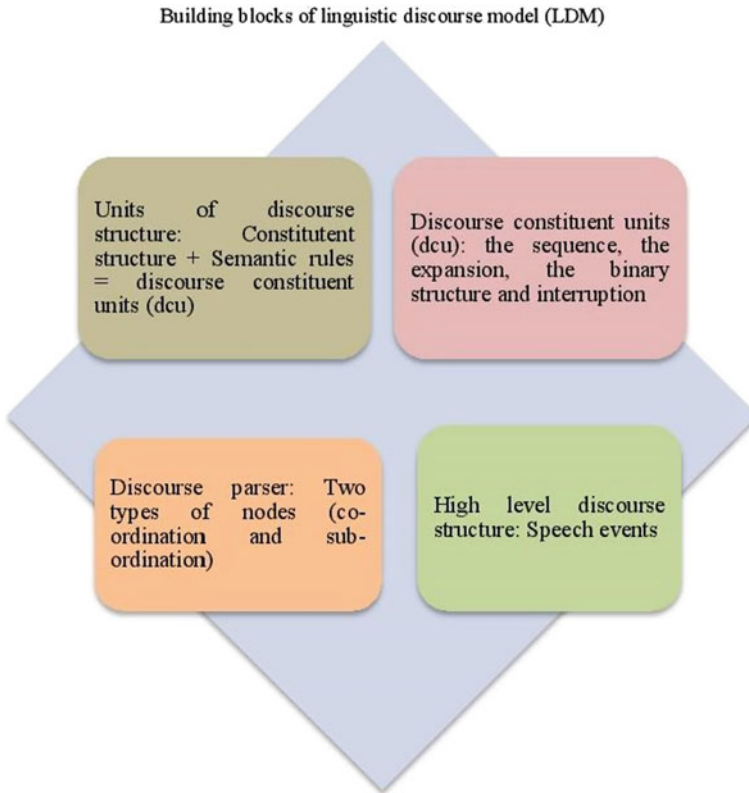


Fig. 2 Linguistic Discourse Model (LDM)

4 Local and Global Focus: From Beginning to Recent Tradition

Since 1970s task structure and dialogue structure have been enumerated in understanding the discourse structure. In general, a task and a dialogue can be categorized into sub-tasks and sub-dialogues to study the focus and focal points. Moreover, it has been argued that definite noun phrases (pronominal and non-pronominal) are significant to specify the focus position (Grosz 1977, p. 10–33). In the context of anaphor processing, it is assumed that focus preferences (such as questions, indefinites, subject/object and verbal elements with ellipsis) play an important role in focusing. On the other hand, a text may contain six focus registers like discourse focus (DF), actor focus (AF), potential discourse focus (PDF), potential actor focus (PAF), discourse focus stack (DFS), and actor focus stack (AFS) to understand the definite anaphora. Based on these six focus registers, we can state the claims in Table 1 [5].

Table 1 Sidner's Claim for Six Focus Registers

Principles	Explanation
Principle of proximity	More recent NPs must be preferred
Pronouns assumed as full NPs	Pronouns must be preferred more in focus
Preference for NPs in matrix and embedded clauses	NPs must be preferred in contrast to other elements
Preference for subject more	Subjects must be preferred but not applicable everywhere
Preference for accusatives object NPs	Objects as accusatives preferred more
Preference for anaphora	Cataphora must be followed by anaphora

For resolving definite anaphora³ in English, Sidner has proposed six focus registers and also brought some principles regarding focusing in Table 1. It has shown that noun phrases are more preferred than pronouns and accusative objects and also anaphors in contrast to cataphora in the list.

With Sidner's focusing principles, it is necessary to understand the discourse markers in a discourse structure. It has been argued that there are four levels (semantic, interpersonal/goal oriented, attentional/thematic and rhetorical) to be used for structuring a discourse. They are one type of cues that must fully be shared between a speaker and a hearer during spoken discourse [6]. Related focusing, we find that an intonation is an important factor in studying discourse structure in Japanese. An intonation and its prominence in relation to referring expressions express local and global focus in Japanese discourse structure [7]. While the focus system like explicit focus and implicit focus found in narratives. An explicit focus is an actor oriented, which is portrayed by names, pronominals and an implicit focus is a type of situation fillers, which is identified by definite descriptions. It is a fact that coherent inferences in a narrative or text generally depend on the accurate distinction between explicit and implicit focus [8].

As earlier Sidner suggested about focus registers, it is found that pronouns and its forms eligible for focusing. The category of personal pronouns not only stand for nouns cross-linguistically however they appear such as referring expressions, anaphors, cataphors, etc. in natural language. Moreover, it is not surprising to see that Southeast Asian languages (like Burmese, Thai and Japanese) do not have personal

³ The following D1 as adapted from Sidner (1979) shows the bold underlined part is definite NP anaphora (Sidner 1979, p. 97).

D1 I want to have a big party with lots of guests.

The party ought to be on Saturday so everyone can come.

In this instance (4), the party is found as definite NP anaphora in English.

pronoun system. A speaker from these languages may select only nouns to communicate different purposes. Even though, it is found that demonstratives from interrogatives and from indefinites can be separated from functional point of view. Demonstratives apply to indicate back or previously mentioned expressions in the deictic use. While interrogatives and indefinites may be considered for new information when they behave like anaphors.

Definite descriptions may also consider in the form of referring expressions those have been explored through Dale and Reiter’s incremental algorithm and support vector machine [9]. Interestingly, it is found that what we have our thoughts and ideas can be expressed through referring expressions. They bring out them in surrounding the world and fix the labels to introduce the spoken and written discourse [10]. Regarding referring expressions, a key word aware network has been applied for image segmentation and it works according to attentional and contextual knowledge [11]. In fact, referring expressions (pronoun/anaphor) usually find in a speech and they are important to see coherence and coreference both. Sometimes, we human become puzzle lack of wrong interpretation of referring expressions. It is true in the case of human–machine interaction platform. Robots is a good example here. They may be trained to resolve the puzzle related referring expressions and may be selected for model purposes through Bayesian framework [12]. On the other hand, some studies have shown generation of referring expressions in a knowledge graph. In this context, we cannot ignore RE-miner algorithm that has been executed for investigating referring expressions in different datasets [13].

5 Preparing Focus Choices in Ek Kahani

We take three dialogue conversations (part-A is related with Channan and Sukh, part-B is associated with Alafnur and Sukh and the part-C is again related with Channan and Sukh) in “*Ek Kahani*” written by Sukhdeep. See the part-DA, DB, and DC.⁴

⁴ Note that DA = Dialogue (A), DB = Dialogue (B) and DC = Dialogue (C).

Part-A (Dialogue between Channan and Sukh)

ਚੰਨਨ : ਅੱਜ ਸੋਏ ਨਹੀਂ ਤੁਸੀਂ ਹਲੇ

Chanman: Today, **you** have not slept yet

ਸੁਖ : ਨਹੀਂ [Omitted] ਬਸ ਸੌਣ ਹੀ ਲੱਗਦਾ ਸੀ, **ਅਲਫ਼** ਡਰ ਜੋ ਗਈ ਸੀ

Sukh: No I just fell asleep, **Alf** got scared

ਚੰਨਨ : ਅੱਛ, **ਪਿੰਡ** ਤਾਂ ਅੱਜ ਵਾਹਲਾ ਮੀਂਹ ਸੀ, **ਸ਼ਹਿਰ** ਵੀ ਐਨਾ ਹੀ ਸੀ

Chanman: Well, it was raining heavily in the **village** today, the **city** was the same

ਸੁਖ : ਹਾਂ ਸ਼ਾਮ ਨੂੰ **ਚਾਰ ਵਜੇ** ਹੋਂਟਿਆ

Sukh: Yes, it was stopped at **4:00PM** evening time

ਚੰਨਨ : [Omitted] ਇੱਕ **ਗੱਲ** ਪੁੱਛਣੀ ਸੀ ਜੀ

Chanman: One **thing** ask to please

ਸੁਖ : ਹਾਂ ਦੱਸ

Sukh: Yes tell me

ਚੰਨਨ : **ਮੈਂ** ਦੇ ਕੇ ਦਿਨ ਪਿੰਡ ਜਾ ਆਵਾਂ, **ਮੰਮੀ** ਕਾਫ਼ੀ ਕਹਿ ਰਹੇ ਨੇ

Chanman: **I** will go to the village in couple of days, **Mom** is saying for longer time

ਸੁਖ : ਹਾਂ ਰਾਂ ਕੋਈ ਗੱਲ ਨਹੀਂ, [Omitted] ਕੱਲ ਨੂੰ ਹੀ ਚੱਲੇ ਜਾਇਓ

Sukh: Okay, no problem, tomorrow you can go

ਚੰਨਨ : ਜੇ **ਤੁਹਾਡੇ** ਕੋਲ ਟਾਇਮ ਹੈ **ਤੁਸੀਂ** ਨਹੀਂ ਛੱਡ ਕੇ ਆ ਸਕਦੇ, ਪਤਾ ਕੀ ਗੱਲ ਸੀ, **ਵੀਰਾ** ਕਿਤੇ ਗਿਆ

ਹੋਇਆ, **ਪਾਪਾ** ਨੂੰ ਕਾਹਨੂੰ ਐਵੇਂ ਤਕਲੀਫ਼ ਦੇਣੀ ਆ

Chanman: If **you** have time then **you** cannot go there, actually **brother** has gone somewhere, and I don't want to disturb **father**

ਸੁਖ : ਨਹੀਂ ਨਹੀਂ ਕੋਈ ਗੱਲ ਨਹੀਂ, **ਮੈਂ** ਛੱਡ ਆਵਾਂਗਾਂ, **ਮੰਮੀ** ਨੂੰ ਪੁੱਛ ਲਿਆ ਸੀ

Sukh: No problem, **I** will go there, have already asked from **Mom**

ਚੰਨਨ : **ਹਾਂਜੀ**, ਪੁੱਛ ਲਿਆ ਸੀ

Chanman: **Yes**, have been asked

ਸੁਖ : ਕੋਈ ਨਹੀਂ, ਜਿਸ ਦਿਨ **ਮੰਮੀ** ਨੇ ਕਹਿ ਦਿੱਤਾ, **ਮੈਂ** ਫੋਨ ਕਰ ਦੇਵਾਂਗਾ, ਲੈ ਵੀ **ਮੈਂ** ਹੀ ਆਵਾਂਗਾ

Sukh: No problem, when mother will inform to me, I will make a call and will also bring her

ਚੰਨਨ : ਠੀਕ ਆ ਜੀ, ਹੁਣ **ਤੁਸੀਂ** ਠੀਕ ਰਹਿਣੇ ਹੋ

Chanman: Okay fine, now are you fine

ਸੁਖ : ਹਾਂ ਪਹਿਲਾਂ ਨਾਲੋਂ ਫ਼ਰਕ ਹੈ

Sukh: **Yes**, it's better now

ਚੰਨਨ : ਵੈਸੇ ਜੇ [Omitted] ਬੁਰਾ ਨਾ ਮੰਨੇ ਤਾਂ ਦੱਸ ਸਕਦੇ ਹੋ ਤਕਲੀਫ਼ ਕੀ ਆ

Chanman: If you don't mind let me know what happened

ਸੁਖ : **ਚੰਨਨ ਤੂੰ** ਐਵੇਂ ਨਾ ਟੈਨਸ਼ਨ ਲਿਆ ਕਰ, ਹੁਣ ਠੀਕ **ਮੈਂ**

Sukh: **Channan**, **you** don't take any tension, now **I** am fine

ਚੰਨਨ : ਜੀ, [Omitted] ਦੁੱਧ ਚੱਕ ਲਵੋ... ਠੰਢਾ ਹੋ ਰਿਹਾ

Chanman: Please have milk otherwise it will become cold

ਸੁਖ : ਠੀਕ ਹੈ

Sukh: Okay

Part-B (Dialogue between Alfanur and Sukh)

ਅਲਫਨੂਰ : ਤੁਹਾਡਾ ਸੁਭ ਨਾਮ ਦੱਸ ਸਕਦੇ ਹੋ?

Alfanur: Can you tell me **your** good name?

ਸੁਖ : ਹਾਂ ਬਿਲਕੁਲ, ਪਰ ਇੱਕ ਸ਼ਰਤ ਤੇ

Sukh: Yes sure, but on one condition

ਅਲਫਨੂਰ : ਰਹਿਣਦੇ
Alfanur: Stay tuned

ਸੁਖ : ਸੁਖਦੀਪ

Sukh: **Sukhdeep**

ਅਲਫਨੂਰ : ਪੂਰਾ ਨਾਮ

Alfanur: Full name

ਸੁਖ : ਬੀ ਐਸ ਆਰ

Sukh: **B.S. R**

ਅਲਫਨੂਰ : ਤੁਸੀਂ... !!! ,... ਲੇਖਕ ਸਾਬ.....

Alfanur: **You**...!!!,....Author saab

ਸੁਖ : ਤੁਸੀਂ ਉਹੀ ਅਲਫਨੂਰ ਹੋ

Sukh: **You** are the same Alfanur

ਅਲਫਨੂਰ : ਹਾਂਜੀ... [Omitted] ਕਿਵੇਂ ਓ ਜੀ

Alfanur: Yes.... How are you

ਸੁਖ : ਵਧੀਆ ਬਸ... ਤੁਸੀਂ ਦੱਸੋ

Sukh: Well... **You** tell me

ਅਲਫਨੂਰ : ਵਧੀਆ ਜੀ... [Omitted] ਹੋਰ ਘਰ ਕਿਵੇਂ ਨੇ ਸਾਰੇ

Alfanur: Well... how about all the others in house

ਸੁਖ : ਵਧੀਆ ਜੀ... [Omitted] ਆਪਣੇ ਦੱਸੋ

Sukh: Well... tell about **yourself**

ਅਲਫਨੂਰ: ਵਧੀਆ... ਮੈਨੂੰ ਤੇ ਐਵੇਂ ਸੀ ਤੁਸੀਂ ਭੁੱਲ ਗਏ

Alfanur: Well... **you** forgot about **me**

ਸੁਖ : ਕਿਹਾ ਸੀ ਆਖਰੀ ਸਾਹ ਤੀਕ ਤੇ ਨਹੀਂ , ਉਸਤੋਂ ਬਾਅਦ ਕੁਝ ਸਾਰੇ ਨਹੀਂ

Sukh: Said that not until the last breath, not all after **that**

ਅਲਫਨੂਰ : ਅੱਛਾ ਜੀ, ਮੈਂ ਸੁਣਿਆ ਸੀ ਤੁਹਾਡਾ ਵਿਆਹ ਹੋ ਗਿਆ

Alfanur: Ok, I heard **you** got married

ਸੁਖ : ਹਾਂਜੀ, ਦੋ ਸਾਲ ਹੋ ਗਏ, ਇੱਕ ਬੇਟੀ ਵੀ ਆ ਗਈ ਹੁਣ ਤੇ

Sukh: Ok, it has been two years now and a daughter has arrived

ਅਲਫਨੂਰ : ਅੱਛਾ ਜੀ ਕੀ ਨਾਮ ਆ ਬੇਟੀ ਦਾ

Alfanur: Ok, what is daughter's name

ਸੁਖ : ਪਤਾ ਤਾਂ ਹੈ

Sukh: you know better already

ਅਲਫਨੂਰ : ਸੱਚੀ ਕਿ

Alfanur: Sure that

ਸੁਖ : ਜਬਾਨ ਦੇ ਕੇ ਮੁਕਰਨਾ ਸਾਨੂੰ ਸੋਭਦਾ ਨਹੀਂ ਆ...ਫੇਰ ਵੀ ਸ਼ਾਇਰ ਸੀ... ਉਹਨਾਂ ਦਿਨਾਂ ਚ

Sukh: Denying with the tongue does not beautify us...was still a poet..in those days

ਅਲਫਨੂਰ : ਜਾਣਦੀ ਹਾਂ ਮੈਂ... ਆਪਣੇ ਤੋਂ ਜਿਆਦਾ ਤਹਾਨੂੰ

Alfanur: I know that... more than **you**

ਸੁਖ : ਪਤਾ ਹੈ, ਤਾਹੀਂ ਤਾਂ ਤੁਸੀਂ ਵੀ ਨਹੀਂ ਭੁੱਲੇ... ਮੈਂ ਵੀ ਸੁਣਿਆ ਸੀ, ਤੁਹਾਡੇ ਵਿਆਹ ਬਾਰੇ

Sukh: You know, **you** have not forgotten...I also heard about **your** marriage

Part-C (Dialogue between Channan and Sukh)

ਚੰਨਨ : ਹੈਲੋ ਜੀ [Omitted]

Channan: Hello G [Omitted]

ਸੁਖ : ਹਾਂ ਜੀ

Sukh: **Yes please**

ਚੰਨਨ : [Omitted] ਪਹੁੰਚ ਗਏ ਜੀ

Channan: [Omitted] have been reached

ਸੁਖ : ਹਾਂ ਪਹੁੰਚ ਗਿਆ ਸੀ

Sukh: **Yes, it was**

ਚੰਨਨ : ਠੀਕ ਹੋ **ਤੁਸੀਂ**...ਦਵਾਈ ਧਿਆਨ ਨਾਲ ਲੈ ਲੈਣੀ

Channan: Okay **you** ... take the medicine carefully

ਸੁਖ : ਹਾਂ ਠੀਕ ਹੈ... **ਮੈਂ** ਸ਼ਾਮ ਨੂੰ ਕਰਦਾ ਗੱਲ, ਕਾਫ਼ੀ ਗਾਹਕ ਆ ਰਹੇ ਨੇ

Sukh: Yes, that's right... **I** will talk in the evening, many customers are coming

ਚੰਨਨ : ਠੀਕ ਆ ਜੀ

Channan: **Okay**, that's right

ਸੁਖ : ਠੀਕ ਆ

Sukh: **Okay**, fine

Above descriptions in the part-A, B, and C contain particularly explicit focus such as named entities like Channan, Sukh and Alafnur. Secondly, they may be substituted with pronouns and again forms the explicit focus only in each dialogue. Moreover, we have also searched some gaps and spaces that may be filled up with named entities in the place of omitted spaces.

5.1 Results and Discussions

We have seen that part-A, B, and C have been selected for generalizing focus at dialogue level. In general, part-DA contains total 191 words where the Channan has a choice for 101 words while Sukh has free to use 90 words during the conversation. In part-DB, they have total no of words are 183 and Alafnur has the capacity to utilize 105 words and Sukh has to complete his conversation within 78 words. Similarly, in the third part-DC, they have total 36 words. Channan has to satisfy with only 16 words whereas Sukh keeps 20 words repository for communication purpose. After this lexicon description, we argue that there are 10 times noun categories have been applied in part-A dialogue. However, a similar results can be found in the case of pronouns in the part-B dialogue. In part-C, we have also more elements are pronouns in contrast to nouns. However, we have taken both (nouns and pronouns) such as players by determining the explicit focus here. It is shown in Figs. 3, 4 and 5.

Here, we have seen that Channan has been used about 101 words out of total 191 in Fig. 3. Whereas, Sukh has got success to utilize his own dialogue with 90 words.

In part-B, we have observed that Alafnur has selected around 105 words out of total 183 in Fig. 4. On the other hand, Sukh has kept 78 words in her repository.

In Fig. 5, we have studied that Channan takes 16 and Sukh has chosen 20 words out of total 36 words.

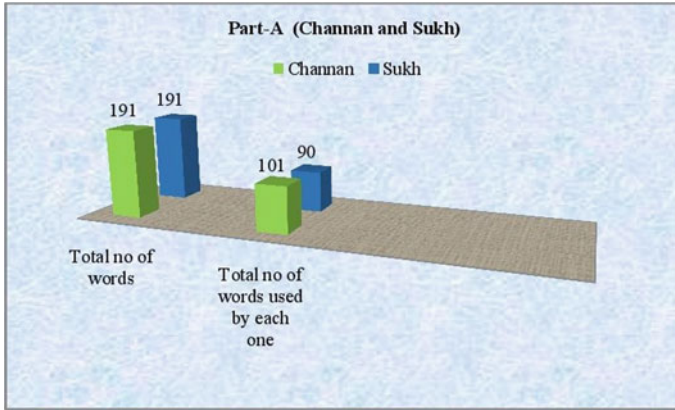


Fig. 3 Dialogues between Channan and Sukh

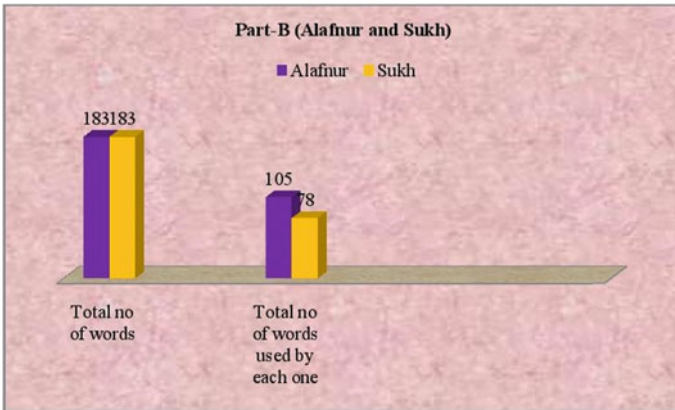


Fig. 4 Dialogues between Alafnur and Sukh

Based on previous discussions, we tried to search local and global focus. We come to know that 20 proper names and eight pronouns find as local focus and for global focus, there are only three pronouns have been received in part-DA. Similarly, we find 24 proper names and seven pronouns in local focus and there are only five pronouns without any proper name available in global focus in the part-DB. Further, we notice that about eight proper names and two pronouns may be judged as local focus and only you pronoun is considered as global focus in part-DC. Figure 6 shows the total no of local and global focus entries.

We may argue that local and global focus may be chosen through various discourse structure models and by noticing the proximity, preference, and salience like factors. In fact, we find out especially explicit focus that come up with prime actors like Channan, Sukh, Alafnur and so on. It is fascinating that proper names and pronouns

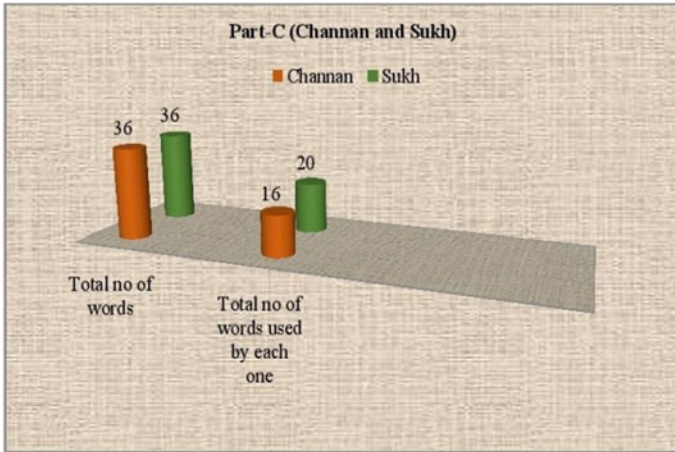


Fig. 5 Dialogues between Channan and Sukh

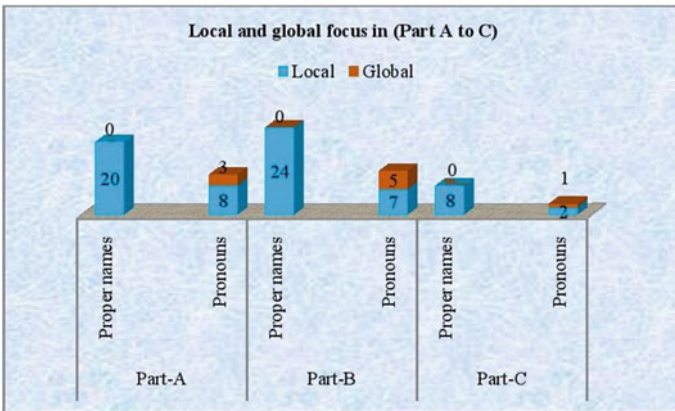


Fig. 6 Representation of Local and Global Focus with Proper Names and Pronouns

both consider as local focus. On the contrary, it is surprising that we have not found a single proper name at global focus level in any dialogue (DA, DB, DC) part.

It is an interesting that we have tried to search local and global focus in Punjabi Ek Kahani. Here, we want to mention that there is no work before available in Punjabi so far. So that, first we must collect no of local and global focus examples and present them in a formal way. As Grosz and Sidner (1977, 79) have proposed focusing mechanism and about coherence in a discourse structure, we also make an attempt to understand choice based coherence for local and global focus among prime actors and players in dialogues. All actors/players have been agreed to use proper names and pronouns for more intended local focus. Whereas, it is likely to notice that nouns, pronouns, and anaphora have been controlled by balanced proximity principle

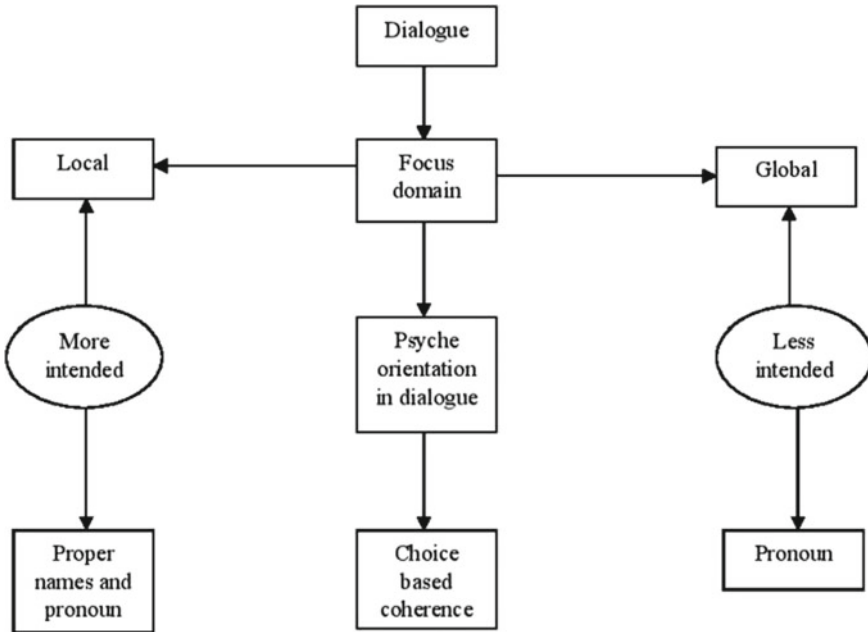


Fig. 7 Interaction between Dialogue and Focus Domain

and under preference criteria. Through the investigation, it is found that pronouns are more recurrent categories comparatively proper names even they are less in numbers. Moreover, we do not claim for any intonation marker behind local and global focus as already pointed out by Venditti [7]. Like a key word aware proposal of Ferrari et al. [11], we also argue that either focus or pronouns and proper names may describe the flow of different events in dialogue. Another important point is that accurate and proper selection of each focus form in dialogue may also contribute to place coherence and coreference at a time such as suggested by Chen and Fragomeni [12]. Figure 7 shows dialogue, focus domain and related concepts.

6 Conclusion and Future Works

We have started with discussing the referring expressions in the context of discourse structure and coherence. We find that notions like local and global focus may be searched in Punjabi also like English, Japanese, Korean languages. For the purpose, we study only three dialogues in “Ek Kahani”, which is written by Sukhdeep. First, we manually count the total no of words used by each actor during the dialogue exchange. Secondly, we go on to study the local and global focus. We conclude that local focus may be assumed for proper names and pronouns both however global

focus does not appear with proper names. In future, we may try to study remaining dialogues to concrete our understanding more about focusing mechanism from all possible perspectives. We will also plan for algorithm and model the system for Punjabi.

Acknowledgements I would like to warmly thank to Vanita Chawadha who helped and supported me to discuss focusing in dialogues.

References

1. Jespersen O (1923) *Language: Its nature, development and origin*. H. Holt Press, London
2. Benveniste E (1971) Subjectivity in language. *Probl Gener Linguist* 1:223–230
3. Linde C (1979) Focus of attention and the choice of pronouns in discourse. In: Givón T (ed) *Syntax and semantics: discourse and syntax*, vol 12. Academic Press, New York, pp 337–354
4. Polanyi L (1988) A formal model of the structure of discourse. *J Pragmat* 12:601–638
5. Carter D (1987) *Interpreting anaphors in natural language texts*. University of Michigan, Halsted Press
6. Hovy EH (1995) The multifunctionality of discourse markers. In: *Proceedings of the Workshop on Discourse Markers*, Egmond-aan-Zee, The Netherlands
7. Venditti JJ (2000) *Discourse structure and attentional salience effects on Japanese intonation*. Doctoral dissertation, The Ohio State University
8. Rickheit G, Habel C (eds) (2011) *Focus and coherence in discourse processing*, vol 22. Walter de Gruyter, New York
9. Gelbukh A (ed) (2014) *Computational linguistics and intelligent text processing*. In: *Proceedings of the 15th international conference, CICLing 2014, Kathmandu, Nepal, 6–12 April 2014*, vol 8404. Springer
10. De Ponte M, Korta K (eds) (2017) *Reference and representation in thought and language*. Oxford University Press, Oxford
11. Ferrari V (eds) (2018) *Computer vision–ECCV 2018*. In: *Proceedings of the 15th European conference, Munich, Germany, 8–14 Sept 2018*, vol 11209. Springer
12. Chen JY, Fragomeni G (eds) (2019) *Virtual, augmented and mixed reality. applications and case studies*. In: *Proceedings of the 11th international conference, VAMR 2019, Held as Part of the 21st HCI International Conference, HCII 2019, Orlando, FL, USA, 26–31 July 2019, Part II*, vol 11575. Springer
13. Pan JZ (2020) *The semantic web–ISWC 2020*. In: *Proceedings of the 19th International semantic web conference, Athens, Greece, 2–6 Nov 2020, Part I*, Springer Nature

Developing Products for the Elderly: PUIA Design Taxonomy



Neha Yaragatti and Ravi Kumar Gupta

Abstract Increase in the elderly population over the years presents both challenges associated with their wellbeing and opportunities for growth and fulfilment. Due to a reduced functional capacity, elderly users do not achieve the required task efficiently with products currently used. Hence, there is a need to develop products which are designed considering requirements, and conditions of the elderly to aid their Activities of Daily Living (ADL). This paper reviews the works in the field of product design for the elderly with an aim of identifying the taxonomies used in the design process. The need for a general design taxonomy while designing products for the elderly is identified. A taxonomy is developed with Product, User, Interaction, and Activity as main categories and its usage is demonstrated by applying it to redesign of handwash dispenser.

Keywords Product design · Senior citizen · Elderly · Aged people · Taxonomy · Customization · ADL · ICF

1 Introduction

With the dawn of a new decade, the year 2020 marks the beginning of the Decade of Healthy Ageing (2020–2030), which is an opportunity to bring together people and societies from every corner of the world for a collaborative and synergistic action to improve the lives of the elderly population [1]. According to the World Health Organization (WHO), by the year 2050, the world population aged 60 years and above is expected to hit the 2 billion mark by increasing the world proportion to nearly 22% from 12% in 2015 [2]. As a person ages, his/her functional capacity decreases which

N. Yaragatti · R. K. Gupta (✉)

CAD Lab, Department of Mechanical Engineering, SAMM, Manipal University Jaipur, Jaipur 303007, India

e-mail: ravikumar.gupta@jaipur.manipal.edu; ravikumar.gupta@manipal.edu

R. K. Gupta

Department of Mechanical and Manufacturing Engineering, Manipal Institute of Technology Bengaluru, Manipal Academy of Higher Education, Manipal 576104, India

poses various challenges to the elderly and reduces their adaptation to ever changing environment [3, 4]. But the longer life can mean increasing opportunities, growth, joy, and vitality which can provide a chance to pursue long neglected interests and contribute to the overall development of society. Hence population ageing can be an opportunity to improve the products and services for aged people which can enable good health and better quality of life for their complete lifetime [5].

Younger users are functionally well defined and adapt to any products they use. When designing for the general population, designers they may not give a thought about how satisfactory the results of the design are when used by the elderly. Aged population are often sidelined and used only in the design of assistive and niche products like disability aids. So, most of the products used by common population do not explicitly consider the needs and desires of the elderly [6, 7].

Despite the consistent effort of researchers to provide comfort and independence for the elderly, their requirements are not completely understood and met. The requirements differ based on the type of product, but it is important to understand certain conditions of the elderly to establish better design goals. Hence there is a need for a generic product development method for designing products for elderly.

To contribute to this ongoing research, this paper reviews the works related to product design for the elderly and presents a Product-User-Interaction-Activity (PUIA) taxonomy based on product functions and features. The taxonomy usage is demonstrated by applying it to redesign of handwash dispenser for the elderly. PUIA taxonomy helps in establishing design goals and improvements required in the existing product based on the needs of elderly and can be applied to a product which is to be designed to for the elderly.

2 Review on Products Designed for Elderly and Taxonomies Used

Aging can cause elderly inconvenience in using everyday objects that are not specifically designed for them. This section will review some design projects that have contributed to the ongoing research and identify taxonomies used in the design process.

2.1 Products Used in Daily Activities

Lilja et al. demonstrated that elderly people's performance of some activities of daily living (ADL) like mobility, hobbies, shopping, and social contacts could be related to problems of support in the environment. In every activity, there were people who, wanted to perform some activities but were rated as not having the ability to do so,

needed more functional training of the products and services, or assistance [8]. With better products, elderly can carry out their daily activities more efficiently.

Studies conducted by Raviselvam et al. [9, 10] focused on using elderly as lead users in the design of everyday objects. The International Classification of Functioning, Disability and Health (ICF) codes were used to study body part functions. The elderly ignored some of the tasks due to design complexity of everyday objects. Based on the needs and suggestions shared by elderly participants, water bottle cap, soda can, mattress and sewing needle were redesigned and on an average, 89% of the general population participants preferred redesigned products over existing ones [9, 10].

Based on the ergonomic simulation of typical nail clipping postures, Wu et al. [4] redesigned nail clipper with a power grasp handle of knife angle 114 degree between the handle and normal line to cutter edge (to maintain neutral wrist angle), and a pedal plate (to reduce lumbar angle and ease the toenail clipping process). They stated that with age, hand pinch strength decreases, and finger and toenails become dry, hard, and thick making it difficult for elderly to clip their nails. Taxonomy developed includes nail clipping postures—two-point pinch, lateral pinch, and grasping hold; toenail clipping postures—leg crossed posture, sole supinated posture, and sole pronated posture. The new clipper was rated better in terms of comfort and satisfaction by elderly participants [4]. Neutral posture is important in product design for elderly.

Dekker et al. [11] explored the types and usage of supports by the Dutch elderly in toilet environment. A test frame consisted adjustable supports (vertical, front, and side supports) and a height-adjustable toilet bowl. Taxonomy developed for user tests includes type of support preferred while sitting down, standing up, and during the task, heights preferred to hold the support, and the way force is applied with each support. Vertical supports are preferred for sitting down and standing up, during toilet use side supports are also valued [11]. Providing supports lets the body muscles assist each other during movement, which can improve the elderly's task efficiency.

Demirbilek et al. [12] proposed Usability, Safety, Attractiveness Participatory (USAP) design model to capture the voice of the users and applied it for designing door handles for elderly. The USAP model categorizes relationship between elderly's requirements, design limitations, and technical requirements. User needs include: accidents related to doors, physical aspects, key and keyhole, other than key, opening door to a visitor, door operations—elbow operated levers if hands are full/dirty, foot operated door, and if no door situations [12]. Factors leading to accidents and injuries and alternate body part usage are interesting aspects to consider in the design.

Koppa et al. [13] demonstrated a set of refrigerator design guidelines for elderly women who live alone. Their study consisted of two parts: (1) a simulation to analyze postures during the refrigerator use with five types of pre-designed shelves (2) build-it-yourself session where the users arranged the interior configuration of the refrigerator according to their needs. Taxonomy developed includes comfort rating for each type of shelf, number of shelves used, preferred heights of shelf and container locations based on which, three design configurations for refrigerator interior were proposed. As the elderly participants preferred varying number of shelves, types,

and locations for items, flexibility of product usage must be an important design goal [13].

Guan [14] demonstrated leisure chair design recommendations for the elderly. Safety, comfortableness, adjustability, portability, appearance, and auxiliary function were identified as the product attention factors (product aspects, the user pays attention to during the activity) for leisure chair and mapped to the leisure activities. The disadvantages, material features, and types of existing leisure chairs used by the elderly were also listed. Based on this research and study, Guan recommended some design considerations [14].

2.2 Taxonomy for Elderly Product Design

The literature review provided a good insight into the design approaches followed by various researchers and designers. Due to content limitations, only few products were discussed which cover most of the important aspects of daily living—personal care, toilet environment, living space, kitchen environment, essential and leisure activities. Taxonomies like Activities of Daily Living (ADL), ICF codes, and taxonomies based on surveys and questionnaires have been used to guide the designers throughout the design process. ADL and ICF are widely used in the medical research as the terms rely solely on the user's performance and capacity. They help narrow down the activities performed by elderly and body functions related to the activity but do not relate the products with the user. Some products were designed based on surveys and questionnaire and relied on taxonomies that were specific to the product.

The previous sections provided a brief review of the products designed for elderly which included design approach followed, and taxonomy used. The next section demonstrates the newly developed taxonomy for elderly product design.

3 PUIA Taxonomy for Designing Products for Elderly

In design, taxonomy helps in understanding subject specific concepts and creates a vocabulary for the same. Vocabulary helps in organizing the components of concepts, making it easier to find or come back to them throughout the design process. Considering voice of the elderly, analyzing their current situation and environment related to the activity, and observing their interaction with the existing products are important for the design process. Due to the elderly's contrasting experiences and lifestyles, demographic, and cultural changes, they differ greatly from one another and do not have similar requirements and interests [15]. Hence, there is a need to develop a generic taxonomy to facilitate the research related to the product and elderly conditions.

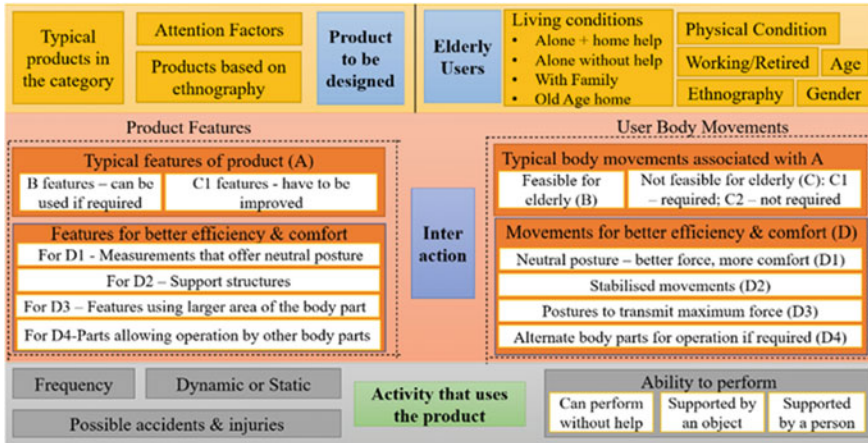


Fig. 1 Product—user—interaction—activity (PUIA) taxonomy

Based on the literature review, design considerations for the elderly are identified, and existing products are analyzed for the use of the elderly against application, ease of usability, fulfilment of functionality. PUIA (Product-User-Interaction-Activity) taxonomy is developed to guide designers in the product design process for elderly. PUIA taxonomy helps in considering special requirements of elderly, their living conditions, and relate factors associated with user body movements to product features. The PUIA taxonomy has four major categories as depicted in Fig. 1: Product to be designed, Elderly Users, Interaction, and Activity with their further classifications.

3.1 Product to Be Designed

Once the product which is to be designed (A) (see Fig. 1) is identified, designer must identify the typical products available in the market. In certain cases, products differ based on the ethnography. Ethnography is the study of people in their own environment based on their cultures, habits, differences, etc. Analysis of such products will help in the preparation of survey questionnaire and interviews and help in understanding user interaction with the product. Product attention factors are the aspects of product that the user pays attention to during activity. These factors can be used to measure the features of the product which need to be addressed from the end user’s point of view [14].

3.2 Elderly Users

Details of target users are crucial aspects of the design process. For the elderly users, details such as age, gender, physical condition are usually collected and analyzed. Apart from these, living conditions of elderly can reflect on their socio-cultural aspects, emotional wellbeing, special needs, and in some cases the extent of product requirement. Whether elderly users are working, non-working or retired can help designers understand their skillset and ability to perform the target activities. Ethnographic details of elderly users can help understand their ways of life and products they currently use.

3.3 Interaction

Product-user interaction is subdivided into product features and user body movements. The typical body movements associated with the product are to be identified and categorized as feasible for the elderly (B) and not feasible (C) as presented in middle panels of Fig. 1. The not feasible movement (C) are further divided into required (C1) for the new design and not required (C2). The corresponding product features associated with these body movements are categorized as B features and C1 features. Since, B features are associated with movements feasible for the elderly, they can be considered only if required. C1 features are associated with the not feasible but required movements, so these must be improved to provide better design solutions. Interaction category also houses a set of suggested body movements for better task efficiency and comfort (D), and the corresponding product features as depicted in middle panels of Fig. 1. Neutral postures (D1) during the product usage and task performance transmit better force, provide better surface contact and comfort to the elderly [4]. For D1, the corresponding product features include product dimensions which support the neutral posture of the body parts and joints involved. Stabilized body movements (D2) are bound to enhance user safety and improve task efficiency. Providing support structure whether as a part of the product or where the product is to be used or placed can be a way to achieve this. Not every product is designed to support postures that provide better grip and transmit maximum force from user (D3). For elderly, such postures must include a large area of the body part (for example, using the whole palm instead of a couple of fingers, both hands instead of one hand, etc.). Lastly, using alternate body parts (D4) are considered if required [12].

3.4 Activity that Uses the Product

Analyzing the activity is as important as analyzing target users and product. Frequency of the activity can provide information about product specific details

(e.g. a spoon is used daily, multiple times, irrespective of the user background) and user specific details (e.g. shopping—how many times a user does shopping, amount of items bought each time). If any activity is performed frequently, the problems associated with it must be minimal to avoid the adverse effects in the long run [16]. Nature of the activity—dynamic like walking, lifting or static like sitting, reading, watching or a combination of both [14], provides a good picture of the product-user interaction. Accidents and injuries related to the activity must be analyzed to establish design goals which reduce or eradicate their possibility. Since they do not happen frequently, we tend to neglect the effects. But for elderly users, even a single and small injury can cause great discomfort and can be fatal in the long run [12]. Target users’ ability to perform the activity helps identify their special needs.

3.5 Advantages of PUIA Taxonomy

Comparative study of PUIA taxonomy with ADL, ICF, and other design approaches used in designing products for the elderly is explained in Table 1. As shown in the table, ADL and ICF taxonomies are more relevant for medical professionals rather than the product designers. Most of the other taxonomies used by the designers are usually developed based on interviews and discussion with the elderly, and study about the product to be developed. In contrast to these taxonomies, PUIA taxonomy incorporates all the major aspects of the product design process for the elderly and is not product specific.

Table 1 Comparison of PUIA Taxonomy and other taxonomies/methods for elderly products

Taxonomy/Method	Features	Observations
ADL [3]	Activities performed in daily life	Only activities
ICF [9, 10]	Body functions, body structures, activities and participation, environmental factors, personal factors	Product is not considered, not very relevant to design field
Taxonomy from study/interview [4, 11, 13]	Depends on the product to be designed	Very product specific
PUIA taxonomy	Typical products, details of activity that uses the product, details of elderly users, their ability to perform the activity, design considerations based on body movements involved	Generic taxonomy for elderly users, body movements, elderly users, activities, and suggests design improvements

4 PUIA Taxonomy Applied to Redesign of Handwash Dispenser

A typical handwash dispenser is considered for elderly usage as shown in Fig. 2a. User presses top of the dispenser to pump out handwash liquid. When pressure is applied, air is pushed out of the tube of the dispenser bottle. The pressure difference creates a suction effect and draws the liquid soap back up the tube. This liquid is then released into the user’s hand. The PUIA taxonomy usage is demonstrated by applying it to the design of portable press down handwash dispenser for the elderly as shown in Fig. 3. The steps followed to redesign existing typical handwash dispenser as follows.

- i. Product category research as illustrated in the taxonomy.

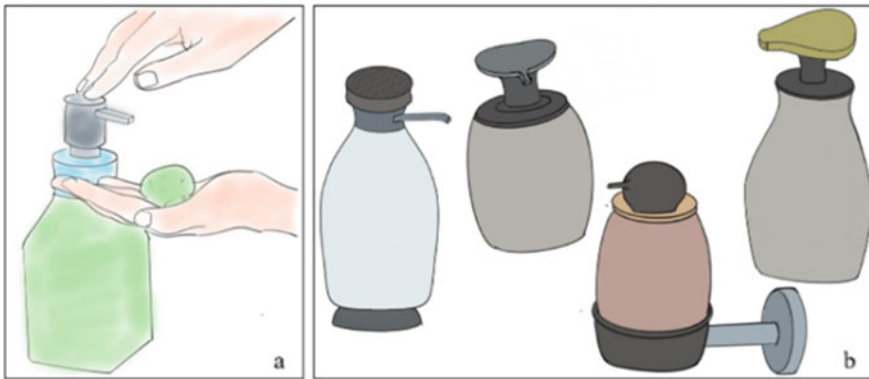


Fig. 2 a Typical handwash dispenser, b ideation sketches for new design

Press Down Handwash Dispenser	Attention Factors	Typical products in the category	Products based on ethnography (India)	Elderly Users-100	Living conditions	Physical Condition
	<ul style="list-style-type: none"> portability appearance easy operation stability easy refill 	<ul style="list-style-type: none"> wall mounted automatic press down dispensers 	<ul style="list-style-type: none"> Handwash liquid makers offer their own press down dispensers and refill packs. Press down dispensers that come with bathroom accessory set. 	Alone + home help - 20 With Family - 53	Alone without help - 25 Old age home - 2	<ul style="list-style-type: none"> 30 - normal 15 - walking aid 5 - wheelchair
				Gender	Working/Retired	Ethnography
				<ul style="list-style-type: none"> 70 - female 30 - male 	<ul style="list-style-type: none"> 20 - working 45 - retired 35 - modern family background 	<ul style="list-style-type: none"> 30 - traditional Rajasthani family 40 - semi traditional background 30 - modern family background

Product Features		User Body Movements		Activity that uses the product Washing the hands
Typical features of product (A)		Typical body movements associated with A		
B features - can be used if required Has to be refilled	C1 features - have to be improved Press down feature must be made easier as the elderly may not be able to transmit required force easily	I N T E R A C T I O N	Feasible for elderly (B) Movements associated with refilling the dispenser Not feasible for elderly (C) C1 - required - press down with fingers/palm C2 - not required - NA	Frequency Very frequent (4-8 times/ day) Dynamic or Static Both - Static body posture with hand movements
Features for better efficiency & comfort For D1 - Measurements that offer neutral posture - NA For D2 - Support structures <ul style="list-style-type: none"> Dispenser holder which is mounted on the wall Suction rubber attached at the bottom For D3 - Features using larger area of the body part Handle for power grasp and then press down instead of small surface for pressing down by the fingers For D4 - Parts allowing operation by other body parts Optional foot operated dispensing mechanism		Movements - better efficiency & comfort (D) Neutral posture - better force, more comfort (D1) - NA (press down feature does not disturb the neutral feature of the wrist joint) Stabilised movements (D2) - While pressing the dispenser, due to shaky hands of the elderly, the dispenser may topple and displace the palm suddenly which can cause an injury Postures to transmit maximum force (D3) - A power grasp posture of the palm instead of finger/palm press down Alternate body parts for operation if required (D4) - Foot		Possible accidents & injuries <ul style="list-style-type: none"> dispenser may topple and displace the palm suddenly Leaking of handwash liquid which makes the surface slippery Ability to perform <ul style="list-style-type: none"> Can perform without help of other person Object support- walking stick

Fig. 3 PUIA taxonomy applied to redesign of handwash dispenser

- ii. Analysis of the details of elderly users (described based on assumptions).
- iii. The interaction category presents the problems associated with press down action of the typical handwash dispensers available in the Indian market which offer a very small surface area for pressing. Since elderly lack the required strength for the movement, product features are suggested to improve efficiency of the activity.
- iv. Activity presents frequency of washing hands, its nature, and accidents and injuries associated with it. Users' ability to perform the activity is assumed in the taxonomy.
- v. Based on the taxonomy, some design concepts are sketched as shown in Fig. 2b.

The PUIA taxonomy can assist in the product design process by providing insights on the problems of elderly which need to be addressed and the corresponding product features to solve these problems. This is a general taxonomy which can be applied to any product used in the activities of daily living of the elderly. The newly developed product features must be designed such that the body movements of the elderly happen efficiently and smoothly. For this, more comprehensive design guidelines based on all the body movements and actions which happen while carrying out daily activities must be developed. Hence there is a need for a more detailed design taxonomy to closely link the needs of elderly users and their physical conditions to the product features, applications, and functionalities.

5 Conclusion

Ageing is a very complex phenomenon. The plight of ageing is just one side of the coin. By implementation of adequate strategies and development products and services that promote user safety, wellbeing, and social inclusion, the elderly can spend their extra years of life in vigor and comfort. This not only benefits the elderly individual but also helps in the healthy development of the society. With more and more product design projects being implemented for the elderly, there is a need for a good design taxonomy to guide the designers. After reviewing certain products designed for the elderly, this paper presented a generic product design taxonomy, the **Product-User-Interaction-Activity (PUIA)** taxonomy. The taxonomy usage was demonstrated by applying it to the case of redesign of handwash dispenser. Future work includes development of a more meticulous design taxonomy comprising of product design recommendations for all the body movements associated with the activities of daily living of the elderly, and design of products for the elderly based on the newly developed taxonomy.

References

1. WHO Homepage. <https://www.who.int/ageing/decade-of-healthy-ageing>. Last accessed 2020/10/28
2. WHO Homepage. <https://www.who.int/news-room/fact-sheets/detail/ageing-and-health>. Last accessed 2020/10/28
3. Laukkanen P, Era P, Heikkinen RL, Suutama T, Kauppinen M, Heikkinen E (1994) Factors related to carrying out everyday activities among elderly people aged 80. *Aging Clin Exp Res* 6(6):433–443
4. Wu HC, Chiu MC, Hou CH (2015) Nail clipper ergonomic evaluation and redesign for the elderly. *Int J Ind Ergon* 45:64–70
5. WHO Homepage. <https://www.who.int/westernpacific/news/feature-stories/detail/addressing-the-needs-of-ageing-populations>. Last accessed 2020/10/28
6. Hannukainen P, Hölttä-Otto K (2006) Identifying customer needs: disabled persons as lead users. In: International design engineering technical conferences and computers and information in engineering conference, pp 243–251. ASME, Philadelphia
7. Demirkan H, Olguntürk N (2014) A priority-based ‘design for all’ approach to guide home designers for independent living. *Archit Sci Rev* 57(2):90–104
8. Lilja M, Borell L (1997) Elderly people’s daily activities and need for mobility support. *Scand J Caring Sci* 11(2):73–80
9. Raviselvam S, Wood KL, Hölttä-Otto K, Tam V, Nagarajan K (2016) A lead user approach to universal design—involving older adults in the design process. *Stud Health Technol Inform* 229:131–140
10. Raviselvam S, Noonan M, Hölttä-Otto K (2014) Using elderly as lead users for universal engineering design. In: Universal design, pp 366–375
11. Dekker D, Buzink SN, Molenbroek JF, de Bruin R (2007) Hand supports to assist toilet use among the elderly. *Appl Ergon* 38(1):109–118
12. Demirbilek O, Demirkan H (2004) Universal product design involving elderly users: a participatory design model. *Appl Ergon* 35(4):361–370
13. Koppa RJ, Jurmain MM, Congleton JJ (1989) An ergonomics approach to refrigerator design for the elderly person. *Appl Ergon* 20(2):123–130
14. Guan S (2011) Study on the leisure chair design of elderly people. *Adv Mater Res* 215:131–135
15. Pericu S (2017) Designing for an ageing society: products and services. *Des J* 20(sup1):S2178–S2189
16. de Wit M, Demirbilek O (2003) Shopping and the elderly: a universal design case study. In: 2nd inclusive design conference, pp 25–28. UNSWorks, Sydney

A GWO Tuned Probabilistic Roadmap Approach for Coarse Mapping of Humanoid Robot in Inclined Terrain



Abhishek Kumar Kashyap, D. R. K. Parhi, Saroj Kumar, and Anish Pandey

Abstract Navigation for a humanoid robot in inclined terrain is a challenging activity in robotics. The goal of current research is to explore possible paths and optimize the footstep and identify routes that are optimum in reference to path length covered by the robot. A hybrid approach of Probabilistic Roadmap (PRM) and Grey wolf optimization (GWO) is proposed for humanoid NAO in terrain with an inclined plane and static obstacles. The sensory data such as obstacle distance in the right direction (RD), left direction (LD), and front direction (FD) are fed to the PRM approach, which provides stable walking for a humanoid robot with an interim driving angle (IDA). For optimum navigation and footstep adjustment for the inclined plane, the GWO approach is utilized. The proposed hybrid approach offers optimal driving angles (ODA) to navigate an inclined plane and guarantees the shortest distance. Simulation in flat terrain using the proposed approach and standalone approaches has been performed in a 3D simulator. The obtained convergence curve, travel distance, and time spent show that the NAO meets the objective in all situations, but that GWO tuned PRM approach is preferable to this objective. Further, the proposed approach has been analyzed in inclined terrain. Based on these results, the designed approach guarantees robustness and effectiveness.

Keywords Inclined terrain · Humanoid robot · Obstacle avoidance · WEBOT · Optimal driving angle

1 Introduction

Automation has become a significantly rising concept in the past several decades, influencing nearly every area of life. Thus, the robots that are autonomous and are

A. K. Kashyap (✉) · D. R. K. Parhi · S. Kumar
Mechanical Engineering Department, National Institute of Technology, Rourkela, Odisha 769008, India

A. Pandey
School of Mechanical Engineering, Kalinga Institute of Industrial Technology, Bhubaneswar, Odisha 751024, India

© The Author(s), under exclusive license to Springer Nature Singapore Pte Ltd. 2022
B. B. V. L. Deepak et al. (eds.), *Applications of Computational Methods in Manufacturing and Product Design*, Lecture Notes in Mechanical Engineering,
https://doi.org/10.1007/978-981-19-0296-3_11

111

needed in many areas have become more and more necessary. The planning of motions for an individual humanoid robot is one of the essential tasks for smart control. It includes designing an impact-free route for a humanoid robot as it travels from the initial location to the final position in an obscure environment. Along with the robotic field, their application touches the field of bioinformatics, medicine, and virtual reality. A humanoid robot is preferred over other robots, as it is more efficient in performing tasks that a human perform. Several kinds of research are being carried out on stabilization and coarse mapping in various terrains. A few of them are discussed here.

Robot guidance is a trendsetting concern, and several types of research on various types of robots on complicated terrains have been conducted [1–7]. The presence of multiple degrees of freedom finds it challenging to regulate. The dynamics [8] of humanoid robots is essential to describe to understand the behavior of their body. Their complex structure can be simplified using 3D linear inverted pendulum model (LIPM) [9]. Enhanced variants of the reference design focused on LIPM has been recorded using the Zero Moment Point (ZMP) Condition in the modeling phase [10]. Zhu et al. [11] have suggested the concept of using the ZMP parameter to produce a LIPM method that is relatively robust. In the single support phase (SSP), they see it obey first-order functions through the heel to the toe. In [12], a cuckoo search technique is used to calculate the optimum route planning for a moving robot in an uncertain area or a partly defined, multiple static barriers. Authors in [13] are being approached for mobile robots to enhance self-position by passive visual landmarks. It allows the usage of relatively cheap hardware elements such as cameras, sensors, etc. to locate and make image processing easier by preventing complete amplification and geometric image adjustment. An enhanced Distance-Bug method consisting of the deliberate layer and the responsive layer in two layers is suggested at [14]. An optimum action horizon accompanies the recommended solution of an updated visibility diagram for trajectory tracking in an area rich in obstacles [15]. Multiple robot management in a single terrain is a challenging activity and involves implementing the regulation to resolve contradictory situations. The hybrid controller application consisting of a dynamic window approach and teaching–learning-based optimization approach has been implemented by Kashyap et al. [16].

Various strategies direct the humanoid robot to the goal defined. However, in working with robots, imbalance may arise while dealing with several obstacles and inclined surfaces in obscure terrains. The independent approach is capable of overcoming the problem but at the cost of high computational complexity. PRM approach has been used to provide a stabilized walking and interim driving angle to guide the robot toward the goal. When obstacles and inclined planes come in the path of navigation, footstep adjustment is essential for navigation on inclined planed. It is performed by using the GWO approach, which provides the final driving angle. The proposed approach shows superiority while comparing with GWO and PRM approach for navigation in flat terrain. This is further applied to inclined terrain to confirm its robustness. This hybridization is intended to avoid local mini-mapping and to result in reduced computation complexity.

The research is presented as follows. Section 2 explains the mentioned optimization methods. The hybridization of the proposed approach for robot control is presented in Sect. 3. Section 4 describes the outcomes of the simulation in flat and inclined planed. Finally, Sect. 5 deals with the conclusion and future evaluation.

2 Architecture of Optimization Approaches

Probabilistic Roadmap (PRM) and Grey wolf Optimization (GWO) approach has been preferred as the optimization methodology in this study. The GWO solution is centered naturally and can overcome global minimum criteria while overcoming barriers, and the PRM approach is intended to ensure an optimum path during navigation.

2.1 Probabilistic Roadmap Approach

Lydia E et al. [17] suggested the PRM approach is part of the techniques for sampling at the beginning of the 1990s. It depicts the correlation of the trajectory diagram in the configuration region, the collision identification of the sampling targets, and checks if neighboring sample targets can be appended.

PRM is classified primarily into two phases. A large number of robot configurations are sampled at random during the offline learning stage, and each and every node searches for neighboring nodes and connects for a road map. In the online query level, an online mapping mechanism is utilized to check for a feasible option from the road map as per the initial point, the goal point, and road map data. The following are two levels.

2.1.1 Offline Learning Stage

The central feature of the PRM method is the offline learning process, which is the procedure of creating a route network, thus deciding if the method is primarily employed in static conditions or if the variability of environmental variance is low. A projection of the undirected route network $U_r = (A_l, N)$, where A_l is an arbitrary locus of nodes, N is the number of nodes between all feasible two positions. The following are the steps for the design concept:

- (a) Start with selecting the arbitrary locus of nodes A_l number of nodes between all feasible two positions N
- (b) Select an arbitrary taken free arrangement (r)
- (c) Assign A_l^r as the set of members adjacent of r selected from A_l and using the local route scheduler

- (d) Attach the (r, r') limit of the feasible route to the set and delete the collision route.
- (e) The length of the alternate point is somewhat on a specific scale. The rule to pick the alternate points is described as:

$$A_l^r = \{r \in A_l | D(r, r') \leq d_{\max}\} \quad (1)$$

- (f) The distance function D is selected as:

$$D(r, r') = \max_{x \in robot} \|x(r') - x(r)\| \quad (2)$$

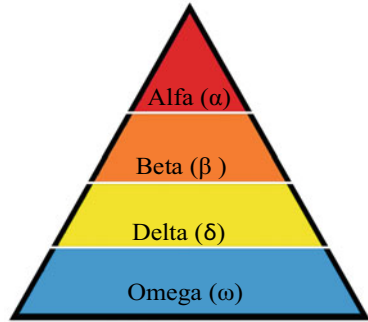
2.1.2 Online Query Stage

The unguided route network $U_r = (A_l, N)$ has been developed during the offline learning process. In the investigation process, as per the start location r^s and the goal location, r^g the acceptable route is chosen. The particular mechanism is used to link r^s and r^g nodes with two items r_1, r_2 individually in a network route map and to locate the route connecting r_1 and r_2 in an unguided network map to attach the original and destination locations to a global route. A smooth approach can be utilized to determine the best route once the global route has been acquired.

2.2 Grey Wolf Optimization Approach

Mirjalili et al. [18] have presented the Grey Wolf Optimization (GWO) approach, which is a population dependent evolutionary approach that imitates grey wolve's management mechanism and their hunting framework. Grey wolves choose community living. Each community has an average of 5–12 wolves. A Grey wolf holds the hierarchical structure of a community by splitting the effort between them. The alpha, α , is among the most significant wolves in the tribe. They are the leader of the group. They may be either male or female. The decision to chase, exercise time, rest, and so on is their duty. The members of the pack must determine the decisions and accept the alpha by keeping their tails down. The alpha wolf is known as the superior wolf in the group, and the group mates must obey all his/her commands. The next type of wolf is the beta β ; this allows the wolf α to sustain the whole group. The betas are secondary wolves that support the alpha make decisions. Whenever the alpha seat is vacant, the leading wolf of beta is assumed to be the alpha. The beta enhances the alpha orders all over the group and brings alpha guidance. Another class of grey wolves within the group is called the delta δ wolf. They operate quite continuously as security officers on the region's borders, and these wolves migrate

Fig. 1 Hierarchy of grey wolf



to the borders of the territory. They guard the group, help alpha and beta in hunting and feeding the group and take care of sick, tired, and injured wolves in the group. The last category is the omega ω . They are new-born wolves who watch the alpha α , beta β , and delta δ wolf and acquire their ability. The hierarchy of the grey wolf is described in Fig. 1.

2.2.1 Hunting Architecture of Grey Wolves

The grey wolves always follow the group for hunting and communicate via howling jointly to follow the leaders’ instructions in the pack. There is a single hulling tone for every pack. This behavior is utilized to transfer information about the prey’s position. When a grey wolf pack recognizes such a style, the beta and Alpha wolves instantly chase to locate the hurling point. The following are comprised of the mathematical formula encircling activities:

$$\vec{S} = \left| \vec{Q} * \vec{X}_a(t) - \vec{X}(t) \right| \tag{3}$$

$$\vec{X}(t + 1) = \vec{X}_a(t) - \vec{P} * \vec{S} \tag{4}$$

X_a is the target vector, and X shows the vector of location for a grey wolf, and P and Q are the coefficient vector of present iteration t . The following calculations are given for vectors P and Q :

$$\left. \begin{aligned} P &= 2 * \vec{p} * \vec{r} - \vec{p} \\ Q &= 2.r \end{aligned} \right\} \tag{5}$$

where elements in an iteration p are reduced linearly from 2 to 0 and r are random vectors in $[0, 1]$. Generally, the hunting is directed by the alpha. Beta and delta could sometimes be involved in hunting. It is believed that the alpha-, beta-, and delta have stronger information about the possible position of prey in the statistical

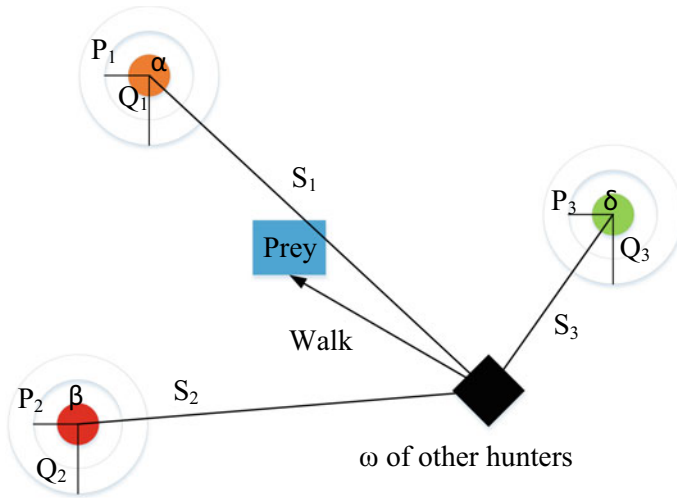


Fig. 2 Hunting process of grey wolf by encircling prey

model of hunting activity of grey wolves. The first three optimal approaches have been preserved, and the remaining entity must upgrade its locations to the top search agents' locations, as described in the following equations are demonstrated in Fig. 3.

$$\vec{S}_\alpha = \left| \vec{Q}_1 * \vec{X}_\alpha - \vec{X} \right| \tag{6}$$

$$\vec{S}_\beta = \left| \vec{Q}_2 * \vec{X}_\beta - \vec{X} \right| \tag{7}$$

$$\vec{S}_\delta = \left| \vec{Q}_3 * \vec{X}_\delta - \vec{X} \right| \tag{8}$$

Proceed toward prey (Fig. 2)

$$X_1 = X_\alpha - P_1 * S_\alpha \tag{9}$$

$$X_2 = X_\beta - P_2 * S_\beta \tag{10}$$

$$X_3 = X_\delta - P_3 * S_\delta \tag{11}$$

$$\vec{X}(t+1) = \frac{X_1 + X_2 + X_3}{3} \tag{12}$$

The flowchart explaining the GWO approach in the coarse mapping of the humanoid robot is explained in Fig. 3.

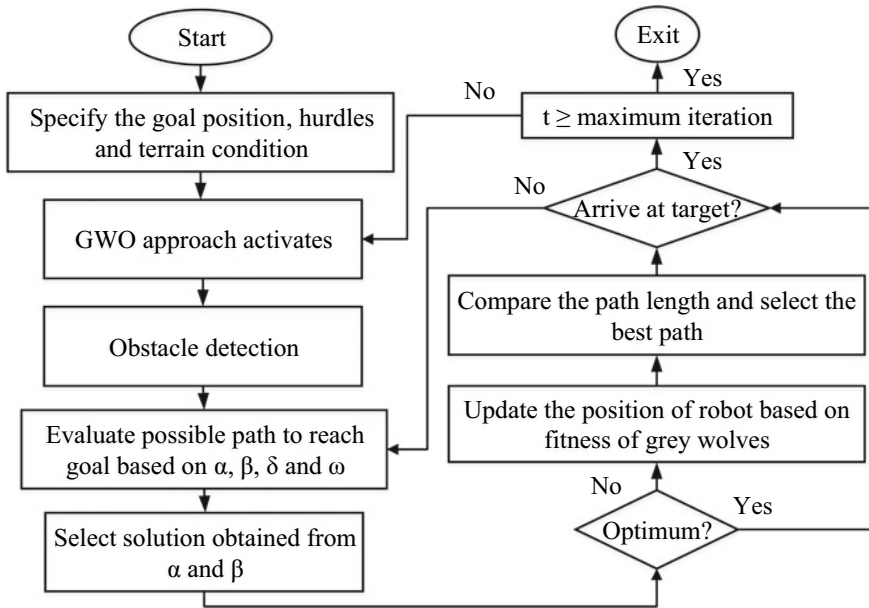


Fig. 3 Flowchart of GWO approach for coarse planning of humanoid robot

3 Enhancement of PRM Algorithm Using GWO Approach

The hybridization of a classical approach and population-based approach is carried out to remove the constraint of the single technique. The hybridizing process is shown in Fig. 4. This could solve both global and local concerns and lead the robot through the appropriate driving angle to the target while avoiding obstacles. PRM and GWO approach is involved in obtaining the solution. Details from sensors (a range of barriers from all directions), providing stable travel on an even and inclined surface, are fed to the PRM approach that provides an interim driving angle. In order

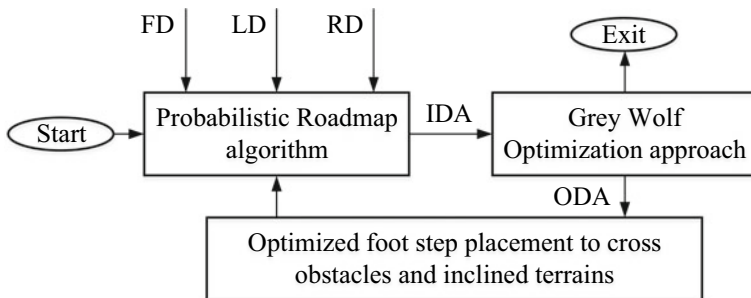


Fig. 4 Mechanism of tuning of PRM model by GWO approach

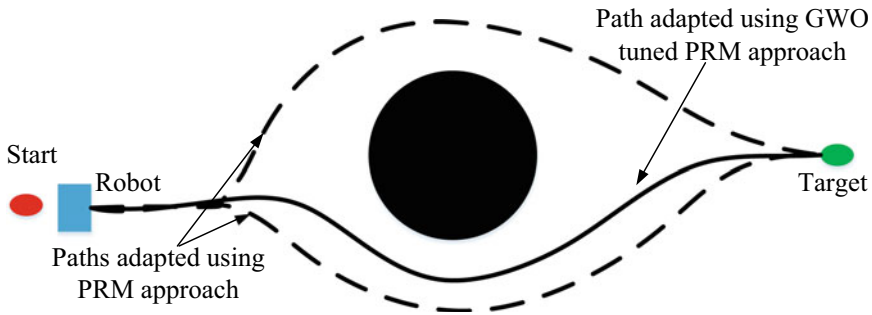


Fig. 5 Selection mechanism of optimum path using GWO tuned PRM approach

to ensure the optimal angle for driving and maximum stability while facing obstacles and inclined planes, footstep adjustment is essential. In order to get this, the interim driving angle is fed to GWO, which provides an optimum driving angle.

It adjusts the placement of the foot. If it is optimum and the robot reaches the target, the operation exit. Otherwise that angle is again supplied to PRM, and the cycle repeats until the termination criteria are obtained. This hybridization will enable the robot to approach and take turns closer to the obstacle. The systems comprise of a balanced walking across the even and inclined surface and an ideal driving angle for avoiding obstacles. The selection of optimum path using the GWO tuned PRM approach is explained in Fig. 5. The start, target, and obstacle positions are provided. The path designed using the PRM approach from both sides is designed. The tuning process provides an adjustment of footsteps using the GWO approach, which guides the robot closest to the obstacle and takes an optimum driving angle to reach the target. It decreases the path length, time spent, and subsequently computational complexity.

4 Implementation of GWO Tuned PRM Approach and Result in Navigation on Even and Inclined Terrain

A GWO methodology has been employed to tune the PRM model. Its installation in the humanoid navigation has been conducted in this segment on even and inclined terrain. The result is achieved and compared. In contrast with individual methods.

4.1 Coarse Mapping of Humanoid NAO in Even and Inclined Terrain Using GWO Tuned PRM, GWO, and PRM Approaches

The simulation has been performed in even terrain using GWO, PRM, and GWO tuned PRM approach. A 3D simulator, WEBOT, has been preferred. It replicated the joint motions and sensors reading of real NAO. It provides the navigational data, i.e., travel length and time spent directly from the interface. Figure 6 shows the snapshot of the result obtained by implementing the proposed and individual approach in a humanoid robot. The result shows that the robot crosses obstacles and successfully achieved the target.

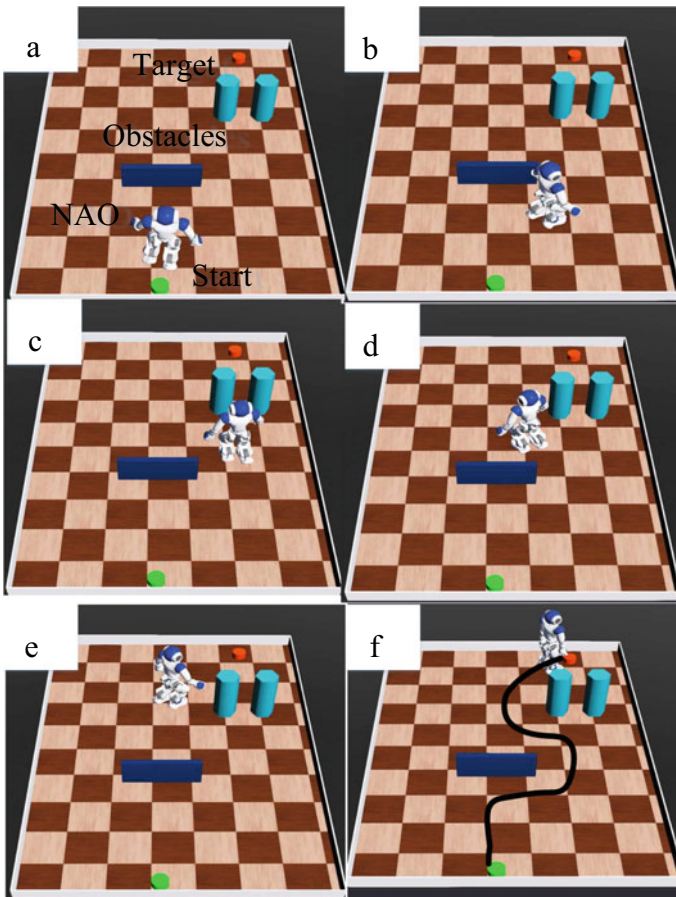


Fig. 6 Implementation of proposed methodology in even terrain

The data has been recorded from the WEBOT simulator, as discussed above, for GWO tuned PRM approach. The same has been done for GWO and PRM approaches. The deviation of path length and time spent has been recorded in contrast to the result obtained by implementing the proposed approach and displayed in Tables 1 and 2. It has been obtained that the deviation of around 17.2 and 19.59% has been obtained for the PRM approach for travel length and time spent, respectively. And for the

Table 1 Deviation of travel length (cm) for PRM and GWO approach against GWO tuned PRM approach for even terrain

S. No.	GWO tuned PRM	PRM	GWO	Deviation w.r.t GWO tuned PRM (%)	
				PRM	GWO
1	213.6	247.6	223.2	15.92	4.49
2	216.5	260.7	226.1	20.42	4.43
3	212.3	246.3	231.4	16.02	9
4	214.2	248.2	223.8	15.87	4.48
5	224.5	258.5	234.1	15.14	4.28
6	222.9	265.9	235.3	19.29	5.56
7	221.7	255.7	231.3	15.34	4.33
8	226.1	267.1	235.7	18.13	4.25
9	224.2	268.7	244.1	19.85	8.88
10	213.1	247.1	236.3	15.95	10.89
Avg	218.91	256.58	232.13	17.2	6.06

Table 2 Deviation of time spent (s) for PRM and GWO approach against GWO tuned PRM approach for even terrain

S. No.	GWO tuned PRM	PRM	GWO	Deviation w.r.t GWO tuned PRM (%)	
				PRM	GWO
1	56.33	68.81	61.7	22.16	9.53
2	54.18	66.66	58.54	23.03	8.05
3	61.33	71.35	66.7	16.34	8.76
4	61.09	73.57	65.46	20.43	7.15
5	58.37	69.47	63.74	19.02	9.2
6	55.98	68.46	61.35	22.29	9.59
7	62.87	71.45	69.24	13.65	10.13
8	59.59	72.07	64.96	20.94	9.01
9	61.09	74.67	66.46	22.23	8.79
10	58.19	67.34	62.17	15.72	6.84
Avg	58.91	70.39	64.04	19.59	8.71

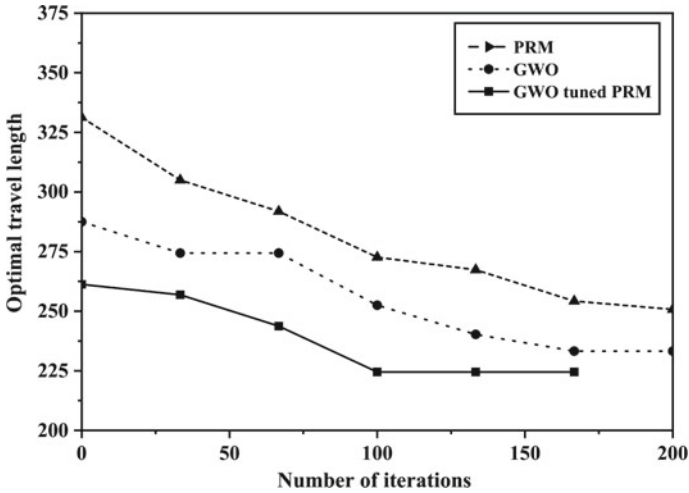


Fig. 7 Relation between deviation curve of GWO, PRM, and GWO tuned PRM approach based on optimal travel length

GWO approach, deviation of 6.06% and 8.71% has been obtained for travel length and time spent, respectively. The convergence curve showing the relation between all three approaches has been obtained and displayed in Fig. 7. The result shown in tabular form and convergence curve shows that the robot reaches the target with minimum path length and lesser iterations using the proposed approach. It is better than both the PRM and GWO approach. But the GWO approach shows a comparable result. Therefore, both approaches have been compared in inclined terrain to check the effectiveness of the approach.

The terrain has been designed having a start, goal point and inclined with 5 degree angle, as shown in Fig. 8. The robot is trained with both approaches and guided toward the target. In many iterations, the robot fall using the implementation of the GWO approach. But in all cases, the robot reaches the target using GWO tuned PRM approach. The data has been collected and compared with each other, as shown in Table 3. The average deviation of 8.68% and 20.87% has been recorded, which shows the superiority of the proposed approach.

5 Conclusion and Future Work

The route designing of humanoid robots has recently been transformed into an essential part of research in the implementation of autonomous surveys. The analysis of humanoid robots in an even and inclined environment with some static barriers has been performed during this study. The developed GWO tune PRM approach is organized by using the PRM model tuned by GWO. The coarse mapping method

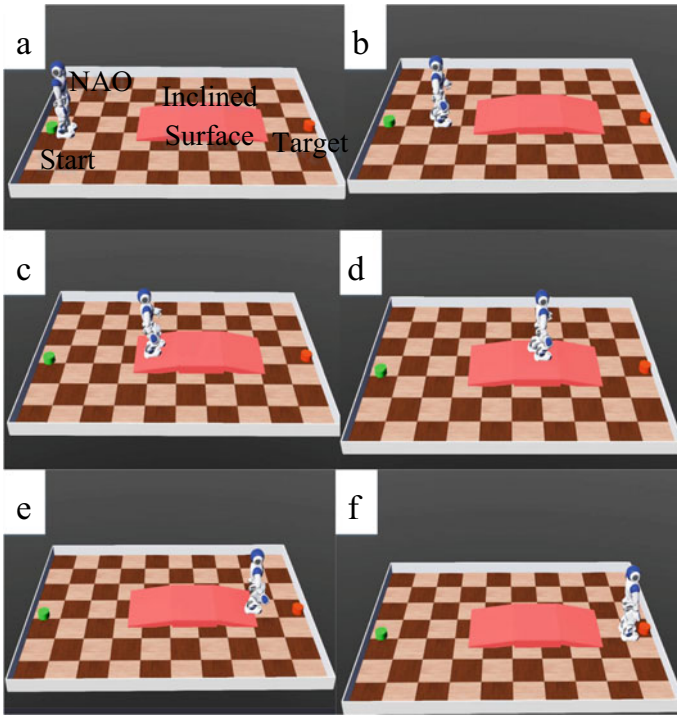


Fig. 8 Implementation of GWO tuned PRM approach in inclined terrain

Table 3 Comparison of travel length (cm) and time spent (s) using GWO tuned PRM and GWO approach for inclined terrain

S. No.	GWO tuned PRM		GWO		Improvement (%)	
	Travel length	Travel time	Travel length	Travel time	Travel length	Travel time
1	293.9	99.25	320.4	121.04	9.02	21.95
2	296.8	100.81	323.2	121.95	8.89	20.97
3	292.6	98.76	318.7	120.41	8.92	21.92
4	294.5	99.91	319.3	120.84	8.42	20.95
5	304.8	108.2	332.6	130.11	9.12	20.25
6	303.2	107.52	330.7	128.84	9.07	19.83
7	302	104.29	326.6	126.04	8.15	20.86
8	306.4	110.18	331	132.33	8.03	20.1
9	304.5	107.98	327.7	129.76	7.62	20.17
10	293.4	99.01	321.2	120.49	9.48	21.69
Avg	299.21	103.6	325.14	125.19	8.68	20.87

using a hybrid technique and individual approach has been performed under simulated conditions for even and inclined terrain. Initially, it PRM approach provides an interim driving angle that starts the navigation toward the target. Further, the foot-step adjustment is made by the GWO approach, which provides an optimum driving angle. It has been implemented on humanoid NAO for navigation in even terrain and compared against the individual approaches.

The deviation and convergence curve shows the effectiveness of the proposed approach is high. It is again compared with the GWO approach in inclined terrain as it shows the comparable result in even terrain. It shows that the developed approach is both efficient and provides maximum stability. Therefore, it could be utilized to guide humanoid robots in difficult terrain as a robust strategy. The path representing multiple humanoid robots in a single domain can be explored in the future, and other approaches can be used to hybridize with the developed controller.

References

1. Pandey KK, A Pandey, Chhotray A, Parhi DR (2016) Navigation of mobile robot using type-2 FLC. In: Lobiyal DK, Mohapatra DP, Nagar A, Sahoo MN (eds) Lecture notes in electrical engineering, vol 396. Springer India, pp 137–145
2. Pandey A, Kashyap AK, Parhi DR, Patle BK (2019) Autonomous mobile robot navigation between static and dynamic obstacles using multiple ANFIS architecture. *World J Eng* 16(2):275–286
3. Kashyap AK, Pandey A (2018) Different nature-inspired techniques applied for motion planning of wheeled robot: a critical review. *Int J Adv Robot Autom* 3(2):1–10
4. Kashyap AK, Pirewa Lagaza K, Pandey A (2018) Dynamic path planning for autonomous mobile robot using minimum fuzzy rule based controller with avoidance of moving obstacles. In: 2018 International conference on recent innovations in electrical, electronics & communication engineering (ICRIECEE). IEEE, pp 3330–3335
5. Kashyap AK, Pandey A (2020) Optimized path planning for three-wheeled autonomous robot using teaching–learning-based optimization technique. In: *Advances in materials and manufacturing engineering*, 49–57
6. Lagaza KP, Kashyap AK, Pandey A (2020) Spider monkey optimization algorithm based collision-free navigation and path optimization for a mobile robot in the static environment. In: *Advances in mechanical engineering*, pp 1459–1473
7. Kumar PB, Muni MK, Parhi DR (2020) Navigational analysis of multiple humanoids using a hybrid regression-fuzzy logic control approach in complex terrains. *Appl Soft Comput* Published online, 106088
8. Kashyap AK, Parhi DR, Kumar S (2020) Dynamic stabilization of NAO humanoid robot based on whole-body control with simulated annealing. *Int J Human Robot* 17(03):2050014
9. Kashyap AK, Pandey A, Chhotray A, Parhi DR. Controlled gait planning of humanoid robot NAO based on 3D-LIPM model. *SSRN Electron J*
10. Kajita S, Kanehiro F, Kaneko K et al (2003) Biped walking pattern generation by using preview control of zero-moment point. In: 2003 IEEE International Conference on Robotics and Automation (Cat. No. 03CH37422), vol 2. IEEE, pp 1620–1626
11. Zhu C, Tomizawa Y, Luo X, Kawamura A () Biped walking with variable ZMP, frictional constraint, and inverted pendulum model. In: *Proceedings—2004 IEEE International Conference on Robotics and Biomimetics. IEEE ROBIO*
12. Mohanty PK, Parhi DR (2016) Optimal path planning for a mobile robot using cuckoo search algorithm. *J Exp Theor Artif Intell* 28(1–2):35–52

13. Rostkowska M, Skrzypczyński P (2015) Improving self-localization efficiency in a small mobile robot by using a hybrid field of view vision system. *J Autom Mob Robot Intell Syst*
14. Zhu Y, Zhang T, Song J, Li X (2012) A new hybrid navigation algorithm for mobile robots in environments with incomplete knowledge. *Knowl Based Syst*
15. Kim SH, Bhattacharya R (2007) Multi-layer approach for motion planning in obstacle rich environments. In: *Collection of technical papers—AIAA Guidance, Navigation, and control conference*
16. Kashyap AK, Parhi DR, Muni MK, Pandey KK (2020) A hybrid technique for path planning of humanoid robot NAO in static and dynamic terrains. *Appl Soft Comput* 96:106581
17. Kavragi LE, Švestka P, Latombe JC, Overmars MH (1996) Probabilistic roadmaps for path planning in high-dimensional configuration spaces. *IEEE Trans Robot Autom* 12(4):566–580
18. Mirjalili S, Saremi S, Mirjalili SM, Coelho LDS (2016) Multi-objective grey wolf optimizer: A novel algorithm for multi-criterion optimization. *Expert Syst Appl* 47:106–119

Path Optimization and Control of Mobile Robot Using Modified Cuckoo Search Algorithm



Saroj Kumar, D. R. K. Parhi, Abhishek K. Kashyap, and Vikas

Abstract Cuckoo search (CS) algorithm is a nature-inspired metaheuristic optimization algorithm. This algorithm is rooted on the brood parasitism of cuckoo bird. The modified algorithm is applied on path optimization of mobile robot in unknown space. The optimization algorithm is getting the primary inputs from the sensors of mobile robot. The inputs are obstacles distance and heading angle. For authentication of proposed algorithm, simulation in V-rep software and real-time experiment through Khepera-III robot is performed. The results acquired by the simulation and experiments are equated with each other and observed a good promise between both the results as the difference in results is less than 5%.

Keywords Optimization · V-rep · Mobile robot · Navigation

1 Introduction

Nowadays, mobile robotics is becoming an emerging trend in the field of artificial intelligence due to the efficiency of mobile robot to do the cultured responsibilities such as human's responsibilities. Actually, the mobile robot is programmable controlled device and having the efficiency to perform the single as well as multitask during navigation. For smooth navigation, it is required to move in an optimized path and avoid the obstacles in unknown environment. Many researchers have been worked on optimized path and obstacle avoidance strategy, but still, it is required to improvise. Namely, Mohanty and Parhi [1] have proposed a cuckoo search (CS) algorithm for path planning of mobile robot. MATLAB software platform has been used for the simulation purpose. Joshi et al. [2] have proposed a detailed review on cuckoo search algorithm. Mareli and Twala [3] have proposed an optimization approach of many engineering problems using cuckoo search algorithm. Many other techniques are also available which has focused on navigation of mobile robot such as Pandey et al. [4] have proposed an ANFIS controller for navigation of mobile

S. Kumar (✉) · D. R. K. Parhi · A. K. Kashyap · Vikas
Robotics Laboratory, Department of Mechanical Engineering, National Institute of Technology,
Rourkela, Odisha 769008, India

© The Author(s), under exclusive license to Springer Nature Singapore Pte Ltd. 2022
B. B. V. L. Deepak et al. (eds.), *Applications of Computational Methods in Manufacturing and Product Design*, Lecture Notes in Mechanical Engineering,
https://doi.org/10.1007/978-981-19-0296-3_12

125

robot. Rawat et al. [5] have proposed a Mamdani fuzzy logic technique for path planning of mobile robot. Simulation and experimental results are compared for authentication purpose. Muni et al. [6] have proposed rule-based technique for path planning of humanoids in unknown environment. Pandey and Parhi [7] have proposed behavioral-based neural network for path planning of mobile robot. Salgotra et al. [8] have proposed an improved cuckoo search algorithm for the optimization of many engineering mathematical functions. Patle et al. [9] have proposed a path planning of mobile robot using firefly algorithm in uncertain environment. Kumar et al. [10] have proposed a hybrid controller of regression analysis and ant colony optimization for path planning of multiple robots in unknown environment. Yang and Deb have proposed cuckoo search algorithm. Raynoldes et al. proposed Levy flight scheme for cuckoo search algorithm. Kumar et al. [13–15] have proposed different artificial techniques for control of mobile robot in unknown terrains.

2 Overview of Modified CS Algorithm

Yang and Deb [11] have developed the cuckoo search algorithm in 2009. This algorithm is widely used as an optimization algorithm for many purposes such as robotic path planning, mathematical function optimization, and engineering problem optimization. Cuckoo search algorithm is based on the parasitic egg laying behavior of cuckoo bird. Generally, cuckoo bird lays their eggs in host bird nest to hatch the egg. If the host bird found the eggs are not their own, then either kicked out the eggs from nest or destroys the nest and starts a new brood elsewhere (Fig. 1).

To increase the productivity of cuckoos, many species of cuckoo bird lays their eggs according to the eggs of host bird eggs. They can change either their color or pattern for laying the eggs in host nest with some idealized assumptions [12]:

1. Nest host chosen randomly and cuckoo bird lays one egg at a time.
2. The quality eggs with best nest will be carried forward to the next generation.
3. Number of host nest is fixed, and probability to find the cuckoo's egg by the host bird is $P_a^e [0, 1]$.

With this case, the third assumption may be minimized by the rounding off the approximate values such as P_a . It can be observed that laying of each cuckoo egg is

Fig. 1 Nest with cuckoo egg



a solution. The egg, which have more fitness value that egg survives, and other are destroyed, so each survived egg is solution for an optimization problem. The Levy flight distribution is a type of arbitrary walk in terms of path length according to heavy probability distribution. The Levy flight follows a law of power for calculation of step length (Y) that can be mathematically described as;

$$Z = Y^{-\psi} \quad (1)$$

where 'Z' is the Levy function and ' ψ ' is the variable which ranges in $1 < \psi < 3$. For $\psi \geq 3$, the search path corresponds to a Brownian motion, and $\psi < 1$ behaves as non-normalized distribution.

Now, this case can be extended to laying of more than one cuckoo eggs, and it is treated as the set of solutions in complex situation. New solution ($S^{(a+1)}$) for general case of cuckoo algorithm is generated at ' i ' cuckoo than Levy flight performed as

$$S_i^{(a+1)} = S_i^a + \beta \oplus \text{levy}(Z) \quad (2)$$

where ' β ' is a variable which is ranges from $0 < \beta \leq 1$. Generally, ' $\beta = 1$ ' is considered. The arbitrary walk is a Markov chain where the next step totally depends upon the immediate last step (S_i^a) of chain. The product \oplus means the entry-wise multiply.

3 Effectiveness Analysis of Proposed Technique

The effectiveness of the proposed technique is tested in two ways such as V-rep simulation and real-time experiment with Khepera-III robot, which are described below.

3.1 Analysis Through V-Rep Simulation

The V-rep simulation is carried out in a complex environment of $240 \times 160\text{cm}^2$ size as shown in the figures below. The simulation results with comparison between simulation and real-time experiment are depicted in Tables 1 and 2. The simulation graph is shown in Fig. 2.

Table 1 Path length in simulation and corresponding experiment

No. of run	Path length (in cm)		% Difference
	In simulation	In experiment	
1	278.91	290.86	4.11
2	279.96	292.64	4.33
3	282.52	295.86	4.51
4	273.26	284.12	3.82
5	275.63	286.53	3.80
6	279.43	290.53	3.82
7	283.71	295.47	3.98
8	274.69	288.42	4.76
9	279.91	290.97	3.80
10	278.12	293.73	5.31
Average =	278.61	290.91	4.23

Table 2 Execution time in simulation and corresponding experiment

No. of run	Execution time (s)		% Difference
	In simulation	In experiment	
1	19.11	19.98	4.35
2	19.68	20.57	4.33
3	19.36	20.12	3.78
4	18.76	19.64	4.48
5	19.42	20.31	4.38
6	19.73	20.46	3.57
7	19.67	20.51	4.10
8	18.97	20.04	5.34
9	19.29	20.24	4.69
10	19.73	20.73	4.82
Average =	19.37	20.26	4.38

3.2 Analysis in Real-Time Environment Through Khepera-III Robot

The real-time experiment is carried out through Khepera-III robot under laboratory conditions. The environment is created same as the V-rep environment, and it is perceived that the robot successfully reached the target point. The results are depicted in Tables 1 and 2. The real-time experimental graph is shown in Fig. 3.

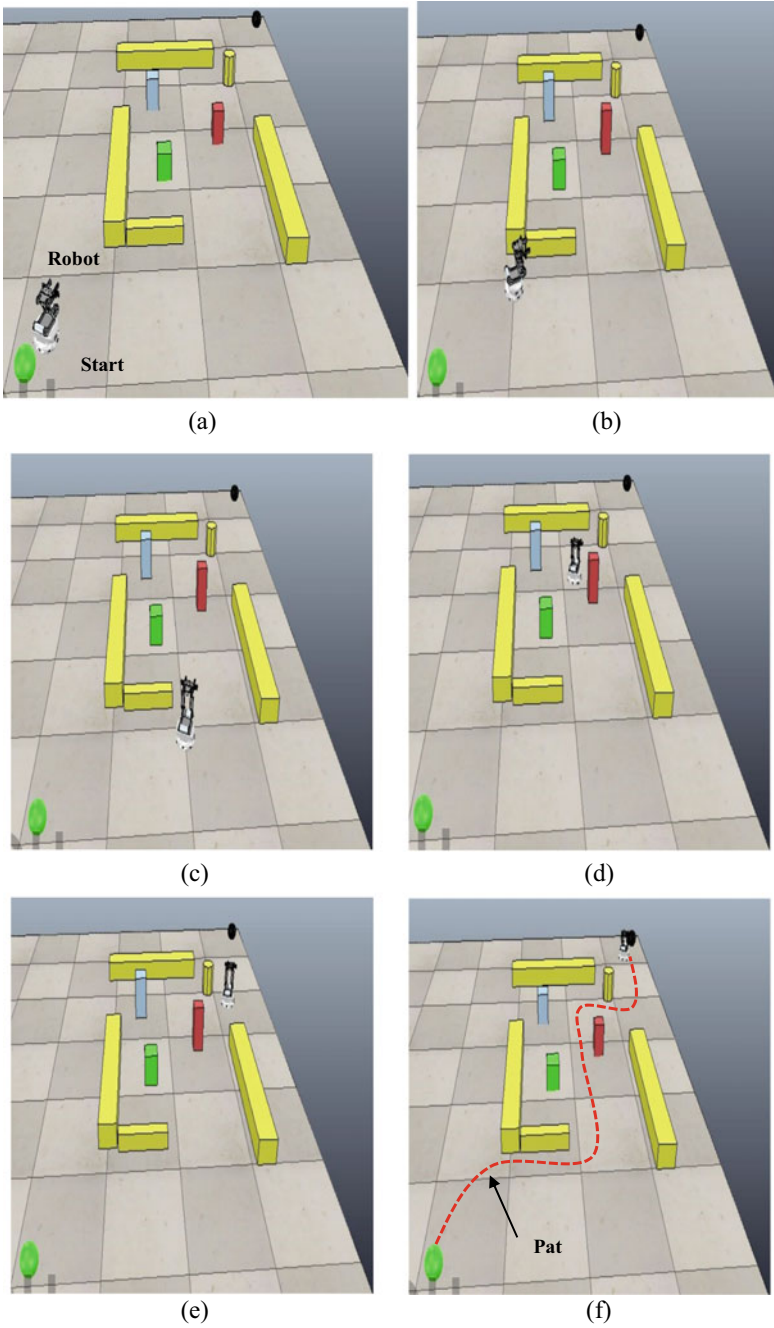


Fig. 2 V-rep simulation using Khepera-III robot

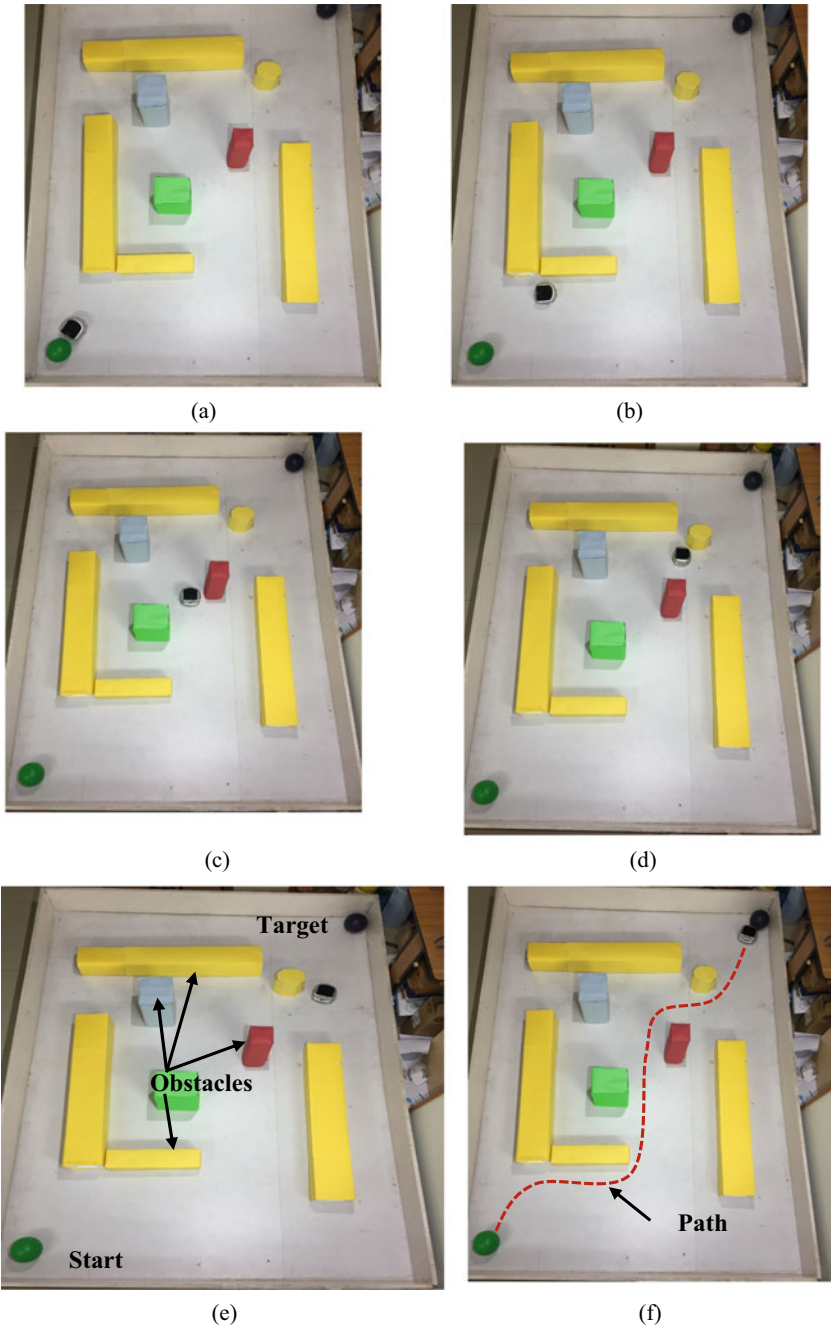


Fig. 3 Real-time experiment through Khepera-III robot

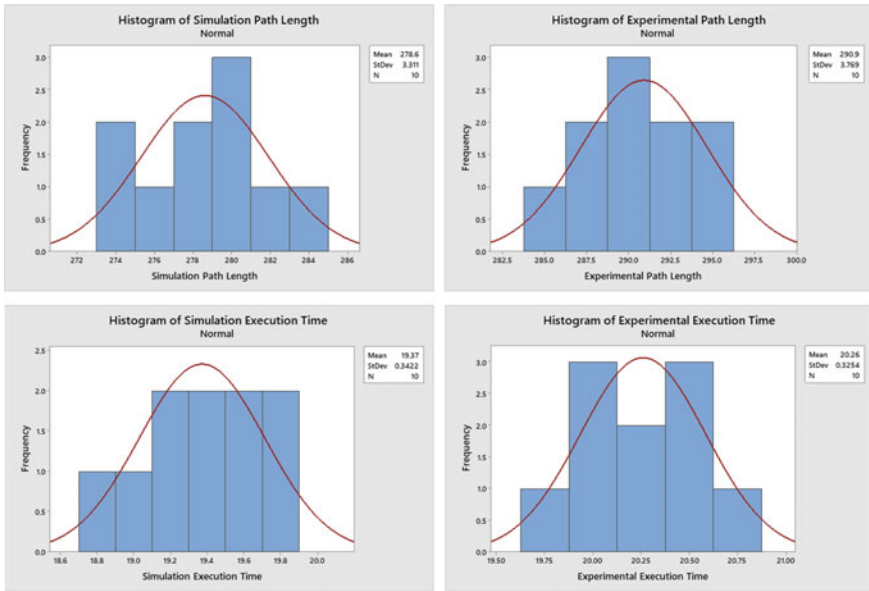


Fig. 4 Histogram of obtained results

3.3 Analysis Through Statistics

The statistical analysis is carried out on Minitab software, and the graphs are formulated with the simulation and experimental results. The normality test is performed with the selection of “Anderson–Darling” test and found the statistical data are normal distribution (Figs. 4 and 5).

4 Conclusions

CS algorithm is an optimization algorithm, and this algorithm is successfully applied in path optimization of mobile robot. During navigation robot achieved their target without any collision. The results analysis says that this algorithm can be applied in the field of mobile robotics where path planning will be a prime consideration. In future, this algorithm may be elaborated for dynamic environment.

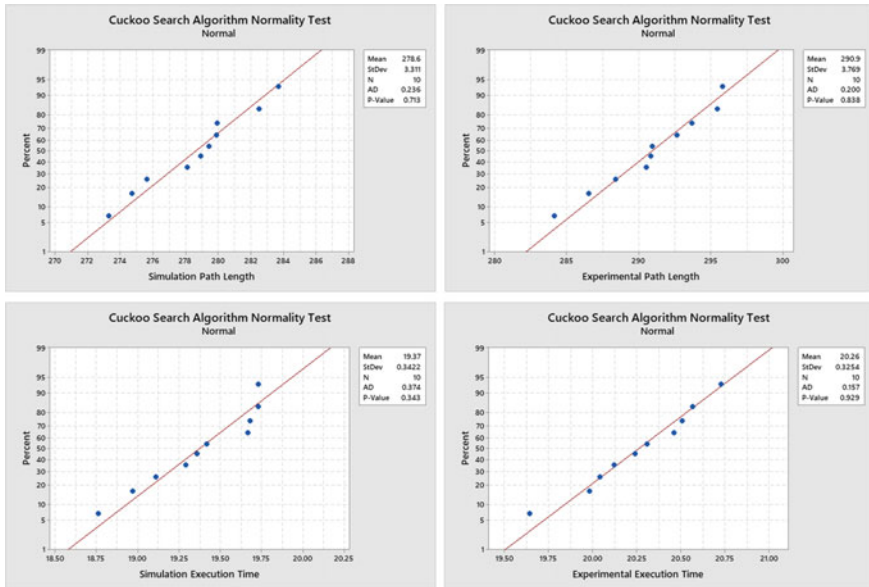


Fig. 5 Normality test of obtained results

References

1. Mohanty PK, Parhi DR (2016) Optimal path planning for a mobile robot using cuckoo search algorithm. *J Exp Theor Artif Intell* 28(1–2):35–52
2. Joshi AS, Kulkarni O, Kakandikar GM, Nandedkar VM (2017) Cuckoo search optimization—a review. *Mater Today Proc* 4(8):7262–7269
3. Mareli M, Twala B (2018) An adaptive Cuckoo search algorithm for optimisation. *Appl Comput Inform* 14(2):107–115
4. Pandey A, Kumar S, Pandey KK, Parhi DR (2016) Mobile robot navigation in unknown static environments using ANFIS controller. *Persp. Sci.* 8:421–423
5. Rawat H, Parhi DR, Priyadarshi BK, Pandey KK, Behera AK (2018) Analysis and investigation of Mamdani fuzzy for control and navigation of mobile robot and exploration of different AI techniques pertaining to robot navigation. In: *Emerging trends in engineering, science and manufacturing (ETESM-2018)*. IGIT, Sarang
6. Muni MK, Kumar PB, Parhi DR, Rath AK, Das HC, Chhotray A, Pandey KK, Salony K (2020) Path planning of a humanoid robot using rule-based technique. In: *Advances in mechanical engineering*, pp 1547–1554. Springer, Singapore
7. Pandey KK, Parhi DR (2019) Trajectory planning and the target search by the mobile robot in an environment using a behavior-based neural network approach. *Robotica*, pp 1–15
8. Salgotra R, Singh U, Saha S (2018) New cuckoo search algorithms with enhanced exploration and exploitation properties. *Expert Syst Appl* 95:384–420
9. Patle BK, Pandey A, Jagadeesh A, Parhi DR (2018) Path planning in uncertain environment by using firefly algorithm. *Defence Technol* 14(6):691–701
10. Kumar PB, Sahu C, Parhi DR (2018) A hybridized regression-adaptive ant colony optimization approach for navigation of humanoids in a cluttered environment. *Appl Soft Comput* 68:565–585
11. Yang, X-S, Deb S (2009) Cuckoo search via Lévy flights. In: *2009 World congress on nature & biologically inspired computing (NaBIC)*, pp 210–214. IEEE

12. Reynolds AM, Rhodes CJ (2009) The Lévy flight paradigm: random search patterns and mechanisms. *Ecology* 90(4):877–887
13. Kumar S, Pandey KK, Muni MK, Parhi DR (2020) Path planning of the mobile robot using fuzzified advanced Ant Colony Optimization. In: *Innovative product design and intelligent manufacturing systems*. Springer, Singapore, 1043–1052
14. Kumar S, Parhi DR, Muni MK, Pandey KK (2020) Optimal path search and control of mobile robot using hybridized sine-cosine algorithm and ant colony optimization technique. *Ind Robot* 47(4):535–545
15. Kumar S, Parhi DR, Kashyap AK, Muni MK (2021) Static and dynamic path optimization of multiple mobile robot using hybridized fuzzy logic-whale optimization algorithm. *Proceedings of the Institution of Mechanical Engineers, Part C: J Mech Eng Sci* 235(21):5718–5735 <https://doi.org/10.1177/0954406220982641>

A Braitenberg Path Planning Strategy for E-puck Mobile Robot in Simulation and Real-Time Environments



Bhaskar Jyoti Gogoi and Prases K. Mohanty

Abstract An efficient method for path planning of mobile robots is being proposed in this paper. The robot is tested to navigate through different types of obstacle to reach the final goal point. To detect and avoid obstacles a Braitenberg vehicle method is used. The implementation of this method can be performed without using much expensive equipments or any kind of complex structures. For the mobile robot, the simulation has been performed using E-puck robot. It is very important for the robot to have the ability to locate and approach its final destination point. Till date there are many different types of techniques available for path planning. In this paper Braitenberg vehicle is being studied and implemented by considering the coordinates of the robot and the destination point. The behaviour of the robot has been tested in a simulated environment using the software Webots and the results are further validated with real-time experiment by using the same environments to check the robot's efficiency. During Simulation and real-time experimentation process few complications were identified and it has been successfully resolved.

Keywords Braitenberg vehicle · Goal point · Starting point · Obstacle avoidance · Path planning · E-puck mobile robot

1 Introduction

It is very important for a robot to be aware of the surrounding environment and respond accordingly to avoid any encounter whilst navigating to a goal point. In recent times the application of mobile robotics has widely increased in the areas like, space exploration, security, distribution of goods in places like warehouse, medical and personal assistance, etc. To perform these tasks, it is very important for the

B. J. Gogoi (✉)

Department of Electronics and Communication, The Assam Kaziranga University, Jorhat, Assam 785006, India

P. K. Mohanty

Department of Mechanical Engineering, National Institute of Technology, Arunachal Pradesh, Itanagar 791112, India

robot to be able to read its surrounding constantly and process the data precisely. Braitenberg vehicles use simple input data from proximity sensors that are attached to the robot to detect obstacles and perform complex behaviours to avoid it. Therefore in this work Braitenberg vehicles are implemented for obstacle avoidance.

Till date there has been lots of research work done on the path planning of mobile robots using different types of methods like wall following method [1], fuzzy methods [2], virtual target method [3]. But the Braitenberg vehicle approach makes the path planning simple and effective. Here in this paper, the robot has been programmed in such a way that it reacts and shows different reactions to different environments by taking input readings from the sensors and implementing Braitenberg vehicle method. The movements on the robot is basically controlled by controlling the motor speed of each wheels. There are many different types of classical techniques that are used for path planning, such as cell decomposition (CD), roadmap approach (RA), neural network (NN) and Voronoi diagram [4]. In cell composition technique the configuration space is transformed into non-overlapping cells and it uses connectivity graphs to travel across the cells to reach the goal [5]. In the roadmap approach it connects the free spaces and forms a network of many one-dimensional curves [6]. The Artificial neural network is made up of many layers and elements connected with each other. These connections are given importance based on other weightage and it can make a system learn on its own [7]. The Voronoi diagram divides the plane with x number of points into polygons and the point in every polygon is always closer to its generating points [8].

In this paper the current coordinates and the coordinates of the goal point are used to estimate the time required to reach the final destination with a constant speed. The Braitenberg vehicle 2a is used to avoid the obstacles on its way. Braitenberg vehicle method is simple and yet effective for a vehicle to show complex behaviours. The simulation results are briefly verified by comparing with the real-time experimental results. This paper is briefly organised as: at Sect. 2 Braitenberg vehicle concepts is briefly discussed. At Sect. 3 how the robot will behave and move towards its final destination. At Sect. 4 the paths followed by the robot is presented using simulation environment. Real-time experiment results of the E-puck robot are mentioned in the Sect. 5.

2 Braitenberg Vehicles

The book “Vehicles: Experiments in synthetic psychology” is written by Valentino Braitenberg in 1984 and it describes about experiments on how complex behaviour can be attained using simple structured machines [9]. In this book he had considered a simple “piece of machinery” as the brains of the animals. This made him to think vehicles as animals with its own nature. Using the different connections and system structure of vehicles, he tried to show the internal structure and basic working of the animals. These machines with simple structure show amazing complex behaviours. That is why these are used to study for Computational Neuroscience.

In Braitenberg Vehicles how a vehicle reacts to the environment is dependent on the connections of sensors to motors and even these connections can alter the reaction of the vehicle [10]. Based on these connections the Braitenberg Vehicles show different behaviours like fear, aggression, liking and love. In order to provide the vehicles with various abilities to cope with the environment different types of Braitenberg Vehicles are used with wide variety of stimulus like, light, darkness, free space infant of the robot, etc.

To better understand here are some of the simplest examples of Braitenberg's vehicles:

2.1 Vehicle 1

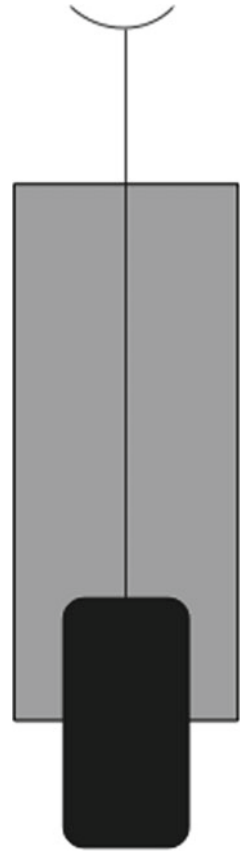
The vehicle 1 of Braitenberg vehicle has one sensor and one wheel, where the wheel is being stimulated by the sensor proportionally. The vehicle 1 is capable of moving only in one direction. It cannot show more complex behaviour or take turns. Depending on the stimuli this vehicle can move forward and backward or stand still. The concept of Braitenberg Vehicle can easily be understood by the beginners. The vehicles with more sensors and wheels can show more complex behaviours and are more sensitive towards the environment. Figure 1 shows the basic diagram of a Braitenberg vehicle 1.

2.2 Vehicle 2

The Vehicle 2 of Braitenberg vehicle contains of two wheels and two sensors. Here each sensor is connected with each wheel in a pair form. Depending on the readings of sensors the corresponding wheel's movements are controlled. Now as we have two sensors and two wheels, there will be two different types of wiring and therefore will have two types of Vehicle 2 i.e., Vehicle 2a and Vehicle 2b.

2.2.1 Vehicle 2a

In Vehicle 2a the sensor on the right side is wired with the right wheel and the sensor on the left side is wired with the left wheel. This vehicle can also be said as symmetric vehicle and it shows negative behaviour. To better understand its behaviour let us consider a situation where there is a light source on the right side of the vehicle. Now the right sensor will have higher readings than the left sensor and thus the right wheel will turn faster and as a result the vehicle will turn towards left, away from the light source. This behaviour is better suited for the escape situations. Another way the Vehicle 2a can be used to move towards the light, away from the dark. As shown in the Figure the “+” sign means that, higher the reading of the sensor, faster the

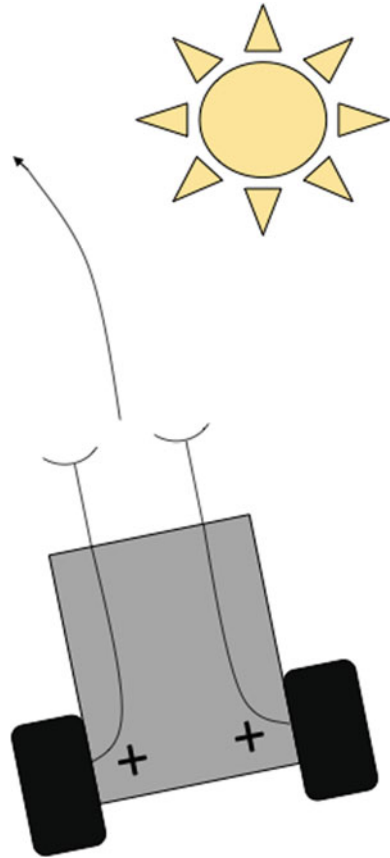
Fig. 1 Braitenberg vehicle 1

motor rotates. But the “-” sign indicates, higher the sensor reading, slower the motor rotates. Now assuming, if the vehicle is moving directly towards the light source then it might hit the source as both the sensor readings are increasing simultaneously. But if the light source is at the side of the vehicle then the motor of that corresponding side will move faster and the vehicle will move away from the source [11]. Figure 2 shows how Braitenberg vehicle 2a reacts to a light source.

2.2.2 Vehicle 2b

For Vehicle 2b the right sensor is connected with the left motor and the left sensor is connected with the right motor. Or we can say that the sensors and motors are connected inversely. Now considering the light source present on the right side, the higher reading will be shown on the right sensor and low reading is shown on the left sensor. Figure 3 represents the vehicle 2b. From the figure we can see that the left motor is connected with the right sensor and as the right sensor will have higher

Fig. 2 Braitenberg vehicle
2a

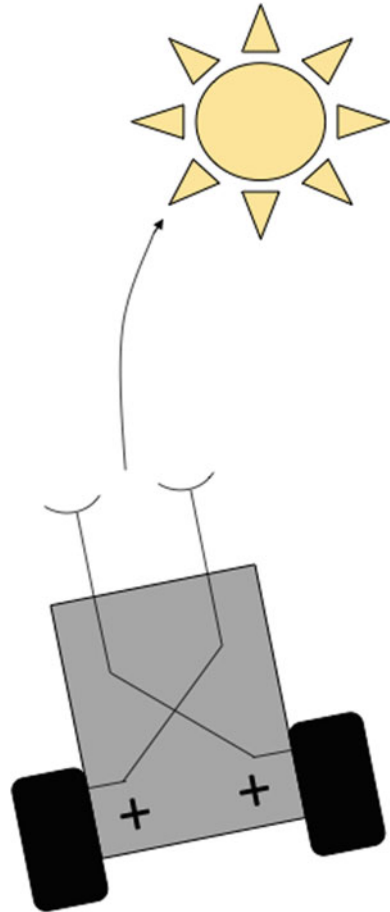


reading the left motor will rotate faster than the right motor. So, as a result the vehicle will move towards the light.

2.3 Vehicle 3

Vehicle 3 of Braitenberg vehicle is similar to that of the Vehicle 2. It has two sensors and two wheels. Similarly, this vehicle can be of two types Vehicle 3a and Vehicle 3b depending on the types of wiring between sensors and wheel. The only thing that separates Vehicle 3 from Vehicle 2 is that motors will move slowly when the reading is high. In other words, this vehicle slows down when faces the light and under certain conditions it might stop in front of the light source [11].

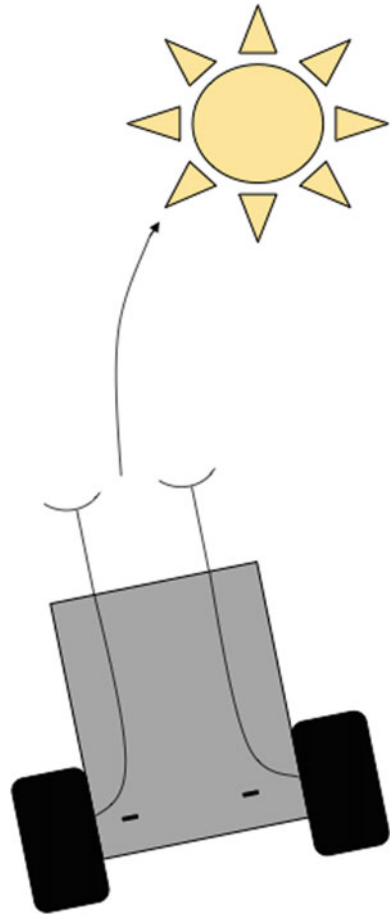
Fig. 3 Braitenberg vehicle
2b



2.3.1 Vehicle 3a

The Vehicle 3a has its right sensor wired with right motor and left sensor wired with the left motor. To better understand this vehicle, let us consider a light source on the right side of the vehicle and when right sensor readings increase the right wheel rotation decreases and as a result the vehicle will turn towards the light source [12]. And when the vehicle faces towards the light source then both the right and left sensor's reading will be higher and as a result it will decelerate the motors and will gradually stop in front of the source as shown in Fig. 4.

Fig. 4 Braitenberg vehicle
3a



2.3.2 Vehicle 3b

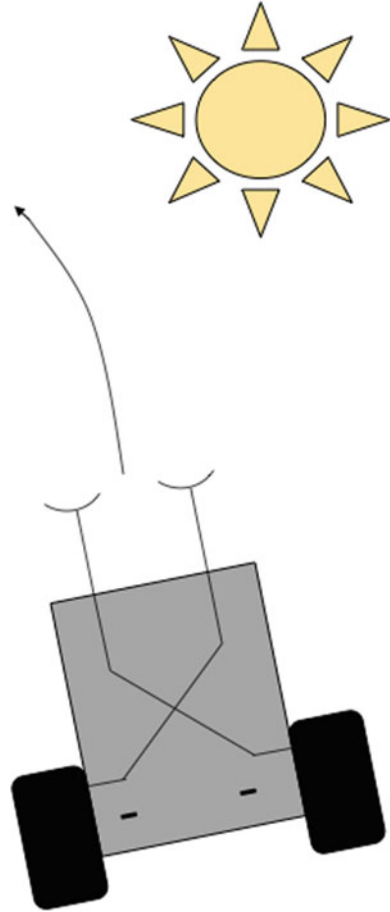
In vehicle 3b the right sensor connected with the left wheel and left sensor is connected with the right wheel. To understand its behaviour, the action of the vehicle 3a is shown in the Fig. 5. From the figure we can see that the vehicle is moving away from the light source.

The relation between the sensor values and the velocity of wheels can be established by the following equation:

$$v_s = f\left(\sum_1^n \omega_i \times d_i\right) \tag{1}$$

Here the ω_i is the weight value and its value depends on the problem feature. d_i is the sensor value and f is the maximum velocity function of the wheels [13].

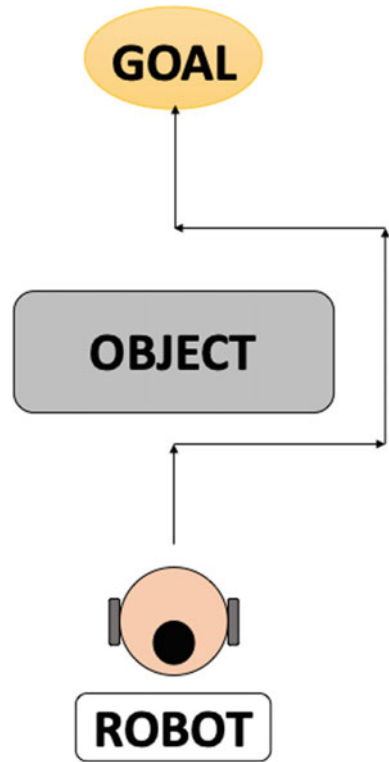
Fig. 5 Braitenberg vehicle
3b



3 Navigation and Obstacle Avoidance Architecture Using Braitenberg Algorithm

In this work there are three main steps play a critical role for the E-puck robot to navigate through an environment, whilst avoiding the obstacles and reach the goal point. These are, rotating and facing towards the goal point—move forward whilst detecting the obstacle on its way—if obstacle is detected avoid it using Braitenberg vehicle concept. To better understand the situation through Braitenberg vehicle's view using block diagram, let us consider the goal point as GOAL and obstacles as OBJECT. Now the GOAL is the destination where the robot wants to go and tries to avoid the OBJECT which lies in front of the GOAL. Now considering these situations, the robot follows the path as shown in Fig. 6 to reach the goal point without any disturbance [13].

Fig. 6 Path followed by the Robot to avoid simple obstacle



With a little modification Braitenberg Vehicle 2a is used to successfully avoid the obstacle. There are a total of eight sensors mounted on the robot and each of the sensors are set with certain threshold value, such that when the threshold value exceeds the robots consider it as an obstacle detected. At first the robot makes a rotation at the starting point to face towards the goal point. After facing towards the goal point the robot starts to move forward with all the sensors activated, and the data collected from the sensors are being processed instantaneously at real time. Whenever an obstacle is detected the robot is brought to stop and then take respective moves that are required to avoid the obstacle. Once the obstacle is cleared the robot again stops and makes a required degree of rotation to face towards the goal point and then moves towards the goal [14]. Figure 7 shows the general actions performed by the robot.

Whilst programming the obstacle avoidance steps for the robot, different types of situations are taken into consideration. The robot will act differently for different types of obstacles. Although the robot is capable of overcoming any obstacles, under certain circumstances it also has the probability of infinitely repeating the same path without making any actual progress towards the goal point. Therefore, it is very important to consider such situations by observing the obstacle patterns where the robot is more likely to fall into such loops.

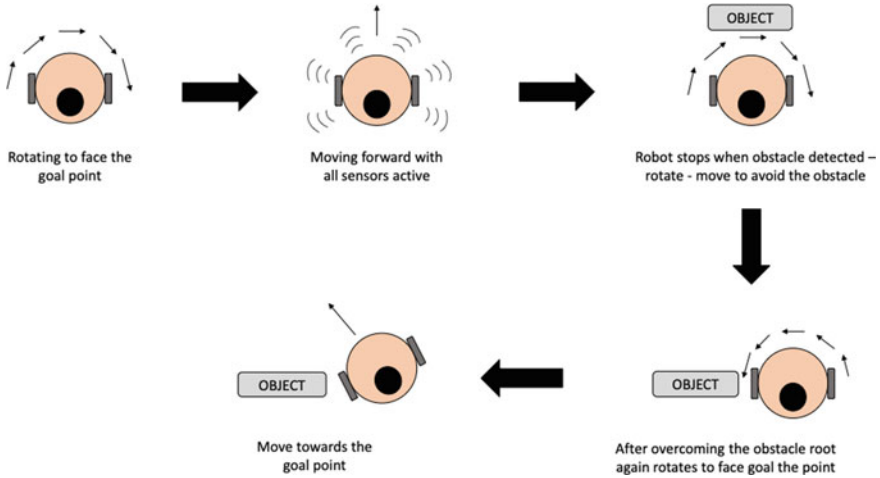


Fig. 7 Steps Performed by the Robot to avoid obstacle

There are different types of ways to implement path planning on a robot such as, Potential field [15] and Navigation function (NF1) [16]. In potential field technique a virtual potential field created around the robot. The concept is that the goal point will have an attractive field and that the robot will reach the goal point by following the field. Or we can say that the robot moves like a ball rolling downhill. But in this work a different approach is made. Initially a goal point will be set and then the robot will rotate to face towards the goal point before moving forward. Then the robot will check its current location and by using the co-ordinates of the current location and final destination the robot will calculate the time required to reach the goal point. And then the robot will start moving forward for the calculated amount of time. If it encounters any obstacles on its way, then the robot will perform the required sets of instructions to overcome it and after this the robot will again rotate towards the goal point and calculate the amount of time required to reach and then move forward.

4 Simulation Results

An open-source software “webots” is used for the simulation of path planning using E-puck robot [17]. The programming languages compatible for this platform are C, C++, python and MATLAB. Webots is a prototyping environment where we can simulate our ideas to see how it will behave in a real-time environment. It is even widely used for both educational and research purposes. In this platform we can consider all types of physical properties like velocity, joints, friction, mass, friction coefficient, etc. for simulation. We are able to build and create any kind of physical situation by using many inbuilt nodes like objects, humans, vehicles, robots, etc.

This platform also gives us the ability to custom build any structure if it is not pre-uploaded [18]. We can build 3-D objects outside of the Webots platform using any CAD software and then import it to the simulation environment [19].

The robot used for the simulation is E-puck robot. This robot weighs 150 g, it has a battery, 2 stepper motors, 8 infrared sensors that can measure range up to 4 cm, a camera with a resolution of 640×480 , 3 omni-directional microphones, an accelerometer, a gyroscope, 8 red LEDs, 1 green LED, speaker, switch and remote control. Figure 8 shows the look of e-puck robot in the simulation environment.

Different types of environments are used to test the path planning of the E-puck robot using Braitenberg vehicle. It is very important to know how the robot behaves in different kind of situations, so that we can update and modify robot's behaviour for better outcome. For the simulation basically an e-puck robot, a rectangular arena and different shapes of obstacle are used. Infrared sensors are used for the robot to be able to detect obstacles and monitor its surroundings. Initially only a goal point is set for the robot and then the robot will move on its own towards the final destination by overcoming any obstacle on its way.

Simulation environment-1 A wall like obstacle is placed in the arena and the robot has to overcome it to reach the goal point. Figure 9 shows the path followed by the robot.

Simulation environment-2 For simulation environment-2 a random puzzle like obstacle is placed around the goal point. Figure 10 shows the path followed by the robot to reach its goal point.

Simulation environment-3 In this environment U-shaped obstacle is placed in front of the goal point. It is one of the obstacles where the robot keeps repeating an infinite loop without actually overcoming the obstacle. It gets stuck inside the U-shaped obstacle. So to overcome these type of obstacle a different approach has to be made. At first the robot needs to detect that there is an L-shaped obstacle in front of it, as shown in Fig. 11. Following steps can be used to overcome these kind of obstacles:

Fig. 8 Simulated E-puck robot



Fig. 9 Simulation environment-1

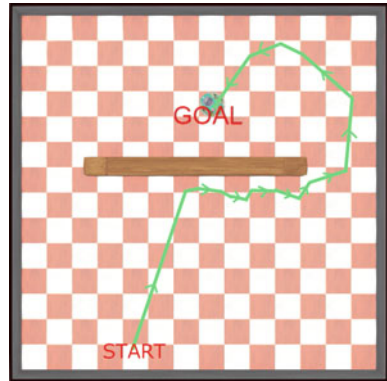


Fig. 10 Simulation environment-2

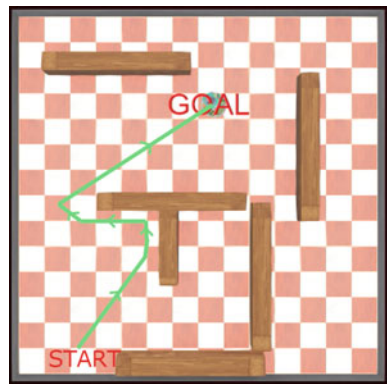
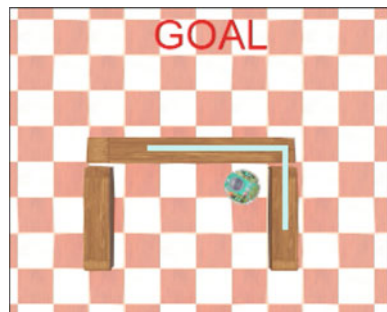


Fig. 11 Detection of the L-shaped obstacle



detecting the L shape → then the robot needs to rotate left or right for 100 degree, depending upon the type of L → for any amount of time move forward → next, a man stops and rotates right or left for an angle of 45° (If no obstacle is found on the way/If obstacle is found, then avoid the obstacle and then move forward) → and

Fig. 12 Simulation environment-3

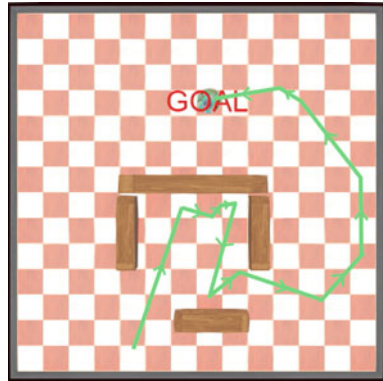
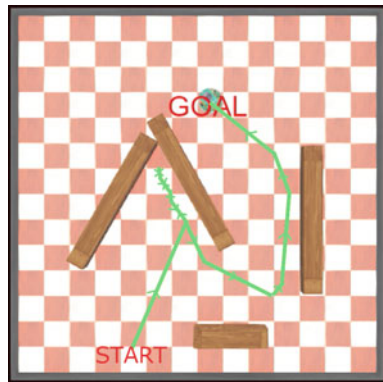


Fig. 13 Simulation environment-4



then move forward. Using these steps it is found that the robot can avoid U-shaped obstacle successfully. The final path followed by the robot is shown in Fig. 12.

Simulation environment-4 In this environment a “V”-shaped obstacle and a few random obstacle are placed in front of the goal point. Here the robot has to overcome the “V” shape, and in order to do that, the robot has to detect that there is no path at its sides or in front of the robot. After detecting the type of obstacle the robot will turn 180° and try to overcome the obstacle. It has been observed that the robot passed through all the obstacles without any problem. Figure 13 shows the path followed by the robot.

5 Experimental Results Using Braitenberg Algorithm

To further validate the simulation result an experimental study has been done. For this experimental study the same environments are used as in the simulation, so that

the validation can be done more precisely. The robot used for real-time navigation has the specifications as mentioned in the Table 1. Real-time experiments are shown in Figs. 14, 15 and 16.

Through laptop the programming for the robot to navigate has been uploaded. Then the robot starts moving towards the goal point by navigating and avoiding various obstacles in the set environment. It has been found that the path followed by the robot in simulated environment and real-time experiment is similar and the percentage of error is very less as presented in Table 2.

Table 1 The specification of the robot used for real-time navigation

S. No.	Component name	Technical specification
1	Processor	Linux core running on a 800 MHz ARM Cortex-A8 processor
2	RAM	512 MB
3	Flash	512 MB with 4 GB additional data
4	Speed	1 m/s maximum
5	Sensors	5 Ultrasonic sensors with measuring distance with 25 cm–2 m, 8 IR proximity and ambient light sensors with measuring distance up to 25 cm
6	Battery	3400 mAh, 7.4 V Lithium Polymer
7	Communications	Bluetooth 2.0 EDR, 802.11 b/g WiFi, 1 USB 2.0 device
8	Size	Height: 58 mm, Diameter: 140 mm
9	Payload/weight	2000 g (max.) 540 g
10	Applications	C/C++

Fig. 14 Path obtained through in of Fig. 9

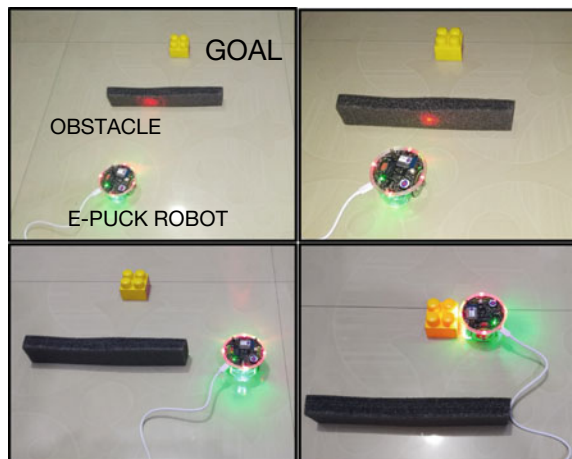


Fig. 15 Path obtained in experiment of Fig. 10

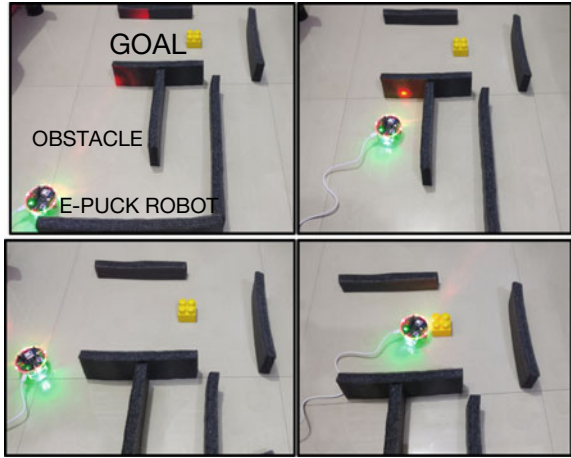


Fig. 16 Path obtained in experiment of Fig. 12

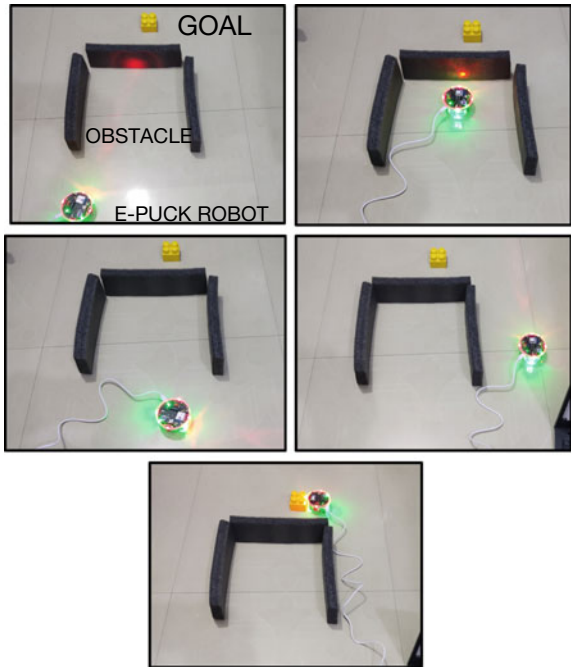


Table 2 Results and comparison of path length and time taken to reach the goal point

S. No.	Fig. No.	Path length (in pixels)		Time duration (in s)	
		Simulation	Experiment	Simulation	Experiment
1	Figures 9 and 14	1430	1509	33	46
2	Figures 10 and 15	1895	1980	59	71
3	Figure 12 and 16	1799	1849	54	68

6 Conclusions

The simulation result of the E-puck robot is also being verified by experimenting the E-puck robot in those environments in real time. The following points can be extracted from the experiment on the path planning method:

1. We needed a simple and effective approach for the path planning of mobile robotics, and it is found that Braitenberg vehicle approach is one that fits the most and also it is easy to implement.
2. Webots software is used for the simulation of the robot and later the results have been verified by performing real-time experiments.
3. The E-puck robot is being examined under different types of environments so that its efficiency to reach the goal point and response towards obstacles can be reviewed. And it can be concluded that the robot is capable of reaching its goal point whilst avoiding obstacles.
4. In this work the current coordinates of the robot and its goal point coordinates along with obstacles avoidance patterns are used to determine the path.
5. Currently static obstacles are used for experimenting but in future with more enhancements dynamic obstacles can also be considered.
6. Using E-puck robot real-time experiments are performed and it is compared to the simulation results. Whilst comparing it shows a very small variation between the path trajectory of simulation and real-time experiments.

In future the proposed algorithm will be compared with other existing algorithm and dynamic obstacles will be considered in place of static obstacles. The proposed methodology is simple and can easily be modified to adapt into many different scenarios.

References

1. Bemporad A, Marco MD, Tesi A (1997) Wall-following controllers for sonar-based mobile robots. In: Proceedings of 1997. IEEE International Conference on Decision and Control, vol. 3, pp. 3063–3068 (1997)
2. Wang M, Liu (2005) Fuzzy logic based robot path planning in unknown environment. In: 2005 International conference on machine learning and cybernetics. <https://doi.org/10.1109/icmlc.2005.1527055>
3. Lining S, Rui L, Weidong W, Zhijiang D (2011) Mobile robot real-time path planning based on virtual targets method. 2011 In: Third international conference on measuring technology and mechatronics automation. <https://doi.org/10.1109/icmtma.2011.429>
4. Zafar MN, Mohanta JC (2018) Methodology for path planning and optimization of mobile robots: a review. *Procedia Comput Sci* 133:141–152. <https://doi.org/10.1016/j.procs.2018.07.018>
5. Milos S (2007) Roadmap methods vs. cell decomposition in robot motion planning. In: Proceeding of the 6th WSEAS international conference on signal processing, robotics and automation. World Scientific and Engineering Academy and Society (WSEAS), p 127e32
6. Siegwart R, Nourbakhsh IR, Scaramuzza D (2004) Introduction to autonomous mobile robots. MIT-Press, pp 1–12

7. Sung I, Choi B, Nielsen P (2020) On the training of a neural network for online path planning with offline path planning algorithms. *Int J Inf Manag* 102–142. <https://doi.org/10.1016/j.ijinfomgt.2020.102142>
8. Bhattacharya P, Gavrilova ML (2007) Voronoi diagram in optimal path planning. In: 4th International symposium on Voronoi diagrams in science and engineering (ISVD 2007). <https://doi.org/10.1109/isvd.2007.43>
9. Braitenberg V (1984) *Vehicles. Experiments in synthetic psychology*. The MIT Press
10. Smart PR (2020) Planet Braitenberg: experiments in virtual psychology. *Cogn Syst Res*. <https://doi.org/10.1016/j.cogsys.2020.06.001>
11. Rano I (2012) A model and formal analysis of Braitenberg vehicles 2 and 3. In: 2012 IEEE International conference on robotics and automation. <https://doi.org/10.1109/icra.2012.6224583>
12. Rano I (2011) On the convergence of Braitenberg vehicle 3a immersed in parabolic stimuli. In: 2011 IEEE/RSJ International conference on intelligent robots and systems. <https://doi.org/10.1109/iros.2011.6094521>
13. Shayestegan M, Marhaban MH (2012) A Braitenberg approach to mobile robot navigation in unknown environments IRAM 2012. *CCIS* 330, pp 75–93
14. Yang X, Patel RV, Moallem M (2006) A Fuzzy–Braitenberg navigation strategy for differential drive mobile robots. Received 5 Mar 2004. Accepted: 2 May 2006. Published online: 21 Sept 2006
15. Orozco-Rosas U, Montiel O, Sepúlveda R (2019) Mobile robot path planning using membrane evolutionary artificial potential field. *Appl Soft Comput* 77:236–251. <https://doi.org/10.1016/j.asoc.2019.01.036>
16. Yuan F, Twardon L, Hanheide M (2010) Dynamic path planning adopting human navigation strategies for a domestic mobile robot. In: 2010 IEEE/RSJ International conference on intelligent robots and systems. <https://doi.org/10.1109/iros.2010.5650307>
17. Guyot L, Heiniger N, Michel O, Rohrer F (2011) Teaching robotics with an open curriculum based on the e-puck robot, simulations and competitions
18. Michel O (2004) Cyberbotics Ltd. Webots™; professional mobile robot simulation. *Int J Adv Robot Syst* 1(1), 5. <https://doi.org/10.5772/5618>
19. Junk S, Kuen C (2016) Review of open source and freeware CAD systems for use with 3D-printing. *Procedia CIRP* 50:430–435. <https://doi.org/10.1016/j.procir.2016.04.174>

Experimental Investigation on the Performance of the Novel 3D-Printed Micro-Cross Axis Wind Turbine



V. S. Surya Prakash , P. S. V. V. Srihari , P. S. V. V. S. Narayana ,
G. Udaysai, P. S. S. Rajesh, and K. Venu

Abstract Cross axis wind turbine which is a combination of both vertical and horizontal axis wind turbine is effective in extracting wind energy in urban regions. In this study, a novel CAWT with auxiliary blades arranged on its vertical components is proposed. The performance parameters such as co-efficient of torque, co-efficient of power, and co-efficient of moment of a 3D-printed scaled models are evaluated by conducting wind tunnel experiments. From the results of this study and the results used for validation of the work from the literature, it was found that arranging the auxiliary blades on the vertical configuration showed enhancements of the torque, power, and moment by 19.55%, 46.3%, and 21.78%, respectively, at 12 m/s wind velocity. This improvement results in better self-starting abilities over the standard vertical axis wind turbine models which make its design suitable for extracting wind energy potential in the urban regions with random turbulence and wind characteristics.

Keywords 3D printing · Cross axis wind turbine · Performance coefficients · Self-starting · Vertical axis wind turbine · Wind turbine

Abbreviations

Ω	Angular velocity (rad/s)
D	WT rotor diameter (mm)
A	WT rotor area (mm ²)
V	Wind velocity (m/s)
P	Air density (m ³ /s)
HAWT	Horizontal axis wind turbine

V. S. Surya Prakash (✉) · P. S. V. V. Srihari · G. Udaysai · P. S. S. Rajesh · K. Venu
Department of Mechanical Engineering, Aditya College of Engineering & Technology,
Surampalem, Andhra Pradesh, India

P. S. V. V. S. Narayana
Department of Mechanical Engineering, Aditya Engineering College, Surampalem, India

© The Author(s), under exclusive license to Springer Nature Singapore Pte Ltd. 2022
B. B. V. L. Deepak et al. (eds.), *Applications of Computational Methods in Manufacturing
and Product Design*, Lecture Notes in Mechanical Engineering,
https://doi.org/10.1007/978-981-19-0296-3_14

VAWT	Vertical axis wind turbine
CAWT	Cross axis wind turbine
SLS	Selective laser sintering
AM	Additive manufacturing
WT	Wind turbine
TSR	Tip speed ratios
C_P	Power coefficient
C_T	Torque coefficient
C_M	Moment coefficient
DMM	Digital multimeter
DAQ	Data acquisition system

Subscripts

P	Power (W)
T	Torque (N m)
M	Moment (N m)
F	Flap
D	Chord
S	Slit

1 Introduction

Harnessing energy-utilizing renewable energy technologies reduces the dependence on non-renewable energy technologies such as fossil fuels. The depletion of the fossil reserves and the rise in population create a huge energy demand globally. To fulfil this ever-increasing demand for electricity, many countries adopted renewable energy technologies to meet energy demand and to generate inexhaustible and clean energy. Today, wind energy technologies are one of the fast-growing renewable energy technologies globally. Srihari et al. [1–5], the total wind capacity was increased significantly from 1995 and was reported as 434 GW at the end of the year 2015. Global wind energy may reach 2000 GW by the end of the year 2030, which will be quenching the global electricity's need by 18–20% [6]. The demand can be met easily if the available wind energy potential from urban regions is converted to electricity.

Urban terrains have huge wind availability in which small-scale wind turbines (WTs) can be utilized for effective conversion of wind energy to electricity. Though small-scale horizontal axis wind turbines (HAWT) have high efficiencies, their performance is greatly affected by unfavourable factors of wind such as low

wind speed, irregular turbulence, and wind direction in urban regions. Specifically designed vertical axis wind turbine (VAWT) may perform well under these unfavourable conditions, but the power coefficient (C_p) of these turbines is very low. And the safety standards for the small-scale VAWTs are not fully developed due to a lack of experimental and real-time test data.

The increase in the number of rotor blades affects the VAWT performance coefficient [7]. H-Type VAWTs with high solidity are prone to vibrations with high amplitude during testing which result in the whirling mode of the turbine. These large vibrations cause resonance of the whole turbine structure which makes it impossible to measure the aerodynamic loads on the blades. The residual vibrations can be damped by using band filters during testing [8].

Various researchers have studied the VAWTs and HAWTs designs and performance parameters. Small, multipurpose WTs are developed, and their performance was reported. Despite many models proposed by various researchers, there are many disputes regarding the performance and starting characteristics of small VAWTs [9].

Pitch control of the VAWTs may improve the starting torque characteristics of the VAWTs but be limited to TSR [10]. The major disadvantages of the VAWTs are their self-starting characteristics which affect their overall performance and low efficiency in extracting wind energy. The design of CAWT has advantages over VAWT and HAWT. The CAWT can work on unpredictable wind conditions in the urban region such as oncoming wind direction, irregular turbines, and wind velocity.

In our previous work, the proposed novel micro-VAWT having slats and flaps arrangement to the main rotor blade showed the improvement in the starting torque characteristics compared to the standard micro-VAWT [1]. In this study, a novel micro-CAWT with slats and flaps on its vertical component has been proposed, and experimental analysis was carried out in an open-circuit wind tunnel. The prototyped scaled models of the VAWT base model, VAWT with configuration [2], and proposed CAWT are manufactured by SLS, AM technique and is tested. The results of the CAWT with the proposed configuration are validated with the results obtained from these two-reference prototype micro-turbine models.

2 Blade Characteristics and Rotor Design

The micro-CAWT proposed in this study has three horizontal configuration blades connected to three vertical configuration blades having a set of five aerofoils. The vertical configuration sets are situated at an angle 120° from each other. The vertical configuration blades are made by using DU-06-W200 aerofoil and the horizontal configuration blades by NACA 0018.

The blade characteristics of the horizontal configuration of novel CAWT are represented in Fig. 1. The design parameters of the horizontal configuration blade sets are represented in Table 1.

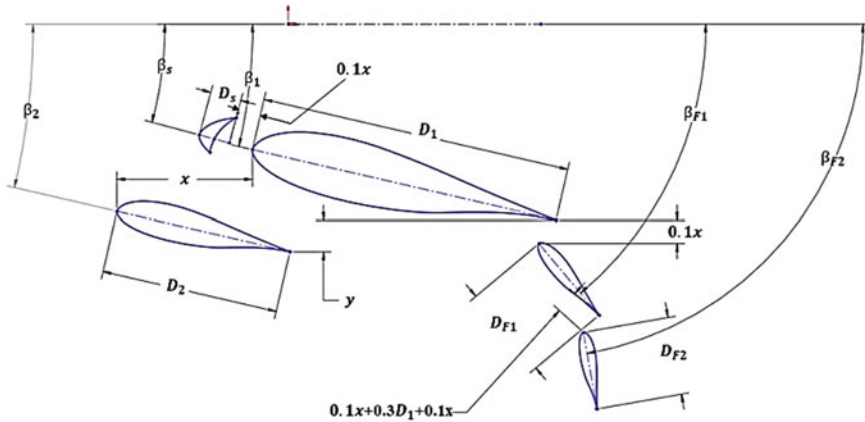


Fig. 1 Novel CAWT blade characteristics of horizontal configuration

Table 1 Horizontal configuration characteristics

Parameter	Notation	Value
Chord lengths (mm)	D_1	47.22
	D_2	26.92
	D_s	4.722
	D_{F1}	14.13
	D_{F2}	11.82
Distance (mm)	x	17.94
	Y	13.72
Distance (mm)	$0.1x$	1.791
Distance (mm)	$0.1x + 0.3D_1 + 0.1x$	17.75
Angle of attack (degrees)	β_1	13.0°
	β_2	13.0°
	β_s	15.0°
	β_{F1}	50.0°
	β_{F2}	80.0°

The three models considered in this study are modelled in SOLIDWORKS and are fabricated by SLS, AM technique by using nylon 66 as filler material. The micro-WT models in isometric view are represented in Fig. 2a–c. The dimensions of these models are tabulated in Table 2.

The rotor models are manufactured by SLS and AM technique, and the AM models without shafts are shown in Fig. 3a–c. The coupling of shafts to the AM rotor models is done by means of Allen screws, and to the one end of the shaft, the generator unit is attached by means of shaft couplings. The generator is fitted to the

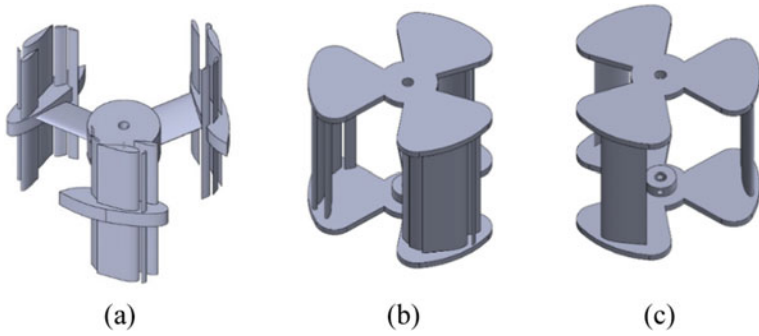


Fig. 2 Isometric views of micro-turbines **a** with proposed configuration **b** with Srihari et al. [3] configuration **c** with standard configuration

Table 2 Micro-WTs dimensions

Configuration	Rotor parameter	Value
Proposed, Srihari et al. [5] and Standard	Swept area	0.030 m ²
	Diameter	200.0 mm
	Height	150.0 mm

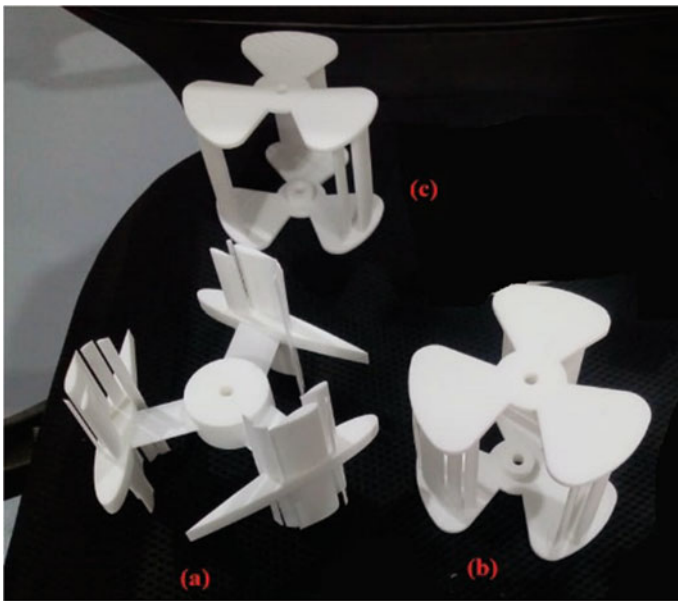


Fig. 3 AM rotor models **a** with proposed configuration **b** with Srihari et al. configuration [4] **c** with standard configuration

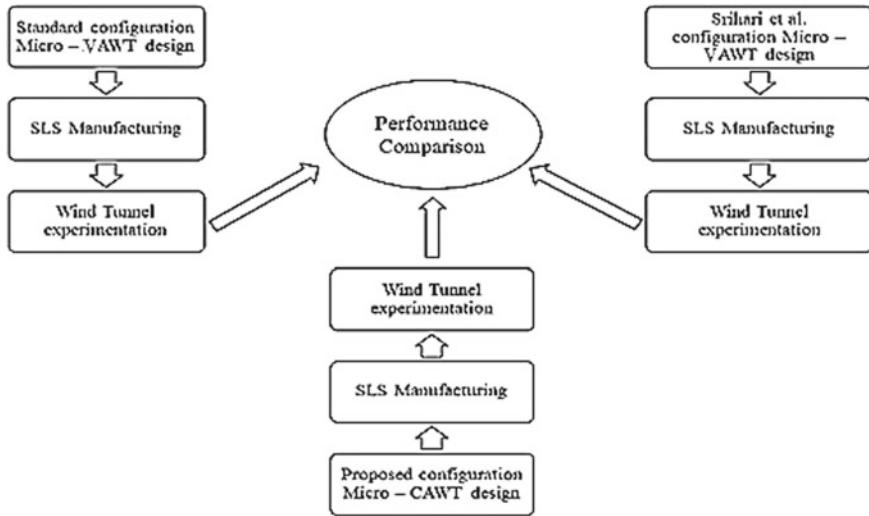


Fig. 4 Scheme of research

base, and the other end of the shaft is fitted to the bracket in the wind tunnel during experimentation.

The fabricated VAWT rotors with the proposed configuration in this study, the VAWT model with Srihari et al. [5] configuration, and base VAWT are coupled by using Allen screws and shaft couplings to the generator. The research schematic flow chart of the study is presented in Fig. 4.

3 Performance Parameters

The non-dimensional performance parameters used to compare the performance of WT rotors under investigation are C_p , C_τ , C_m , and TSR [12–14]. The parameters are calculating by using the following formula

$$\text{TSR} = \frac{2\omega D}{4V} \quad (1)$$

$$C_p = \frac{10P}{5\rho AV^3} \quad (2)$$

$$C_\tau = \frac{10P}{5\rho ARV^2} \quad (3)$$

$$C_m = \frac{2C_p}{2(\text{TSR})} \quad (4)$$

4 Experimental Setup

The fabricated WT models are tested in an open-circuit wind tunnel. The function parameters of the wind tunnel are 0.4–20 m/s and work at an optimal temperature of 80° C by providing good repeatability characteristics, uniform flow characterizes, and feedback characteristics. The wind velocity in the tunnel is regulated by regulating the speed of the fan coupled to a synchronous AC motor through the belt drive system by using a frequency inverter.

The schematic of the data acquisition from the turbine models in the text section of the wind tunnel and the wind tunnel used in this study are represented in Fig. 5a, b, and the schematic of experimentation is represented in Fig. 6. The instruments used in this study are shown in Table 3.

The performance of the WT was calculated using the brushless motor which acts as a generator that is connected to the turbine rotor. The generator power out was

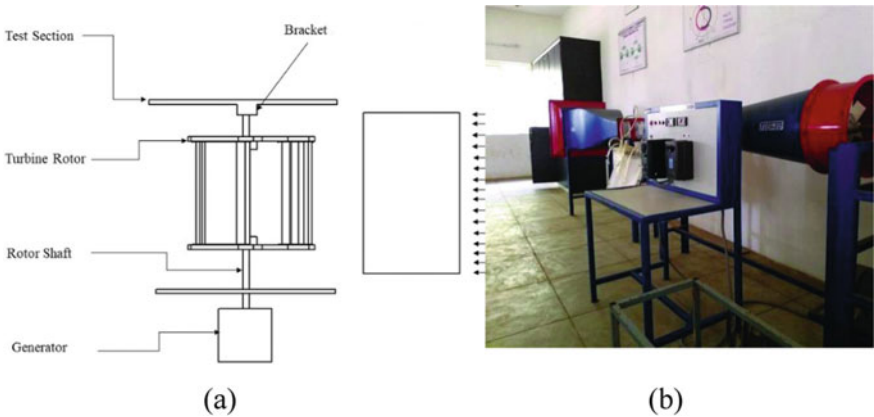


Fig. 5 a Schematic of the data acquisition in text section b wind tunnel used

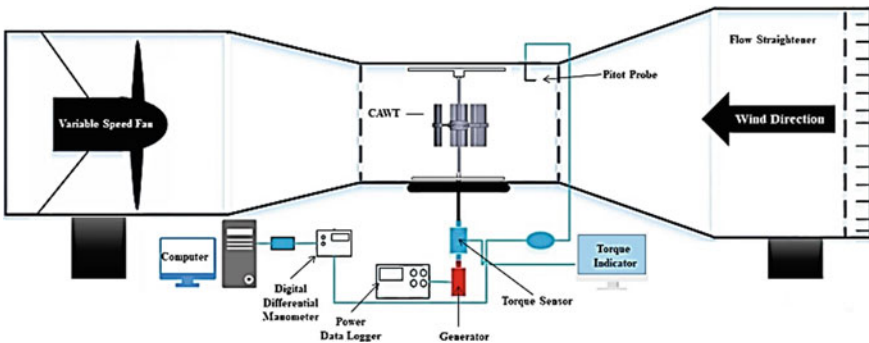


Fig. 6 Experimentation schematic

Table 3 Instrumentation

Experiment	Test	Level of accuracy
Pitot tube	Wind velocity	± 0.10 mmH ₂ O
Non-contact tachometer	Rotational speed	$\pm 0.10\%$
Brushless motor	Generator	$\pm 0.10\%$
Torsion cell	Torque	$\pm 0.10\%$
DMM data logger	Data logging	40.0 ppm (timing accuracy)

logged by using the DMM data logger, by using a photo tachometer the torque was measured, and by using a 0–20 N m torsion load cell, and the torque was evaluated.

The micro-CAWT characteristics curves are plotted from the logged data from the data loggers at every imposed value of air velocity in the test tunnel.

5 Results

The experimentation results in this study are reported in terms of dimensionless performance parameters. The average of acquisition data for 110 s of observations with 5 s of sampling time from the DAQ system is used in the construction of plots.

The plots with air velocity as a function for C_p , C_T , and C_M for the micro-CAWT with proposed configuration, micro-VAWT with Srihari et al. configuration [5], and base configuration are shown in Figs. 7, 8 and 9.

Fig. 7 C_p versus velocity plot

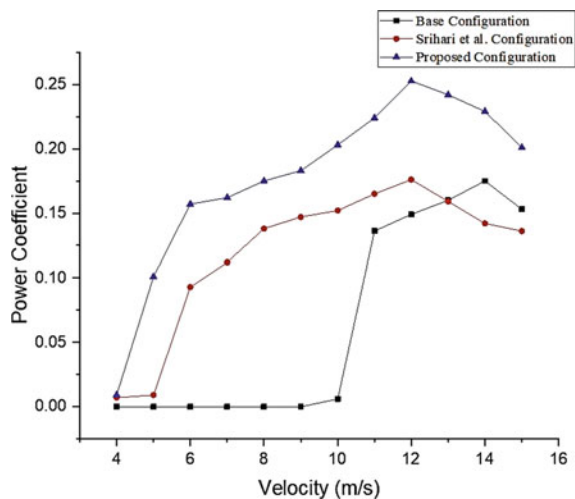


Fig. 8 C_T versus velocity plot

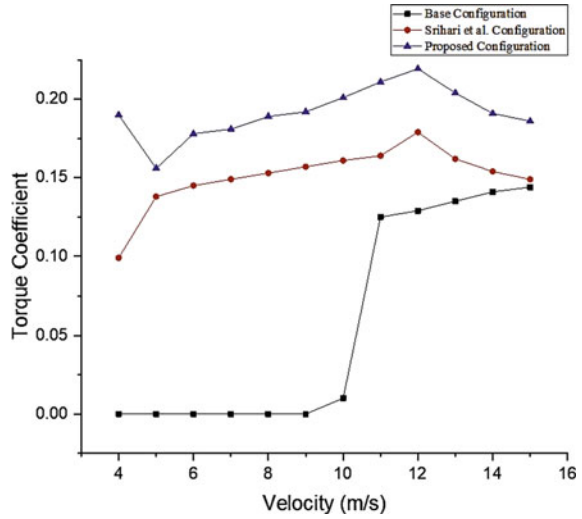
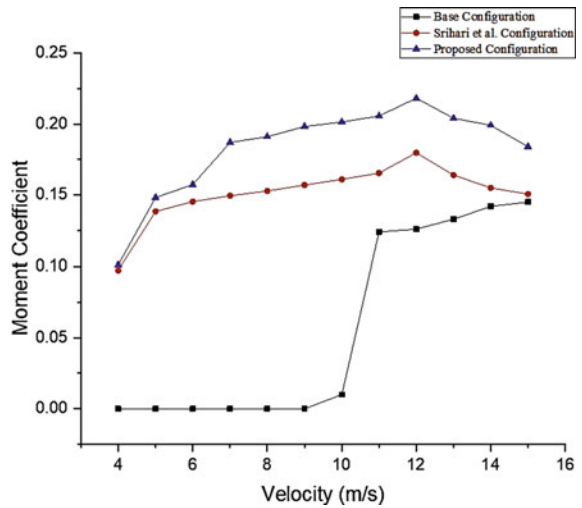


Fig. 9 C_M versus velocity plot



6 Conclusion

The auxiliary blade profile arrangement on the vertical configuration showed a great improvement in the overall performance of the micro-CAWT proposed in this study. The micro-CAWT proposed in this study shows higher values of C_p , 0.257 at 11 m/s. Whereas, the micro-VAWT proposed by Srihari et al. [3–5] shows C_p of 0.1705 at 12.1 m/s, and the standard VAWT shows C_p of 0.143 at 15.0 m/s. The values C_T and C_M for proposed micro-CAWT are 0.214 and 0.218, whereas for micro-VAWT

proposed by Srihari et al. [3–5] are 0.180 and 0.179 at 12 m/s and for micro-VAWT with base configuration are 0.144 and 0.145 at 15 m/s.

Following are the enhancements observed in the performance parameters:

1. The torque coefficient of the proposed micro-CAWT enhanced by 19.55% at 12 m/s wind velocity.
2. The power coefficient of the proposed micro-CAWT enhanced by 46.3% 12 m/s wind velocity.
3. The moment coefficient of the proposed micro-CAWT enhanced by 21.78% at 12 m/s wind velocity.

This enhancement in performance parameters shows indicates better self-starting abilities over the standard VAWT models which make its design suitable for the extracting wind energy potential in the random turbulence and wind characteristics regions.

Disclosure Statement The author declares that they have no potential conflicts.

References

1. Srihari PSVV et al (2019) Influence of slat and flaps arrangement on the performance of modified Darrieus wind turbine. In: AIP Conference Proceedings 2200(1): 020012
2. Srihari PSVV et al (2019) Experimental study on vortex intensification of gravitational water vortex turbine with novel conical basin. In: AIP conference proceedings, vol 2200(1), p 020082
3. Ebenezer NS, Srihari PSVV, Prasad CR, Appalaraju P, Tatahrishikesh A, Teja BS (2020) Experimental studies on damping behavior of nickel electroplated A356.2 alloy. *Mater Today Proc* 27(2):1038–1044. ISSN 2214-7853. <https://doi.org/10.1016/j.matpr.2020.01.388>
4. Srihari PSVV et al (2019) Experimental study on a shell and tube heat exchanger with novel self-agitating inserts. In: AIP conference proceedings, vol 2200(1), p 020039
5. Srihari PSVV et al (2019) Thermal performance investigation of MMC heat sinks for low CTE electronic components cooling. In: AIP conference proceedings, vol 2200(1), pp 020024
6. Gipe P (2004) *Wind power: renewable energy for home, farm, and business*. Chelsea Green Publisher
7. Li, Q., Maeda, T., Kamada, Y., Murata, J., Furukawa, K., Yamamoto, M. (2015). Effect of a number of blades on aerodynamic forces on a straight-bladed vertical axis wind turbine. *Energy* 90, 784795.
8. McLaren K, Tullis S, Ziada S (2012) Measurement of high solidity vertical axis wind turbine aerodynamic loads under high vibration response conditions. *J. Fluid Struct.* 32:1226
9. Kumar R, Raahemifar K, Fung AS (2018) A critical review of vertical axis wind turbines for urban applications. *Renew Sustain Energy Rev* 89:281–291. ISSN 1364-0321. <https://doi.org/10.1016/j.rser.2018.03.033>
10. Miao J, Liang SY, Yu RM, Hu CC, Leu TS, Cheng JC et al (2012) Design and test of a vertical axis wind turbine with pitch control. *Appl Mech Mater* 338343
11. Hirahara H, Hossain MZ, Kawahashi M, Nonomura Y (2005) Testing basic performance of a very small wind turbine designed for multi-purposes. *Renew Energy* 30:12791297
12. Krogstad, P.-Å., Lund, J.A., 2012. An experimental and numerical study of the performance of a model turbine. *Wind Energy* 15, 443457.
13. Cho T, Kim C (2012) Wind tunnel test results for a 2/4.5 scale MEXICO rotor. *Renew Energy* 42:152156

14. Monteiro JP, Silvestre MR, Piggott H, Andre JC (2013) Wind tunnel testing of a horizontal axis wind turbine rotor and comparison with simulations from two Blade Element Momentum codes. *J Wind Eng Ind Aerod* 123:99106
15. Ebenezer NS et al (2020) Mechanical and microstructural characterization nickel electroplated metal matrix composites. *Mater Today Proc* 27:1278–1281
16. Stanley Ebenezer N et al (2020) Experimental studies on damping behavior of nickel electroplated A356.2 alloy. *Mater Today Proc* 27:1038–1044

Novel Application of Electrolysis on Vehicle: Hydrogen Fuel Cell



Pavan Kumar Rejeti, Subrat Kumar Barik, and S. Balakrishna

Abstract The present world is looking for an alternate fuel source to reduce the use of conventional resources. This paper introduces a new technique to use the hydrogen produced by electrolysis used as fuel for the vehicle. The fuel is HHO gas (hydrogen and hydroxide) which is generated by electrolysis. This paper also introduces a special kind of technology, in which renewable energy sources like solar energy and H_2O are used to generate HHO gas. This fuel is having economical usefulness for our automobile industry. It will increase the efficiency of the engine and also reduce the emission to the environment. In this paper, the production rate of HHO gas which is influenced by the parameters like voltage, current, space between electrodes, time variation, and electrolyte concentration has been observed. In this research, the generation rates of wet and dry cells were also monitored.

Keywords Fuel cell · Electrolysis · Renewable energy

1 Introduction

HHO may be a well-liked and familiar gas generated within the fuel cell by the electrolysis of water. It consists of a mixture of two H_2 and O_2 gases. The basic chemical equation for conversation of water to HHO gas is $H_2O \rightarrow HHO$. The dissociation of water into hydrogen and oxygen is linked to electrolytic cells with a direct current aid. $2H_2O(g) + \text{Energy} \rightarrow 2H_2 + O_2 + \text{Power}$. By using the catalyst the chemical process may easily be speeded up and the selected compound does not

P. K. Rejeti (✉)

Department of Mechanical Engineering, NITR, Rourkela, Odisha, India

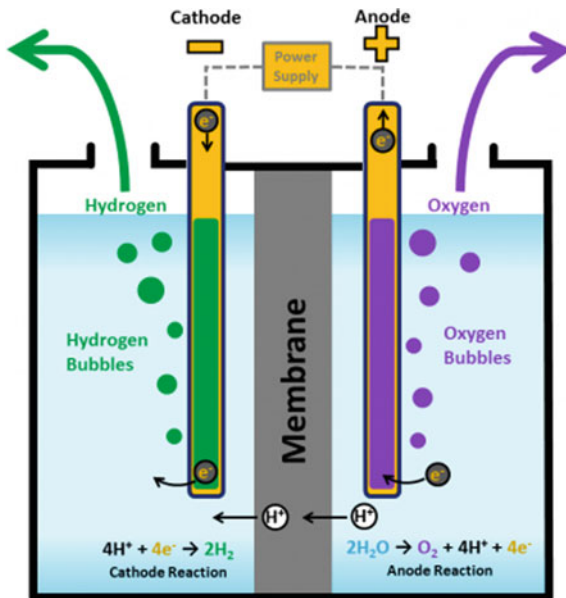
S. K. Barik

Department of Mechanical Engineering, Centurion University of Technology and Management, Gajapati, Odisha, India

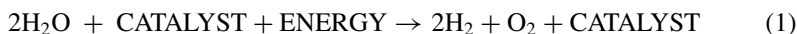
S. Balakrishna

Department of Mechanical Engineering, Sri Sivani College of Engineering, Srikakulam, Andhra Pradesh, India

Fig. 1 Electrolysis process



change its property during the process. The main aim of the catalyst is to reduce the amount of conversion energy available. The following chemical equation describes the function of the catalyst [1, 2].



As a result, electrolysis (Fig. 1):



This is completely not harmful to nature and this does not emit carbon dioxide. This technology can be installed in all kinds of engines like cars, trucks, buses ... etc. [3–5].

For HHO gas production the most principle is electrolysis in which the water splits into 2 hydrogens and 1 oxygen molecule. The hydrogen and hydrogen oxide gas is an extra boosting to the engine. Less relative molecular mass and high calorific value of HHO gas facilitate to enhance the potency of the engine. It is an extremely burnable gas and in the electrolysis method, it is the simplest for the generation. This method is clean and having less quantity of wastage and fewer emission. The speed of hydrogen is 0.098–0.197 ft/min (3–6 cm/min), the hydrogen gas is three times quicker than the other gas and oil explosion. Once a spark is generated in one end of the combustion cylinder, the gasoline is having a short period in the combustion cylinder and if it is not absolutely burnt in this time period then it simply goes out through exhaust and is lost. It is also desirable to ignite all of the gasoline when

it is under maximum compression in the combustion cylinder to induce the most quantity of energy out of it. Once the piston starts moving down the energy transfer from the explosion to the engine becomes less efficient. The hydrogen's higher burn temperature and explosive force are the foremost effective output so it cleans the soot that gathers within the engine (its like maintaining the engine uniformly) and you can achieve better mileage and less oil changes with a cleaner engine [6–8].

Using deep sub Debye length gap electrochemical cell, electrolyte free pure water electrolysis has been achieved when the gap between cathode and anode is even smaller than the length of electrical molecule motion, the double layer region of two electrodes will overlap with each other, resulting in a uniformly high electrical field distributed within the line gap. Such a strong electric field will greatly boost the transport of ions within the water, increase water self-ionization further and sustain the continuation of the total reaction and display little resistance between two electrodes [9–11].

So we are making a complete setup where HHO gas is used as fuel which is produced by the electrolysis process. Water is acting as secondary indirect fuel because from there only HHO gas is produced. Hence use of HHO gas is not only effective but also eco-friendly.

1.1 Effect of Emission to the Environment of HHO Gas

Adding HHO to an internal combustion engine leads to a quicker, additional combustion of the present fuel. Quicker and additional thorough combustion means additional energy is transferred mechanically to the engine, rather than wasted heat through the exhaust. This incorporates a positive impact not solely on power and fuel economy however conjointly on emissions [12, 13]. The quicker flame propagation speed of hydrogen is answerable for this and is commonly compared to a large “spark plug” within the engine that ignites all the flammable fuel. In summary, vehicle emissions are commonly comprised of five gases (the sixth applies to diesel-fuelled engines) [14, 15],

- HC
- NOX
- O₂
- CO
- CO₂

The elements of these are coming out of HHO gas can be reduced to maximum extend by different processes.

2 Methods of HHO Generation (Fuel Cells)

Generally, the HHO fuel cells are prepared in different ways. This electrolysis process is carried out in two ways those are HHO Wet fuel cell and HHO Dry fuel cell.

In this process, we have considered stainless steel as an electrode material because its having high corrosive resistance and good conductivity and also most important factor is the cost of material is less compared to other material like copper, aluminum, etc. [11, 12].

2.1 Preparation of HHO Wet Fuel Cell

Hydrogen and hydroxide gas will generate by the electrolysis process in this process the different elements are used they are described below.

1. Stainless steel plates
2. Glass container
3. Plastic strips
4. Bubbler

2.1.1 Experimental Procedure

The eight electrolysis plates are about 0.8 mm thick and 160 mm × 200 mm stainless steel. A 10 mm gas vent hole is drilled in each plate as shown in Fig. 2. The level of the electrolyte is always about 25 mm below the vent hole of the leg. In the bottom corner of each plate, 3 mm dia, liquid level equalization holes are drilled in such a way as efficiency loss due to current leakage between cells, but makes electrolyte filling and level equalization much simpler. A tiny SS component is welded to the two end plates for electrical contact, the arrangement of steel plates is like electrode which cathode, and anode and these plates having some of the electrode gap 2–3 mm gap, in this gap will be maintained at constant. The electrode cell will dip in the container and passing the electricity through the electrode then the H₂O will split into hydrogen and hydrogen oxide. In this cell, the production rate is very low compared to the dry cell and the construction of the wet cell as the following diagram.

2.2 Preparation of HHO Dry Cell

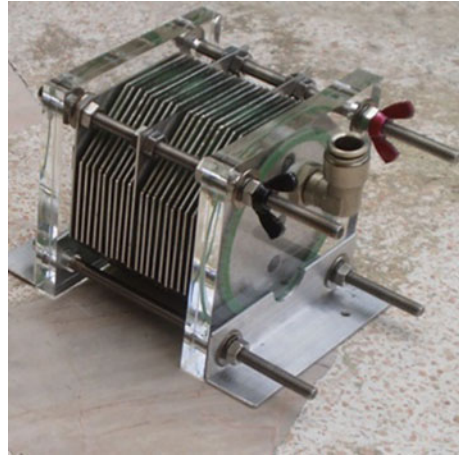
Hydrogen and hydroxide gas will generate by the electrolysis process. In this process, the different elements are used those are stainless steel plates with grade 316 L and battery of 12 V 5 A and hoses and electrical cables and fiber plates, ammeter and voltmeter and rheostat which are connected as per circuit diagram. The dry cell can



Fig. 2 Experimental set up

be operated on electrolysis. The electricity is passing through the electrodes then the hydroxide is generating on anode and hydrogen is generating on cathode then finally we will get a new form of gas HHO.

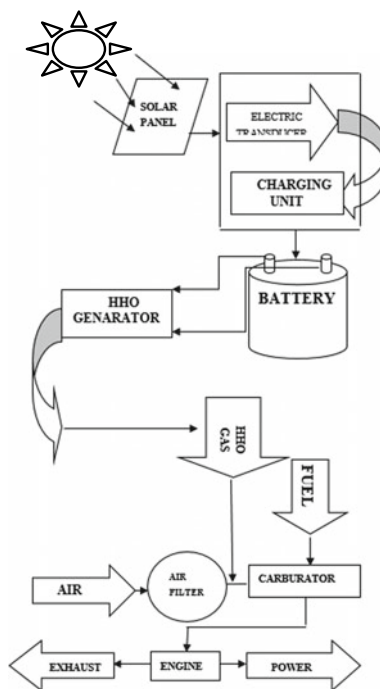
In preparation of dry cell first of all the stainless steel is made electrodes as per dimensions, the shape the electrode is an octagon shape. Its side length is 30 mm and the radius is 55 mm. According to the number of plates the production rate will be dependent, because the area of contact is increasing then increasing the production rate of HHO gas The stainless steel electrodes are chosen as its material composition relatively insert properly in alkaline solution in which the electrodes can be drilled by drilling machine the hole size is diameter 10 mm and each plate having two holes, on a hole is water flow and another hole is flowing of gas in this dry cell, total number of plates are 21 plates are used in 5 plates required to electricity by using D.C battery is arranged in an alternative manner in the cathode and another one is the anode. Then arrange these electrodes while the gap will be kept constant that is 2–3 mm. This gap will be covered with O-rings. Finally, a dry cell can be arranged by using nut and bolts, before arranging the cell, both sides are covered with fiber plates. It helps to control the leakage of water, and both ends can be arranged with nozzles by passing water and HHO gas for removing saturation of gas by using a muffler (Fig. 3).

Fig. 3 Dry cell

2.3 Flow Chart of Cyclic Process of HHO Generation

The process is carried out with the generation of HHO by renewable energy sources like solar energy and water; those are utilizing cyclically. The connections are developing as following block diagram. This block diagram shows clearly the process of generation of HHO gas, the sun energy focusing on the solar panel in which the intensity of energy is converted into electrical energy by using the charging unit it is connected to the battery it stores the DC electrical energy. Then the DC supply is connected to electrode cell, one is connected with positive terminal and another one is connected with negative terminal and finally, HHO gas will be generated it will supply to intake manifold it's construction will be following in block diagram. And at a time fuel and brown gas will supply to the engine in the combustion chamber it will burn at maximum power developing in the engine, because of the HHO gas atomic weight is very less so it is having high calorific value so it will burn 2–3 times faster than the gas oil (petrol). In the flow diagram finally the maximum output will be developing, the crankshaft will be connecting with a crank which is rotating at high speed, this crank will be connecting with a sprocket this is attached to the back wheel hub of the bicycle with proper alignment then finally the power can transmission to rear wheels (Fig. 4).

Fig. 4 Flow chart of the cyclic process of HHO generation

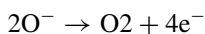
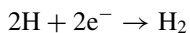
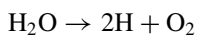


3 Testing and Results

3.1 Experimental Calculations

The experimental calculations have been carried out by two steps with room temperature and taking 1 atm pressure.

1. Half-reactions take place at the anode and the cathode.



2. Calculation of the number of moles of electrons that are transferred.

- Ampere \times Time = Columbus
- 1 F = 96,485 Columbus
- 1 F = 1 mol of electron

The following are the calculations that have been made to see the amount of hydrogen and oxygen gas is produced inside the final prototype HHO generator over an hour. The electric current is the driving factor in this calculation considering the motorized bicycle alternator is sending an average of 90 amps to the generator.

$$90 \text{ A} \times 3600 \text{ s} = 32,4000 \text{ coulmbus}$$

$$32,4000 \text{ coulmbus} \times \frac{1 \text{ faraday}}{96485 \text{ colum}} = 3.3580 \text{ faraday}$$

$$3.3580 \text{ faraday} \times \frac{1 \text{ mole electron}}{1 \text{ faraday}} = 3.3580 \text{ faraday}$$

From the stoichiometry taken from the balanced half-reactions, we obtain the moles of hydrogen and oxygen produced.

$$3.3580 \text{ mole } e^- \times \frac{1 \text{ mole } H_2}{2 \text{ mole } e^-} = 1.679 \text{ mole } H_2$$

$$3.3580 \text{ mole } e^- \times \frac{1 \text{ mole Oxygen}}{4 \text{ moles of } e^-} = 0.8395 \text{ mole } O_2$$

Using the ideal gas equation $PV = nRT$ we get the value of the volume of each gas

$$V = nRT/P$$

where

n = number of moles

R = Boltzmann constant = 0.08206

T = Temperature in Kelvin = 300 K

- The volume of hydrogen gas:

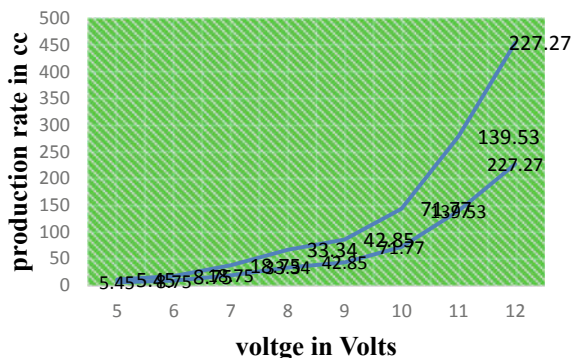
$$\frac{1.169 \text{ mole } H_2 \times 0.08206 \text{ L atm/mole K} \times 298}{1 \text{ atm}} = 41.05 \text{ L of } H_2.$$

The volume of oxygen gas:

$$\frac{0.8395 \text{ mole } O_2 \times 0.08206 \text{ L atm/mole K} \times 298}{1 \text{ atm}} = 20.529 \text{ L of } O_2$$

These calculations have shown that for a current of 90 A during 1 h, the calculations of electrolysis of water yield 41.05 L of hydrogen gas and 20.529 L of oxygen gas.

Fig. 5 Effect of production rate with change voltage



3.2 Effect of Production Rate with Change Voltage

The production of hydroxyl is influenced by the applied voltage. With a 0.1 mol concentration of KOH, the hydrogen evolution reaction and oxygen evolution reaction can be examined over a flat plate stainless steel electrode at room temp. of 27 °C. The applied voltage ranges from 5 to 12 V and the resulting graphs shows that the rate of output of hydrogen gas rises steadily with increased applied voltage. The likely explanation is that the uniform charge density increases on the flat plate electrode surface (Fig. 5).

3.3 Effect of Production Rate with Change Current

The production of hydroxyl is influenced by the applied current. With the same condition taken before the resultant graph as shown below shows that the rate of production of hydrogen gas gradually increases with the increase in applied current. The reason is the uniform charge density increases on the surface of the flat plate electrode. As shown in the Fig. 6 the production rate also depends on the current. At constant voltage, as current increases gas production rate also increases the production rate of HHO gas varying of the production rate with constant voltage remaining

Fig. 6 Effect of production rate with change current

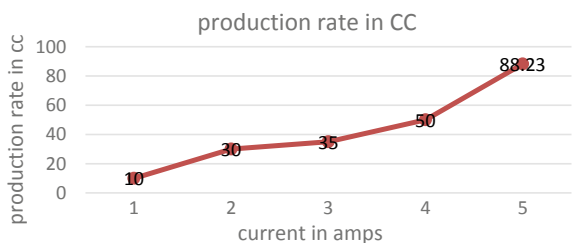
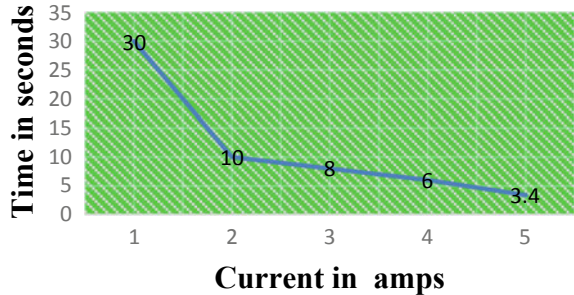


Table 1 Effect of production rate with change current

Current (A)	Production rate (cc)
1	10
2	30
3	35
4	50
5	88.23

Fig. 7 Current with a graph time variation

constant at 12 V, the experimental values are taken by generation rate of HHO gas (Table 1).

3.4 Effect of Time on Production Rate

Analysis of the continuous output of hydroxyl gas for flat plate electrodes with a continuous increase in electrolysis time is very interesting. The rate of output of hydroxyl gas increases steadily at the beginning of electrolysis and becomes maximum within 5 min. After that, very little variation in the rate of gas output fluctuates. The results obtained are illustrated in Fig. 7. It is observed that the output of hydroxyl gas is initially reached to a maximum of 200 cc/min and thus achieves a stable state. Under current experimental conditions, the overall output of the stainless steel electrode has shown a reasonable degree of stability by performing the experimental procedure then obtaining the following values, the time variance at constant voltage with the variation of current with time changes.

3.5 Current and Voltage with Time Variation

See Figs. 7 and 8.

Fig. 8 Voltage with time variation graph

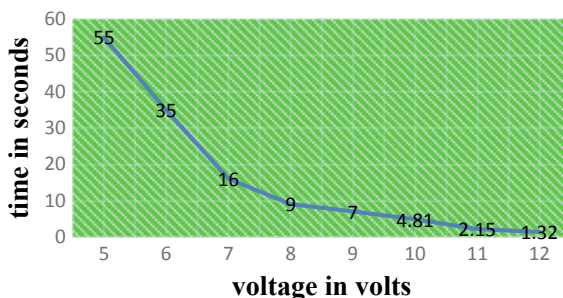


Table 2 Effect of electric concentration

S. No	Amount of fuel consumption	Distance covered
1	50 ml	1.218 km
2	100 ml	2.436 km
3	150 ml	3.412 km

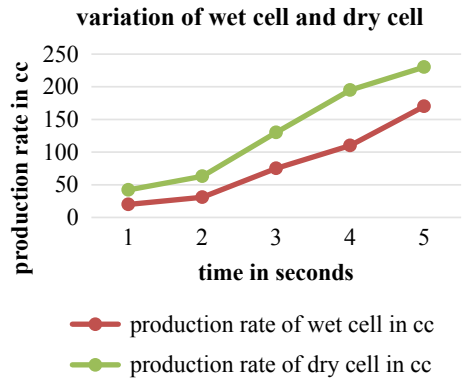
3.6 Effect of Electrolyte Concentration

The concentration of the electrolyte is carried by constant voltage 12 V battery and 3 A current is adjusted by the rheostat connected parallel to the load and the digital multimeter connected in series to the electrolyte at constant current. In this system, the concentration of the electrolyte is an increase from 0.1 to 2 mol concentration in rainwater, the catalyst increases the ionic conductivity of rainwater increases. In pure water, no electrons flow into that water, so with the increased conductivity of rainwater, the resistance of the overall electrolyte system is reduced thus reduces the effect of the over voltages value on electrode load. The acidic and alkali solution used to be limited and by the practical applications, it will be affected by corrosion of the electrode surface, the hydroxyl gas production gradually increases with increasing the electrolyte concentration (Table 2).

3.7 Analysis of Wet and Dry Cell

The analysis of wet and dry cells have concluded that the main difference in production rate in the wet cell production rate is low compared to the dry cell, the production rate of these cells at varying time are discussed as in Fig. 9.

Fig. 9 Analysis of dry and wet cell



3.8 Analysis of Mileage with and Without Brown Gas

Total distance covered without brown gas is = 7.066 km

Total distance covered with using brown gas is = 13.385 km

$$\begin{aligned} &\text{Percentage of increasing efficiency} \\ &= \frac{13.385 - 7.066}{7.066} \times 100 = 85.9\% \end{aligned}$$

From the above data considering the mileage of vehicle increasing with 80–90% with the engine mixing of fuel and brown gas, and also some of the modifications to consider the above design modification takes place in the system to increase the efficiency of the engine (Tables 3 and 4).

Table 3 Mileage without brown gas

Time (s)	Wet cell production rate in cc	Dry cell production rate in CC
5	20	42
10	31	63
15	75	130
20	110	195
25	170	230

Table 4 Effect of production rate with change current

S. No.	Amount of fuel consumption with brown gas	Distance covered
1	50 ml	2.150 km
2	100 ml	4.715 km
3	150 ml	6.515 km

4 Conclusion

The cylinder pressure is increased once combining with HHO and the amount of flame development and fast combustion was shortened. With the rise in HHO content, the cyclic variations were reduced, combustion stability is improved. Partial burning and alternative abnormal combustion phenomena are controlled. The generated gas is mixed with fresh air simply before getting into the mechanical device. The exhaust is sampled by a gas analyzer and therefore the exhaust constituents and their concentrations are evaluated. Therefore the subsequent conclusions may be drawn.

- HHO cell can be simply integrated with existing engine systems
- The combustion potency has been increased once HHO gas has been introduced to the air/fuel mixture, consequently reducing fuel consumption.
- The concentration of oxide has been reduced to fifty percent.
- The typical concentration of carbon monoxide gas has been reduced to twenty percent.
- The nitrogen oxide concentration is reduced about fifty four percentage.

Brown' gas (HHO) has recently been introduced to the motorcar business as a replacement supply of energy. The current work proposes the look of a replacement device connected to the engine to integrate associate HHO production system with the internal combustion engine. The planned HHO generating device is compact and might be put in within the engine compartment. The auxillary device was designed, made, integrated and tested on an IC engine.

The research shows a positive aspect of the use of HHO gas as an alternative fuel. From the last years, scientists are inventing so many renewal sources which will replace the use of petrol and diesel. Here we have tried the same thing but differently. Previously hydrogen gas is stored in the tank from outside and being used as fuel for vehicles. Here we have attached the setup to the vehicle so that both generation of HHO gas and its use in the engine can be obtained. Various practical tests conformed about the increment in the acceleration of the vehicle. It helps economically for the present and future generation, for reducing the utilization of petrol and diesel, now HHO gas generated by renewable energy sources like H₂O with help of electricity, in future other researches can avail to get it from different sources. It is not only eco-friendly but also helps in increasing in the life of engine oil more than 2–3 times than normal one and also shows the variation in the mileage of 2 stroke petrol engine with brown gas and without brown gas, that is reducing the consumption of petrol is less up to 60–70% and also reducing the emission to the environment up to 0.2 ppm (parts per million). The generation of HHO gas by dry cells compared to the wet cell method is increasing the production rate up to 50–60%. The HHO is compatible with all bikes and scooters below 1000 cc. Further research will glow the hidden side of this method.

References

1. Derbeli M, Barambones O, Sbita L, Derbeli M, Barambones O, Sbita L (2018) A robust maximum powerpoint tracking control method for a PEM fuel cell power system. *Appl Sci* 8:2449
2. Kerviel A, Pesyridis A, Mohammed A, Chalet D, Kerviel, A, Pesyridis A, Mohammed A, Chalet D (2018) An evaluation of turbocharging and supercharging options for high-efficiency fuel cell electric vehicles. *Appl Sci* 8:2474
3. Choi H, Shin J, Woo J (2018) Effect of electricity generation mix on battery electric vehicle adoption and its environmental impact. *Energy Policy* 121:13–24
4. Eriksson ELV, Gray EMA (2017) Optimization and integration of hybrid renewable energy hydrogen fuel cell energy systems—a critical review. *Appl Energy* 202:348–364
5. Hosseini SE, Wahid MA (2016) Hydrogen production from renewable and sustainable energy resources: promising green energy carrier for clean development. *Renew Sustain Energy Rev* 57
6. Das LM (2016) Hydrogen-fueled internal combustion engines. *Compend Hydrog Energy* 177–217
7. Hosseini SE, Andwari AM, Wahid MA, Bagheri G (2013) A review on green energy potentials in Iran. *Renew Sustain Energy Rev* 27:533–545
8. Ayad MY, Becherif M, Henni A (2011) Vehicle hybridization with fuel cell, supercapacitors and batteries by sliding mode control. *Renew Energy* 36:2627–2634
9. Giorgi L, Leccese F (2013) Fuel cells: technologies and applications. *Open Fuel Cells J* 6:1–20
10. Offer GJ, Howey D, Contestabile M, Clague R, Brandon NP (2010) Comparative analysis of battery electric, hydrogen fuel cell and hybrid vehicles in a future sustainable road transport system. *Energy Policy* 38:24–29
11. Aceves SM, Berry GD, Weisberg AH, Espinosa-Loza F, Perfect SA (2006) Advanced concepts for vehicular containment of compressed and cryogenic hydrogen. In *Proceedings of the 16th world hydrogen energy conference 2006 (WHEC 2006)*, Lyon, France, 13–16 June 2006
12. Hibino T, Kobayashi K, Ito M, Ma Q, Nagao M, Fukui M, Teranishi S (2018) Efficient hydrogen production by direct electrolysis of waste biomass at intermediate temperatures. *ACS Sustain Chem Eng* 6:9360–9368
13. Davis C, Edelstein B, Evenson B, Brecher A, Cox D (2003) Hydrogen fuel cell vehicle study. Presented at the Panel on Public Affairs (POPA), American Physical Society, 12 June 2003
14. Bhosale AC, Mane SR, Singdeo D, Ghosh PC (2017) Modeling and experimental validation of a unitized regenerative fuel cell in electrolysis mode of operation. *Energy* 121:256–263
15. Atkinson K, Roth S, Hirscher M, Grünwald W (2001) Carbon nanostructures: An efficient hydrogen storage medium for fuel cells. *Fuel Cells Bull* 4:9–12

Influence of Process Parameters on Microstructural and Mechanical Properties of Friction Stir Processed AA6063/Zn Composite



Pavan Kumar Rejetti and Sandhyarani Biswas

Abstract The main aim of this research is to modify the microstructure and mechanical properties of the AA6063 alloy by reinforcing zinc using friction stir processing (FSP). In this paper zinc (Zn) powder particles are used as a reinforcement in the material of AA6063 by the process FSP. In this paper, the effect of FSP process parameters such as tool rotational speed, feed rate on the tensile strength, microhardness and surface roughness of AA6063 was studied. The results obtained in this study proved that FSP significantly modifies the microstructure, tensile, microhardness and surface roughness of the AA6063/Zn alloy.

Keywords Aluminium alloy · Friction stir processing · Microstructure · Mechanical properties

1 Introduction

On the basis of friction stir welding (FSW), which was invented in 1991 by TWI (The Welding Institute) of the United Kingdom the friction stir processing is obtained. The material is in a solid state through the Friction stir processing (FSP) so is called as a solid-state process. FSP consists of a cylindrical tool with a pin in relation with the plate thickness. The tool can be moved in required direction when the pin has penetrated in the plate and the shoulder is intercourse to the plate. The plate starts melting below its actual melting point because of the generated heat by the intense penetration of the pin and as a result, the grains in that area will be recrystallized. To homogenizing and refining the grain microstructure of the metal plate FSP is considered as an emerging and result oriented process. In the super plasticity era, friction stir processing is marked as a beneficial process as it uplifts the super plasticity in many aluminium alloys. FSP is therefore both a thermal process and a plastic deformation even though there is no bulk fusion. Thermocouple measurements during FSP of aluminium alloys suggested that, in general the temperatures are reached in

P. K. Rejetti (✉) · S. Biswas

Mechanical Engineering Department, National Institute of Technology Rourkela, Rourkela, Odisha, India

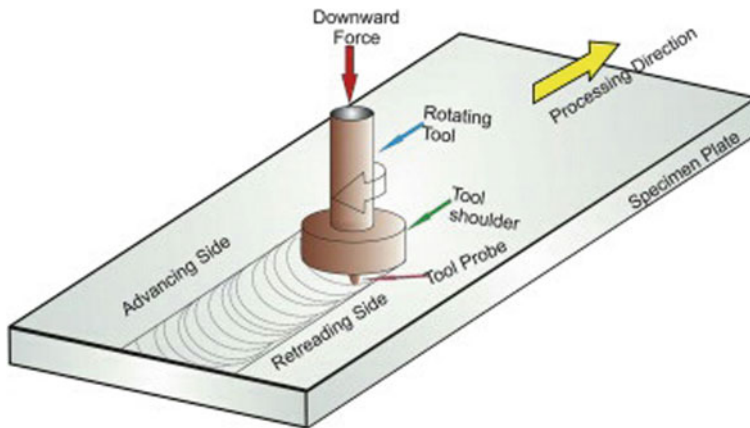


Fig. 1 Schematic illustration of FSP

below 500 °C, this temperature is below the melting point of aluminium alloys (Fig. 1).

2 Literature Review

Sen et al. are examined that the impacts of FSP parameters on elasticity of AA6063 aluminium combination prepared plates. The outcomes show that the process parameters are rotational speed (RS), and cross speed (TS) is the main factor in the elasticity of FSP aluminium compound [1].

Chandan et al. are researched that the impact of FSP measure boundaries on microstructure and effect quality of AA6063. From those investigations, the triple-pass FSP test demonstrated exceptionally fine consistently appropriated composite silicide's in a grid of aluminium with no break to that of a solitary pass, two pass, the base metal which additionally coarse microstructure and second pass have finely disseminated silicide's yet not uniform. A solitary pass microstructure demonstrated some surface imperfections with the conveyance of silicide shows intermittence. So the mechanical properties are legitimately identified with the fine microstructure. The effect quality doesn't show any improvement, the effect obstruction of the FSP test had been diminished when contrasted with the base metal [2].

Joyson Abraham et al. are explored that the FSP strategy is to create SiO₂ particulate fortified AA6063 composites. The different grooves are used to fill the SiO₂ particles (0, 5 and 10 vol.%). The metallurgical characteristics, hardness were enhanced after FSP because of the change in the microstructure. Perceptions show that, hardness is expanded because of the alteration, separating, and merging of the SiO₂ fragments at the mix region. It is observed as that the equal scattering of SiO₂ is resulted in high hardness, complex microstructure adjustment because of FSP [3].

Amirtharaj et al. are researched that the AA6063 surface property is adjusted by strengthening B_4C molecules through FSP. The appropriation of B_4C molecules into the surface is significant for the great surface property. Distinctive tool pin shapes, for example, threaded cylindrical and square pin are utilized to break down the best circulation of B_4C into the outside of the base metal through various additive packing strategies. A solitary pass FSP with tool revolving speed 1200 rpm, travel speed 40 mm/min, and axial power 10 kN are kept consistent. The microstructure of the FSP sample prepared with the square pin profile tool shows fine molecule conveyance of B_4C than the round and hollow pin profile tool [4].

Saravanan et al. are researched that the Magnesium MMCs have generally excellent mechanical and physical properties, for example, high quality, low thickness and high damping limit [5].

Vikash et al. are considered that the impacts of process parameters in FSP on the rigidity of AA6063. In the FSP, the vital properties such as elasticity, grain size of the structure and hardness are upgraded. The tool pin, shoulder of the device has a huge part in the arrangement of frictional heat. Tool revolving speed and pass over speed greatly affect FSP. With an expansion in instrument cross speed, the rigidity increment. With an expansion in tool traverse speed, the grain size likewise diminished [6].

Rathee et al. are exploring the blend of AA6063/SiC surface composites through FSP is given. A solitary pass FSP was completed on AA6063-T6 plates with SiC reinforced particles utilizing consistent tool rotational speed of 1120 rpm and differing cross velocities of 30, 40, and 50 mm/min with the 2° tilt angle of tool. Optical microscopy was utilized to consider the impact of traverse speed on the microstructure of the created surface composites [7].

Gan et al. "Development of microstructure and hardness of aluminium after Friction stir Processing": In the stir region, fine equated out grains are acquired because of complete recrystallization. The thermomechanical influenced region (TMAR) consists not many equated molecules because of inadequate strain deformation. The heat affected region (HAR) holds a similar structure as the base material. The hardness graph shows a "U" shape because of a nearby material mellowing happening in the SR, due to heat delivered by the FSP [8]. Rao Santha et al. investigated tensile and microhardness properties of AA6061/TiB₂ metal matrix composite fabricated by FSP and the tool rotational speed is the major influenced parameter to improve the UTS and microhardness [9]. Salavaravu et al. investigated that the tool rotational speed is the major effect on tensile strength, microhardness and surface roughness of the AA6063 FSW joints [10]. Zhao et al. have investigated that UTS were not upto that of the BM at lower tool movement speeds for each single and double pass FSP. With increasing tool movement speed, the UTS exaggerated bit by bit then became more than that of the BM. The strain values were all not upto that of the BM [11].

It had been summarized from the literature that influence of Zinc particles on the microstructure and mechanical properties of composites by FSP was not rumored. Further, several researches are targeted on solely mechanical properties. Thus a trial was created to manufacture the AA6063/Zn composite by FSP and investigated the

result of process parameters i.e. tool rotational speeds and feed rates on mechanical properties and microstructure of composites.

3 Experimental Procedure

The material used in this work is AA6063 the chemical compositions and mechanical properties are placed in Tables 1 and 2. The aluminium alloy AA6063 plates are prepared for conducting FSP in the dimensions of $250 \times 60 \times 6$ mm in size is shown in Fig. 2a, b. In this process, different tool rotation speeds are 1000, 1200, 1400, 1600 rpm and different tool feed rates are 22, 45 mm/min and constant tool tilt angle 1° are used. The reinforced material is Zinc microparticles that are used and it is shown in Fig. 3. The non-consumable taper cylindrical tool is made of high-speed steel tools and the dimensions of the tool pin are 6 mm diameter, 5.8 mm length and 18 mm shoulder diameter. The plates are prepared for FSP for different sizes of holes drilled by drilling machine on the AA6063 work plates and to fill up the holes with the reinforced material Zinc, those work plates are shown in Fig. 4.

After FSP, the processed plates are shown in Fig. 5. The samples are taken for the investigation of tensile strength, microhardness and microstructures. The tensile specimens are prepared as per ASTM-E8 standards to the required dimensions which are horizontal to the direction of FSP as shown in Fig. 6. The tensile test is conducted on UTS-INSTRON 9900. Microhardness is conducted on the cross-section of the FS processed plate. The microstructural observation was carried out at a cross-section of the stir zone to the FSP processed direction.

Table 1 AA6063 chemical composition

Elements	Mg	Si	Fe	Mn	Cu	Cr	Zn	Zr	Ti	Al
wt %	0.45	0.35	0.15	0.02	0.010	0.09	0.04	0.02	0.02	Balance

Table 2 Mechanical properties of AA6063 aluminium alloys

Alloy	Temper	Proof stress 0.20% (MPa)	Tensile strength (MPa)	Shear strength (MPa)	Elongation A50 (%)	Hardness Brinell HB	Hardness Vickers HV	Fatigue endur. limit (MPa)
AA6063	T6	210	245	150	12	75	80	150

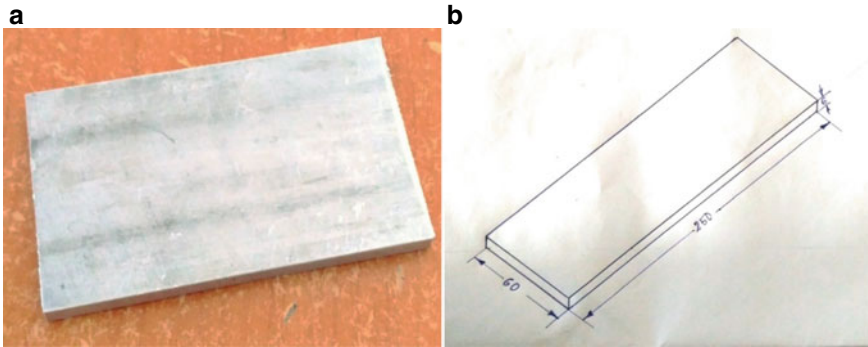


Fig. 2 a AA6063 plate. b Dimensions of plate

Fig. 3 Zinc powder



4 Results and Discussion

4.1 Mechanical Properties

4.1.1 Effects of Process Parameters on Tensile Strength

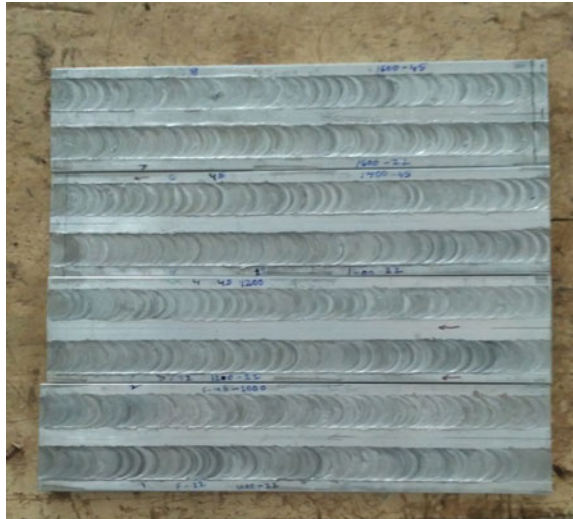
Transverse tensile strength properties of FSW joints are represented in Fig. 7. Three specimens were tested at every condition giving averagely three results. The joint made-up with a tool rotation speed of 1600 rpm and feed rate of 45 mm/min showed higher tensile strength compared to other joints made up by another tool speeds and feed rates. When put next to the feed rate of 22 mm/min with the feed rate of 45 mm/min, the tensile strength is raised with the surge in motility speed.

The tensile strength at 1600 rpm is higher when compared to other speeds i.e. 1000, 1200, 1400 rpm. At the higher tool rotational speed (1600 rpm), the sufficient heat is generated in between tool and workpiece, the base material is going to plastic deformation state and the reinforced particles are stirred properly in stirred zone.

Fig. 4 Filled with zinc reinforcement



Fig. 5 After FSP



4.1.2 Effects of Process Parameters on Microhardness

The results of microhardness testing of FSP zone shows that the hardness in the Nugget zone is less compare to the base material zone. The FSP zone is softer than



Fig. 6 Specimens for tensile test (ASTM-E8)

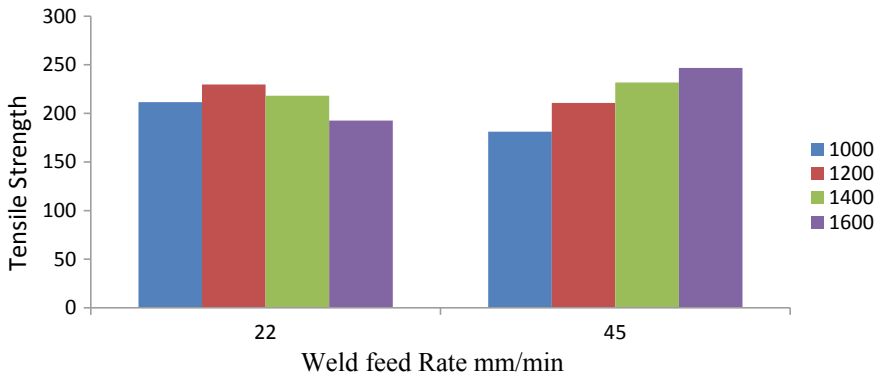


Fig. 7 Effect of tool feed rate on ultimate tensile strength

base material zone and the microhardness is increasing with increase in tool rotational speed.

The feed rate 22 mm/min having high microhardness compared to the feed rate 45 mm/min. The reason of microhardness is high at low feed rates high heat is generated the material is stirred properly. The microhardness results are shown in Fig. 8.

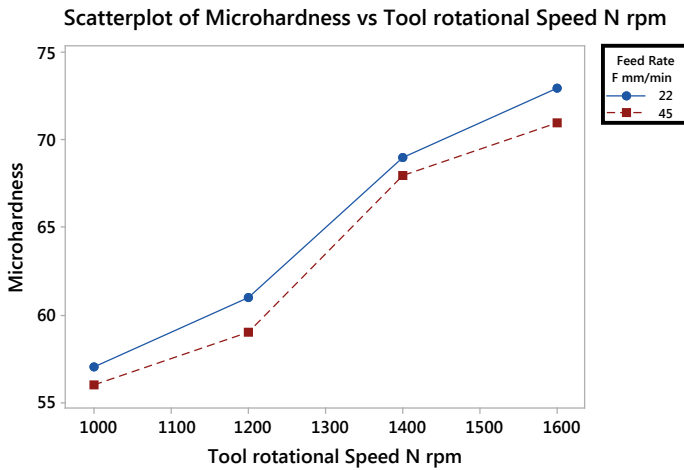


Fig. 8 Effect of tool rotational speed versus microhardness

4.1.3 Effects of Process Parameters on Surface Roughness

The surface roughness is the measure of the finely spaced micro irregularities on the surface. The surface roughness is related to the appearance of the processed plate. The tool rotational speed increases as the surface roughness value decreases. The feed rate increases as the surface roughness value increases. The reason is the sufficient heat is generated and material is stirred properly in the stir zone. The FSP plates are shown in Fig. 5. The surface roughness is low at tool rotational speed of 1600 rpm and feed rate 22 mm/min, the results are exhibit in Fig. 9.

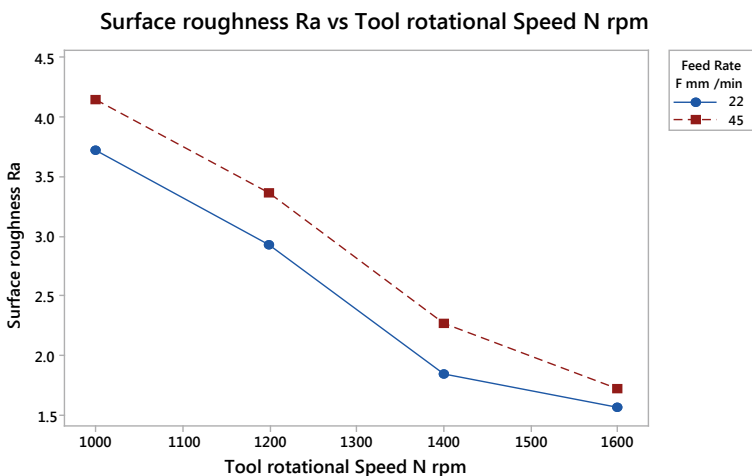


Fig. 9 Effect of tool rotational speed versus surface roughness

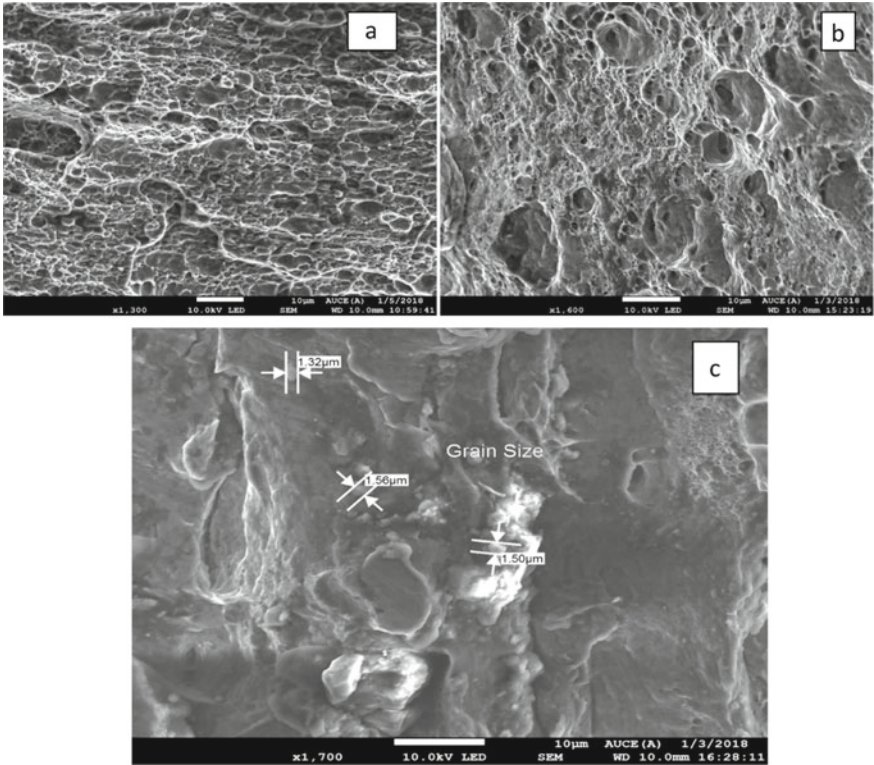


Fig. 10 a SEM micrographs of parent material. b FSP at 1600 rpm and 45 mm/min. c SEM micrographs grain size FSP at 1600 rpm and 45 mm/min

4.2 Microstructure Evaluation

The microstructures obtained from SEM of both base material and FSP plates are represented in Fig. 10a, b respectively. In result it is observed that the grain structure of base material is found to be coarsed whereas in FSP plates the grain structure is homogenous. In FSP plates the size of grains have reduced as shown in Fig. 10c. The material flow, severe plastic deformation and high temperature give a result as more grain refinement and recrystallization in FSP plates. The alloy is showing fine dimples in it which further gives a great impact on increase of mechanical properties.

5 Conclusion

In this study, an attempt has been made to inspect the effects of friction stir processing on the composite of AA6063/Zn. From this piece of work, several conclusions are

attained. The average tensile strength is improved than the base metal. Greater tensile strength is achieved at high rotational speeds of 1600 rpm and feed rate of 45 mm/min respectively. The microhardness and surface roughness are occurred at the high tool rotational speed and low feed rate. For changing the microstructure of AA6063-T6 alloy and homogenized grain structure FSP is considered as a better process.

References

1. Sen U, Sharma K (2016) Effects of process parameters of friction stir processing on tensile strength of AA6063 aluminium alloy. *JSRSET* 2(2):785–789
2. Singh CD, Singh R, Kumar N (2014) Effect of FSP multipass on microstructure and impact strength of AA6063. *AIJRSTEM* 140–145
3. Joyson Abraham S, Chandra Rao Madane S, Vettivel SC (2016) Wear behavior of SiO₂ particulate reinforced AA6063 surface composites using friction stir processing. *Int J Adv Eng Technol VII(II)*:321–325
4. Amirtharaj D, Rajamurugan G, Sivachidambaram S, Dinesh D. Wear and microstructural characteristics of friction stir processed aluminium 6063
5. Saravanan RA, Surappa MK (2000) Fabrication and characterization of pure magnesium-30 vol.% SiC P particle composite. *Mater Sci Eng A* 276(1):108–116. [https://doi.org/10.1016/S0921-5093\(99\)00498-0](https://doi.org/10.1016/S0921-5093(99)00498-0)
6. Vikash R, Kaushik N (2016) Microstructure evolution of friction stir processed aluminium alloy 6063. *Int J Res Educ Sci Methods (IJARESM)* 4(8). ISSN: 2455-6211. Impact Factor: 2.287
7. Rathee S, Maheshwari S, Siddiquee AN, Srivastava M. Fabrication of AA6063/SiC surface composite via friction stir processing
8. Gan WY, Zhou Z, Zhang H, Peng T (2014) Evolution of microstructure and hardness of aluminium after friction stir processing. *Trans Nonferrous Met Soc China* 24:975–981
9. Rao Santha D et al (2017) Process parameters optimization for producing AA6061/TiB₂ composites by friction stir processing. *Strojnický Casopis* 67(1):101–117. <https://doi.org/10.1515/scjme-2017-0011>
10. Salavaravu LR, Dumpala L (2020) Multi-objective optimization of submerged friction stir welding process parameters for improved mechanical strength of AA6061 weld bead by using Taguchi-L18-based gray relational analysis. In: Voruganti H, Kumar K, Krishna P, Jin X (eds) *Advances in applied mechanical engineering. Lecture notes in mechanical engineering*. Springer, Singapore. https://doi.org/10.1007/978-981-15-1201-8_103
11. Zhao H, Pan Q, Qin Q, Wu Y, Su X (2019) Effect of the processing parameters of friction stir processing on the microstructure and mechanical properties of 6063 aluminum alloy. *Mater Sci Eng A* 751:70–79

Self-sustainable Toilet System



Adithya Kameswara Rao, S. Karthi, K. Vedhanarayan, A. Ssmrithi,
P. Niranjana Kumar, Kevin Mathew Thomas, and Mayank Kapur

Abstract Sanitation in India has become one of the major national problems that need to be tackled urgently. The absence of a proper sewage system exposes our ecosystem to its harmful effects and becomes nothing more than open defecation. Open defecation, which is currently widely practised adds to the incremental risk of many diseases such as UTIs, diarrhoea, and cholera. In general, sanitation refers to providing facilities and services for the safe disposal of human waste. The safe disposal of human excreta is of paramount importance for low-income populations' health and welfare and the prevention of pollution to the surrounding environment. Our project implements an innovative yet feasible closed-loop sanitation system that reduces sewage generation whilst producing essential fuel, construction material, and fodder components.

Keywords Sanitation · Open defecation · Closed-loop sewage treatment · Sustainability

1 Introduction

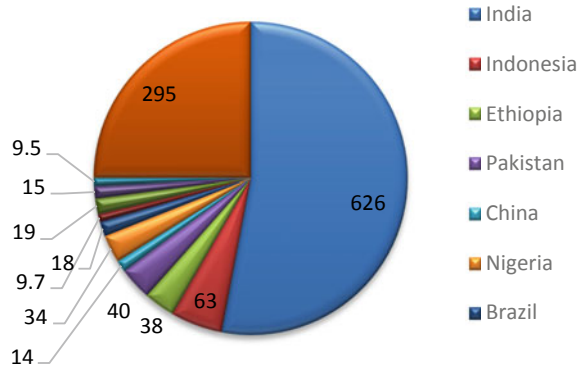
1.1 Background

Hygiene in India has been one of the critical national challenges to be resolved as a matter of urgency. Without a proper sewage system, our environment is vulnerable to its adverse effects. Open defecation, which is currently widely practised adds to the incremental risk of many diseases such as UTIs, diarrhoea and cholera. In general, hygiene applies to the provision of proper handling of human wastes. The appropriate handling of human excreta is of vital significance for low-income communities' health and well-being and the prevention of environmental degradation.

A. Kameswara Rao (✉) · S. Karthi · K. Vedhanarayan · A. Ssmrithi · P. Niranjana Kumar
Production Engineering, National Institute of Technology, Tiruchirappalli, Tiruchirappalli, India

K. M. Thomas · M. Kapur
Mechanical Engineering, National Institute of Technology, Tiruchirappalli, Tiruchirappalli, India

Fig. 1 Share of open defecators by country, in millions [2]



About 60% of the 1.2 billion people in the country are still defecating in the open. More than 1 million toilets have been built since then. Studies have shown that even where constructed, the vast majority, particularly in rural areas, are not used. In some situations that is because clean water and sewers are still not connected to the bathroom. More specifically, however, there has not been a health education initiative to change transparency and sanitation culture in the region.

The social and economic effects of open defecation are various. It can build a vicious disease loop and high healthcare expenses. Repeated bouts of diarrhoea are the leading cause of children's malnutrition. According to WHO statistics, 827,000 people die each year from inadequate water and hygiene in low and medium-income countries, comprising 60% of all diarrheal deaths. In 432,000 of these deaths, inadequate sanitation is considered to be the primary cause. The fatalities of 297,000 children under five could be prevented by better sanitation and hygiene [1]. This needs real-life on-site sanitation solutions (Fig. 1).

Our product minimises sewage generation and thus contains an alternative waste processing device necessary for sustainable waste management. It also reflects the dire need for sustainable infrastructure and identifies the consequences of an intact human nutrient cycle (Fig. 2).

A realistic solution to the current unsustainable system is an intact human food cycle. Our product takes account of this challenge and provides high hygiene standards by converting slurry to reusable flush water and dried faeces, thereby preventing waste products from being released. The product also overcomes the limitations of sewage systems that require massive facilities and high maintenance. These challenges emphasise the socioeconomic challenges of maintaining facilities and treatment of flushed water.

Our product reduced sewage production and produced critical resources for food, building materials, and fodder compounds by handling waste efficiently. By using safe disposal practices in urban slums, we mitigate the environmental effects of uncongenial sanitation disposal and inappropriate drainage systems while ensuring the availability of essential sanitation services to underprivileged sections. The adverse environmental impact of waste is greatly minimised by optimising flush

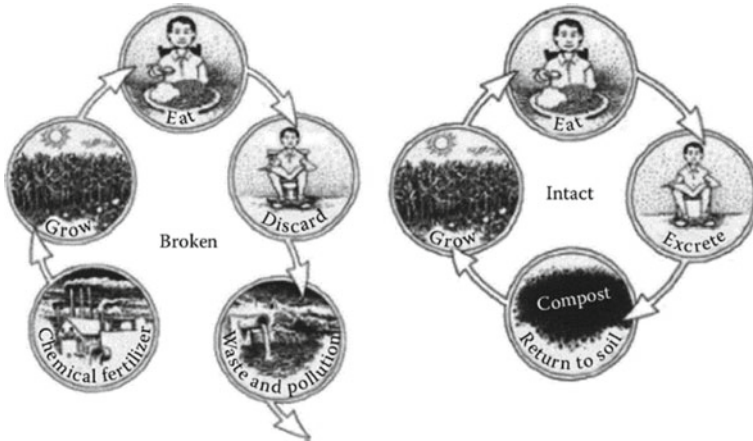


Fig. 2 Human nutrient cycle [3]

water and faecal matter in safe and usable forms. A closed-loop system is provided. It has a tremendous effect as it is aimed at all areas that lack access to toilets.

Rapid implementation of this modern off-grid sanitation system could dramatically reduce the human and economic burden of unsafe health care worldwide, including the deaths of half a million children under the age of 5 per year and more than \$200 billion wasted results of healthcare expenses and reduced wages.

1.2 Existing Solutions

Dry San Hygienic Rural Toilet: The Dry San Hygienic Rural Toilet [4] is a squat-based toilet system with three ports, constructed by IIT Bombay for solids, urine, and washing water. This technology was developed for populations in India with less access to flushing water because liquids’ isolation from solid waste enables them to be decomposed aerobically over time and eventually be used as manure.

Sani Solar Toilet System: Sani Solar Toilet [5] is a comprehensive sanitary solution with a capability of up to five persons built for a single household. It operates without electricity and water. Without external drainage facility, the sanitation waste is collected, processed, and sanitised. This product has a method in which the liquid and solid excreta are stored in individual spaces. To minimise its weight and scent, solid waste is dried using solar radiation.

Nano Membrane Toilet: The toilet [6] was created by a team in Cranfield University at the Melinda and Gates Foundation’s reinvention of the toilet expo, in the form of an environmentally friendly low-cost toilet for the underprivileged. The bathroom treats the waste in a thermal chamber where solid is vaporised to volatile gases.

Table 1 Drawbacks of the existing solutions

Existing solutions	Drawbacks
Dry San Hygienic Rural Toilet	<ul style="list-style-type: none"> • There is a separate urinary and faecal matter opening in this toilet. The design expects people to sit in a specific way • The device is readily vulnerable to collapse because of the people's incompetence, resulting in holes being blocked • Need to be maintained regularly. The composting phase of the faecal matter is disrupted, especially during the rainy season • The composting technique is prolonged, and the results are reached after six months
Sani Solar Toilet System	<ul style="list-style-type: none"> • The functionality of the system relies on the continually varying external environmental influences • Requires periodic maintenance • Operates only in hot climates, since solar power is climate-prone
Nano Membrane Toilet	<ul style="list-style-type: none"> • The toilet is flushed only if the toilet seat is set flat • The mechanisms that follow are dependent on the toilet seat being shut, which cannot be necessarily expected from every user. If the user fails/forgets to shut it down, the system's whole objective is lost • The efficiency of the mechanism employed in separating the faeces and urine is still under research • To convert faeces into gases via pyrolysis process, it needs massive quantities of hot energy

1.3 Novelty of the Proposed Solution

Our solution is environmentally friendly and also requires minimum efforts to be put in by the user. The extra padding added increases the versatility of the toilet. Our system optimises the usage of renewable resources while maintaining efficiency at the same time. Due to the closed water cycle, people living in water-scarce areas can use the toilets with its full function. Vacuum extraction requires minimal energy, and it eliminates much of the water in the system. Any inefficiencies that lead to a loss of water in the system is recharged by the water present in liquid wastes, minimising the need for additional inputs. Our solution becomes a better product by addressing the drawbacks in Table 1.

2 Technical Design

2.1 Overview

We intend to resolve this problem by designing a self-sustainable, environmentally, and user-friendly waste-free system that includes an efficient and economic sewage treatment process explained hereafter for waste treatment and transformation into a

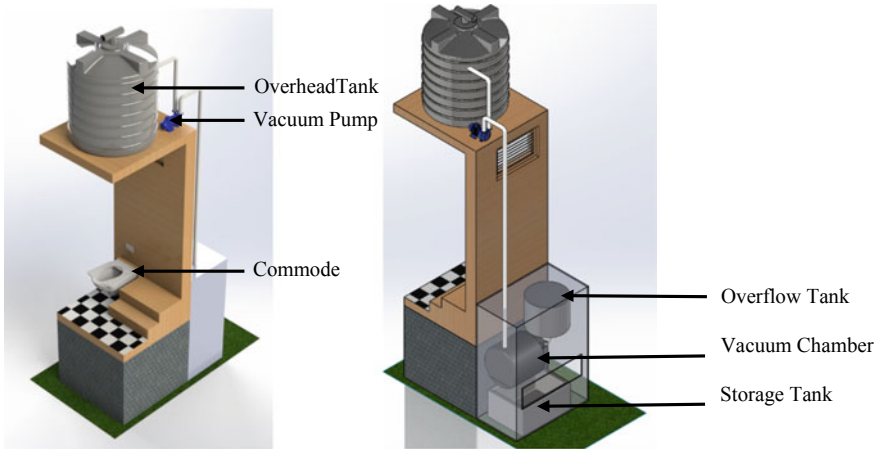


Fig. 3 Isometric view of the entire system

helpful product. The system handles waste within a low pressure vacuum chamber, thereby reusing the water and drying the solid waste, ensuring maximum efficiency. An automated flush is incorporated as it requires less effort and user support while maintaining routine toilet cleaning. The device is also versatile enough to be used in Western and Indian ways made possible by the attached paddings. Our product reduces sewage generation whilst producing essential resources for fuel, construction material, and components for fodder (Fig. 3).

2.2 Principle

Water boils when the vapour pressure equals the pressure in the surroundings. Since the pressure and the temperature are both directly proportionate, water would have a higher boiling point at high pressure and a lower boiling point at low pressure. The water continues to boil at a temperature below 100 °C when maintained below ambient conditions using a vacuum. The boiling point is lowered to 273 K by keeping the pressure under 0.006 atm.

$$P = \exp(20.386 - 5132/T) \tag{1}$$

2.3 Waste Management

Biogas: Dried faeces are combusted to produce biogas via the pyrolysis process. The biogas produced is a rich source of fuel [7].

Construction Material: Bricks with dry faeces increase the brick's thermal insulation property and decrease the weight. Additions of faecal matter up to 20% do not make a significant practical difference [7].

Animal's Protein Supply: Pilot modules for feeding Black Soldier Fly larvae with faeces are being created. The mature flies will then be a protein source for chickens [7].

3 Components Description

3.1 Commode with Customized Paddings

The toilet bowl designed is modified to be used as either western or eastern type by switching the padding to an upright or horizontal position. The paddings have a small intrusion at the bottom to fit the toilet bowl. The toilet is intentionally wall mounted for ease of cleaning the ground [8]. Additionally, steps on one side can be used to climb and sit on the toilet when it is to be used in a squatting position in eastern toilets.

The bowl incorporates a piezoelectric sensor [9] under the seat to sense pressure or intensity changes. The bowl is 15 in. longer than usual, so that urine always falls inside the bowl when used as both eastern and western type latrines. The top of the bowl is placed 16 in. above the ground level considering ergonomics.

3.2 Overflow Tank

Along with the flush water, the faeces enter the overflow tank where it momentarily stays until it reaches a certain height. The tank is fitted with a floatation-based valve control to allow faeces to escape the tank into the vacuum chamber at regular intervals. The maximum quantity of faeces with flush water and urine that are collected in the overflow tank is 90 L approximating the volume of slurry peruse to be about 9 L, the time taken per cycle to be 56 min and the average time a person takes in the bathroom to be 6 min.

3.3 Automated Flush

The flush is triggered by sensing the individual withdrawal's weight through a piezo-electric sensor [9] below the toilet bowl. This reduces the possibility of an unflushed condition, which is among the most significant unhygienic open defecation factors.

3.4 Overhead Tank

The overhead tank is mounted on the roof, serving as a reservoir for the reused flush water and an open-air condensing chamber for the vacuum tank's vapour. The tank is also linked to a chimney to maintain constant atmospheric pressure in the tank, which is essential for the open-air condensation. The tank is painted black on its outer surface to act as a solar heater to replenish the lost heat due to the possible leakage of heat in the accumulated water caused by rapid evaporation and condensing cycles.

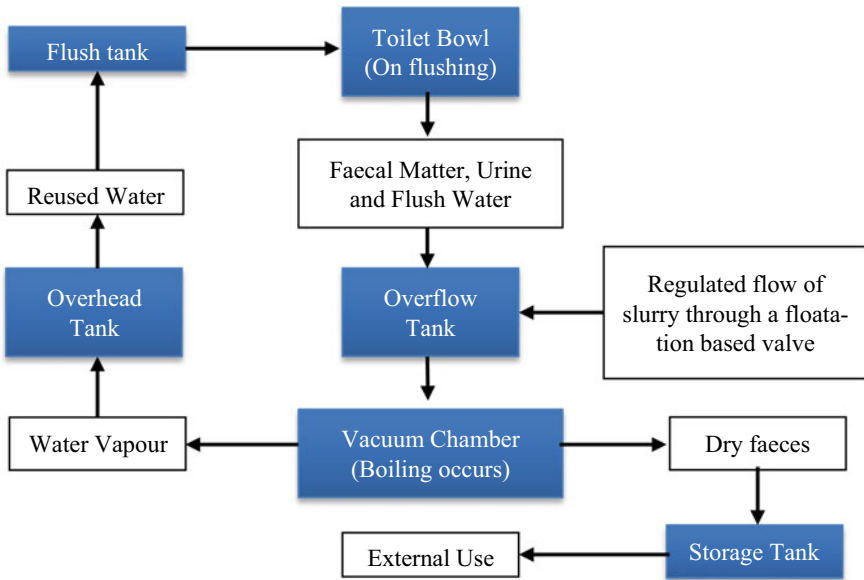
3.5 Vacuum Chamber

The vacuum tank is the chamber in which the slurry is subjected to low pressure where the water begins to boil at room temperature because the reduced pressure is less than the vapour pressure of water at room temperature (25 °C). A mechanical valve avoids the additional entry of slurry from the overflow tank. The tank comes with other equipment such as a humidity sensor that senses the need to turn off the vacuum pump and a vacuum control unit to re-pressure the device as it is not possible to recover the initial conditions with the inflow of slurry from the overflow. The tank is made of steel painted black and not in any adiabatic condition, thereby maintaining the slurry inside higher than room temperature.

3.6 Vacuum Pump

An external vacuum pump [10] is set up where the suction end is fitted to the vacuum chamber and the free end to the overhead tank. The pump maintains the low pressure inside the chamber, which is the cause of boiling and acts as a water pump to the overhead tank.

4 Workflow Diagram



5 Simulation and Analysis

5.1 Volumetric Analysis

Considering the law of conservation of mass before water boiling and vacuum pump activation.

Initial volume of water: X L

At 25 °C and 1 atm pressure,

Molar volume of 1 mole of water vapour = 18 ml

At operating conditions (0.0313 atm and 25 °C),

Molar volume of 1mole of water vapour = 0.57 L

Let the suction rate of the pump be V L/min,

Actual volume occupied by water vapour,

$$X * 1000 \text{ ml} * 0.57 \text{ L}/18 \text{ ml} = X * 31.667 \text{ L}$$

Net time taken for pump to completely evacuate the system,

$$X * 31.667 / V \text{ min}$$

The specifications of the pump used are: Suction rate [10] = 67 L/s

$$\text{Volume of tank} = 120 \text{ L}$$

$$\therefore \text{Time taken} = 55 \text{ min}$$

Average time taken for a person to defecate = 5–6 min.

$$\text{Volume of water flushed} = 7.5 \text{ L}$$

$$\text{Volume of slurry} = 9 \text{ L}$$

Approximated time to fill overflow tank: $(120 \text{ L}/9 \text{ L}) * 5 \text{ min} = 70 \text{ min}$.

\therefore The time taken by the process to complete (55 min) is well within limits.

5.2 CFD Analysis

The boiling of the slurry was simulated and tested in Ansys Fluent.

Given conditions:

$$\text{Volume flow rate} = 60 \text{ L}/\text{min}$$

$$\text{Internal operating pressure} = 0.006 \text{ atm}$$

The simulation shows the different stages inside the chamber (Fig. 4).

5.3 Validation

A basic model has been set up to verify the feasibility of the concept. The model employed a glass jar, a vacuum pump connected with a pipe. The glass has been tightly sealed using a rubber seal to ensure the vacuum operation is smooth. The

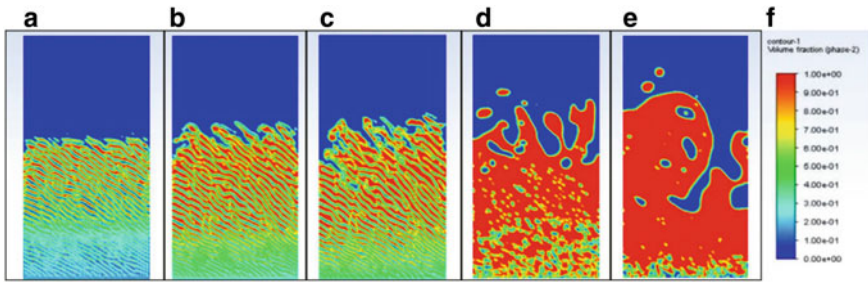
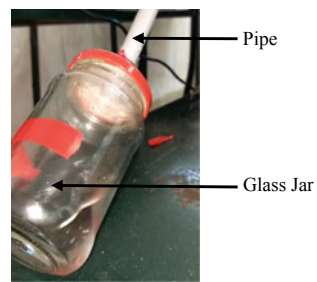


Fig. 4 Different stages occurring in the vacuum chamber. **a** Boiling starts. **b** Bubbles rise. **c** Solid moves down. **d** Steam rises. **e** Water content is removed. **f** Legend

Fig. 5 The basic set up consisting the jar and the pipe



glass is filled with water and some edibles to simulate the experimental conditions. The water evaporated successfully leaving behind the solid particulate. Figure 5 showcases the setup.

5.4 Cost Analysis

See Table 2.

5.5 Material Analysis

See Table 3.

Table 2 Cost of different components used in the system

S. No.	Components	Cost (Rs.)
1	Water tank	7225
2	Vacuum pump	4000
3	Overflow tank	3000
4	Vacuum chamber	7400
5	Commode	4195
6	Valve	1200
7	Electronic equipment (sensor + light + exhaust + fan)	150 + 1000 + 70 + 400
8	Structural cost	3000
	Total	31,640

Table 3 Materials used for different components in the system

Components	Material used
Commode	Ceramics
Padding	HDPE plastic
Pipes	PVC
Overhead tank	PVC
Vacuum chamber	Stainless steel

6 Results

6.1 Advantages

- The versatility of the toilet is increased. The extra padding added can be used as both eastern and western type latrines.
- As it is not essential to make flush water as clean, it can be flushed again. The water does not contain any harmful pathogen due to rapid evaporation and condensation. Our system optimises the usage of renewable resources while maintaining efficiency at the same time. Due to the closed water cycle, people living in water-scarce areas can use the toilets with its full function.
- The automated flush system reduces the risk of unflushed toilets, one of the critical unhygienic causes in currently operated public toilets. The mounted automatic flush of sensors removes the need for daily servicing, which is not the case in most existing systems.
- Because vacuum extraction eliminates much of the water in the system, any inefficiencies that lead to a loss of water in the system is recharged by the water present in liquid wastes, minimising the need for additional inputs.
- As moving parts are not in close contact with the faecal elements, the system is less likely to be polluted.

- The installation and further repairs are not required or expensive as the separation is done. Our system is environmentally friendly and also requires minimum efforts to be put in by the user.
- Dried poop can be used in rural areas to feed insects that can, in turn, be used to provide chickens with food or help turn the dried slurry into manure.

6.2 Future Prospects

- The equipment depends on an external power supply for the vacuum pump and other equipment to operate. An alternate power source to the toilet has to be provided.
- The device needs to be rendered more suitable for handling other items such as plastics, sanitary towels, etc.

References

1. World Health Organization (2018) Sanitation [Internet]. Fact sheet, p 1. Cited 17 Dec 2018. Available from: <https://www.who.int/news-room/fact-sheets/detail/sanitation>
2. World Health Organization. Sanitation [Internet]. Fast facts. Available from: https://www.who.int/water_sanitation_health/monitoring/jmp2012/fast_facts/en/
3. Jenkins JC (2005) The humanure handbook: a guide to composting human manure. Joseph Jenkins, Inc., White River Junction, VT. Distributed by Chelsea Green Pub.
4. Munshi K (2013) Dry sanitation system. Patent application No. 3711/MUM/2013
5. 3P Technik sanitation homepage. <https://3psanitation.de/the-product-sani-solar/?lang=en>
6. Ravndal K, Hennigs J, Barrington D, Collins M, Engineer B, Kolios A, Mcadam E, Parker A, Talaia P, Tiereny R, Tyrrel S, Williams L (2018) Human user testing of the nano membrane toilet
7. Wikipedia. https://en.wikipedia.org/wiki/Reuse_of_excreta
8. Hindware homepage. <https://www.hindwarehomes.com/>
9. Changzhou right measurement and control system co homepage. <http://www.ritcl.net/>
10. Advanced research systems homepage. <https://www.arscryo.com/vacuum-pumping-systems>

Novel Water-Conserving Faucet Attachment



Adithya Kameswara Rao, R. Jayendran, P. Niranjana Kumar,
J. Sudarsana Jayandan, and K. Harikrishna

Abstract Water wastage can be attributed to people's lethargy and laxity while using water. Water lost every day by taps and faucets is around 125 million litres in India, critically important to a country that does not have access to clean water for its 163 million inhabitants. Our product reduces water wastage when people utilize taps and faucets for their daily activities and controls the time of water flow during operation for more efficient usage of the limited freshwater resources. It also encourages users to utilize their limited resources effectively and efficiently in a time-bound manner.

Keywords Water conservation · Faucet attachment · Torsional springs · Non-concussive faucets

1 Introduction

1.1 Background

WWF states that two-thirds of the world is to be impaired by the scarcity of freshwater by 2025 [1]. UN-INWEH, a think tank of the United Nations, predicts that the world's demand and supply will be at 40% water deficits [2].

15.7% of water is used through faucets, 26.7% is used for toilet and bathing purposes, and 13.7% of water is wasted through leakage. A concussive, manually closed faucet can waste up to 1 L of water per day. Every Indian, on average, waste 0–45 L of water per day, which amounts to about 30% of the water requirements of a person per day [3].

The water wasted through taps and faucets, per day, in India amounts to about 125 million litres, which is deeply concerning for a nation where 163 million people have no access to clean water [3]. Worldwide, already more than 2 billion people live

A. Kameswara Rao (✉) · R. Jayendran · P. Niranjana Kumar
Production Engineering, National Institute of Technology Tiruchirappalli, Tiruchirappalli, India

J. Sudarsana Jayandan · K. Harikrishna
Mechanical Engineering, National Institute of Technology Tiruchirappalli, Tiruchirappalli, India

in areas of water stress. And UN-INWEH estimates that 40% of people will come under water stress in the next decade [2].

Water mismanagement has become a primary concern in our households and the public amenities, especially when it hits hard during summer. One of the major causes is our lethargy and laxness to close taps, especially during chores like face wash, handwash, brushing and so on. Existing faucets designed for water conservation, such as percussive faucets, faucet aerators, and automatic taps, have shortcomings of their own.

We cannot control the time and amount of water flow during each operation, which leads to inconvenient usage of water-conserving faucets. This further leads to the wastage of freshwater and reluctance to adopt such water-conserving devices. Our product addresses the aforementioned problem.

Our product is a non-concussive, retrofittable attachment for the existing taps, which allows us to regulate water flow for each application, which significantly reduces the wasting of water.

1.2 Existing Solutions

Faucet Aerators [5]: Aerators are small attachments fixed at the end of the faucet. It regulates water flow and increases pressure, therefore conserving water and preventing the splashing of water. It can reduce the water flow rate significantly, but the manual closing design adding with people's lethargy leads to water wastage.

Percussive Faucets [6]: Faucets work based on push-button mounted on a spring. The water is released, and the spring is squeezed when the top is pushed down. The water source is steadily closed as the spring retracts. The time at which the water flow is stopped cannot be changed, and the user might push the button multiple times to procure water of their requirement. This results in a massive loss of water used.

Automatic Faucets [7]: Sensors on the neck of the faucet senses the hand and releases water by opening the solenoid valve. The faucet stops releasing water when the hand is pulled away from the sensor. This automated tap is more disadvantageous as it ceases during washing movements. The solenoid valve is vulnerable to water backflow, and a broken valve leads to water leakage. The solenoid valve, therefore, requires a high degree of maintenance. Because of the factors mentioned above, users find these sensor faucets extremely uncomfortable.

Water Atomizer [8]: This is a retrofittable attachment to the tap's mouth, which atomizes water. Nozzles help utilize the water flowing through with maximum efficiency for our purposes. However, it does not address people's lethargy, who turn on the tap and let it flow frivolously and impetuously. Also, it is very costly.

Table 1 Comparison with existing solutions

Existing solutions	Drawbacks	Our solution
Faucet aerators	Leads to water wastage due to absence of self-closing capability	Has self-closing capability
Percussive faucets	The time of the water flow cannot be changed, hence it might have to be pressed multiple times	Time of flow can be controlled intuitively by the extent of rotation of the lever
Automatic faucets	Requires heavy maintenance as it incorporates solenoid valve and is very costly Involves electrical components which are susceptible to damages	Requires low maintenance Fully mechanical Inexpensive
Water atomizer	Absence of self-closing capability and is very costly	Offers self-closing capability at a very low cost

1.3 Comparison

Table 1 represents the existing solutions and their drawbacks.

1.4 Novelty of the Proposed Solution

Our solution utilizes a constant torque spring which enables the user to intuitively operate the faucet for the required time. It also offers non-concussive features at a very low cost addressing aforementioned drawbacks.

2 Technical Design

2.1 Overview

Our solution as shown in Fig. 1 is not to replace current taps because removing them will create waste, take time and expense. Our approach aims instead to act as a retrofittable system for existing taps that enable them to be auto-closing within a time interval and be water-conserving. We use a constant torque spring to retract the knob right as soon as it is left at any angle. This helps ensure that when the user turns the lever, the knob retracts back at a constant speed, giving the user sufficient time to use the running water. The turn of the knob defines the time and volume of the water flow. The user will be able to determine the time interval at which the tap closes intuitively, thus uses only the appropriate amount and conserves water in the process.

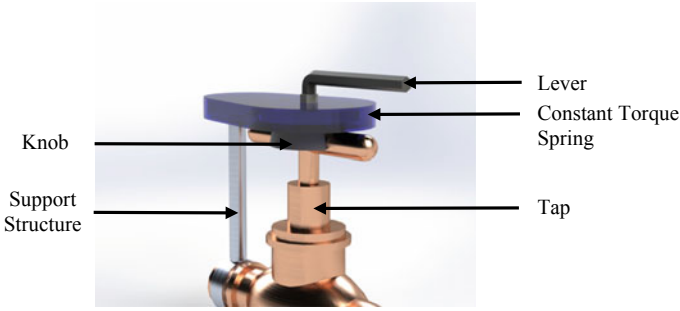


Fig. 1 Isometric view of the attachment

2.2 Principle

The torque of the torsional spring (Fig. 2) is calculated with the formula given below.

$$T_{spring} = K(\theta_i - \theta_o) \tag{1}$$

where

K = Stiffness of the spring.

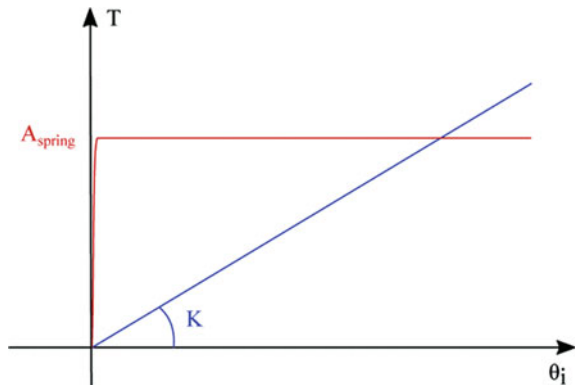
θ_i = Initial position of the spring.

θ_o = Final position of the spring.

For a constant torque spring, the sum of the torques for each turn must match the output torque. There is an intrinsic constraint to the spring, and the following is written:

$$T_o(t) - (\sum T_{spring,i}) = h(x, t) = 0 \tag{2}$$

Fig. 2 Torque versus angle for a constant torque spring (red) and linear spring (blue) [4]



Output torque is a function of time and sum of the torques is directly proportional to deflection [4]. The amount of deflection by the knob defines the time at which the knob returns to the original position. In other words, the amount by which you deflect determines the amount by which the water flow stops.

2.3 Design Parameters

The torque required to open/close the knob entirely is constant. Time of water flow depends on the angle turned. The characteristics of the attachment can be modified by altering the design parameters [9].

- Spring stiffness (K): The stiffness of constant torque spring can be increased to provide the same amount of deviation (θ) for larger torque.
- Spool distance (S): Spool distance is the distance between the storage drum and the output drum. It should be greater than the sum of radii of both the drum. Decreasing spool distance decreases the drum diameter and coil diameter (Constituting one arm of the pivot) and hence provides higher torque for the same amount of deviation (θ).
- Length of lever arm: By increasing the length of the lever arm (Constituting the other arm of the pivot), higher torque can be generated for the same amount of deviation (θ) provided by the user.

3 Components Description

3.1 Lever

The lever lets the user control the turning of the tap. It is connected to the larger drum of torsional spring placed inside the casing.

3.2 Casing

The blue region shown in Fig. 3 represents casing. It consists of the constant torque spring and the cap. The whole case is mounted on the tap so that it is not rotated by turning the lever.

Fig. 3 Lever along with casing

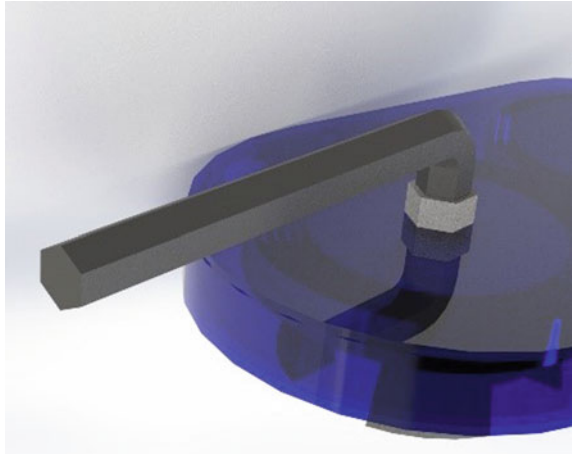


Fig. 4 Cap



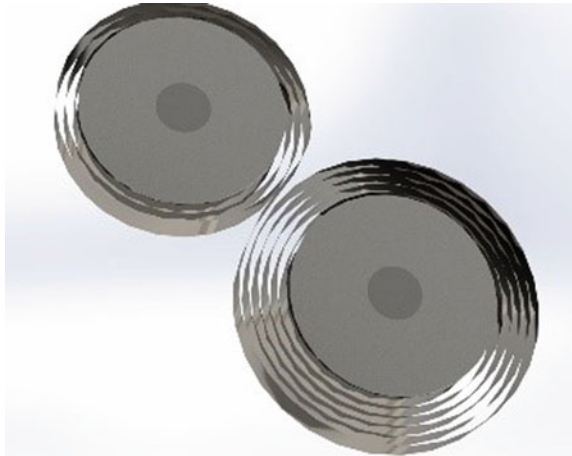
3.3 Cap

The cap as shown in Fig. 4 serves as a link between the tap and the attachment. It is compatible with the different knobs of existing faucets. It connects the knob of the tap to the larger drum of the constant torque spring.

3.4 Constant Torque Spring

Constant torque spring as shown in Fig. 5 is a flat pre-stressed strip of spring material shaped into a spiral with a nearly constant radius and stored on a compact output drum.

Fig. 5 Constant torque spring



The inherent stress resists the loading force when the strip is stretched/shortened, similar to the typical extension spring, except at an almost constant speed. The free end of the coil is attached to a larger storage drum to achieve a steady torque. The constant torque is generated as the storage drum always wants to maintain its natural curvature and hence imposes a constant counter torque for the movements induced in the output drum. When connected to the tap’s knob, it retracts slower and jerklessly, allowing the user more time to use the tap. They work almost constantly during turns, making it incredibly productive and helpful with any turn. A standard torsional spring cannot be used in its place as the time period remains almost the same irrespective of the max extension given. In other words, the more we rotate faster, the faster would be its retraction time.

4 Analysis and Results

4.1 Cost Analysis

Table 2 represents the bill of materials and the estimated price of the proposed system.

4.2 Water Savings

The flow rate was calculated by finding the time taken to fill a 1 L bottle.

$$\text{Time taken to fill 1 L bottle} = 9.25 \text{ s}$$

$$\text{Flow rate} = 1/9.25 = 0.1081 \text{ L/s}$$

Table 2 Cost of different components used in the system

S. No.	Components	Cost (Rs.)
1	Constant torque spring	25
2	Plastic casing	10
3	Lever	20
4	Cap	30
5	Support structure	25
	Total	110

Average time when water is wasted while brushing = 10.36 s.

Average water wasted while brushing [10] = Flow rate * Time = 0.1081 * 10.36 = 1.12 L

Population of India = 1,352,500,000

Total amount of water that a single resident can save per year:

Amount Wasted * Total days in a year = 408.8 L

4.3 Advantages

- Compatible with different types of faucets and taps.
- Simple, inexpensive, and uses less number of parts, hence is reliable.
- Requires less maintenance and no expense or electricity to run the device.
- It can be operated very easily.

5 Conclusions

Observing the analysis results, the proposed solution offers a retrofittable attachment enabling self-closing feature to the existing faucets by employing a constant torque spring. Significant amount of water can be conserved at an investment of very low cost.

References

1. World Wild Life, <https://www.worldwildlife.org/threats/water-scarcity>
2. United Nations University, <https://inweh.unu.edu/a-starting-point-to-solve-the-global-water-crisis/>

3. Indian Education Diary, <https://indiaeducationdiary.in/every-indian-wastes-45-litres-water-per-day/>
4. Saerens E, Furnémont R, Ducastel V, Crispel S, Vanderborght B, Lefebvre D (2019) Energetic advantages of constant torque springs in series parallel elastic actuators. In: 2019 IEEE/ASME international conference on advanced intelligent mechatronics (AIM), Hong Kong, China, pp 62–67. <https://doi.org/10.1109/AIM.2019.8868883>
5. Ruhnke G (1988) Faucet aerator. (U.S. Patent No. 4,789,103). U.S. Patent and Trademark Office
6. Wang C-A (2012) Percussive sprinkler with flow regulation functions. (U.S. Patent No. US20120241539A1). U.S. Patent and Trademark Office
7. Rahman SAMM, Al Mamun MA, Ahamed NU, Ahmed N, Ali MS, Islam MM (2014) Design of automatic controlling system for tap-water using floatless level sensor. In: 2014 IEEE international symposium on robotics and manufacturing automation (ROMA), Kuala Lumpur, pp 18–21. <https://doi.org/10.1109/ROMA.2014.7295855>
8. Wolfe JE (1996) Liquid atomizing nozzle (U.S. Patent No. 5,520,331). U.S. Patent and Trademark Office
9. Vulcan Spring Guide, https://www.vulcanspring.com/wp-content/uploads/2019/02/Vulcan_Spring_Design_Guide.pdf
10. Karabrahimoğlu A, Karabekiroğlu S, Unlu N (2017) Estimation of wasted water during tooth brushing determining the rate of taps open in Konya, Turkey

Novel Design of Selective Action Knee Assistive Device



Kulkarni Atharva Kumar, S. M. Deepshikha, Kevin Mathew Thomas, Kunal Yadav, Navneeth Rajiv, K. Rohit Surya, and K. Vedhanarayan

Abstract Problems such as knee osteoarthritis and weakening of leg muscles lead to difficulty and pain in walking for some people in their old age. This paper talks about a new product that aims to assist people suffering from such problems in walking while also trying to minimize further damage and reducing the pain associated with walking. The idea discussed uses the person's body weight force through the landing foot to store energy in a torsional spring via a Bowden cable that engages with the knee joint only when the foot is in contact with the ground. It consists of two main modules, one to be worn at the knee and the other at the foot. The sensing of foot landing and lifting determines timing of engagement and disengagement of the spring with the joint and thereby the action of assistive extension moment on the knee. The idea was modeled through CAD, its parameters optimized and the ability of components verified through simulations.

Keywords Walk assist · Osteoarthritis · Orthotics · Product design

1 Introduction

Knee problems start to become more and more common as people inch toward old age with multiple studies showing radiographic prevalence of more than 20% in Asians above the age of 60 years [1]. Knee pain can be caused due to acute injuries or can be a result of a complicated medical condition. It can be localized to one part of the knee or diffuse throughout the knee. A few of the major reasons for knee pain are osteoarthritis (OA), spinal stenosis, shin splint, grade 2 and grade 3 sprain and tendonitis.

K. A. Kumar · S. M. Deepshikha · K. M. Thomas · K. Yadav · N. Rajiv (✉) · K. Rohit Surya · K. Vedhanarayan

National Institute of Technology Tiruchirappalli, Tiruchirappalli, India

The knee itself is made up of three compartments:

- lateral compartment, located on the outer side of the knee
- medial compartment, located near the middle of the knee on the inner side
- patellofemoral compartment, formed by the kneecap and part of the femur.

The NIAMS found OA to be the most common form of knee arthritis [2]. The effect of OA on a knee can be seen in Fig. 1. OA of the knee that affects only the medial compartment or only the lateral compartment is also called unicompartmental arthritis. Between medial and lateral compartments of the knee, OA is more commonly seen in the medial than lateral compartment [3], possibly because of heavier loading in the former. Without diagnosis and treatment, medial compartmental OA can lead to serious complications that can affect your mobility. Treatment ranges from medication and physiotherapy to surgery and injections.

Some existing solutions for knee braces involve springs. However, there is a need for a mechanism that disengages the spring at the swing phase which involves a greater flexion angle [5] so that it doesn't affect the flexion and extension of the knee when the foot is off the ground. Electrically powered solutions for knee braces largely focus on complete paralysis and their common limitation is the overall increase in weight and motor positioning.

Our solution concentrates on realigning a Varus knee [6] and reducing the impact forces during heel strike. Unloading the knee joint may result in improved soft-tissue repair [7]. It's also a passive assistive mechanism that doesn't affect stride and only assists the extension of the knee in the stance part of the gait cycle. The mechanism works by sensing heel strike and only engages during heel strike. Implementation

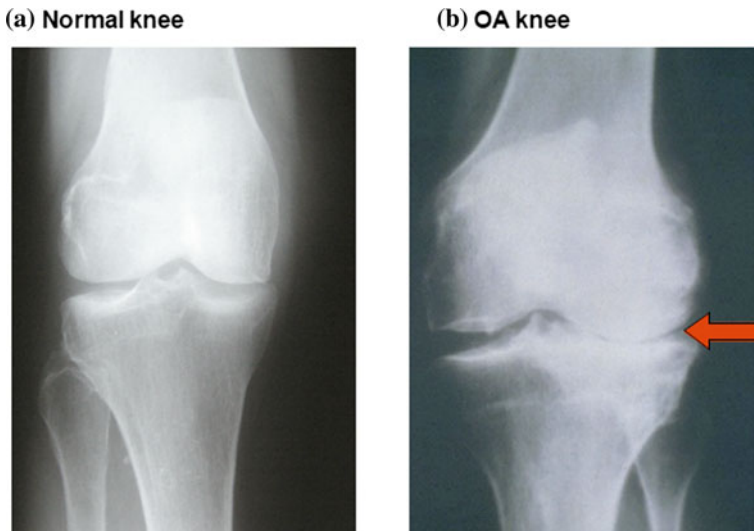


Fig. 1 Smooth joint space in a normal knee compared to narrowing joint space in an OA affected knee [4]

of this assistive mechanism with unloading the knee can provide neuromuscular retraining benefits [8].

2 Proposed Design

The proposed design (as seen in Fig. 2) aims to achieve the following objectives:

- Partially shift load from medial compartment to the lateral side
- Reduce initial shock forces experienced at heel strike
- Reduce the effort required to extend the knee using an assistive mechanism to support knee extension when the foot is on the ground.

Shifting of the load is achieved through a structural solution involving an adjustable structure that exhibits behavior analogous to a diaphragm spring. Application of a calculated force on the knee joint introduces opposite reaction forces at the mid-shin and mid-thigh. Thus a 4-point contact system is established and realignment of the knee in the Valgus is carried out.

Once the flap comes in contact with the ground, the landing force from the foot is transmitted via cable to the mainspring. The angular displacement of the flap is recorded by a potentiometer. Energy is stored by pre-tensioning of the spring at heel strike and at maximum flap flexion, a pair of internal and external gears connecting the spring and the thigh links is engaged. Once engaged, energy at the flexion of the knee is stored. The mechanism gives back a moment that assists the extension moment of the knee that is otherwise completely produced by the muscles. This provides assistance in the stance phase—the phase of walking when the foot is on the ground.

The flap at the foot mechanism is connected to a main torsion spring at the knee using a Bowden cable. Table 1 explains the various components used in the mechanisms and their brief functioning.

The occurrence of events and the working sequence is depicted through flowcharts in Fig. 3.

3 Calculations and Analysis

Keeping the mechanism design, we modeled the overall system using a set of equations depicting the forces and moments involved. The geometric relations between forces at the foot mechanism are shown in Fig. 4. These equations could then be used for optimizing parameters of the overall design. It was desired that the maximum possible knee extension moment be provided by the main spring. This would be provided by the energy loading rotation developed in the spring during flexion of the knee while the foot is on the ground and during transfer of the body weight force from the foot mechanism via the cable. Of these the former is a result of the person's gait

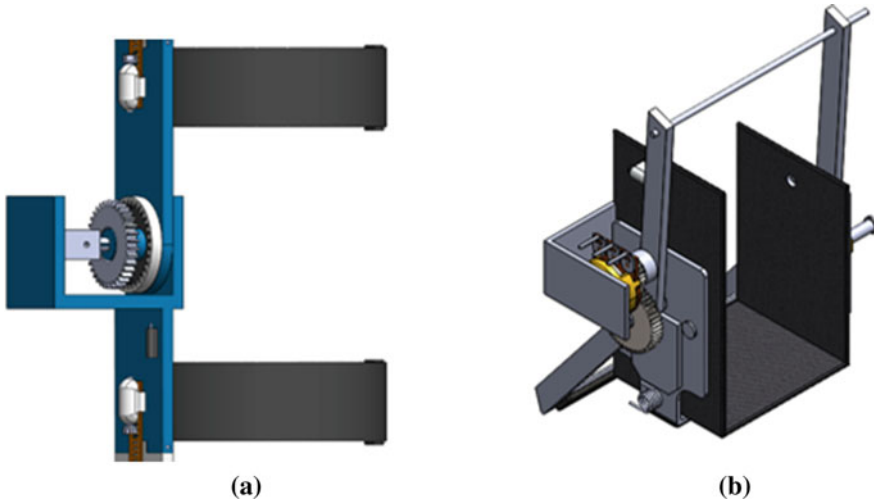


Fig. 2 CAD image of the mechanisms at the knee (a) and at the foot (b)

while the latter can be maximized through optimizing the variables in the equations. This must be done consider two major constraints. The first being that there is a limit to the bodyweight force that can be transferred along the foot and the second being that dimensions of the flap mechanism at the foot not be the cause of discomfort or forceful change in foot movement during walking. Hence, the total horizontal distance projected by the flap and the maximum vertically downward extension of the flap from the lowest point of the person’s footwear were limited.

The nomenclature for the variables used is as follows:

- L—Projected horizontal length
- l_1 —Length OA
- l_2 —Length OB
- α —Initial angle between OA and horizontal
- β —Initial angle between OB and horizontal
- γ —Angle rotated by the mechanism
- T_c —Tension in the string
- r_o —Radius of the torsional spring at which cable acts
- θ —Angle rotated by the torsional spring
- τ —Torque applied on the torsional spring.

The overall displacement of the cable at the main spring is assumed to be vertical and of equal angles above and below the horizontal. Equating the length of cable travel at its two ends gives us an expression relating the angle changes at the flap.

$$2r_o \sin \frac{\theta}{2} = l_1 \gamma$$

Table 1 Components and their functionalities

Component	Functionality
Foot links	Present in the foot mechanism to receive the heel strike motion
Thigh and shin links	There are 4 links. A hinge connects the two shin links and another hinge connects the two thigh links. The lower thigh link has an internal gear which is coaxial with the external gear on the shin link
Internal gear and external gears	This is to transfer motion and engage the mechanism at heel strike
Torsional spring (main)	This spring is pre-tensed at heel strike and further stores energy during flexion during stance stage. The energy is released to aid extension of the knee
Torsional spring	This is to make the links in the foot mechanism go back to their original position
Spline shaft and sleeve	This allows the external gear to move axially on the shaft attached to the shin link and not rotate with respect to it
Solenoid	To engage and disengage the internal and external gears
Breathable fabric	To allow evaporation of sweat to avoid the accumulation of sweat and discomfort
Potentiometer	To measure displacement of the flap
Linear worm drive	This is to make the 2 links on the shin and the thigh to bend with respect to each other on tightening of the hose clamp. This applies the realigning moment on the knee
Lithium polymer battery (11.1 V)	Power supply for electrical components
Arduino Nano	To process input and actuate
Relay	Switching power and step down
Bowden cable	To transfer motion from the heel strike to rotate the gears and tighten the torsional spring
Jumpers, wires, diodes and soldering board	To connect all electrical components and power control

$$\therefore \theta = 2 \sin^{-1} \frac{l_1 \gamma}{2r_o}$$

The tension in the cable can be expressed as a function of the angle turned by the spring.

$$T_c = \frac{\tau}{r_o \cos \frac{\theta}{2}}$$

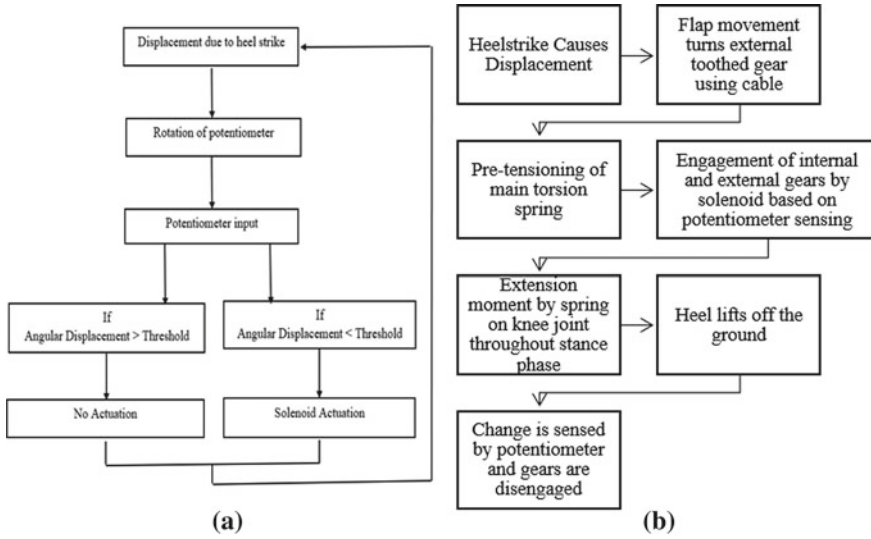
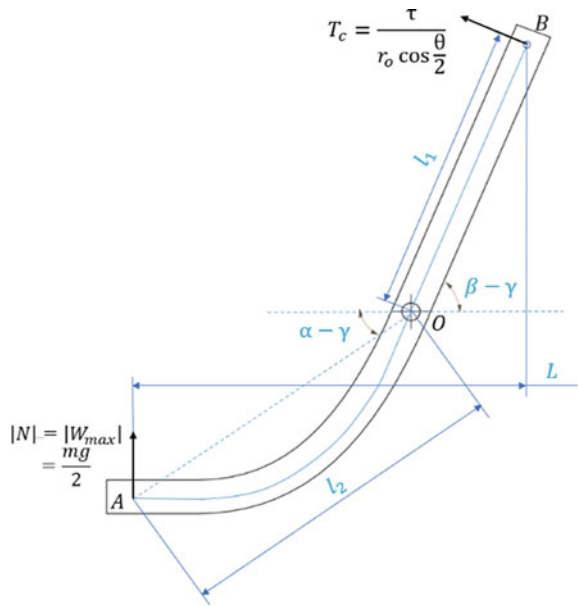


Fig. 3 Working sequence of a Solenoid actuation, b force transfer

Fig. 4 The geometry and the forces involved at the foot flap mechanism



Balancing the moments about O, which is assumed to be at the due to normal reaction at the ground and the tension in the cable, we get an expression for the normal reaction at the ground.

$$T_c l_1 = N \cos(\alpha - \gamma) l_2$$

$$\therefore N = \frac{T_c l_1}{\cos(\alpha - \gamma) l_2}$$

The normal reaction and the cable tension forces can then be used to calculate the forces at the hinge O, which are eventually the forces experienced by the foot, as the vertical and horizontal forces

$$F_{p,v} = N + T_c \cos(\beta - \gamma)$$

$$F_{p,h} = T_c \sin(\beta - \gamma)$$

The vertical force is a limiting factor as mentioned earlier in this section, while the combination of the two forces is used to determine and verify the structural integrity of the flap hinge and its geometry.

Structural simulations were carried out in ANSYS Static Structural module as seen in Fig. 5 for some structurally important parts while also attempting to minimize

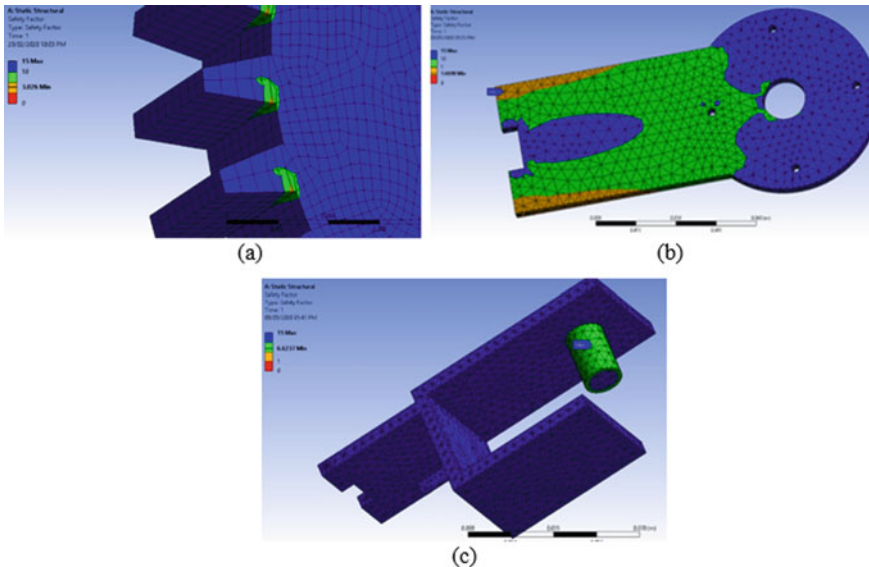


Fig. 5 Structural Simulation in ANSYS for **a** the external toothed gear, **b** the lower thigh link, **c** the upper shin link

their weight by altering their dimensions. The tooth thickness of the gears and their spacing was optimized by trial error to allow for structural integrity and smooth engagement and disengagement. The cross sectional dimensions of the links were also modified by trial and error to reduce their weight while ensuring they are able to bear the bending moment about the axis normal to their plate surface. For the spline shaft, commercially available diameter specifications were modeled and their ability to transmit the required torque was verified.

4 Discussion

Knee pain is a common complaint among adults and is most often associated with general wear and tear of cartilage from daily activities like walking, bending, standing and lifting. Athletes who play sports that involve jumping or quick pivoting are also more likely to be victims of knee pain. A knee injury can affect any of the tendons, or fluid-filled sacs that surround the knee joint as well as the bones, cartilage and ligaments that form the joint itself.

Whatever may be the reason for an individual's knee pain, it holds them back from the complete extent of mobility. A large fraction of people over the age of 40 are prone to develop pain in knee joints after walking for a short distance or time. This commonly occurs with some chronic diseases, like diabetes, heart disease and obesity, and can make it harder for people to manage these conditions. Osteoarthritis occurs due to the deterioration of cartilage that cushions the ends of bones in your joints. The complete wearing of cartilage leads to the rubbing of bones as they have direct contact between them. Osteoarthritis is the most frequent joint disease with a prevalence of 22–39% in India [9], making it the second most common rheumatologic problem.

Our product aims to help patients reduce the effect of ailments such as swelling, weakness, pain, instability and inability to bear the weight in the knee. In the long term, since the impact load is reduced and all the above-stated symptoms due to our daily activities are reduced, the spine is also protected from injuries. Our device doesn't take support from the hip, unlike some other products, making it usable by pregnant women also. Using this would reduce the consumption of painkillers, anesthetics, electrical impulses, etc. that one has to take for pain relief.

Most of the products in the prosthetic/orthotic market (as seen in Fig. 6) employ static knee reinforcements/knee braces that aim to slow down the movement or dampen sudden shock forces. These include prophylactic, functional and patellofemoral knee braces which mainly target diseases concerning the knee joint by slowing down movement (like flexion) rather than assisting. The cost of these products ranges from INR 10,000–35,000. A small segment of the market provides a robotic solution that mobilizes both the disabled and the amputees. Such a product is the Cbrace [10] with a price tag of about \$90,000 that is roughly ₹6,500,000. Our solution targets people in the 1–3 stages of osteoarthritis, whereas most products in the market help only those who opt out of operation in the 4th stage. There are no



Fig. 6 Existing products (a) CBrace [11], (b) Levitation spring loaded tech [12], (c) Paragon polycentric knee caliper Supra [13]

viable solutions other than arthroplasty which not only is as expensive as ₹300,000 but also has side effects.

Most other existing knee assist mechanisms are engaged throughout and take energy from the flexion of the knee which means they also hinder this bending motion of the knee. On the other hand, our mechanism only works during the stance phase of the gait and remains inactive when the foot is off the ground. It also reduces impact loading on knee due to impulsive forces experienced during heel strike. This selective aid makes sure that it doesn't come in one's way while walking. It's a mechanical system that provides the user free range of motion and doesn't restrict their natural gait pattern.

5 Conclusion

Research into this area has brought to light the many shortcomings of the already existing products in the field and has given rise to new ideas to address the prevailing issue of knee osteoarthritis. This product will reduce impact during heel strike and only be active during the stance phase of the walking cycle. This means it does not

oppose the flexion of the knee during the stride phase, which is a much larger flexion as compared to when one's foot is on the ground. The product is not motorized so the user is free to move their leg without restriction. The mechanism assists the natural walking motion of the person all the while reducing wear and tear of the knee whilst considering an affordability aspect in contrast to existing products in the market.

Acknowledgements We would like to thank our institute, the National Institute of Technology Tiruchirappalli, Tiruchirappalli, India and the Student Centre for Innovation in Engineering and Technology (SCIENT), NIT Tiruchirappalli for their support and encouragement.

References

1. Hunter DJ, Bierma-Zeinstra S (2019) Osteoarthritis. *Lancet* 393:1745–1759
2. <https://www.niams.nih.gov/health-topics/osteoarthritis>
3. Vincent KR, Conrad BP, Fregly BJ, Vincent HK (2012) The pathophysiology of osteoarthritis: a mechanical perspective on the knee joint. *J Injury Funct Rehabil* 4(5 Suppl):S3–S9
4. Sofat N, Beith I, Anilkumar PG, Mitchell P (2011) Recent clinical evidence for the treatment of osteoarthritis: what we have learned. *Rev Recent Clin Trials* 6(2):114–126
5. Frigo C, Rabuffetti M, Kerrigan DC, Deming LC, Pedotti A (1998) Functionally oriented and clinically feasible quantitative gait analysis method. *Med Biol Eng Comput* 1998(36):179–185
6. Cherian JJ, Kapadia BH, Banerjee S, Jauregui JJ, Issa K, Mont MA (2014) Mechanical, anatomical, and kinematic axis in TKA: concepts and practical applications. *Curr Rev Musculoskel Med* 7(2):89–95
7. van der Woude J-TAD, Wiegant K, van Roermund PM, Intema F, Custers RJH, Eckstein F, van Laar JM, Mastbergen SC, Lafeber FPJG (2017) Five-year follow-up of knee joint distraction: clinical benefit and cartilaginous tissue repair in an open uncontrolled prospective study. *Cartilage* 8(3):263–271
8. Johnson A, Starr R, Kapadia B, Bhave A, Mont M (2012) Gait and clinical improvements with a novel knee brace for knee OA. *J Knee Surg* 26(03):173–178
9. Pal CP, Singh P, Chaturvedi S, Pruthi KK, Vij A (2016) Epidemiology of knee osteoarthritis in India and related factors. *Indian J Orthopaed* 50(5):518–522
10. Pröbsting E, Kannenberg A, Zacharias B (2017) Safety and walking ability of KAFO users with the C-Brace[®] orthotronic mobility system, a new microprocessor stance and swing control orthosis. *Prosthet Orthot Int* 41(1):65–77
11. <https://www.ottobock.in/orthotic-supports/solution-overview/c-brace/>
12. <https://springloadedtechnology.com/product/levitation-knee-brace/>
13. <http://www.pmr.in/knee-brace-supra>

‘Saarathi’—Novel Design and Prototype of Single Person Operated Casualty Evacuation Stretcher



Karthi Saran, Kunal Yadav, Yash Prakash, Nithin Subhash, Amritha Suresh, and Siddharth Mahesh

Abstract It is a well-known fact that our soldiers put their lives on the line for us, fighting in extreme conditions away from their homes. Hence, any armed forces have to retrieve a soldier who is injured in battle and bring him back to the base camp for treatment. The evacuation needs to be done as fast as possible to ensure that the patient’s injuries do not aggravate. As a result, the evacuation needs to be carried out immediately and while the battle is still going on. The injured soldier is kept on a stretcher by the evacuation personnel and brought back. Today’s stretchers require multiple people to operate the stretcher and get back the patient. This essentially means putting the lives of multiple combat medics at risk while saving a soldier. Saarathi serves to minimise the number of lives put at risk during evacuation. Saarathi is a uni-operational stretcher—it requires only one person for complete operation. This means that only one person has to risk their life to go into the battlefield and evacuate casualty instead of five or six people.

Keywords Casualty evacuation · Uni-operational · Stretcher · Armed forces · Foldable · Variable reclination

1 Introduction

The army is the primary institution that protects a nation from both internal and external threats. Hence, it must have a fool-proof system that can ensure maximum safety, security, and support to the brave-hearted soldiers. One of the significant threats to the soldiers’ lives during the battle is the unavailability of efficient medical transport systems that can transport them from the battle zone to a safe area, where primary aid can be provided. If this medical treatment is given within the first one hour of succumbing to the injury, also known as the ‘*golden hour*,’ the chances of the soldier’s survival without any permanent physical disability/deformation is 85% [1] as shown in Fig. 1. The rescuer is often under threat of enemy attack

K. Saran (✉) · K. Yadav · Y. Prakash · N. Subhash · A. Suresh · S. Mahesh
National Institute of Technology Tiruchirappalli, Tiruchirappalli, India

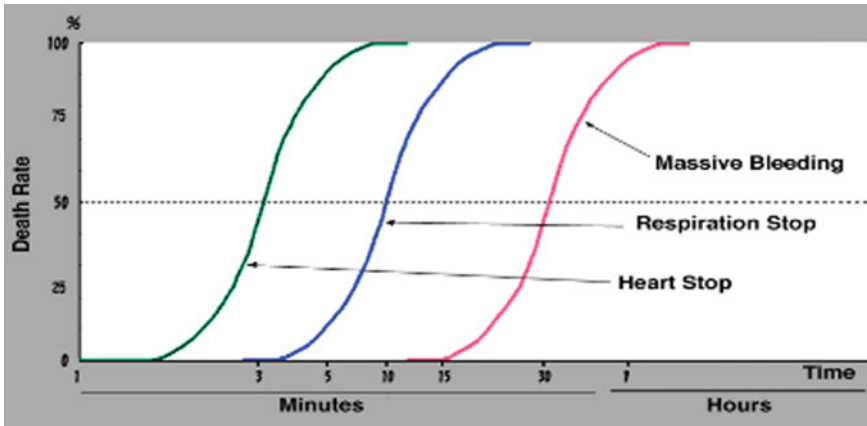


Fig. 1 The golden hour principle in medicine [1]

throughout the rescue operation. Simultaneously, the injured has to be loaded onto a stretcher/sled/litter—whichever can get them to safety the fastest. Recent times have also witnessed a dire shortage in the number of combat medics leading to the soldiers' reduced survival rate. Most stretchers of today require multiple people for operations [2, 3]. Hence, if the number of rescuers per injured soldier is cut down to one from three to four in the existing solutions, more lives can be saved while risking a lower number of lives. Care must be given so that the injured soldier's injuries are not aggravated during transportation. Also, rough and uneven terrain must not be a barrier to the rescuer while transporting the injured. Saarathi provides a holistic solution to all the issues mentioned above and improves the existing defence stretchers. It is a novel solution whose idea and design development thought process as well as concepts are discussed in this paper in an effort to make the design functionally capable as well as convenient to operate and efficient in cost and weight.

2 Literature Survey

Several types of stretchers are available in the market at a wide range of costs and effectiveness. The Clinic Extero [4] stretcher can be operated by a single person and is easy to fold and operate. However, it requires at least two people for loading. It is also bulky to be carried into a battlefield and unfit for rough and uneven terrains. The EL3000 Military Emergency stretcher [5] has support structures and wheels for support but faces similar problems. It requires multiple people for loading the injured person, is bulky and difficult to steer in uneven terrain. It offers only one resting position to the injured and is not foldable. The Mule II [6] makes steering easier in rough and rocky terrain but it too has some problems that limit its ability for our purpose. Having a single wheel makes it harder to balance and it again requires

at least 2 people for loading while offering only one resting position. Innovative stretchers without wheels such as the Lenify Stretcher [7] and the Ferno Lifesaver [8] are compact and lightweight but often require two or more people for complete operation. Hence, there is a need for a foldable, compact, lightweight stretcher that requires just one person to operate and easy to manoeuvre in rough terrain.

3 Thought and Ideation Process

Upon researching various existing stretcher designs through journal papers and patents and speaking to medical professionals in hospitals, we came across all the shortcomings of existing stretcher designs (Fig. 2). Interaction with war veterans and army officers gave insights regarding existing military evacuation techniques, stretchers used by the army and their availability in the market. After analysing all the procured information, the problem statement was framed based on the following factors:

- An injured person's survival rate depends on whether he's evacuated within the first hour of succumbing to injury. The first hour after the injury is termed as the 'Golden Hour' [1] and most of the existing evacuation methods do not have the speed and efficiency in catering to this requirement.
- The existing medical stretchers cannot be used for military purposes due to their large size and uneven terrains of the battlefield.
- Different injuries require corresponding positions at which the injured person to place for medical comfort. This can prove vital to the survival of the wounded.
- It is physically and medically inefficient for one person alone to rescue an injured person and hence more than one person is required for evacuation.
- The entire load of the injured patient has to be borne by the rescue operation experts while transporting the patient to safety. This requires immense human effort as well as increases the time required to relocate the patient. This could potentially make the rescuers feel tired which could potentially risk their own safety.



Fig. 2 Some of the existing stretchers, **a** EL3000 [5], **b** Clinic Extero [4], **c** The Mule II [6], **d** Lenify [7], **e** Ferno Lifesaver [8]

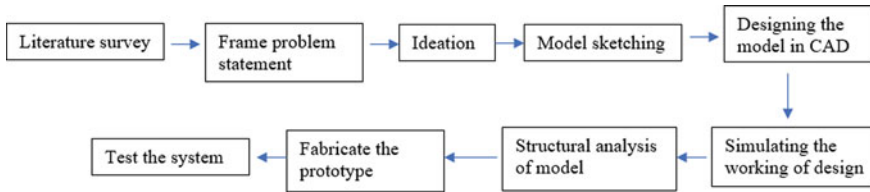


Fig. 3 The workflow process undertaken

- The existing methods of rescue operations during a battle causes secondary injuries to the soldier as well as the patient.
- A single common stretcher model is not suitable for all terrains as the locomotive ability differs with each stretcher. If the wrong stretcher is used on a terrain, it could transfer unnecessary loads in the form of shock to the patient which could aggravate the injury and potentially break the stretcher.

Hence, after carefully analysing, the following objectives were framed. The situation needs a novel form of stretcher that can be metamorphosed into suitable positions to carry the patient across all forms of terrain without discomforting the patient. The patient must be well secured without jeopardizing his safety. The stretcher must be operable by an individual who must be able to deploy the stretcher and carry the patient to safety without spending much time and without exerting too much effort which can be achieved by redistributing the load to the ground. Finally, the stretcher must be developed (as per Fig. 3) with minimum cost and should be foldable in order to transport it easily while being suitable for a variety of situations.

4 Proposed Design

4.1 Development of the Design

Based on the required impact points of the proposed design, the following requirements have to be satisfied.

The ability of a stretcher to be operated by a single person is determined by the magnitude and the location of the acting mass of the patient that the rescuer is supposed to transport. Hence, to reduce the force and torque required to be generated by the rescuer and increase his ability to carry, control and manoeuvre the stretcher, the centres of gravity of the cumulative masses are brought closer to the rescuer and lower to the ground. This is achieved by a radical change in position of the patient on the stretcher. The stretcher is designed to be reconfigurable and deployable at the disposal of the user using a parallelogram mechanism with a single degree of freedom. Additional to achieving this primary requirement, this functionality helps

to load the patient on to the stretcher and shift his position with minimum effort and time spent by a single person.

The stretcher is designed shown in Fig. 4 for the rescuer to carry the load on his shoulders with the use of his upper body muscles while allowing him to use his limbs freely. The rescuer stands in between the legs of the patient facing away from him holding the stretcher with the back straps and the handles by his side. This position is locked, and it ensures that the tipping moment on the rescuer is minimised to be able to efficiently carry the loaded stretcher. Furthermore, a pair of wheel rods (4) are required to redistribute the effective load of the stretcher from the rescuer to the ground while allowing mobility across all terrains. The height of the tire rods is made adjustable to customise the stretcher to suit the rescuer and this can be done well in advance to the rescue operation to save time. An angle locking mechanism is used to adjust and lock the inclination of the wheel rods (4) with respect to the seat frame and the angle is adjusted to effectively distribute the load to the ground.

The retractability function of the stretcher is extended to completely fold the stretcher to make it portable for transport so that the stretcher can be used for various situations including disasters and wars. The foldability of the stretcher is achieved using the same mechanism which is incorporated to the seat frame with additional back and leg support (2) for the injured. A central bar is provided about which the seat frame and the suspension tires are mounted with a locking mechanism to lock both the seat frame position and the wheels independently.

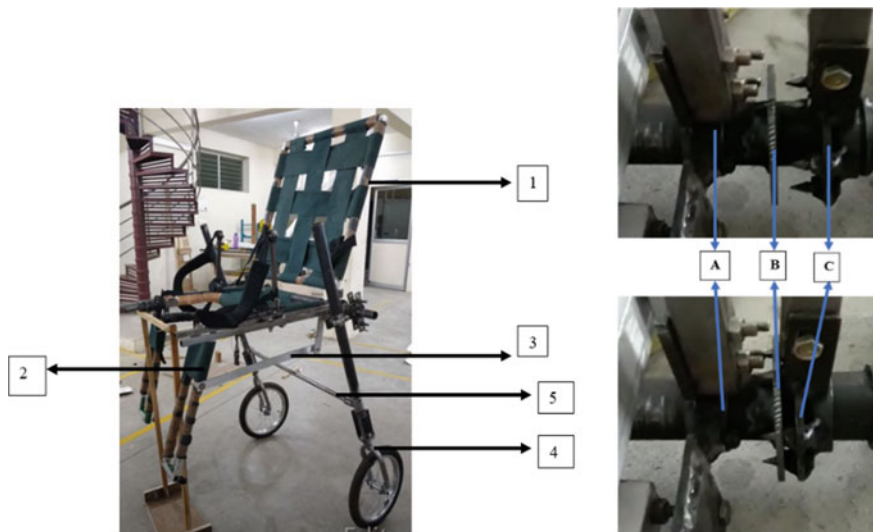


Fig. 4 The reclination subsystem components

4.2 Reclination Subsystem

The reclination angle between the back support (1) and the base (11) can be adjusted to provide more orientations in which the patient can be carried depending on the type of injury to the patient as well as the comfort of both the rescuer and the patient.

The back support (1) and the leg support (2) are both connected with the base (11) and an auxiliary link (3) rod to form a parallelogram link such that all 4 linkages are allowed to pivot about its adjacent linkages. The base (11) provides the necessary structure for the patient to sit and the parallelogram linkage allows both back support (1) and leg support (2) to move in accordance with each other such that, when the back support (1) moves back in a lying down position, the leg support (2) comes upwards to make the stretcher an equivalent to a bed. The same kind of movement in the opposite direction allows for the back support (1) to come up in a chair like position, the leg support (2) also goes down by an equal measure.

The angle reclination capability of the stretcher has been designed to allow the stretcher to fold into a compact form which can be easily carried into a battlefield as a backpack. The reclination angle of the stretcher is locked by using a new, innovative locking mechanism. Since the parallelogram linkage is a four-bar mechanism, when the angle between the base (11) and the back support (1) is locked, it automatically locks the leg support (2) as well. To provide a support structure to mount the mechanism, the main cylindrical bar (10) is used on which the mechanism is mounted. The linkage of the back support (1) is attached to a free disk (A) which is revolute about the main cylindrical bar (10). Another long linkage (7) is attached to this disk (A) which forms one part of the handlebar system such that this linkage (7) of the handlebar and the back support (1) becomes the extensions of disk (A) which in turn is free to revolve around the main cylindrical bar (10).

The handlebar system as shown in Fig. 5 consists of 2 such long linkages (7) (6) that are dimensionally symmetric links attached to each other at approximately their



Fig. 5 The reclination handlebar linkages

centre point to pivot about each other. A spring (8) is attached between the 2 links (7) (6) of the handlebar system such that when they are pressed together about the pivot point, the spring (8) is extended and when released will automatically return the 2 linkages (7) (6) to their original orientation about each other. Now, 2 more disks are introduced namely disk (B) and disk (C) on the main cylindrical bar (10) such that their orientation allows disk (B) to be placed in between disk (A) and disk (C). Disk (B) has 12 holes precisely laser cut at equal spacing along its circumferential area. The third disk (C) is joined with the second linkage (6) of the handlebar system such that disks (A) and (C) are part of the handlebar system and are allowed to revolve about main cylindrical bar (10) on either side of disk (B). Disk (C) which forms an integral part of the system has modifications to it such that as the linkages (7) (6) of the handlebar system pivot, there is enough clearance between disk (C) and the main cylindrical bar (10) for the disk to move linearly with the main cylindrical bar (10). Furthermore, disk (C) is provided with 6 pin like protrusion along its circumferential area which are spaced equally and similar to that of disk (B).

Hence when all 3 disks are mounted on the main cylindrical bar (10), the entire parallelogram mechanism of the reclining system including the base (11), the back support (1), the leg support (2) and the auxiliary bar (3) are mounted on the main cylindrical bar (10) along with the handlebar system including the 2 spring mounted pivotable linkages (7) (6). When the handlebar system is engaged by the user to pivot, disk (C) moves linearly away from disk (B), allowing the user to adjust the reclination angle and once he has adjusted it, he can release the handlebar system which will in turn return to the original position owing to the spring (8). Once the spring (8) returns, the pins of disk (C) automatically fit into the holes of disk (B) as disk (C) is made to move linearly towards disk (B). As disk (B) is welded neither would the disk (C) be able to rotate and due to the pivot joint in the handle bars, it constrains the two parts of the handle to remain in the same plane thereby restricting the disk (A) to rotate and effectively locking the reclination angle. This will arrest further linear movement about the main cylindrical bar (10) as well the angle of reclination.

Since 12 such holes are provided on disk (B), the stretcher allows possible reclination angles as multiples of 30° . When the angle is 0° , the stretcher is at its completely folded position and when it is at 180° , it metamorphosis into a bed like structure. The parallelogram mechanism disallows the angle to go past 180° owing to physical hindrance between the linkages and the ideal position for transporting the injured is found to be between 45° and 90° . Hence, when the reclination angle is to be changed the handlebar linkages (7) (6) are pushed together which makes the disk (C) to slide out of disk (B) and allows it to rotate about the main cylindrical bar (10) thereby allowing disk (A) to rotate as well and by its extension allows the back support (1) to change the reclination angle. The same mechanism of reclination angle lock is given on both sides in order to prevent any bending in the back support (1) due to unbalanced torque.

4.3 Wheel Locking System

As mentioned before, a pair of wheels are provided on either side of the stretcher with the primary aim to redistribute load to the ground and provide the necessary suspension effect for the comfort and safety of the user while he is transported. The suspension wheel system consists of 2 long rods that are attached to each other with a common rod such that they are parallel to each other. At the end of these rods, we have a suspension system with a uni-wheel attached. These rods are mounted on the central main cylindrical bar (10) adjacent to the reclination system. These suspension wheels need to be fixed when the stretcher is deployed and must be locked in its position while carrying the patient. To lock its position, one needs to arrest the distance between the tip of the tire and the main cylindrical bar (10) depending on the height of the rescuer as well as the angle of these suspension wheel rods (4) about the main cylindrical bar (10). In the ideal situation where the terrain is flat and suitable, majority of the load on the rescuer from the stretcher is re-distributed to the ground using the pair of suspension wheels rods. In the scenario of uneven terrains, the wheels can be retracted and locked at different heights to give the necessary clearance between the wheel and the ground to avoid the imbalance and hinderance caused for mobility as shown in Fig. 6. The height of the suspension wheels can be adjusted and locked in position using an eccentric cam lock mechanism.

Adjusting the Wheel Rod Angle The angle of the wheel is locked using almost the same arrangement of disks on the main cylindrical bar (10). A disk similar to disk (C) namely disk (F) is introduced on the main cylindrical bar (10). The disk (F) has 6 similar protrusions that are equally spaced. This disk is allowed to move linearly along the main cylindrical bar (10) for a certain distance. The disk has a nut and bolt configuration (9) where the bolt is attached to fixed plate on the main cylindrical bar (10) and the bolt passes through disk (F). The nut on the other side of the disk is used to tighten and temporarily restrict the linear movement of disk (F). The length of the bolt determines the certain distance that disk (F) can linearly move. The same nut and bolt configuration (9) is responsible for arresting the disk (F) from

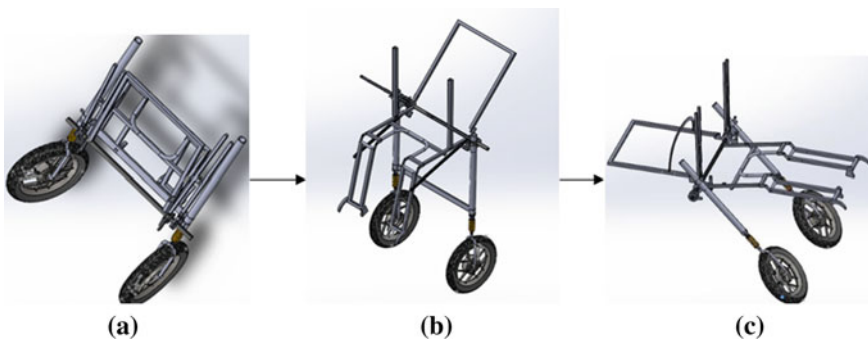


Fig. 6 a Folded, b retracted and c fully extended positions of the stretcher

revolving about the main cylindrical bar (10) since the bolt passes through the disk parallel to the main cylindrical bar (10). Hence the disk cannot revolve about the main cylindrical bar (10). The suspension wheel rods (4) are attached to a disk (G) similar to disk (B) which has 12 equally spaced holes. The configuration mounted on the main cylindrical bar (10) is such that disk (G) is placed between disk (F) and fixed plate to which the bolt is attached. There are solid structures fixed to the main cylindrical bar (10) on either side of disk (G) which disallow it to move linearly on the main cylindrical bar (10) while it is allowed to revolve about it. To fix the angle, the nut and bolt configuration (9) is released, and disk (F) is pulled back such that the 6 protrusions are detached from the hole of disk (F). Now the disk (F) which is directly attached to the suspension rod is rotated to the necessary angle and then disk (F) is re-attached to disk (G) using the protrusions. The nut and bolt configuration (9) are now tightened to fix the entire system in place. The wheel angle locking mechanism is provided only on one side unlike the prior arrangement where it was provided on either side. Since the wheels are connected by a common connecting rod (5) and are parallel to each other, the change of angle in one-wheel rod (4) by a certain angle will result in the motion of the other wheel by the same angle as shown in Fig. 7. There are no handles required for locking since it is locked well in advance and is not operated upon while the stretcher is moving. The rescuer is not using the stretcher when the wheel angle needs to be locked.

Adjusting The Wheel Height (Fig. 8) The wheel rod (4) is also given a degree of freedom in its vertical direction. The wheel rods (4) are housed on a ring to which an eccentric clamp lock is attached. The ring encircling the wheel rod (4) can be made to tighten or loosen against the outer surface of the wheel rod (4) by toggling the eccentric clamp lock.

This plays a vital role in providing clearance from the ground to the stretcher body on very rough terrain. The necessity of clearance can be emphasised by the fact that

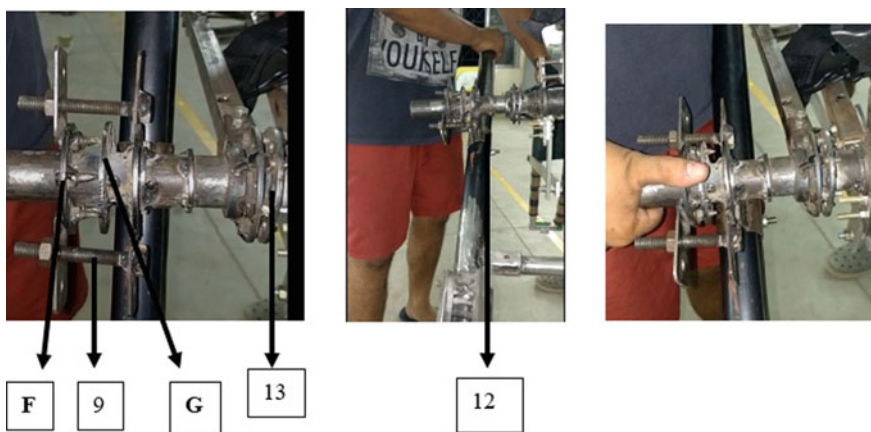


Fig. 7 Wheel rod adjusting mechanism

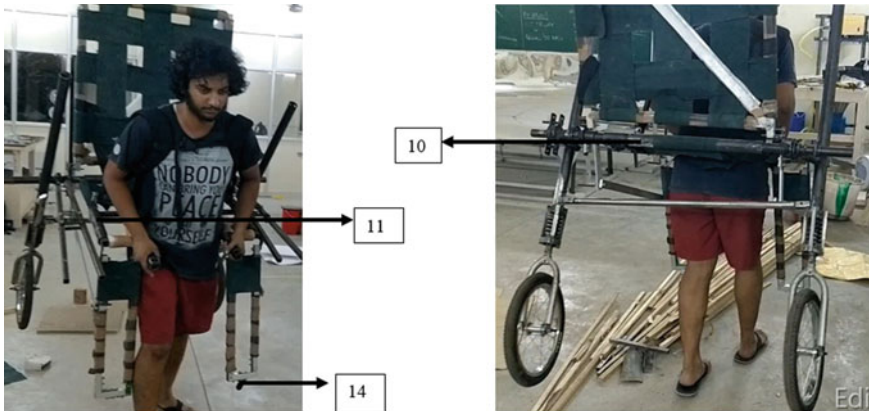


Fig. 8 Wheel rod height adjustment mechanism

in the case of a ditch or a bump in the road or a stream of water being encountered, the presence of the wheel can prove to be a hinderance. If the ground contacts were only the feet of the rescuer, the obstacle can be easily surpassed. Hence, the retraction of the wheel after loosening is key to passing through very rough terrain. The retraction can be done either by pulling the wheel rods (4) up or by letting the stretcher body drop down by the needed clearance due to the natural weight of itself and the patient after the clamp lock is released. Once the desired height is achieved, one can manually toggle the clamp to fix its position.

4.4 Loading Mechanism

Loading is the process of strapping in the injured on the stretcher and lifting the whole stretcher from the ground. The uniqueness of the project which makes it ideal is that it requires just a single person to lift and strap the patient from ground and onto the stretcher. Once the rescuer reaches the patient, he initially adjusts the suspension wheels rods to the desired height. Once that is completed, the folded stretcher is deployed into its full extension as a flat and bed like structure where the leg support (2), the base (11) and the back support (1) are all parallel to each other. The suspension wheel rods (4) are also laid flat beside the reclining system and the entire stretcher is laid on the ground. Now the injured is made to lie flat on the stretcher with his thighs rested on the base (11) and his torso resting on the back support (1). He is strapped to stretcher for his safety. Now, the claws (14) provide the base (11) of the leg support (2) are fixed to the ground temporarily and the flat stretcher with the injured person is pivoted about its point of contact to the ground to a particular height. Now, holding the stretcher in position, the angle of the wheel rods (4) are fixed using the wheel locking mechanism based on the rescuer such that

the stretcher is made to balance by itself with the claws (14) and the suspension wheel rods (4) both supporting the structure to the ground. Now the rescuer moves to the front of the stretcher and places himself in between the legs of the injured. He wears the backstrap of the stretcher and using the handlebar system, lifts the claw (14) of the leg support (2) from the ground and uses the same handlebar to adjust the reclining angle. Now he is ready to carry the injured person of the field for loading the stretcher is lifted from the back support (1) by the rescuer. The whole process of loading a patient on the stretcher takes an average of just about 36 s which is much lesser than many of the other stretcher options.

4.5 Some Features of the Product

- **One-man armed** Saarathi can be operated and manoeuvred by a single person unlike other stretchers which requires 2 or 4 people.
- **Reclining mechanism** Saarathi has a novel and optimised mechanism for changing the angle of the recliner seat. It can provide multiple suitable positions for the patient to rest on. The protrusions on the rotating plate locks themselves to the holes in the fixed plate and this force is provided by the spring (8) attached to the handle.
- **Height adjustment** (Fig. 9) The ground clearance of the seat structure can be varied according to the person who is carrying to fit his height and comfort.

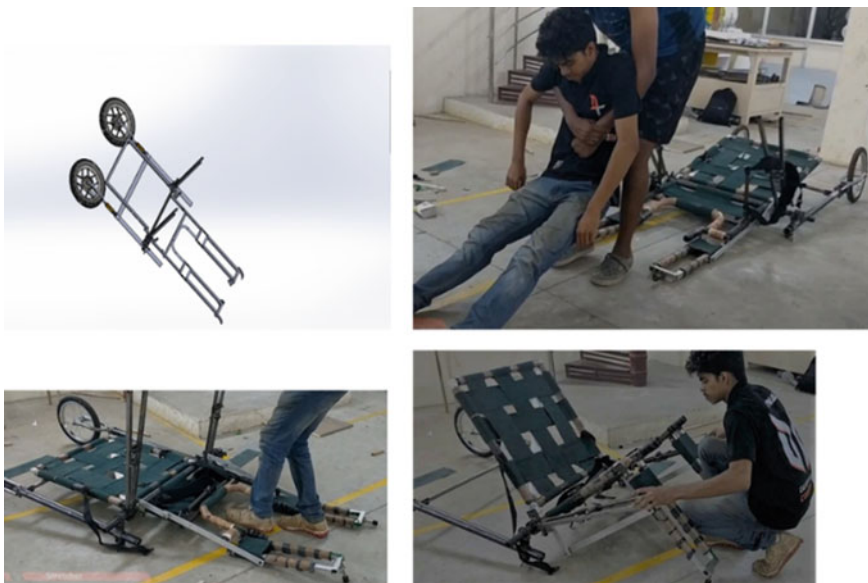


Fig. 9 The stretcher laid out on the ground

Also, the wheels can be retracted completely from the ground to help the rescuer manoeuvre easily across big obstacles where wheels cause a hindrance.

- **Suspension** (Fig. 9) The wheel rods (4) come with built in suspension to reduce the shock absorbed by the injured person on the stretcher.
- **Angle of wheel assembly** The angle of the wheel rod (4) with respect to the seat can be changed and fixed at 8 possible angles. This helps the rescuer to change the wheel according to the plane of travel and also maintain the centre of mass and balance of the system.
- **Foldability** The whole system can be unfolded and put to shape quickly. It's designed in a way that the parts' planes don't coincide each other. It's a highly compact system which when folded can be worn as a bag pack and taken into battlefield making it highly portable. It is engageable with the end frame members and a bed portion in the form of a flexible sheet supported by the frame. Each side frame member comprises at least two rigid tubular sections with the end of one tubular section being foldably connected to the end of the next adjacent tubular section as in The Foldable Casualty Carrier [9].

5 Analysis

Considering the fact that one of the requirements of this product is the ability to be moved and carried around with minimal ease for timely evacuation, the weight of the stretcher becomes an important factor. Hence, structural simulations were carried out in ANSYS Static Structural module to determine the dimensions of the parts to be used considering the commonly available materials mild steel and aluminium in an effort to minimise the weight of the overall stretcher [10]. Made from mild steel, the crucial load bearing parts discussed in this section are the reclination angle locking disk, the wheel rod, the wheel ring and the main cylinder. Corresponding analysis results are Figs. 10, 11 and 12.

The wheel rod has to transmit the load from the stretcher which includes the weights of the patient and the stretcher itself to the wheel so that it can be distributed

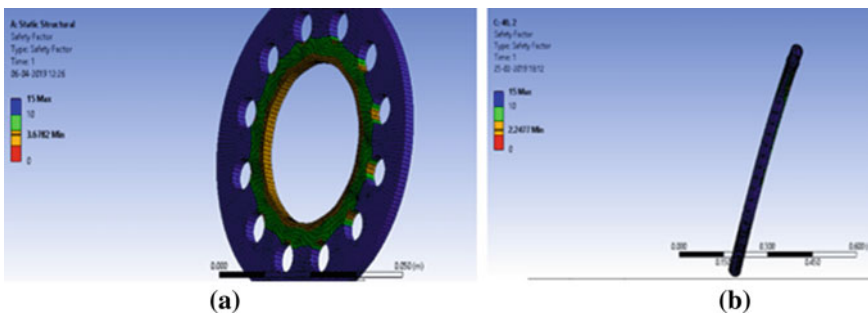


Fig. 10 Structural simulations for **a** reclination angle locking disk, **b** wheel rod

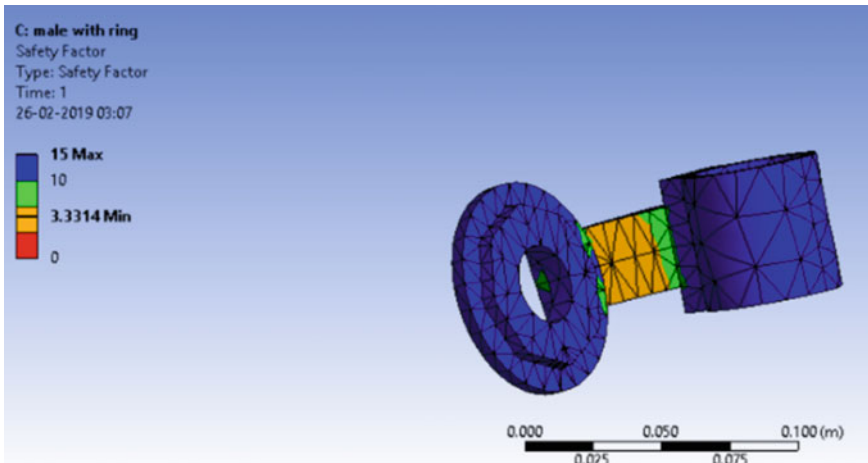


Fig. 11 The wheel ring subjected to 1000 N downward force

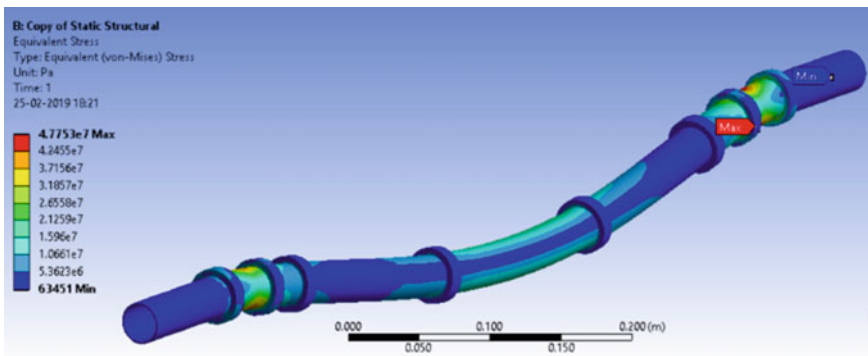


Fig. 12 The main horizontal cylinder subjected to bending

to the ground. The major consideration would have been the stress incurred in the wheel rod upon impact loading when the stretcher has to travel across a depression in the ground. Taking the weight of the stretcher and the patient combined to be a high estimate of 100 kg, the weight on each wheel rod would be 500 N.

The reclination angle locking disk interlocks with the revolute disc connected to the handle. When locked, the weight of the back of the patient is acting on the back support. The back support is rigidly attached to the handle linkage. This transmits the moment caused by the centre of gravity of the back acting on the back support being offset from the vertical of the main cylinder to the locking disk. It was analysed considering the weight acting on the back support to be 40 kg and the distance of the centre of gravity of the weight from the main cylinder being 40 cm when the stretcher is flat.

The wheel ring controls both the degrees of freedom of the wheel rod. The wheel rod is held in its vertical position by the clamp lock on the ring. This transfers all vertical loads to the ring. The sliding joint between the wheel rod and the ring ensures that the angle of the ring with the main cylinder is the same as the angle of the wheel rod. As discussed about the wheel rod above, it was also simulated considering a force of 1000 N upon impact loading on each ring clamp.

The main cylinder is mainly subject to bending moments due to 3 sets of forces. They are the downward weights from the seat frame bars welded to it—300 N each, the downward forces from the reclination angle locking disks that support the back—400 each and the reaction forces from the wheel rod rings.

Through these simulations, relatively optimised dimensions of the parts such as pipe thickness, diameter, plate thickness and hole diameter were arrived at to reduce the weights of the parts while also verifying their structural integrity.

6 Discussion

The novel design presented in this paper allows operation of the stretcher requiring only one person and potentially solves several issues faced by some of the already existing stretcher designs that aim to do the same.

It is a stretcher that puts lower number of lives at risk during rescue operations. Existing methods of carrying a stretcher include:

- Five-person team: For easier load distribution and quick movement.
- Four-person team: Not used in case of a spine trauma
- Two-person team: Not used in case of any trauma

The design allows it to be used by a single person while allowing sufficiently ergonomic patient transportation. This can drastically reduce the number of people involved in the rescue operations which means the available human resource can be optimised to save more lives in the same time. This can be viewed in two ways as the same number of combat medics can rescue a larger number of soldiers, or the same number of soldiers to be rescued require a lesser number of combat medics. In one way, the number of lives put at risk is reduced, while in another, the number of lives saved increases, each noble in their own right.

The suspension wheel rods drastically reduce the load on the rescuer which in most situations can cause physical injury. The load being distributed to the ground drastically reduces the risk of the rescuer getting injured and also saves him a lot of effort.

The stretcher firmly secures the patient in his medically required inclination position according to the type of his injury using the reclining mechanism. This novel feature is not present in conventional stretcher in which the patient even stands a chance of falling out during the rescue operation. The chances of such unfortunate situations are minimal in this.

The wheel rods have a suspension system attached to them which considerably reduces the shock transmitted to the injured patient when moving across rough terrains. This further reduces the risk of aggravating his injury while making him relatively more comfortable.

The time consumed for rescue operation is lowered since the stretcher requires merely 36 s for it to be deployed, load the injured on the stretcher, lift him up, fix the suspension wheel rod angle and then use the recliner mechanism to fix his position and carry the patient to safety. All of this can be achieved with a single person.

Economically, the provision of casualty evacuation services is one that can consume a lot of capital. Since the requirement is of very high skill professional doctors also trained in combat, the number of people willing to take up the job is insufficient. This results in increased cost to a government in recruiting personnel for the same. The widespread use of Saarathi would reduce these costs. Although the pay for one person would need to be higher due to the increased training required, the number of people required would significantly reduce.

Disaster management can be a field of valuable scope for this stretcher design. When people are not available in abundance to assist in rescuing a trapped person in distress, the provision of this stretcher allows it to be used by a single person itself to carry out the rescue operation. It is designed to be used in all types of terrains that one can potentially encounter during a calamity which includes debris, ditches, roads etc.

7 Conclusion

The article aims at highlighting the features of the proposed design of a novel stretcher that can be operated by a single person to rescue injured people. The stretcher can be reclined into suitable positions for carrying the injured based on the type of injury he has suffered while distributing the load of the patient to the ground using the suspension wheel rods. Apart from reducing the number of people required for the process, the foldable nature of the stretcher allows for it to be used under all circumstances such as calamities and disasters. The novel stretcher was designed, and its structure was analysed for safety using CAD software packages and the prototype was subsequently fabricated.

Acknowledgements We would like to thank the Student Centre for Innovation in Engineering and Technology (SCIENT) Lab, NIT Trichy and our institute, NIT Trichy for the provision of facilities for developing the prototype as well as their support and encouragement.

References

1. The Golden Hour Principle, [https://en.wikipedia.org/wiki/Golden_hour_\(medicine\)#/media/File:Golden_hour_graph.png](https://en.wikipedia.org/wiki/Golden_hour_(medicine)#/media/File:Golden_hour_graph.png)
2. Military casualty evacuation, https://link.springer.com/chapter/10.1007/0-387-22699-0_5
3. https://armypubs.army.mil/epubs/DR_pubs/DR_a/pdf/web/ARN17834_ATP%204-02x2%20FINAL%20WEB.pdf
4. Clinic Extero Stretcher, <http://www.medirol.eu/Products/Ambulance-Rescue/Ambulance-Stretchers/Stretchers-Transporters/Clinic-Extero-en.aspx>
5. EL3000 Stretcher, <https://www.medicalexpo.com/prod/faretec/product-68475-742084.html>
6. Mule II Stretcher, <http://www.ferno rescue.com/products/basic-rescue/litter-wheels-stretcher-carriers/traverse-stretcher-carriers>
7. Lenify Collapsible Emergency Stretcher, <https://www.tuvie.com/lenify-collapsible-emergency-stretcher-by-danny-lin/>
8. Ferno lifesaver rescue stretcher, <http://www.ferno rescue.com/products/basic-rescue/rescue-stretchers/ferno-lifesaver-rescue-stretcher>
9. Foldable casualty carrier, <https://patents.google.com/patent/US3886606A/en>
10. Aluminium in lightweight design, https://www.researchgate.net/publication/269451363_Aluminium_in_Innovative_Light-Weight_Car_Design

Review on the Application of CGP to Improve AZ31 Mg Alloy Properties



A. Muni Tanuja, Anoop Kumar, and B. Nageswara Rao

Abstract Constrained groove pressing (CGP) is a method of severe plastic deformation (SPD) techniques. It is being used to enhance mechanical properties and reduction in grain size. In CGP method, the specimen of sheet metal has been subjected to a shear deformation repetitively by utilizing a set of grooved and flat dies. CGP method can be applied to low carbon steel, aluminum, copper, nickel, brass, and titanium. By applying this method, improved properties of the materials can be expected. An attempt has been made in the present work to study the effect of CGP passes on microstructure, micro-hardness, tensile strength, and yield strength of AZ31 magnesium alloy.

Keywords Constrained groove pressing (CGP) process · Severe plastic deformation (SPD) · Mechanical properties · Sheet metal · Shear deformation

1 Introduction

Production of nano-structured or ultrafine grain (UFG) materials through micro-structural refinement of 100–500 nm with SPD process has captured many researchers for past couple of decades [1]. SPD process involves introduction of plastic strains through hydrostatic pressure with nominal changes in cross-sections [2]. The metals or alloys processed by SPD have non-porous structures and possess good physical as well as mechanical properties and are influential in automobile and

A. Muni Tanuja (✉) · B. Nageswara Rao
Department of Mechanical Engineering, Koneru Lakshmaiah Education Foundation, Green Fields, Vaddeswaram, Guntur, Andhra Pradesh 522502, India
e-mail: tanujamech@cvsr.ac.in

A. Muni Tanuja
Department of Mechanical Engineering, ANURAG University, Venkatapur, Ghatkesar, Hyderabad, Telangana 500088, India

A. Kumar
Department of Mechanical Engineering, Sri Datta Institute of Engineering and Science, Ibrahimpatnam, Hyderabad, Telangana 501510, India

aeronautical industries [3–6]. Major advantages of UFG materials are due to good processability at low temperatures and high strain-rate super plasticity [7]. Various processes for SPD and manufacturing of materials with UFG microstructure are as follows: equal channel angular pressing (ECAP); high pressure torsion (HPT); equal channel angular rolling (ECAR); repetitive corrugation and straightening (RCS); cyclic extrusion compression (CEC); accumulative roll-bonding (ARB); constrained groove pressing (CGP); and continuous high-pressure torsion (CHPT) processes [3, 4]. Amidst these processes, ECAR, RCS, ARB, and CGP have been applied in case of sheet metals [8]. UFG sheets are being used in automobile and aeronautical sectors.

ARB process induces intense straining of the material with only 50% decrease in thickness of the end product. From the experiments carried by Lee et al. [9] on ultra-low carbon IF steel, refinement of structure was not found. Moreover, the formation of sub-grains with low-angle boundaries caused low ductility and high strength. This process is laborious and more time-consuming.

RCS method utilizes rolling to procure strain in the material. Though the process is simple and has ability for multiple number of cycles, tensile stress on free surfaces induces defects, cracks, micro and even nano-voids. Therefore, very large strains cannot be applied which is the major aspect of an efficient SPD technique [10].

CGP technique can be utilized for creating homogeneous strains throughout the samples and also for large sheets [11]. CGP process applies repetitive shear plastic deformation on the work piece using alternative pressings with a set of corrugation and flattened dies [12]. For each CGP pass, a strain (of 1.16) on the sheet with grain refinement was imposed. The obtained microstructure has good shear bands [13, 14].

Because of good ratio of strength, weight, better formability, and exceptional resistance to corrosion, magnesium alloys are extensively utilized in automobile, aerospace, and constructional sectors. Due to hexagonally close packed (HCP) structure, Mg alloys exhibit less ductility at room temperatures [7]. There is a possibility of improving the mechanical properties through refinement of microstructures by alloying with distinctive elements, heat treatment, and thermo-mechanical processing [11]. Good amount of research has been carried out on upgrading the mechanical properties of Al and its alloys using SPD techniques [15]. Processed materials by CGP show unique and fair properties. Hence, CGP is being used in aerospace, automobile, energy, defense, and bio-medical sectors for producing several components and also for major constructions with improved safety.

Despite the fact that CGP is useful SPD method, it has certain drawbacks also. With increased CGP passes of the sheet metal, as the dies are made of sharp profiles, micro-cracks may appear on the specimen's surface and leading to reduction in strength, ductility, and toughness of the material. This paper briefly highlights on the application of CGP method in enhancing the properties of AZ31 Mg alloy and its limitations as well.

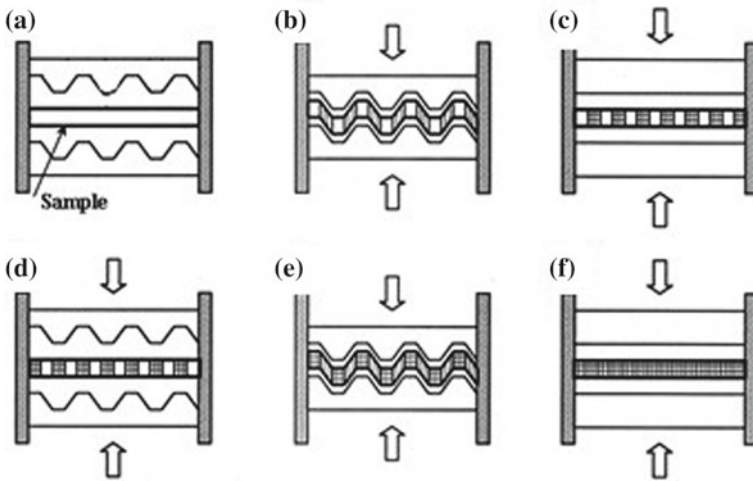


Fig. 1 Schematic diagram of CGP process [7]

2 Methodology

The CGP procedure is one among the promising SPD processes which can bring about UFG sheets. It can be utilized for manufacturing of sheet metals and its alloys. Figure 1 shows the illustrative diagram of CGP process and its array of pressings. Each cycle consists of four passes (in which, two passes for grooved die and the other two passes for flattened die). Initially, a sample sheet in Fig. 1a is arranged in the space between the upper and lower dies with grooves. In the first pass, the specimen is pushed by a set of grooved dies as in Fig. 1b. For the second pass, the specimen (grooved) is flattened with two flat dies as in Fig. 1c. Later, the second pass, the work sheet is turned by 180° over the axis which is perpendicular to plane of the sheet as in Fig. 1d. The un-deformed regions (if any) can be well deformed in next pressing due to dissymmetry of the grooved die as in Fig. 1e. Lastly, a steady distribution of strain, plastic in nature can be achieved all over the sheet by a set of flat dies as in Fig. 1f [7].

3 Influence of CGP Process Parameters

3.1 Temperature

Yogesha et al. [12] have investigated the tensile and fracture behavior of Al-Mg alloy (AA 5052) applying cryo-rolling and post-deformation annealing. Deformed samples (of 90% reduction of thickness) show enhancement in strength (291 MPa),

hardness of value 110 HV in CR samples. Strength of 313 MPa and hardness of 122 HV are achieved in cryo-groove-rolled specimens. This is on account of large density of misplacement and reduced size of the grains. Post-annealing of the sheets (of 90% shrinkage of thickness) leads to enhancement in ductility and fracture toughness. The cryo-groove rolled and samples after the process of annealing have exhibited good fracture toughness of 142 kJ/m^2 when compared with that of cryo-rolled sheets of 29 kJ/m^2 due to grains of large size and dips detected in TEM and fractographic studies.

Fong et al. [14] have considered AZ31 magnesium alloy plate and subjected to CGP process in three deformed cycles at temperatures from 503 to 448 K. The micro-structural stability of the material is investigated through annealing carried isothermally at temperature from 473 to 623 K for various time intervals. The first cycle is performed at $503 \pm 5 \text{ K}$, while the second and third ones are at $448 \pm 5 \text{ K}$. They have noticed exceptional grain growth at 623 K indicating more regular distribution of grain size. XRD analysis shows that the peak intensity ratio observed is lower at 623 K.

Liu and Chen [16] have observed that processing of a high deformed material below recrystallization temperature can restore its ductility and toughness with significant influence of precipitates within the matrix. Hence, straining intensifies the desired condition for further precipitations. More annealing temperatures result in generation of a consistent recrystallized structure and appreciable drop in micro-hardness when compared to those for as-cast Mg alloy. Properties of AZ31 strips are improved through high temperature CGP process [17].

3.2 Groove Angle and Width

Groove angle and width are major processing parameters in CGP. Moradpour et al. [18] have considered the gap in between the top and bottom dies equal to thickness of sheet (of 3 mm) having 45° groove angle. It is noted that groove width has prominent impact on cracking propagation in the sheet.

Moskvichev et al. [19] have found 45° groove teeth angle as optimal in obtaining the plastic strain accumulation. The size of height of teeth, width, thickness, and space between teeth is reported as 1.5 mm. They have observed the accumulated strain enhancement proportionally with increasing number of pressing cycles.

Wang et al. [20] have demonstrated the importance of the parameters of die structure like groove width and its angle for analyzing the microstructure, distribution of strain, and mechanical properties of material. Best combination of the process parameters provides optimal solution.

3.3 Friction

When the specimen is subjected to SPD, strength decreases due to generation of cracks on surface. Hence, the influence of friction between die and sheet must be examined. Moradpour et al. [21] have made investigations on wear resistance, weight loss morphology, and friction coefficient of worn surfaces. The wear resistance is prominently increased by CGP-CR process and evolution of UFGS.

4 Influence of CGP on Mechanical Properties

Table 1 presents achieved mechanical properties after CGP process of AZ31 Mg alloy.

Zimina et al. [7] have made investigations on the microstructure and micro-hardness mapping with UFG structure through CGP by twin-roll casting of AZ31 Mg strips. 90% drop in grain size and 43% increase in micro-hardness of the specimen were found after the CGP.

Fong et al. [14] have processed AZ31 (Mg alloy) plate adopting the CGP process under three cycles of deformation and at temperature from 503 to 448 K. The method yields 1.8 μm grain size with homogeneous UFG microstructure. An increase of 38% was noticed in yield strength of the material.

Moradpour et al. [18] have made comparative studies on the microstructure and micro-hardness of the constrained groove pressed and annealed as-cast specimen. The material exhibits heterogeneous structure. It is restored by fine and constant recrystallized structure sub-sequential aging at 450°C for a period of 10 h. The size of the grains in the surface layer is smaller (10–20 μm) than that in the sample (200 μm). The micro-hardness values are up to 85 HV0.1, which are 20% more than that of the TRC strip.

Wang et al. [20] have performed CGP of AZ31, Mg alloy sheets at room temperature, 423 K, 473 K, 523 K, and 573 K to examine the cracking behavior and the significance of number of passes and working temperature on the mechanical properties and microstructure. The mean grain size is reduced by 59%, micro-hardness increased by 11%, ultimate yield strength increased by 33%, tensile strength enhanced by 9%, and percentage of elongation is 18.5%.

Moradpour et al. [21] have carried out CGP-CR process on Al–Mg alloy and implemented up to two pressings at room temperature for developing the plastic strain of 4.64. Up to two pressings of CGP-CR process, they have observed appearance of UFGS with a mean sub-grain size reduction up to 95%, enlarged tensile strength of 7.5%, and 71% increase in hardness.

Lin et al. [22] have made investigations on the grain refining and there by affecting the properties of AZ31 Mg alloy using advanced technology of warm constrained groove pressing (WCGP). The effective distribution of strain in the sheet is found to be uniform and consistent after completing fourth stage CGP process at 473 K. The

Table 1 Mechanical properties of AZ31 (Mg alloy) before and after the CGP process

Process	Size of Specimen	Method	Properties	CGP process	
				Before	After
Twin-roll casting (TRC) [7]	Sheet of size 70 × 50 x 5.6 mm ³	Specimen heated to 450 °C for 10 min before each step	Microstructure (μm) Micro-hardness (HV0.1)	200 67	20 96
CGP for three deformation cycles [14]	Ingot of size 30 × 40 × 80 mm ³	Specimen subjected to Isothermal Annealing at 473 to 623 K	Yield strength YS (MPa) Activation energy (kJ/mol)	175 92	242 27.8
Twin-roll casting (TRC) [18]	Sheet of size 70 × 50 x 5.6 mm ³	Specimen is aged at 450 ⁰ C for 10 hr	Microstructure (μm) Micro-hardness (HV0.1)	200 45	15 55
Hot rolling [20]	Sheet of size 100 × 100 x 2 mm ³	Specimen fullyannealed at 573 K for 1 hr	Mean grain size (μm)	6.92	2.81
			Micro-hardness (HV)	66.8	73.9
			YS (MPa)	181	240
			Tensile strength UTS (MPa)	270	295
CGP-crossroute (CGP-CR) for two cycles [21]	Sheet of size 72 × 72 × 3 mm ³	CGPed at room temperature	Mean grain size (μm)	50	2.5
			Hardness (HV)	55.5	95
			UTS (MPa)	226	243
Warm CGP [22]	Sheet of size 44 × 44 × 2 mm ³	Specimen is annealed at 550 K for 1 hr	Microstructure (μm)	20	9
			Micro-hardness (HBW)	55.84	69.16
			YS (MPa)	132	155
			UTS (MPa)	240	285
CGP for four cycles at elevated temperatures [23]	Sheet of size 60 × 60 × 3 mm ³	Specimen annealed at 320 °C for 2 h and furnace cooled	Average grain size (μm)	50	4
			UTS (MPa)	235	325

grain size is decreased up to 55%; hardness is increased by 24%, an increase in yield strength by 17%, and tensile strength by 19%.

Thuy et al. [23] have used AZ31 (Mg alloy) strips of $60 \times 60 \times 3 \text{ mm}^3$ for CGP for four cycles at elevated temperatures. They have observed UFG structure and maximum grain size reduction of 92% in the highest deformation regions. They are able to achieve an increase in strength up to 38% and elongation of 35%.

5 Advantages and Limitations of CGP Method

5.1 Advantages

CGP method can be applied to sheet metal processing which is a major advantage over the SPD processes like ECAP, HPT, and ARB. The dimensions of the specimen during CGP do not change as observed in case of constrained groove rolling (CGR) process. Due to this, tensile stresses do not develop in the specimen which is an added advantage with CGP technique. ARB process requires a bonding between two plates, due to which the mechanical properties of the specimen may degrade because of interfacial bonding [24]. Hence, CGP process provides a good alternative to ARB technique.

A significant change in specimen thickness can be observed in the specimen worked by RCS process which is not observed in case of CGPed specimens.

5.2 Limitations

The CGP technique has certain disadvantages also. The number of passes that the sheet metal has to undergo is limited because of the sharp die profile, due to which micro-cracks can appear on the specimen surface decreasing the mechanical properties like strength, ductility, and toughness [25].

6 Conclusions

Constrained groove pressing method is a SPD process, which is being adopted as a strengthening technique for sheet metal processing. This paper briefly presents on the recent advances in CGP process with the following conclusions:

- The size of the grains decreases by increasing the no. of CGP pressings. The degree of grain refinement in the first stage is rapid and decreases for the successive passes.

- From the tabulation, it is evident that the sample grain size can be decreased even up to 95%, if processed through CGP-cross route process.
- Micro-hardness values of AZ31 magnesium alloys when processed through hot rolling CGP can be increased as low as 11%.
- The mechanical property, yield strength of the work material can be increased up to 38%, when specimen is subjected to three deformation cycles of CGP.
- The tensile strength of the material can be enhanced up to 38%, when the CGP process is done at elevated temperatures.

7 Research Gaps

The Ballistic properties have a major role in defense sectors. CGP process can improve these ballistic properties. Materials having good ballistic properties are preferred in army vehicles and associative equipments, security cars, etc. Processing of these materials by CGP technique will definitely enhance mechanical properties [26].

Materials like armor steel possesses high strength and have wide applications in aerospace and defense sectors due to their explicit properties. Armor steel is being used in producing army vehicles. Structural efficiency (i.e., strength to weight ratio) also gets enhanced through processing of the armor steels adopting the CGP technique [27]. Hence, there is a possibility of realizing the lightweight materials for improving the portability of the vehicles and maintenance of protection standards as well.

Further, research on CGP can defeat limitations of this process. Future work can be carried in order to enhance the strength, ductility, and toughness of the material by combining CGP with certain heat treatment methods like quenching, annealing, and tempering.

References

1. Valiev RZ, Islamgaliev RK, Alexandrov IV (2000) Bulk nanostructured materials from severe plastic deformation. *Prog Mater Sci* 45:103–189
2. Lavernia EJ, Han BQ, Schoenung JM (2008) Cryomilled nanostructured materials: processing and properties. *Mater Sci Eng A* 493:207–214
3. Khodabakhshi F, Kazeminezhad M, Kokabi AH (2011) Mechanical properties and microstructure of resistance spot welded severely deformed low carbon steel. *Mater Sci Eng A* 529:237–245
4. Khodabakhshi F, Kazeminezhad M, Kokabi AH (2012) Resistance spot welding of ultra-fine grained steel sheets produced by constrained groove pressing: optimization and characterization. *Mater Charact* 69:71–83
5. Khodabakhshi F, Kazeminezhad M, Kokabi AH (2014) On the failure behaviour of highly cold worked low carbon steel resistance spot welds. *Metal Mater Trans A* 45:1376–1389

6. Khodabakhshi F, Kazeminezhad M, Kokabi AH (2015) Metallurgical characteristics and failure mode transition for dissimilar resistance spot welds between ultra-fine grained and coarse-grained low carbon steel sheets. *Mater Sci Eng A* 637:12–22
7. Zimina M, Bohlen J, Letzig D (2014) The study of microstructure and mechanical properties of twin- roll cast AZ31 magnesium alloy after constrained groove pressing. *IOP Conf Ser: Mater Sci Eng* 63:012078. <http://iopscience.iop.org/1757-899X/63/1/012078>
8. Nazari F, Honarpisheh M (2018) Analytical model to estimate force of constrained groove pressing process. *J Manuf Process* 32:11–19
9. Lee S-H, Saito Y, Park K-T, Shin DH (2002) Microstructure and mechanical properties of ultra-low carbon IF steel processed of accumulative roll-bonding process. *Mater Trans* 43:2320–2325
10. Asghari-Rad P, Nili-Ahmadabadi M, Shirazi H, Nedjad SH (2016) A significant improvement in the mechanical properties of AISI 304 stainless steel by a combined RCSR and annealing process. *Adv Eng Mater*. <https://doi.org/10.1002/adem.201600663>
11. Nazari F, Honarpisheh M (2019) Analytical and experimental investigation of deformation in constrained groove pressing process. *Proc Inst Mech Eng C: J Mech Eng Sci* 233(11):3751–3759
12. Yogesha KK, Kumar N, Joshi A, Jayaganthan R, Nath SK (2016) A comparative study on tensile and fracture behaviour of Al–Mg alloy processed through cryorolling and cryo groove rolling. *Metallogr Microstruct Anal* 5:251–263. <https://doi.org/10.1007/s13632-016-0282-0>
13. Pouraliakbar H, Jandaghi MR, Heidarzadeh A, Jandaghi MM (2018) Constrained groove pressing, cold-rolling, and post-deformation isothermal annealing: consequences of their synergy on material behavior. *Mater Chem Phys* 206:85–93
14. Fong KS, Tan MJ, Ng FL, Danno A, Chua BW (2017) Microstructure stability of a fine-grained AZ31 magnesium alloy processed by constrained groove pressing during isothermal annealing. *J Manuf Sci Eng* 139(8):081007-1–9
15. Sajadi A, Ebrahimi M, Djavanroodi F (2012) Experimental and numerical investigation of Al properties fabricated by CGP process. *Mater Sci Eng A* 552:97–103
16. Liu K, Chen XG (2015) Development of Al–Mn–Mg 3004 alloy for applications at elevated temperature via dispersoid strengthening. *Mater Design* 84:340–350
17. Zimina M, Bohlen J, Letzig D, Kurz G, Pokova M, Knapek M, Zrnik J, Cieslar M (2015) The study of the behavior of constrained groove pressed magnesium alloy after heat treatment. *Acta Phys Pol, A* 128(4):775–778
18. Moradpour M, Khodabakhshi F, Eskandari H (2018) Microstructure–mechanical property relationship in an Al–Mg alloy processed by constrained groove pressing-cross route. *J Mater Sci Technol* 34(8):1003–1017. <https://doi.org/10.1080/02670836.2017.1416906>
19. Moskvichev E, Kozulin A, Krasnoveikin V, Skripnyak VA (2018) Numerical simulation of deformation behavior of aluminum alloy sheets under processing by groove pressing method. *Matec Web Conf* 143(1):01011. <https://doi.org/10.1051/mateconf/201714301011>
20. Wang Z, Guan Y, Wang T, Zhang Q, Wie X, Fang X, Zhu G, Gao S (2019) Microstructure and mechanical properties of AZ31 magnesium alloy sheets processed by constrained groove pressing. *Mater Sci Eng A* 745:450–459. <https://doi.org/10.1016/j.msea.2019.01.006>
21. Moradpour M, Khodabakhshi F, Eskandari H, Haghshenas. M (2019) Wear resistance and tribological features of ultra-fine-grained Al-Mg alloys processed by constrained groove pressing-cross route. *J Mater Eng Perform* 1235–1252. <https://doi.org/10.1007/s11665-019-3859-3>
22. Lin P, Tang T, Zhao Z, Wang W, Chi C (2017) Refinement strengthening of AZ31 magnesium alloy by warm constrained groove pressing. *Mater Sci* 23(1):84–88. <https://doi.org/10.5755/j01.ms.23.1.14392>
23. Thuy PT, Hue DTH, Ngung DM, Quang P (2019) A study on microstructure and mechanical properties of AZ31 magnesium alloy after constrained groove pressing. *IOP Conf Ser: Mater Sci Eng* 611:012005
24. Fathy A, Ibrahim D, Elkady O, Hassan M (2018) Evaluation of mechanical properties of 1050-Al reinforced with SiC particles via accumulative roll bonding process. *J Compos Mater* 1–10

25. Xue K-M, Liu M, Yan S-L, Wang Z, Hua Y-L, Li P (2018) Synergic improvement of plasticity and strength of Al-Zn-Mg-Cu alloy by grain refinement and precipitates redistribution using cyclic extrusion compression. *Adv Eng Mater* 1800140
26. Siddesha HS, Shantharaja M (2014) Optimization of cyclic groove pressing parameters for tensile properties of Al6061/sic metal matrix composites. *Procedia Mater Sci* 1929–1936
27. Saeidi Googarchin H, Teimouri B, Hashemi R (2018) Analysis of constrained groove pressing and constrained groove pressing-cross route process on AA5052 sheet for automotive body structure applications. *Proc IMechE Part D: J Automob Eng, IMechE* 1–17

T-Ceres—An Automated Machine for Any T-Shirt to Bag Conversion



S. Premkumar, Yash Prakash, Burhanuddin Shirose, K. M. Dhivakar, Mayank Kapur, L. N. Puthiyavan, and Ssmrithi Arul

Abstract Carry bags are one of the most used utilities in modern lives. Majority of the carry bags are made of plastic. Every day, 25,940 tons of plastic waste is produced in India gives way to environmental damage such as pollution, threat to marine life due to their inappropriate disposal methods. An alternative to these plastic bags is cloth bags but the environmental impact due to the manufacturing of a single cloth bag is equal to that of 104 plastic bags. So, a whole new system/invention is dearly needed that meets the demand of consumers and keeps in mind the environmental impact. To address these consequences, T-Ceres, our solution converts used T-shirts to cloth bags. This automated machine stitches the base of the T-shirt cuts the sleeves and widens the neck of the T-shirt to convert it into a carry bag. By doing this, we are extending the life of the cloth, thus reducing the amount of waste and harm generated due to fast fashion while eliminating the effect of manufacturing new cloth bags as well as replacing the single-use plastic bags in the modern market.

Keywords Environment · Recycling · Automatic cloth bag converter

1 Background Research

1.1 Introduction

Carry bags are one of the most used utilities in modern lives. Most of the carry bags are made of plastic. Manufacturing of these plastic bags has an enormous advantage over other alternatives in terms of environmental impact and the production cost. There is no doubt that plastic bags shadow other alternatives in terms of manufacturing cost and environmental impact in the process, but the biggest issue with using plastic bags is their disposal. They are not biodegradable and their negative impact on almost all the ecosystems is well known. Data collected from small businesses [1] shows we

S. Premkumar (✉) · Y. Prakash · B. Shirose · K. M. Dhivakar · M. Kapur · L. N. Puthiyavan · S. Arul
National Institute of Technology Tiruchirappalli, Trichy 620015, India

© The Author(s), under exclusive license to Springer Nature Singapore Pte Ltd. 2022
B. B. V. L. Deepak et al. (eds.), *Applications of Computational Methods in Manufacturing and Product Design*, Lecture Notes in Mechanical Engineering,
https://doi.org/10.1007/978-981-19-0296-3_22

247

use about 160,000 plastic bags per second and the rate is only increasing. This vast multitude of use of plastic bags demands the manufacturing sector to be at par with it hence, manufacturing of plastic bags is a trillion-dollar industry. This puts another hurdle in the way of plastic ban. So, a whole new system/invention is dearly needed that meets the demand of consumers and keeps in mind the environmental impact. Currently, there is no existing product in the market to address this issue, thus making our solution the first of its kind. At the same time, the use of cost-effective alternatives for laser cutting and pneumatic approaches makes the product much more feasible.

1.2 Background Data

According to data available from Vogue institute of art [2], in 2017 only 2.6 million tons out of 17 million tons of clothing produced was recycled. The rest ends up in landfills or are incinerated. One of the major problems is that natural fibers are decomposable but when mixed with synthetic fibers, the synthetic components inhibit the decomposition of natural components. Adding to the woes is the fact that most of the fabric today is a blend of natural and synthetic fibers. Figure 1 shows cloth disposal distribution.

Fig. 1 Disposal of cloth waste [3]

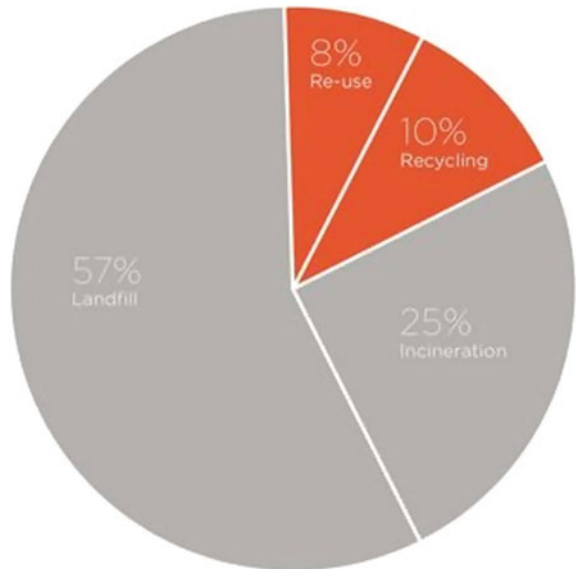


Fig. 2 Portion of T-shirt making into a plastic bag



2 Approach

2.1 Problem Statement

To design and fabricate an automated, compact, and user-friendly machine that converts used T-shirts to carry bags.

2.2 Our Solution

Our Product: T-Ceres addresses the reckless use of plastic bags by consumers all over the world by providing them an alternative by converting used T-shirts into cloth bags. Therefore, we use it to its maximum while also preventing manufacturing of new cloth bags which otherwise will cause adverse effects on the environment.

Figure 2 shows what operations T-Ceres is going to perform of the T-shirt thus making it into a plastic bag.

The machine cuts the base of the T-shirt right below the clamp and the excess part is disposed into a bin while the sleeves are cut and the neck is widened; thus, the widened neck becomes the mouth of the cloth bag.

3 Technical Report

3.1 Components

The proposed machine consists of following parts as represented in Fig. 3.

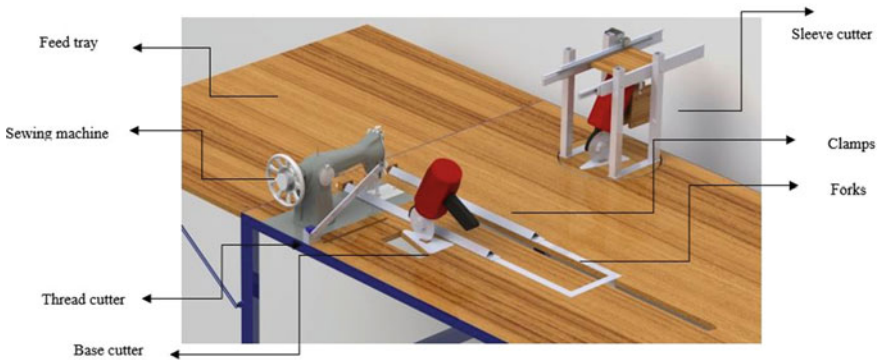


Fig. 3 Component placement

Platform

This is the base for the whole mechanism, is made of wood, and is mounted on the support structure which is an L-Frame. The whole platform is divided into two segments for ease of maintenance. A slot runs across the table through which the connector reciprocates.

Forks

The clamps are connected by a U-shaped structure called fork. The fork facilitates the movement of the clamped T-shirt past the platform through the other components.

Lead Screw

Lead screw is responsible for pulling the forks along with the T-shirt forward through each component. It is powered by a stepper motor (NEMA-23 10 kg-cm) and is connected to the forks via a connector (a simple vertical link) that runs through the slot and fits onto the fork assembly perpendicularly.

Clamps

Clamps as shown in Fig. 4 are devices used to hold the T-shirt firmly so that it prevents the T-shirt from slipping during different operations. In this machine, there are two clamps that are used to hold the T-shirt in two different locations—one at the chest and the other at the hem of the T-shirt. The clamp is designed in such a way that it can accommodate T-shirts of any size. It consists of male and female links having a V-shaped profile. This profile holds the T-shirt firmly during various operations. The clamps are locked using snap locks.

Base Cutter

Base cutter as shown in Fig. 5 is an electrical rotary cutter that cuts the excess part off the hem of the T-shirt to achieve the size required for the bags. It is moved back and forth using a rack and pinion mechanism.

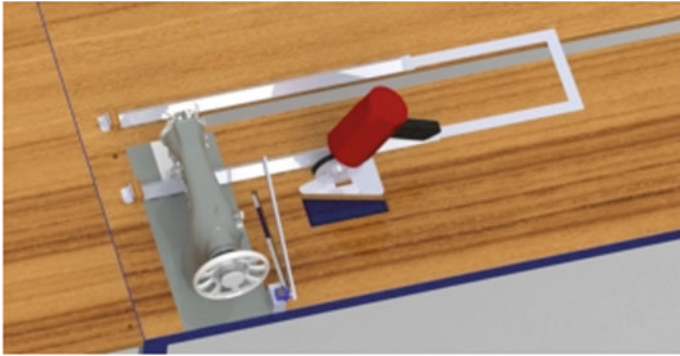


Fig. 4 Clamps and forks

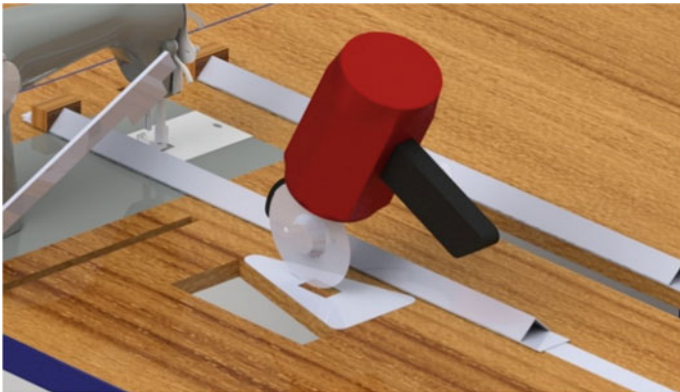


Fig. 5 Base cutter

Sewing Machine

A traditional sewing machine as shown in Fig. 6 which is powered by a motor is used to stitch along the hem of the T-shirt. The sewing machine is placed on the platform next to the base cutter.

Thread cutter

It cuts the extra thread running out of the needle and bobbin of the sewing machine after stitching and is placed next to the sewing machine. A blade is attached to the shaft as shown in Fig. 7 which is actuated by a motor. The blade while rotating goes through a dedicated slot in the platform thus ensuring the thread is cut properly.

Sleeve cutter

The sleeve cutter as shown in Fig. 8 is similar to the electric rotary fabric cutter that rips the sleeves off from the T-shirt and widens the neck of it for ease of handling.

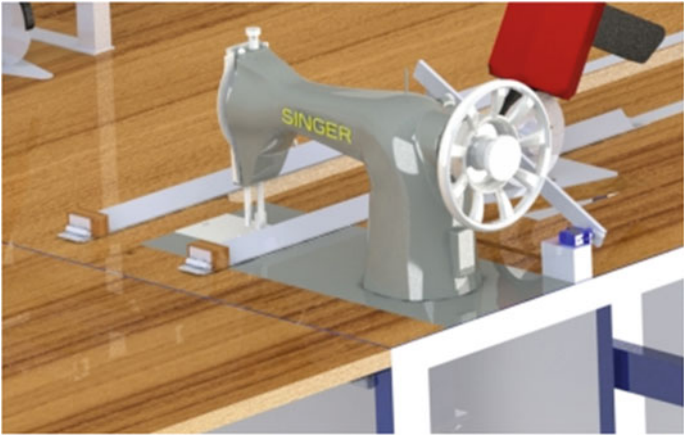


Fig. 6 Sewing machine



Fig. 7 Thread cutter

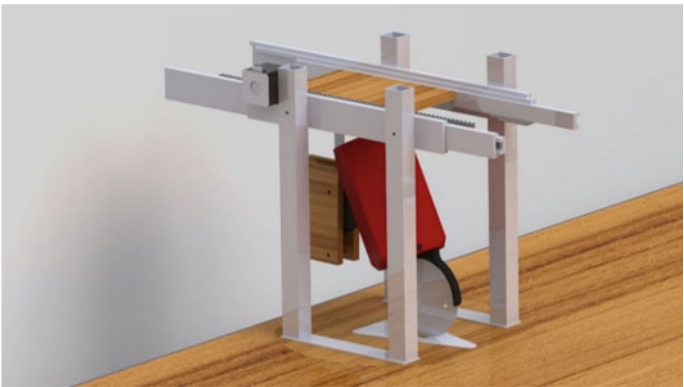


Fig. 8 Sleeve cutter



Fig. 9 Feed tray

The cutter is attached to a wooden plank which is attached to side supports (metal rods). There is a rack attached on top of it which is coupled to a pinion connected to a stepper which moves it forward. This assembly rests on a circular platform which is placed inside a hole of same dimension.

Feed Tray

It is a wooden extension of the platform as shown in Fig. 9 hinged to the start of the frame where the T-shirt is placed and fed into the machine. This part is made foldable for the ease of maintenance and accessibility to the base cutter and sewing machine.

IR Module

An IR module is placed right before the sewing machine at a predetermined distance from it. The IR module is used to measure the time T-shirt takes to travel across it and as we know the speed of the lead screw, we can know the length of the T-shirt which is used as explained in the working.

Stepper Motors

Two Stepper Motors are used to rotate the lead screw which in turn propagates the forks and therefore the T-shirt forward and moves the rack forward by rotating the pinion to move the sleeve cutter back and forth.

Servo Motors

Two Servo Motors are used to facilitate the movement of the blade in an arc that cuts the extra thread that comes from the sewing machine and to rotate the rack and pinion setup of the sleeve cutter through a fixed angle.

4 Working

The T-shirt is placed on the feed tray and clamped. As the stepper motor rotates the lead screw, the forks along with the T-shirt start moving forward. The IR module senses the T-shirt as it passes. The sewing machine starts after some delay and starts stitching on the part of T-shirt just above the upper clamp. Using the inputs from the IR module, we stop both the sewing machine as well as the lead screw once the sleeve comes right below the sleeve cutter. The sleeve cutter starts operating and makes an inclined cut first and then the straight cut. The lead screw and sewing machine start again until the next sleeve comes right under the sleeve cutter. The same inclined cut is made and then the sleeve cut. Coding ensures that the two inclined cuts meet at a point making a “V”. The thread cutter also operates simultaneously and cuts off the extra thread attached to the needle. The user can then open the casing from the side, open the locks and take out the T-shirt.

5 Work Flow

The flow process of the proposed system is shown in Figs. 10 and 11.

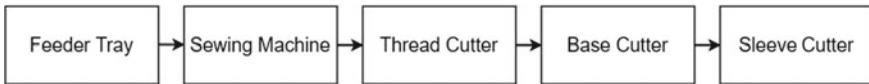


Fig. 10 Workflow of the machine

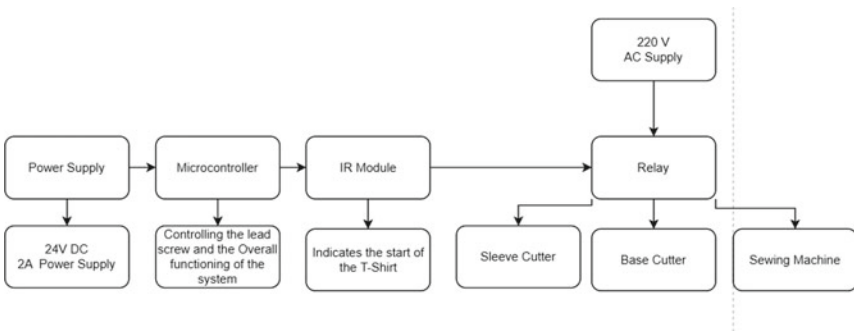


Fig. 11 Power flow of the machine

Table 1 Components and specifications

Components	Specifications
Feeder tray	Rectangular tray attached to the platform Length 800 mm, breadth 1200 mm, Thickness 18 mm
Fork	Aluminum structure that connects clamps to the lead screw length 250 mm, connector 150 mm, thickness 6 mm
Sewing machine	Sewing machine of base dimensions Length 440 mm, breadth 180 mm
Base cutter	Base cutter of dimension dimensions Length 200 mm, breadth 100 mm
Sleeve cutter	Sleeve cutter assembly is attached on a rotatable platform of diameter 30 mm
Platform	A plywood platform of dimensions length 1200 mm, breadth 1200 mm, thickness 18 mm
Clamp	Aluminum V-shaped structure of length 600 mm thickness 6 mm
Lead screw	Mild steel Lead screw of length 1000 mm with triangular threading

Table 2 Electrical components

Electrical components	Specifications
Stepper motor	Nema 17: 4 V-1.2 A per coil, 3.2 kg-cm—used for translation of sleeve cutter [4] Nema 23: 3.2 V-2.8 A per coil, 10.3 kg-cm—used for rotation of Lead Screw [5]
Microcontroller	Arduino UNO R3
Servo motor	SG90: 4.8 V-10 mA, 2.5 kg-cm—used for thread cutting Jx PS-5521: 4.8 V-3A, 19.3 kg-cm—used for rotation of sleeve cutter assembly
Relay	4 Channel relay control Board: 5VDC-10 A—used for controlling the sub-assemblies
IR module	RKI-3141: 5VDC-20 mA—used for sensing the width of the T-shirt

6 Power Flow

7 Specification Chart

See Tables 1 and 2.

8 Cost Analysis

Estimated cost of the proposed system (Fig. 12) in Indian rupees is illustrated in Table 3.



Fig. 12 T-Ceres

Table 3 Cost Estimate

Component	Requirement	Cost (INR)
Wood	(8 ft * 4 ft)	2000
Steel frame (2 mm thick)	19.19 kg (pipes and L columns)	4221
Sewing machine	1	2000
Electric cutter	2	8800
Aluminum (forks)	120 cm	100
Lead screw	1	250
Thread cutter (blade)	1	5
Welding	-	1000
Stepper motor	2	2100
Servo motor	2	1700
Relay	1	140
Wires	-	150
IR module	1	35
Arduino	1	250
Miscellaneous		100
Total		22,851

9 Emergency Situations

In case of a failure in any of the components there are three cases of emergency scenarios that can occur in the system:

Before the IR module: If any of the components fail before the T-shirt reaches the IR module placed before the base cutter, the forks are brought back to the initial position, and none of the components following its function.

During Stitching: If there is a failure during the stitching operation the sleeve cutter mechanism is switched off and the stitching operation is completed by moving the forks forward.

After Stitching: If there is a failure in any of the components after stitching, the forks are taken to the end position while all other components are shut down.

10 Conclusion

The product clearly will have a great impact on society as it provides a feasible, viable, accessible, ecological, economical alternative to plastic carry bags. The biggest advantage is tackling the huge menace caused by irresponsible, inefficient disposal of plastic carry bags which does not have a clearer alternative. The business model seems to be an effective one with only improvements required in logistics. The load-carrying capacity also ensures the large lifetime of the bag. Moreover, keeping in mind the growing awareness among people, this product ensures that it gives a platform to contribute toward saving the planet.

References

1. <https://www.thebalancesmb.com/textile-recycling-facts-and-figures-2878122>
2. <https://www.voguefashioninstitute.com/how-to-recycle-waste-clothes>
3. <https://www.commonobjective.co/article/fashion-and-waste-an-uneasy-relationship>
4. <https://www.cuidevices.com/product/resource/nema17-amt112s.pdf>
5. <https://datasheet.octopart.com/NEMA23-17-15PD-AMT112S-CUI-Devices-datasheet-141001913.pdf>

Automatic Attendance Monitoring System (AAMS)



Abhinav Santosh Pandey, Kumar Mayank Verma, Tanya Verma, and Abhay Kumar

Abstract As We Know Marking Attendance manually is something that takes more time and also leads to distraction of class whilst taking attendance. This form of taking attendance didn't guarantee the safety of the whole data. So, we automated this system by creating an Automated Attendance Monitoring Application that will manage all the tasks related to attendance marking. This application is based on facial recognition technology which is nothing but identification of a particular person by peculiar features of their faces and it functions as a clear identifier of anyone (Matilda and Shahin in 2019 IEEE international conference on system, computation, automation and networking (ICSCAN), pp. 1–4, 2019[1]). As computer vision (CV) is growing day by day as it is technology that takes images/videos as its input and performs classification of images, detection and recognition of given input images (Deeba et al. in Int. J. Adv. Comput. Sci. Appl. 2019[2]). Its functionality is simply we had to move our camera into room and it will detect the faces and later train the images by our pre-trained model i.e. Haar Cascade Files and then recognizes every face and marks the attendance by matching with stored images data in firebase and stores attendance in csv file and this will save time and hence will avoid fake proxies.

Keywords Face recognition · Computer vision (CV) · Firebase · Local binary pattern histogram · Haar cascade file

1 Introduction

Machine Learning the word only tells that we are automating the machine by using some technologies or some algorithms that are used to train machines at various levels and parameters. Facial Recognition is one of the parts of the machine learning domain which is increasing nowadays in various fields. Face is the most important part of the human body to recognize anyone on basis facial peculiar features [1]. We have also seen various research works done in the field of facial recognition and many

A. S. Pandey (✉) · K. M. Verma · T. Verma · A. Kumar
School of Computing Science Department, Galgotias University, Greater Noida, India

researchers have proved this technology is one of the best technologies in the field of machine learning and image processing. Student attendance marking has been a quite headache for instructors since it wastes the time and also distracts the students from the ongoing topic in class and majorly the problem of fake proxies. So we had found an easy and simple alternative for this manual way of marking attendance that is to automate this manual attendance marking system by applying facial recognition technique. There are various researches and models had been made already in this topic and they had successfully implemented them also. Like [3] proposed a system which is based on this similar face recognition technique but in terms of accuracy their models are little lacking when compared to models proposed by [4].

we all know that facial extraction is done either by image processing or by feature extraction and both these techniques are really good in their terms but if we talk about accuracy, feature extraction tops this technique and this is the speciality of our proposed model that we had implemented an automated monitoring application which uses this feature extraction from the face and we had succeeded very well in comparison of other techniques available. Hung [5] proposed a facial recognition attendance marking model based on neural networks and had used a support vector machine as an image classifier algorithm which is quite good in terms of getting accurate results.

But when it comes to which classifier algorithm we had used in our model then we had just used one of the best and efficient algorithms i.e. LDA (linear discriminant analysis) which reduces the high dimension image space into low dimension space and we knew that for image processing high dimension is not good so we had come up with this algorithm which is good as compared to [5] in both terms execution time and space.

There are different facial recognition algorithms but the main three which are being used many times in different technologies for facial extraction are (1) Eigenfaces Method, (2) Fisherface Method, (3) Linear Binary Histogram Pattern Method which is also clearly seen in one of article by Jeong JP in IAAS [10]. In the first two methods the algorithm considers image as eigenvector and evaluates results on the basis of extracted features but there was a problem in these methods that if light of the room is low or if a student or person is far than these methods were unable to give exact results. Then we had used Linear Binary Histogram Pattern Method which has quite much roots in 2D image analysis and also it's one of the important features that it compares image pixel by pixel which is very different from the previous researches as compared to accuracy and time of the algorithm.

In today's world there have been a lot of advancements in the biometric attendance system. Like we can see fingerprint-based attendance system which was quite interesting when it was introduced and till today many are using this technology for their attendance marking application and for various security purposes but it has come up with some security threats like anyone can get your fingerprint and easily scan and can enter to manipulate any kind of important things whether it is office or some institution [6]. The main objective of this paper is to make an automated application which will provide ease in terms of marking attendance. Firstly, we will place camera in front of faces and then our algorithm for facial recognition will detect the face

and then it will be converted into various greyscale images which is specialty and uniqueness of our project and then with the pre-trained model it will be trained and after this by using LDA we will reduce the dimensionality of our image by image processing and then applying linear binary histogram pattern algorithm to recognize the face and then our application will redirect to firebase to match the data stored in bucket in firebase and then matches the image features in the firebase and marks the attendance on the basis of matched image and this data will be stored in separate csv file.

We had a very well defined introduction part of our work so far and now the rest part of our research work will consist of comparative study of the given technology, methodology, analysis of our working application, results and conclusion at last.

2 Comparative Study of Face Recognition

As we already know that marking attendance via face recognition is not a new topic to write as there are various applications, papers and journals published or developed on this attendance monitoring system and they were quite good projects in every aspect. Mehta et al. [7] proposed one of the best models for automated-based attendance system by using video inputs of the classroom and in this they introduced an interesting factor of two levels of authentication which was really a good idea and it was working unless the video inputs were clearly given to algorithm but when there is dark in classroom due to power cut then video inputs were unable to perform face detection and recognition and also unable to see the faces of students and this was main failure behind this model and whilst talking about our model there is not any kind of drawback of light as we had tested our model in dark light it was working fine as we had used image processing which converts image into grayscale images and stores the each and every pixel of face so when light is dim also we can just take picture and recognize it by comparing pixel by pixel of given image.

Further to these, the face recognition model by using convolutional neural networks (CNN) for attendance monitoring is the best model ever made in terms of speed and time of application. We had seen that this works with one of the pre-trained models to get the feature of machine Learning as used by [5] in their paper also. But only problem with this application that it was capable of extracting only eyes, ears and nose features which have low recognition problem and due to which many have moved to another method for face recognition methods like eigenfaces, fisherfaces and lot more algorithms.

PCA (principal component analysis) is another method that is used in attendance monitoring algorithms as Pentland proposed this idea in 1991. This PCA uses eigenvectors and eigenvalues for reduction in dimension of an image and it will train the data in small space. Its functionality is somewhat similar to our model in which we had used LDA for reducing the image dimension. As [8] uses this principal component analysis in his paper but to overcome this PCA problem he used another machine

learning classifier to overcome the problem raised by PCA and that MAP-MRF classifier was working with PCA very well and successfully. However, Eigenfaces was also very effective when it comes to face recognition but PCA was more popular that time for this technology. Also Principal component analysis was used for facial feature extraction and dimensionality reduction. Nguyen et al. [9] proposed a model based on fingerprint automatic model for recognizing the faces but this was with limitations that it requires both face and fingerprint which was very time consuming task for teacher as well as students.

Now, talking about one of famous algorithms for recognizing faces is by using dlib in python which is nothing but a simple face recognition API provided by ageitgey and this API works in real time for recognizing the faces even it can recognize the multiple faces successfully in every condition. It simply takes the faces from image and converts them into encodings and then uses support vector classifier which is pre-trained model to train those dataset and then successfully recognizes those faces by using API but when it comes to large datasets it lacks in this field because SVC gives very accurate results when there is small datasets but for large datasets it is showing inaccuracy in its performance and this is the reason this method is only used for small datasets. Sovitkar and Kawathekar [6] described this problem into his paper also and gives a proper explanation about the limitations of this method.

3 Proposed Methodology

AAMS application works in several phases and these phases are interdependent on every phase. Our application functions in 4 stages involving getting images into dataset creation module and then training those datasets in various conditions and after that matching all the trained datasets with the images stored in separate folder where all the greyscale images of students along with the IDs are stored and then on basis of matched datasets marking the attendance successfully and presenting in the form of sheets with the help of firebase is one of the uniqueness of our software and working module of AAMS application.

- A. *AAMS Architecture*: The architecture of AAMS application consists of only three modules (Fig. 1) i.e. first one is image capturing module, then image processing algorithms and last but not least database part which is maintained by Firebase in AAMS.
- B. *AAMS Dataset Creation*: We will begin the process of capturing video from the dataset. After using the haar cascade frontal face xml file the process of feature detection will begin as shown in Fig. 2. At the end the sample face image count will be initialized to zero. The loop will begin and the image frame will be captured and converted to grayscale image. Then each face will be looped separately and cropped into a rectangular frame. The sample face image will be increased. Then in the dataset folder our image will be saved that is stored

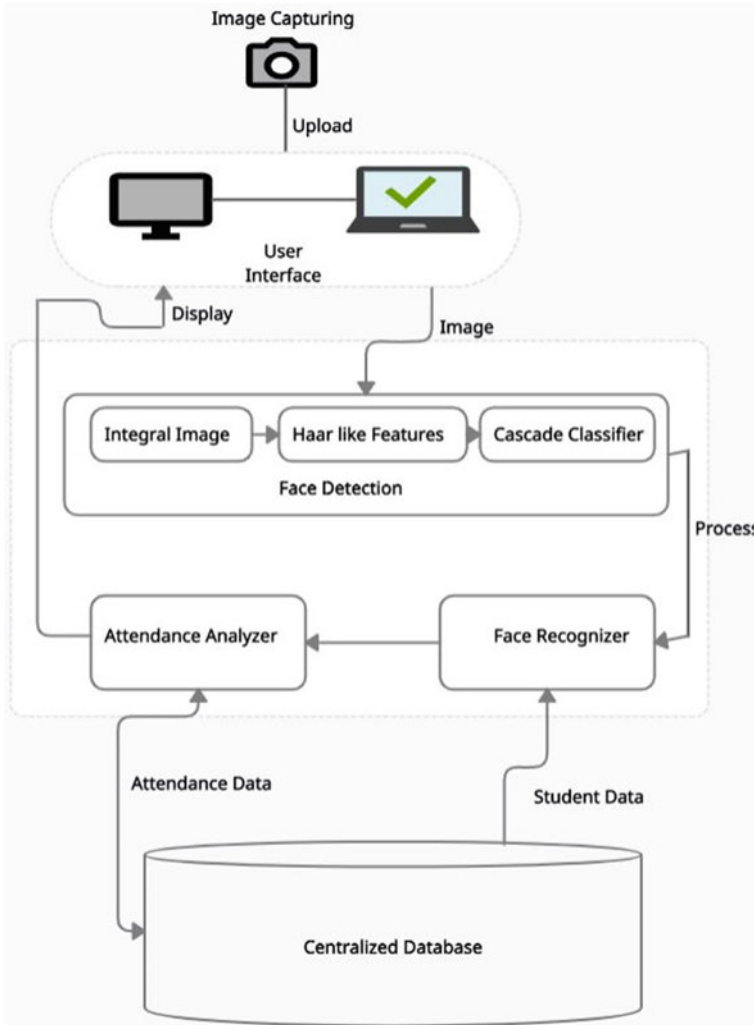


Fig. 1 AAMS architecture by Abhinav Pandey Jan 2021

in the OS path. The video frame would hence be displayed with a rectangular frame over the face of the student.

- C. *AAMS Dataset Training:* To detect the faces we have used the Haar cascade file and also to do the process of training our pre-trained model. Hence different features of the face will be extracted like nose, eyes, cheeks. We have defined functions for getting the associated faces and face ID with the available image. At this point we have to train our model on the faces and face ID parameters in the yml file. The application will be trained every time when we want to take attendance of class and up to now we had trained for 60 dataset which



Fig. 2 Different sets of data created whilst AAMS dataset capturing by Abhinav Pandey Jan 2021

average number of students in class got an accurate results upto 95% and for big datasets we are trying to build an upgraded version of this which has trained as many as datasets in one time only.

- D. *AAMS LBPH Recognizer Module*: This Module is main thing that we had used in our application which is completely different from other papers. The main function of this module is that it recognizes images by feature extraction by comparing the middle pixel of an image with its neighbouring pixels and storing in form of binary numbers (Fig. 3) and this is the main reason behind accuracy of our application.

Further, this algorithm will convert those trained image datasets into grayscale images Refer to (Fig. 4) and after merging those images we will get histogram features of images which have every features of a face of a particular dataset Refer to (Fig. 5).

- E. Haar Cascade xml File is used as pre-trained model for our AAMS application which is also a feature classifier of an image during the recognizing phase of an image.
- F. Google Firebase is used as Database support for our application which automatically stores datasets in its bucket and does the process of all dataset matching with results which is one of the advantages behind our AAMS application.

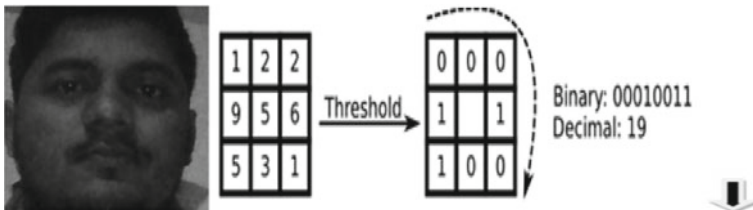


Fig. 3 Image in form of matrix whilst recognizing phase by Abhinav Pandey Jan 2021

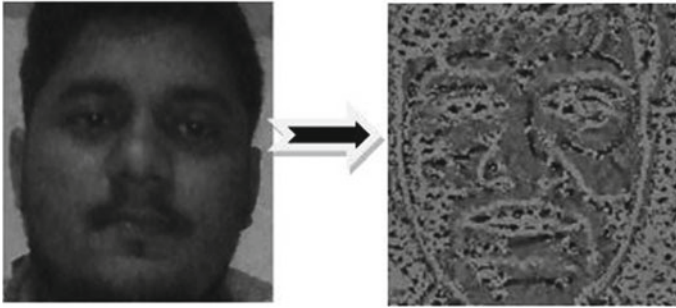


Fig. 4 Image and grayscale image

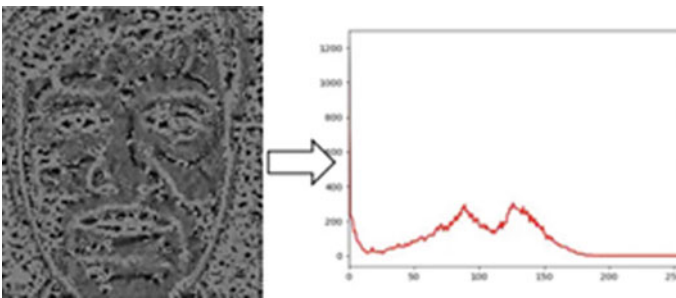


Fig. 5 Grayscale image and histogram representation of an image

4 AAMS Analysis

Now, coming towards analysis part we did an analysis by giving this application to various schools and collected point of views of various teachers and students regarding our application and these views are depicted in form of Table 1.

Table 1 Analysis amongst teachers and students for AAMS application

Experiment taker	AAMS point of Views	Satisfied Yes/NO
Teachers from various schools	Most of them had good views on AAMS. They told us that it gives accurate results when they try in their classes	Yes
Students views	They also find this interesting but some students were complaining about this as they thought automating everything will result in a lack of interest in the classroom	60% Yes 40% Not satisfied
Parents view	Every parent were satisfied with AAMS as they were happy that their children will not skip classes with this application	Yes

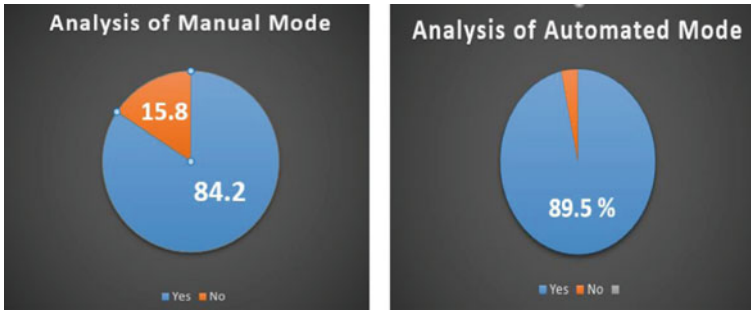


Fig. 6 Manual mode analysis versus automated mode analysis

We had also made a pie chart representation of AAMS about views on manual mode and automated mode of attendance and it is depicted in Fig. 6.

5 Results and Tests of AAMS

To check the efficiency of AAMS we had tested it on 30 students with 90 different images and we got an efficiency of above 95% and also seen that when our face orientation is incrementing it decrements the rate of recognition.

1. Face Detection Module involving the detecting face and storing it for training. Firstly, by starting with capturing images it will show up the User Interface part which is made with the help of tkinter module in python.
2. The Face Recognition module is done by using a local binary histogram algorithm and for feature extraction we had used a haar cascade classifier which would automatically train those datasets and recognize them and then gives it to firebase for final results.

Figure 7 shows the Grayscale Images result after extraction from the face and then start recognizing the image phase.

Table 2 illustrates the results after testing on a set of 30 Different persons with 90 different Images.

6 Conclusion

This Work is made for enhancement in the field of marking attendance by instructors and by applying various algorithms and methods this application was successfully made and tested also. This image recognition technology is being used by many but most importantly it is different from others in every aspect as we have used very efficient algorithms which should be required to make an application work efficiently

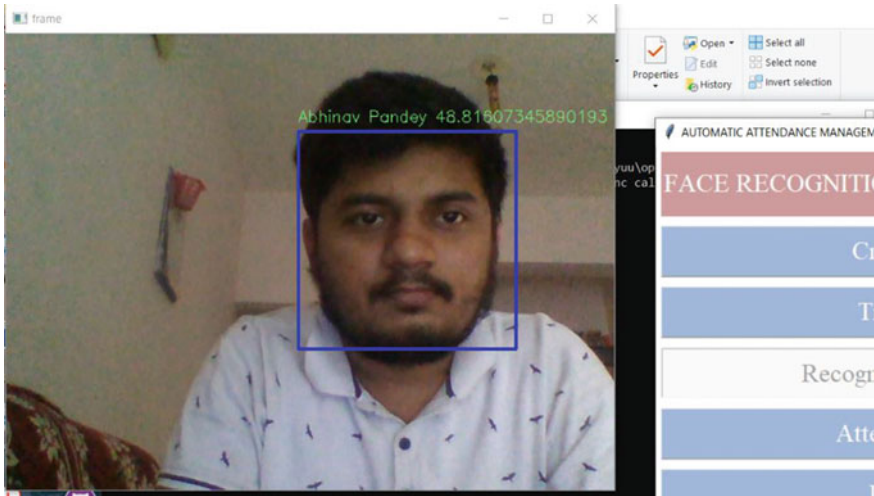


Fig. 7 Image recognition

Table 2 Analysis results of proposed approach

Module tests	Expected output	Observed output	PASS/FAILED
Create dataset module	Connects with the camera and creates different datasets	The camera started and captured the images for dataset training	PASS
Train module	It will train the images with help of haar cascade files and thereby get executed for extraction	Images trained properly and extracted for recognition purposes	PASS
Recognize module	Here the LBPH algo will work and the image will be recognized and stored in a csv file	Image recognized properly and displayed in csv file successfully	PASS

and this is the main motive of every application around the globe that it should be efficient.

For further future work, we are trying to apply big data so that it will be able to recognize around as many people in the room and also try to add extra features like sending automatic messages to parents regarding attendance of their students.

Acknowledgements This Proposed work/paper is solely done by Galgotias University Students and we would like to thank Galgotias University for Mentoring whilst making this project and special thanks to *prof. Abhay Kumar*.

References

1. Matilda S, Shahin K (2019) Student attendance monitoring system using image processing. In: 2019 IEEE international conference on system, computation, automation and networking (ICSCAN), pp 1–4. Pondicherry, India. <https://doi.org/10.1109/ICSCAN.2019.8878806>
2. Deeba F, Memon H, Dharejo F, Ahmed A, Ghaffar A (2019). LBPH-based enhanced real-time face recognition. *Int J Adv Comput Sci Appl* 10. <https://doi.org/10.14569/IJACSA.2019.0100535>
3. Shah K, Bhandare D, Bhirud S (2021) Face recognition-based automated attendance system. In: Gupta D, Khanna A, Bhattacharyya S, Hassanien AE, Anand S, Jaiswal A (eds) International conference on innovative computing and communications. *Advances in intelligent systems and computing*, vol 1165. Springer, Singapore. https://doi.org/10.1007/978-981-15-5113-0_79
4. Saharan A, Mehta M, Makwana P, Gautam S (2021) Automated attendance management using hybrid approach in image processing. In: Khanna A, Gupta D, Pólkowski Z, Bhattacharyya S, Castillo O (eds) Data analytics and management. *Lecture notes on data engineering and communications technologies*, vol 54. Springer, Singapore. https://doi.org/10.1007/978-981-15-8335-3_34
5. Hung BT (2021) Face recognition using Hybrid HOG-CNN approach. In: Kumar R, Quang NH, Kumar Solanki V, Cardona M, Pattnaik PK (eds) *Research in intelligent and computing in engineering*. *Advances in intelligent systems and computing*, vol 1254. Springer, Singapore
6. Sovitkar SA, Kawathekar SS (2020) Comparative study of feature-based algorithms and classifiers in face recognition for automated attendance system. In: 2020 2nd international conference on innovative mechanisms for industry applications (ICIMIA), pp 195–200. Bangalore, India. <https://doi.org/10.1109/ICIMIA48430.2020.9074917>
7. Mehta R, Satam S, Ansari M, Samantaray S (2020) Real-time image processing: face recognition based automated attendance system in-built with “two-tier authentication” method”. In: 2020 international conference on data science and engineering (ICDSE), pp 1–6. Kochi, India. <https://doi.org/10.1109/ICDSE50459.2020.9310090>
8. Majumdar S, Bose A, Das P (2021) A novel approach for face recognition using modular PCA and MAP–MRF classifier. In: Bhattacharjee D, Kole DK, Dey N, Basu S, Plewczynski D (eds) *Proceedings of international conference on frontiers in computing and systems*. *Advances in intelligent systems and computing*, vol 1255. Springer, Singapore. https://doi.org/10.1007/978-981-15-7834-2_17
9. Nguyen LT, Nguyen HT, Afanasiev AD et al (2021) Automatic identification fingerprint based on machine learning method. *J Oper Res Soc China*. <https://doi.org/10.1007/s40305-020-00332-7>
10. Jeong JP, Kim M, Lee Y, Lingga P (2020) IAAS: IoT-based automatic attendance system with photo face recognition in smart campus. In: 2020 international conference on information and communication technology convergence (ICTC), pp 363–366. Jeju Island. <https://doi.org/10.1109/ICTC49870.2020>

Coronavirus Visual Dashboard and Data Repository: COVID-19



M. Arvindhan, Mohit Bhatia, Nishant Sinha, and Tarun Kumar

Abstract This research paper talks about the site advancement and the most hazardous and pandemic infection COVID-19. We are additionally examining the Steps followed for making a site. We analyze diverse site advancement web applications. What is more, we examine a daily existence cycle and system of advancement of web applications. In this report, different audit papers' results likewise included for comprehension of issues can be looked at by the client for making a site and furthermore the issues looked by this infection. This Research Paper discusses the advances utilized in the improvement of site, JavaScript, HTML, CSS and clarified in outcome its usefulness with its structures (i.e., Nodejs, Expressjs) with screen captures. It is trusted it will give a valuable system for managing the cycle.

Keywords JavaScript · HTML · CSS · Advancement · Nodejs · Expressjs · COVID-19

1 Introduction

COVIDs are a group of infections that will cause sicknesses, for example, respiratory illness, Serve acute respiratory syndrome (SARS), and geographic territory respiratory disorder (SEAS). In 2019, another COVID was distinguished in light of the fact that the clarification of the sickness scourge began in China. The infection is currently said on the grounds that the serious Coronavirus 2 respiratory syndrome (SARS-COV-2). The sickness it causes is called Coronavirus 2019 (COVID-19). In March 2020, the COVID-19 scourge is announced destructive sickness by the World Health Organization (WHO). General wellbeing gatherings, including US disease control and prevention centers (CDC), and screen pandemic updates and show on their sites. These gatherings have additionally distributed proposals to forestall and treat the sickness.

M. Arvindhan · M. Bhatia (✉) · N. Sinha · T. Kumar
SCSE Galgotias University, Gautam Budh Nagar, Greater Noida, UP, India

© The Author(s), under exclusive license to Springer Nature Singapore Pte Ltd. 2022
B. B. V. L. Deepak et al. (eds.), *Applications of Computational Methods in Manufacturing and Product Design*, Lecture Notes in Mechanical Engineering,
https://doi.org/10.1007/978-981-19-0296-3_24

Coronavirus visual Dashboard And data Repository may well be a platform where everyone can see the most recent updates of the coronavirus and acquire updates to prevent these diseases it also tells us the protection Measures and thus the Symptoms of the virus within the physical structure, by which you will be ready to be safe or prevent meeting those people with the symptoms of coronavirus. It also contains some data of your nearby hospitals and also the helpline numbers that are issued by the Indian Government. It also contains the entire number of cases and also the recovery Rate and thus the No of deaths within the globe. And also updates you on the foremost recent status of the virus on the daily basis. Be Safe and Happy.

Website Development resembles a structure of house, i.e., prior to building a house, we get some information about arrangement, permit, administer a study of geographical and permit from city, design (i.e., blueprints). And the things that are needed for the site improvements are configuration, fitting language, internet browser, and so forth [1].

Most necessary thing for an online site is selecting a programming language. Mostly web design is done using HTML and CSS. For web designing not necessarily high-level knowledge of HTML is required. We use JavaScript for animations and making our website more interactive which also looks good [2].

Our idea gives everyone an idea about how to be safe in this dangerous period and keep them updated by the giving them current status of the virus. The Purpose of the “CORONAVIRUS VISUAL DASHBOARD AND DATA REPOSITORY: COVID-19” is to give awareness about the most dangerous disease known as Coronavirus. And give them a brief introduction to the Web Development. As there are many websites related to COVID-19 and also most of them are issued or made by who or any country Government But all in the there is a high level of knowledge given about the virus and its cause but most of the people are not used to that kind of high-level knowledge and even cannot understand that. So, our website gives a brief Knowledge about the virus in simple way they can understand and also, we give them the simplest website by which if any coder wants to do work in web development then they can simply understand and also can have a simple knowledge of the web development.

Website Development Process:

Various Steps consider in Website Development Process:

- Analysis
- Requirements
- Invention and Development
- Content Writing
- Coding
- Advancement
- Maintenance and Update

As Fig. 1 shows the entire Roadmap of our Projects.

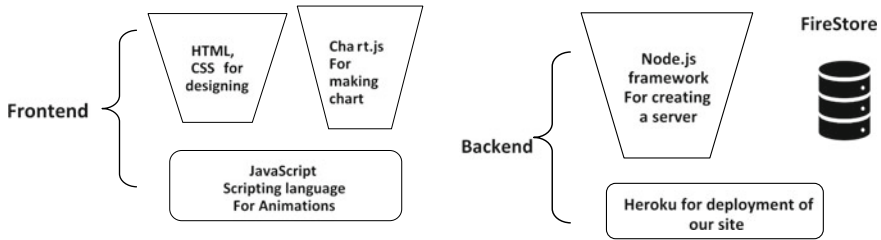


Fig. 1 Architecture

1.1 Analysis

Right off the bat, we comprehend the site prerequisite for creation, including web composition and Website styling, the Web pages utilized, site content and for recommendation and conversations, a legitimate space accessible on a site for effectively agreeable [3].

1.2 Requirements

Predicated on Requisite, set up a draft assignment of destinations to be created incorporating the sitemap and a progression of fluctuated measure.

1.3 Invention and Development

Invention and Development play a significant role in Web Development. We created a logo for our site as shown in Fig 5. Designing plays a vital role in the web development. And it also decides how is our website or web application looks and at what place is for what thing [3].

1.4 Content Writing

Composing of substance is a huge piece of making a site and assumes a vital function to give as much as data about the what is the motivation behind making a site. Content composed by a more expert requires more unadulterated, simple, and exact substance.

Table 1 Timeline of objectives achievements

S. No.	Activity/objective	Duration
<i>Front end</i>		
1	Designing the landing page (HTML AND CSS)	3 Weeks
2	Implementation of markup language (CSS)	2 Weeks
3	Implementation of animations and responsiveness language (JavaScript)	3 Weeks
<i>Backend</i>		
1	Setting up the server	1 Week
2	Creating a login and signup form	2 Weeks
3	Connecting to the database (FireStore)	2 Weeks
4	Improving our websites	3 Weeks

1.5 Coding

Beginning of the coding of a Web Pages is started using CSS, HTML, JavaScript contents, and different advances of WWW (internet), for drawing of the realistic and text substance, we write code of website page reliably like as site page plan. Coding of a web page is stacking fast program and list gives us rank rapidly. Each site of a web website takes a particular title, interesting meta labels as catchphrases and depictions. We can make connections of inner with catchphrases of site to investigate the program positioning and route. In this manner improve the site quality code by utilizing strategies and instruments reliable with site norms.

1.6 Advancements

The headways are in like manner a vital advance for site to attention to the people groups. To turn out to be greater, we will do site advancement that is recorded underneath: E-mails, Social media, Weblogs, Articles, Blog, Advertisements, Networks.

Table 1 represents the steps to make websites and time taken or the explanations of Fig. 1

1.7 Maintenance and Update

For better operation, our developer and also other users can suggest and monitor the website from time to time. We also can make it as an open-source project like there are many developers in our country who can give us more ideas that what new content we can add or what we can do to improve our site by deploying either in Heroku or GitHub [3].

2 Related Work

Kamini et al. [4]: This paper additionally portrays the utilization of MERN stack for speaking with IoT (web of things) gadgets. JavaScript is utilized as scripting language for customer-side programming that runs in any strong program.

Ninan et al. [5] the objective of this paper is to take a gander at the use of applying the interpersonal interaction advances in Education Institutes.

According to Taylor et al. [6], proposed deal with “A User Center Website Development Approach” during this paper distinguish the client prerequisites for the site, that is a prerequisite for information on the shifted necessities after its plan of site and vital methods utilized. Fundamentally, site highlights rely on the shifted kind of site clients. Chiefly those strategies utilized in this kind of site go under the client-focused plan of site.

COVID-19: Viral–Host Interactome Analyzed by Network Based-approach Model to Study Pathogenesis of SARS-CoV-2 Infection. During this examination, an organization-based model was created with an expectation to characterize atomic parts of pathogenic aggregates in human COVID contaminations [7]. A superior comprehension of the pathophysiology identified with COVID-19 is critical to upgrade treatment modalities and to create successful counteraction procedures. The subsequent example from this investigation may encourage the strategy for structure-guided drug and indicative examination with the possibility to spot expected new natural targets.

The Hallmarks of COVID-19 Disease [8]. A nitty–gritty investigation in comprehension of the epidemiological, virological, and clinical attributes of COVID-19 and a conversation of the possible focuses with existing medications for the treatment of this arising zoonotic sickness.

Chisnell and Redish [9], Both recognized these requests and got back with another turn on using personas and heuristics that thinks about age, yet the limits, wellness customer. The ensuing stage was to apply the model. There are 50 objections are picking regions of data than money-related clinical consideration and recreation exercises: Sites that are likely going to be used by a more settled experienced childhood in the run of the mill course of their day.

3 Research Methodology

System and route utilized for a site improvement are distinctive for various clients, most thoughts state the correct method of site advancement is created by the engineers according to the necessity in own methodology [10].

Necessities of a large portion of the sites had not changed by time and cost and something else is that we need a web-worker space and cost to store the site on the web-worker documents cannot store at on the worker of nearby. Basically, we need to know all about a web browser for creating a website like Google Chrome, Microsoft

edge, Firefox, etc. We also need the basic knowledge of HTML, CSS, and JavaScript. Our idea gives a simple way to understand the concept of web development and also gives an information about the existing virus COVID-19. That is how to prevent it and the safety precautions.

Hypertext Markup Language (HTML) is the standard markup language for reports intended to be shown in an internet browser. It is utilized to make a structure for a site.

Cascading Style Sheets (CSS) is a template language utilized for depicting the introduction of a report written in a markup language, for example, HTML. It helps us to style the html document or website to show it attractive like making a background, changing fonts, styling images, etc. it also used to make the site responsive using media queries i.e., the site is can be viewed on both desktop and mobile without any font dissimilarity.

JavaScript regularly contracted as JS is a programming language that adjusts to the ECMAScript determination. JavaScript is elevated level, regularly in the nick of time gathered, and multiparadigm. It has wavy section grammar, dynamic composing, model-based item direction, and top of the line capacities. It is used for the both front end and backend. For front end we use it for animations and, tracking the HTML and for backend it uses for client-server.

In this work, we are using to use a JavaScript framework known as Nodejs for creating a server. For this presentation, we use HTML to code our site content and diverse symbol that we need on our site looks, we use CSS for content planning of the site. Those symbols we need on the front as a few pages title, for these titles we have different sections like Home, About, Contagion, Symptoms, precautions, Cases and contact section. The work is about to generate rules that will be used for the users and the students to know the basic knowledge of web development and also it gives us the knowledge of the virus known as Coronavirus or COVID-19 which is most dangerous virus spreads all over the world. And also get to know how to use APIs for the information according to the requirements.

3.1 Objectives

The objectives associated with the work are given here:

- (1) The target of work is giving an update to every one of new technologies in the web development.
- (2) The goal of the work is to give a stepwise information or knowledge for making a website.
- (3) The goal of work is to incorporate the different strategies for streamlining work.
- (4) The target of work is to improve the precision and strength of work.
- (5) Our Main Motto is to develop such kind of platform that no one in the world is still unaware of this disease.

- (6) As our title says “Coronavirus Visual Dashboard” which means it tells us or update us from the latest status in the coronavirus days and the “Data Repository” means the Data of the coronavirus like the Symptoms, Safety measures, and some information about what to do if you feel u are infected or the information of the hospitals for the check-up.
- (7) Our idea gives everyone an idea about how to be safe in this dangerous period and keep them updated by the giving them current status of the virus.
- (8) It also helps everyone to understand the processes that take place in the web development and how interesting is this.
- (9) Our idea gives them brief of web development and to work is done in the field.

3.2 Scope

- (1) The degree and centrality work is given here under. In existing work, no worker space is utilized and no cost utilization for DNS will be utilized.
- (2) Applying the JavaScript Coding with help and certainty detail on various phases of plans will improve the precision. Client will be ready to infer all the clearer perceptions with respect to standpoint of site, effectively can add content.

4 General Approach

Our first approach is to try to deploy our site to Heroku and the hosting is also done by Heroku. Through Heroku users can easily navigate to our site as Heroku provides us a domain for our site and it can be seen easily by the developer and users can clone the source code from the Heroku in their local system for the further reference. Heroku is a holder-based cloud Platform as a Service (PaaS). Engineers use Heroku to send, oversee, and scale present-day applications. It is a platform where various user can deploy their projects with ease and also helps to run the modern applications as shown in Fig 2.

5 Result

In view of this work, we have made an intelligent, responsive, and usable site. In the wake of utilizing these stunning and fast mindful things expansion, presently we can ready to choose every one of those things in this work. For creating our own Server Nodejs structure is utilized in JavaScript language.

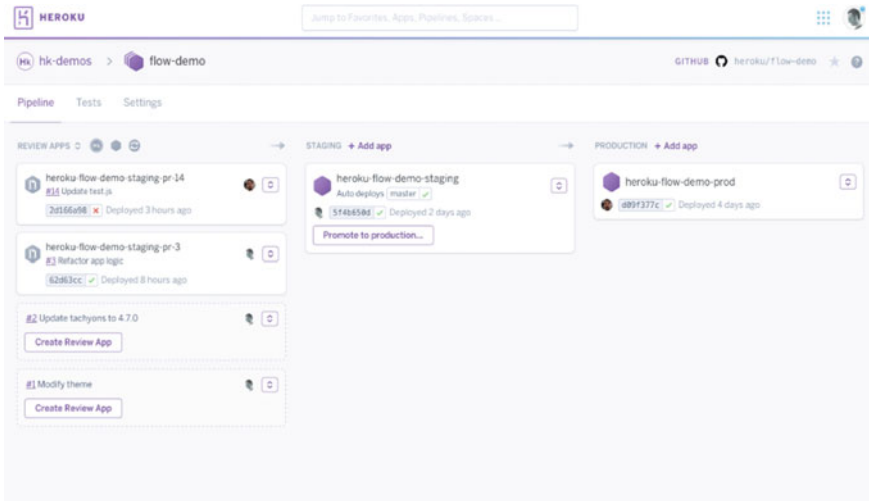


Fig. 2 Screenshot of Heroku deployment

5.1 Index Code:

For website design, we have written code in HTML and CSS. The things we can see on the Homepage of the website are done using HTML and CSS. Now let's see the screenshot of the same in Fig 3.

5.2 Standpoint of List Document

In index file, all the labels like overview, Contagion, Symptoms, etc. will be reflected on the Homepage of the website.

Firstly, we go to the Heroku where we deploy our site and this provides us a link or a domain for navigating to our home page as shown in Fig. 4.

5.3 Content Preview on a Website

In the image, we added some contents related to COVID-19 (logo as shown in Fig. 5) such as symptoms, precautions, and daily based increase and decrease of the cases and recovery or deaths cases of whole world. Apart from this, we use API for our project for requesting the information of cases in the world by which we can navigate the latest status of COVID-19 in whole world as represented in Figs. 6 and 7.

```
index.html X style.css
index.html > html > body > div.container > div.container > div.container > form
1 (<DOCTYPE html>)
2 <html>
3
4 <head>
5 <title>Covid19 </title>
6 <meta name="viewport" content="width=device-width, initial-scale=1.0">
7 <link rel="stylesheet" href="https://cdnjs.cloudflare.com/ajax/libs/materialize/1.0.0/css/materialize.min.css">
8 <link rel="stylesheet" type="text/css" href="css/style.css">
9 <script src="https://cdn.jsdelivr.net/npm/chart.js@2.8.0"></script>
10 <link rel="stylesheet" href="https://cdnjs.cloudflare.com/ajax/libs/font-awesome/4.7.0/css/font-awesome.min.css">
11 </head>
12
13 <body>
14 <header id="overview">
15 <div class="container">
16 <div class="row">
17 <div class="col s12 m6 s5">
18 <div class="logo">
19 <a href="#"></a>
20 </div>
21 </div>
22 <div class="col s12 m6 s7">
23 <div class="mainmenu">
24 <ul>
25 <li><a class="active" href="#overview">Overview</a></li>
26 <li><a class="" href="#contagion">Contagion</a></li>
27 <li><a class="" href="#symptoms">Symptoms</a></li>
28 <li><a class="" href="#prevention">Prevention</a></li>
29 <li><a class="" href="#cases" class="btnmenu">Cases</a></li>
30 <li><a class="" href="#contact" class="btnmenu">Contact</a></li>
31 </ul>
32 </div>
33 </div>
34 </div>
35 </div>
36 </div>
37 </div>
38 </div>
39 </div>
40 </div>
41 </div>
42 </div>
43 </div>
44 </div>
45 </div>
46 </div>
47 </div>
48 </div>
49 </div>
50 </div>
51 </div>
52 </div>
53 </div>
54 </div>
55 </div>
56 </div>
57 </div>
58 </div>
59 </div>
60 </div>
61 </div>
62 </div>
63 </div>
64 </div>
65 </div>
66 </div>
67 </div>
68 </div>
69 </div>
70 </div>
71 </div>
72 </div>
73 </div>
74 </div>
75 </div>
76 </div>
77 </div>
78 </div>
79 </div>
80 </div>
81 </div>
82 </div>
83 </div>
84 </div>
85 </div>
86 </div>
87 </div>
88 </div>
89 </div>
90 </div>
91 </div>
92 </div>
93 </div>
94 </div>
95 </div>
96 </div>
97 </div>
98 </div>
99 </div>
100 </div>
```

Fig. 3 Screenshot of lines of code

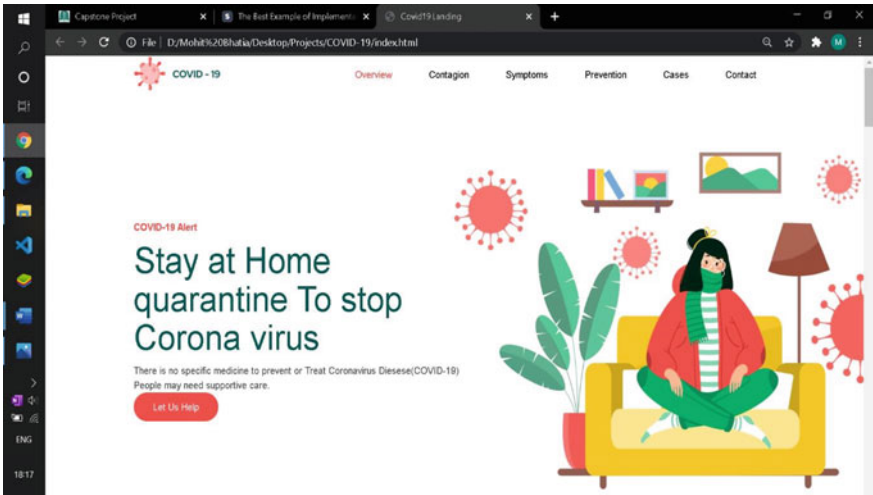


Fig. 4 Outlook of home page

Fig. 5 Logo



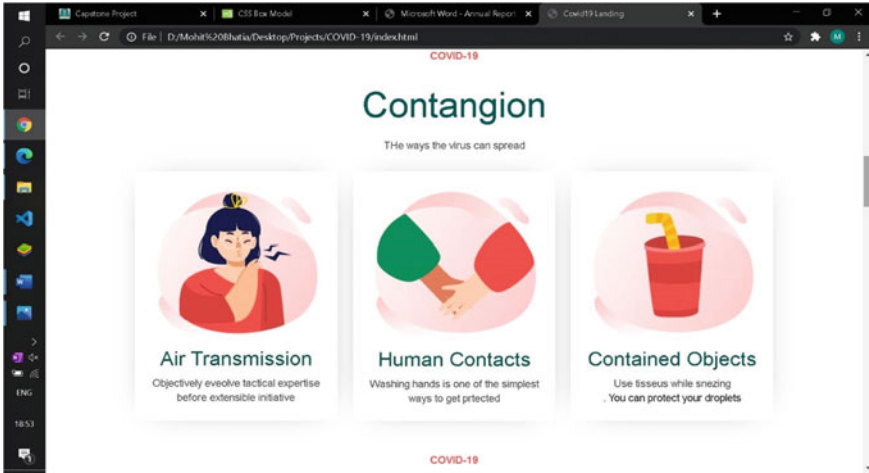


Fig. 6 Content outlook—contagion

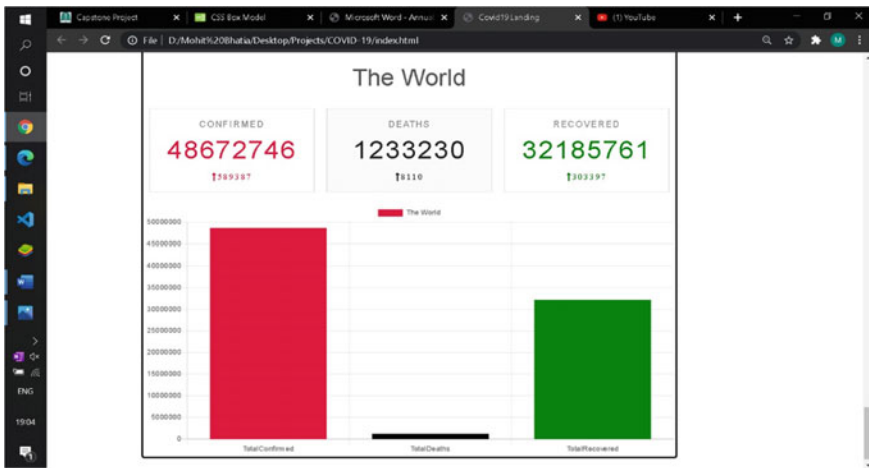


Fig. 7 Content outlook-case

6 Future Work

Since a lot of work was done on the front-end part of the project, there are many improvements that can be made in the backend. Since, also we can add some new features like we can make chatbot which checks that we are safe or not, login signup page for our project.

This project can also be improved regarding how it would communicate with users and also add some new features. And in the front end, we can improve the UI of the front end of the site and also navigate the different sections.

It will also be useful to make the system accessible through a mobile platform and also, we can create a mobile App as our new project for the same using the React naïve which is a framework for naïve apps.

7 Conclusion

We are attempting to build up a site utilizing HTML, CSS, and JAVASCRIPT. For web composition, we will utilize the JAVASCRIPT and HTML language and for more intuitive way we will utilize CSS Scripts.

We have created a dashboard and data repository for coronavirus in which everyone can see the latest updates in the status of this disease and also can take some safety features to prevent this disease and also helps them to find their nearby hospitals which take the COVID-19 patients and also give them the helpline numbers issued by the government for the same.

References

1. https://github.com/RamiKrispin/coronavirus_dashboard
2. Kumari P, Nandal R (2017) A research paper on website development optimization using XAMPP/PHP. *Int J Adv Res Comput Sci* 200–215
3. Pelletier JS, Tessema B, Frank S, Westover JB, Brown SM, Capriotti JA (2020) Efficacy of povidone-iodine nasal and oral antiseptic preparations against severe acute respiratory syndrome-coronavirus 2 (SARS-CoV-2). *Ear Nose Throat J* 1–5
4. <https://www.who.int/emergencies/diseases/novel-coronavirus-2019>
5. <https://covid19.who.int/>
6. <https://www.mohfw.gov.in/>
7. <https://journals.asm.org/content/covid-19>
8. <https://www.worldometers.info/coronavirus/>
9. Dana Chisnell and Janice (Ginny) Redish (February 1, 2005), “Designing Web Sites for Older Adults: Expert Review of Usability for Older Adults at 50 Web Sites”, AARP, aarp.org/olderwisewired
10. Rajesh C, Srikanth KK (2014) Research on HTML5 in web development. *Int J Comput Sci Inf Technol* 5–6

Influence of Drop Weight Low-Velocity Impact on Thin Panels Study by Numerical Simulation and Experimental Approach



I. Ramu, K. V. G. R. Seshu, P. Srinivas, and P. SenthilKumar

Abstract The present work is to study the deformation behaviour of the thin panels by using the drop weight impact machine. The impact test machine is model in 3D experience. The developed model imported into simulation software to conduct the numerical experiments of the impact response of deformation. Aluminum material is considered to perform the mathematical analysis for the specimen. In simulation results of the impact response of strain for different thinness, values are observed. Similarly, the deformation to various velocities is observed. The new drop weight machine is designed and fabricated to conduct the tests in this study. Drop weight impact tests are conducted for the varied thickness of thin panels by the experimental investigation. The validation of the numerical results to the experimental results is observed and there are good agreement between them. The difference between those is due to the frictional and other losses negligible in numerical simulation.

Keywords Impact test machine · Impactor · Low velocity · Thin panels · Deformation

1 Introduction

Several studies have observed the thickness of the panel presents a significant role in the impact analysis of thin plates. The velocity of the impact is conflicting with a low-speed impact test. The effect of the lightweight with the impact force may cause damage to the panel. In general, the higher the acceleration and ability to effect a lesser impact longer. The ability to recreate the conditions under which real-life components would be subject to impact loading is another significant advantage of using drop-weight impact tests over other standard tests.

I. Ramu (✉) · K. V. G. R. Seshu · P. Srinivas
Faculty of Mechanical Engineering, Vishnu Institute of Technology Bhimavaram, Bhimavaram,
Andhra Pradesh 534202, India

P. SenthilKumar
Faculty of Mechanical Engineering, BV Raju Institute of Technology Narasapur, Narasapur,
Telangana, India

Winkel and Adams [1] research the impact analysis relating to the composite material by experiments. New Drop-weight Machine for Concrete Materials is investigated by Banthia et al. [2]. Cantwell and Morton [3] deals with the drop test system for small, quickly supported composite laminates to analyze their impact efficiency. Gunawan et al. [4] addressed the formation of a lower load shock experiment. It is planned to validate quantitative simulations of impact charges on crush boxes that absorb kinetic energy during crashes as an experimental data facility.

Sharma et al. [5] investigated the effect of energy absorbers on various materials and structures at low speed. Galdino et al. [6] deals with the construction of a system with a drop weight effect on composite materials. Composite materials were analyzed, and laminated structure effects were also investigated. Few researchers review the design and development of drop weight impact machines, Chandrashekhar et al. [7] has reviewed the model analysis of impact machines. Numerical and experimental correlation of laminate with low velocity impact analysis has studied by [8–10].

The present study describes the development of a low-velocity impact test machine. The developed experimental invention is used to test the thin panels with a wide range of impact speeds and energies. Experiments were conducted to determine the deflection of individual thin panels by varying the impact load. The numerical simulation also carried with different impact loads in the simulation software. The experimental and numerical study of deflection on thin panels due to impact loads were carried out for various cases.

2 Numerical Methodology

When an impulse charge is applied to a structure by the burst load, it induces an immediate change in velocity: the momentum is absorbed, and the material absorbs kinetics that is transformed into energy while the structure deforms.

The traditional way of measuring energy absorption is calculating kinetic energy before and after impact by equations as

$$\frac{1}{2}mv_1^2 - \frac{1}{2}mv_2^2 = \int Fdy \quad (1)$$

where m is the impactor mass, F is the force, y is the force due to displacement, velocity of impactor before and after impact are v_1 and v_2 , correspondingly.

In drop weight tests the impactor is the key part to design and its material selection. We considered impactor material is steel and its density is 7900 kg/m^3 . Mainly this impactor is divided into three sections. Hemispherical end of 18 mm diameter cylinder with 9 mm radius tip, 50 mm diameter cylindrical part in middle and 45 mm diameter cylindrical part.

Volume of Section 1 = $\pi r_1^2 h_1 + 2/3 \pi r_1^3$.
 Volume of Section 2 = $\pi r_2^2 h_2$.
 Volume of Section 3 = $\pi r_3^2 h_3$.
 Total volume = sum of three section volumes.
 Mass = Total volume \times density.
 Velocity of freely falling object = v

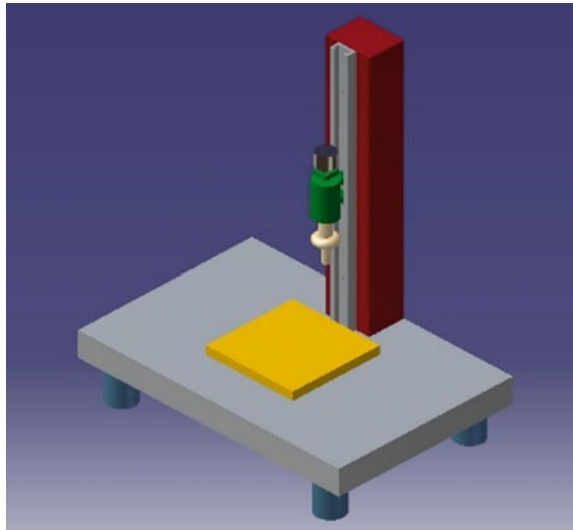
$$v = \sqrt{2gh} \tag{2}$$

where, g is the acceleration due to gravity and h is height of fall.

To conduct numerical and experimental analysis the velocity of freely falling weight is obtained from Eq. (2).

Design is the very important aspect to fabricating a device. We have used CATIA software to model the device. The model consists of many components such as impactor, electromagnet, rails, stand and specimen etc. During design of equipment in CATIA, we considered a frame of 1.6 m height and inserted impactor inside it. So that it could slide freely from top to bottom. We placed a table below the frame of height 250 mm and a supporter of dimension 150 mm \times 150 mm to keep the specimen upon it. The diagrammatic representation of the isometric view of model of the alignment of impactor is shown in Fig. 1.

Fig. 1 Low impact testing machine model



3 Experimental Methodology

The low-speed impact testing is allowed by the drop weight impact system. A vertical steering column, an electromagnet, and an impactor are included in the equipment. A cross-section of the impactor is to insert in a column and smoothly slides due to gravity force. Through changing the direction of the electric magnet, the position of the impactor can be changed. The electro-magnet was adjustable in the height of 1.5 m. Nevertheless, since the support frame of the rail is lower than the bottom of the track, the impact height could be higher than 1.5 m. The maximum impact height of 1715 mm is determined in this study. On the support plate, the exemplars were pre-tight using a square four-bolt steel frame. A-frame, as shown in Fig. 2a, supports the support structure on the ground.

There is a circular 80 mm diameter hole in the centre of the frame. A steel impactor with a radius of 9.6 mm and a weight of 8048 g and another radius weight of 60 mm has a hemispherical shape. Figure 2b shows the impactor, and Fig. 2c shows the rail that controls the impactor.

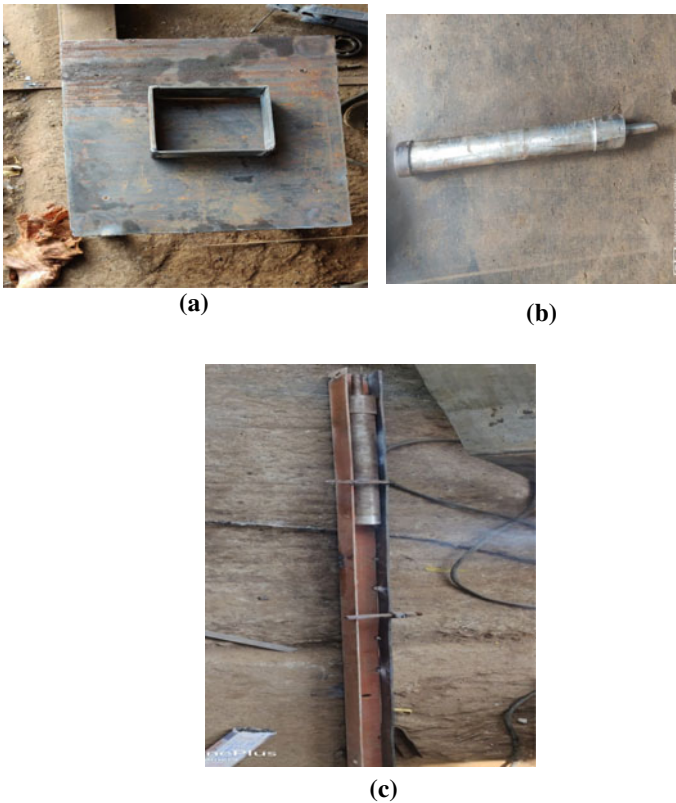


Fig. 2 a Bottom specimen supporting structure, b impactor, c frame to guide of impactor

Drop Weight Impact Test method was to reduce the weight in a vertical direction, with a tube or rail to guide it during the “free fall.” Once again, with known height and weight, the impact energy can be measured. There was no way to calculate impact speed in the early days. In the guidance system, the engineers had not to recognize friction. The only tests that could be obtained were pass/fail results since the weight that was either stopped dead or destroyed entirely in passing on the test specimen.

4 Numerical Results and Discussions

While doing simulation of impactor in simulation, we have divided impactor into mainly two parts with hemispherical tip of 18 mm, 50 mm and 45 mm diameter respectively. Similarly the displacement of an object after the impact test is obtained from the numerical simulation using the tool called as explicit dynamics in simulation. The numerical and experimental results are carried out by using simulation software and prepared impact response test machine, respectively. The velocity of impactor is varied and calculated the displacements of thin aluminum sheets of size 0.5 mm using analysis software simulation. Similarly, the experiments are conducted with different heights of impactor and finds the displacements of the objects due to drop weight. The deformation of experimental and numerical results are represented in Table 1.

We have done experimental calculation on different thickness of aluminum sheets by varying height. There is a great impact for larger height and deformation is also more. Similarly we have done simulation so that we could verify the errors. The variation readings obtained by experimental and simulation on 1 mm thick aluminum sheets are shown Table 2.

In contrast to the static loading conditions, various materials can behave in quite different ways. In deciding its response also is how the kinetic energy is distributed throughout the part. The diagrammatic representation of 0.5 mm thick aluminum sheet is shown in Fig. 3. We conducted a simulation test on the specimen of dimension 150 × 150 mm in simulation software with parameters of velocity, deformation, weight and thickness, material. Diagrammatic representation of the simulation model on aluminum sheet thickness 0.5 mm and applied velocity 5.1 m/s is shown in Fig. 3a.

Table 1 Simulation and experimental deformation results of 0.5 mm thick aluminum sheet

S. No.	Velocity (m/s)	Height (m)	Simulation deformation (mm)	Experimental deformation (mm)
1	4.4	1	0.0158	0.01
2	4.6	1.1	0.034	0.02
3	4.8	1.2	0.053	0.04
4	5.1	1.3	0.14	0.09

Table 2 Simulation and experimental deformation results of 1 mm thick aluminum sheet

S. No.	Velocity (m/s)	Height (m)	Simulated deformation (mm)	Experimental deformation (mm)
1	4.4	1	0.02	0.01
2	4.6	1.1	0.04	0.03
3	4.8	1.2	0.05	0.04
4	5.1	1.3	0.08	0.07

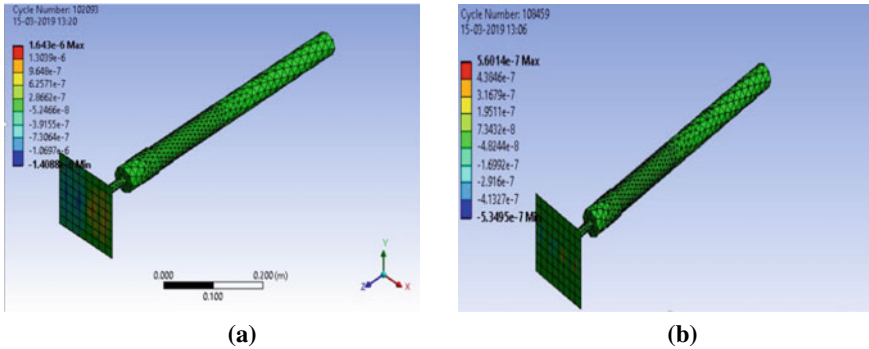


Fig. 3 **a** The simulation model on aluminum sheet thickness 0.5 mm and applied velocity 5.1 m/s, **b** the simulation model on aluminum sheet thickness 0.5 mm and applied velocity 4.8 m/s

Figure 3b illustrate the impact response diagram in simulation of 0.5 mm thin sheet and the impactor. The velocity 4.8 m/s is considered in this analysis and its deformation result and its values are shown in Fig. 3b.

We have plotted a graph between experimental deformation results and simulated deformation results which is shown in Fig. 4. In the graph we can compare the deformation result between experimental and simulation values. There is a slight variation between them.

The plotted graph between experimental deformation results and simulated deformation results is shown in Fig. 5. In the graph we can compare the deformation result

Fig. 4 Comparison between experimental deformation results and simulated deformation results of 0.5 mm thick aluminum sheet

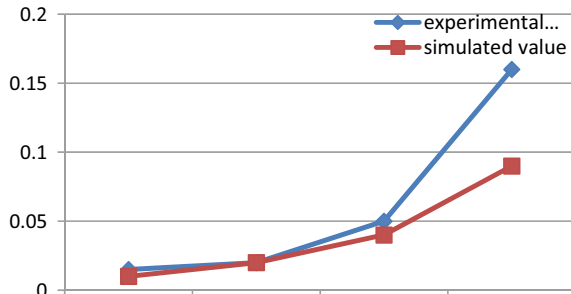
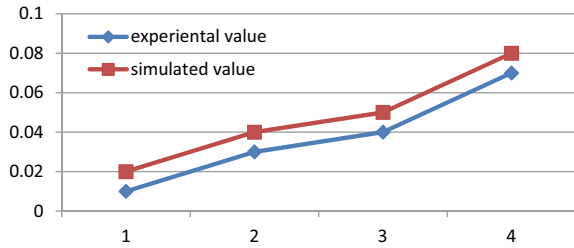


Fig. 5 Comparison of deflection between the experimental value and simulated value of 1 mm thick aluminum panel



between experimental and simulation values. There is a slight variation between them.

The variation results obtained by experimental and simulation on 1 mm thick aluminum sheet are shown in Fig. 5. There is a great impact for larger height and deformation is also more. Similarly the simulation has been done so that it could verify the errors obtained. Plotted graph between experimental deformation results and simulated deformation results is shown in Fig. 5. In the graph we can compare the deformation result between experimental and simulation values. There is a slight variation between them.

5 Conclusion

A drop weight testing system thrived, allowing the impact load to be applied to a specimen at a max. Speed of 4 m/s and a variable weight up to 8 kg. The low-speed impact test is performed with drop-weight impact equipment, and the findings are reported in this article. The resistance to impact and failure of the aluminum sheets are investigated. Different heights of the impactor and the varying thickness levels of the specimen determine the performance of the impact test apparatus. The use of the experimental setup of drop-weight machine provides useful to test the low velocity impact on the thin panels. The increased thickness of sheets of aluminum means a slight increase in the energy consumption of aluminum foil. The theoretical and experimental values are precisely the same as small differences.

References

1. Winkel JD, Adams DF (1985) Instrumented drop weight impact testing of cross-ply and fabric composites. *Composites* 16(4):268–278
2. Banthia N, Mindness S, Bentur A, Pigeon M (1988) Impact testing of concrete using a drop-weight impact machine. *Exp Mech* 29:63–69
3. Cantwel WJ, Morton J (1991) The impact resistance of composite materials—a review. *Composites* 22:347–362

4. Gunawan L, Dirgantara T, Putra IS (2011) Development of a dropped weight impact testing machine. *Int J Eng Technol* 11(6):98–104
5. Sharma A, Karthik D, Hemanth Kumar J, Naveen H E (2017) Design and fabrication of drop weight impact testing machine. *Imperial J Interdisplanery Res* 3(6):1121–1127
6. Galdino F, da Silva RG, de Amorim WF (2013) Development of a machine per drop weight impact for composite materials. In: 22nd international congress of mechanical engineering, Ribeirao Preto, SP, Brazil
7. Shende CJ, Sahu AR, Deshmukh AV (2015) Modeling and analysis of hammer of impact testing machine: a review. *Int J Mech Eng Robot Res* 4(1):350–354
8. Lawrence Sy B, Fawaz Z, Bougherara H (2019) Numerical simulation correlating the low velocity impact behaviour of flax/epoxy laminates. *Compos Part A Appl Sci Manuf* 126:105582
9. Sun M, Chang M, Wang Z, Li H, Sun X (2018) Experimental and simulation study of low-velocity impact on glass fiber composite laminates with reinforcing shape memory alloys at different layer positions. *Appl Sci* 8(2405):1–15
10. Tuo H, Lu Z, Ma X, Zhang C, Chen S (2019) An experimental and numerical investigation on low-velocity impact damage and compression-after-impact behavior of composite laminates. *Compos Part B Eng* 167 (15):329–341

Analysis of Segmental Vibration Transmissibility of Seated Human



Veeresalingam Guruguntla and Mohit Lal

Abstract The present study improves the effectiveness of Wan and Schimmels model by minimizing the least square error between experimental and analytical. The vibration transmissibility from source, i.e., seat to various human body parts such as head and neck, upper torso, lower torso and viscera are analyzed for seated human without backrest condition. The human segmental, i.e., mass, stiffness, and damping properties are tuned/optimized with firefly algorithm (FA) to obtain goodness of fit. The goodness of fit value obtained by Wan and Schimmels is compared with and without FA. With this analysis it could be concluded that the biomechanical properties optimized/tuned with FA must be used instead of proposed by Wan and Schimmels to make human dummies for better performance and efficiency.

Keywords Human body modeling · Firefly algorithm · Biodynamic response · Mathematical model

1 Introduction

Whole-body vibration (WBV) is the study of vibration exposure of workers or drivers in the industrialized world while operating small to heavy machinery, automobiles, and equipment/tools. WBV may lead to many side effects that can cause temporary or permanent health issues, which may impact human vision and activities like sketching and typing [1–5]. Both driver and passengers experience vibration while traveling in automobiles. The level of intensity of exposed vibration may rely on the duration of exposure and amplitude. The need for transportation is highly demanded in daily human life. In such cases monitoring human health and level of vibration exposure human segments is mandatory. These problems have caused extensive research to

V. Guruguntla (✉) · M. Lal
Industrail Design Department, National Institute of Technology, Rourkela, India
e-mail: 518id1001@nitrkl.ac.in

M. Lal
e-mail: lalm@nitrkl.ac.in

model the human body and understand segment's biodynamic response. A study [6] has recently revealed that most of the biodynamic responses are observed through experimental works, but less weightage is given to modeling the human body and segmental vibration transmissibility. The present study worked in this direction and briefly analyzed the each segmental vibration transmissibility values.

Literature example [7] started modeling the human being in the nineteenth century by referring to mechanical impedance experimental data. In that human being treated as a single lumped mass as a rigid type and established one degree of freedom (*df*) model. Apart from several sources of vibrations like an automobile, power tools, and machinery, ship shock motions can also play a versatile role in increasing human discomfort and injury. A phenomenon is developed to study the impact of ship shock motion and created a two *df* human model in [8]. Later on in [9] four *df* human model developed and further it utilized to study the ride comfort of four-wheel automobile [10] and quarter car model [11]. A similar kind of modeling is performed in studies [12, 13], but the degree of accuracy with experimental data is not that much attractive. A real human ten *df* human model is developed, and natural frequencies of various human segments are observed in [14, 15].

The literature review identified that a large amount of experimental study was carried out under real-time scenario [6]. The human body is modeled from one *df* to several *df* [1] in seated and semi-supine posture conditions [16]. But none of the studies focused on grabbing the exposure limits of human segments. The current article is focusing on this direction. The present article work is divided into two stages in the first stage. Methodology is proposed to improve the effectiveness of Wan and Schimmels model [9]. In the second stage, it analyzed the transmissibility values of various human segments. The obtained results can deliver the basic idea of the dynamic response of human segments.

2 Modeling

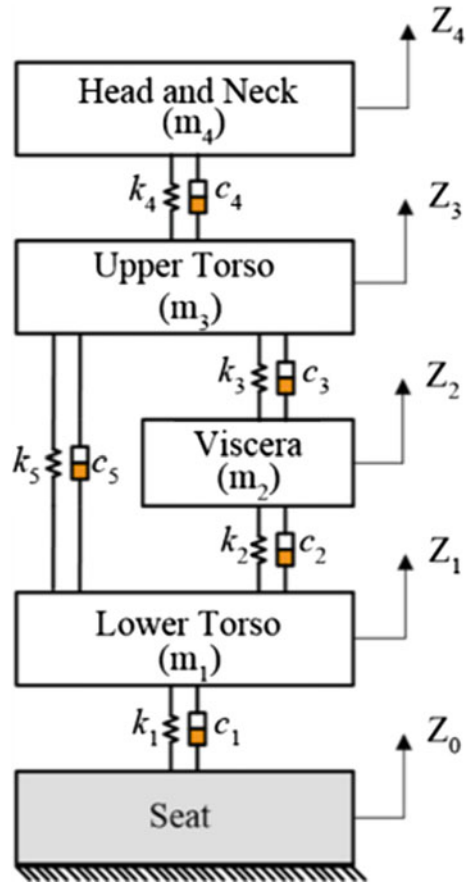
2.1 Wan and Schimmels Model

Figure 1 represents a four-degree of freedom human model proposed by Wan and Schimmels [9]. Here m_1 to m_4 , k_1 to k_4 and c_1 to c_4 represent the segmental mass, stiffness and damping, respectively. z_1 to z_4 resulting displacements due to external excitation z_0 .

2.2 Method of Evaluation

The equation of motion for each segment of Fig. 1 can be obtained with Newtons' II law and the overall systems' equation of motion can be written as

Fig. 1 The schematic diagram of Wan and Schimmels model



$$[M]\{\ddot{z}\} + [C]\{\dot{z}\} + [K]\{z\} = \{f_z\} \tag{1}$$

where $[M]$, $[C]$, and $[K]$ are assembled mass, stiffness and damping matrices, respectively. The size of each matrix is 4×4 and the force vector $\{f_z\}$ is 4×1 .

Equation (1) can be represented in the frequency domain as

$$(-\omega^2 M + j\omega C + K)Z = F_Z \tag{2}$$

The biodynamic response functions seat to head transmissibility (SH) is “through the body” whereas, apparent mass (AM) and impedance (IM) are “to the body” vibration properties that can be calculated as

$$SH = \frac{Z_4}{Z_0} \tag{3}$$

$$AM = \frac{F_d}{a_d} \tag{4}$$

$$IM = \frac{F_d}{V_d} \tag{5}$$

where F_d , a_d , and V_d are the force, acceleration, and velocity at driving location.

2.3 Optimization Technique

The present study utilized the objective function that minimizes the error between experimental and analytical magnitude values of “to the body” and “through the body” functions with FA and may be represented as

$$obj_{min} = \sum_{i=1}^N (SH_1(f_i) - SH_2(f_i))^2 + (AM_1(f_i) - AM_2(f_i))^2 + (IM_1(f_i) - IM_2(f_i))^2 \tag{6}$$

The subscripts “1” and “2” of SH, AM, IM indicate experimental and analytical readings and “N”, indicating a number of practical/experimental reading. The boundary conditions applied to the model is taken from [9]. The tuned/optimized human segmental properties with and without FA are compared in Table 1.

Table 1 Comparison of optimized parameters of Wan and Schimmels model [9] with and without FA

Parameter	Without FA	With FA
m_1	36	38.85
m_2	5.5	3
m_3	15	13.92
m_4	4.17	5.1
k_1	49,340	149,504.66
k_2	20,000	10,815.27
k_3	10,000	280,174.96
k_4	134,400	80,180.62
k_5	192,000	23,910.41
c_1	2475	3470.64
c_2	330	947.76
c_3	200	3438.38
c_4	250	2617.03
c_5	909.1	3020.49

The optimized parameters from Table 1 are utilized to calculate the biodynamic responses “to the body” and “through the body” defined in Eqs. (3), (4) and (5), and corresponding results are presented in Figs. 2, 3, and 4. The result reveals that FA shows well matching with experimental results. The calculated goodness of fit

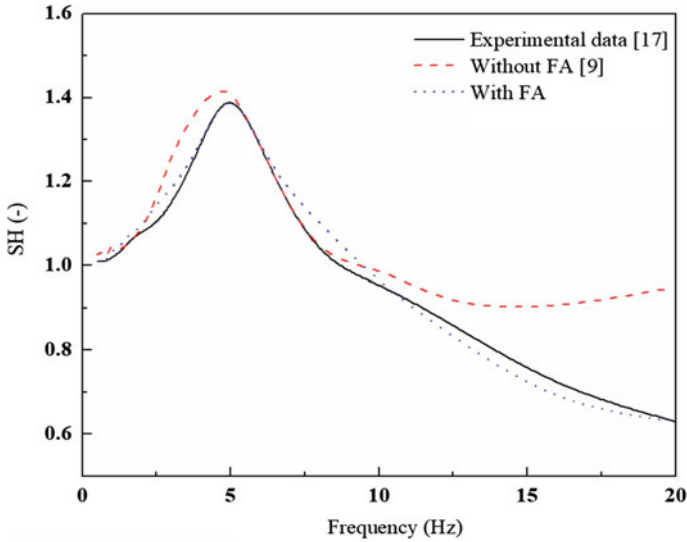


Fig. 2 Seat to head transmissibility

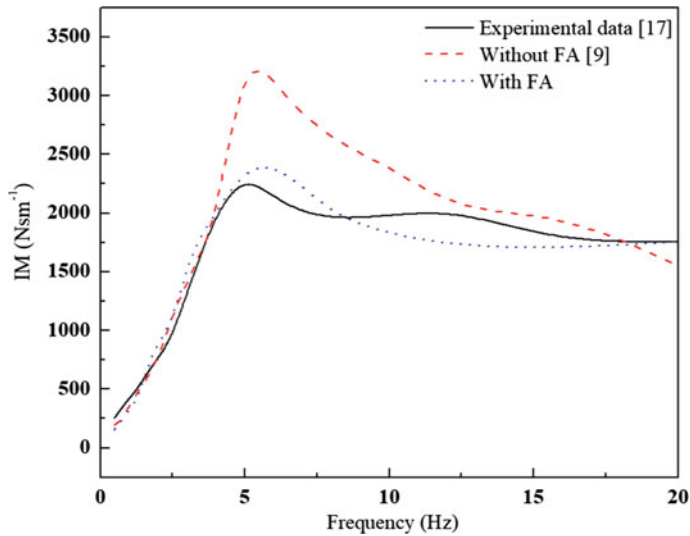


Fig. 3 Impedance

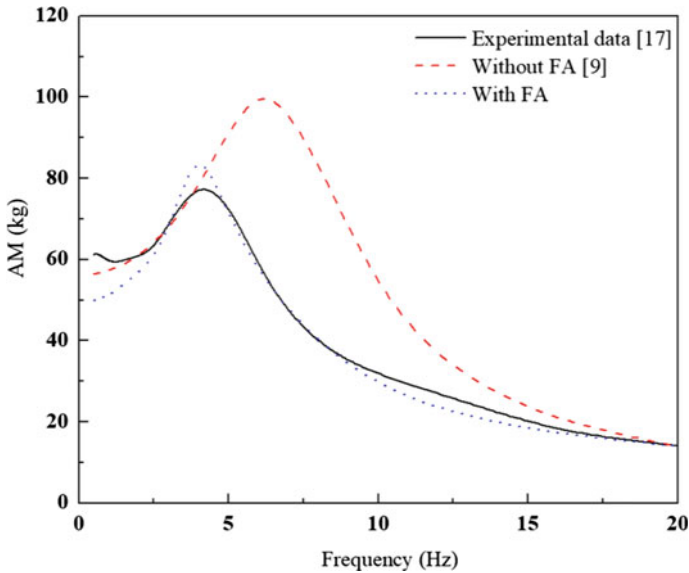


Fig. 4 Apparent mass

for SH is 92.35% compared to 91% for Wan and Schimmels model [9]. On the other hand, IM and AM values increased from 80.10%, 86.80% to 89.86%, 90.64%, respectively. The overall goodness of fit value improved from 85.90% to 90.95%. Furthermore, the amount of vibration transmitted from the seat to various human segments is estimated and presented in Fig. 5. From Fig. 5 it can be seen that the vibration transferring to different segments is varying, and maximum for lower torso and minimum to the head at the resonance frequency.

3 Conclusion

In this article, an optimization technique is proposed to improve the effectiveness of the biomechanical model. An optimization technique (FA) is utilized to optimize the human segmental properties of Wan and Schimmels model. The overall goodness of fit value estimated with optimized segmental properties improved effectiveness of the model from 85.90% to 90.95%. Also, segmental vibration transmissibility analysis reveals that except the resonance frequency zone, minor changes are noticed in the rest of the frequency.

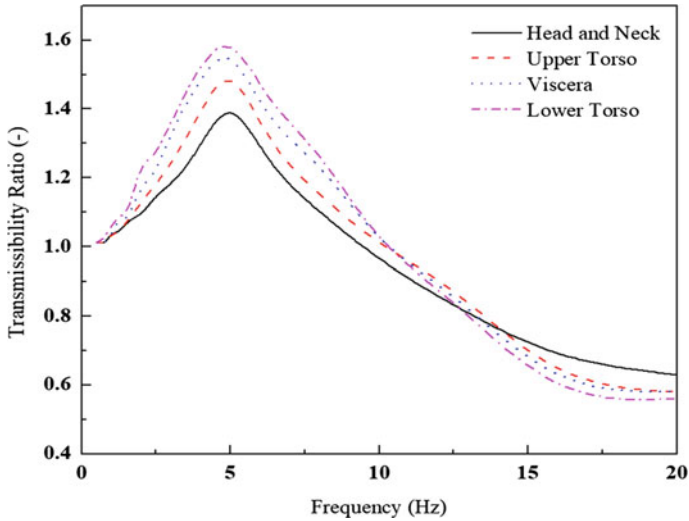


Fig. 5 The segmental vibration transmissibility

References

1. Liang CC, Chiang CF (2006) A study on biodynamic models of seated human subjects exposed to vertical vibration. *Int J Ind Ergon* 36(10):869–890
2. Bhiwapurkar MK, Saran VH, Harsha SP, Goel VK, Berg M (2010) Influence of mono-axis random vibration on reading activity. *Ind Health* 48(5):675–681
3. Corbridge C, Griffin MJ (1991) Effects of vertical vibration on passenger activities: writing and drinking. *Ergonomics* 34(10):1313–1332
4. Khan MS, Sundstrom J (2007) Effects of vibration on sedentary activities in passenger trains. *J Low Freq Noise Vib Act Control* 26(1):43–55
5. Bhiwapurkar MK, Saran VH, Harsha SP (2011) Quantitative evaluation of distortion in sketching under mono and dual axes whole body vibration. *Ind Health* 49(4):410–420
6. Rakheja S, Dong RG, Patra S, Boileau PE, Marcotte P, Warren C (2010) Biodynamics of the human body under whole-body vibration: synthesis of the reported data. *Int J Ind Ergon* 40:710–732
7. Coermann RR (1962) The mechanical impedance of the human body in sitting and standing position at low frequencies. *Hum Factors* 4:227–253
8. Liu XX, Shi J, Li GH, Le X, Zhao B, Yue M, Ke W (1998) Biodynamic response and injury estimation of ship personnel to ship shock motion induced by under water explosion. In: *Proceeding of 69th shock and vibration symposium*, vol 18, pp 1–18
9. Wan Y, Schimmels JM (1995) A simple model that captures the essential dynamics of a seated human exposed to whole body vibration. *Adv Bioeng* 31:333–334
10. Reddy PS, Ramakrishna A, Ramji K (2015) Study of the dynamic behaviour of a human driver coupled with a vehicle. In: *Proceedings of the institution of mechanical engineers, part D*, vol 229, pp 226–234
11. Singh D (2019) Ride comfort analysis of passenger body biodynamics in active quarter car model using adaptive neuro-fuzzy inference system based super twisting sliding mode control. *J Vib Control* 25:1866–1882
12. Bai XX, Xu SX, Cheng W, Qian LJ (2017) On 4-degree-of-freedom biodynamic models of seated occupants: lumped-parameter modelling. *J Sound Vib* 402:122–141

13. Singh I, Nigam SP, Saran VH (2015) Modal analysis of human body vibration model for Indian subjects under sitting posture. *Ergonomics* 58:1117–1132
14. Guruguntla V, Lal M (2020) An improved biomechanical model to optimize biodynamic responses under vibrating medium. *J Vib Eng Technol* 1–11
15. Guruguntla V, Lal M (2021) Development of novel biodynamic model of the seated occupants. In: *Research into design for a connected world*. Springer, Singapore
16. Govindan R, Saran VH, Harsha SP (2020) Low-frequency vibration analysis of human body in semi-supine posture exposed to vertical excitation. *Eur J Mech A/Solids* 80:103906. <https://doi.org/10.1016/j.euromechsol.2019.103906>

Early Detection of Sepsis Using LSTM and Reinforcement Learning



R. Dhanalakshmi, T. Sudalaimuthu, and K. R. Radhakrishnan

Abstract The delay in predicting sepsis is possibly life-threatening and to procure restrictions in medical resources. The prediction of sepsis in patients having no sepsis and prediction of sepsis in the earliest for patients having sepsis is the concept of predicting the sepsis with good quality acts as the key source of this work. The foremost objective is to create a platform in this digitized environment using the Machine Learning and Deep Learning model to detect the deterioration of sepsis in the patient before it's too late. This work aims to predict sepsis sequentially using Long Short Term Memory (LSTM) an RNN model that helps to learn the order dependencies and clinical detection of sepsis 6 h before using the clinical data. Further Reinforcement Learning is applied to label the data for accurate matching.

Keywords Sepsis · Reinforcement learning · LSTM · RNN

1 Introduction

Infections in the human body are common in nature but the response of the body to the infections is different. Some humans may have high immunity and some may have low in nature. The level of immunity decides the cause and severeness of the diseases. Apart from the immunity the early stages of identification, detection, and diagnosing the diseases also decide the disorders. One such severeness is early sepsis detection using physiological data. Through many causes, the human body reacts to infections. The infections are of different means (like contaminated food or water, and even via the bite of an insect.). Once the human body was infected it may lead

R. Dhanalakshmi (✉)

Computer Science Engineering, KCG College of Technology, Chennai, India

T. Sudalaimuthu

Computer Science Engineering, Hindustan Institute of Technology and Science, Chennai, India

K. R. Radhakrishnan

Information Technology, St. Joseph's College of Engineering, Chennai, India

e-mail: radhakrishnankr@stjosephs.ac.in

to diseases infections. One such disease is sepsis it may form a life-threatening issue if not noticed at an early stage. People having sepsis are also found with any chronic illnesses (such as diabetes, kidney disease, cancer, high blood pressure, and HIV). Adults or seniors are easily affected by sepsis if they have problems with urinary tract infections. To fight infection human body naturally releases chemicals into the bloodstream. The cause of sepsis happens in the stage when the response of the human body goes out of balance due to the chemical reactions in some cases it may lead to multiple organ damage. Statistics are taken globally, each year 6 million people specifically in the USA, every year huge amount (270,000) of people die due to sepsis and as per regulations of the government, act hospital spends 24 billion every year. This work concentrates on detecting sepsis from the base of clinical data. Further, this paper continues in the stream of previous work, methods, experiments, and implementation platform of proposed work in detail.

1.1 Surveys

As the treatment gets delayed for an hour approximately 4–8% of mortality increases. The implementation and the source for this sepsis detection were also considered to be happening in the industry sector like IBM Watson, AWS Sagemaker, Google Cloud ML. This provides the platform for research to detect, identify, predict, and classify the diagnosis of sepsis with clinical and nonclinical data set.

The research field for sepsis started to improve in the diagnosis of detection at an early stage by the implementation of various methods and techniques. The field study and the research was tested with different patients in clinical sectors. It was evaluated with different metrics and with various raise and low parameter values. Futoma et al. [1] suggested a method for detecting sepsis very suitable for sampling irregularly as of Gaussian Process adapter was applied as endwise learning framework, (6) later trained by classifier Long Short-Term Memory (LSTM). Lea et al. [2], was publicized to outclass sequential learning sectors namely parallelism, memory efficiency, and evaluation metrics through the conventional Recurrent Neural Network (RNN) architectures [3] “LiSep LSTM”; a neural network Long Short-Term Memory predicts the septic shock in patients during the hospital stay to the earliest of 20 h. [4] Combined form of CNN and LSTM was suggested to record the blood values and the circulatory antibiotics for the prediction before 24 h in advance on to the metrics of AUROC range from 0.8 to 0.7. Another combined combination of a lazy learner and deep learning manipulates by the time series distances [5]. It was framed as the supervised time series classifier to detect sepsis on a period of 7 h before sepsis arrival.

2 Background

2.1 Recurrent Neural Network

The RNN is a category of Artificial Neural Network (ANN) which gives the previous output as additional input with the given input. To predict the layers of the output it is possible for Recurrent Neural Network by saving the outputs of the specific layers and applying them back to the input layers.

Recurrent Neural Network (RNN) is also considered to be a sector of Artificial Neural Network that have as many interconnections with nodes between them, it can also form a temporal structure with the directed graph. This leads to the formation of temporal behavior in a dynamic pattern. From the base of the feed-forward neural network, RNN can inherit the memory of its internal state to generate inputs in the form of different length sequences (Fig. 1).

2.1.1 Long Short Term Memory (LSTM)

For framing the texts, we get the labels and additional features as input using this with the help of Long Short Term Memory (LSTM) a distinct type of Recurrent Neural Network (RNN) we will be predicting the text or sentence which describe the video (Fig. 2).

The impulse signals either finite or infinite of the recurrent neural network have the possibility of extra storage classes that can also be controlled directly by the presence of the neural network. These storage classes also act as an exchangeable to alternative graphs or networks that may include either feedback loops or time delays. This is named as gated memory or states and section of Long Short-Term Memory (LSTMs).

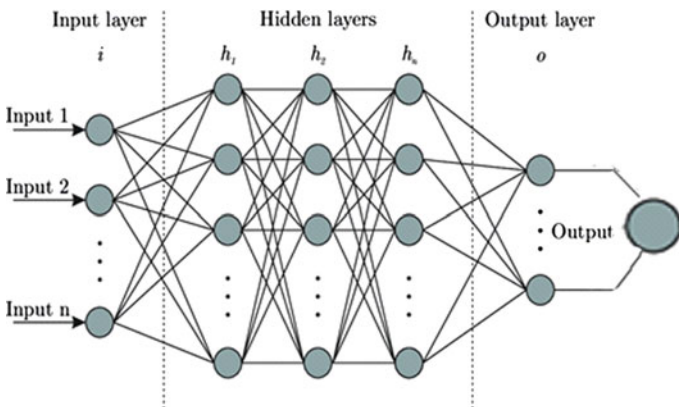
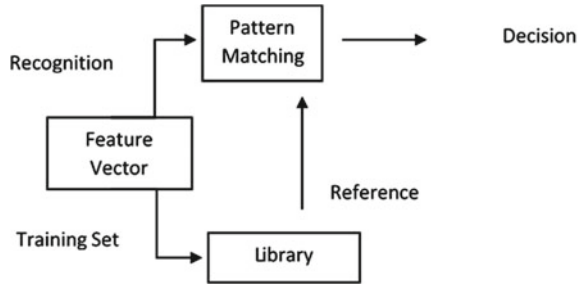


Fig. 1 Recurrent neural network architecture

Fig. 2 The general framework of LSTM methodology



The major use of Long Short-Term Memory (LSTM) was stated to neglect the issue of vanishing gradient problem. Generally, LSTM gets improvements using “forget gates”, it is said to be recurrent gates. Using the concepts of either explode or vanishing backpropagation errors can be prevented in LSTM. As a replacement, errors can stream backward utilizing virtual layers without any limit. This event means that discrete time series of more than thousands or even millions of earlier events that happened can be learned by LSTM. Due to this LSTM can work for lengthy delays within the specific events and also can handle high and low-frequency component signals.

RNNs use LSTM to solve issues like vanishing gradient that infers sequences and does not gather the past input for the long-term sequences. This LSTM can learn long-term dependencies and their corresponding identification formats with input, output, and past gate controls. The gates are adjusted by a sigmoid unit that learns during training where it is to open and close. The dataset that is needed for training RNN deep learning model is a list of object lists from a list of images with a list of text describing this list of images. The accuracy of this RNN model is dependent on the amount of dataset used for training.

2.2 Reinforcement Learning

This is one type of learning in a Machine Learning algorithm that helps the agents to detect the behavior of the model to make the proper labeling of the data during the decision making process. Here policy optimization model-free reinforcement learning is used so that it can directly learn the policy functions to map the state to action with no uncertainty.

The policy gradient is generally modeled with the parameters $(\theta, \pi\theta(als))$. Θ acts as the reward in the policy gradient so any algorithms can be applied to optimize the θ .

$$J(\theta) = \mathbb{E}_{\pi} [r(\tau)] \tag{1}$$

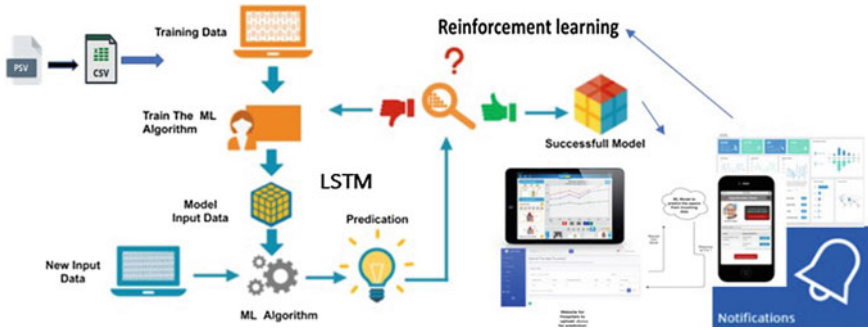


Fig. 3 Architecture design of proposed work

From the Formula (1) $J(\theta)$ is the function of policy that determines the weight of the neural network, \mathcal{E}_π is expected policy, τ is the expected future value, and $r(\tau)$ is the total reward or trajectory of the policy function.

3 Proposed Approach

3.1 Architecture Description

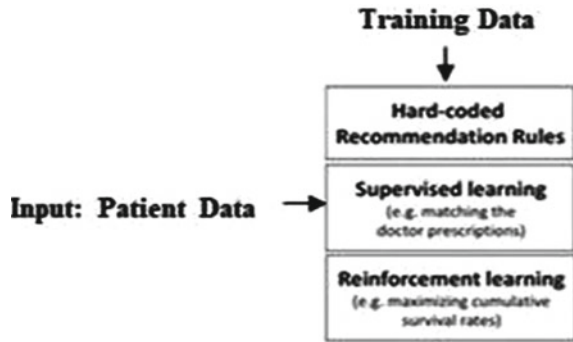
1. Converting the input dataset from .psv extension to .csv file or the .csv is obtained it can be directly given as input.
2. The converted dataset is fed to training data, trains the Machine Learning algorithm to get a model input data that makes a standard Machine Learning algorithm of the Long Short Term Memory (LSTM).
3. Training the ML algorithm happens with the concept of reinforcement learning
4. On the other base, new input data was given to the Machine Learning algorithm for prediction. The predicted values are considered as the input to reinforcement learning of step 3 to train the ML algorithm.
5. The outcomes are visioned in the form of mobile application notifications and in the dashboard of the hospital web application (Fig. 3).

3.2 Training Model Description

After the conversion of the prescribed coded format of input data, the training model is used to convert the categorical features to one-hot encoding and scaling the continuous features. The continuous features are trained by machine learning models, and the Auto Encoders (AE) are trained by Deep Learning models (Fig. 4).

The procedural perspective for policy gradient used in this work is stated below,

Fig. 4 The perspective of the training model



1. Initialize the policy parameter θ at random.
2. Generate one trajectory on policy π_θ : $S_1, A_1, R_2, S_2, A_2, \dots, S_T$.
3. For $t = 1, 2, \dots, T$:
 - (i) Estimate and return G_t ;
 - (ii) Update policy parameters: θ

3.3 Feature Extraction and Prediction in LSTM

For training the network we use back-propagation which is the essence of neural net training. Based on the loss function (error rate) from the earlier epoch the weights of the neural network are fine-tuned and also grow in generalization to make the model reliable (Fig. 5).

The functionalities and the fealties of both the models are given below:

1. Continuous Features: The continuous features are generated in the form of feature engineering, few features are selected under two categories: (a) converted to categorical and (b) unchanged features. The features that need conversion to categorical have three different classifications namely normal, abnormal, and

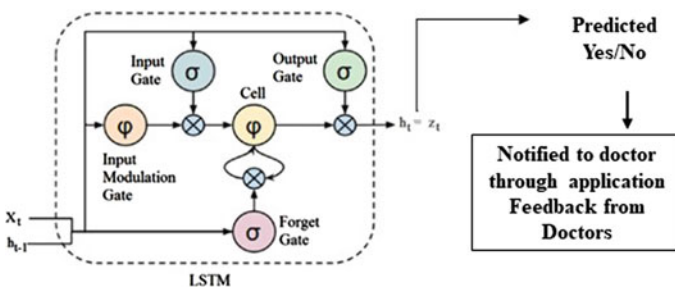


Fig. 5 The general framework of LSTM and prediction modeling

missing. Heart Rate, O2stat, Temperature, SBP/DBP, Respiratory rate, and Age falls in the first category, Gender, Hospadmtime (Hospital admission time), and ICU LOS (ICU Length of Stay) is said to be the unchanged category.

2. Auto Encoders: For high-class imbalance used by the use cases of anomaly detections, autoencoders produce good results. Treating the classes in different manners like classes in negative states as anomaly and classes in positive states for the process consideration, Auto Encoders has better performance than the traditional methodology. In healthcare or medical representation having an average precision of 7% is measured to be a favorable ratio.

3.4 Implementation and Experiments

Once after prediction is done as quick as the data provided, it'll respond within a minute by sending the notification to concerned devices like the doctor's mobile/PC, and the indication is shown concerning ward number. The data is also shown in brief with an analytics dashboard that'll help the doctor to take decisions and treat the patient faster.

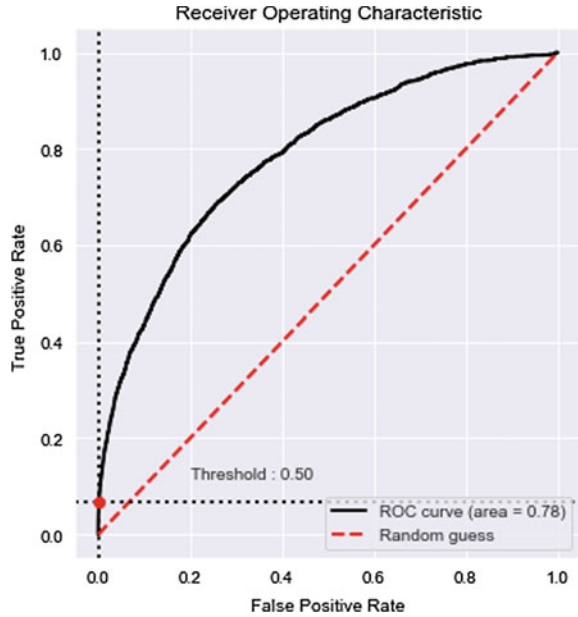
The outcome is visualized by the development of two different patterns one on the display on the dashboard of the hospital website applications for the preferable of doctors, and the other on the display on the alert mechanism in the mobile application. The design on both was generated using the platforms; Angular, ML5 js, Runway, Flutter, Android Studio. The message notification in the mobile application was designed using; Python-Flask. The model design for the machine learning framework was implemented in the platform; Python (Major Libraries: sci-kit-learn, Keras, Tensorflow, NumPy, Pandas).

From the working of LSTM methodology, the value of θ is tested in different values. Ranging from 0.1 to 0.7. According to the trajectory policy value $\pi\theta$ the performance of the features, the selection was considered to be good enough and its result is measured in form of ROC and Precision and Recall Curves.

3.5 Results and Discussions

Metrics or measurements chose for the evaluation is very important. Considering the accuracy alone will not be sufficient or good enough for the prediction models it's known that the maximum of the models uses the accuracy as the major measure and also proves to be better or even high sometimes. Comparing to CNN-LSTM method measured by AUROC in previous work scores 0.879 with the period 3 h and 0.752 in 24 h. Applying reinforcement learning in Recurrent Neural Network for the prediction will provide an outcome of better accuracy. The linear discriminant and the Support Vector Machine are used for the classification of the data for the results of the prediction. The results were measured by the metrics Receiver Operating

Fig. 6 ROC measurement

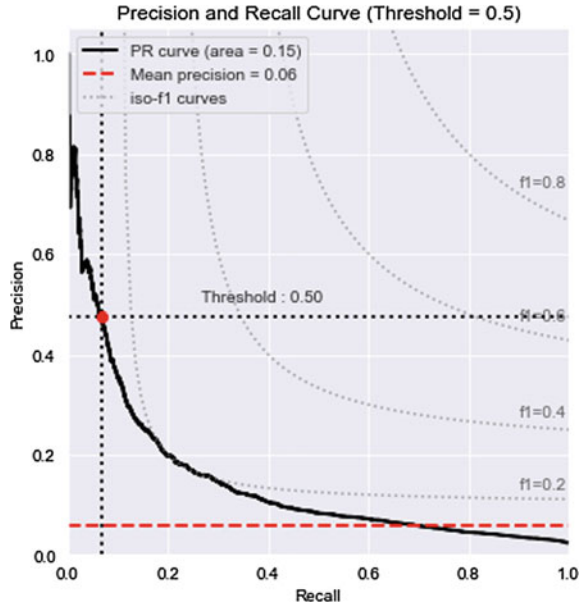


Characteristics (ROC), precision, and Recall Curve (RC) was considered with the threshold value of 0.5. The plot shows the accuracy of above 95% in the early detection of sepsis. Reinforcement is also enabled to improve accuracy, precision, and recall. The ROC was calculated using the True Positive and False Positive rates (Figs. 6 and 7).

4 Conclusion

In recent years, some solutions have been devised to help people in detecting sepsis in the medical environment. But it is not that efficient to recognize the earliest of sepsis our purpose is to provide a robust and easy system for doctors and people to recognize as early as possible. Our proposed system uses a Recurrent Neural Network (RNN) and reinforcement learning for better accuracy. This work was implemented in high technologies with the features on successful detection, a notification will be sent to the respective staffs and generation of detailed reports in dashboards.

Fig. 7 Precision and recall curve metric with threshold value 0.5



References

1. Futoma J et al (2017) Learning to detect sepsis with a multitask Gaussian process RNN classifier. In: International conference on machine learning, pp 1174–1182
2. Lea C et al (2017) Temporal convolutional networks for action segmentation and detection. In: IEEE conference on computer vision and pattern recognition (CVPR), pp 1003–1012
3. Fagerström J, Bång M, Wilhelms D, Chew MS (2019) LiSep LSTM: a machine learning algorithm for early detection of septic shock. *Sci Rep* 9. Article No. 15132
4. Lauritsen SM, Kalør ME, Kongsgaard EL, Lauritsen KM, Jørgensen MJ, Lange J, Thieson B (2019) Early detection of sepsis utilizing deep learning on electronic health record event sequences. *Artif Intell Med* [arXiv:1906.02956v1](https://arxiv.org/abs/1906.02956v1)
5. Moor M, Horn M, Rieck B, Roqueiro D, Borgwardt K (2019) Early recognition of sepsis with Gaussian process temporal convolutional networks and dynamic time warping. In: Proceedings of machine learning research, vol 106, pp 1–IX
6. Bai S et al (2018) An empirical evaluation of generic convolutional and recurrent networks for sequence modeling. *arXiv preprint* [arXiv:1803.01271](https://arxiv.org/abs/1803.01271)
7. Li SC-X, Marlin BM (2016) A scalable end-to-end Gaussian process adapter for irregularly sampled time series classification. In: Advances in neural information processing systems, pp 1804–1812
8. Reyna M, Josef CS, Jeter R (2020) Early prediction of sepsis from clinical data: the PhysioNet/computing in cardiology challenge. *Crit Care Med* 48(2):210–217
9. Singer M et al (2016) The third international consensus definitions for sepsis and septic shock (Sepsis-3). *J Am Med Assoc (JAMA)* 315(8):801–810
10. Sarah I, Soundarya K, Dhanalakshmi R, Deenadayalan T (2020) DYS-I-CAN: An Aid for the Dyslexic to improve the skills using Mobile Application. In: 2020 International conference on system, computation, automation and networking (ICSCAN), pp 1–5. <https://doi.org/10.1109/ICSCAN49426.2020.9262375>
11. Siva Rama Rao AVS, Dhana Lakshmi R (2017) A survey on challenges in integrating big data. In: Deiva Sundari P, Dash S, Das S, Panigrahi B (eds) Proceedings of 2nd international

- conference on intelligent computing and applications. *Advances in intelligent systems and computing*, vol 467. Springer, Singapore. https://doi.org/10.1007/978-981-10-1645-5_48
12. Secretariat W (2017) Improving the prevention, diagnosis and clinical management of sepsis. http://apps.who.int/gb/ebwha/pdf_files/WHA70/A70_R7-en.pdf?ua=1
 13. Futoma J, Hariharan S, Sendak M, Brajer N, Clement M, Bedoya A, O'Brien C, Heller K (2017) An improved multi-output Gaussian process RNN with real-time validation for early sepsis detection. arXiv preprint [arXiv:1708.05894](https://arxiv.org/abs/1708.05894). <http://arxiv.org/abs/1708.05894v1>
 14. Futoma J, Hariharan S, Heller K (2017) Learning to detect sepsis with a multitask Gaussian process RNN classifier. arXiv preprint [arXiv:1706.04152](https://arxiv.org/abs/1706.04152)
 15. Nemati S, Holder A, Razmi F, Stanley MD, Cliord GD, Buchman TG (2018) An interpretable machine learning model for accurate prediction of sepsis in the ICU 46(4):547–553. <https://doi.org/10.1097/ccm.0000000000002936>
 16. Sainath TN, Vinyals O, Senior A, Sak H (2015) Convolutional, long short-term memory, fully connected deep neural networks. In: 2015 IEEE international conference on acoustics, speech and signal processing (ICASSP), IEEE. <https://doi.org/10.1109/icassp.2015.7178838>
 17. Shickel B, Tighe P, Bihorac A, Rashidi P (2018) Deep EHR: a survey of recent advances in deep learning techniques for electronic health record (EHR) analysis. arXiv preprint [arXiv:1706.03446](https://arxiv.org/abs/1706.03446). <https://doi.org/10.1109/JBHI.2017.2767063>

Design of Cost-Effective Bamboo Reinforced Manhole Cover; A Step Toward Sustainable Development



Shilpa Kewate, Manisha Jamgade, and Madhulika Sinha

Abstract In India, many open Manholes have been death traps for pedestrians, especially during monsoon. Steel reinforced manhole cover and mild steel manhole cover have a good resale value due to which these Manhole covers are in danger of being stolen it may cause accidents due to open Manhole left on the road. This may harm the lives of the public and animals walking on roads. This research work aims to design an environment-friendly sustainable manhole cover by using bamboo as an alternative material to steel. This newly developed product is cost-effective. In this paper, experimental testing for load resisting capacity as per IS (5) of a bamboo reinforced Manhole cover and steel-reinforced Manhole cover is carried out. Also, cost-effectiveness between both the Manhole cover is presented in this paper. This research work approaches to contribute toward sustainable development of green alternative material to steel.

Keywords Design · Cost-effectiveness · Bamboo reinforcement · Sustainable development

1 Introduction

The Manhole cover is the lid of the Manhole openings to a sewer system or inspection chamber [3]. Generally, Manhole covers are located on pavements and roads. It should be strong and durable to resist the load and impact of pedestrians and vehicles

S. Kewate (✉) · M. Jamgade · M. Sinha
Department of Civil Engineering, Pillai HOC College of Engineering and Technology, Rasayani,
Maharashtra 410207, India
e-mail: shilpakewate@mes.ac.in

M. Jamgade
e-mail: mjavgade@mes.ac.in

M. Sinha
e-mail: madhulik@mes.ac.in

[1]. These covers are normally made up of cast iron and concrete to bear the large loads [4].

The purpose of the Manhole cover is to avoid accidentally falling anyone or anything into the Manhole cover. And the Manhole cover allows the authorized person for repair and maintenance work. Theft of manhole cover for scrap value is the common issue associated with Manhole covers. It causes road accidents and several health hazards.

Steel reinforced Manhole cover and mild steel Manhole cover have a good resale value due to which these Manhole covers are at risk of being stolen which may cause accidents due to open holes left on the road [11]. In 2012, the New York Times reported that based on the existing commodity prices for iron and steel, a stolen Manhole cover might fetch more than \$30, but it costs the municipality about \$200 to bring back each. Governments of Asian Countries like India and China have taken the initiative to replace the steel Manhole covers with concrete covers. But the thefts persisted since concrete covers were also stolen for the rebar inside the concrete [9]. The open holes of a Manhole cover may disturb the lives of residing people due to bad odor and arises various diseases. Figure 1 shows an accident caused due to missing Manhole cover on the road.

Many researchers are working on the possibility of the use of bamboo as a structural element. Bamboo is the fastest-growing plant. It has enormous economic potential. From ancient times bamboo is used in the construction of bridges and houses. This research work approaches to design cost-effective Bamboo reinforced manhole cover which would contribute to sustainable development and also green alternative material to steel.

The novelty of this research work is about a totally newly developed product, 'Bamboo Reinforced Manhole Cover'. Bamboo is first time used as a substitute material to steel in the production of a Manhole cover. Even though many researchers



Fig. 1 Accident due to missing manhole covers [2]

have work on the use of bamboo as a substitute material in different structures but it is used first time in a Manhole cover. Bamboo has the potential of both environmental benefits as well as means of employment generation.

1.1 Types of Manhole Cover

- (a) Fiber-reinforced plastic
- (b) Glass-reinforced plastic
- (c) Reinforced cement concrete
- (d) Cast iron
- (e) Steel fiber reinforced concrete
- (f) Ductile iron.

1.2 Grades of Manhole Cover

The various grades of manhole cover, their grade, and use purpose are shown in Table 1

2 Bamboo

The fastest-growing plant on the earth is Bamboo. On degraded land also bamboo can be grown and harvested rapidly. Bamboo possesses high strength to weight ratio and

Table 1 Grade of manhole cover [5]

Grade	Grade designation (Load resist capacity)	Use/purpose
Light duty	LD-2.5 (25 kN)	Residential and institutional complexes/areas with pedestrian, inspection chambers
Medium duty	MD-10 (100 kN)	Service lanes/roads, on pavements used under medium-duty vehicular traffic, car parking areas
Heavy duty	HD-20 (200 kN)	Institutional/commercial areas/carriageways/city trunk roads /bus terminals with heavy-duty vehicular traffic of wheel load between 50 and 100 kN and parking areas and manhole chambers for road pavement
Extra heavy duty	EHD-35 (350 kN)	Carriageways in commercial/industrial/port areas/warehouses/godowns where frequent loading and unloading of trucks/trailers, slow to fast-moving vehicular traffic for wheel loads up to 115 kN

tensile strength. Bamboo has the potential to use as a reinforcement material [12]. Bamboo does not have natural durability. Durability of bamboo can be enhanced by soaking, drying, and applying water proof coating and sand [7].

An author in [8] has conducted an experimental investigation on tensile strength test on a variety of diameter sizes of steel and bamboo bars. Tensile results show that as the size of bamboo bars increases the tensile strength also increases.

Past study [10] have studied bamboo which can be a suitable replacement for steel. Bamboo can play a very important role in developing rural areas due to its cost-effectiveness. Also, the author has shown the advantages, disadvantages, treatments, and mechanical properties of bamboo.

An experimental investigation [6] on a bamboo reinforced slab of size $1000 \times 1000 \times 50$ mm with different cross-sectional shapes of bamboo. Four different types of the slab were cast with mild steel-reinforced, circular bamboo reinforced, square bamboo reinforced, and triangular bamboo reinforced; these slabs were tested for single point load on center with all sides simply supported. From the test results, the load-resisting ability of the square bamboo reinforced slab is 25% as compared to the mild steel slab.

Ahmad et al. [2] have investigated bamboo fibers in concrete cubes and bamboo reinforced beams of size $750 \times 150 \times 150$ mm. For concrete cubes, 1% bamboo fibers with varying sizes were tested for compression test. Three types of beams were cast plain concrete, singly bamboo reinforced and doubly bamboo reinforced beam which was tested for flexural strength. The test results of the compression test on bamboo fibers cubes show double the strength as compared to plain concrete cubes. From the flexural test results, the doubly reinforced bamboo beam has shown the best results as compared to others.

3 Experimental Program

Literature survey reveals that bamboo cannot be used directly as reinforcement in concrete thus bamboo has to be properly selected, seasoned, and treated before using. Also the flowchart showing the experimental program for the preparation process of bamboo reinforced manhole cover is shown in Fig. 2.

3.1 *The Casting of the Manhole Cover*

According to the literature, survey bamboo cannot be used directly as reinforcement in concrete thus bamboo has to be dried to reduce moisture content, then after spitted vertically into strips form as per desired dimension (area) the cross-sectional area of single bamboo strips taken as 78.5 mm^2 . Strips are then coated with coal tar and sprinkled sand on them which are well dried for 48 h. This makes the bamboo withstand water absorption and termites and a sprinkling of sand makes a good bond

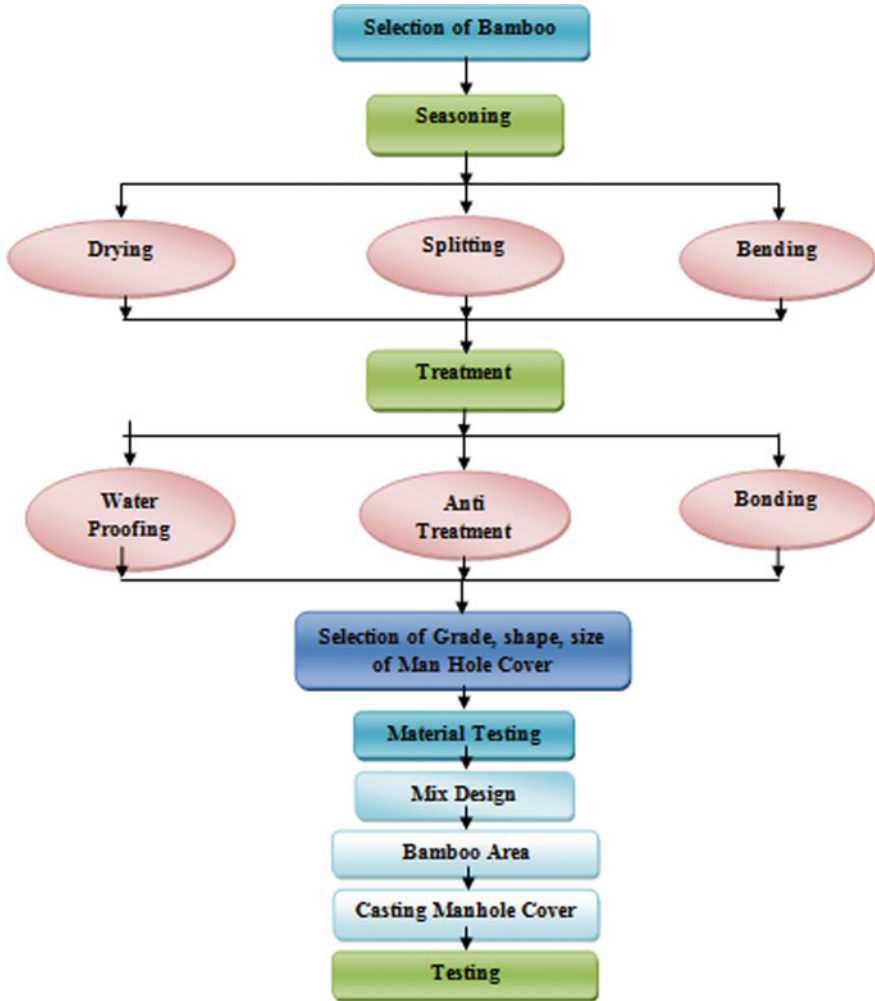


Fig. 2 Flowchart of experimental work

with concrete. Bamboo mesh tied with binding wire and then cast with M30 grade concrete. Figure 3 shows an experimental set up for testing of Manhole cover.

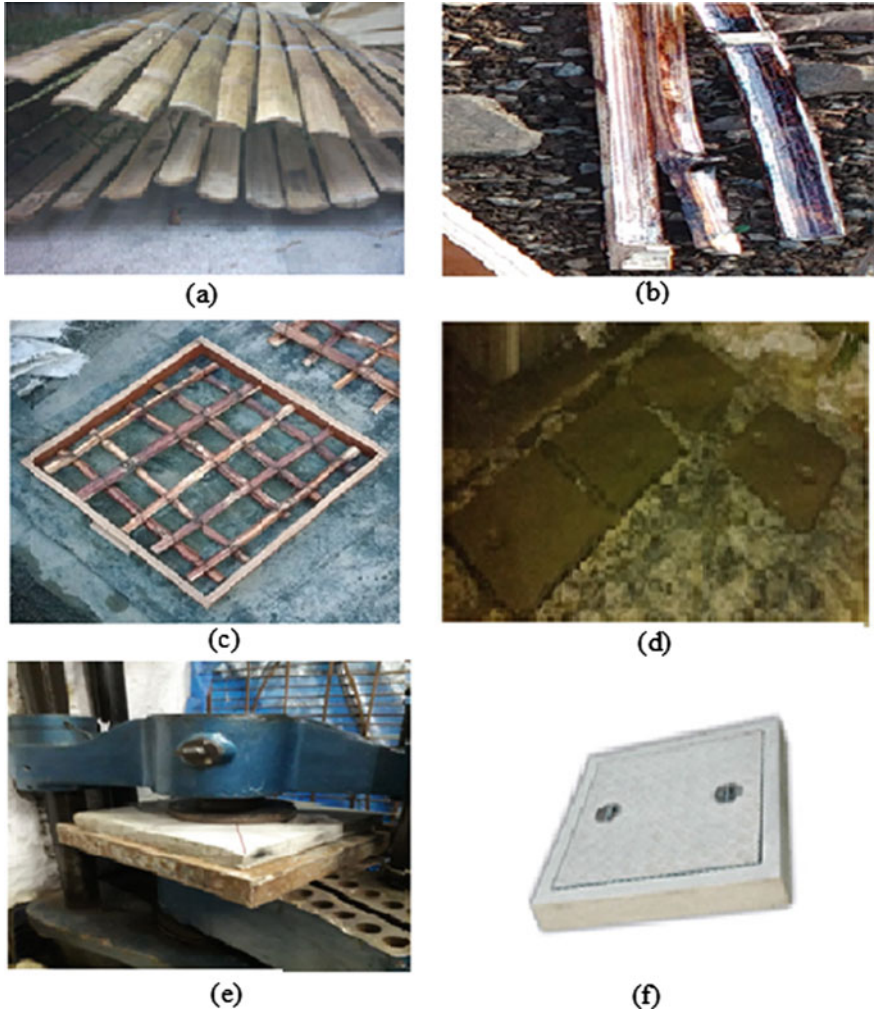


Fig. 3 Experimental setup, **a** splitting of bamboo, **b** bamboo strips coated with coal tar **c** bamboo mesh for manhole cover, **d** casting of Manhole cover, **e** test setup for testing of manhole cover in UTM, **f** final product

4 Results

4.1 Load Resisting Capacity of Manhole Cover

Load test on Manhole cover is done in Universal testing machine (UTM). In this test application of target load is considered with the use of 300 mm diameter circular block (plate) positioned on a manhole cover at its geometrical center and load application is

Table 2 Load test results (load resisting capacity) of manhole cover

Particular	Dimension (mm)	Reinforcement	Load (kN)	Average load (kN)
Case 1—light-duty steel reinforced manhole cover	510 × 510 × 50	Steel	25	25
	510 × 510 × 50	Steel	25	
	510 × 510 × 50	steel	25	
Case 2 - light-duty 3% bamboo reinforced Manhole cover	510 × 510 × 50	3% Bamboo	18	20
	510 × 510 × 50	3% bamboo	19	
	510 × 510 × 50	3% bamboo	23	
Case 3- Extra heavy-duty steel reinforced Manhole cover	600 × 600 × 100	Steel	350	
	600 × 600 × 100	Steel	350	
	600 × 600 × 100	Steel	350	350
Case 4- Extra heavy-duty 3% bamboo reinforced Manhole cover	600 × 600 × 100	3% bamboo	62	65
	600 × 600 × 100	3% bamboo	65	
	600 × 600 × 100	3% bamboo	68	

done as per IS code (5) recommendation. As per IS (5), the minimum load resisting capacity of light-duty Manhole cover should be 25 kN and heavy-duty Manhole cover should be 350 kN. Table 2 shows the load resisting capacity of Manhole cover.

In experimental work, the four cases of Manhole cover are considered.

Case 1: light-duty steel reinforced manhole cover of size 510 × 510 × 50 mm in which three samples were cast and tested for load resisting capacity and also for other analysis.

Case 2: light-duty 3% bamboo reinforced Manhole cover of size 510 × 510 × 50 mm in which three samples were cast and tested for load resisting capacity and also for other analysis.

Case 3: Extra heavy-duty steel reinforced Manhole cover of size 600 × 600 × 100 mm in which three samples were cast and tested for load resisting capacity and also for other analysis.

Case 4: Extra heavy-duty 3% bamboo reinforced Manhole cover of size 600 × 600 × 100 mm in which three samples were cast and tested for load resisting capacity and also for other analysis.

4.2 Cost Effectiveness

The total cost of case 2 bamboo reinforced manhole cover is 36% less than as compared to case 1 steel reinforced cover.

Table 3 Cost analysis of case 1—light-duty steel reinforced manhole cover

Case 1—light-duty steel reinforced manhole cover	Concrete M30 (cum) (Rs. 5000/cum)	Reinforcement (kg.) (Rs. 50,000/ton steel)	Treatment coal tar	Total (Rs.)
Quantity	0.013	2.01	–	
Price Rs	65	100.5	0	165.5

Table 4 Cost analysis of light-duty 3% bamboo reinforced manhole cover

Case 2—light-duty 3% bamboo reinforced manhole cover	Concrete M30 (cum) (Rs. 5000/cum)	Reinforcement (Rs. 100 per bamboo)	Treatment coal tar	Total (Rs.)
Quantity	0.013	Less than 1/3 bamboo used	Rs. 10	
Price (Rs.)	65	30	10	105

Case 1 light-duty steel reinforced manhole cover

Table 3 shows the cost analysis of case 1, size 510 × 510 × 50 mm light-duty steel reinforcement Manhole cover.

Case 2 light-duty 3% bamboo reinforcement:

Table 4 shows the cost analysis of case 2, size 510 × 510 × 50 mm light-duty bamboo reinforcement Manhole cover.

From cost analysis given in Tables 3 and 4 it is observed that the total cost of a light-duty bamboo reinforced manhole cover (Newly developed Manhole cover) is 36% cheaper as compared to a light-duty steel reinforced manhole cover (existing Manhole cover). This newly developed product is cost-effective and it will contribute toward sustainable development of green alternative material to steel. However, the further experimental investigation should be conducted to enhance the load-carrying capacity of the bamboo reinforced Manhole cover.

5 Conclusions

Light-duty bamboo reinforced Manhole cover is cost-effective and it will contribute toward sustainable development for a green alternative material to steel. Bamboo is not suitable for heavy-duty bamboo reinforced Manhole cover as its load carrying capacity is far behind the permissible limit as per IS (6). RCC and steel Manhole cover is being in danger of stealing as it has good scrap value in the black market which is a cause of many accidents and health problems. Bamboo reinforced manhole cover can be a solution to this problem as it has zero scrap value and the load-carrying

capacity of the bamboo reinforced Manhole cover is nearby the Permissible limit as per IS (6). However, the further experimental investigation should be conducted to enhance the load-carrying capacity of the bamboo reinforced Manhole cover.

6 Future Scope

The strength of bamboo reinforced light-duty Manhole cover can be enhanced further with the addition of fibers in concrete. Also, the use of Ferro-cement mesh with bamboo reinforcement may show improvement in the strength of the bamboo reinforced light-duty manhole cover.

References

1. ASTM C478 (2000) Specification for precast reinforced concrete manhole sections. ASTM Standards Source, Philadelphia, USA
2. Ahmad S, Raza A, Gupta H (2014) Mechanical properties of bamboo fibre reinforced 2 concrete. In: 2nd international conference on research in science, engineering and technology (ICRSET), Dubai
3. BS 497 (2006) Specification for manhole covers, road gully gratings and frames for drainage purposes. British Standards Source, London, UK
4. BS 7903 (1997) Guide to selection and use of gully tops and manhole covers for installation within the highway. British Standards Source, London, UK
5. Indian Standard 12592 (2002) Precast concrete manhole cover and frame. First revision
6. Khan I (2014) Bamboo Sticks as a substitute of steel reinforcement in slab. *Int J Eng Manage Res* 4(2):123–126
7. Muhtar (2020) Precast bridges of bamboo reinforced concrete in disadvantaged village areas in Indonesia. *Appl Sci* 10(20):7158
8. Ogunbiyi A et al (2015) Comparative analysis of the tensile strength of bamboo and reinforcement steel bars as structural member in building construction. *Int J Sci Technol Res* 4(11):47–52
9. OÑA M, Soltanzadeh F, de Sousa C, Barros JAO (2015) Exploring the use of HPFRC and GFRP grids for the production of manhole covers. In: *Fibre concrete*, Prague, Czech Republic
10. Patil S, Mutkekar S (2014) Bamboo as a cost effective building material for rural construction. *J Civ Eng Environ Technol* 1(6):35–40
11. Haggar SE, Hatow LE (2009) Reinforcement of thermoplastic rejects in the production of manhole covers. *J Cleaner Prod* 17:440–446
12. Weifeng Z, Jing Z, Guobin B (2012) Application technology of bamboo reinforced concrete in building. *Appl Mech Mater* 195–196:297–302

Design and Development of a Trolley for the Finishing Department of Garment Industry to Enhance Feeding Helper Productivity



M. Rajesh and N. V. R. Naidu

Abstract The paper deals with the design and development of an efficient material handling equipment for the finishing department of a garment industry. In the finishing department a feeding helper routinely moved between the helper desk, semi-finished garment bin, buttoning machines, individual pressing table and eventually the packing section. Due to this it was very difficult for the helper to supply the garments to the operators in time. Hence, it was very much essential to reduce the number of trips made by the feeding helper. A customized trolley was designed and developed for bulk handling of garments. The trolley had two compartments namely a basket on the top for holding pre-pressed garments and two racks at the bottom for placing the stacks of pressed garments. After implementing the trolley in the finishing department the number of feeding helper trips from 23 to 11 which resulted in an enhanced labor productivity up to 109%.

Keywords Material handling equipment · Productivity · Garment industry

1 Introduction

Garment industry is one among the highest revenue generating industries of the nation [1]. More and more countries getting into the trade demands efficient, reliable and high quality garment producers. In today's competitive world a manufacturer needs to cut down the production cost in order to keep the product cost at low [2, 3]. The garment manufacturers are finding different ways to lower the production cost without compromising on the quality of the product [4, 5].

Generally, a garment industry has three main departments namely the cutting, sewing and finishing and a list of auxiliary departments like personnel, industrial engineering, merchandising, administrative, security, stores, mechanic, housekeeping etc. The conversion of fabric to garment begins at the cutting department where the

M. Rajesh (✉) · N. V. R. Naidu
Ramaiah Institute of Technology, Bengaluru 560054, India
e-mail: mrajeshiem@msrit.edu

© The Author(s), under exclusive license to Springer Nature Singapore Pte Ltd. 2022
B. B. V. L. Deepak et al. (eds.), *Applications of Computational Methods in Manufacturing and Product Design*, Lecture Notes in Mechanical Engineering,
https://doi.org/10.1007/978-981-19-0296-3_29

317

fabric is cut against a pattern and these cut pieces are moved to the sewing department where the pieces are sewed to form a semi-finished garment which further moves to the finishing department where the finishing touches are given for having an aesthetically pleasing garment.

Even after a tremendous scientific development in the field of garment manufacturing, majority of work is still manually done [6]. The Indian manufacturers are more and more adapting several techniques to reduce the production costs, one of which is the use of material handling system [7]. James apple [8] describes "Material handling as the movement of materials, manually or mechanically in batches of one item at a time within the plant. The movement may be horizontal, vertical or the combination of horizontal and vertical."

According to William Gant Ireson [9] the cost of material handling is as much as 20–25% of the total cost of converting the raw material into the finished product. These factors alone are sufficient to establish that the material handling system should be given an exhaustive study whenever a new factory is being planned or an existing one is being remodeled.

2 Literature

There are not so many papers published in the past pertaining to the material handling equipment in garment industry. However various technical papers and books in relevance to the area of research were reviewed. Much of the research was based on improving productivity through the use of technology and training manpower. No research discussed on how to enhance productivity by adopting material handling equipment design in garment industries.

Garment manufacturers are searching for ways to identify and eliminate hidden costs that are draining out cash resources [10]. Longer lead time and high inventory are nothing but different forms of waste in the manufacturing environment [11]. Waste elimination is one of the most effective ways to increase profitability in manufacturing [12]. Abhilasha [13] discusses the wastes in the apparel industry namely over production, waiting, transportation, inventory, processing and product defect. A waste can therefore be defined as any unnecessary input to or an undesirable output from a system.

Many factories observe transportation of raw and finished goods as wastes. The prime reason for this type of waste is a poor layout of the factory floor and material handling facilities [14]. In order to eliminate transportation waste, the improvement must be made in the areas of layout, methods of handling and housekeeping. In the garment industry, it is not unusual to see carrying of fabric rolls to and fro from stores, semi-finished components bundles being shuttled to and fro in the sewing line, sewn garments juggled around the finishing departments for different processes like thread trimming, spotting, etc. these are different forms of transportation waste, resulting from unclear instructions, poor layout of equipment and processes and confused

material flow. By streamlining material flows through the use of material handlers, the transportation time could be reduced.

ILO defines Productivity as the ratio of output to input [15]. Productivity expresses the relationship between the quantity of goods and services produced (output) and the quantity of labor, capital, land, energy and other resources to produce it (input). The term productivity can be used to assess or measure the extent to which a certain output can be extracted from a given input. According to Mathur [16], productivity improvement is possible through industrial engineering techniques. He says the productivity concept can be applied with equal success in every sphere of human life, whether the aim is to reduce consumption of resource or to increase industrial output or to reduce time required to do a job. Industrial engineering techniques maximizes productivity by suggesting layout, methods improvements, material handling alternatives, etc. that would allow the worker to produce more.

3 Objective

The work aims at designing and developing material handling equipment for a garment industry using material handling principles.

4 Problem Description

During the work-in-process (WIP) stage, a garment is subjected to a lot of in-house movement i.e. material traffic from one section to another section in the industry. The traffic can be greatly reduced by carefully studying and analyzing the present system and by adopting industrial engineering tools and techniques.

5 Data Collection

Data is required in the initial stage so as to understand the present working conditions and data is required in final stage to evaluate the proposal. It is common to sight workers moving at irregular intervals between a number of points in the working area, with or without material [17]. This situation occurs very often in the industry when bulk material is being fed or removed i.e. an operative is attending to two or more machines or operators. The movements can be recorded as a travel chart. A travel chart is a tabular record for presenting quantitative data about the movements of workers, materials or equipment between workstations over any given period of time.

5.1 Present Handling Methods and Equipment

Excessive material handling expense and/or inadequate material handling capacity are the two conditions that frequently cause a company to consider the installation of a new system and dispose-off the present facilities. This may be due to poor utilization of the present equipment or an existing layout that prevents proper utilization of the material handling equipment.

In the finishing department a feeding helper (similar to a messenger) collects and distributes garments in various sections namely buttoning, pressing and packing. The feeding helper made a number of trips carrying a small number of garments carried on her shoulder from one station to another, i.e. from the helper desk to semi-finished garment bin to each of the buttoning machines to every individual pressing table and to the packing section as shown in Fig. 1.

As a result, there were a lot of movements between the stations; due to this it was very difficult for the helper to feed the garments to the operators. The feeding helper's task was recorded as number of trips made between each station using a travel chart as shown in Table 1.

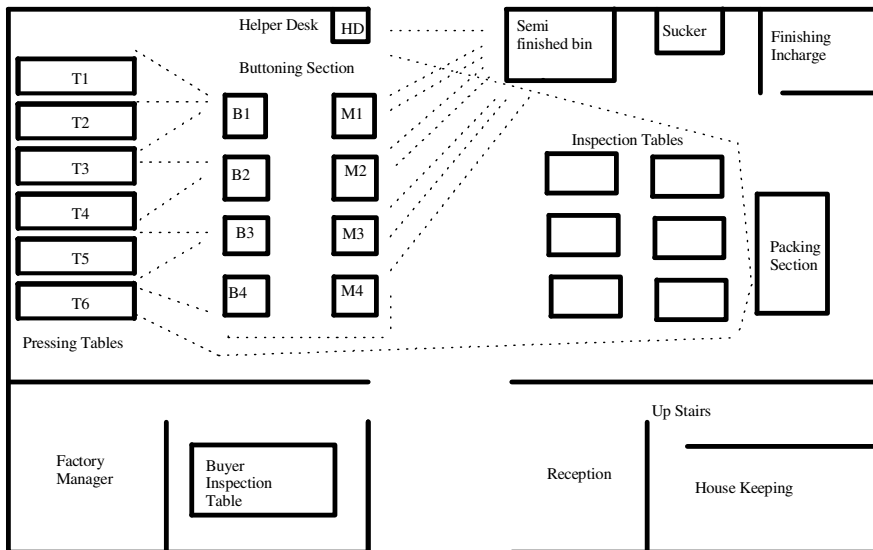


Fig. 1 Movement of feeding helper in present layout

Table 1 Number of trips made in present method

		FROM										
		HD	Bin	Buttoning				Pressing				
				M1	M2	M3	M4	T1	T2	T3	T4	Packing
TO	HD											✓
	Bin	✓		✓	✓	✓						
	M1		✓						✓			
	M2		✓							✓		
	M3		✓								✓	
	M4		✓									
	T1			✓								
	T2				✓							
	T3					✓						
	T4							✓				
	Packing								✓	✓	✓	✓

6 Analysis

While understanding the importance of minimizing transportation, cause and effect diagram [18] shown in Fig. 2 a specialized idea organizing technique helped in identifying potential causes to investigate.

Critical examination shown in Table 2 is the systematic analysis of the information about a problem, procedure or activity. It has two stages which consist of primary

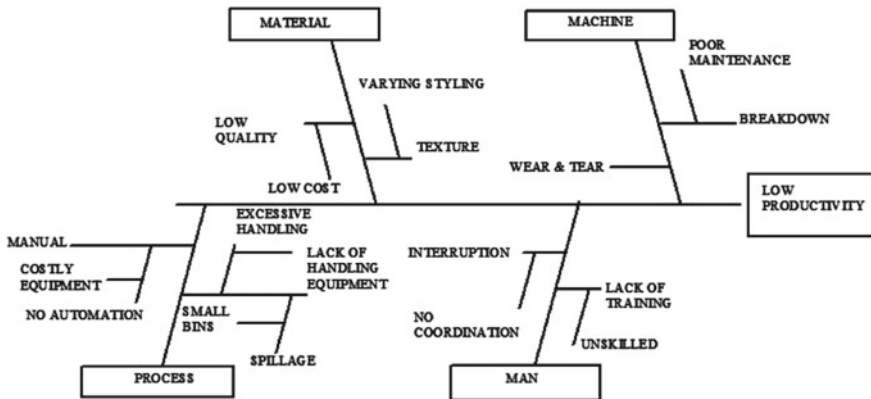


Fig. 2 Cause and effect diagram

Table 2 Critical examination sheet of finishing section

Critical examine—questioning technique				
	Primary questions		Secondary questions	
PURPOSE	WHAT is done?	WHY is it done?	WHAT else could be done?	WHAT should be done?
	Garments are distributed by a feeding helper	Done to feed the operators	Operators can do by passing it Design a material handling equipment	Design a material handling equipment
PERSON	WHO does it?	WHY does THAT person do it?	Who ELSE might do it?	Who SHOULD do it?
	A feeding helper does it	The work activity involves in distributing	An additional helper Feeding helper with a work aid	Bulk handling by the feeding helper
MEANS	HOW is it done?	WHY is it done THAT way?	How else COULD it be done?	How SHOULD it be done?
	Done manually by carrying on shoulder	To load all operators in batches	Might be done by a trolley	By designing a trolley

questions and secondary questions. Answers to primary questions indicate the facts and the answers to secondary questions point the alternatives.

6.1 Interpretation

After an exhaustive study of the present handling methods, it was noticed that some activities performed by the operators in various sections contributed toward the ineffective time and unwanted movements, i.e. a number of unwanted trips were made by the feeding helper in the finishing department. All these appear simple but when considered on a large scale this leads to a major problem and this cannot be ignored. Hence, it was important to eliminate or minimize these unwanted movements. On evaluating the alternatives based on several parameters like the material, movement, supervision, path, speed, power requirement, load and space, trolley was selected as the material handling equipment that suits the plant under study, as this alternative can handle bulk, do not require power to operate, simple and cheap at cost.

Table 3 Product parameters

Parameter	Product dimensions in finishing department
Size of product	12" × 9" × 1.5" to 15" × 10" × 1.5"
Volume	5.45–6.5 cu in
Weight	250 g (average)
Bundle size (units/bundle)	5 units/bundle

6.2 Factors Influencing the Design

The size of the product, its weight and the volume to be handled will, to a great extent, determine the type of equipment to be used and the number of units required to meet the production capacity. All the above variables change from one department to another i.e. The number of units handled in cutting or sewing department was in bundles of 10 units whereas in finishing department it was in bundles of 5 units. Hence, an ergonomically designed [19] material handling equipment must be used to transport the required number of units between the workstations. Table 3 lists the product parameters.

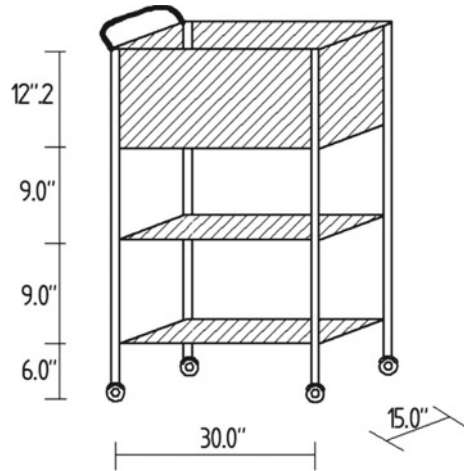
6.3 Design Details

The trolley was designed based on the product size in the finishing department. It ranged between 12" X 9" X 1.5" and 15" X 10" X 1.5" depending on the buyer specification. Table 4 provides the necessary trolley design details.

Hence, the designed trolley shown in Fig. 3.

Table 4 Calculation of trolley specification

Design parameter		Value
Trolley width (W)	=	15" (max dimension of pressed garment as per buyer specification)
5 units each from 6 ironers is stacked in 2 racks, the length of trolley (L)	=	10" (length of each unit) × 3 stacks
The height of each rack (H _r)	=	1.5" × 5 units + 1.5" clearance for stacking
Basket volume required for containing 5 units each for 4 button hole machines	=	6.5 ³ (volume of each pre pressed unit) × 20 units
The height of basket H _b	=	5492 cu in/(30" × 15")
Total height of trolley Considering ergonomic height in design	=	12.2" + 9" + 9" + 6" ground clearance

Fig. 3 Trolley specifications

6.4 Function of the Proposed System

- The semi-finished garments were loaded into the upper compartment (the basket) and the trolley was pushed to the buttoning section, the garments were unloaded and the buttoned garments were reloaded into the basket and the cart was pushed to pressing section.
- In pressing section, at each of the tables the helper issued garments from the top compartment and collected the pressed garments. The collected garments were neatly stacked on the racks of the trolley.
- The trolley was then pushed to the packing section for delivering the pressed as shown in Fig. 4.
- The number of trips made by the feeding helper was recorded in the travel chart as shown in Table 5.

7 Economic Analysis

The economic analysis was done as shown in Fig. 5 and the results indicate that the organization can make savings if the material handling equipment was adopted in the finishing department. Also there was no or very little maintenance cost which all add-up to the net savings. In the present method the management was planning to hire an additional operator

i.e. cost of employing = Rs 20000/ – per month

From the proposed method i.e. on using the trolley there was no need for an additional operator [20].

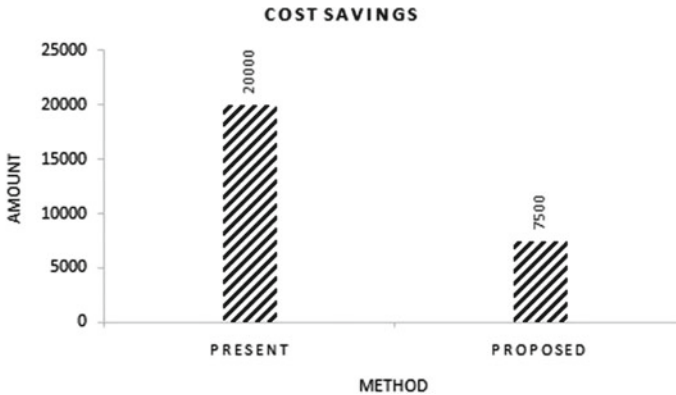


Fig. 5 Economic analysis to compare present and proposed methods

Hence, direct savings to company = Rs 20, 000/ – per month

Therefore, savings per day = Rs 20, 000/26 working days

= Rs 769.23 per day

Cost of equipment (prototype) = Rs 7500/–

Therefore, paybackperiod = investment/contribution

= Rs 7500 Rs/Rs 769.23/day

= 9.75 days

8 Results

The results shown in Fig. 6 indicate the proposed material handling equipment reduced the number of trips made by the feeding helper from 23 to 11 trips per cycle, which is a significant improvement. Comparatively, the feeding helper's performance increased from handling 2.17 units per trip to 4.55 units per trip in a work cycle. This resulted in the enhancement of labor productivity up to 109%.

9 Conclusions

Time study was analyzed for identifying the unwanted activities that added up to the total work content and it was observed that the designed material handling equipment eliminates the piling up of work. In finishing section, the feeding helper was making several trips between stations in order to feed the operators; with the designed trolley, the feeding helper was making only a few trips to complete the work.

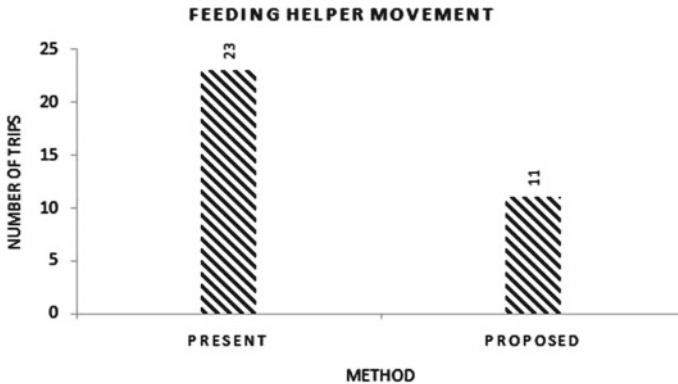


Fig. 6 Graph of number of trips made by the feeding helper

The management finds this an easy solution as it avoided the hiring of additional heaper and also it was simple and inexpensive to develop. The results show that the proposed workplaces with trolley reduced the ineffective time involved in the job while enhancing productivity up to 109%.

References

1. Nayak PA (2005) Does India gain from the enlarged EU market? Textile committee, ministry of textiles, Government of India, 3, India
2. Gardas BB, Raut RD, Narkhede BA (2018) Modelling the challenges to sustainability in the textile and apparel sector: a Delphi-DEMATEL approach. *Sustain Prod Consumption* 15:96–108
3. Santos PMM, Campilho RDSG, Silva FJG (2021) A new concept of full-automated equipment for the manufacture of shirt collars and cuffs. *Rob Comput Integr Manuf* 67:1–12
4. Finn Johnson A (2005) The outlook for Europe's position in global economy. *Non-Woven World* 2:80–83
5. Onut S, Kara SS, Mert S (2009) Selecting the suitable material handling equipment in the presence of vagueness. *Int J Adv Manuf Technol* 44:818–828
6. Sumeet Thapar A (2004) Appropriate technology combined with well-trained manpower creates quality. *Apparel Online* 1:21–22
7. Hellmann W, Marino D, Megahed M, Suggs M (2019) Human, AGV or AIV? An integrated framework for material handling system selection with real-world application in an injection molding facility. *Int J Adv Manuf Technol* 101:815–824
8. James Apple Z (1977) *Plant layout and material handling*, 2nd edn. Wiley, New York
9. William Grant Ireson Z (1959) *Factory planning and plant layout*, Englewood cliffs, 4th edn. Prentice Hall, NJ
10. Pradeep Jha A (2005) Incentive an intelligent way to become more profitable. *J Stitch World* 3:12–14
11. Nayak R, Padhye R (2018) Introduction to automation in garment manufacturing. *Autom Garment Manuf* 1–27
12. Gries T, Lutz V (2018) Application of robotics in garment manufacturing. *Autom Garment Manuf* 179–197

13. Singh A, Panghal D, Jana P (2019) Automatic seam ripping system. *Proc Manuf* 30:98–105. In: 14th global congress on manufacturing and management, Brisbane, Australia
14. Sutharsan SM, Prasad MM, Vijay S (2020) Productivity enhancement and waste management through lean philosophy in Indian manufacturing industry. *Mater Today* 33(7):2981–2985
15. George Kanawaty Z (2007) *Introduction to work study*, 4th edn. International Labor Organization, Geneva
16. Mathur G (1993) Productivity improvement using methods engineering. A case study. *Indus Eng J* 22(9):18–22
17. Capodaglio EM (2017) Occupational risk and prolonged standing work in apparel sales assistants. *Int J Indus Ergon* 60:53–59
18. Daniels S (1997) Back to basics with productivity techniques. *Work Study* 46(2):52–57. ISSN: 0043–8022
19. Juran JM (1995) *Quality planning and analysis*, 3rd edn. Mc Graw-Hill, Delhi
20. Jocelyn D, Abad A (2018) Ergonomics and simulation-based approach in improving facility layout. *J Indus Eng Int* 14:783–791. <https://doi.org/10.1007/s40092-018-0260>

Optimization of Dynamic Capacity of Deep Groove Ball Bearing by Using Genetic Algorithm



Krapa Bhanuteja, Mummina Vinod, and Duvvuri Vamsee Krishna

Abstract Deep Groove Ball Bearings (DGBB) is designed to operate at high speeds by supporting high radial load, minimal axial load and subjected to dynamic loads continuously. The objective in this work is to predict the optimum design parameters to maximise the dynamic load carrying capacity of DGBB at various contact angles. The complexity of the internal geometry of a DGBB and the associated constraints make non-traditional optimization techniques a suitable methodology for arriving at the optimum design parameters. We used genetic algorithms (GAs) technique present in the MATLAB to obtain optimum design parameters to maximise dynamic capacity (C_d) at various contact angles 5° , 10° , 15° and 20° . Thus, obtained values of the dynamic capacity (C_d) are compared with the values of the standard catalogue values. The significant thing in the present work is, the contribution of contact angle (α) is considered in detail over the objective function.

Keywords Deep groove ball bearing (DGBB) · Contact angle · Dynamic load carrying capacity and Genetic algorithm

1 Introduction

Bearing is a member of a machine that transfer loads between two moving machine members. DGBB is one of the classifications of rolling contact bearing, where balls are rolling elements and placed inside the groove of inner and outer raceways. In conventional optimization methods [1] are deterministic and only a few design variables related to internal geometry are used due to convergence and complexity problems.

The wide use of rolling contact bearings Changsen [2] has promoted many scholars to study simple and naive techniques of calculating optimal values to associated design parameters. Optimizing the diameter and length of a journal bearing at a specified speed and load is done by Asimow [3]. Weighted sum of the shaft twist and

K. Bhanuteja (✉) · M. Vinod · D. V. Krishna
Vishnu Institute of Technology, Bhimavaram 534202, India

frictional loss were considered for the minimization of objective function. Optimization of the radial clearance, the length of bearing and the average viscosity of the lubricant using gradient-based search was carried by Seireg and Ezzat [4]. Weighted sum of temperature rise for the quantity of lubricant oil feed to the bearing were considered to minimize the chosen objective function. Applications of optimization methods in the design of mechanical systems and elements, includes journal bearings, pressure vessels, rotating discs, gears, bending and torsion of shafts, beams under longitudinal impact, elastic contact problems and distributions of load is done by Seireg [5]. Chakraborty et al. [6] used genetic algorithm to optimize the dynamic capacity of rolling element bearing by keeping contact angle zero.

1.1 Genetic Algorithms in Mechanical Design

To exploit GAs [7] a plenty of applications have been known in mechanical engineering. Choi and Yoon [8] have designed an automobile wheel bearing system with various design parameters by GAs. Chakraborty et al. [6] used genetic algorithm to optimize the rolling element bearing performance, this is the first literature to use continuous design parameters of rolling contact bearing in GAs. Genetic algorithm application in the design of turbo machineries and aeronautics was reviewed in detail by Periaux [9].

Genetic algorithm is a stochastic optimization technique and its uniqueness is to avoid the traps of local minima or local maxima. In optimization problems the search space area is huge and a major advantage of genetic algorithms is its ability to explore the different locations in the search space. Considering this advantage GAs was chose for this work.

1.2 Macro-Geometry of DGBB

Outer appearance of DGBB is simple, but the load carrying capacity can depends mainly on their internal geometry. Performance and life of bearing mainly depends on the internal geometry. The width of bearing (B_w), bore diameter (d) and outer diameter (D_o) are completely defines the outer geometry. Internal geometry of DGBB is defined by the parameters they are, number of balls (Z), ball diameter (D_b) and the pitch diameter of the bearing (D_m) as shown in Fig. 1.

1.3 Contact Angle ' α '

The contact angle for DGBB is determined by the geometry relationship between the radial clearance and the radii of inner and outer grooves. The initial contact angle, α

Fig. 1 Macro-geometry of DGBB

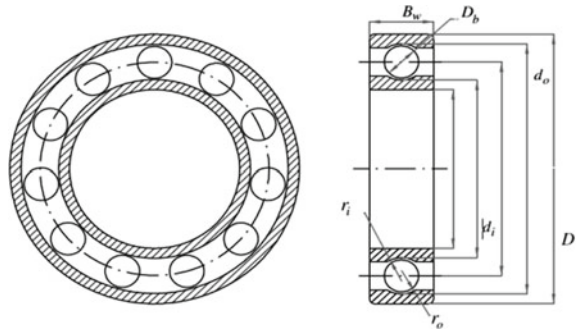
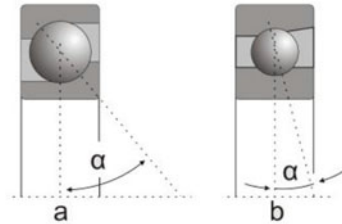


Fig. 2 Contact angle



$= 0^\circ$, is the initial contact angle when the axial load is zero. Application of any axial load to the bearing will change this contact angle. Several researchers worked on the optimization of DGBB but most of the work was done to optimize the dynamic capacity at contact angle, $\alpha = 0$. In the present work optimum dynamic capacity at various contact angles 5° , 10° , 15° and 20° as in Fig. 2 was predicted. Design of a machine part can be improved by taking the design variables of part geometry and constraints associated with the boundary conditions.

2 DGBB Dynamic Capacity Optimization Problem

Bearings are subjected to dynamic loads, which affects the life of the bearings. Longest fatigue life is important for DGBB. Optimizing of dynamic load carry capacity of bearing improves there fatigue life. DGBB are designed mainly to withstand the radial load, but by changing the point of contact between the ball and the raceways allow them to withstand the axial loads. This will impact the dynamic capacity of the DGBB. The complete internal geometry of a bearing is taken as design parameters with associated constraints.

2.1 Design Variables

The internal bearing geometry dimensions are considered for design parameters. The design vector consisting of the design variables of DGBB is

$$X = [Z, D_m, D_b, f_i, f_o, K_{D \max}, K_{D \min}, e, \alpha, \varepsilon] \tag{1}$$

These design variables are part of objective function and the constraints considered. Out of these design variables D_b, Z, D_m, f_i, f_o pertain to the internal geometry of the DGBB, while, $K_{D \max}, K_{D \min}, e, \varepsilon$ are constraints parts and enter into design space.

2.2 Objective Function

Among different objective functions for rolling element bearings, the dynamic capacity (C_d) plays a key role in fatigue life of a bearing.

Objective function for dynamic load rating is expressed as [2, 6]

$$\begin{aligned} \max[f(x)] &= \max[f_c Z^{2/3} D_b^{1.8}] D_b \leq 25.4 \text{ mm,} \\ &= \max[3.647 f_c Z^{2/3} D_b^{1.8}] D_b > 25.4 \text{ mm,} \end{aligned} \tag{2}$$

where

$$\begin{aligned} f_c &= 37.9 \left[1 + \left\{ 1.04 \left(\frac{1 - \gamma}{1 + \gamma} \right)^{1.72} * \left(\frac{f_i(2 * f_o - 1)}{f_o(2 * f_i - 1)} \right)^{0.41} \right\}^{3.33} \right]^{-0.2} \\ &* \left[\gamma^{0.3} * \frac{(1 - \gamma)^{1.39}}{(1 + \gamma)^{0.33}} \right] * \left[\frac{2 f_i}{2 f_i - 1} \right]^{0.41} \\ \gamma &= D_b * \cos \alpha / D_m \end{aligned}$$

Here factor, γ , is a dependent parameter. For DBGG contact angle, α is taken as 5, 10, 15 and 20 degrees in the present work. By careful observation of objective function, the dynamic capacity depends up on the ball diameter and the number of balls.

2.3 Constraints for Design Parameters

The bounds of these design parameters from an internal geometry are expressed below.

Number of balls in the bearing depend on the diameter of ball should satisfy the following requirements [2] and maximum tolerable assembly angle (\emptyset_0) depends on geometry of bearing.

$$2(Z - 1) \sin^{-1} \left(\frac{D_b}{D_m} \right) \leq \emptyset_0$$

$$g_1(X) = \frac{\emptyset_0}{2} \sin^{-1} \left(\frac{D_b}{D_m} \right) - Z + 1 \geq 0. \tag{3}$$

Constraints 2 and 3: Ball diameter D_b is bounded within the outer and inner diameter of the bearing associated with the maximum and minimum values of the constants of the ball diameter.

$$K_{D \min} D - d/2 \leq D_b \leq K_{D \max} D - d/2$$

where $K_{D \max}$ is maximum and $K_{D \min}$ is minimum value constants of the ball diameter [2], Constraint conditions are given by

$$g_2(X) = 2D_b - K_{D \min}(D_o - d) \geq 0, \tag{4}$$

$$g_3(X) = K_{D \max}(D_o - d) - 2D_b \geq 0. \tag{5}$$

Constraints 4, 5: Pitch diameter D_m is bounded within the outer and inner diameter of the bearing. Mobility is important for ball bearing.

Therefore,

$$g_4(X) = D_m - (D_o + d)(0.5 - e) \geq 0, \tag{6}$$

$$g_5(X) = (D_o + d)(0.5 + e) - D_m \geq 0, \tag{7}$$

where e is mobility constant [2].

Constraint 6: Usually the D_{avg} is less than the related D_m of a ball bearing.

$$g_6(X) = 0.5(D_o - D_m - D_b) - \varepsilon D_b \geq 0. \tag{8}$$

Constraints 7 and 8: The radii of groove curvature of the outer raceway and inner raceway of a DGGB should be more than $0.515 D_b$ [6], this make sure that the ball rolls freely on raceways with no interference.

Therefore,

$$g_7(X) = 0.52 \geq f_i \geq 0.515, \tag{9}$$

$$g_8(X) = 0.53 \geq f_o \geq 0.515. \tag{10}$$

2.4 Optimization Procedure for Genetic Algorithm

We used genetic algorithm in MATLAB for solving this optimization problem. Objective function is coded in MATLAB at common line. Constraints are defined as vectors and for launching genetic algorithm parameters initial population count is given, number of generations, crossover fraction, mutation fraction, mutation function, crossover function and the stopping criteria are mentioned.

3 Results and Conclusions

Table 1 shows the dynamic capacity of DGBB at contact angle $\alpha = 0^\circ$ for various outer diameters and the results are compared with the standard catalogue [10]. Tables 2, 3, 4 and 5 shows the dynamic capacity of DGBB at contact angle $\alpha = 5^\circ, 10^\circ, 15^\circ$ and 20° , respectively for various outer and inner diameters and behaviour change of dynamic capacity at these angles are noted and represented in Fig. 3. $e = 0.1, KD_{min} = 0.5, \varphi_0 = 4.7124$ radians, $KD_{max} = 0.8$, and $\varepsilon = 0.1$ [1, 6]. The genetic

Table 1 Dynamic capacity (C_d) at $\alpha = 0^\circ$

d (mm)	D_o (mm)	D_b (mm)	D_m (mm)	Z	f_i (mm)	f_o (mm)	C_d (N)	C_s (N) [10]	λ
10	30	5	20	8	0.52	0.53	5786.8	3580	4.2
15	35	7.58	20	7	0.52	0.53	6910.8	5870	1.6
20	47	8.93	26.8	8	0.52	0.53	10,718	9430	1.4
30	62	11.76	36.7	9	0.52	0.53	18,352	14,900	1.8
40	80	12.98	47.5	9	0.52	0.53	25,397	22,500	1.4
50	90	15.43	60	10	0.52	0.53	36,226	26,900	2.4
60	110	19.62	82	11	0.52	0.53	57,654	40,300	2.9
70	125	20.5	94	11	0.52	0.53	68,010	47,600	2.9
80	140	22.19	105	12	0.52	0.53	79,895	55,600	2.9
90	160	24.16	120	12	0.52	0.53	95,954	73,900	2.1

Table 2 Dynamic capacity (C_d) at $\alpha = 5^\circ$

d (mm)	D_o (mm)	D_b (mm)	D_m (mm)	Z	f_i (mm)	f_o (mm)	C_d (N)	C_s (N) [10]	λ
10	30	5	20	8	0.52	0.53	5791.1	3580	3.9
15	35	7.58	20	7	0.52	0.53	6,952.3	5870	1.6
20	47	8.9	26.8	8	0.52	0.53	11,547	9430	1.8
30	62	11.7	36.7	9	0.52	0.53	16,407	14,900	1.3
40	80	12.9	47.5	9	0.52	0.53	24,960	22,500	1.3
50	90	15.43	60	10	0.52	0.53	40,008	26,900	3.2
60	110	19.62	82	11	0.52	0.53	54,095	40,300	2.4
70	125	20.5	94	11	0.52	0.53	66,093	47,600	2.6
80	140	22.19	105	12	0.52	0.53	79,403	55,600	2.9
90	160	24.16	120	12	0.52	0.53	91,326	73,900	1.8

Table 3 Dynamic capacity (C_d) at $\alpha = 10^\circ$

d (mm)	D_o (mm)	D_b (mm)	D_m (mm)	Z	f_i (mm)	f_o (mm)	C_d (N)	C_s (N) [10]	λ
10	30	5	20	8	0.52	0.53	5,827.7	3580	4.3
15	35	7.58	20	7	0.52	0.53	7,044.7	5870	1.7
20	47	8.93	26.8	8	0.52	0.53	10,880	9430	1.5
30	62	11.76	36.79	9	0.52	0.53	14,634	14,900	0.94
40	80	12.98	47.5	9	0.52	0.53	24,971	22,500	1.3
50	90	15.43	60	10	0.52	0.53	40,131	26,900	3.3
60	110	19.62	82	11	0.52	0.53	56,877	40,300	2.8
70	125	20.5	94	11	0.52	0.53	66,538	47,600	2.7
80	140	22.19	105	12	0.52	0.53	80,139	55,600	2.9
90	160	24.16	120	12	0.52	0.53	90,056	73,900	1.8

algorithm parameters used are: maximum generations = 20, crossover probability = 0.5, population size = 100, mutation probability = 0.15 and elite count as 70.

In order to measure the improvement in the fatigue life of the DBGG designed using GAs as against the available standard values, the below relation has been used [6].

The below equation is used for measure the fatigue life of the DGBB

$$\lambda = \frac{L_d}{L_s} = \left(\frac{C_d}{C_s} \right)^3 \tag{11}$$

Table 6 shows the comparison of GAs with Amended Differential Evolution Algorithm (ADEA), for outer diameter 30, 35, 47 and 80 mm and got better optimum

Table 4 Dynamic capacity (C_d) at $\alpha = 15^\circ$

d (mm)	D_o (mm)	D_b (mm)	D_m (mm)	Z	f_i (mm)	f_o (mm)	C_d (N)	C_s (N) [10]	λ
10	30	5	20	8	0.52	0.53	5,844	3580	4.3
15	35	7.58	20	7	0.52	0.53	7,093	5870	1.7
20	47	8.93	26.8	8	0.52	0.53	11,679	9430	1.8
30	62	11.7	36	9	0.52	0.53	18,595	14,900	1.9
40	80	12.9	47.5	9	0.52	0.53	28,136	22,500	1.9
50	90	15.43	60	10	0.52	0.53	40,201	26,900	3.3
60	110	19.62	82	11	0.52	0.53	57,737	40,300	2.9
70	125	20.5	94	11	0.52	0.53	68,432	47,600	2.9
80	140	22.1	105	12	0.52	0.53	79,224	55,600	2.8
90	160	24.16	120	12	0.52	0.53	95,390	73,900	2.1

Table 5 Dynamic capacity (C_d) at $\alpha = 20^\circ$

d (mm)	D_o (mm)	D_b (mm)	D_m (mm)	Z	f_i (mm)	f_o (mm)	C_d (N)	C_s (N) [10]	λ
10	30	5	20	8	0.52	0.53	5,889.2	3580	4.4
15	35	7.58	20	7	0.52	0.53	6856.6	5870	1.5
20	47	8.9	26.8	8	0.52	0.53	10,023	9430	1.2
30	62	11.7	36.7	9	0.52	0.53	17,853	14,900	1.7
40	80	15.5	57	9	0.52	0.53	35,120	22,500	3.8
50	90	15.43	60	10	0.52	0.53	37,151	26,900	2.6
60	110	19.62	82	11	0.52	0.53	55,776	40,300	2.6
70	125	20.5	94	11	0.52	0.53	69,021	47,600	3
80	140	22.1	105	12	0.52	0.53	78,788	55,600	2.8
90	160	24.16	120	12	0.52	0.53	94,474	73,900	2

values in ADEA. But for remaining outer diameters GAs got best optimum values. Hence by observing the optimum values in the Table 6 GAs given the best optimum values for most of the outer diameters.

Table 7 illustrates the optimum contact angle value for the particular outer diameter. For the outer diameter 30 mm maximum dynamic capacity is achieved at contact angle $\alpha = 20^\circ$. Similarly, for remaining outer diameters, contact angle where maximum dynamic capacity achieved was tabulated. In present work only five different contact angles (α) are chosen and optimization studies are limited only at those particular contact angles ($\alpha = 0, 5, 10, 15, 20$). However an idea about the performance of DGBB at any other intermediate contact angles (α) could not be concluded. Therefore, the future work can be extended in a direction where the behaviour of DGBB at any chosen contact angles (α) within the range of 0° to 20° (α) can be performed.

Fig. 3 Dynamic capacity at different D and contact angles

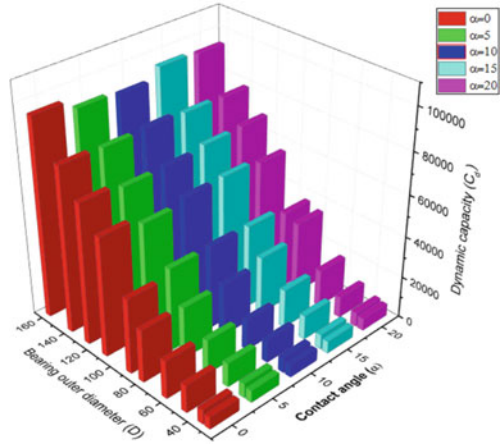


Table 6 Compared results of GA with ADEA [11] and catalogue for dynamic capacity

d (mm)	D_o (mm)	GAs	ADEA [11]	C_s (N) [10]
10	30	5787	6032.33	3580
15	35	6911	7059.09	5870
20	47	10,718	12,100.7	9430
30	62	18,352	18,113.2	14,900
40	80	25,397	27,144.3	22,500
50	90	36,226	29,174.5	26,900
60	110	57,654	43,620.9	40,300
70	125	68,010	53,452.6	47,600
80	140	79,895	64,968.9	55,600
90	160	95,954	81,862.5	73,900

Table 7 Optimum dynamic capacities at different D_o and contact angles

Bearing outer diameter (D) (mm)	Optimum contact angle (α) (Degrees)	Maximum C_d (N)
30	20	5889.20
35	15	7093.00
47	0	10,718
62	15	18,595
80	20	35,120
90	15	40,201
110	15	57,737
125	20	69,021
140	10	80,139
160	0	95,954

References

1. Rao SS (1996) *Optimisation theory and applications*, 3rd edn. Wiley, NY
2. Changsen W (1991) *Analysis of rolling element bearings*. Mechanical Engineering Publications Ltd.
3. Asimow M (1966) *Introduction to engineering design*. McGraw Hill, New York
4. Seireg A, Ezzat H (1969) Optimum design of hydrodynamic journal bearings, transactions of ASME. *J Lubr Technol* 91(3):516–523
5. Seireg A (1972) A survey of optimisation of mechanical design. *Trans ASME J Eng Indus* 94(2):495–599
6. Chakraborty I, Viany K, Nair SB, Tiwari R (2003) Rolling element bearing design through genetic algorithms. *Eng Optim* 35(6):649–659
7. Rao BR, Tiwari R (2007) Optimum design of rolling element bearings using genetic algorithms. *Mech Mach Theory* 42(2):233–250
8. Choi DH, Yoon KC (2001) A design method of an automotive wheel bearing unit with discrete design variables using genetic algorithms. *J Tribol Trans ASME* 123(1):181–187
9. Periaux P (2002) *Genetic algorithms in aeronautics and turbomachinery*. Wiley, New York
10. Shigley JE (1986) *Mechanical engineering design*. McGraw-Hill Book Company, New York
11. Rana P, Patel J, Laiwani DI (2019) Design-parameter optimization of a deep-groove ball bearing for different boundary dimensions, employing amended differential evolution algorithm, artificial intelligence applications and innovations. In: 15th IFIP WG 12.5 international conference, AIAI 2019, Hersonissos, Crete, Greece, May 24–26, 2019.

Suitability of Hybrid Aluminium Metal Matrix Composite Material to Replace Cast Iron in Automobile Components



Mohammad Habibullah, N. V. V. Manikanta, A. Varun, and M. Praveen

Abstract Hybrid Reinforcement technology is in response with the most in-demand attractive characteristics like high ductility, good corrosion resistance, light in weight, and high strength to weight to meet ever more demanding service requirements from the transport, the aerospace, the automotive sector, and the marine industry. In this advancement, an effort has been made to assess the mechanical properties of Al6061 alloy composites having varying weight percentages of (2–4–6%) Silicon carbide, pulverized Fly ash was cast with the help of liquid metallurgy technique-stir casting. The developed specimens were machined as per ASTM standards for testing of mechanical properties such as Tensile, Flexural, Izod impact, Rockwell hardness at room temperature. From these tests of Hybrid Metal matrix alloy Al6061-SiC-Fly ash samples test data was collected. Further Design and Analysis was conducted by choosing an automotive component—Steering Knuckle Component to validate the experimental values obtained for HMMC, structural analysis, Equivalent elastic strain, and vibrational analysis was performed.

Keywords Hybrid metal matrix composite (HMMC) · Silicon carbide (SiC) · Fly ash · Steering knuckle component

1 Introduction

Evolution of advanced engineering materials for different engineering applications, especially for transport, aerospace and engineering applications are the regions which demand light weight, high strength, and good influencing properties. HMMC are materials in which two discrete types of particulates are added as reinforcements.

M. Habibullah (✉) · N. V. V. Manikanta · M. Praveen
Department of Mechanical Engineering, Vishnu Institute of Technology, Bhimavaram, Andhra Pradesh, India

A. Varun
Department of Mechanical Engineering, B. V. Raju Institute of Technology, Narsapur, Telangana, India

Hence desired properties such as higher strength values, resistance to wear, corrosion, fatigue are manifested.

Jaswinder et al. [1] the significant enhancement in composite was observed, whilst during the solidification phase, indirect strengthening was proposed by the thermo variance between the reinforcing phase with matrix alloy. Krishna et al. [2] a relative uniform distribution of particles was found in the composite, with clusterings in few areas, Hybrid composites were fabricated by stir casting. Hima Gireesh et al. [3] it was revealed that strengthening of the mechanical properties was accomplished due to the inclusion of different reinforcement materials. Effect on properties with varying weight percentage of reinforcement materials was found significantly correlated. Kumar et al. [4, 5] it was observed that tensile strength increased with addition of fly ash content also it contributed by amount of fly ash weight in Al matrix resulted in less wear. The value of tensile strength, hardness, and toughness with increase in weight percentage of SiC was investigated. Vijayarangan et al. [6, 7] steering knuckle is considered to be one of the key components of the vehicle suspension system. It undergoes several interactions under various conditions and types of varying loads, leading to fatigue failure. It is made up of cast iron. Computer Aided Engineering is used to design component and static analysis was performed by restricting the steering knuckle and by adding load it was observed due to calliper setup, horizontal reaction, perpendicular reaction, weight of the vehicle, and steering reaction. Vivekananda and Haitham et al. [8, 9] cast iron can be ideal for steering knuckle component but Metal Matrix Composites (MMCs) have a capability due to their higher strength and weight limitation ratio to replace conventionally used cast iron. By conducting structural, fatigue, vibration analysis it was observed potential capability of Metal Matrix Composite steering knuckle component. Dusane et al. [10] a 3D CAD model of modified steering knuckle component was developed using modelling software and the static and design analysis was performed through Analysis software. It was designed to understand its behaviour under operational conditions. All frame tests were performed on 6061-T6 aluminium alloys. In this Present experimentation was focused on validating HMMC specimens via casting and mechanical testings, readings obtained were exported to analysis software to validate experimental results and developing an Automotive crucial component to verify suitability of HMMC material to replace cast iron.

2 Materials and Methodology

In this research work a well-known Alloy Al 6061 is chosen as the metal matrix base and as reinforcing material pure fine powder type SiC and Fly ash are considered. Synthesis of Hybrid metal matrix composite was carried out with the aid of a stir casting technique. During the process stirring is carried out to prevent reinforcement particles from agglomeration thus by improving the homogeneous distribution of reinforcement particles in the matrix. A weighted quantity of The Al6061 alloy was

put in an electric furnace in a graphite crucible vessel and melted. The temperature increased to 850 °C steadily. A mild steel impeller with 630 rpm was forced to generate a Swirling effect. SiC and Fly ash reinforcements are adequately combined and pre-heating was provided at 450 °C to remove any humidity may be present. The reinforcement particles are then added into the melt when the vortex in the melt is formed. The stirring shall be continued for 5 min after the reinforcement has been added so that homogeneous distribution of the reinforcement can be accomplished. The slurry is then moved to the metal mold, where it is left to rest at room temperature. There are many factors that have a direct Impact on the stir-cast composite characteristics. Factors such as the geometry of the agitator such as blade angle, agitator time, stirring rate, pouring rate, melting temperature etc., to produce a better batch of compound properties. The whirling parameters were chosen as 12-min whirring periods, 3 bladed stirrers with a 30° blade angle, and stirrer immersion in the molten mixture is two-thirds of the melt in order to optimize a uniform particle distribution into the melt. The experimental samples have now been cast.

3 Experimental Details

Properties	Gray cast iron
Tensile strength (MPa)	250
Young modulus (GPa)	105
Hardness (HB)	179–202

Knuckle component is generally manufactured by cast iron; the following are mechanical properties of cast iron.

3.1 Mechanical Testings

The developed specimens were further machined as per ASTM E-8, D-790, D-256, E-18, for experimental evaluation of results obtained from Mechanical Tests like Impact, Hardness, Tensile, and Flexural testing.

The Tensile tests, Flexural test for the five samples were performed and readings were plotted in Figs. 1 and 2. The breaking load and tensile strength and Flexural stress of sample 3 have been found to be higher than in other samples, this is because high quantities of ceramic presence as reinforcement, i.e., silicon, Fly ash. The Izod impact test was conducted to the composites and energy absorptions are shown in Fig. 3. Sample 1 has been found to absorb more energy than others because it contains low amount of SiC addition which makes it ductile for more energy absorption. The Rock well hardness test was employed to find the composite material hardness and

Fig. 1 Yield stress for HMMC specimens

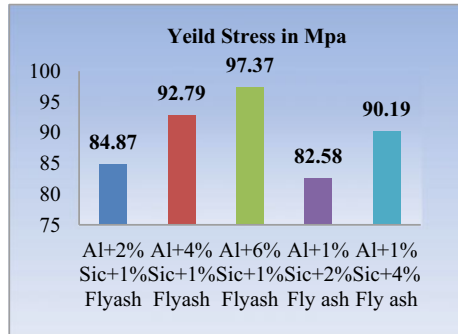


Fig. 2 Flexural stress for HMMC specimens

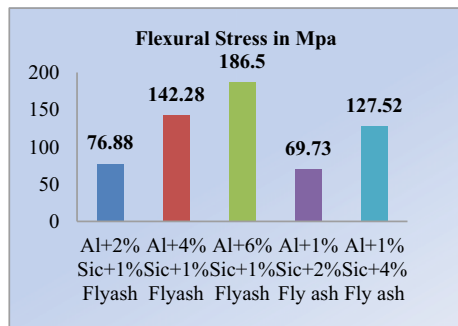
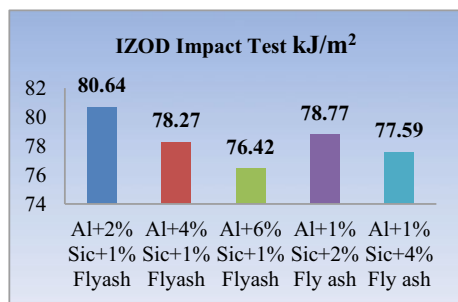


Fig. 3 IZOD impact values for HMMC specimens



the results are shown in Fig. 4. Because of the high volume of silicon carbide and fly Ash, the hardness of Sample 3 is greater than for other samples.

4 Numerical Analysis

By selecting a four-wheeler light weight vehicle, a knuckle component from a real-time model via reverse engineering dimensions was collected [7], by using 3D

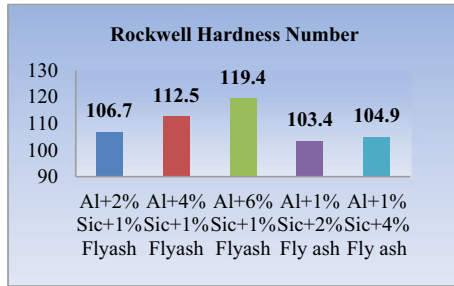


Fig. 4 Rockwell hardness for HMMC specimens

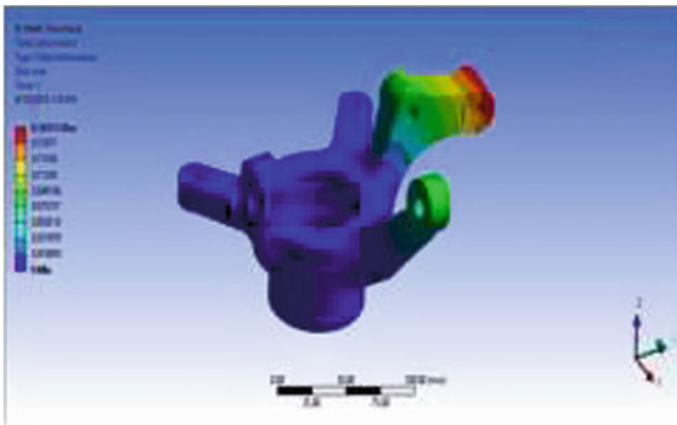


Fig. 5 Deformation of cast iron steering knuckle component

modelling software steering knuckle component was developed by considering all the geometrical parameters which is shown in Fig. 5.

4.1 Structural Analysis

In Fig. 6 there is a complete deformation (Al + 6% Sic and 1% Fly Ash) of the steering knuckle, at the end of the strut, there is maximum deformation. Figure 7 shows the deformation of the steering knuckle component’s CI and HMMC material. Compared to CI materials, HMMC materials are maximally deformed. Both components are minimally deformed. The two are safe; they have a deformation of less than 1 mm (Fig. 8).

Figure 9 indicates stresses on the steering knuckle components (Al + 6% Sic and 1% Flyash) when the force was exerted on each face of joint. The relation between strut and hub causes additional stresses. The whole section is firmly below the design

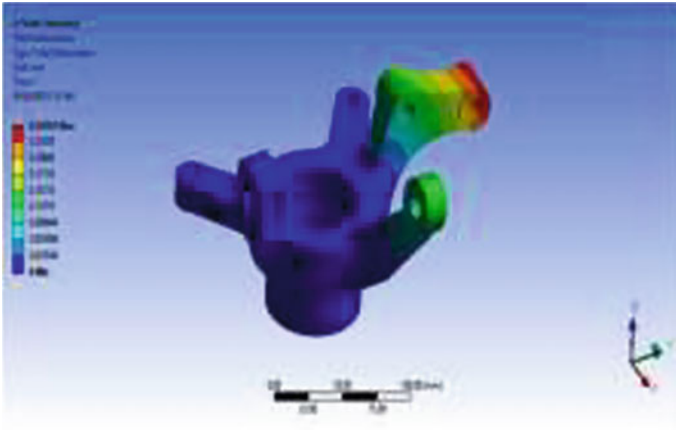


Fig. 6 Deformation of HMMC steering knuckle component

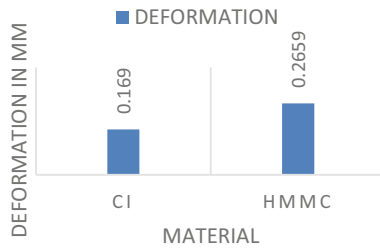


Fig. 7 Deformation of steering knuckle component

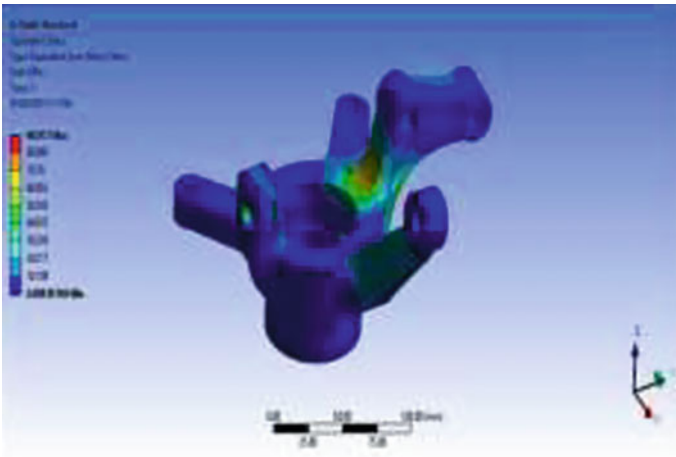


Fig. 8 Stress on cast iron steering knuckle component

threshold. However, in the sharp corners of the strut there are most stresses developed. HMMC material is safe in compliance with the material yield strength (Fig. 10).

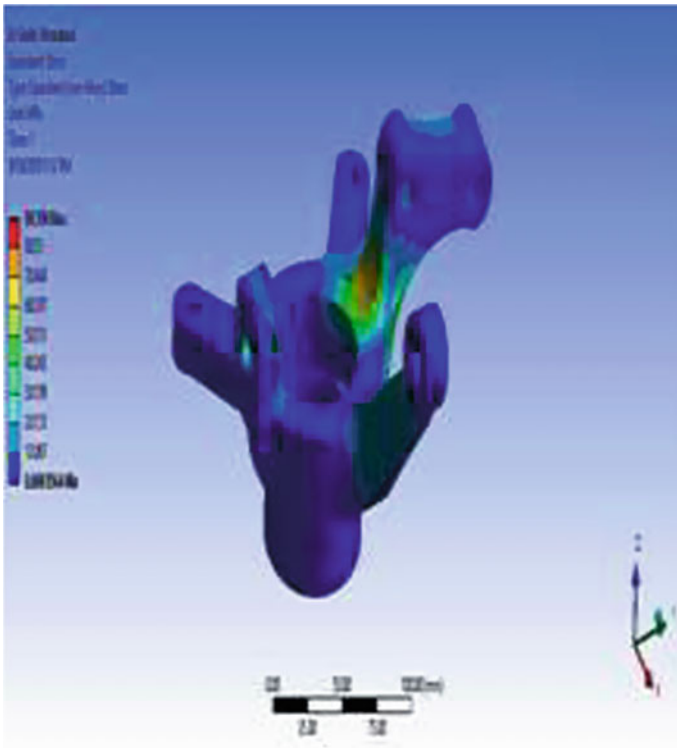
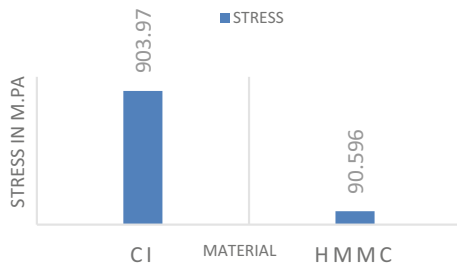


Fig. 9 Stress on HMMC steering knuckle component

Fig. 10 Stress in steering knuckle component



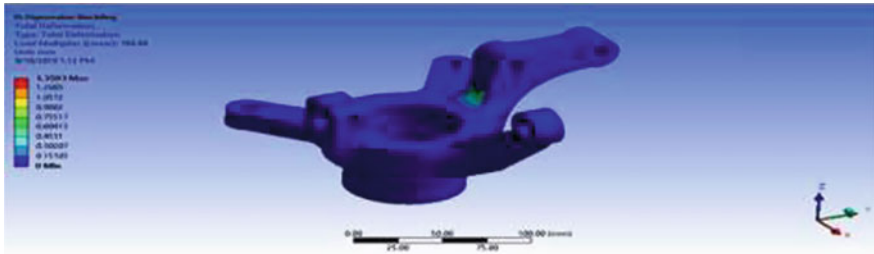


Fig. 11 Critical load on HMMC steering knuckle component

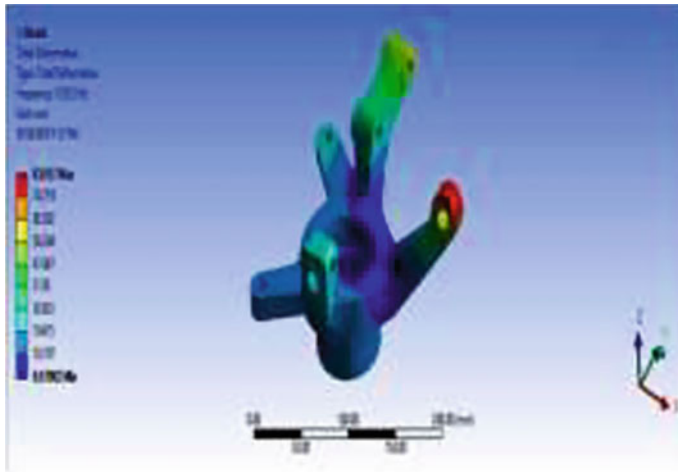


Fig. 12 First mode of cast iron steering knuckle component

4.2 Buckling Analysis

Figure 11 illustrates the critical load and breakdown mode of the steering knuckle component. Crack can be started at the site of the suspension installation Upper Arm/Strut Mount. Critical load was found to be 764 times the load added, thereby maintaining a secure structure (Fig. 12).

4.3 Vibrational Analysis

Figure 13 above represents the natural frequency and shape of the steering knuckle component at first mode. The restriction of the model boundary condition is in space. The structure bends in X-direction at 1630,3 Hz.

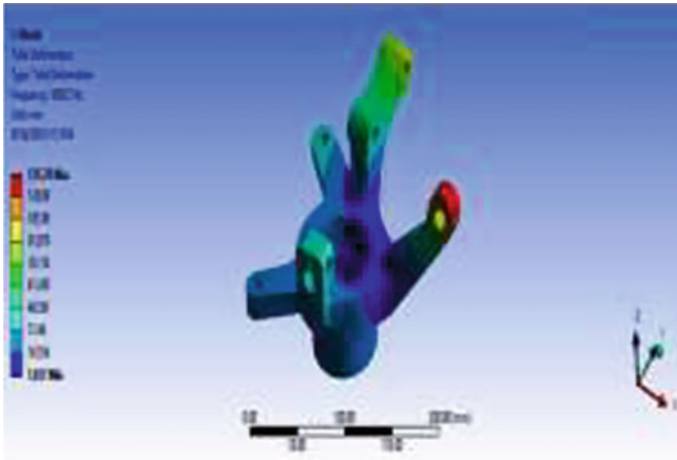


Fig. 13 First mode of HMMC steering knuckle component

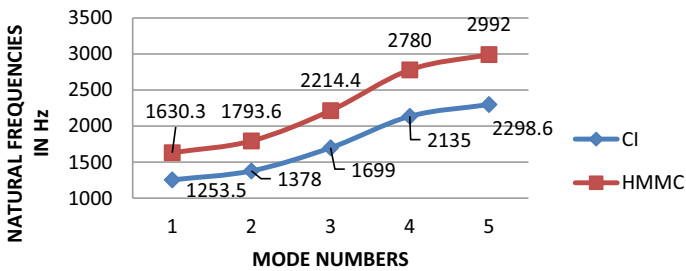


Fig. 14 Natural frequency of steering knuckle component

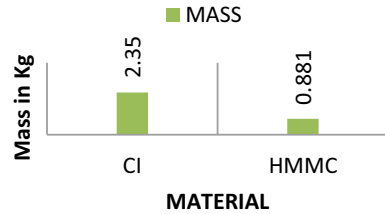
Figure 14 implies the natural frequency for steering knuckle component. If it is more then it indicates it is having more stiffness. HMMC material from the above graph signifies more normal frequencies than CI materials.

HMMC knuckle is Validated to the performance of Cast Iron knuckle (2.35 kg) [8] with an increase of mass from 0.881 kg. Thus the weight is reduced by 62.08% from Cast Iron. Figure 14 illustrates the steering knuckle Component mass. We can decrease the demand fuel consumption if we minimize weight (Fig. 15).

5 Conclusion

It was detected that tensile strength increases up to 12.8%, during tensile testing specimens, having 6% of SiC with 1% of Fly ash exhibits brittle factor. If we apply

Fig. 15 Mass of steering knuckle component



the SiC and Fly ash as reinforcement, the hardness of the specimen is continuously increasing. The increase in flexural strength is noticed, since the increase in ceramic reinforcements. Reduction in the impact strength is observed by increasing the reinforcement.

Numerical analysis of steering knuckle component to validate the experimental test results was studied by structural analysis. Whilst maximum deformation is at the end of strut region for both of the materials also stress development was mostly concentrated at the hub contact region. Buckling analysis for HMMC steering knuckle component revealed that crack initiation was found to be at max critical load at suspension mounting region. From vibrational-Modal analysis it was observed HMMC to have higher Frequency Stiffness. Weight reduction was the major motto to satisfy in this study hence a great variation in strengthening mechanical properties was observed.

References

1. Singh J, Chauhan A (2015) Characterization of hybrid Aluminium matrix composites for advanced applications review. *J Mater Res Technol* 170
2. Krishna MV, Xavior AM (2014) An investigation on the mechanical properties of hybrid metal matrix composites. *Proc Eng* 97:918–924
3. Hima Gireesh C, Durga Prasad KG, Ramji K (2018) Experimental investigation on mechanical properties of an Al6061 hybrid metal matrix composite. *J Compos Sci* 4
4. Kumar V, Gupta RD, Batra NK (2014) Comparison of mechanical properties and effect of sliding velocity on wear properties of Al 6061, Mg 4%, fly ash and Al 6061, Mg 4%, graphite 4%, fly ash hybrid metal matrix composite. *Proc Mater Sci* 6:1365–1375
5. Sharma VK, Singh RC, Chaudhary R (2017) Effect of fly ash particles with aluminium melt on the wear of aluminium metal matrix composites. *Eng Sci Technol Int J* 20:1318–1323
6. Vijayarangan S, Rajamanickam N, Sivananth V (2013) Evaluation of metal matrix composite to replace spheroidal graphite iron for a critical component, steering knuckle. *Mater Des* 43:532–541
7. Yadav S, Mishra RK, Ansari V, Lal SB (2016) Design and analysis of steering knuckle component. *Int J Eng Res Technol* 5
8. Vivekananda R, Mythra Varun AV (2016) Finite element analysis and optimization of the design of steering knuckle. *Int J Eng Res* 4

9. Ibrahim HM, Gopi Krishna Mallarapu M (2016) Deformation finite element studies and fabrication of Al6061 alloy/fly-ash/Sic hybrid composites. *Adv Res J Sci Technol* 19:2349–1845
10. Dusane SV, Dipke MK, Kumbhalkar MA (2016) Analysis of steering knuckle of all terrain vehicles (ATV) using finite element analysis. *IOP Conf Ser Mater Sci Eng* 149:012133

Design and Analysis Studies in Pellet Extrusion Additive Manufacturing Processes



Abhishek Patel, Krishnanand, and Mohammad Taufik

Abstract In today's generation 3D printing is one of the most trending technologies, by using 3D printers manufacturing complicated parts becomes easy and accurate which is difficult to manufacture by conventional manufacturing methods. 3D printing is based on additive manufacturing, in solid-based additive manufacturing, two types of processes are used namely fused filament fabrication and pellet extrusion. In this paper detailed study of pellet-based screw extruder is carried out, several papers are studied which tells about development of pellet extruder, modeling of screw, design of extruder, controlling the process parameters in pellet extruder, energy-based modeling method for screw used in pellet extruder. Knowledge gained from this study can be used in improving pellet extruder and precise control over process parameters for improved printing quality.

Keywords 3D printing · Additive manufacturing · Fused filament fabrication · Pellet extrusion

1 Introduction

Additive manufacturing (AM) is a process in which product is made in layers by depositing layers of material one above the other, materials such as plastic, concrete, metal, and even composites can be used. Lack of wastage of material in AM reduces cost of manufacturing and hence can be used for value parts. S Scott and Lisa Crump [1] firstly patented for the detailed study of fused deposition modeling (FDM) later in 1984 Charles W. (chuck) Hull [2] developed first robotic 3D printer and in 1989 FDM was patented by S. Scott and Lisa Crump and co-founded Stratasys, Ltd for 3D printer manufacturing. Wankhade and Bahaley et al. [3] developed a filament extruder.

A. Patel · Krishnanand · M. Taufik (✉)
Department of Mechanical Engineering, Maulana Azad National Institute of Technology (MANIT), Bhopal 462003, India
e-mail: mohammad.taufik@maint.ac.in

© The Author(s), under exclusive license to Springer Nature Singapore Pte Ltd. 2022
B. B. V. L. Deepak et al. (eds.), *Applications of Computational Methods in Manufacturing and Product Design*, Lecture Notes in Mechanical Engineering,
https://doi.org/10.1007/978-981-19-0296-3_32

351

Additive manufacturing is broadly classified into three main categories namely powder-based, liquid-based, and solid-based additive manufacturing [4, 5]. Since for tissue engineering most of starting materials are in powder form, powder-based additive manufacturing process is attractive and practical. These processes include Selective laser melting (SLM), Selective laser sintering (SLS), and Electron beam melting (EBM). In liquid-based additive manufacturing, most of these manufacturing systems build parts in a vat of photocurable liquid resin, an organic resin that cures or solidifies under the effect of exposure to light, usually in the UV range. The light cures the resin near the surface, forming a thin hardened layer. These processes include Stereolithography apparatus (SLA). To create part or prototype solid-based additive manufacturing process uses solid as primary medium. These processes include fused deposition modeling (FDM) and Laminated object manufacturing (LOM). Solid-based additive manufacturing process is further classified as filament-based and pellet-based additive manufacturing processes [6]. Additive manufacturing has wide range of applications including automobile, medical, aerospace, construction, fashion, and accessories.

1.1 Fused Filament Fabrication

In this additive manufacturing, process part is produced by adding material layer by layer. This additive manufacturing process has emerged as it has advantages of improved speed to supply new products to market, enabling part consolidation, increase design complexity, and lower manufacturing cost. This method is very useful for producing low quantities of customized parts that are difficult to produce by machining or molding process. In this process, material is continuously fed in the form of filament as shown in Fig. 1a.

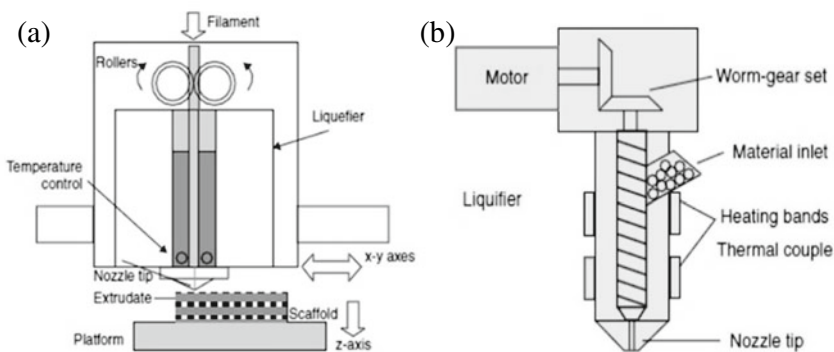


Fig. 1 **a** Schematic of fused filament fabrication process; **b** schematic of pellet additive manufacturing [7]

1.2 Pellet Extrusion Additive Manufacturing

In this manufacturing process, raw material is directly fed to extruder in the form of pellets. This type of extruder has the advantage of lowering manufacturing costs as compared to fused filament fabrication. Principle of pellet-based extrusion is shown in Fig. 1b. Manideep et al. [8] has developed a new type of pellet-based screw extruder which reduces cost of manufacturing. Pellet-based extruder uses a screw to feed, transport, and melt the material inside a barrel and forces the material out to be extruded at desired temperatures. Despite pellet extruder being complex, it is used in additive manufacturing because it has several advantages.

This study presents the review of designs of pellet extrusion systems. Pellet extrusion has a number of advantages over filament extrusion. It decreases the overall cost of part fabrication by eliminating the filament manufacturing cost and reusing the waste material. Flexible material could also be used as feed material. It also provides flexibility in changing the material and color during the fabrication process.

2 Design of Pellet Extruder

Freeform filament extrusion printing is most commonly used but because of limitation on materials to be readily available in filament form such as biopolymers, materials blend a new type of extruder is developed. Screw based pellet extruder is developed which can extrude mixes of biopolymers like PLA, the system has advanced features like liquid cooling, control of temperature, and controlled feeding of pellets and parts are printed and testing is done to demonstrate the utility of extruder.

Main parts of pellet extruder are hopper, screw, barrel, and nozzle. Hopper is used to store the feed material; cylindrical hopper is used to reduce conveying problems as square hopper corner causes feeding problem. Whyman et al. [9] also use a drip-feeding mechanism to correctly feed the required quantity of material for consistent print quality and avoiding extruder from jamming. Extruder screw or auger is the major part of extruder which is used to transport pellets to the heating region and then finally push the molten material out of nozzle [10]. The extruder screw is divided into three zones as shown in Fig. 2a, zone for transportation, zone for melting, and zone for mixing here melt is under high pressure before coming out from nozzle. Too high temperature at inlet of screw may result in melting the material at inlet and jamming the system it also burns the material and it becomes less viscous at outlet, whereas to low temperature prevents extrusion because of low rate of melting resulting in jamming. Variation of pressure along length in three section screw is shown in Fig. 2b. Variation of pressure for auger drill bit is shown in Fig. 2c.

Shearing in material is used as major source of heating in large extrusion systems but in this project an external power source, an electric heater is used for heating. Whyman et al. [9] used cooling system with closed-loop using automotive-grade coolant to prevent the sticking of pellets on hot spots and blocking of extruder. In

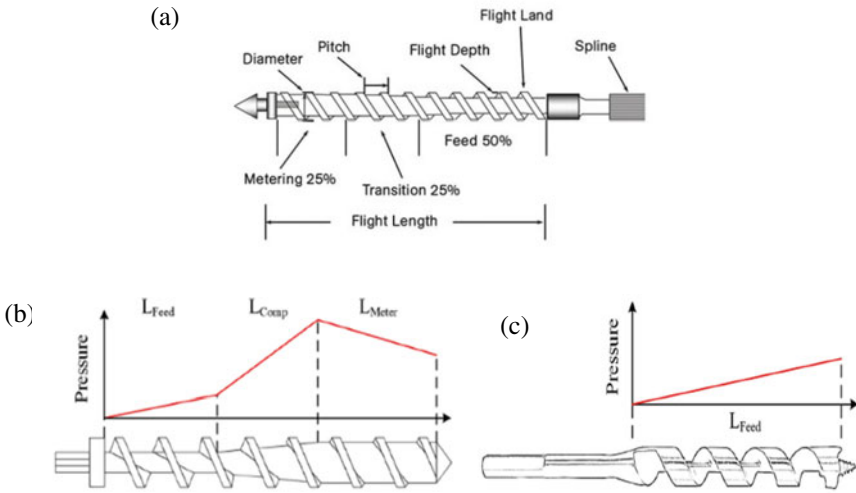
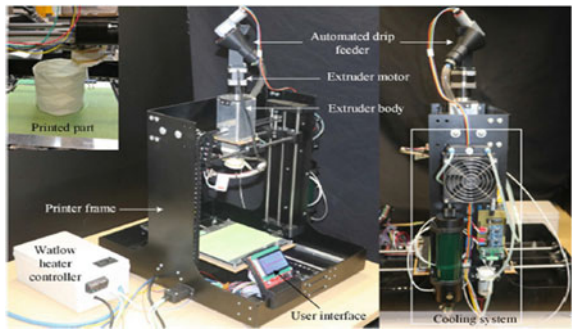


Fig. 2 a Design of screw or auger [11]; b pressure profile of screw and c pressure profile of an auger bit [9]

order to have complete control over the printing sensors for screw speed monitoring, barrel temperature, pressure of die head, power consumed, and even for vacuum pressure measurement are used. Printer along with its components is shown in Fig. 3. In case of pellet extrusion, screw speed is an important process control parameter along with other parameters like layer height, nozzle temperature, print speed, nozzle diameter, and bed temperature.

Fig. 3 Pellet extrusion-based 3D printer [9]



3 Mathematical Model of Pellet Extrusion

In pellet extrusion system design of screw plays an important role. Various pressure along the length of screw is crucial to decide the torque of motor. Heater is used to melt the pellets in melting zone. So, power requirement for heater as well as calculations of heat utilization and heat dissipation should be concern for energy consumption optimization. The pressure profile along the screw is shown in Fig. 2 and backpressure is given below:

$$\text{Back Pressure} = \Delta P_{\text{Feed}} + \Delta P_{\text{Comp}} + \Delta P_{\text{Meter}} \tag{1}$$

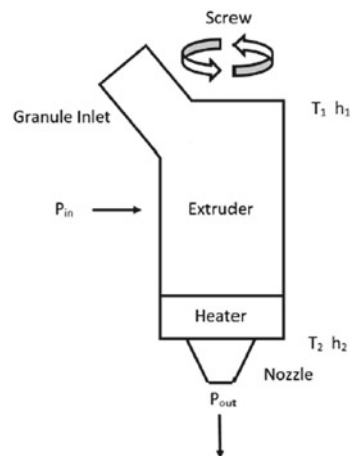
$$\Delta P_{\text{Feed}} = \frac{dP}{dZ} L$$

3.1 Power Analysis

Drotman et al. [12] presented an energy-based modeling method for pellet-based screw extruder used in 3D printing. Their work is based on energy balance between screw work done, heat energy dissipated by heater at nozzle, and extruded product enthalpy. Their model is helpful in developing a dynamic model for a controller capable of accurate flow control based on preview of extrusion rate. This model described material output flow rate in extruder nozzle in terms of screw speed and melting temperature distribution of material along the extruder barrel.

Change in specific enthalpy between two stages 1 and 2 as shown in Fig. 4, are rewritten as enthalpy change in melting (constant pressure) and forming (constant

Fig. 4 Schematic of screw extruder process for power analysis [12]



temperature) are shown in equations below:

$$\Delta h = h_2 - h_1 = \Delta h_{\text{melt}} + \Delta h_{\text{form}} \quad (2)$$

$$\Delta h = \bar{C}p(T_2 - T_1) + h_f + \frac{(P_2 - P_1)}{\bar{\rho}} \quad (3)$$

$$P_{\text{out}} = \dot{m}\Delta h = \dot{m}\Delta h_{\text{melt}} = \dot{m}(\bar{C}p(T_2 - T_1) + h_f) \quad (4)$$

Here average heat capacity is $\bar{C}p$, specific enthalpy of fusion is, h_f , and pressure at Stage 1 and Stage 2 are P_1 and P_2 , respectively. Heat change can be written as:

$$\Delta Q = \dot{Q} - \dot{Q}_{\text{losses}} = \frac{V^2}{R} + mfV_{\text{barrel}} \left(\frac{\pi DN}{H} \right)^{n+1} - \dot{Q}_{\text{losses}} \quad (5)$$

$$P_{\text{losses}} - \dot{W} = \dot{Q} - P_{\text{out}} = \left(\frac{V^2}{R} + mfV_{\text{barrel}} \left(\frac{\pi DN}{H} \right)^{n+1} \right) - (\dot{m}(\bar{C}p(T_2 - T_1) + h_f)) \quad (6)$$

The left side of Eq. 6 is lumped as one parameter and can be found out by known values on right side of equation. Here system is controlled by two variables T_2 and N . Values obtained by experiments are V and \dot{m} , other terms on right-hand side of equation are known. For different values of T_2 and N , \dot{m} is measured and a lookup table is created to find the relationship between T_2 , N and \dot{m} . At any given temperature and screw speed \dot{Q} and $P_{\text{losses}} - \dot{W}$ are found by interpolation to calculate P_{out} and this is how \dot{m} is determined. Polylactic acid pellets are used as material for printing as it has low melting point. Three test temperatures are 180, 190, and 200 °C. Three screw speeds are 1 RPS, 2 RPS, and 3 RPS and their observations are shown in Fig. 5a, b.

4 Material Extrusion Calculations [3, 10]

Volumetric flow rate (Q) is shown as a function of three types of flow: drag flow which is caused due to turning of screw, pressure flow that opposes the system flow, and filtration flow are due to loss of material in clearance of screw cylinder. Volumetric flow is shown by Eq. 7.

$$Q = \left(\frac{\alpha K}{K + \beta + \gamma} \right) \eta \quad (7)$$

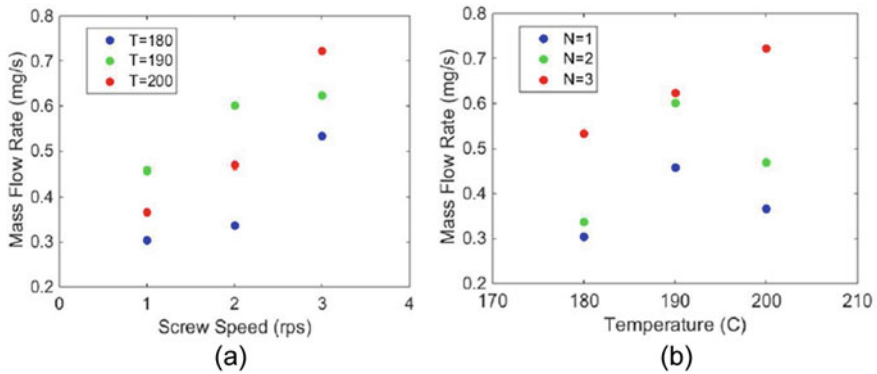


Fig. 5 a Mass flow rate vs. Screw speed at different temperatures; **b** Mass flow rate versus temperature at different screw speeds [12]

In Eq. 7 α is coefficient of drag flow, β is coefficient of pressure flow, γ is coefficient of filtration flow, K is geometrical head constant and η is speed of spindle.

$$\alpha = \frac{\pi \times m \times D \times h \times \left(\frac{t}{m} - e\right) \times \cos^2 \theta}{2} \quad (8)$$

where D is diameter of screw, t is pitch, h is Initial channel depth, ϕ is helix angle, e is ridge width and m is number of channels.

$$\beta = \frac{m \times h^3 \times \left(\frac{t}{m} - e\right) \times \sin \theta \times \cos \theta}{12 \times L} \quad (9)$$

$$\gamma = \frac{\pi^2 \times D^2 \times \delta^3 \times \tan \theta}{10 \times e \times L} \quad (10)$$

Here d is clearance of fillet

$$k = \frac{\pi \times d^4}{128 \times L} \quad (11)$$

$$d = D - (2 \times h)$$

Power required for melting the plastic is calculated by Eq. 12

$$P = \rho \times Q \times C \times (t_m - t_0) \quad (12)$$

where ρ is density, Q is volume flow rate, C is specific heat, t_m and t_0 are melting and inlet temperatures.

Motor torque required for turning the screw is calculated by Eq. 13

$$T = \frac{P \times 60}{2 \times \pi \times N} \quad (13)$$

Stress in hopper σ is calculated by Janssen's assumption Eq. 14

$$\sigma = K \times P_v \quad (14)$$

Normal compressive stress P_v is calculated by Eq. 15

$$P_v = \frac{\rho g D}{4\mu K g_c} \left(1 - \exp\left(-\frac{4z\mu K}{D}\right) \right) \quad (15)$$

where, g_c = constant for gravity conversion, ρ is density, K is Janssen constant, μ is wall friction coefficient.

5 Conclusion

Major disadvantage of fused filament fabrication is that raw material is supplied in the form of filament, production of filament from raw material has to be carried out separately which adds to the cost of manufacturing, and sometimes it is not possible to produce filament from raw material and hence its application is restricted. While in pellet-based extrusion there is no need to separately produce the filament instead raw material is supplied in the form of pellets. To make use of this advantage of pellet extruder for reduced manufacturing cost advanced extruder can be developed but very limited literature is available for pellet extruder and hence a lot of scopes is available for innovation and improvement of pellet-based extruder.

Acknowledgements This work was supported by the Science and Engineering Research Board (SERB)—DST under its Start-up Research Grant (SRG) scheme [Grant number: SRG/2019/000943].

References

1. Crump S Scott (1992) Apparatus and method for creating three-dimensional objects. U.S. Patent 5, issued June 9:121–329
2. Chuck Hull invents Stereolithography or 3D printing and produces the first commercial 3D printer: history of information. <https://www.historyofinformation.com/detail.php?id=3864>, Last accessed 2020/12/30
3. Wankhade MH, Bahaley SG (2018) Design and development of plastic filament extruder for 3D printing. *IRA-Int J Technol Eng* 10:23 (2018). ISSN 2455-4480
4. Krishnanand SS, Taufik M (2020) Design and assembly of fused filament fabrication (FFF) 3D printers. *Mater Today Proc* (2020)

5. Taufik M, Jain PK (2017) Characterization, modeling and simulation of fused deposition modeling fabricated part surfaces. *Surf Topogr Metrol Prop* 5, 045003
6. Taufik M, Jain PK (2020) Part surface quality improvement studies in fused deposition modelling process: a review (2020)
7. Reddy BV, Reddy NV, Ghosh A (2007) Fused deposition modelling using direct extrusion. *Virtual Phys Prototyp* 2:51–60
8. Manideep P, Subbaratnam B, Harsha M (2019) Design and development of pallet extruder. In: *AIP Conference Proceeding* 2200
9. Whyman S, Arif KM, Potgieter J (2018) Design and development of an extrusion system for 3D printing biopolymer pellets. *Int J Adv Manuf Technol* 96:3417–3428
10. Singh S, Taufik M, Jain PK (2014) Development of extruder head for fused deposition process. *J Eng Sci Manag Educ* 7:1–5
11. von Krogh P (2017) Direct pellet extruder developed for LEDC 3D-print with recycled plastics
12. Drotman D, Arbor A, Bitmead R (2017) Control-oriented energy-based modeling of a screw extruder used for 3D printing. In: *Proceedings of the ASME 2016 dynamic systems and control conference DSCC2016*, pp 1–7
13. Albu SC, Nuțiu E (2019) Study on designing the extruder for 3D printers with Pellets. *Acta Marisiensis Ser Technol* 16:19–22

Intelligent Flooring Systems in Interiors-Exploring the Impact on Well-Being



Zeba Shaikh, Tamanna Naaz, and Banafsha Rajput

Abstract Need for artificial intelligence in interior design is growing day after day with the advancement of technology over time. Accordingly, implementation of AI tools in smart cities has laid the foundation for harmony and alliance development. AI bridges the differences between practicality and ideas. Internet of things (IoT) and advanced technologies have brought enormous revolution in the field of AI and have unveiled impressive solutions. Intelligent materials perform a vital role in sustaining user-friendliness and environmental success of the smart interiors through their actions and their properties. The use of innovative technology focused on smart materials has the potential to rapidly boost building sustainability. Floor is an essential component of any interior since it is the first physical interaction a person would have with the room, it can dramatically change space easily, and it forms a base for the space and will ultimately affect its overall performance. Interiors with smart finished floors can be designed with advanced and responsive materials powered by AI. The influence on the construction and design stages of intelligent material systems and the study of how to build architecture with great technology to facilitate. A thorough review of three eccentric genius and bright materials installed to the interior of buildings underneath the finished floors. The study explores the purpose and significance of unique AI-based materials in the construction of smart interiors and their commitment to enhancing the indoor environment and living experiences through advanced technology. It also analyzes the health impact that can occur through the application of these intelligent materials on the inhabitant of the space.

Keywords User comfort · Intelligent flooring systems · AI · Smart Interiors

Z. Shaikh · T. Naaz · B. Rajput (✉)
Amity University Dubai, Dubai, United Arab Emirates
e-mail: brajput@amityuniversity.ae

Z. Shaikh
e-mail: zebaS@amitydubai.ae

T. Naaz
e-mail: tamannaN@amitydubai.ae

1 Introduction

The AI resources are emerging in a new and more efficient way that relies on the growth of technology in all walks of life, especially in the domain of architecture and interior design. AI has incredible transformative potential with the proper application, and how it constantly affects human interaction and life on a global scale [1]. The supervening advancements have resulted in new interpretations and a wide range of dimensions regarding smart building technology, a key phenomenon leading to implementation in intelligent interiors [2]. Internet of things (IoT) and technological advancement are indeed the backbone of intelligent interiors that can be used in the indoor environment like the interoperability, predictive analytics, data integration, sensorization, and connectivity. Generations ago, the domotics has opened the way to new digital systems that offer solutions, linking more and more components in intelligent constructions. The implementation of AI in handling the intelligent buildings infrastructure helps in interpreting and collecting information from the domotics devices, predicting user activity, offering maintenance statistics, and improving security and confidentiality [3]. Furthermore, building systems through intelligent design solutions have the potential to enable intelligent materials, intelligent building services, and intelligent construction to provide desired features for surrounding systems, thus improving diverse strategies, enhancing healthier and secure lifestyles, and utilizing advanced knowledge with the advancement in technologies. In order to build futuristic design that provides latest demands without undermining new generations, bright innovations could perhaps be considered highly intertwined with sustainable development. Architects and interior designers with updated technology, skills, abilities, and tools acknowledge that it analyzes and create data that saves time and energy by integrating smart and advanced solutions in interior spaces. Smart interior is an interior or a space that gets magnified and reinforced due to the influence of modern technology on our day-to-day life and surrounding spaces and smart interior design is a process of integrating functionality, innovations, and aesthetics. The aim of intelligent interiors is to provide safety and security, effectively manage space functions, save time and energy, and enhance home management and quality of life. As per description given in the international journal “Alexandria Engineering Journal”, smart interiors are interiors that employ AI-based sustainable design strategies to improve the future of construction design industries, and the participation of the occupants of space through the dynamic strategies is indeed a prerequisite for smart interiors.

Four factors leading to define smart interiors and their AI-powered IoT approaches which are identified by Deakin and Al Waer are:

- Using wide range of digital and electronic innovations in the construction of effective interiors.
- To enhance the indoor environment by implementing Information and Communication Technology (ICT) and Artificial Intelligence (AI).
- Integration of government system to increase productivity within ICT.

- Introducing laws and regulations that bond or unite humans and ICT to foster creativity and broaden their awareness.

A smart interior should be an interior space that not only has ICT but also implements advanced technology in a manner that has a positive effect on the inhabitants [4].

1.1 Novelty of the Research Paper

The core objective of this paper is to discover how IoT technologies can be effectuated to provide user comfort and protection in smart interiors. Many researches have been done on effects of AI in other fields of life like society, global environment, etc. but very few works speak about its implementation in interior spaces. Individuals interact the most with the interiors, so designing it innovatively and making it smart by using AI technologies is of key importance. With adequate research and analysis of the latest AI technological systems available today in the market, this study can be used to develop and design smart-futuristic interiors that provide optimum comfort and user care, ultimately making life easy.

2 Impact of AI on Intelligent Interiors and Human Health

As with many other changes in life, as artificial intelligence continues to change the state of environment, there will always be positive and negative effects on the society/ social environment.

By the use of AI analytics, AI can make the buildings highly adaptive, intelligent, and agile, helping them optimize operations, lower costs, and minimize inefficiencies across building platforms. Benefits of AI-enabled systems are collecting data on daily basis, like signing in or out of staff, logistical operations, floor occupancies, and contractor traffic, which could help to enhance the ambient temperature. Systems equipped with firefighting, access control, and surveillance system, in various buildings operations that can be accomplished, avoiding accidents that could negatively affect buildings.

One of the major threats in a smart building is due to the cybercriminals, whose primary aim is to achieve economic benefit, from their actions and also make an impression and spread fear. Tools like “Shodan” already exist that allow anyone to expose unauthorized IoT devices hooked up publicly to the internet. Using this tool, one can find billions of domotics systems in their lists, along with data used by the hacker. It implies that, after discovering it through a search, anyone can gain control of a BAS. In the web browser, finding and copying IP addresses will create an access interface where username and password are needed to enter. The hacker can gain access to the network monitoring panel, which contains data identical to

the details available to the firms engaged inside the intelligent interiors, whether it is a default password or can be fractured easily by a brute force attack. Once access is granted, the hacker could request network access, enabling them to monitor the building operations and then demand ransom in using the system that enables them to stay anonymous in return for not shutting down the building, such as cryptocurrency. As a consequence, the odds of a cybercriminal launching an attack on an intelligent interior with cryptography are already a fact.

3 Significance of AI Systems in Intelligent Interiors

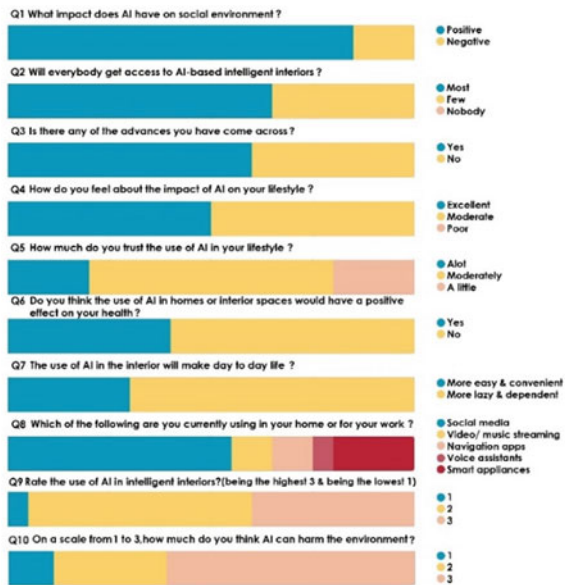
3.1 IoT in Intelligent Interiors

AI systems and their production techniques can cover a comprehensive range of benefits and improvements in the architecture and design world. Consequently, the inclusion of advanced systems into structures is very essential. Therefore, a questionnaire was carried out to determine the demand for AI systems.

57 users, consisting of undergraduates and graduates, professors, and others uae citizens, replied to this questionnaire.

Therefore this survey was to study the need and importance of AI systems and the analysis on how is the interaction of humans and their health (Fig. 1).

Fig. 1 Review of questionnaire on significance of AI systems in Intelligent Interiors



3.2 IoT in Social and Health Care

IoT allows the possibility of sensing and controlling objects remotely through network technologies. Study programs are based on linked devices and the partnership they build between the sectors of ICT and health, social care, and well-being (HSCWB). IoT should endorse a transition from paroxysmal disease interventions to preventive treatment and well-being solutions in HSCWB. The IoT should be a supporter of health care that is cost-effective and of high quality. The goal is to achieve healthy years of life and greater health and social protection quality. In examining the duties and economic opportunities for market-driven artificial intelligence solutions enabled by smart devices. Technological and market fields are distinguished by the research method. On the basis of these trends to illustrate how market opportunities have been approached from a market network perspective. Not all essential problems can be understood at a mere firm level when launching an IoT operation. In basic context, alliance can be utilized,

- i. To increase the quality of current health and social service programs without the initial intention of expanding the variety of services provided, or to enhance the productivity of current services.
- ii. To establish creativity and differentiation, without disrupting the narrative logic of current services of HSCWB.

4 Significance of AI Systems in Intelligent Interiors

For several years at least, intelligent materials have become incredibly important due to great advances in material engineering, appearing in various applications of architecture and interior design as well [5]. In particular, advances are of great importance in the domains of designed materials, artificial intelligence, and adaptive structural control [6]. It makes these materials appealing to architects and interior designers, both from a visual and a technical perspective, because of their original and distinctive properties [5].

Three intelligent materials are described below focusing on originality and necessity, which are identified for their innovative technologies (Fig. 2).

1. CNF-Based TENG



Fig. 2 Sectional working of CNF-FEP-based TENG. Author’s image

2. ELSI® Smart Floor
3. BIGS- RFID-Based Intelligent Floor.

4.1 CNF-Based TENG

A triboelectric nanogenerator (TENG) is an innovative form of energy, first seen in 2012 by Wang et al., operating fundamentally on the theories of electrostatic induction and triboelectric effect [7]. It is used to harness multiple forms of potential energy that are usually wasted [7].

The working theory of TENG is based on two different surfaces that are oppositely charged. The positive materials in TENG are cellulose nanofibrils (CNF) thin films, which are extremely transparent, flexible, and biodegradable and possess ideal surface roughness and piezoelectric properties. They are coupled with FEP (fluorinated ethylene propylene) to fabricate TENG devices that demonstrate comparable results that are indicated by synthetic polymer-based TENG devices. Further CNF-based TENG is integrated inside a fiberboard that is composed of recycled cardboard fibers, generating a high voltage power board using eco-friendly timber extracted materials through the chemical-free cold-press process. If subjected to an ordinary human step, the fiberboard generates an electrical output of up to ~30 V and ~90 μ A.

4.1.1 Components and Installation Process

It comprises fabricated CNF-FEP based TENGs film and manufactured power fiberboard.

Assembly of TENGs/Fabrication of CNF-FEP Based TENGs Film

Demonstrating the performance and design of TENGs as follows: CNF thin film was fixed to the center of PET/ITO substrate, as the top electrode. Whereas the bottom electrode FEP was located on the other PET/ITO substrate. Both the electrodes were separated by spacers and secured with copper tapes.

Manufacturing of Power Fiberboard:

Through mechanical stirring a uniformed mixture was formed, recovered fibers from cardboard were diluted in water. Vacuum sucking pressured the mixture thru the screen, leaving a moist mat. During vacuum sucking, the CNF-FEP based TENG whose edges were sealed and inserted in the wet plant. The mat was sandwiched between coil plated and release papers. Further, it was sent for 60 min under a

pressure of 100 MPa for cold pressuring. The mat obtained was then dried under a pressure of 50 lb weight for 24 h at 65 °C.

4.1.2 Application Possibilities

Fabrication of TENGs requires two oppositely charged materials in TENGs. Metals, polyamides, zinc oxide, and indium tin oxide (ITO) are typical positive materials in TENG and polyethylene terephthalate (PET), polydimethylsiloxane (PDMS), polyvinylidene fluoride (PVDF), polytetrafluoroethylene (PTFE) and fluorinated ethylene propylene (FEP) are negative materials in TENG.

Manufacturing of power fiberboard can be done with any eco-friendly natural wood-extracted materials which have magnificent integrity on mechanical impacts and also have excellent recyclability.

4.1.3 Properties

1. Unique and sustainable energy source
2. Eco-friendly
3. High efficiency
4. High power density
5. Cost-effective manufacturing process
6. Lightweight
7. Low cost, and
8. Great manufacturability.

4.2 *ELSI® Smart Floor*

Thanks to the new innovation and creativity seen in AI and computing fields, it is no wonder that such a product like an Elsi Smart Floor has finally arrived on market. The Elsi Monitoring System is a state-of-the-art smart flooring solution, a one-of-a-kind validated approach to minimize falls and increase protection in healthcare facilities [8]. The biggest reward is the fact that it has been verified to be the first and only system on the market that provides cost savings for its consumers and according to prevailing challenges and features, offers solutions for safety and well-being [9].

Elsi Smart Floor is an embedded sensor and linked hardware device that operates together to detect and track the movement of human bodies relative to their floor positions [10, 11]. The system can be used to acquire status checks for those who need 24/7 supervision. It is also possible to incorporate surveillance systems already in operation with an intelligent floor, integrating them to provide complete clarity of status and location of any given resident [10] (Fig. 3).

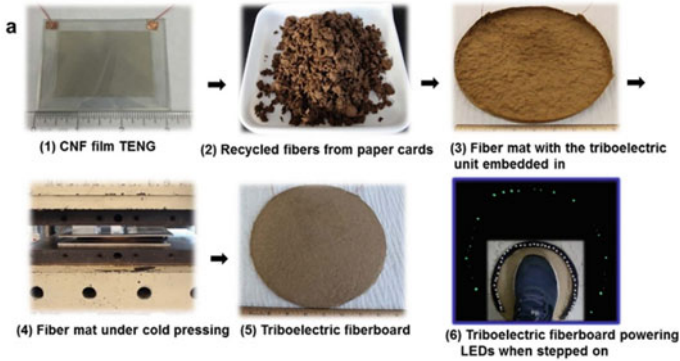
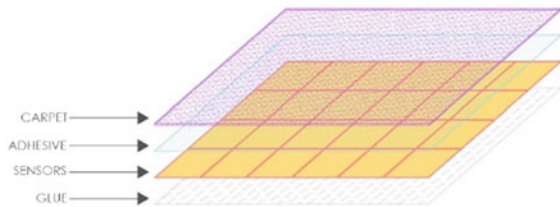


Fig. 3 Chemical-free cold pressing of power-fiberboard [16]

Fig. 4 Study of layers in depth of Elsi® Smart floor. Author’s image



4.2.1 Components and Installation Process

The “Quick and Easy” Elsi® Smart Floor can be installed either in current or new facilities.

The installation of intelligent floor is identical to the traditional linoleum carpet installation, i.e., it is designed in the same manner as the traditional top floor carpets are designed. It is laid quickly and efficiently, and the top floor carpet is completely protected, giving it long life span.

It comprises sensor sheets, cards, and top floor covering. Installation procedure starts with gluing on the entire floor for the sensors to be installed. Once the installation of sensors is complete, “test phase” is conducted to check all the sensor sheets are working properly or not. It is tested with a metal detector which gives the track reading of footsteps. Installation of adhesive sheets is placed for the underlayment of carpet and welding is done to acquire clean-finished flooring. Cards and plinths are laid on the skirting of the room which is the second part of the monitoring system are placed. The cards are covered and the connections are placed intact (Fig. 4).

4.2.2 Application Possibilities

The underlayment of sensor system remains the same. But for the top floor covering the options are of four different types; carpets, tiles, parquet, and linoleum. It is applicable to clinics, hospitals, and hospices as it helps to improve operational activities. It is also installed in residential areas which maintain an aesthetically pleasing, home-like environment with healthcare services.

Properties

1. Fall detector
2. Reliable
3. Safety and Security of the residents
4. Capacitive sensing
5. Conductance sensing
6. Easy and Quick to install
7. Cost and time saving
8. Invisible
9. Reduction of routine checks
10. Saving scarce resources
11. Improve residents privacy
12. Improved Quality of life
13. Pays itself back in 12–18 months
14. Aesthetically pleasing (Fig. 5).



Fig. 5 System operation of Elsi® Smart floor [9]

4.3 *ELSI® Smart Floor*

BIGS- RFID-based solution is an indoor positioning system that helps visually impaired people to navigate [12]. The Blind Interactive Guide System (BIGS) is used in buildings for blind people. The IPS system helps to capture the user's current location information, generates a unique id number, helps navigate blind person to its final destination and the user can disable the wireless connection if they want privacy so that the server does not receive any data from the user. The BIGS is also fitted with the wireless LAN Blind Interactive Guide System using RFID-based IPS (Indoor Positioning System) to enable the user to be linked to the system to be monitored by the building's security staff [13].

These "navigation aids" are buried under the finished floor to build the workspace in a way that allows and facilitates accurate navigation and positioning over broad distances with absolute precision [14].

4.3.1 **Components and Installation Process**

There are two parts to the system: the intelligent floor and the portable terminal unit. The intelligent floor is a building floor where a passive RFID tag transmits a specific ID number to the individual tile of the floor. An embedded machine fitted with an RFID reader like an input device is the portable terminal unit [13]. Radio-frequency Identification (RFID) technology guarantees that readers and tags (also called transponders) communicate wirelessly. These are the two crucial parts of the RFID systems. Tags are of two types such as active and passive. Only the electrical charge transmitted by reader drives the passive transponders and it does not require additional battery [15].

To recognize the user's current location, calculate the user's direction, identify voice commands, and deliver voice messages. There are two key constraints of using RFID-based solutions:

- (a) It takes more time and effort to reconfigure the positioning area than other solutions, such as vision-based systems, and
- (b) Users are usually guided only by predefined paths [12].

4.3.2 **Application Possibilities**

In a dense, area-wide network thousands of RFID transponders, which are deployed under the regular flooring and serve almost as radio beacons, the "intelligence" of floor [14]. Due to its unique and navigating aspect, it is installed in hospitals for blinds, banks, and residence of blind people (Figs. 6 and 7).

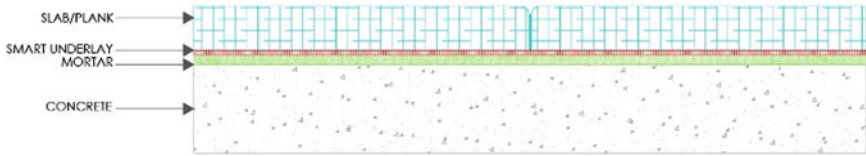
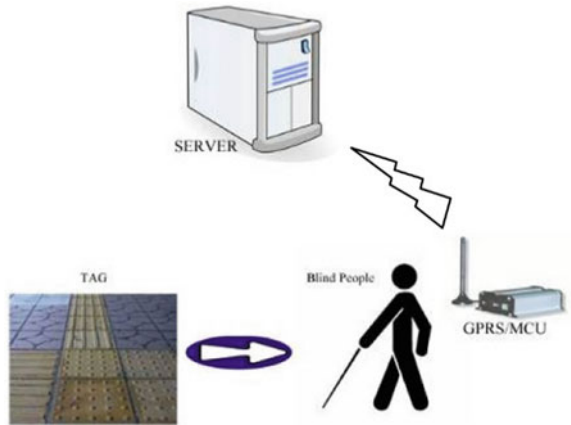


Fig. 6 Conceptual detail of BIGS- RFID-Based Intelligent Floor. Author’s images

Fig. 7 Technical functioning of BIGS- RFID-Based Intelligent Floor [17]



Properties

1. Recognize the current location of the user
2. Navigate user
3. Calculate user direction
4. Identify audio commands
5. Deliver audio messages
6. Object tracking
7. Supports and enable reliable navigation
8. Absolute accuracy
9. Serve as radio beacon
10. Obtain the current location data of the user
11. User privacy
12. Small size and low cost

5 Comparative Analysis

To build a deeper understanding of the three materials given below is an analytic study that has been compared below with different distinction criteria (Table 1).

Table 1 Comparative analysis table of three intelligent finished floor system

S. No	Criteria	CNF-FEP Based TENG	ELSI® Smart Floor	BIGS RFID-based Intelligent Floor
1	Requirement	Eco-friendly fiberboard with piezoelectric properties that harvest and store energy when an individual steps on it	Its approach is to detect and minimize falls and increase protection for users	It is an IPS system used in an interior to capture present location information of the user's, develop unique id numbers, navigation aids are added below the flooring to direct blind user's to its desired destination
2	Strength	Durable due to lightweight, flexible and fibrous piezoelectric material that can be integrated with any natural wood recycled board	Lifespan depends on the usage of material as it has captivated and conductance sensing and is also aesthetically appealing	Durability depends on IPS system tracking and storing of data
3	Use	Can be applied on horizontal plane	It can be applied on both vertical and horizontal planes	It can be applied on both vertical and horizontal planes
4	Characteristics	Eco-friendly Renewable energy source High power density Great manufacturability	Invisibility Reliability Security of scarce resources Better quality of life	Help to navigate, recognize, and tracking information of the user Detected audio commands Help to deliver voice notes
5	Comfort	If this system used as flooring will provide: Harvest energy by stepping on the plane Provide renewable energy to small devices	If this system used as flooring will provide: User privacy Enhancement in routine checks	If this system used as flooring will provide: Store user information Navigate user to required destination User privacy

(continued)

Table 1 (continued)

S. No	Criteria	CNF-FEP Based TENG	ELSI® Smart Floor	BIGS RFID-based Intelligent Floor
6	Restrictions	Consumption of energy Installation complication	-No restrictions-	Restrictions are yet to be found
7	Fabrication	CNF- based TENG is a wet mat that is sandwiched between coil plates and release papers under cold pressing method. Dimensions- 20 cm dia and 4.5 mm thick	Sensors are equally similar to the ones found in tablets and touchpads	Portable terminal unit is an embedded machine that acts as an input device with a RFID reader fitted with it
8	User Comfort	It generates adequate electrical energy that can be used for other user functions; such as charging phones, etc	In sectors like hospitals and healthcare homes, it is highly beneficial choice to detect and reduce the case of falls and provide user protection	It can help to locate people (especially blind people) indoors by generating and tracking their profiles and navigating their motion in the interior spaces. In general terms, if you use this system can help to reduce the risk of lost cases

6 Discussion and Conclusion

The dream of future smart technology is now a reality that exists in each one of the enclosed spaces we live in, particularly in the developed countries and Middle East. With the development of IoT things and advances in this field, our life has become much more convenient and effortless. Artificial intelligence is a marvelous tool that makes interiors better, futuristic, and aesthetically appealing for its uses, however, one of the most neglected aspects of smart technology is its effect on health and well-being. When certain intelligent systems and materials are incorporated the standard of living enhances to a great extent. Floors are generally any individual’s first physical encounter with any social environment whether exterior or interior and has overall effect on efficiency. The use of such intelligent systems in flooring would enhance the technicality and efficiency of any building interior. Considering that

it is also essential to study and evaluate the direct and indirect effect it has on a habitant's health. An attempt has been made to analyze three intelligent flooring systems and their behavior with regards to their health aspect when used in interior spaces. The behavior of these systems varies across factors like usage installation and maintenance. Accordingly, appropriate study with regards to the health factor needs to be undertaken in order to ensure the Holistic well-being of the habitant in interior spaces.

References

1. Sweet J (2020) Artificial intelligence. Accenture (Online). Available: <https://www.accenture.com/ae-en/insights/artificial-intelligence-summary-index>
2. Appio FP, Lima M, Paroutis S (2019) Technological forecasting and social change. *Underst Smart Cities Innov Ecosyst Technol Adv Soc Challenges* 142:1–14
3. Qualetics Data Machines, Inc. (2019) How AI & IoT is driving intelligence and automation in smart homes. 28 November 2019 (Online). Available: <https://qualetics.com/how-ai-iot-is-driving-intelligence-automation-in-smart-homes/#:~:text=AI%20in%20Smart%20Homes,enhance%20data%20security%20and%20privacy>; Mathur N (2019) How AI is transforming the smart cities IoT? (Tutorial) 23 March 2019. (Online). Available: <https://hub.packtpub.com/how-ai-is-transforming-the-smart-cities-iot-tutorial/>
4. Konarzewska B (2017) Smart materials in architecture: useful tools with practical applications or fascinating inventions for experimental design? *IOP Conf Ser Mater Sci Eng* 1–8
5. Spillman WBJ (1992) The evolution of smart structures/materials. In: *European conference on smart structures and materials*, pp 97–113
6. Rathore S (2018) A critical review on Triboelectric Nanogenerator. In: *IOP conference series: materials science and engineering*, pp 1–17
7. Active healthcare, Elsi smart floor systems: falls prevention monitors (Online). Available: <https://activehealthcare.co.nz/products/patient-transfer/falls-prevention-monitors/elsi-smart-floor/>
8. MariCare (2015) Safety—security—savings. In: *Smart sensor system*, pp 1–7
9. Stehr M (2018) What is an Elsi smart floor and what are its benefits? 21 May 2018 (Online). Available: <https://www.hlshealthcare.com.au/what-is-an-elsi-smart-floor/>
10. 4Healthcare (2018) Elsi smart flooring (Online). Available: <https://www.4healthcare.com.au/our-products/fallsprevention/elsi-smart-floor/#smart>
11. Guerrero LA, Vasquez F, Ochoa SF (2012) An indoor navigation system for the visually impaired. *Sensors* 2012:1–23
12. Na J (2006) The blind interactive guide system using RFID-based indoor positioning system. In: *Telecommunications and computer engineering*, pp 1–2
13. Prassler E, Kämpke T, Kluge B, Strobel M (2008) Services robots navigating on smart floors. In: *Recent progress in robotics*, pp 1–2
14. Regus M, Talar R, Labudzki R (2019) Indoor positioning and navigation system for autonomous vehicles based on RFID technology. In: *IOP conference series: materials science and engineering*, pp 1–14

15. Chunhua Y, Hernandez A, Yua Y, Cai Z, Wanga X (2016) Nano energy. In: Triboelectric nanogenerators and power-boards from cellulose nanofibrils, pp 103–108
16. Chumkamon S, Tuvaphanthaphiphat P, Keeratiwintakorn P (2008) BIGS. In: A blind navigation system using RFID for indoor, pp 1–3

Impacts of Integrating High-Tech and IoT Developments for Workplace Performance



Zehra Hafizji, Banafsha Rajput, and Amna Rafi Chaudhry

Abstract In today's modern world there is no surprise that technology has become such a vital force for any organization in the business environment. The suitable technology can actually enhance the overall market efficiency and performance of a company, as well as augment company-wide employee productivity, dedication, communication, and sense of responsibility. One of the most browsed subjects by modern day-workers was "How to increase workplace productivity?" nowadays. Highly dynamic, flexible tasks and growing workloads are causing workers across various sectors to actively search for productivity solutions in the workplace. Productivity throughout the workplace is a phenomenon that affects virtually all main company metrics such as operating expenses, sales, retention, and turnover of staff, as well as the satisfaction of consumers and clients. Technology is an aspect that is constantly advancing. New technologies are being designed to help organizations increase productivity and make the job enjoyable for the workers. The aim of this study was to look at the scope of the demand for incoming high technology and how it affects the productivity of a daily worker. Implementation of technology may vary from workers conducting various tasks not only mentally but also physically to increase their focus. In order to achieve the most effective way of functioning, we need to find suitable ways throughout this analysis to address the challenges faced by employees.

Keywords Productivity · Workplace · Activities · Office · Corporates · IoT

Z. Hafizji (✉) · B. Rajput · A. R. Chaudhry
Amity University Dubai, Dubai, United Arab Emirates
e-mail: zehraH@amitydubai.ae

B. Rajput
e-mail: brajput@amityuniversity.ae

A. R. Chaudhry
e-mail: achaudhry@amityuniversity.ae

1 Introduction

For several employees, office space is more likely to be a second home as they spend most of their time in the office 8–9 h per day, which often affects an individual's mental and physical health that eventually contributes to the success of the employee toward the job. The concept of “workplace,” is changing as digital and connected technologies redefine what is possible. The smart device helps many to have a versatile workspace and will remain a primary way to connect and communicate. New ways of working together, sharing information, and business results are provided by the convergence of the physical market with technological networks and devices. With employee wearable devices that are already here, self-driving cars that are expected to be seen on the roads within the next 3–5 years will continue to extend the boundaries of the mobile workforce. The systems have evolved over the same time, by keeping up with the latest trends and selecting the integrated and smarter. By enhancing efficiency and productivity and creating a workforce collaboration environment, interconnection with smart machines and analytical tools will transform the company. As devices continue to bind employees, they construct an atmosphere that is more than an office and develops a mutual knowledge community. Health in the workplace, productivity of workers, maintenance of resources, and the development of a comfortable environment tie together to form an ideal workplace.

The main purpose of this paper is to find out the effects of IoT apps and technologies and how their implementations would facilitate comfort and increase productivity among the user in a workplace. While several researchers have been working on effects of IoT on business, society, and global change, there have been very few researchers reporting on the impacts of IoT on the users and their environment. The key requirements for the design of an effective smart technological space would be mainly considering the users and their behaviors around the technology. This data is very useful in the design of user-friendly spaces.

Many researchers compared IoT in different aspects. Though there is similar work, the present work shows the latest use and upgradation of diverse IoT apps available in the market which could be used for multiple purposes. In the present work, “Effects of Integrating High-Tech and IoT Developments for Workplace Performance” is studied exclusively.

2 Defining Productivity

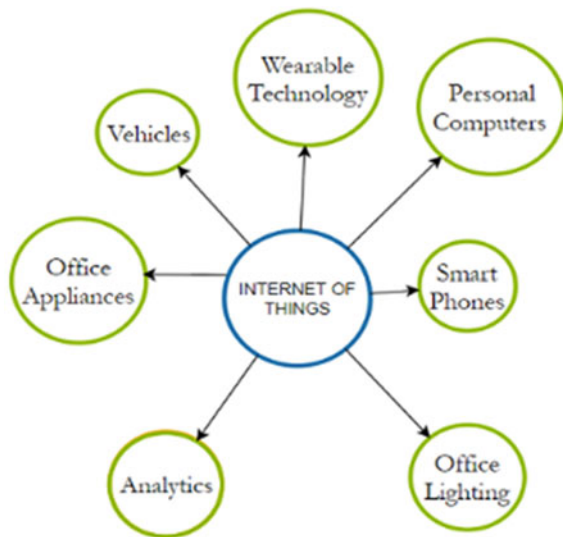
The workplace climate is the most important factor in employee productivity, while office furniture is the secondary factor affecting high-rate efficiency and productivity. Artificial and natural conditions that are appealing to humans, including factors such as decor, noise, lighting, room planning, affect their efficiency. The positive atmosphere directly affects the attitude of the worker and increases the quality of working with customers [1]. Productivity is a percentage of how well an organization

(or employee, company) converts into input funds for goods and services (labor, machinery, machines, etc.) In this case, we consider output growth as when there is less absenteeism, less workers finish early and less breaks; while performance increases can be calculated by the number of products in a factory setting employees are viewed as the assets of the company as well as the product or service, a company’s customer base, and may build a business or destroy it. As such, an organization should invest in its workforce but still hope to earn a return on that investment through the productivity of its employees.

3 Technology at Workplace

Internet of Things (IoT) seems to see physical objects being connected to the internet enabling people to either be remotely controlled or to retrieve and share information and communicate without having to involve a human being (Fig. 1). Throughout the workplace, IoT can encompass a variety of types of equipment and technologies such as smart objects, robotic systems, and artificial intelligence to increase efficiency and improve business performance [2]. IoT technology software allows every single product that is distinctly recognizable via its embedded software framework and that can communicate within the current network infrastructure. Recently, it has become prominent in this tech-centric corporate environment, which has sought to extend the role and impact of technology remarkably in every facet of life [3]. This allows several more touchpoints to be gathered, shared, and evaluated through the entire range of business activities. In addition, the IoT provides an unrivaled approach to

Fig. 1 Workspace IoT.
Author’s image



data on goods, operations, and individuals. Data retrieved and collected are being analyzed to identify work mindsets for workers, user preferences, and organizations. Therefore, businesses must make strategic decisions about database management and aim to strike the right balance among belief, security, and confidentiality issues [4].

3.1 Smart Office

As already stated in this report, smart office is an IoT applicability category. Originally, IoT was applied to specific traceable and compliant linked objects with RFID, technology, radio frequency identification. Further technical elements, including sensors, actuators, GPS systems, and mobile devices, were connected with IoT afterward.

There is currently a single concept of IoT as a dynamic global network system with separate set-up capabilities based on common and compliant communication protocols where identities are allocated to virtual and physical “items” with virtual personalities and physical attributes using smart interfaces while being incorporated into the information network.

With the smart office concept becoming an IoT category as a rising number of companies are moving toward the smart office environment, this transition has two hampering factors. First is the energy usage issues that modern smart offices need, and secondly the privacy concerns and malicious attacks. But somehow, this does not seem to deter companies from introducing smart office environments with different features and solutions around the world [5].

Although IoT provides the second aspect, cost, and pain, while increasing efficiency, a way to reduce waste, the greatest attraction of this technology revolution is for us to lead a healthier, more productive, and better quality of life on earth [6].

3.2 IoT Apps Fall into the Following Broad Categories in the Smart Digital Workplace

- Environmental—Includes “smart” lighting, HVAC, fittings such as automated shades, furniture, and similar systems, all of which are related to a Building Management System (BMS)
- Security—Includes physical user access, surveillance cameras along with recording/processing equipment, fire suppression, and other monitoring and safety-related systems
- Mobile—Includes smart apps for consumers, dedicated devices, mobile PoS, and many more

- Application-focused—Includes Wireless markers, area occupancy monitors, digital signs, AV, collaboration as well as other user-focused tools and systems
- Other—The ever-declining costs of highly advanced IoT devices make sure that more device types, in categories apart from the examples given, remain constantly connected.

There is also interconnectivity, transparency, and data sharing with many of the applications being brought into the IoT world, but still, the systems and devices operate on their own unmonitored networks. A perfect example of this is the traditional Physical Access Control System (PACS) which controls doors or systems. The landscape is evolving today. One of the drivers of IoT implementation and incorporation in the enterprise is the need to enhance the experiences and cybersecurity programs powered by executive management, IT, corporate real estate, HR, and other business functions [7].

4 Scope of IoT

The Internet of Things is perhaps the largest technological phenomenon that is taking place right now. Within the next five years, IoT will give us the most disruption and perhaps the most potential. IoT is set to transform and modify the world we have come to know and your career and personal life is certain. The most highly rated advantage of an IoT-enabled approach is the capacity to increase the users' efficiency [8]. When every person wants to communicate with other items or objects, an intelligent IoT network is created. IoT technology is evolving with more creative innovations and tremendous growth for smart offices to boost living standards [9].

IoT has the ability to maximize system and process efficiency, save time for people and businesses and enhance quality of life. The technology offers us distinct opportunities like:

- Improve business processes
- Maintenance preparation
- Improved utilization of assets
- Improved productivity [8].

5 IoT's Impacts in Workplace

IoT-enabled innovations have changed industries and will continue to do so from any angle, from operations and procedures to customers and outcomes. Smart devices have made it possible for teams to be better equipped with simpler and more efficient methods and digital efficiency in the workplace [10].

5.1 Company, Economy, Work Skills, and Society Impacts

The rapid spread of connected systems and devices from one for each person today to 10 systems for each person in the future will create numerous new start-up opportunities and create an atmosphere across the IoT sector [7]. Business success is important to IT as it directly affects the processes from which they produce and receive value to earn a profit. The most critical consideration for a company that adopts technology is to control the technology's life cycle [11]. This may also contribute to the development of additional services or industries, such as IoT and smart systems manufacturing, monitoring and quantification systems, decision-making and data management systems, and security technologies, in order to ensure safe usage and to resolve IoT privacy issues [7].

Adoption of IoT will also lead to the introduction of innovations for big data and analytics that can provide a framework for realistic decision-making. More opportunities can be created by the large number of apps combined with the high volume, speed, and architecture of data sets, especially in security areas, data storage management, servers, data center networks, and data analytics. In addition to understanding industry-specific use trends, consumer preferences, and innovative marketing techniques, this implies skills such as knowledge of business science, math, and statistics, imaginative design for end-user visualization, big data applications, programming and development of large scalable systems, and awareness of devices used in IoT ecosystems would be in demand [7].

5.2 Impacts on How and Where One Works

Technology is being used to help employees to work or to oppress them. Yes, both of these results reflect the introduction of modern technology, as we must therefore see. Theoretical and psychological studies will help inform solutions to this issue.

In truth, the acceptance and implementation of technology in the workplace are determined by at least four factors. Next, are they comfortable to use, and natural? The human-to-technology interface, which can be measured in terms of efficiency, effectiveness, and user satisfaction, is affected by functionality.

If technology is to motivate workers at work, it should promote self-motivation and well-being, key elements of the principle of self-determination; enhance productivity; and promote satisfaction in the workplace, organizational engagement, and habits of employee citizenship. When technology leads to a loss of power, dignity, and interdependence, there are feelings of injustice. That, in turn, leads to stress, demoralization, and negative activities in the workplace.

5.3 Impacts on Jobs

Computer technology, of course, is not necessarily the very first technology to have an effect on jobs. Technology has long replaced humans, often creating new and increased skill jobs in its course, from steam engines to robotic welders and ATMs. Affected workers with outdated qualifications are still affected, but the total number of jobs has never declined over time.

6 Key Developments of Work and Organization in Technology

In the course of human history, the effects of technology are well established. Based on their respective core technological infrastructures, the growth and advancement of society can be divided into three eras: the agricultural period, the industrial age, and the digital era. The drive to learn new ideas and skills was greatly affected by the development of these periods. Nevertheless, these have all been required and permitted by new economic structures, revolutionary revolutions, cultural transformations, and working models [12]. Therefore, the future smart workspace will include everything from fundamental tasks, such as turning the coffee machine on whenever the office door is opened, to more complex ones [13].

People are based on an infrastructure containing new technology and communications in the digital age. That is, because of the properties of digital goods, the unit cost of nominal or incremental output steadily decreases, whereas the sum of most other manufacturing factors remains constant. When uploading, accessing, transmitting, and storing online technology, regardless of location or time, boundaries and geographical distances are no longer as relevant as they have ever been, and entirely new, invisible digital spaces are now open [12]. Smart lighting systems or automated windows and doors allow you to monitor the light's strength and color, as well as to maximize the amount of waste. When there is one in the bed, the lights turn off automatically [14].

7 Case Study-Industrial Basis

The Edge Headquarters, Amsterdam.

The workspace combines technology, sustainability, and well-being, focused on the digital infrastructure of "Edge" that links controls of the indoor spaces via a unified system of the iCloud. Several ideas culminated in a "no-office" idea, which would shape the office into an "unconventional garden" giving priority to user productivity. Employees can configure anything from lighting to temperature via the Edge app, find their peers and recognize available working space. The work of designer, Fokkema &

Fig. 2 “Urban zone” space [21]



Fig. 3 Bar counter leading to meeting rooms



Partners had to be a mirror of this hyper-personalization inside. The outcome is a room that facilitates a “personal user journey” through the three zones” of nooks and corners. The first (Fig. 2) is a “home space” for relaxing and lounging. The second (Fig. 3) is a biophilic “living room” for reflection and reading. And the last one an “urban zone,” complete with two board rooms and a tech playground. It is proposed that staff make their way to the bar for meetings or a game of foosball [21].

8 Changes in Smart Office Environment

It had not been that convenient at all to move from a conventional old-fashioned workplace to a modern office. Among all the challenges faced by organizations is the struggle to gain consumer acceptance and approval of emerging technologies, and the question of how to sustain an optimal level of productivity and results. Since technology may be fresh and unfamiliar to some non-technology-updated workers, some workers may be a misfit with the introduction of new technology and may feel uncertain about their employment. This also leads to alienation from work and resistance to improvements, making it more difficult to embrace technology [15].

Technology impacts profoundly on the essence of office work. Using technology, the normal tasks performed by hand are already executed. Technology removed the original hiring process through the use of technology applications and software such as Hotjobs.com Ltd.'s Resumix6 program. This reduced recruiting expenses by more than 50%. Whereas, this does not indicate that technology has minimized the need for further jobs. The technology generates far more work than it does away with. Regardless of the sectors, the advent of the technology industry has produced millions of "digital employments" for workers in ICT industries and advanced users in workplaces [16].

9 Draws Backs of IoT in the Workplace

9.1 Security

Protection is the biggest concern associated with the production of IoT by far. The total attack surface is far greater than a conventional network architecture, as each system is linked to a larger edge computing network. Many devices move between different networks to make matters worse, likely picking up malware along the way that lets cybercriminals circumvent those security measures.

Overcome: Organizations should design their networks to protect against possible threats to establish protocols of security and authentication that subject device to rigorous inspection and refuse them automatic access to potentially sensitive information.

9.2 Technical Requirements

It must function as a single, unified system in order for an IoT network to provide value to a company. The truth, from a technological point of view, is that the IoT is often fragmented and lacks interoperability.

Overcome: Platforms must be able to work across devices, regardless of the brand, manufacturer, or industry, to combat this. A major IoT hurdle is overcoming compatibility problems, but emerging businesses are beginning to allow increased interoperability through open-source growth.

9.3 Constraints of Time

It can be a lengthy and expensive undertaking for corporations to roll out IoT ventures. Rapid technological shifts mean that businesses run the risk that every new technology system will become outdated even as it is being installed.

Overcome: Businesses need to try to remove as many of the stumbling blocks as possible from the business development phase in order to benefit from the advantages of a new IoT system in order to allow a quick and effective implementation. They must also ensure that they collaborate with competent service providers who are able to meet their expectations for technology and make agile solutions possible.

10 Smart Office IoT Systems

Smart office approaches together with a security system can save your staff time and energy on day-to-day activities such as room management, visitors, and asset management.

10.1 R307 Sensor with Fingerprint

This system includes visual fingerprint scanners such as biometric identification security systems, high-performance DSP devices, high-speed fingerprint matching technology, high-dimensional Display chips as well as other features like, image processing, scan storage. The scanner reads the unique fingerprint of every employee whenever it is time to log in or out.

10.2 LDR Sensor

It is essentially a photocell that operates entirely on the belief in photoconductivity. Characteristically the passive component is a resistor whose resistance rate decreases as the light asset decreases. Usually, this optoelectronic system is integrated into light fluctuating sensor circuits and switching circuits that are light and dark [17]. Smart lighting is increasingly evolving and has the possible additional business effect of providing management with a strong understanding of space usage, in addition to energy savings [18].

10.3 Temperature & Moisture Monitor DHT11

A very low-cost digital temperature and humidity monitor. To test the ambient air, a capacitive humidity sensor, as well as a thermistor, are used and a digital signal is sprayed on the data pin [17]. The ability of workers to change their temperature in the workplace reduces temperature problems and increases the effectiveness and efficiency of employees [18].

10.4 ESP32 Slot (Wireless Chip System)

It is a special wireless dual-core chip device. Bluetooth 2.4 GHz and Wi-Fi composition chip fitted with TSMC extreme 40 nm low-power technology. It is intended to achieve the finest power and RF efficacy, seeing longevity, flexibility, and reliability in a wide range of applications and power circumstances. To ensure that data use is ethical and compatible with the specific objective of data collection, specific processes, protocols, and communications must be in place [17].

10.5 Automated Office Facilities

The futuristic smart workspace would also provide an idea of communications, workflows, and resources requiring physical and information equipment for staff scripting. Varied computer machines and software for digitally producing, gathering, processing, manipulating, and relaying the office information required to perform basic functions [18].

There is an increasing variety of different devices (notepads, tablets, smartphones, and smartwatches) that people use in their everyday working lives and bring to their workplace too. There are a variety of ways that leaders in the digital world can exploit this phenomenon by bringing these issues together in the digital and physical workplaces [18]. To be able to discharge sufficient employees, a smart office must be built with one thing in mind [17]. Employees would also like the similar digital experience as users always do. Also, workers feel comfortable challenging technology limits into their personal lives, playing with things like smartwatches, health monitoring software, and other smart devices [19] (Table 1).

Table 1 Comparative analysis table of smart office IoT systems

S. No	Criteria	Fingerprint sensor	Ldr sensor	Temperature and moisture monitor	Wireless chip system	Automated office facilities
1	Need	Antiqued time and attendance systems do not monitor workers' output accurately. The data generated can be used to track the hard-working staff. Along with increased security	Bad working lighting can lead to eye pain, tiredness, fatigue, and mistakes. More lighting can cause glare headaches and tension. These sensors are used for measuring the intensity of light	It helps employees to make requests to have the office room warmed or cooled from their mobile or Web browser. More temperature controls will improve morale and efficiency	It can interact with other devices to provide Wi-Fi and Bluetooth networking via its SPI / SDIO or I2C / UART interfaces	Office automation can perform almost all of the tasks faster. It facilitates the employees with lesser workload and increases productivity
2	Performance	High performance, easily accessible	Their tolerance in the dark is very powerful, often up to 1 M, but when the LDR sensor is exposed to light, the resistance decreases greatly	Electronic sensors should have a precision of $\pm 0.5^\circ\text{C}$ or better	Runs at 160 or 240 MHz and performs at 600 DMIPS	Office automation helps businesses to increase their productivity and revenue
3	Complexity	The biometric data is not complex for an employee	The level of complexity of the sensor varies widely	It is complex as the sensors are susceptible to drifting	Able to manage more complex tasks	The larger an office, the more complicated the system gets

(continued)

Table 1 (continued)

S. No	Criteria	Fingerprint sensor	Ldr sensor	Temperature and moisture monitor	Wireless chip system	Automated office facilities
4	Application	<ul style="list-style-type: none"> • Logical control of access • Regulation of physical access • Time and attendance • Monitoring 	Such resistors are often used as light sensors, and application of LDR includes primarily alarm clocks, street lights, work station light intensity meters, and warning circuits	Enabling us to “feel” or detect any physical changes to that temperature that generates an analog or digital result	It is the microcontroller for the IoT Node Reducing workload communication system on the central application device	Used for functions like Management of data Exchanging data More accuracy
5	Security	High-security door lock, Safeguarding assets from unauthorized employees or guests	The sensor’s resistance decreases when light falls on the LDR sensor, which causes an alarm to be activated to give the user an alert	Health security	It is a secure boot	Moderately secure, but prone to hacking threats
6	Data	Minimum 100 persons, with 500 dpi/256 resolution	No data saved or required	Data is stored to detect any kind of airborne illness	Memory is up to 520 KiB SRAM	Many people can modify data at the same time, as the handling capacity is more

11 Co-Working Office Space Layout with IoT Integrated Technologies

In the last century, the design of offices has bounced between rigid structures and dynamic layouts, each with limited success. However, the office has moved from a place of development to a place of engagement with the emergence of a new autonomous workforce. Coupled with this are techniques of spatial computation that measure spaces with a more human approach. With the construction of a new-built collective workspace, the combination of the two gives rise to a new office typology illustrated.

11.1 Intelligent Interiors for Co-Working Space Design

(a) Solar shading systems for front facade

Natural sunlight and passive solar heat are better used by buildings with large areas of glazing. Solar shading louvers can be oriented to increase natural light levels while mitigating glare, providing the building with optimum natural light quality during the daylight hours throughout the year and reducing the need for artificial lighting as much as possible.

Application: This technology would help the co-working space move toward minimizing energy usage, optimizing the use of natural light without the problems of glare or excessive solar heat gain as well as making the indoor habitat live in the correct amount of sunlight.

(b) Switchable electric glass

Smart glass or switchable glass is glass or glazing whose properties of light transmission change when voltage, light, or heat are applied (Fig. 4).

Application: These switchable glasses would be used in meeting rooms and private working cubicle spaces to provide complete privacy to the users. Also serving as an HD working screen which would help in simultaneous working or discussions reducing the need for traditional whiteboards and making the aesthetic of the space stand out.

(c) Space management software

Workspace optimization is possible through the study of data on the occupancy of workspaces and meeting rooms. Sensors record occupancy at various times and days and monitor the users' movements. The room grid offers an overview of up to nine room resources by showing details about each room's current occupancy status, location and room name, and the time before the occupancy status changes.

Application: As the potential of co-working space increases (Figs. 5 and 6), it becomes much more important to be able to gain insights into space usage, increase employee efficiency and satisfaction, and be smarter about building management.

Fig. 4 Functioning of switchable glass

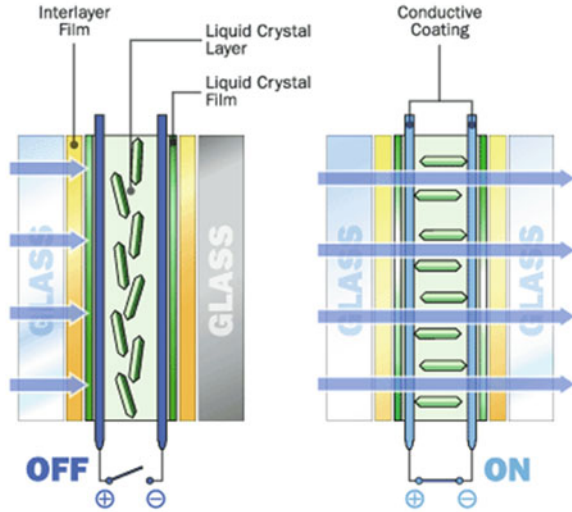


Fig. 5 Touch operating smart panel



Fig. 6 Smart panel with additional features

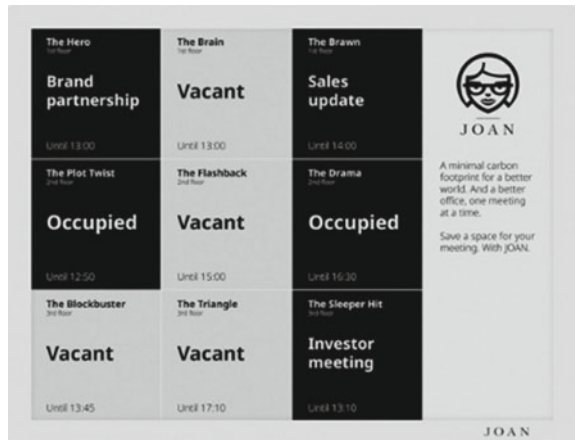




Fig. 7 Smart water control leak net that navigates to the damage

(d) Smart water controller (Fig. 7)

A more resilient and effective water supply system can be created by smart water management systems, minimizing costs and improving sustainability. Digital meters and sensors, supervisory control and data acquisition (SCADA) systems, and geographic information systems provide high-technology solutions for the water field.

Application: It will be applied in the landscaping areas with plants and trees that cannot be handled manually so smart systems can provide reliable and up-to-date information that enables water managers to make informed and systematic, rather than ad hoc, decisions. These will automate duties and reduce criteria for staffing.

(e) Building environmental control systems

If someone works with a manual thermostat in an office, then they will know how hard it can be to reach the perfect room temperature.

A thermostat is a feature that forms part of the controls of space, helping to maintain a predetermined, steady temperature. The room automation stations and room controls are composed of room temperature controllers. Regulation of the air conditioning system is taken over by users as shown in Fig. 8.

Fig. 8 Smart control panel to operate temperature of different rooms



Fig. 9 Smart technology integrations in co-working space. Author’s image



Integrated room temperature sensors compare the actual measured room temperature with the specified set points and, by heating or cooling, change the temperatures to the demand.

Application: This technology shown in Fig. 9 can be applied in all commonly shared spaces like co-working, co-creating, lounge, and training rooms that require individual comfort while working. Making it more easily usable by installing the automated control system apps on their phone.

12 Discussions and Conclusion

Technology is crucially important in every field. Organizations need to adopt and implement technology at all levels in order to compete effectively. Employees are every organization’s most valuable asset. Organizations should make plans that make it easier for their workers to do their job; it will lead to increased customer service and improved productivity. Investment in modern technologies will have a positive effect on employee performance; it will increase their quality and productivity. IoT-driven solutions would allow management and employees to work more in far less time. Such IoT-enabled software and devices could also be linked to a centralized network that allows a business to monitor the workplace and its workflows more easily. Controlling lighting and temperature, smart devices, and services help workers find silent spaces to think about and demonstrate ways to communicate collaboratively with employees. While IoT’s effect has started to evolve and achieve definitive results in areas such as industrial and manufacturing services, choosing smart devices at the office is an ideal option for smooth business. If it comes to incorporating some technologies into the workspace, however, it is better to pick something that will give you the best value for money. Start low, and then grow. Technology is strong

and can at first be intimidating because of all the knowledge and data that it has to offer.

References

1. Akhtar N, Ali S, Salman M, Ijaz A (2014) Interior design and its impact on of employees' productivity in telecom sector. *J Asian Bus Strategy* 9:9
2. McLellan C (2018) ZDNet, ZDNet, 1 March 2018 (Online). Available: <https://www.zdnet.com/article/optimising-the-smart-office-a-marriage-of-technology-and-people/>
3. Barman A, Das MK (2018) Internet of Things (IoT) as the future smart solution to HRM. In: International conference, Assam
4. Mähler V, Westergren UH (2019) Working with IoT—a case study detailing workplace digitalization through IoT system adoption. Sweden
5. Saleh A, Munoz M (2018) Knowledge transfer in smart office environment, Sweden, 2018
6. Iyengar S (Online) Impact of Internet of Things (IOT) on IT, business and our lives. Available: <https://channels.theinnovationenterprise.com/articles/8745-impact-of-internet-of-things-iot-on-it-business-and-our-lives>
7. Aruba networks (2017) IoT and the smart digital workplace: opportunities and challenges
8. Attaran M (2017) The internet of things: limitless opportunities for business and society. *J Strat Innov Sustain* 12(20) (2017)
9. Shaikh SA, Kapare AS (2017) Smart office area monitoring and control based on IoT. *IJERCSE* 4(4):5
10. Roe D (Online) CMS Wire, 3 April 2019. Available: <https://www.cmswire.com/digital-workplace/how-iot-impacts-the-digital-workplace/>
11. Pfano M, Beharry A (2016) The effect of modern office technology on management performance. *Probl Perspect Manage* 14(2)
12. Cascio WF, Montealegre R (2016) How technology is changing work and organizations (2016)
13. Buchanan J, Kelley B, Hatch A (2015) Digital workplace and culture
14. Aleksandrova M (Online) IoTforall.com, 11 May 2018. Available: <https://www.ietfforall.com/iot-smart-office-applications/>
15. Huthamah YA, Alruwayyeh A (2018) The effects of technology in the modern office work environment. *Int J Eng Sci* 3(3):7
16. Abbas J, Muzaffar A, Mahmood HK, Ramzan MA, Rizvi SS (2014) Impact of technology on performance of employees (a case study on allied Bank Ltd, Pakistan). *World Appl Sci J* 29
17. Arun S, Likith AR, Dharshan K, Srinivasa N (2019) Smart office monitoring system using IOT. *Int Res J Eng Technol* 6(4):5
18. Aggarwal A, Rozwell C (2018) Make your digital workplace employeefriendly with these six IoT best practices, Gartner
19. CGI (Client Global Insights) (2018) Changing the workplace to empower your digital workforce

Recognition of Dubious Tissue by Using Supervised Machine Learning Strategy



G. S. Pradeep Ghantasala, D. Nageswara Rao, and Rizwan Patan

Abstract Bosom malignancy is the primary stage of disease detection. Classifiers are thus constantly wanted with higher accuracy. A highly accurate classifier gives fewer opportunities to misinterpret a malignant growth patient. This paper explores how the concept of strategic recession is portrayed in a modified, enhanced manner. For minimizing cost efficiency, both inclination plunge and propelled streamlining are used. The theory, which is a sigmoid capacity, involves a weighing dimension of β . The weighting variable depends on the number of highlights, dataset size, and the type of simplification method used. Through correctly estimating β , which is part of the quantity and type of enhancement systems used, the accuracy of the bosom disease position is fundamentally improving. By increasing precision, affectability, and specialty, the achieved results are promising.

Keywords Cancer · Malignancy detection · Support vector machine · Fine needle aspiration · Artificial neural network

1 Introduction

Bosom disease is a disease in the bosom tissue cells caused by a harmful tumor. A threatening tumor is the array of malignant growth cells that can expand into a tissue or spread far away [1]. Uncontrolled increase in bosom tissue cells is bosom development malignant growth. A collection of cells that quickly divide may set up a bump or create mutilations. The method causes of life among women, which legitimately follows lung disease, were bosom malignant growth. Bosom malignancy is a genuine illness that can surely reduce the pace of death early identification. A review of the latest evidence reveals that after 5 years of testing, the stamina rate was 88% and

G. S. Pradeep Ghantasala (✉) · D. Nageswara Rao
Department of Computer Science and Engineering, Chitkara University Institute of Engineering and Technology, Chitkara University, Punjab, India

R. Patan
Department of Software Engineering and Game Development, Kennesaw State University, Marietta, USA

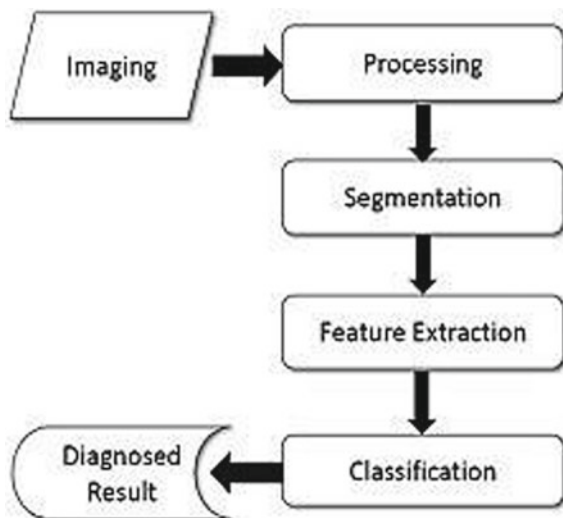
after 10 years of reducing 80% [1]. Popular for identifying bosom malignancy are AI classifiers. There have been some academic projects there. A measurement classifier called —Strategic Regression|| has been modified here to more accurately determine the risk or the benignity of the tumor cell. Computer-aided conclusion (CAD) has finished up an exchange as typical clinical work for recognizing verification of bosom danger on specific test sites mammograms. This seems to be the beginning for CAD associated with and huge inside the differential finding and disclosure of different sorts of irregularities in restorative pictures obtained in a few assessments by utilization of diverse imaging modalities. Truly, in restorative imaging and characteristic radiology, CAD provided one of the basic subjects examined [2].

2 Related Work

In Feng et al. [2] proposed a malignant growth recognition method utilizing clinical inter-preferable highlights. This calculation chips away at K mean bunch and division idea. This comprises such a large number of phases resembling division of cells, highlight taking out, and order strategy intended for the improvement methodology. The first picture be situated separated into portions by utilizing picture division idea of picture handling. In the highlight extraction stage, the highlights are removed from the divided pictures. At last, apply order methods like KNN as well as SVM [3] grounded classifiers, and the outcomes are watched for different pictures and they chose highlights rundown of pictures (Fig. 1).

In Sun et al. [3] proposed another pre-processing procedure for distinguishing lung malignant growth. In this paper, we had another clamor expulsion system for

Fig. 1 Proposed model structure



the input picture to decrease the commotion contrast for info and yield picture. In [4], Hospedales proposed a picture investigation strategy for recognizing malignant growth cells and to check the quantity of cells that drive o disease in unique pictures. The calculation comprises four significant advances like preprocessing, order, bound regions, and cellular checking. In the preprocessing evacuation of clamor, identification was accomplished for a unique picture. Also, the first picture was characterized utilizing KNN [1] calculation after that it will gather into similar bunch esteem. Thirdly, we check the basic cells whichever depend on the yield commencing the second stage [5]. The nearby threshold calculation is utilized for isolating the assured core. The outcomes are great as for blunder proportion and Standard Deviations, in [6]. Thilagavathi et al. exhibited another strategy for checking red platelets utilizing the change procedure. This calculation is utilized for assessing red platelets. This calculation is displayed in 5 phases. Preprocessing, division, picture obtaining, include extraction and checking. In division discover the lower and upper edge esteems and the immersion picture is utilized for preprocessing and apply essential XOR activity for two paired pictures. All in all computerized mammography is one of the main procedures to analyze malignant growth. Such a large number of calculations were proposed dependent on the different grouping issues for the advanced mammography picture. In this different highlight are extricated utilizing the fundamental documentation and are utilizing different standard systems. Around thereof the tumor is determined by utilizing a calculation called MLE [7]. Screwing mammography is probably the most effortless approach to a conclusion the bosom malignancy. By this we discover the edges, smoothening the edges of the picture. At last ascertain the dimension of conveyance, tissues in a picture shorn of division [8]. Nano technology additionally contributes quick also sensitive areas for malignant growth cells. The nano gadgets could remain utilized to recognize cells also murder the tainted cells in a hominoid body. Mello suggested two strategies for distinguishing malignant growth cells in a humanoid body [8]. These two strategies depend happening the distinctive shading. The info picture stays in the RGB shading organization also it is changed obsessed by the HSL shading exemplary. HSL shading model is pragmatic to the binarization. Separating is accomplished on behalf of the binarization picture to smoothen the edges of the picture [9, 10] (Fig. 2).

Tumors can be listed in two wide-ranging cases of breast cancer (Fig. 3) illustrations the interior erection commencing a breast image.

- (a) Benign (Non-cancerous): Benign cases are known as non-cancerous, i.e., non-life-threatening opportunities, which may lead to cancer. In the case of an immune system called a “sac,” benign tumors normally are separated from further cells and distant commencing the body easily.
- (b) Malignant (Cancerous): Cancer twitches with irregular cell growing and may binge or assault tissue adjacent quickly. The heart of malignant tissue is usually significantly greater than normal tissue, which in subsequent phases will jeopardize life.
- (c) Cancer is always cancer that destroys health. Proper cancer treatment saves the lives of people. A highly important move toward the further treatment of cancer

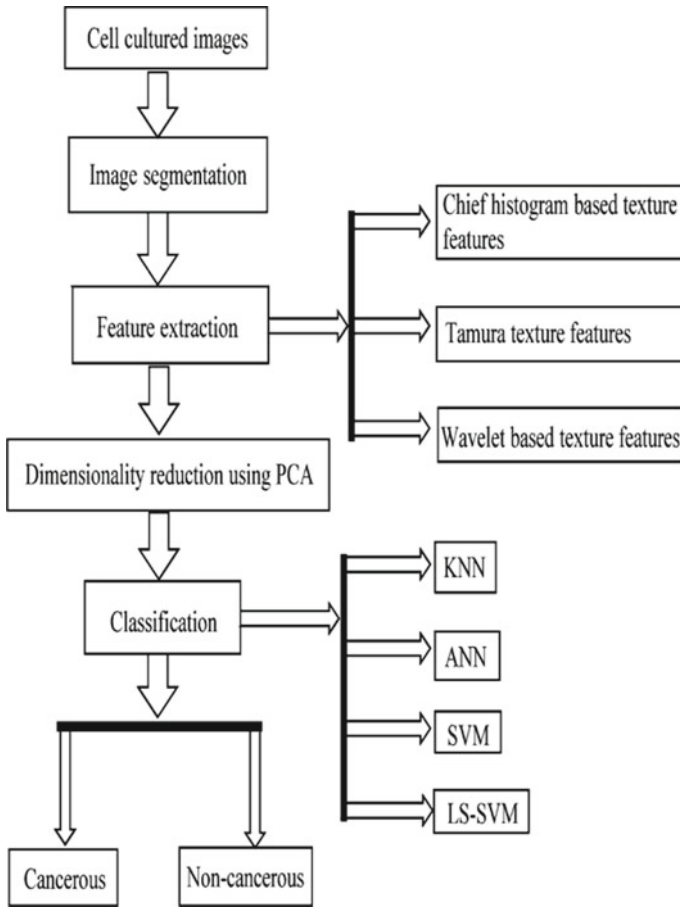


Fig. 2 Flow chart shows the pattern recognition system of breast and normal cell classification

is distinguishing healthy, benign, and malignant tissues. Imaging the intended expanse of the body allows the surgeon and the general practitioner to promote detect benign and malignant diseases. The view of the desired part of the body can be obtained more accurately through sophisticated modern imaging techniques. Medical imaging methods can be classified into two groups centered on the dispersion of the membrane and tissue impairment.

- (d) Noninvasive.: Using an imaging technology similar to SUV (SONAR) in the high-frequency domain, Karl developed an ultrasonic signal system that comprehends a central processing unit (CPU) transducer and screen module as well as some other peripheral devices. Ultrasound: This technology uses similar techniques to SUV (SONAR). This tool can take 2D and 3D images. Exceptions are the creation of a heat bubble around the intended tissue. Ultrasonic procedures have no side effects.

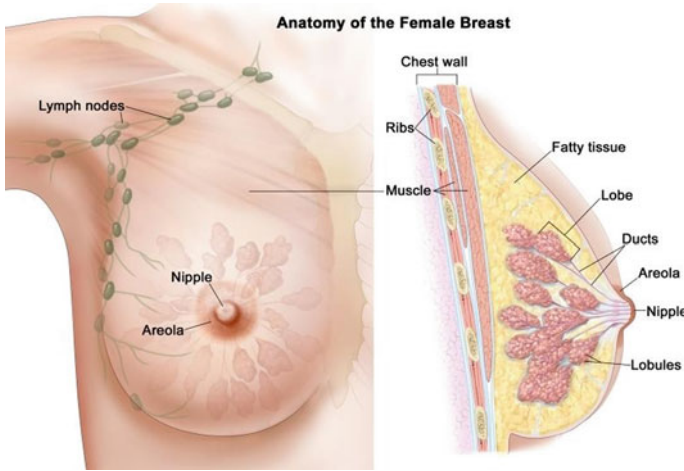


Fig. 3 The female breast anatomy

Fig. 4 Demonstrate benign and malignant mammographic photos (examples of noninvasive image)



(e) Invasive. Histopathological pictures (biopsy pathology): histopathology is a tissue microscopy science. A patient needs to take a variety of surgical precautions to perform the histopathological review. Histopathological images are taken from histopathological tissue (see Fig. 4)

3 Proposed Algorithm

In this section, the proposed algorithm is being discussed.

- (a) Step1: Cancer causes various types of tissue changes; tissue can ultimately cause a change in its physical properties, such as a change in density or porosity if cancer occurs in the tissue itself. Such shifts can be seen in the medical image

as a warning. The role of the learning algorithm is to determine whether a given tissue is cancerous and to select that signal.

- (b) Step2: In segmentation, feature extraction, and grading steps the ML algorithm is applied. The support vector machine (SVM) is one of the best-known and most powerful ML algorithms.
- (c) Step3: SVMs are useful to take in one of two classes a large number of features and discriminate inputs.
- (d) Step4: When trained, SVMs reveal the line or frontier with the greatest margin of separation.
- (e) Step5: This concept can be extrapolated to a wider range of features (or dimensions) in which the line of separation turns into a hyperplane. Give SVMs useful for image processing because of the large number of features which can be combined mathematically.

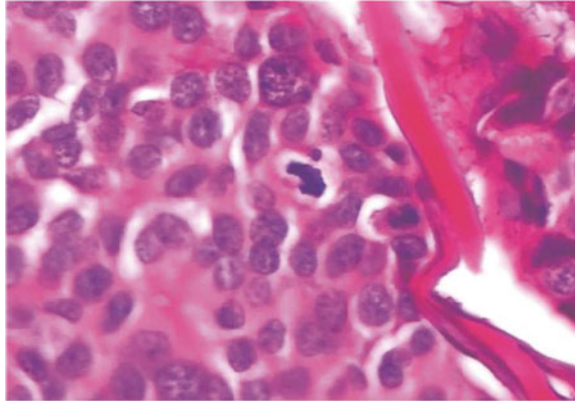
The proposed algorithm consists of diverse stages to categorize cancer cells, calculating cancer cells inevitably. The proposed model assembly is revealed in Fig. 1.

4 Model for Proposed Algorithm

The main objective of this research was to identify cells from cell photographs from breast and other cancer cells by using image processing and AI techniques. Our proposed design for pattern recognition was shown in Fig. 1.

- (a) Image preprocessing: The image preprocessing order is intended to improve the image and to lower the dot without losing the main highlights of BUS images.
- (b) Image segmentation: Image segmentation isolates the image into districts not protected then isolates objects from base. For highlight removal, the disadvantages of the injuries are shown.
- (c) Extraction and collection of features: This is to monitor a list of bosom sores capabilities that can accurately identify wounds, non-sore, or benevolent and risks. The space of the element might be incredibly huge and complicated, so it is important to remove and select the best points. The extraction tool is a process used to obtain different functions from the reduction of image and dimensionality. We used three different techniques for extracting texture from each segmented picture (Chip histogram-based texture, Tamura texture characteristics, and wavelength-based texture)
- (d) Classification: The suspect premises are arranged into different classes, for example, friendly discovery and harm, based on selected features. The primary purpose of this work was to identify breast cancer and non-cancer cells in cell images using scanning and AI techniques. Figure 2 showed our proposed

Fig. 5 Demonstrate benign and malignant histopathological images (examples of invasive images)



pattern recognition architecture. Initially, we added the cells from the context of the object segmentation techniques. From each of the images was extracted the different segmental features, Tamura layout, chip histogram features, and wavelet dependent texture features. The segmentation and abstraction of the object were done with MATLAB in a trendy way. We also merged them to create a list of features to remove all this information. Clear representation is given in Figs. 3, 4 and 5 for the data classification.

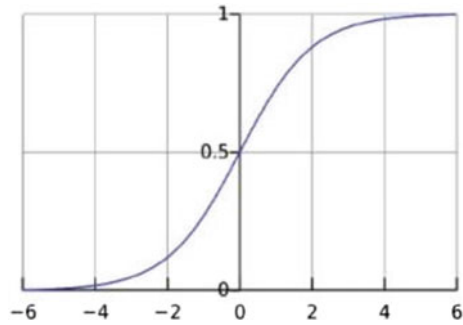
- (e) For example, various AI techniques have been read for more characterization, including straight-discriminatory investigation (LDA), SVM, in addition to artificial neural network (ANN).
- (f) Numerical contemplations: Logistic regression models are typically not as much of numerical and take less time to train compared to ANNs

5 Sigmoid Capacity

As of its non-linearity and computational uncomplicatedness of the subordinate, sigmoid capacity is the most commonly used capability in feed-forward neurotic systems [11, 12].

Sigmoid capacity is the structure's calculated capacity this sigmoid power maps the estimate of the scale from 0 to 1 as shown in Fig. 6. Data sets and their features sigmoid capability have the structure and order specifications for the team. Data sets are required. Dataset is a network that speaks to different highlights. All of the data are provided on different highlights. That section of the dataset refers to the tumor tissue component, and each column tells the number of incidents. Some three kinds of data sets are widely used to classify the malignancy of the bosom.

- (a) Wisconsin diagnosis breast cancer (WDBC)- Each data set of the WDBC has its degree of subtlety [13]

Fig. 6 Sigmoid function

Characteristics: number of ID, diagnosis (M = malignant, B = benign), and 10 true highlights: radius, texture, perimeter, area, smoothness, compactitude, concave, symmetric and fractal concavity [13, 14]. These highlights are a digital image of fine-needle aspiration (FNA) bosom mass. The characteristics of the cells are shown in the picture Fig. 5. At the point where the snake center determines the length of the spiral line segment, subtract the snake concentration distance. The absolute separation of the snake from the back is the atomic limit. The distance from the actual nucleus is determined when the out-stream length of the snake core is contrasted with the single focus of the snake. The whole isolation is the atomic layer of the snake concentration.

Wisconsin prognosis breast cancer (WPBC)- The features of the databases set of WPBC [15] are as follows: ID, the result (recurred, n = no repeat), texture, radius, area, perimeter, compactness, smoothness, and color (SCF), concave focus, symmetry and fractal (CFM), time (r = repeat time, n = SIFF) for each cell basis are recorded in a range of 3 to 33 genuine highlights. The 34 and the 35 status of the lymphatic hub. 34 tumors.

Wisconsin breast cancer (WBC) - Considerable cells in the bunch thickness is usually assembled in monolayers, whereas cancer cells are routinely collected on a multilayer basis. While the malignant growth cells suit as a fiddling in the uniformity of cell size/form. This is why these parameters are important when it comes to whether or not the cells are destructive [12, 13, and 15].

Attributes have 3 attributes, with 3 segments in an information collection, according to the properties of the WDBC / WPBC datasets. Where refers to the configuration default value, S refers to the default and n refers to the sample length. A major decision in building an order model is considerable progress. It is desirable to restrict the number of information qualities in a classificatory so that large, high-performance models are less computational. The two-component selection procedures suggested in this paper were chi-square tests and Central Component Investigation (CCI)

6 Result

Results acquired as of the classical system: The classic calculated relapse starved of the weighted sigmoid work leads to the taking after yield parameters when connected to a dataset with 12 highlights as shown in Fig. 7.

For testing purposes, the parameters were kept indistinguishable for each of the two approved subsets as shown in Fig. 8. We have considered the following parameters:

- (1) Erector Rate: 0.0429
- (2) Sensitivity: 0.9944
- (3) Specificity: 0.8333
- (4) Conspicuous lattice: 178 1 9 45 4.

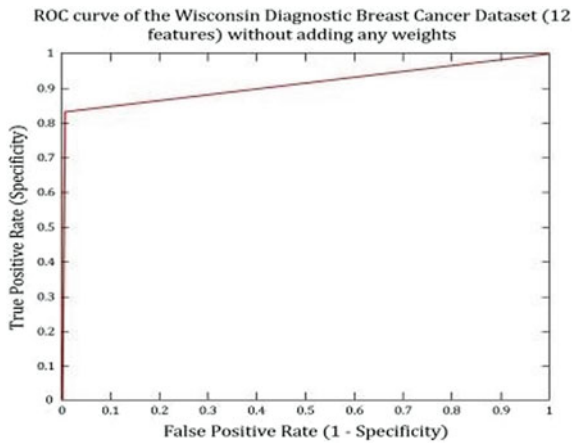


Fig. 7 Result of all the classic dataset method

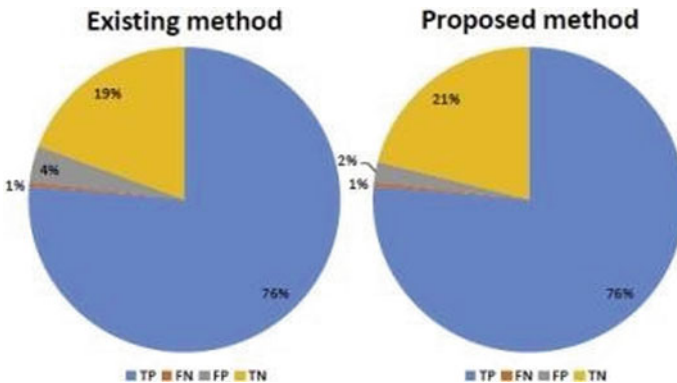


Fig. 8 Sections of the uncertainty grid from current and planned larger dataset strategy

7 Conclusion

After a special load expansion for both datasets, the proposed adjusted sigmoid power effectively improved the display. The pattern of the size of the weighted variable is tracked to maintain the improvement process. With the number of highlights in the dataset, the greatness of the weight is included. Comparative recreations are done to retain the same size but to change the process of development. The estimate of the dynamic loads is also considered to be different under such conditions, which concludes the way that this factor is a component of the information and the improvement process.

References

1. Siegel RL, Miller KD, Jemal A (2019) Cancer statistics, 2019. *CA A Cancer J Clin* 69:7–34
2. Feng Y et al (2018) Breast cancer development and progression: risk factors, cancer stem cells, signaling pathways, genomics, and molecular pathogenesis. *Genes Dis* 5(2):77–106. <https://doi.org/10.1016/j.gendis.2018.05.001>
3. Sun Y-S et al (2017) Risk factors and preventions of breast cancer. *Int J Biol Sci* 13(11):1387–1397
4. Jing-Hao Xue D (2010) Michael Titterington, On the generative–discriminative tradeoff approach: Interpretation, asymptotic efficiency and classification performance. *Comput Stat Data Anal Comput Stat Data Anal* 54(2):438–451
5. Hospedales TM, Gong S, Xiang T (2013) Finding rare classes: active learning with generative and discriminative models. *IEEE Trans Knowl Data Eng* 25(2):374–386
6. Akram M et al (2017) Awareness and current knowledge of breast cancer. *Biol Res* 50(1):33
7. Han Z-Z, Liu P-G, Mao J (2017) A novel method of extracting and classifying the features of masses in mammograms. In: 2017 12th international conference on computer science and education (ICCSE), pp 227–231
8. Salama GI, Abdelhalim MB, Zeid MA (2012) Experimental comparison of classifiers for breast cancer diagnosis. In: 2012 7th international conference on computer engineering and systems (ICCES), Cairo, 2012, pp 180–185
9. Tang J, Rangayyan RM, Xu J, Naqa IE, Yang Y (2009) Computer-aided detection and diagnosis of breast cancer with mammography: recent advances. *IEEE Trans Inf Technol Biomed* 13(2):236–251
10. Ghantasala GP, Kallam S, Kumari NV, Patan R (2020) Texture recognition and image smoothing for microcalcification and mass detection in abnormal region. In: 2020 international conference on computer science, engineering and applications (ICCSEA), pp 1–6. IEEE, 2020
11. Zhou X et al (2012) Invasive ductal breast cancer metastatic to the sigmoid colon. *World J Surg Oncol* 10:256
12. Patan R, Ghantasala GP, Sekaran R, Gupta D, Ramachandran M (2020) Smart healthcare and quality of service in IoT using grey filter convolutional based cipher physical system. *Sustain Cities Soc* 102141
13. Mert A et al (2015) Breast cancer detection with reduced feature set. *Comput Math Methods Med*
14. Kumari NV, Ghantasala GP (2020) Support vector machine based supervised machine learning algorithm for finding ROC and LDA region. *J Oper Syst Dev Trends* 7(1):26–33
15. Aalaei S et al (2016) Feature selection using genetic algorithm for breast cancer diagnosis: experiment on three different datasets. *Iran J Basic Med Sci* 19(5):476–82

Performance Prediction of Students Using Machine Learning Algorithms



Sai Sudha Gadde, Dama Anand, N. Sasidhar Babu, B. V. Pujitha, M. Sai Reethi, and G. S. Pradeep Ghantasala

Abstract To predict the accurate future performance of the students, we consider the data like student's past and present academic records. It is very important to complete student's academics in a successful way. The problem is to identify the students whose performance is poor in their courses. So according to their performance and capability there will be a chance to take some remedial actions. There are many literatures on predicting the grades and improving their accuracy. In this paper, we predict the final grades using naive Bayes algorithm and linear regression to predict the final performance of students so that we can get more accurate values. It issues a forecast for every student exclusively, when the expected exactness of the prediction is adequate.

Keywords Performance prediction · Linear regression · Naive Bayes algorithm

1 Introduction

Making advanced education moderate has a critical effect on guaranteeing the country's financial flourishing and speaks to a focal point of the administration when making training arrangements [1]. To make school more reasonable, it is consequently urgent to guarantee that numerous more students graduate on time through early mediations on students whose execution will be probably not going to meet the graduation criteria of the degree program on time. Besides, new innovation permits for customized training empowering students to take in more proficiently and giving educators the instruments to help every student separately if necessary, regardless of whether the class is extensive [2]. A basic venture toward powerful intercession is to

S. S. Gadde (✉) · D. Anand

Assistant Professor, Department of Computer Science and Engineering, Koneru Lakshmaiah Education Foundation, Vaddeswaram, Andhra Pradesh, India

Present Address:

N. Sasidhar Babu · B. V. Pujitha · M. Sai Reethi · G. S. Pradeep Ghantasala
Student, Department of Computer Science and Engineering, Koneru Lakshmaiah Education Foundation, Vaddeswaram, Andhra Pradesh, Vijayawada, India

construct a framework that can constantly monitor understudies' scholarly execution what's more, precisely foresee their future execution. For example, when they are probably going to graduate and their evaluated last GPAs, given the present advancement. In spite of the fact that anticipating understudy execution has been widely considered in the writing, it was principally examined with regards to taking care of issues in finishing courses [3].

Using the understudies past execution in all courses that he/she has finished expands multifaceted nature as well as presents commotion in the expectation, in this manner debasing the forecast execution. Evaluations should be shortened in a solitary number or letter how well an understudy could comprehend and apply the information passed on in a course. Along with these it is important for understudies to acquire the vital help to pass and do well. With extensive class sizes at colleges which have experienced a quick improvement in the recent years, it has turned out to be incomprehensible for the teacher also, instructing colleagues to monitor the performance of every understudy independently [4]. This can prompt understudies flopping in a class who could have passed if proper healing moves had been made sufficiently early. We center on foreseeing student's GPAs yet the general system can be utilized for other understudy performance expectation undertakings. In this paper, we used two algorithms, naïve Bayes and linear regression to predict the final grade of the student [5]. Hence, it is very important to use personalized algorithms to predict the performance of understudies to complete their graduation.

We plan a review forecast calculation that finds every understudy the best time to foresee his/her review with the end goal that in view of this expectation, a convenient mediation can be made whether vital. A convenient prediction dependent on the only restricted information from the course itself is trying for different reasons. Initially, most of the students get good scores in their courses but later they may get fewer score because of other reasons. Second, regardless of whether a similar material is canvassed in each year of the course, the assignments and exams change each year. Hence, the education of specific assignments with respect to predicting the last grade may change over the long time. Third, each student will be from different backgrounds (courses, specializations). For a few understudies an exact prediction can be made early dependent on the initial performance evaluations. For example, if a student gets the good score in his/her first three semesters we can easily predict his score as there were no fluctuations but it is not equally same for every student for some students it is difficult to predict.

2 Methodology

In this paper, we used two algorithms, naive Bayes and linear regression to predict the final grade of the student. From these predictions we can get accurate predicted grades, and we can also determine which algorithm is best suitable for these predictions.

2.1 Naive Bayes

Naive Bayes classifier depends on Bayes theorem in which the predictor's independent assumptions are considered. Even for very large datasets it is easy to build naïve Bayesian model with no complex iterative parameters. It is the most frequently used algorithm to improve more developed classified models. We consider past and present scores like CGPA's of every student to build a model for predicting the performance accurately.

$$P\left(\frac{E}{x_1, x_2, \dots, x_n}\right) = \frac{P(E) * P\left(\frac{x_1}{E}\right) * P\left(\frac{x_2}{E}\right) \dots P\left(\frac{x_n}{E}\right)}{\sum_{i=1}^n x_i * P(x_i)}$$

The above equation includes both the chain rule and condition, where 'E' is denoted for the event which is conditioned on $x_1, x_2, x_3, \dots, x_n$. Through this equation we get the outcome which has more probability and satisfies the conditions [6]. We consider past and present scores like CGPA's of every student to build a model for predicting the performance accurately.

2.2 Linear Regression

Linear regression is a type of algorithm which is mainly used for analyzing the future predictions and also to study the relation between two parameters. The main idea of regression and the process is illustrated by Fig. 1, depends on two points. First one is to check whether the two variables considered to predict the output are enough to get efficient outcomes. Second one is to identify the variables which are significant enough to get the outcomes in particular [1, 6–8]. We initially built a linear model by using the past semester CGPA's as dependent variables. Using this model which is built we predict the final grades of students.

From the algorithms which were used for predicting we can determine the algorithm through which we obtained accurate result.

3 Experimental Results

The dataset used to test the method is collected from a private institution. The dataset consists of the student previous academic performance and current academic performance details. Previous performance details consist of student secondary school percentage and intermediate percentage, and the current performance has consisted of overall SGPA till date [9]. We had taken the dataset of the graduates in the year 2013.

Fig. 1 Linear regression

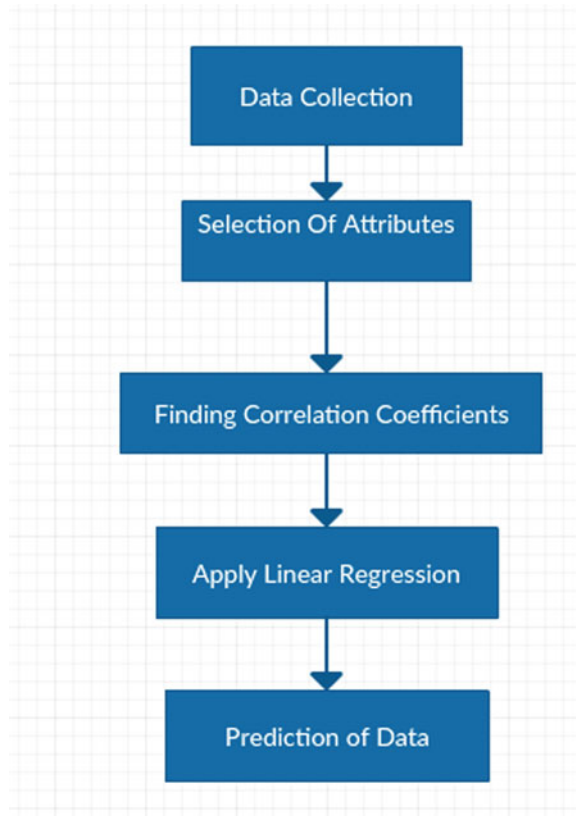
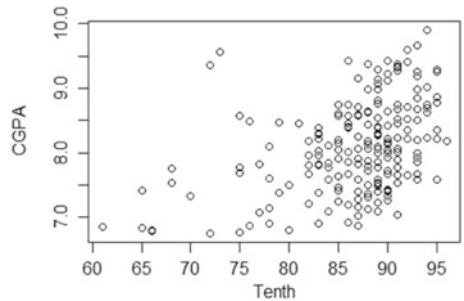


Fig. 2 Correlation between tenth and CGPA



The dataset has 200 professional graduate students who enrolled in the Computer Science and Engineering Stream of Bachelor’s and technology. In the dataset each student’s Id number, name, Tenth marks, Inter marks and current CGPA are mentioned [3]. Due to limitation of the dataset, we use only tenth, inter, and current CGPA percentage as static features.

Figure 2 indicates the correlation between the student’s tenth marks and present CGPA and Fig. 3 represents the correlation between the Inter percentage of the student and the CGPA of the student in the bachelor’s degree. The students having the best score in tenth can also have good percentage in the bachelor’s degree but when we compare the correlation between tenth and CGPA it is less with the correlation between the inter and CGPA. Now we can check the correlation between the current CGPA (SGPA) and the cgpa to use as the best fitting attributes. In Fig. 4 the correlation between the SGPA and CGPA can be clearly visualized [10].

The correlation coefficient between SGPA and CGPA is 0.74503, having high correlation coefficient we do not consider the tenth and inter percentage for the regression. The correlation coefficient between tenth and CGPA is 0.40560 and the correlation coefficient between inter and CGPA is 0.48023. The tenth and inter percentages has less predictive power than the SGPA. The SGPA consists of over all marks of the student in various core or elective subjects. SGPA is having the highest correlation with the CGPA [5].

We performed the data processing on the dataset of the student initially and removed the unnecessary and noisy data from the dataset. Next, we apply linear regression, a supervised algorithm of machine learning algorithms for the classification and regression [11]. The linear regression is used for the regression of large datasets and predict data. Figure 5 illustrates the predicted data after applying the linear regression for the taken dataset. Figure 6 also illustrate the predicted data,

Fig. 3 Correlation between inter and CGPA

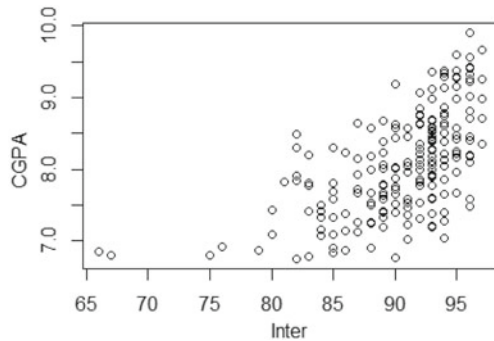


Fig. 4 Correlation between SGPA and CGPA

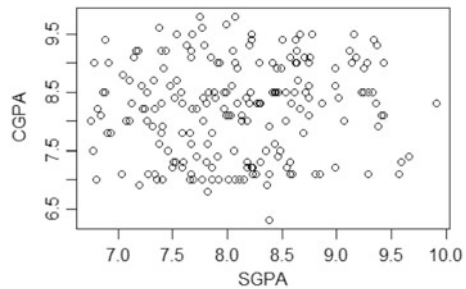


Fig. 5 Predicted data

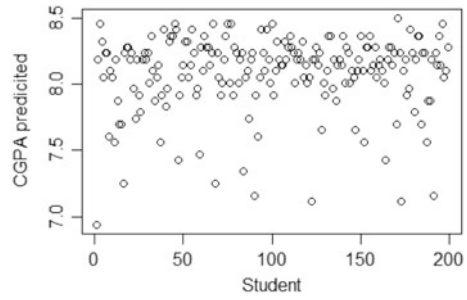
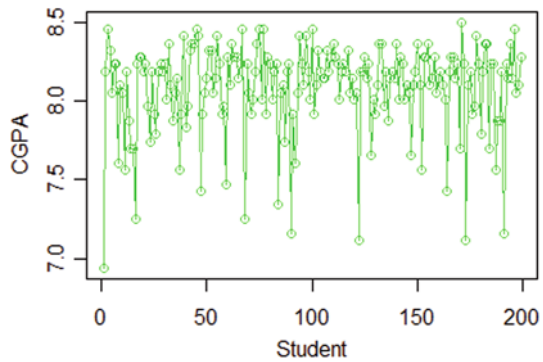


Fig. 6 Linear plot of predicted data



where linear plot is used to the predicted data for better understanding. We also apply naive Bayes algorithm for the prediction. The predicted data is similar to the linear regression and the data is accurate. Both the algorithms predicted the best performance of the student.

4 Conclusion

In this paper, we have used two machine learning algorithms namely, linear regression and naive Bayes for predicting students future performance using current and past performance of the student. Our numerical result show that linear regression is more accurate than naive Bayes. By predicting the student performance we can analyze that wheather the students need any further remedial action that may improve the future performance of the student.

References

1. Anand D, Satyavani AV, Raveena B, Poojitha M (2018) Analysis and prediction of television show popularity rating using incremental K-means algorithm. *Int J Mech Eng Technol* 9(1):482–489
2. Marquez-Vera C, Romero C, Ventura S (2010) Predicting school failure using data mining. In: *Proceedings of 2011 4th international conference on educational data mining*
3. Majeed EA, Junejo KN (2016) Grade prediction using supervised machine learning techniques. In: *e-Proceeding of the 4th global summit on education 2016, Kuala Lumpur, 14–15 Mar 2016*. e-ISBN 978-967-0792-07-1. Organised by <http://worldconferences.net/home>
4. Huang S, Fang N (2013) Predicting student academic performance in an engineering dynamics course: a comparison of four types of predictive mathematical models. *Comput Educ* 61:133–145
5. Brinton CG, Chiang M (2015) MOOC performance predicting via click stream data and social learning networks. In: *Proceedings of 2015 IEEE conference on computer communications (INFOCOM)*, pp 2299–2307
6. A survey on microcalcification identification and classification using CAD System (2015) *Int J Emerg Technol Innov Res* 2(5):186–190. www.jetir.org. ISSN: 2349-5162. Available: <http://www.jetir.org/papers/JETIR1805783.pdf>
7. Pradeep Ghantasala GS et al (2016) *Int J Res Eng IT Soc Sci* 06(09):50–54. ISSN 2250-0588. Impact Factor: 6.452
8. Kumari NV, Pradeep Ghantasala GS (2020) Support vector machine based supervised machine learning algorithm for finding ROC and LDA region. *J Oper Syst Dev Trends* 7(1):26–33
9. Meier Y, Jie X, Atan O, van der Schaar M (2016) Predicting grades. *IEEE Trans Signal Process* 64(4):959–972
10. Xu J, Moon KH, van der Schaar M (2017) A machine learning approach for tracking and predicting student performance in degree programs. *IEEE J Sel Top Signal Process* 11(5)
11. Iqbal Z, Qadir J, Mian AN, Kamiran F. Machine learning based student grade prediction: a case study

Pedal Operated Weeder for Eco-Friendly Management of Aquatic Weeds



R. B. Choudary, B. Ajayaram, A. Ravi Kant, K. D. A. N. V. S. Prakash,
and K. S. Manikanta

Abstract A pedal operated weeder is designed, developed, and tested for harvesting aquatic weeds in small and medium-sized lakes. Harvesting was performed in the lakes in the locality within the Eluru district. The harvests were weighed during the test period at an interval of one hour. Machine capacity and efficiencies were evaluated to assess the performance. The harvest capacities were in the range of 65–222 kg/h averaging at 112 kg/h as against the mean capacity of ~100 kg/h using conventional way. The aquatic weed weeder driven by the pedal is a viable strategy for eco-friendly management of small ponds infested with weeds.

Keywords Aquatic weed · Weeder · Pedal operated system

1 Introduction

Dense growths of algae and other aquatic plants (such as hyacinth, hydrilla, and duckweed) in canals and fish ponds pose a serious threat to aquatic life by depleting the dissolved oxygen, giving rise to reduced survivability of the fish [1, 2]. Their rapid growth rate and adaptability allow them to grow almost anywhere. The production of fishes is affected by the presence of aquatic weeds and worsens as the weeds grow thicker and cover the entire water body. As a consequence of this, the level of oxygen is further reduced leading to suffocation of fishes. Fishes are more vulnerable to the floating and submergible aquatic weeds as they become extremely dense. They block the sunlight from reaching the living plants or algae and prevent photosynthesis. In addition, decomposers further deplete the oxygen levels. The foul smells resulting

R. B. Choudary (✉) · K. D. A. N. V. S. Prakash · K. S. Manikanta
Sasi Institute of Technology and Engineering, Tadepalligudem, West Godavari, Andhra Pradesh
534101, India

B. Ajayaram
L&T Technology Services Limited, Hyderabad, Telangana 500081, India

A. Ravi Kant
National Institute of Technology Rourkela, Rourkela, Odisha 769008, India

from decomposition attract mosquitoes and other parasites to grow in these situations, increasing risks of malaria, yellow fever, and encephalitis.

Weed control is done through use of chemicals such as the herbicides [3]. Although herbicides can be effective in controlling weeds, they also pose a damaging impact on living beings such as wildlife, fish, and desirable plant life. Regular treatment may be required for adequate control of weeds. Despite numerous methods of managing weed, biological control of submersed aquatic weeds still remains an issue as of today [4–6]. Harvesting by hand or using power weeders is an alternative method of weed control, however is expensive [7]. Mechanical control is a viable option to weed control, where vegetation can be removed quickly from flood control structures, bridges, or shipping channels. They can collect floating plants. Crusher boats are used as mechanical weeders in weed harvesting. Special equipment has been designed to cut weeds using a simple cutter, similar to a grass trimmer, to remove weeds from the ponds [8]. The development of an improvised manual aquatic weeder will allow them to remove aquatic weeds at an early stage and deport them to the coast. Weeds that have infested deep into the water bodies require removal of the upper portion of the plant from five to ten feet below the water surface. For better weed control, the same area may need to be treated twice or more [9]. Aquatic weed harvesting at a large scale was tried as an experiment. For example, the San Francisco Estuary Institute (SFEI) organized an experiment for controlling *Eichhornia crassipes* by shredding the water hyacinth at the Dow Wetlands Preserve in Antioch, California [10]. Small, shallow canals, and ponds are often not suitable for large aquatic weeders, commercially available in western countries. Escalating labor costs make aquaculture unprofitable. Most small farmers get work a few days in a year. The development of an improvised pedal aquatic capture system will help eliminate aquatic weeds at an early stage [11]. The farmers can do this work on their own and save labor charges. Thus, the weeder will empower the aqua farmers.

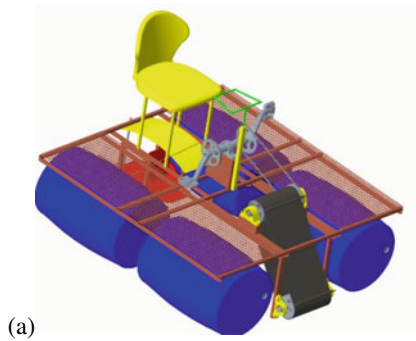
In this work, we have designed a pedal operated weeder for eco-friendly management of aquatic weeds. We have determined the performance of the weeder by conducting initial studies at a lake that is infested mildly with the weeds (majorly the water hyacinth) at Eluru.

2 Materials and Methods

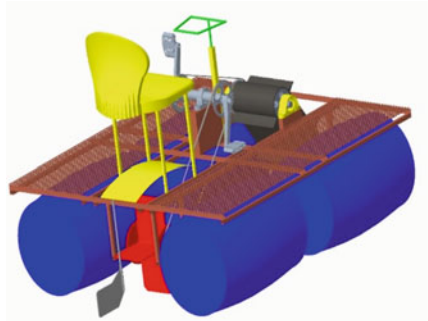
2.1 Design of the Aquatic Weeder

Pedal drive of the aquatic weeder (Fig. 1) was mounted on a raft. The raft was made from recycled plastic barrels. The weeder can be run throughout the day with a little effort. The main frame of the weeder was built in square section MS (size: 25 × 25 mm, thickness: 2 mm). The design employs a variety of “pods” placed between the barrels. The pod system allows the conveyor, drive, propeller, and rudder to be placed directly in the rectangular frame with no likely damage to equipment while taking to

Fig. 1 CAD model of aquatic weeder showing front (a) and rear view (b) together with the prototype (c)



(a)



(b)



(c)

the water. A conveyor belt was placed at the front end of the weeder. It is pedaled by the farmer. The cycling motion is transmitted to the conveyor through a chain mechanism. The conveyor has a provision to be tilted up and down. The conveyor points downward during weed collection and points upward while unloading the weeds on the shore. The propeller attached to the bottom of the raft is operated by pedaling. A rudder was installed at the rear to direct the weeder. An adjustable seat was provided above the propeller. The operator can pedal on the propeller, the conveyor, and direct the weeder comfortably seated on the seat. The seat, steering wheel, and pedals

were ergonomically designed. Some hand tools were ergonomically designed and manufactured to assist the operator in manually picking up leftover weeds.

Conveyor: A lightweight multilayer conveyor belt was used. The reinforcing fabric is made up of polyester.

Propeller: The propeller transmits power by converting rotational motion into thrust. A propeller works by accelerating the water backward.

Raft: A raft is the waterborne structure of a weed weeder. Above the raft are the superstructure and the weed tray. The barrels were purchased from local lubricant retailers. The barrels were air sealed. Four barrels (200 l) were used to support a raft of size 2400×1500 mm. A galvanized iron section was used to make the frame rust free. The total cost of the raft was around Rs. 5000/-, which is relatively cheap for a weeder. The inside diameter and the height of a barrel are, respectively, 572 mm and 851 mm.

Rudder: An outside rudder is attached at the rear of the weeder. The farmer controls the direction of the weeder by turning the handle connected to the rudder by cables. The rudder can be used as a brake by rotating it at right angles to the longitudinal axis of the weeder.

Accessories: The chair has been designed to offer more comfort to the farmer.

Casing: It acts as protective covering for the propeller fitted at the rear end of the weeder. It helps in removing any sprinkling which would sprinkle the water toward the farmer on the seat. Casing is essential for the extended life of the boat. The grill housed in the casing protects the farmer. Good casing increases the life of weeder. The casing is 400 mm in length, and curve has a radius of 700 mm.

Pedals: Basic platform type pedals were used in the weeder. They are commonly found on children's bicycles. The simplicity of use and the lack of specialized shoes are the advantages. However, no power is transferred to the pedals during the upstroke. The feet slips off pedals.

Cutter: A lever operated cutter with a spring loaded blade is mounted in front of the conveyor. A cable connected to the lever pulls the blade down severing the weed mat. On releasing the lever, the springs bring the blade back to its normal position. The cutter is used to care for thick mats of weeds (Tables 1, 2 and 3).

Considering the flow is laminar, the drag coefficient C_D for the long cylindrical body relates as a linear function of Reynolds number Re , and assumes a value close to 0.5 for the drum with conical ends. Further, considering that the resistance from wind is negligible, the pedaling force developed equates the drag force of the weeder. The pedaling force relates to square of the velocity, so at 1 m/s speed, the pedaling force to be developed is close to 64.21 N, and at a higher velocity of 2 m/s, the pedaling forces required are 256.84 N (Table 4).

Table 1 Specifications of the aquatic weeder

Component	Value
Seating	1
Propeller	1
Pedals	1 pair
Conveyor	1100 mm × 450 mm (dimension) 30° (inclination)
Rudder	1
Barrel material	PVC
Conveyor material	Nylon fabric-reinforced rubber belt

Table 2 Principal dimensions of the aquatic weeder

Variables	Description	Value (m)
LOA	Length overall	2.4
LWL	Length of water line	0.69
LBP	Length between perpendiculars	0.54
<i>B</i>	Breadth	1.5
<i>D</i>	Depth	0.2
BWL	Beam on waterline	0.179
<i>T</i>	Designed draft	0.12

Table 3 Hydrostatic data

Variables	Description	Value
W_{ls}	Light ship weight	0.0165 t
W_{dead}	Dead weight	50 t
V_d	Displaced volume	0.006 m ³
ρ_w	Density of freshwater	1.000 t/m ³
ρ_{salt}	Density of salt water	1.025 t/m ³
W_d	Displacement	0.006 t
LCB	Longitudinal center of buoyancy	0.414 m

2.2 Methodology

We define the following terms:

- (1) Machine capacity

$$MC = W/T \quad (1)$$

where W = weight of weeds processed in kg, T = time in hours. It was estimated that 30% of the time is spent in traveling, manual picking, and unloading the weeds. So, to take into account the above, a factor of 0.7 is introduced as a correction to

Table 4 Design details of the weeder

Parameter	Known values	Calculation
Weeder capacity	Drum dia. $D_d = 0.572$ m	Max. weight that can be sustained $V_d = 4\pi R^2 H = 0.8747 \text{ m}^3$ $W_{H_2O} = W_{max}$ $W_{max} = \rho_w V$ $W_{max} = 1000 * 0.8747 = 874.7 \text{ kgf}$
Max. draft	Weight of weeder = 180 kg Weight of human = 70 kg	$W_{harvester} = 180 + 70 = 250 \text{ kg}$ $W_{harvester} = W_{displaced}$ $4\pi R^2 H \rho_w = 250$ $H = 0.243$
Drag force on drum	Cylinder, $C_D = 0.82$ Hemi-spherical, $C_D = 0.42$ Cone, $C_D = 0.5$ Streamline, $C_D = 0.04$	$F_D = 105.3 \text{ N}$ $F_D = 53.94 \text{ N}$ $F_D = 64.21 \text{ N}$ $F_D = 5.14 \text{ N}$

Eq. 1, resulting in assessment of the practicable machine capacity,

$$MC_p = 0.7 * W / T \tag{2}$$

(2) Efficiency

$$\xi = W_{wc} / W_{wp} * 100 \tag{3}$$

where ξ is the percentage machine functional efficiency, W_{wc} is the weight of weed collected in kg, and W_{wp} is the weight of weeds present in the lake loaded into the machine in kg units.

Considering the harvest area, the weeder was tested in few lakes in the Eluru district, Andhra Pradesh. The study was conducted over a course of eight weeks. Field capacity and weeding efficiency were determined. The aquatic weeds were collected with the help of a weeder. The experiment has been replicated ten times. The experiment was conducted for 7 h with one-hour lunch break. The weight of weed was measured in one hour intervals using a stopwatch and weighing machine. The mesh placed on the deck ensures draining of water. The machine capacity (MC) in kg/h, and the efficiency (ξ) were determined using Eqs. 1, 2, and 3, respectively.

3 Results and Discussion

The weight of weeds collected during the test period was determined at an interval of one hour. Excerpts (two weeks) of results of the harvest are presented in Table 5. The amount of weeds harvested was 65 kg/crew-h on day 1 and ranged from a minimum of 65 to 222 kg/crew-h per day (Table 5). While the weeds were unevenly distributed across the lake, the amount of harvest does not indicate the capacity of the weeder, however, provides a good estimate. Further, while performing the work at higher capacity, it does not guarantee the complete elimination of the weeds. Also, the capacity of weeds harvested also depends on the depth of the conveyor below the water surface and width of the conveyor.

The efficiency of the weeder was determined to be 65% as compared to conventional harvesting of 90% efficiency (Table 6). This low value is due to the choice of a narrow conveyor belt width that is housed. A wider conveyor belt will increase the load demand of the cycling which necessitates for increased effort by the individual. Therefore, we made choice for an optimal width of the conveyor. The second reason for the low efficiency is the inability of the weeder to pick up weeds due their

Table 5 Harvesting production in the lakes at Eluru district

Day	Transport loads harvested		Crew harvesting hours		Load per hour		*kg per crew hour	
	W	M	W	M	W	M	W	M
14	9	11	7	6	1.3	1.8	65	80
15	3	10	2	4	1.5	2.5	75	120
16	2	8.5	2	3.5	1.0	2.4	95	115
17	22	8	6	3	3.7	2.7	222	140
18	11.5	2	6	1	1.9	2	95	85
19	6	15	3	7	2.0	2.1	100	105
20	4	7.5	1.5	5	2.7	1.5	135	75
21	12	5	4.5	2	2.7	2.5	121.5	120
22	4	3	1	1.5	2.9	2	145	85
23	16	11	7	5	2.3	2.2	115	110
24	11	6	6	3	1.8	2	90	85
25	9.5	13	5	7	1.9	1.9	95	82.5
Total/avg	110	100	51	48	2.14	2.13	112.8	100.2

W represent weeder and M for manual. Experiment is performed during month of November 2019

Table 6 Machine capacity and efficiency of the weeder

Machine capacity (kg/h)		Machine efficiency (%)	
Conventional	Weeder	Conventional	Weeder
100	112	90	65

entanglement. The present model houses a moderate capacity of weed tray which is sufficient for small lakes without frequent unloading. While for larger lakes, the tray size may need to be increased further.

4 Conclusions

A pedal operated aquatic weeder is designed and tested for harvesting aquatic weeds in the lakes. Due to its relatively small size and weight, it is easy to install and use. The weeder offers a potential solution to small and medium size lakes for the purpose of aquatic weed harvesting. The amount of weeds harvested was 65 kg/crew-h on day 1 and ranged from a minimum of 65 to 121.5 kg/crew-h per day. Though they suffer from lower efficiency of harvesting compared to conventional means, the amount of effort involved is minimized which makes it better than the conventional ones. Worker need not walk into water, and therefore, the work is safe and worker-friendly.

Acknowledgements We express sincere gratitude to NewGen Innovative Entrepreneur Development Cell, Sasi Institute of Technology and Engineering for their support and guidance for carrying out this work.

References

1. Hussner A (2009) Growth and photosynthesis of four invasive aquatic plant species in Europe. *Weed Res* 49(5):506–515
2. Charudattan R (2001) Are we on top of aquatic weeds? Weed problems, control options, and challenges. In: British crop protection council symposium proceedings, 12 Nov 2001, no 77, pp 43–68
3. Durborow R (2014) Management of aquatic weeds. In: Recent advances in weed management. Springer, New York, pp 281–314
4. Hamill AS, Holt JS, Mallory-Smith CA (2004) Contributions of weed science to weed control and management. *Weed Technol* 18(sp1):1563–1565
5. Timmons FL (2005) A history of weed control in the United States and Canada. *Weed Sci* 53(6):748–761
6. Cuda JP, Charudattan R, Grodowitz MJ, Newman RM, Shearer JF, Tamayo ML, Villegas B (2008) Recent advances in biological control of submersed aquatic weeds. *J Aquat Plant Manag* 1(46):15
7. Shelton J, Murphy T (2011) Aquatic weed management: control methods. Shareok.org
8. Janardhan GG, Varghese CS, Babu A, Cherian A (2016) Smart technology in weed removal from lakes. UG project report, no.: 39S_BE_0038. New Horizon College of Engineering, Bengaluru
9. Kimbel JC, Carpenter SR (1981) Effects of mechanical harvesting on *Myriophyllum spicatum* L. regrowth and carbohydrate allocation to roots and shoots. *Aquat Bot* 11:121–127
10. Greenfield BK, David N, Hunt J, Wittmann M, Siemering G (2003) Aquatic pesticide monitoring program: review of alternative aquatic pest control methods for California waters. Unpublished report for San Francisco Estuary Institute
11. McCiagh JC (1977) Pedal power: In: Leisure and transportation. Rodale Press, USA

Ergonomic Evaluation of the Three Implements of the Manual Weeder for Farmers



R. B. Choudary, A. Ravi Kant, B. Ajayaram, and B. Madhuri

Abstract Tools used in farming pose risk for various musculoskeletal disorders since it involves performing operations continuously in an unfavorable posture. In addition, psychosocial factors influence the health of farmers. In this work, three farmer-friendly multipurpose manual weeders were designed and compared with conventional ones, with a view of suppressing the risks for musculoskeletal disorders. Fourteen students participated in the study including questionnaire administered prior to the start and during the study. The volunteers found the second implement of the weeder is more convenient than the rest of the two implements and conventional weeders. Although there is excess energy expenditure, it appears that this excess energy is utilized for the physical work can increase the field capacity of the weeder. In conclusion, the use of the second implement of the weeder could improve the field capacity of weeding while ensuring lower musculoskeletal pain (MSP).

Keywords Ergonomics · Weeder · Heart rate · Musculoskeletal pain

Nomenclature

AHR	Average Heart Rate
ARgHR	Average Resting Heart Rate
AHR	Average Heart Rate
ARyHR	Average Recovery Heart
AWHR	Average working Heart Rate

R. B. Choudary (✉) · B. Madhuri

Sasi Institute of Technology and Engineering, Tadepalligudem, West Godavari, Andhra Pradesh 534101, India

A. Ravi Kant

National Institute of Technology Rourkela, Rourkela, Odisha 769008, India

B. Ajayaram

L&T Technology Services Limited, Hyderabad, Telangana 500081, India

CCR	Cardiac Cost of Recovery
CCW	Cardiac Cost of Work
<i>D</i>	Duration
HR	Heart Rate
MSP	Musculoskeletal pain
PCW	Physiological Cost of Work
RT	Recover Time
TCCW	Total Cardiac Cost of Work
TTW	Total Time of Work

1 Introduction

Weeders are useful tools for farmers, specially designed to ease the task of removing weeds between the plants. Weeding, however, is majorly done by manual means in India in small and medium holdings. The amount of work spent in manual weeding equates to about ~1000 man-h/ha. It is true that mechanization has backed the growth of agriculture thereby contributing to the national growth. However, to take advantage of the development, it is necessary to facilitate use of proper weeding tools by the farmers who work at small farms under constrained budget. Farmers, however, continue to use the old tools for the weeding. Of these, women also contribute to significant farm operations which are full of drudgery [1].

Manual weeding is an intensive task that accounts for about a quarter of the total labor during the cultivation season [2]. It involves removal of weeds such as the *Carthamus oxycantha*, *Cyperus rotundus*, *Saccharum spontaneum*, *Cynodon dactylon*, *Avena fatua*, *Phalaris minor*, and *Parthenium hysterophorus* that normally infest in large capacities [3]. The work demands ample amount of the physical stress where the individual may have to work in a stooped position, performing the plucking in awkward positions, kneeling often, and continuous movement of the arms, wrists, and shoulder. It is essential that the subject is allowed to work at their own pace in a natural posture so as to perform the work efficiently. In continuation to this, tool should be well designed in a manner that suits the operability of the farmers [4]. Ergonomic designs could greatly reduce the drudgery among the farmers by increasing the operability of the tool and the productivity demands of 60–110 man-h/ham for weeding in black heavy soil and 25 man-h/ha in light soil [5].

Through use of a simulator, ergonomics of weeding was analyzed by using a 20–120 N load at increments of 20 N on the field [6]. The study showed that the “*push–pull operation*” of manual weeders results in generating a peak and continuous load (~60 N) with minimal strain. In another study involving women workers in weeding, a full-scale study was performed to evaluate performance of an improvised weeder [7]. It was found that for an average heart rate during the work session at 112.5 beats/min,

the energy expenditure was found to be at an average of 9.16 kJ/min with the improvised wheel hoe. In dry land, the physical demands were evaluated as having the heart rate of 109.47–130.66 and 130.33–147.52 beats/min by using wheel hoe [6]. The oxygen consumption rate of subjects was in the range of 1.389–1.738 l/min with a wheel hoe. Two long handle weeders were tested for their ergonomic suitability in dryland [8]. The physical demands were measured for oxygen consumption rate at 1.38 l/min for the first model and 1.20 l/min for the second model. The study indicates that the physical requirements of the oxygen levels are low with second weeder and is suitable for performing operation over a day-long work. Authors have also taken into consideration the effects of various anthropometric parameters involving stature, elbow, and hand [9]. The study indicated that push force in standing posture was highest among males at 224 N in comparison to females at 143 N, similarly, a pull forces of 218 N (male) and 158 N (female) were registered. The physiological demands were evaluated using cardiac cost 140.2 bpm (male) as against 136.3 bpm (female). In another study [10], the physiological cost of weeding was measured to have a heart rate in the range of 131.0–145.5 beats/min and oxygen consumption rate of 0.80–0.98 l/min. The rate of expenditure of the energy was found to be in the range from 4.01 to 4.90 kcal/min during weeding operation.

In a major study to assess the impact of the tools (which includes—khurpi, wheel hoe, and an improvised grabar) on drudgery, Krishi Vigyan Kendra conducted a survey at two districts of Bihar viz., Vaishali and Muzaffarpur during 2014–17 [11]. The study reported that the improvised grabar was four times more efficient as compared to traditional weeding tools such as khurpi and wheel. The improvised grabar ergonomically suits the farming by avoiding the need for bending or squatting posture during the activity. It reduced the exertion and fatigue and women felt comfortable.

Ergonomic factors play a key role in reducing the drudgery and therefore due consideration has to be given to improvise the tool design [12]. In this paper, the authors evaluated the ergonomics of three adjustable weeders and compared their performance against the age-old weeders used by the farmers such as the crowbar, hand hoe, and the spade.

2 Methodology

2.1 Area of Study

The area of our study is Tadepalligudem, the mandal headquarters of Tadepalligudem mandal in Eluru revenue division, AP. Tadepalligudem is located at 16.8333° N and 81.3500° E and is on National Highway 45. More than 40% of its population depends on agriculture and allied activities for living, although the percentage of the primary sector on the total GDP is slowly decreasing and it counts actually around 20%. This indicates a declining attraction of farming activities when compared to the higher

salaries reachable in other sectors and the better living conditions achievable in urban areas around the city.

2.2 Participants

The study includes volunteers (undergraduate students) from the institute comprising of five females and nine males. The volunteers had an average height of 168.3 (SD = 11.5) cm, an average weight of 76.1 (SD = 10.23) kg and average BMI of 24.4 (SD = 5.23) units. Participants who are unfit for the plowing sessions were excluded from the study. Care was also taken to ensure that the participants are healthy with no history of cardiovascular diseases.

2.3 Experimental Design

The subjects were asked to weed plot 20 * 4 ft. with a conventional hoe. Before beginning the experiment, the soil was sprinkled with water for duration of three hours. The subjects were asked to stop and take rest whenever their heart rate exceeds 130 bpm. After the subjects have finished preparing the soil weeding, they were asked to fill out the Comfort Questionnaire for Hand tools (CQH). Four sessions were conducted every day at 9.00 a.m., 11.00 a.m., 2.00 p.m. and 4.00 p.m. This procedure was repeated for both the conventional hoe (French hoe, Grub hoe) and newly developed ones (weeder 1, 2, and 3) as shown in Fig. 1.

Subjective measurement

To measure localized discomfort we have considered the approach of a body mapping which divides the body into 12 regions [13]. It is a mere representation of the body on a paper, where we chose thermocoal as the material, to capture the discomfort the subject would have felt during the exertion. The rating of discomfort was assessed in terms of first worst, the second-worst, and so on in accordance with a five-point scale [14]. The subject was allowed to refer to the nature of discomfort by fixing a group of



Fig. 1 Three models of manual weeders—weeder 1, 2, and 3. *Note* During the middle of the 30 min work, if the HR increases beyond 130 beats/min, subject were asked to take rest till HR comes to 72 beats/min

pins on the diagram where one pin represents minimum pain and two pins for a higher pain [15]. To ensure that the musculoskeletal problems were captured effectively, assessment was made on the next day morning, since these pains manifested after some time. The discomfort while performing the task was also registered [16].

Measurement of physiological cost

Heart rate is one of the essential parameters for measuring the energy required for performing various types of operations [17]. A heart rate monitor (CooSpo heart rate monitor chest strap sensor with Bluetooth 4.0 ANT+) was used to capture the heart rate of the subject during the work session. The device allows connectivity with the mobile phone using an ANT plus interface. After receiving the data, the physiological parameters were assessed which include—heart rate at rest, while at work, and during recovery [18]. During the study, the heart rate was found to increase quickly with start of the session and reach a steady-state [19]. The energy costs of operation of the selected weeders were computed.

The heart rate monitoring device was tied to the subject and switched on to register the heart rate at a time interval of one minute. In order to bring down the heart rate to normal value, five minutes of rest was given before the experiment. The subject was asked to perform the work session (weeding activity) for duration of 30 min followed by rest for duration of ten minutes. After the task is completed, we switched off the device; while taking care not to remove the device during the recovering until completion of the recovery phase. We registered the heart rate during each phase of the work session which includes—rest, work, and recovery; while operating with conventional tools (French hoe and Grub hoe) and the three new implements of the weeders (Weeder 1, 2, and 3).

The physiological cost of work (PCW) was calculated as,

$$PCW = \frac{\text{Total Cardiac Cost of Work, TCCW}}{\text{Total Time of Work, TTW}} \quad (1)$$

The amount of stress experienced by the circulatory system was assessed as a summation of Cardiac Cost of Work and Cardiac Cost of Recovery,

$$TCCW = CCW + CCR \quad (2)$$

where, CCW is the Cardiac Cost of Work, and CCR is the Cardiac Cost of Recovery.

We adopted following definition for the CCR as the total number of heartbeats, considering values above the resting level, as required by the subject to perform the task. The CCR is defined as the total number of heartbeats, considering values above the resting level, as taken by the subject during the interval from the end of the session to the return to pre-activity state [20].

$$CCW = AHR * \text{Duration of activity} \quad (3)$$

$$\text{AHR} = \text{Average working Heart Rate} - \text{Average resting heart rate} \quad (4)$$

$$\text{CCR} = (\text{Average Recovery HR} - \text{Average Resting HR}) * \text{Duration} \quad (5)$$

where AHR is the average heart rate.

Energy expenditure (kJ/min) was determined using [16],

$$\text{EE} = 0.159 * \text{HR} - 8.72 \quad (6)$$

3 Results and Discussions

The cardiac parameters and field performance parameters are given in Table 1. The musculoskeletal pains reported by the subjects are shown in Table 2. The musculoskeletal pain was “moderate” for ergonomically designed models when compared to conventional tools among the subjects. Majority of pain as experienced by the workers was in the shoulders, legs, lower arm, mid-back, and neck (Fig. 2). The discomfort experienced by the subject is due to the frequent forward bending involved in weeding with French hoe and grub hoe. The vertical posture, however, results in less pain.

The MSPs were found to be more when operating with French hoe, followed by the Grub hoe (Fig. 2). Weeder 1 and 3 contribute to major portion of the MSP among the three implements of the new weeders. The weeder 2 showed reduced MSP in comparison to the others.

The physiological cost of work (PCW) workers for the French hoe averaged 20.21 at an energy expenditure (EE) of 6.97 kJ/min (Figs. 3 and 4). For grub hoe, the PCW and EE were found to be 23.06 and 7.127 kJ/min. Mean PCWs for the three implements of the weeders—1, 2, and 3 were 32.29, 33.65, and 41.27, and EEs were 7.55, 7.59, and 7.53 kJ/min, respectively. The physiological cost of work (Fig. 3) seems to be less in case of conventional tools than in ergonomic weeders. But keeping the higher output of weeders in mind, it can be concluded that more work can be extracted from weeders without straining the worker much.

The energy expenditure is shown in Fig. 4. Among the three implements of the weeder, weeder 1 and 3 resulted in higher energy expenditure; indicating that it may not be suitable due to use of excess energy to perform the weeding. However, given the MSP distribution of the subjects, it appears that they continue to perform the work without straining. The weeder-2 appears to be more convenient to use in terms of the MSP, whereas no significant differences can be found in terms of EE. As per the study, the weeder-2 has the best ergonomic design.

Table 1 Cardiac parameters and field performance characteristics

Tool	ARyHR	ARgHR	RT	CCR	AWHR	AHR	D	CCW	TCCW	TTW	PCW	EE
I1T1	87.43	83.20	7.00	29.60	109.13	25.93	30	778.0	807.60	37	21.83	7.65
I1T2	92.86	81.60	7.00	78.80	111.97	30.37	31	941.4	1020.17	37	27.57	8.08
I1T3	90.14	80.60	7.00	66.80	111.63	31.03	32	993.1	1059.87	37	28.65	8.03
I1T4	86.57	80.40	7.00	43.20	108.00	27.60	33	910.8	954.00	37	25.78	7.48
I2T1	85.86	82.80	7.00	21.40	102.73	19.93	34	677.7	699.13	37	18.90	6.69
I2T2	90.00	87.20	7.00	19.60	104.83	17.63	35	617.2	636.77	37	17.21	7.01
I2T3	87.86	84.80	7.00	21.40	102.40	17.60	36	633.6	655.00	37	17.70	6.64
I2T4	85.14	82.00	7.00	22.00	108.43	26.43	37	978.0	1000.03	37	27.03	7.55
I3T1	84.86	82.00	7.00	20.00	101.53	19.53	38	742.3	762.27	37	20.60	6.51
I3T2	89.00	86.00	7.00	21.00	105.90	19.90	39	776.1	797.10	37	21.54	7.17
I3T3	90.00	87.20	7.00	19.60	107.87	20.67	40	826.7	846.27	37	22.87	7.46
I3T4	86.14	83.20	7.00	20.60	107.27	24.07	41	986.7	1007.33	37	27.23	7.37
I4T1	82.14	79.00	7.00	22.00	108.30	29.30	42	1230.6	1252.60	37	33.85	7.53
I4T2	87.29	84.20	7.00	21.60	108.03	23.83	43	1024.8	1046.43	37	28.28	7.49
I4T3	87.86	84.80	7.00	21.40	115.33	30.53	44	1343.5	1364.87	37	36.89	8.58
I4T4	81.00	77.80	7.00	22.40	102.10	24.30	45	1093.5	1115.90	37	30.16	6.60
I5T1	90.50	87.20	6.00	19.80	109.20	22.00	46	1012.0	1031.80	37	28.66	7.66
I5T2	90.00	87.00	7.00	21.00	109.80	22.80	47	1071.6	1092.60	37	29.53	7.75
I5T3	84.14	81.00	7.00	22.00	108.57	27.57	48	1323.2	1345.20	37	36.36	7.57
I5T4	80.71	77.60	7.00	21.80	107.40	29.80	49	1460.2	1482.00	37	40.05	7.39
I6T1	79.86	76.80	7.00	21.40	102.73	25.93	50	1296.7	1318.07	37	35.62	6.69
I6T2	82.29	79.20	7.00	21.60	102.93	23.73	51	1210.4	1232.00	37	33.30	6.72
I6T3	81.14	78.00	7.00	22.00	111.77	33.77	52	1755.9	1777.87	37	48.05	8.05
I6T4	85.86	82.80	7.00	21.40	116.00	33.20	53	1759.6	1781.00	37	48.14	8.68

4 Conclusions

Three implements of the weeder were tested to assess their performance and convenience compared to conventional ones. The second implement, weeder-2, was found to be more convenient to use due to its lower MSPs and comparable energy expenditure. Though the EE parameters were relatively higher than the conventional weeders, the subjects did not appear to strain. Mean PCW and EE for the second implement were found to be 33.65 and 7.59 kJ/min, respectively.

Table 2 Survey of the musculoskeletal pains during the activity

Tool	Trial	Shoulders	Upper arms	Lower arms	Upper back	Mid back	Lower back	Buttocks	Thighs	Legs
French hoe	I2T1	2								3
	I2T2	3	1	3		3			2	2
	I2T3	3		2		2	1			3
	I2T4	1	1	2		2		1	2	2
Grub hoe	I3T1	4								
	I3T2	2		2			1	1		3
	I3T3	3		2		1				
	I3T4	3	1	1			1			2
Weeder-1	I4T1	3						1	3	
	I4T2	3				1				3
	I4T3			2		2	2			2
	I4T4	1		1				1		
Weeder-2	I5T1									
	I5T2	2	1	2					2	
	I5T3	1								2
	I5T4					1				
Weeder-3	I6T1	2		2			2		2	
	I6T2		1	1				1	2	2
	I6T3	2		2						
	I6T4	2		1		2	1			

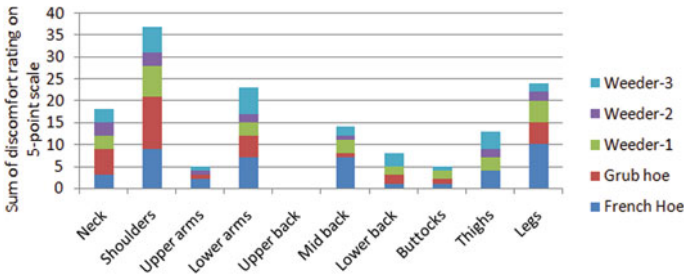


Fig. 2 Distribution of musculoskeletal pains across the various body parts compared for the three implements of the weeder against the traditional ones

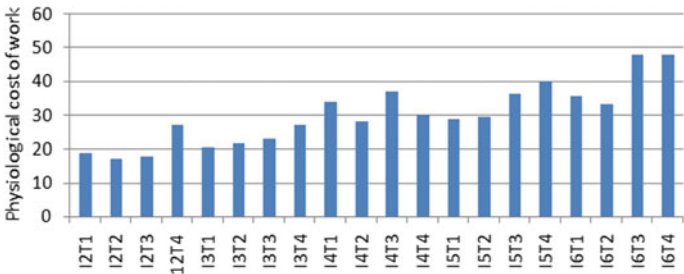


Fig. 3 Physiological cost of work for three implements of the weeder and two conventional weeders; where I denote the implement and T for trial

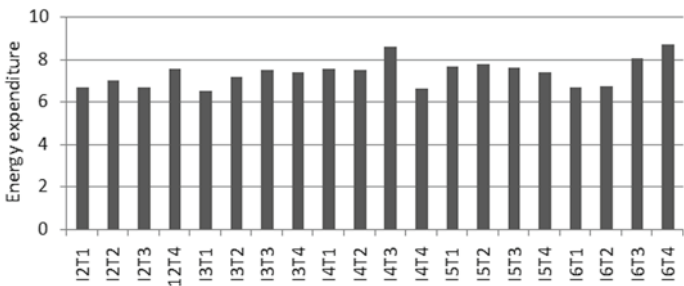


Fig. 4 Energy expenditure for different implements of the weeder

References

1. Singh G (1988) Development and fabrication techniques of improved grubber. *Agric Mech Asia Afr Lat Am* 19:42–46
2. Nag PK, Datta P (1970) Effectiveness of some simple agricultural weeders with reference to physiological responses. *J Hum Ergol* 8:13–21
3. Biswas HS, Ojha TP, Lingle GS (1999) Development of animal-drawn weeders in India. *Agric Mech Asia Afr Lat Am* 30:57–62

4. Grandjean E (1980) *Fitting the task to the man: an ergonomic approach*. Taylor & Francis
5. Singh G (1992) Ergonomic considerations in development and fabrication of manual wheel hoe weeder. *Indian J Agric Eng* 2:234–243
6. Haribabu B, Prakashm RJ, Kumar DA, Prasad P (2015) Ergonomical evaluation of manual and power operated weeders in dry land condition. *Int J Agric Eng* 8:169–174
7. Shilpi V, Shobhanam G, Pachauri CP (2013) An ergonomic study on evaluation of single wheel hoe in reducing drudgery. *Agric Update* 8:665–669
8. Sam B, Regeena S (2015) Development and ergonomic evaluation of long handle weeders for uplands. *Int J Res Eng Soc Sci* 5:1–3
9. Mohanty SK, Jena PP, Mishra JN (2016) Development of dry land weeders with ergonomic principles for higher efficiency. *Int J Innov Sci Eng Technol* 3:340–348
10. Upendar K, Dash RC, Behera D, Goel AK (2018) Ergonomical evaluation of power weeder in wetland paddy condition. *J Pharmacogn Phytochem* 7:2605–2609
11. Shahi V, Shahi B, Kumar V, Singh KM (2018) Performance evaluation and impact of small weeding tools for drudgery reduction of farm women. *J Pharmacogn Phytochem* 5–7
12. Gite LP (1993) Ergonomics in Indian agriculture—a review. Paper presented in the international workshop on human and draught animal powered crop protection held at Harare, pp 19–22
13. Corlett EN, Bishop RP (1976) A technique for assessing postural discomfort. *Ergonomics* 19:175–182
14. Lusted M, Healey S, Mandryk JA (1994) Evaluation of the seating of Qantas flight deck crew. *Appl Ergon* 25:275–282
15. Legg SJ, Mahanty A (1985) Comparison of five modes of carrying a load close to the trunk. *Ergonomics* 28:1653–1660
16. Varghese MA, Saha PN, Atreya N (1994) A rapid appraisal of occupational workload from a modified scale of perceived exertion. *Ergonomics* 37:485–491
17. Cureton TK (1947) *Physical fitness appraisal and guidance*. CV Mosby Co., St. Louis, p 558
18. Tiwari PS, Gite LP (2006) Evaluation of work-rest schedules during operation of a rotary power tiller. *Int J Ind Ergon* 36:203–210
19. Davies CT, Harris EA (1964) Heart rate during transition from rest to exercise, in relation to exercise tolerance. *J Appl Physiol* 19:857–862
20. Saha PN (1976) Practical use of some physiological research methods for assessment of work stress. *J Indian Assoc Physiother* 4:9–13

Blockchain in Smart Healthcare Application



Avnish Vishwakarma, Maniket Kumar, and M. Arvindhan

Abstract A blockchain is a form of distributed ledger technologies, it attracts all stakeholders in many areas, like healthcare application. Its capacity in multi-stakeholders driven sectors such as health is responsible for many investments and studies and implementation. EHR is a system traditionally used to exchange health information between healthcare stakeholders, which exchange has been centralizing power. In this study, an Electronic Health Record (EHR) is an electronic form of clinical history that is kept up by the supplier over the long run and may incorporate the entirety of the key regulatory clinical information applicable to that people care under a specific supplier, including socioeconomics, progress notes, issues, prescriptions. Blockchain is promising to face many EHR challenges, among others which is reliable and secure to exchange data between stakeholders. Several blockchain models in healthcare applications have been published, some are prototype, executed. In our study we encourage PRIZMA framework to explore and evaluate various models. The basic design of our work is that we have to study some research papers and we analyze them found that in the healthcare industry how blockchain is an emerging technology and enhance the performance of industry by using EHR model, Functional Distribution and with the help of technical analysis. EHR, functional distribution and technical study were presented in this study. The technical and architectural analysis was detailed for privacy, security, cost and performance.

Keywords Systematic review · Smart healthcare · Blockchain in healthcare · Electronic health record system

A. Vishwakarma · M. Arvindhan (✉)
School of Computing Science and Engineering, Galgotias University, Greater Noida, Uttar Pradesh, India
e-mail: saroarvindmster@gmail.com

M. Kumar
Computer Science and Engineering, Galgotias University, Greater Noida, Uttar Pradesh, India

1 Introduction

The technology of blockchain is a combination of old-fashioned technology which is popular with white bitcoin paper. Blockchain is now a properly hooked up and ubiquitous technological know-how used from furnish chain administration to fintech. It is poised to trade how the healthcare enterprise manages privateness and healthcare data. In the covid-19 situation in the world, the telehealth turns into an imperative way of caring, it becomes a game-changer in covid-19. The blockchain's sponsors as an alternative to the central system of operating in many other areas that are more than just finance speed, low cost, safety, few mistakes, tolerance of mistakes and the removal of the main point of authority. Blockchain in healthcare application has the power to rework healthcare, placing the patient in the ecosystem of healthcare and increasing the safety, privacy, and secure personal data [1]. This technology could enhance the model for health information shared by making EMR. This technology has transparency and eliminates intermediaries. In Blockchain, the cryptography for verification of the license of transaction and environment. Blockchain technology uses Peer to peer (P2P) network transactions and receive node check messages, if the message is incorrect it does not store them [2]. Then a consensus algorithm works for verification of the data in every block; we call it PoW—Proof of work.

The rest of this article is as per the following. In Sect. 2, arising blockchain and an overview of blockchain in healthcare industry and applications are extensively arranged and the work process from crude information to partners inside medical services. Blockchain design is portrayed. In Sect. 3 we provide work in the prior reviews paper, for which Sect. 4 portrays research methodology in blockchain production network the executives. Section 5 examines late examination of the study findings, Healthcare IoT Infrastructure and Data Security and Artificial Intelligence (Computer-based intelligence).

2 Overview of Blockchain

2.1 *Blockchain in Healthcare Application*

As its core, technical part of the blockchain is beyond the range of this paper. Although, the motive of our discussion is that it is crucial to focus on blockchain concepts, terminologies and features that will make a better understanding of healthcare applications.

The most prominent and remarkable blockchain benefit is to remove centralized third parties in allocated applications. Blockchain is reinventing data modelling due to versatility and ability to secure medical data service. Blockchain becomes the centre of many healthcare industries. In the beginning, all medical data was consolidated into big data which plays a very important role in whole blockchain-based healthcare. The top raw data layer of Blockchain technology is a core framework in chasing to opt

secure architecture as shown in Fig. 1. Healthcare architecture has four components and each has different features. Blockchain platforms which were created and are currently in use for example; Ethereum (Fig. 2), Ripple, and Hyperledger Fabric. Contracts, signatures, wallets, events, membership and Digital assets are the primary components of blockchain in smart healthcare.

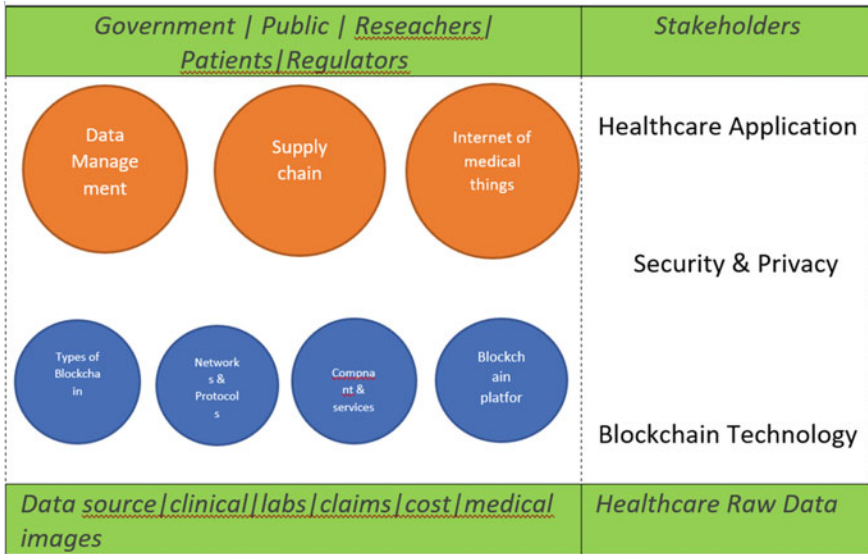
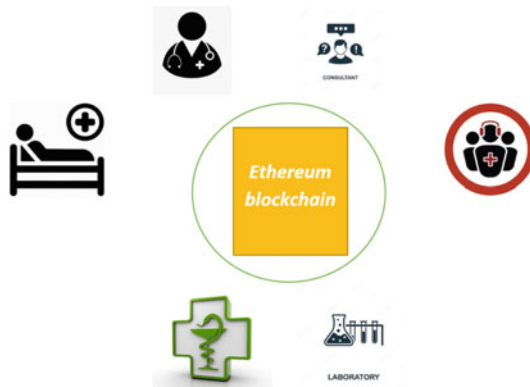


Fig. 1 Functions of blockchain-based healthcare application [2]

Fig. 2 Healthcare data management system [2]



3 Prior Reviews Paper

There are currently various review papers which deal with the application of finance, Internet of Things, energy sectors, government privacy and security in the blockchain domain, in which few review papers denote the application of blockchain technology in healthcare, a wide-ranging criticism of contemporary research on blockchain healthcare application is not covered, like, the work introduced by Mettler gives a short survey of medical services applications that utilize blockchain innovation [3]. The investigation thinks about just three zones, general wellbeing the executives, client situated clinical, and drug forging. In spite of the fact that the investigation was the first to introduce an advanced survey of arising blockchain-based medical services applications, it centres mostly around utilitarian angles and benefits of such innovation. In 2017, Kuo et al. distributed another survey paper on medical care and biomedical applications dependent on blockchain innovation. The work in Kuo et al. for the most part examines customary blockchain innovation (bitcoin highlights) and its design. At that point, the creators depict a few parts of blockchain innovation for the clinical record, the board, protection guarantee measure, biomedical exploration, and wellbeing information record [4]. Also, the creators didn't clarify the specialized perspectives on how the information would be halfway circulated.

4 Research Approach

The Healthcare System involves many stakeholders and it is a very complicated system. In the Healthcare System, Soft System Method is tried and tested method of research action when the requirement of the goal is clarifying its defined system (Checkland and Scholes in 1999), that's why it is best for the domain.

One of the important features of Healthcare Management is the expression of key requirements through the rich picture drawing [5]. It goes through the definition of model root and framework design.

Then the output of the model is validated by some testing by production environment, which means stakeholders conducting interviews that checked whether the blockchain-based healthcare management system can increase the level service and reduced cost. The output after the SHM technique applying, in this case, it will deliver a higher-level service and low-cost outcome [6].

4.1 Step by Step Recording the Data of Patient

In this process, recording the patient's data, you can add more new information related to the patient, but you can't erase the previous data. More the algorithm used in blockchain in healthcare management allows operations to change locally any

patient record, but the data of the initial you will need to get the verification of other users to the entire chain of integrity. All the process will happen automatically. If any information of the patient chain doesn't match the same information on the other system, the data operation is cancelled.

Thus, the whole chain of information must be completed and also no one changed the previous information related to the patient.

On the other hand, there are some advantages. The patient is always sure about his information or data that is safe and can't be changed by any other user. It needs a very important approach to fill the information of patient data. After all, things happen, a mistake happens by the doctor and it can affect the situation unpleasant in future [7].

4.2 Drug Tracking

Everybody knows, in the problem of production in medicine. Blockchain can fix this problem. The transaction between each component to the distributor can be recorded by a chain. Within some second, the system will give permission to easily check the authenticity of drugs, learn from the manufacture and movement history.

5 Study Findings

5.1 EHR Model

Electronic Health Record (EHR), it is a type of digital version of a patient's paper chart of patients. HER are based on real-time, some of the users receive information instantly and securely by patient-centred records [8]. Medical and treatment histories of patients are contained by EHR. The HER system is about building standard clinical data that is collected in the provider office and it can be important for a larger view of a patient's care. It is an important part of health IT and it can contain treatment plans, immunization dates, patient medical history, diagnosis, medication and laboratory and test results. It also gives permission to evidence-based tools that the user can use to make a decision about the care of a patient.

5.1.1 Automate and Modernized Provider Workflow

In faith, the important lineament of an HER record of health information can be managed and created by authorized providers in an illest formed that can be cablevision shared with other providers across many organizations.

EHR systems are built to share patient information with other healthcare organizations, providers and others—such as specialists, laboratories, pharmacies, medical imaging facilities, emergency facilities and workshop clinics and schools—so the records all information from all clinical involved inpatient care [9].

5.1.2 Impact of EHR on Care

Many countries have been radically transformed by the digital world—smartphones, web-enabled devices and tablets have changed our daily lives, and we communicate to others. Medicine is an information-based enterprise. More seamless and greater information flow within a digital care infrastructure, that can be created by electronic health record, leverages digital process and encompasses and can transform the way care is compensated and delivered.

- a. Improve Diagnostic and patient outcomes
- b. Improved care coordination
- c. Improved patient care
- d. Practice care coordination
- e. Improved patient participation.

5.1.3 Advantages of EHR Model

- (1) Helping providers to improve work-life balance and productivity.
- (2) Securely sharing electronic information with other clinic and patient.
- (3) Securely sharing electronic information with patients and other clinicians.
- (4) Enabling the security of patient data and privacy.
- (5) Enabling safer and more reliable prescribing.

5.1.4 What Information Does an Electronic Health Record Contain?

- (1) Medication
- (2) Progress notes
- (3) Administrative and billing data
- (4) Allergies
- (5) Patient demographic
- (6) Immunization dates
- (7) Lab and test results
- (8) Medical histories.

5.2 *Functional Distributions*

Healthcare industries are undergoing clinical innovation items and make their presentation on the lookout, the utilitarian investigation offers an incentive for new items and builds its ability to serve patients consummately. To have a solid relationship tolerant is the way to get the ideal yield by each medical services supplier, yet this time these associations rely upon clinical information from the executives to improve their capacity to treat patients. New information investigation apparatuses joined with various medical care authorities keeping persistent consideration.

Here the terms how a patient-centric CRM system built the relationship with the help of organization data.

Global data makes product design more valuable.

When the healthcare industries provide an offer, it is totally depending on correct diagnostics and proper product design, they need to meet lawful prerequisites. They incorporate usefulness, esteem, multifaceted nature of the plan and by and large execution. As we know that different place has different price value of all medicine and treatment is different but, in this project, we are designing a proper set and considered all the things and all the cost of like medicine, patient treatment, doctor appointment each cost value is similar by using this the patient easily accept all the facilities, in present time as we know that money is everything that's why the accommodation is same. In the event that it cut the expense normally, it has added benefits. In any case, reducing expenses ought not to be the best way to re-design or make any item. Potential item configuration administrations should deal with the accompanying angles if understanding driven CRM is to be constructed [10].

- (1) Most medicated data reduces errors, boosts the quality of controls of servicing for patients from wrong reading and improves payments structure.
- (2) Pouring off an unorganized data which include diagnostics lab tests, patient care records and insurance claims.

5.3 *Technical Analysis*

5.3.1 **Internet of Medical Things**

The Internet of medical things system plays an important job in the improvement of wellbeing and clinical frameworks. With the assistance of the web of clinical things innovation, healthcare apparatus like monitors, body scanners or X-ray and vesture devices can collect, by using this that we can share on the Internet in real-time. For example, with the improvement of artificial intelligence, healthcare providers by using the Internet of medical things we are able to capture the image of small cells and the person who has the right access, only those persons can access all the data.

- *The main source of all the data is patients.*

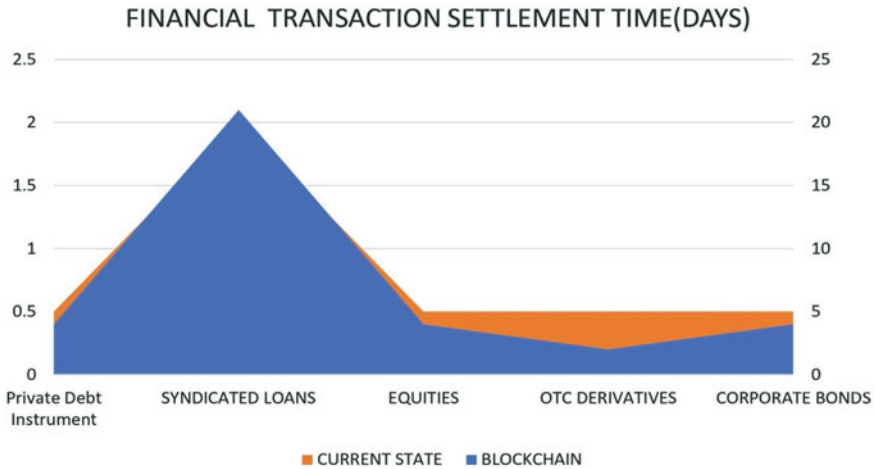


Fig. 3 Trends of blockchain in healthcare financial transaction [10]

- *The Internet of medical things is normally used for generating large scales of data and monitoring patient records (Fig. 3).*

5.3.2 Healthcare IoT and Medical Devices

Internet of Things in healthcare, all the devices are made by using the help of the Internet of Things in this time the machine is automatic. It automatically does everything whatever is required. The data is also machine-generated and the machine-generated data is in an organized way, if we want to read this data we can easily read. For example, many devices are automatic like X-ray machine, there is not any involvement of human beings the machine automatically scans all the thing and generate the data in present time this technology is used for checking coronavirus record the device scan the patient skin and generate the output whether the patient is negative or positive and the data is also updated in real-time, it is very helpful.

5.3.3 Artificial Intelligence

AI also plays important role in smart healthcare system, it is used for like authenticity the person which has valid username and password means if the patient booked an appointment to the doctor by using two things, username and valid id proof, they know the person is authorized. In medical treatment, every machine is automatic because of artificial intelligence, we monitor all the patient activity by using this technology. If a patient wants to book an appointment, medicine, test, or booking seat all the facilities they can access. By the help of artificial intelligence, we can

transfer the record from one place to another place if the receiver end has a valid identity they can access.

6 Conclusion

Our study sets out the answer to the question of the technology of blockchain in healthcare application and their trends. The functional distribution, EHR of blockchain were described and the technical analysis of healthcare classifies as a template through architectures, security, privacy and by performance and cost. In the blockchain platform, we presented a distribution of blockchain, technical analysis of blockchain by reviewed articles, to read published research papers. This study is a summation of the current situation of blockchain in healthcare application and this study shows functional use case of blockchain, and EHR model like health data analytics, data sharing, remote patient monitoring, access control, audit, distributed computing, data storage, data aggregation, electronic medical records, drugs. Our examination shows that blockchain has numerous medical care use cases including the administration of electronic clinical records, medications and drug store network the executives, biomedical exploration and schooling, far off patient observing, well-being information investigation, among others. We also suggest future research also needs to supplement ongoing efforts to determine versatility, waiting for time and security and privacy to use blockchain in healthcare applications.

References

1. Arvindhan M, Anand A (2019) Scheming an proficient auto scaling technique for minimizing response time in load balancing on Amazon AWS cloud. In: International conference on advances in engineering science management & technology (ICAESMT)-2019, Mar 2019, Uttaranchal University, Dehradun. Conversational chatbot with AIML—M. Arvindhan Ahmad Ali
2. Kousik NV, Arvindhan M, Pradeep Ghantasala GS (2019) Clustering algorithm networks test cost sensitive for specialist divisions. *ICTACT J Image Video Process* 10(2)
3. Anand A, Chaudhary A, Arvindhan M (2021) The need for virtualization: when and why virtualization took over physical servers. In: *Advances in communication and computational technology*. Springer, Singapore, pp 1351–1359. Aravindhan M, Singh R, Kathuria K. An efficient technique for scheduling algorithm in real-time environment for optimizing the operating system
4. Singh A (2014) Survey on pLSA based scene classification techniques. In: 2014 5th international conference-confluence the next generation information technology summit (confluence), Sept 2014. IEEE, pp 555–560. A systematic review of blockchain in healthcare: frameworks, prototypes, and implementations. *IEEE Access* (2020)
5. Peng SL, Pal S, Huang L (2020) Principles of internet of things (IoT) ecosystem: insight paradigm

6. Willis B, O'Donohue W (2020) It's not just Murphy's Law: a case study of problematic records transmission. Clin Case Stud 1534650120984238. Treleaven P, Brown RG, Yang D (2017) Blockchain technology in finance. Computer 50:14–17
7. Fanning K, Centers DP (2016) Blockchain and its coming impact on financial services. J Corp Acc Finance 27(5):53–57. Writer's handbook (1989) University Science, Mill Valley, CA
8. It works. H. Benchmark—electronic health record implementation paper
9. <https://channels.theinnovationenterprise.com/articles/functional-analysis-offers-new-product-value-and-services-for-healthcare-industry>
10. Hinterding R, Michalewicz Z, Peachey TC (1996) Self-adaptive genetic algorithm for numeric functions. In: International conference on parallel problem solving from nature, Sept 1996. Springer, Berlin, Heidelberg, pp 420–429

Investigation of Diesel Engine's Performance Using Nano Additives in Biodiesel Blends (B20, B30 and B40)



Bandaru Bangarraju, P. Srinivas, G. Narasinga Rao, and Ch. Bhanuprakash

Abstract This research poses the possibility of using an alternate and renewable fuel (say mustard oil) mustard oil as a renewable and alternative fuel along with alumina as a performance-enhancing nano additive. To cope with this situation of load shedding, we would like to pay attention and promote the use of renewable energy sources. This is also reducing the dependency on import mustard oil that has a high calorific value and it can be cultivated in almost any terrain. So the endeavor is to use this mustard oil as an alternate to regular diesel oil. Biodiesel was prepared, blended with diesel, nano additives were missed and fuel properties viz., viscosity, density were determined within the laboratory with standing operating procedure. An experimental set-up was then carried out using various biodiesel blends prepared from mustard oil to assess the efficacy of a small amount of diesel. As biodiesel houses various properties when compared to diesel, is able to run faster and with a notable variation from its efficiency. Through this work, an attempt was made to the optimum blend is identified by comparing the engine's performance and emission characteristics.

Keywords Blends of biodiesel · Nano particles · Emission · Performance

Nomenclature

TIME	Time taken for 10 cc fuel to be consumed (s)
RPM	Revolutions Per Minute
W1	Load on spring balance 1 (kg)
W2	Load on spring balance 2 (kg)
BP	Engine Brake Power (kW)
m_f	Mass flow rate (kg/min)
TFC	Total Fuel Consumed (kg/h)
SFC	Specific Fuel Consumed (kg/h)

B. Bangarraju (✉) · P. Srinivas · G. Narasinga Rao · Ch. Bhanuprakash
Vishnu Institute of Technology, Bhimavaram 534202, India

© The Author(s), under exclusive license to Springer Nature Singapore Pte Ltd. 2022
B. B. V. L. Deepak et al. (eds.), *Applications of Computational Methods in Manufacturing and Product Design*, Lecture Notes in Mechanical Engineering,
https://doi.org/10.1007/978-981-19-0296-3_40

HI	Heat Input (kW)
FP	Frictional Power (kW)
IP	Indicated Power (kW)
$\eta_{th} \%$	Thermal efficiency (%)
$\eta_{me} \%$	Mechanical efficiency (%)

1 Introduction

A nation's energy consumption is generally regarded as an index of its growth. For social and economic growth, energy is critical. In reality, modern society is highly attached to the availability of resources, and so the entire system relies on it. Efforts are being made to upgrade advanced technology and to develop new approaches to traditional and non-conventional energy sources to meet rising energy demands. The pollution levels are rising at an alarming rate and wish immediate attention.

The sources of biodiesel are vegetable oils, recycled cooking grease/animal. Biodiesel blends (represented as BXX) indicates fuel that's composed of XX% biodiesel and (100 – XX) % diesel fuel. For example, 'B100' is pure biodiesel where as 'B20' represents '20%' biodiesel, '80%' diesel oil. Biodiesel, biodiesel blends are often utilized in Compression Ignition engines like diesel-powered trucks, cars, boats and irrigation systems, electrical generators, mining equipment and in most of the applications where diesel is mainly used. By adding nanoparticles, say alumina (aluminium oxide), at a proportion of Y ppm, the biodiesel blend is named as BXX + YAL.

2 Literature Review

Before advent of first diesel engine functionality, trans-esterification of vegetable oil was existing [1]. In 1893, Augsburg, Germany, prime model of Rudolf Diesel consisting of a flywheel at the base, one 10-foot (3 m) iron cylinder was first to run on its own power. At an injection pressure (280 bar) which is optimum, smoke emissions from fuel borne catalyst (FBC), total hydrocarbon (THC) and carbon monoxide (CO), and added biodiesel decreased by 6.9, 26.6, 52% when compared to biodiesel with no FBC [2]. Biodiesel with diesel fuel, NO_x emissions rised by 5% where as smoke emissions and CO were decreased by 9%, 13% respectively [3]. The engine's performance was increased with biodiesel with various concentration levels of additive (20–80 ppm). The emission levels hydrocarbons, NO_x are seen to greatly be reduced when incorporated with cerium oxide nanoparticles [4]. However, real fuel consumption decreased marginally due to impact of metal-dependent catalyst additives. Enhanced smoke capability and CO emissions of the exhaust gas emission profile decreased by 30.43, 56.42%. Low emissions of NO_x and CO₂ typically have

been assessed using biodiesel fuels [5]. Investigations on influences of biodiesel along the fuel additives (Mn, Ni) emission, diesel engine performance at 12 mol/l, 8 mol/l showed that a decrease in the the pouring point, the biodiesel viscosity is a function of rate of additive [6]. Diesel engine (Direct Injection type) experiments using alumina nano sized particles and carbon nanotubes as biodiesel and diesel additives seen a substantial increase engine performance, decrease in harmful pollutants compared to renewable biodiesel and clean diesel fuel [7]. Kao et al. performed an experiment using diesel blended aluminium nanoparticles and observed a significant increase in combustion and a significant decrease in HC and CO [8]. The blends such as MB20, MB10 are used in without any engine's modification [9]. Higher alcohol blends are directly proportional to thermal efficiency because of lower heat of vaporization. Nevertheless, in both the cases i.e., low/high blends of alcohol, the brake thermal efficiency was observed to greater than the biodiesel [10]. Biodiesel prepared from mustard oil would fetch better results and decided to analyze the performance parameters of mustard biodiesel with alumina nanoparticle additives.

3 Experimental Work

3.1 Preparation of Biodiesel

There are some observations in engine characteristics, when vegetable oils were used as fuels. The major problem is to be looked after during the preparation of biodiesel from non-edible vegetable oils is soap formation. Since they bind the methyl esters to water, the soap decreases the yield. At the washing point, the bonded esters will be washed out, but it will make water separation more difficult and increase water consumption as well.

3.1.1 First Stage (Pre-heating)

To melt the strong fats present in the oil, the filtered oil is taken into a jar and heated to 50 °C. For one hour, the compound is stirred, keeping the temperature at 45 °C.

3.1.2 Second Stage (Base-Catalyzed Reaction)

20 g of potassium hydroxide (KOH) is added to 250 ml of methanol and stirred thoroughly to produce potassium methoxide. In the preheated mustard oil, potassium methoxide is added and stirred at a steady temperature of 50 °C. The mixture is poured into a decanter after one hour and permitted to settle for 12 h.

3.1.3 Third Stage (Washing)

Direct water wash technique is adopted to remove any dissolved impurities from the biodiesel. 23 °C water is pre-heated to a temperature of about 60 °C and is added to the oil with constant stirring. Until the blend becomes uniform, the mixture is stirred. After allowing the mixture for setting with a period of one hour, the water is drained. For dispensing traces of water, the biodiesel is heated to 100 °C and then retained. Figure 1 indicates the processes in chronological order to convert raw oil into biodiesel.

3.2 Nanoparticles as Fuel Additives

To improve fuel consumption and reduce harmful emissions, fuel formulations and additive packs are now being developed. As a possible fuel additive, nanoparticles and microparticles of alumina have also been examined. Alumina, because of its high combustion energy, is known to increase the power output of engines. The efficiency advantage of nanoparticles or alumina is greater than that of microparticles. The properties of suspended nano alumina are more conducive to the occurrence of micro explosions during combustion, helping to mix air fuel and leading to safer, more efficient combustion. Moreover, studies have shown that, with the inclusion of alumina particles, the mean effective pressure increases.

3.3 The Process of Adding Nanoparticles to the Fuel

With the assistance of an ultrasonicator, the method of adding nanoparticles to the fuel is carried out. A predefined mass fraction (say 50 ppm) are disseminated within the biodiesel aiding a ultrasonicator set for half an hour with 20 kHz of frequency. The resultant (biodiesel) and nano additives are known as BIODIESEL + 50NANO are

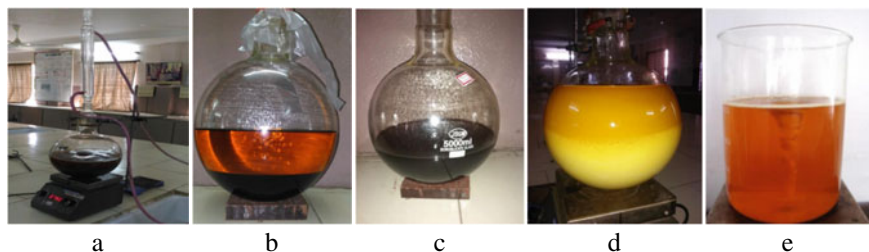
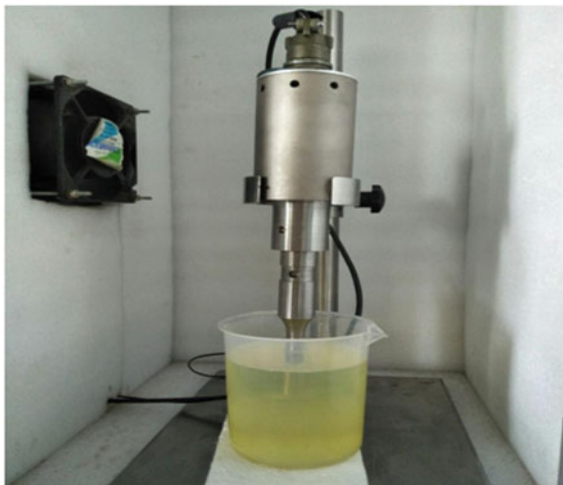


Fig. 1 Various steps involved in bio-diesel preparation **a** complete setup, **b** gravity preparation, **c** glycerin, **d** water washing, **e** dehydration

Fig. 2 Ultrasonicator

now blended together. There are three key components of an ultrasonicator system: Generator, Converter and Horn (also referred to as probe), as shown in Fig. 2. The tip of the probe will longitudinally stretch and contracts during operation. Amplitude is the distance traveled by the tip, based on the user's chosen amplitude setting.

3.4 Characteristic Properties of Fuel

The necessary properties of the ester are defined, after producing the required quantities of methyl ester from vegetable oil. The properties of ester are obtained from experimentation in the laboratory. The viscosity is calculated with the help of Brookfield viscometer, the calorific value is calculated with the help of Bomb calorimeter and the density is calculated with the help of Specific Gravity Bottle. Table 1 shows the results.

From the test results it can be assessed that the biodiesel obtained is fit worthy to implement it into the diesel engine without any potential injection problems. The mustard oil is tested on laboratory with direct injection diesel engine with variable compression ratio, with/without preheating for the engine parameters like performance evaluation, combustion parameters and exhaust gas analysis.

Table 1 Diesel and methyl ester of mustard oil properties

Fuel	Viscosity (cp)	C.V (kJ/kg)	Density (kg/m ³)
DIESEL	0.67	45,500	835
BIODIESEL	0.65	41,300	840
B20	0.666	34,025	821.68
B20 + 25AL	0.638	37,774	821.98
B20 + 50AL	0.62	40,964	823.44
B20 + 75AL	0.6	42,800	824.68
B30	0.694	31,690	825.96
B30 + 25AL	0.664	36,514	826.83
SB30 + 50AL	0.642	39,292	827.41
B30 + 75AL	0.628	42,323	829.54
B40	0.741	30,160	830.44
B40 + 25AL	0.712	32,604	831.66
B40 + 50AL	0.691	33,941	833.45
B40 + 75AL	0.675	41,292	836.27

3.5 Test Equipment

The test equipment used here is a Single Cylinder Compression Ignition engine. Loads are loaded onto the brake drum. A dynamometer (rope brake type) is incorporated to measure engine strength. A measurement board is placed near the engine, which contains readouts for temperature and a clear graduated tube measures the fuel consumption with respect to time. The temperature measurements are made through the usage of thermocouples placed at appropriate places inside the engine. The room temperature is measured prior to the start of the engine (refer to Fig. 3). The load is varied and the readings are taken accordingly and the variation in the exhaust emissions.

3.6 Experimental Procedure

Fuel is prepared at different blends, B20, B30 and B40 separately for experimentation. Alumina is added with the help of ultrasonicator to the prepared biodiesel blends. Now initially run the engine with pure diesel and take the time taken for 10 cc fuel consumption at different loads. The characteristic performance readings were noted and tabulated. The same procedure is repeated with all the fuel mixtures separately for different loads. These parameters are recorded for each blend at various loads and results were plotted.



Fig. 3 Diesel engine test rig

3.6.1 Various Formulae Used for Calculations

$$\text{Brake Power (BP)} = \frac{2\pi NT}{60,000} \text{ kW} \quad (1)$$

$$\text{Indicated power (IP)} = \text{Brake power} + \text{Frictional power (kW)} \quad (2)$$

$$\text{Brake Specific fuel consumption (SFC)} = \frac{\text{Fuel consumption}}{\text{BP}} \text{ (kg/kWh)} \quad (3)$$

$$\text{Mechanical Efficiency} = \frac{\text{BP}}{\text{Indicated power}} \quad (4)$$

$$\text{Brake Thermal Efficiency} = \frac{\text{BP}}{(\text{F.C} * \text{Calorific value of used fuel})} \quad (5)$$

where N and T represents speed in rpm and torque in N-m respectively.

4 Results and Conclusions

4.1 Observations of Biodiesel

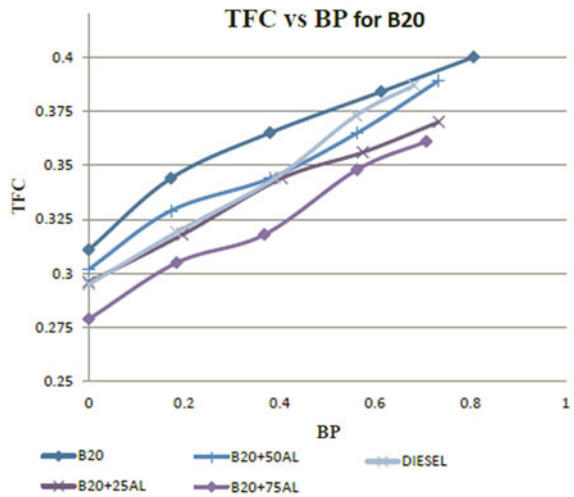
See Table 2.

Similarly we have got the performance parameters for B30 and B40 blends along with the nano particles and the correlation plots for TFC, SFC, η_{th} %, and η_{me} % are drawn against BP for all fuel blends and all variations of biodiesel blends

Table 2 Performance parameters for B20

TIME (s)	95	86	81	77	74
RPM	1506	1497	1491	1493	1489
W1 (kg)	0	1	2	3	4
W2 (kg)	0	0.3	0.45	0.5	0.7
BP (kW)	0	0.172	0.38	0.613	0.807
m_f (kg/min)	0.0052	0.0057	0.0061	0.0064	0.0067
TFC (kg/h)	0.311	0.344	0.365	0.384	0.4
SFC (kg/kW-h)	–	2	0.96	0.63	0.56
HI (kW)	2.943	3.251	3.452	3.631	3.778
FP (kW)	0.269	0.269	0.269	0.269	0.269
IP (kW)	0.269	0.441	0.649	0.882	1.076
η_{th} %	0	5.3	11	16.89	21.37
η_{me} %	0	39.02	58.52	69.5	75

Fig. 4 TFC versus BP for all B20 blends and diesel



with different proportions of nano additives separately. These graphs are depicted in Figs. 4, 5, 6, 7, 8 and 9 and conclusions are made from these graphs.

4.2 Correlation Plots

See Figs. 4, 5, 6, 7, 8 and 9.

Fig. 5 η_{th} % versus BP for all B20 blends and diesel

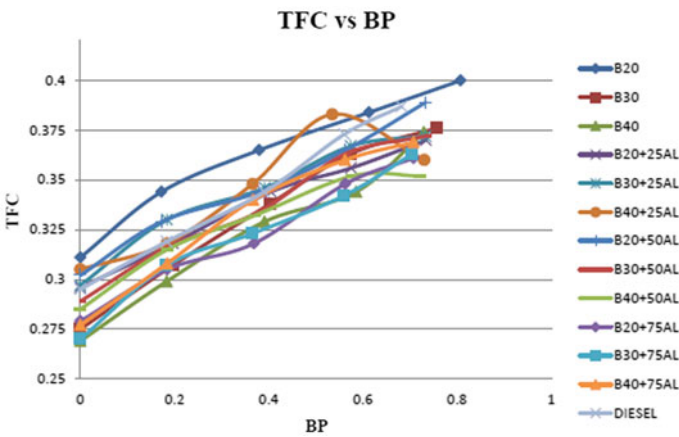
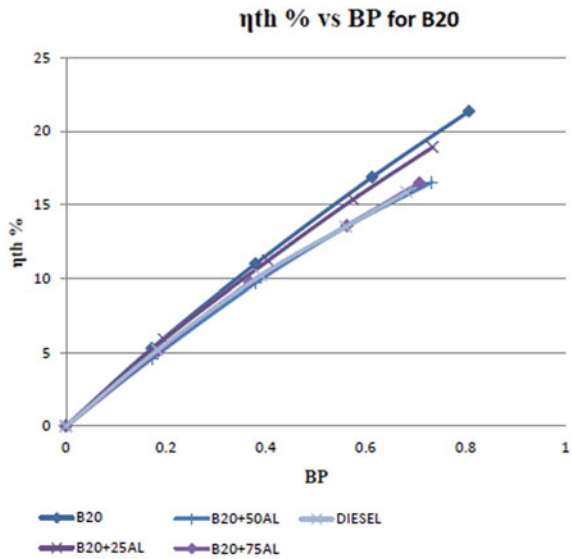


Fig. 6 TFC versus BP for all blends of fuel

4.3 Conclusion

Figure 4 shows that B20 + 75AL has fewer TFC and Fig. 5 shows that B20 has more thermal efficiency compared to diesel. In all fuel blends, it is observed that fuel consumption inversely proportional (Fig. 7) to the load. The thermal efficiencies (indicated) for all blends of biodiesel when compared with diesel were found as higher. Mustard biodiesel blend is comparatively cheaper than diesel. Total fuel consumption is found to be better at higher nano particle blend, i.e., B20 + 75AL,

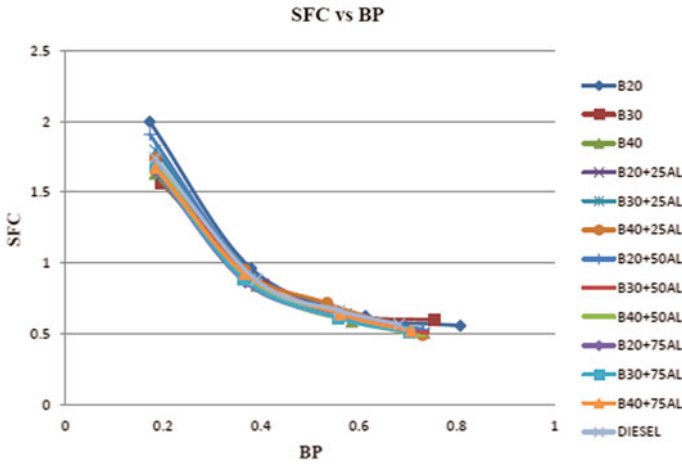


Fig. 7 SFC versus BP for all blends of fuel

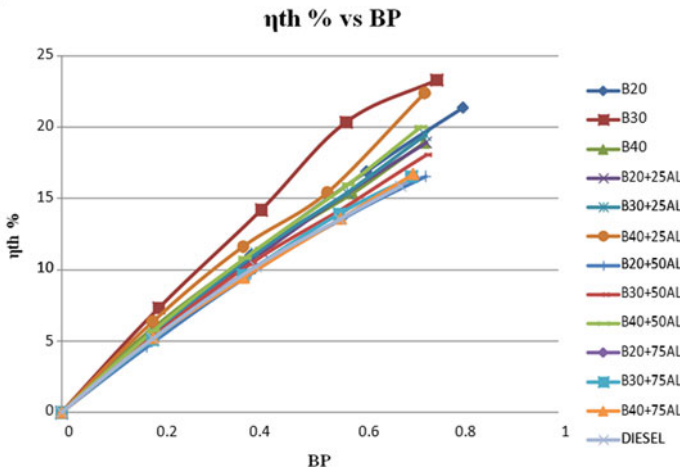


Fig. 8 η_{th} % versus BP for all blends of fuel

B30 + 75AL and B40 + 75AL than biodiesel blends with lesser concentrations of nano additives (Fig. 6). The optimum specific fuel consumption is observed for 50 ppm additives for B40 blend and 25 ppm additives for B30 and B20 blends. From Fig. 9 we can see that there is very small enhancement in mechanical efficiency of biodiesel and its blends but from Fig. 8, its clearly a significant thermal efficiency improvement for blends with addition of nano additives than pure blends of biodiesel and diesel.

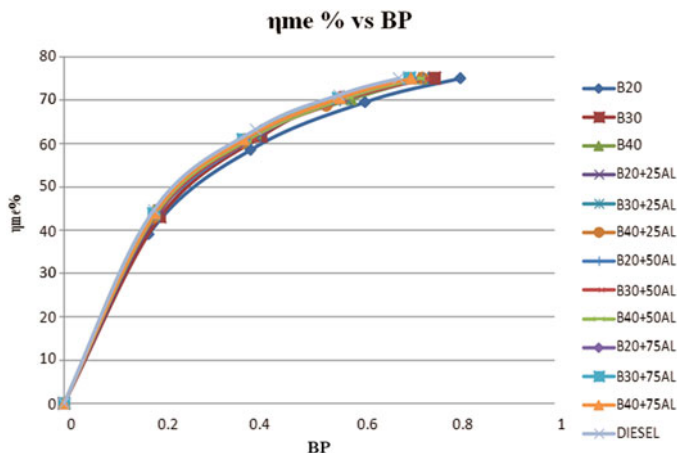


Fig. 9 η_{me} % versus BP for all blends of fuel

References

- Demirbas A (2009) Biorefineries. Green Energy Technol. <https://doi.org/10.1007/978-1-84882-721-9>
- Kannan GR et al (2011) Effect of metal based additive on performance emission and combustion characteristics of diesel engine fuelled with biodiesel. Appl Energy 88:3694–3703
- Guru M, Koca A, Can O, Cinar C, Sahin F (2010) Biodiesel production from waste chicken fat based sources and evaluation with Mg based additive in a diesel engine. Renew Energy 35:637–643
- Sajith V, Sobhan CB, Peterson GP (2010) Experimental investigations on the effects of cerium oxide nanoparticle fuel additives on biodiesel. Adv Mech Eng. <https://doi.org/10.1155/2010/581407>
- Keskin A, Gürü M, Altıparmak D (2008) Influence of tall oil biodiesel with Mg and Mo based fuel additives on diesel engine performance and emission. BioresourTechnol 99(14):6434–6438. <https://doi.org/10.1016/j.biortech.2007.11.051>
- Keskin A, Gürü M, Altıparmak D (2007) Biodiesel production from tall oil with synthesized Mn and Ni based additives: effects of the additives on fuel consumption and emissions. Fuel 86:1139–1143
- Sadikbasha J, Anand RB (2014) Performance, emission and combustion characteristics of a diesel engine using carbon nanotubes blended jatropha methyl ester emulsions. Alex Eng J 53:259–273
- Kao MJ, Ting C-C, Lin B-F, Tsung TT (2008) Aqueous aluminium nanofluid combustion in diesel fuel. J Test Eval 36(2):1–5
- Sajid A, Masjuki HH, Kalam MA, Abedin MJ, Ashrafur Rahman SM (2014) Experimental investigation of mustard biodiesel blend properties, performance, exhaust emission and noise in an unmodified diesel engine. In: ICESD, 19–21 Feb 2014, Singapore
- Jeya Jeevahan S, Sankar L, Karthikeyan P (2018) Comparative investigation of the effects of lower and higher alcohols/bio-diesel blends on engine performance and emissions characteristics of a diesel engine. Int J Ambient Energy. <https://doi.org/10.1080/01430750.2018.1484809>

Cloud Serverless Security and Services: A Survey



A. Arul Prakash and K. Sampath Kumar

Abstract The Serverless has proven to be an exciting new paradigm for deploying applications and services. This is the development of models for application in cloud space with abstraction environment. The term abstraction is an environment where the server has been maintained by the service provider and hidden from the end user. Data in cloud platform itself facing lots of security issues, also here deployment becomes easier which leads more security issues. This paper explores existing serverless platforms for industrial, academic, and open-source projects, identifies key features and use cases, and discusses technology and open challenges and problems. Also discusses the existing security threads, challenges of serverless computing and its solutions.

Keywords Cloud computing · FaaS · Cloud serverless security · Web services · Encryption · Decryption · Authentication

1 Introduction

Amazon AWS (Amazon Web Service) Lambda 2014 Reboot supports serverless processing. Other vendors used the Google Cloud feature, Microsoft Azure feature, and IBM Open Whiskey in 2016. However, this is nothing new without access to a computer server [1]. It was created after the recent development and introduction of virtual machines (virtual machines) and its container technology counterpart. Each step in the abstract level facilitates the IT unit in terms of resource utilization, cost and speed of development and implementation. Among the existing approaches, mobile Backend as-a-Service (MBaaS) is very similar to serverless processing (Fig. 1). Cloud functionality additionally offers a portion of these administrations. This means that some code servers can work for mobile applications without managing the server. For example, face book Cloud and Parse Cloud. Be that as it may, such codes are commonly restricted to serverless [2]. Serverless Computing (Function as a Service)

A. A. Prakash (✉) · K. S. Kumar
Galgotias University, Greater Noida, India

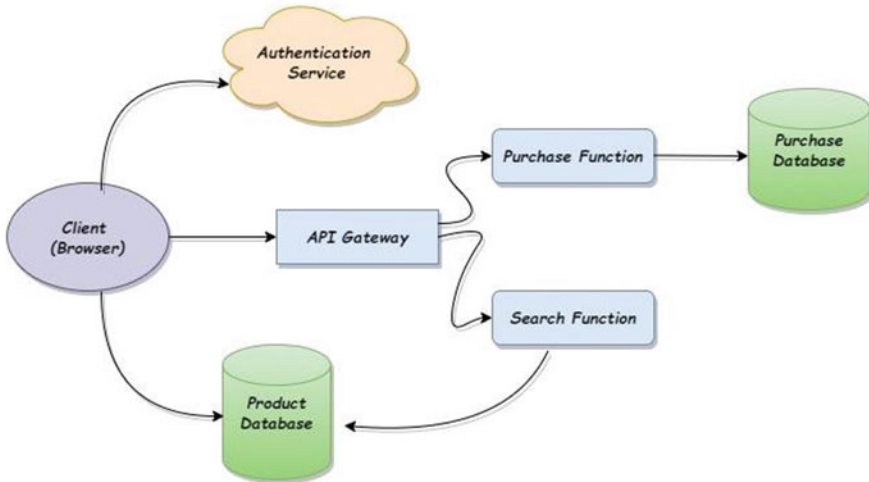


Fig. 1 Serverless system architecture

has been an advantage for many companies: it facilitates code expansion and distribution while increasing the use of server resources, minimizing costs, and reducing security costs. In cloud computing, rather than associations requiring their own workers, cloud administrations give instances of virtual server processing where applications can run. In the serverless model, the administration seed is made one stride further and the server itself. In short, without a server, instead of requiring an old server or repository like other cloud services, a simple operation is performed to obtain specific functions based on event triggers. For example, instead of a long server with no servers, you can activate the e-mail feature whenever you need to send e-mail. The thought without a server was first executed in AWS Lambda, and now the methodology is additionally accessible in the open haze of Microsoft Azure and the Google Cloud Platform (GCP). There are additionally a few open-source alternatives that permit serverless arrangement in private clouds and the Kubernetes Container Orchestra [3].

Serverless platforms promise new capabilities that make scalable micro-services easier and more expensive and represent the next step in the evolution of cloud computing architecture [4]. Many large cloud computing providers, including Amazon, IBM, Microsoft, and Google, recently unveiled serverless computing capabilities. There are many open-source efforts, including the Open Lambda project [5].

A key feature of the serverless platform is knowledge of the event processing system, as shown in Fig. 1, the service must manage a set of user-defined tasks, access HTTP relay events or copy sources to each function. Decide whether to send an event, check the current status of the project or create a new situation, send an event to the function instance, wait for a response, collect logs for the project, and report to the user when the work is no longer needed [6]. The challenge is to achieve

efficiencies based on indicators such as cost, disability, and tolerance of error. The platform will start running quickly and efficiently, and installation will be required. The platform should organize festivals based on event schedules and standards, plan activities, restrict activities, and install unused equipment. In addition, the platform needs to think carefully about how you can measure and manage errors in the cloud environment [7].

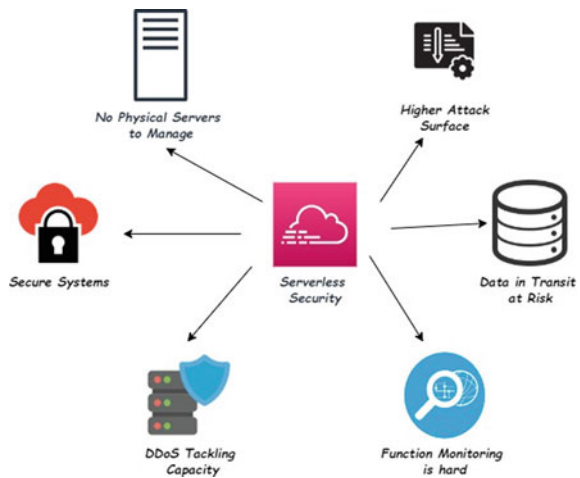
2 Serverless Security

Serverless systems represented in Fig. 2 are a dangerous place if you don't prepare yourself for the best training. There is a threat that wants to hack your system. DDoS attacks, ransomware distributors and all kinds of hackers using improperly configured databases and serverless functionality. This paper explores serverless security issues and concerns (AWS Lambda) and how they can be made worse [8]. In addition to safety training and continuous monitoring has protective limits. We've seen a lot of things that make the serverless security landscape different from the cloud. This is the thing has to be discussed first.

2.1 No Physical Server for Administration

According to today's statistics, many successful exploits in the modern world are caused by server health issues. Many attacks exploit security vulnerabilities that have not been resolved, even though they have been known for months [9].

Fig. 2 Different types of serverless security issues



Symantec believes that by 2020, 99% of the world's exploited vulnerabilities will be detected in more than one year. This is an inherent technical issue and management is not your responsibility when handling service [10]. So, your only responsibility is your data, so you should only choose platforms that you trust. Since the feature is a service, your security is an issue for your service provider. Debugging and keeping the server up-to-date are important skills that your service provider will tackle with precision.

2.2 Reconstruction

Reconstruction is the term which used to isolate the communication from the third party or the intruders. Here is some point which has to be followed when there reconstruction is needed [11].

1. Since the function is stateless, you transfer large amounts of data over the network, which increases the risk of leakage of this information.
2. While it has granular availability and flexibility, it does pose a risk of data leakage. So there are things that are good and bad at the same time. But it should be handled.
3. Encryption is definitely your best friend. Categorizes applications for which data is processed, stored, or transferred. Encrypt all data sent using PFS using a security protocol such as TLS. Or you can implement encryption with instructions like HTTP Strict Traffic Security.

In addition, you should limit the number of functions that each data store can access. Not all functions allow access to all data stores. Specific credentials are recommended for different set roles. Once you have added the ears, it can be difficult to remove them, so it is best to do it slowly and carefully [12].

2.3 Track Unused Functions

As monitoring is a challenging process, it is recommended to keep track of what happens in one job and how it works among other jobs. Like the permissions I mentioned earlier, when you have lots of simple implementations with minimal overhead, it's really hard to remove them after adding work.

In the absence of an accurate monitoring solution, job tracking is not supported. If you have hundreds of these features, each of them is vulnerable because attackers can infiltrate your system and make further progress. Even though the operating costs are very small, the total cost of ownership must be considered.

Although this problem is inherent in serverless ecosystems, current monitoring solutions are designed as complex applications, and their logical interfaces are not

designed to handle the small details of serverless architectures. So it's better to rely on a simple tool like this open source project: [Epson List Lamda Expressions \[13\]](#).

2.4 Safety and Granularity

As said earlier flexibility is good, but at the same time, an attack usually does what you don't want and causes problems with your system. Traditionally, you know that a lot of work involves you and that a protective environment surrounds you. In serverless architecture, each team has its own limitations and you need to use this technology and render it.

This means you should keep track of their contributions and external projects and worry about AWS Lambda storage and its dependent numbers. However, it places a lot of responsibility on the developer and automatically finds an engineer who properly regulates and monitors what a person can and cannot do. The learning curve is about learning these other activities to prevent fatigue, and isolation from test units and experimental development. Since the jobs are called external APIs, you must restrict them for validation [11].

2.5 Multi-Tenancy- a Low-Priority Threat

Multi-Tenancy means that your actions are performed in a service body shared by multiple users. However, the safety of the situation is the priority of any service. However, given the comment posted to Mike Roberts' post on his server, it is speculated that the resident may receive different hosting information due to a hosting error. The chances of this happening are very low, but low expectations are worrisome and cannot be ignored.

3 Serverless Computing Risks

While a serverless computing provides a more flexible and robust way of providing services, it is an alternative to use and may present new risks for the manager. Risks that organizations need to consider include [14, 15]:

Vendor security: Serverless functions run on a supplier's foundation, which could possibly be secure.

Multi-tenancy: Functions in a serverless help frequently run on shared framework that is running code for different clients; that could be a worry with regards to touchy information as illustrated in Fig. 3.

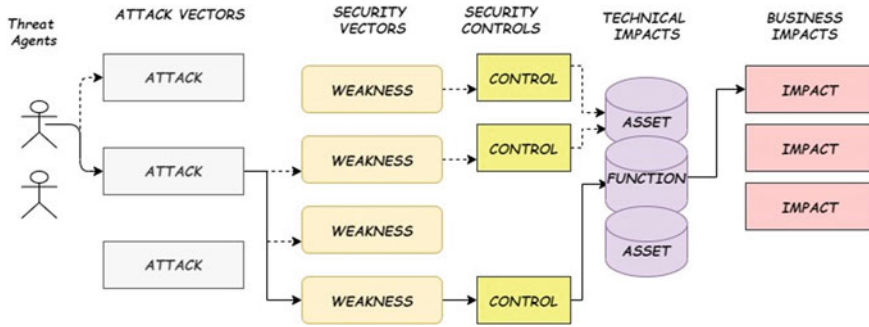


Fig. 3 Serverless computing security common issues

1. *Injection attacks*: In an injection attack, unapproved or sudden substance or information is infused into an application stream; in the serverless model, an injection attack can emerge out of an occasion that the serverless capacity calls to execute.
2. *Encryption*: Serverless functions can frequently shout to databases and other advantaged assets; if the association isn't encoded, information can possibly be spilled
3. *Security misconfigurations*: In request to empower admittance to various assets, a designer might enter access keys, tokens, and passwords straightforwardly into the capacity; not securing those mysteries is a hazard.
4. *Function permissions*: Often serverless functions are granted the same permissions as a server might get. A serverless capacity, be that as it may, requires just an absolute minimum authorization to execute, and overprovisioning consents opens up the capacity to likely hazard.
5. *Component vulnerabilities*: Functions are often based on the supply chain of libraries and third-party components. If one of the items has a known (or unknown) vulnerability, you can use the serverless service [16].

4 Serverless Security and Policies

Serverless security team is tied in with executing proper controls and approaches. Cloud server security arrangements are powerful with regards to cloud computing server examples, however serverless processing requires an extra degree of control, exactness, and deceivability. Serverless computing includes effortlessness and another financial model of cloud computing [17]. By exposing public offerings in the cloud and deploying a serverless application implementation model, companies take on more security responsibility for cloud providers. The company must provide the application layer. Application data access management and monitoring like Forced enforcement actions, error monitoring, security incidents, etc.

However, because serverless computing is a relatively new technology, many development and security teams find it difficult to understand and address the inherent security risks it poses. The vast majority of the current security devices depend on the virtual machines, operating systems, databases and virtual interface system. At the point when application designers decide to expand on a serverless foundation, their center segments are not, at this point changeless and not effectively available. Accordingly, numerous venture security groups have grown new arrangements that work to ensure present day applications and APIs based on serverless structures, for example, Amazon Lambda, Azure Functions, and Google Cloud Functions [18].

4.1 Reduce Serverless Permissions

The greatest danger of serverless computing is the capacity to have a larger number of benefits than would normally be appropriate. Serverless frameworks can fundamentally diminish their assault surface by actualizing a least-benefit model for all dispersed usefulness. It could decrease the quantity of benefits by setting up programmed checks in the organizing condition for jobs being developed. You can likewise profile the conduct of a job to see which benefits the running job really employments. This deceivability permits directors to accelerate access and empower just the benefits they need [19].

1. *Force Authentication*—All functions calling administrations, including inside the cloud supplier, must require access control and verification to restrict hazard. Cloud specialist organizations give best practices to serverless validation. This ought to be trailed by the executive.
2. *Use Cloud Provider Controls*—Cloud suppliers likewise have some underlying administrations that assist clients with distinguishing potential setup mistakes. For instance; AWS Trusted Advisor is a possibility for clients running AWS Lambda.
3. *Activity of Log Function*—Since serverless functionality is event-based and stateless, it's easy to go through most activities while watching real-time activity. Utilizing cloud (or outsider) serverless logging and observing, you can make a helpful review trail when searching for threats.
4. *Monitor Function Layers*—Functions can have numerous layers that call various codes and outsider libraries. By checking the layers, executives can recognize pernicious movement and endeavor section [20].
5. *Consider Third-Party Security Tools*—Serverless platform vendors often perform a lot of security checks, but their scope is usually limited, focusing only on the platform the feature is running on. For the serverless computing an additional layer of visibility control was provided by the different third-party tools and technologies [21].

5 Serverless Computing Security Providers

The market for serverless security tools is generally new, however the business as of now has a few sellers. Serverless innovation commonly includes the utilization of short stateless compartments, so there is some cover with holder security suppliers (see eSecurity Planet’s rundown of significant compartment security suppliers) [22].

- *Aqua Security*—Aqua Security gives an extensive holder and serverless security stage that assists associations with evaluating and decrease serverless hazard.
- *Nuweba*—Nuweba is another individual from serverless system. It will be utilized in February 2019 and has its own security work administration stage, which can be coordinated with serverless administrations of significant open cloud suppliers.
- *Puresec*—PureSec’s Serverless Security Platform is explicitly intended to address serverless security challenges and coordinate with an association’s continuous integration/continuous development (CI/CD) work process.
- *Protego Labs*—Protego Labs is furthermore based on serverless security, hoping to give full lifecycle security from progress through association.
- *Snyk*—The Snyk stage engages relationship to perpetually check functions to help recognize any normal threats.
- *Twistlock*—Twistlock’s foundation gives security to the compartments and as well as serverless functions over the full turn of events and deployment lifecycle [23].

6 Security Challenges of Serverless

Shadow APIs popping up in the corporate environment are especially important when:

1. Cloud providers will be easier, faster, and cheaper to build large applications on the platform.
2. Serverless is a software engineer and DevOps team to develop large-scale end-to-end applications and APIs [24].

Cold start issues and denial-of-service (DoS) attacks can be intimidating. It seems possible because you cannot access the applications without a server and it may take longer for enough containers and databases to respond on time. The latter can lead to unexpected costs.

When many applications are attacked by DoS, the desired result may be that the program can no longer respond to a new request, is blocked, and resources are overloaded due to too many bogus requests made by an attacker. On account of serverless applications, the cloud supplier is liable for scaling enough frameworks to deal with new application demands. In the event that the serverless applications don’t have a furthest breaking point on the scale, the after effect of the DoS assault can put a gigantic money related weight on the program engineer. Thus, the term portfolio denial means that the company cannot bear the high cost of such an attack, but the biggest issue so far seems to be visibility [25].

Asking any IT or security manager how many business applications and APIs have been added to your internet service, you may have more questions than answers. Solicitations consent to make an application without a server. Additionally, of course, it first tends to security issues found in serverless and applications that don't utilize the API. Wireless software is a dead end for most IT leaders and security companies. However, as organizations gain experience and monetary value from using servers, IT and security professionals will begin to gain visibility and understanding of the new threats and potential risks associated with this new architecture [26].

7 Conclusion

Serverless is a term which is most popular now a day because of its usability and flexibility. The word serverless doesn't mean that there is no server besides there exists a server but in terms of end user the server is not a criterion to worry about. It's inbuilt and a user can reply their application without the consideration of the server. In other terms, to deploy the application in cloud it is not mandatory to know about the server. It enhances the integrity of the application. As there are more advantage and flexibility over the application as well there is a drawback when looking for the security. Dealing security in cloud itself a big challenging, now the deployment has also been more relaxed. The deploying become easier since there are few things to be noticed. As I have observed few things about the serverless cloud architectures are (i) The serverless term implies that as the user there is no server because it was maintained by the third party. As all know that when a data stored in a cloud itself faces a security breaches now the server has also become a third party. It is really a situation where all have to think about. (ii) As a user they have some set of architecture and infrastructure in the function or the application. All the features are acceptable by the server which is already inbuilt. In other terms, there is limitation on the applications. (iii) When there is an updating on the function or the application it takes time to approve the same on server side. (iv) It possesses the limitations on the concurrent process as it implies the impacts on the number users at times.

References

1. Aws re: invent 2014 | (mbl202) new launch: Getting started with aws lambda. Retrieved from <https://www.youtube.com/watch?v=UFj27laTWQA>. 1 Dec 2016
2. Azure functions. Retrieved from <https://functions.azure.com/>. 1 Dec 2016
3. Bainomugisha E, Carreton AL, van Cutsem T, Mostinckx S, de Meuter W (2013) A survey on reactive programming. *ACM Comput Surv* 45(4):52:1–52:34 (2013). <https://doi.org/10.1145/2501654.2501666>. <http://doi.acm.org/10.1145/2501654.2501666>

4. Baldini I, Castro P, Cheng P, Fink S, Ishakian V, Mitchell N et al. (2016) Cloud-native, event-based programming for mobile applications. In: Proceedings of the international conference on mobile software engineering and systems, MOBILESoft '16. ACM, New York, pp 287–288. <https://doi.org/10.1145/2897073.2897713>. <http://doi.acm.org/10.1145/2897073.2897713>
5. Bienko CD, Greenstein M, Holt SE, Phillips RT (2015) IBM cloudant: database as a service advanced topics. IBM Redbooks
6. Building Serverless Apps with Webtask.io. Retrieved from <https://auth0.com/blog/building-serverless-apps-with-webtask/>. 1 Dec 2016
7. chalice: Python serverless microframework for aws. Retrieved from <https://github.com/aws-labs/chalice>. 1 Dec 2016
8. Iron.io (2017) Iron.io IronFunctions. Available: <http://open.iron.io/>
9. Cloud foundry and iron.io deliver serverless. Retrieved from <https://www.iron.io/cloud-foundry-and-ironio-deliver-serverless/>. 1 Dec 2016
10. Cloud functions. Retrieved from <https://cloud.google.com/functions/>. 1 Dec 2016
11. Ethereum. Retrieved from <http://ethdocs.org/en/latest/introduction/whatis-ethereum.html>. 1 Dec 2016
12. Google (2017) Google cloud functions. Available: <https://cloud.google.com/functions/>
13. Microsoft (2017) Azure functions. Available: <https://azure.microsoft.com/en-us/services/functions/>
14. Fernandez O (2016) Serverless: Patterns of modern application design using microservices (Amazon Web Services Edition) (in preparation). <https://leanpub.com/serverless>
15. Galactic fog gestalt framework. Retrieved from <http://www.galacticfog.com/>. 1 Dec 2016
16. Google apps marketplace. Retrieved from <https://developers.google.com/apps-marketplace/>. 1 Dec 2016
17. OpenLambda (2017) OpenLambda. Available: <https://open-lambda.org/>
18. Hendrickson S, Sturdevant S, Harter T, Venkataramani V, Arpaci-Dusseau AC, Arpaci-Dusseau RH (2016) Serverless computation with openlambda. In: 8th USENIX workshop on hot topics in cloud computing, HotCloud 2016, Denver, 20–21 June 2016. <https://www.usenix.org/conference/hotcloud16/workshopprogram/presentation/hendrickson>
19. Introducing lambda support on iron.io. Retrieved from <https://www.iron.io/introducing-aws-lambda-support/>. 1 Dec 2016
20. OpenStack. Retrieved from <https://www.openstack.org>. 5 Dec 2016
21. Jira. Retrieved from <https://www.atlassian.com/software/jira>. 5 Dec 2016
22. Learn chaincode. Retrieved from <https://github.com/IBM-Blockchain/learn-chaincode>. 1 Dec 2016
23. The Apache Software Foundation (2017) ApacheOpenWhisk. Available: <http://openwhisk.org/>
24. NGINX announces results of 2016 future of application development and delivery survey. Retrieved 5 Dec 2016
25. LeverOS. Retrieved from <https://github.com/leveros/leveros>. 5 Dec 2016
26. Amazon web services, AWS Lambda. Available: <https://aws.amazon>

Early Prediction of Credit Card Transaction Using Local Outlier Factor and Isolation Forest Tree Machine Learning Algorithms



K. P. Arjun, Godlin Atlas, N. M. Sreenarayanan, S. Janarthanan, and M. Arvindhan

Abstract A credit card is one vital thing nowadays for everyone, even in developing countries. We are using a credit card to pay bills, shop both online as well as offline. With the increase in the use of credit cards, fraud with the credit card is also increasing side by side. Credit card fraud is one of the major crimes nowadays. In this study, we proposed two machine learning models to predict the fraud transaction outbreak in a credit card accurately. Machine learning models can effectively help bankers and customers accomplish this objective because of their quick and accurate recognition efficiency. Our proposed work, we used Isolation Forest (IF) tree and Local Outlier Factor (LOF) algorithms, which used for anomaly detection for detecting fraud transactions. Isolation Forest (IF) tree algorithm randomly selecting credit card features and make a decision tree from a given dataset and finally score calculated as path length of tree to isolate outlier. Local Outlier Factor (LOF) algorithm calculates outliers by computing the local density of given data concerning its neighbors. Those two models trained and tested with the dataset contain 4092 entries of customer's credit card details made by European cardholders. The data sample is consisting of 80% of fraudulent transactions and the remaining is authenticated transaction done by the customer. We compared our two models with all the existing models that used to identify the fraud transactions, and the prediction accuracy reaches 99%.

Keywords Machine learning · Credit card fraud detection · Isolation Forest (IF) · Local Outlier Factor (LOF) · Outlier detection

K. P. Arjun (✉) · G. Atlas · N. M. Sreenarayanan · S. Janarthanan · M. Arvindhan
School of Computing Science and Engineering, Galgotias University, Greater Noida,
Uttar Pradesh, India

M. Arvindhan
e-mail: m.arvindhan@galgotiasuniversity.edu.in

1 Introduction

Credit card is one of vital thing nowadays for everyone, even in all the developing countries. We can use credit card to pay bills, shop both online as well as offline. With increase in use of credit card, fraud with credit card also increasing side by side. Every year millions of dollars loses caused by credit card fraud [1]. Credit card frauds are defined as someone using else credit card for their own use without owner doesn't knowing about it that his card is used. So, it's become very necessary that credit card companies are able to correctly identify fraud transaction very efficiently. Necessary major decision should be taken by credit card companies to avoid and prevent credit card fraud. Credit card companies also make their system more secure so that information is not leaked from their side.

Credit card theft has become one of the biggest offences as days go on. Credit card fraud can happen through online platforms as well as offline. According to Reserve Bank of India total 972 cases are reported in 2017–18. So, it's become very important that banks are correctly able to identify fraud transactions. Around 25 billion dollars are lost in credit card payments all around world in 2018. According to shift credit card processing website The United States is now the leading nation in countries vulnerable to credit card theft (Fig. 1).

Via scams, theft and information by scammers, identity is stolen and thieves can target and obtain your personal information [2]. The third biggest source of financial crime is identity theft. Identity fraud happens as someone uses data to register for a new card or to enter your credit card account, such as name, age, birthday, financial statements, etc. In Fig. 2 represented number of different types of identity thefts and we can clearly understand credit card fraud is the most reported identity theft compared to other types of identity thefts.

The growth in disclosed data attacks in 2019 is 54%. Eight out of 3800 in 2019 data breaches revealed more than 3.2 million documents, i.e. almost 80% of all information exposed so far in 2019, according to the shift credit card processing website. Figure 3 shows the different sector data breaches are represented in pie

Fig. 1 Credit card fraud reported in US

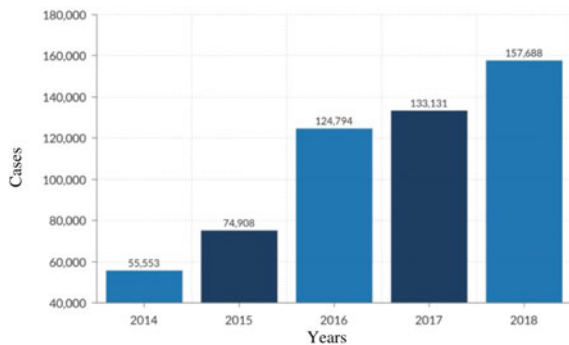




Fig. 2 Identity theft reports by SHIFT on 2018

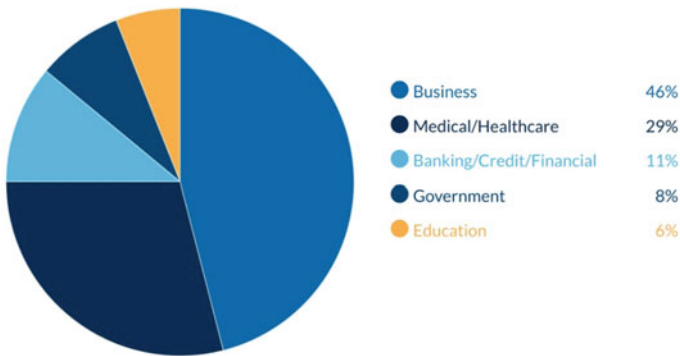


Fig. 3 Data breaches reports in different areas

graph. The top companies are also data breaches that exposed consumer records like Yahoo, Facebook, Marriott, etc. [3].

Credit card fraud can be preventing through various easy ways. Various methods through which we can take precaution for preventing credit card fraud are monitoring your credit card account statement frequently. Keep your wallet secure where you kept your cards and close to you all time. When doing online payment make sure doing through secure website and keep your card details not saved in public computer [4]. During point-of-sale payment method make sure no one see your pin while entering. If you are a victim of credit card fraud then make sure to report of that to your credit card company and if you misplaced your card or lost contact of your bank and closed that card. Final one is changing your card pin regularly over 2–3 months to prevent fraud.

Machine Learning is sub-set of Artificial Intelligence (AI). Machine learning is field of study concerned with the design and development of algorithms and techniques that allows machine learn by it. Machine learning works as similar ways as human learning. In Machine learning, statistical and mathematical methods are used

for learning through datasets. Machine learning can help in many areas where problems are very complex and difficult such as in medical field, banking sector, etc. [5]. Machine learning are applied to our every daily basis such as in Netflix, Amazon as well as Facebook, etc.

Machine learning also plays an important role in providing cyber security. Machine learning easily safeguard against malware, assessing network security, developing secure online transactions as well as online interaction and developing authentication systems. Credit card fraud can be happening in numerous ways. In case of offline credit card fraud, fraudster required credit card physically while, in case of online credit card fraud, fraudster required only details of credit card user. The major challenges fraud detection is [6–9], first one huge large amount of data processed every day and model built that must be fast enough to detect fraud transaction in time. Second is imbalanced dataset i.e., most of the transaction are valid transaction and only few about 0.1% of transactions are fraud transaction. Finally the banking companies are not sharing their fraudulent transaction details because of company's credentials.

2 Literature Survey

Fraud detection for credit card can be done through various techniques such as machine learning techniques, neural networking and data mining. Most commonly ways of detecting fraud in credit card through machine learning is using supervised learning i.e., Decision tree, Random Forest, KNN, etc. There are many researches focus on use of data mining for data processing and data analysis. Research shows development of fraud detection model along with machine learning increases the prediction result.

Setiawan et al. [4], they have used the BPSOSVM-ERT and BPSOSVM-RF which are compared on the several performance metrics. The dataset is used form the LeadingCub which provides the loan dataset and the data issued from 2007 to 2017. The BPSOSVMERT model which produced the accuracy as 64%. Patil et al. [10] they have used the German credit card fraud dataset and the models are used in this approach are logistic regression, decision tree and random forest decision tree with accuracy as 72%, 72% and 76% respectively.

Zheng et al. [5] they have used the Markov chain models for the transaction fraud detection based on total order relation and behavior diversity. In this they have also used the behavior profiles (BPs) that helps in finding the fraud. They have used the dataset from Kaggle and they got accuracy score about 0.912. Kalid et al. [6] they have used the Multiple Classifiers System for the anomaly detection in credit card in which they have used the two datasets as credit card fraud dataset in which they have overlapping class samples and unbalanced class distribution, and another dataset is credit card default payments. In the multiple classifier system, they have used the two models as Naïve Bayes (NB) and C4.5, with this model they got the accuracy

score different for both the datasets as for credit card fraud as 0.99 and for credit card default detection as 0.93.

Makki et al. [11] they have used the imbalanced classification approaches for the credit card fraud detection. Their models used in the approach are LR, C5.0 decision tree algorithm, SVM and ANN which performed well and got the same accuracy score as 96% for all the models. They have used the credit card fraud labeled dataset.

Taha and Malebary [12] they have used the optimized d light gradient boosting machine (OLightGBM). In their approach they have used a Bayesian-based hyperparameter optimization algorithm used to tune the parameters of a light gradient boosting machine (LightGBM). They have used two different datasets; first dataset consists credit card transaction of an owner in Europe and the second dataset is from UCSD-FICO Data mining contest in which it has the real dataset of e-commerce transactions. They got the accuracy 98.04%, precision 97.34% and f-1 score 56.95%.

Itoo et al. [13] they have used logistic regression, Naïve Bayes and KNN models for the credit card fraud detection. They have used the dataset from the Kaggle which provides the dataset for the credit card fraud detection. They got the best accuracy for the logistic regression model with accuracy 0.959.

3 Literature Survey Proposed Model

3.1 Dataset Description

Kaggle provided the dataset which contains transaction made by European credit card-holders. The dataset contains transactions that occur in two days, where it has 492 Fraud transaction and 284,315 valid transactions. Dataset has features V1, V2, V3 ... V28 that are transformed into PCA values due to confidentiality issues. It also contains three more features that are not PCA transform, amount, time and class. Class represents transaction is fraud or valid. If class is 1 then transaction is Fraud while 0 when transaction is valid. Table 1 shows the overall details of credit card fraud problem’s dataset provided by Kaggle.

Table 1 Dataset explanation

Variables	Explanation	Data type	Scale
V1–V28	Confidential data of credit card holders which numerical input variable that is PCA transform	Numerical	Numerical
Amount	Numerical input feature that represents amount debit or credit from credit card	Numerical	Money in euros
Time	Time represents second elapsed between each transaction and first transaction in the dataset	Numerical	Time in seconds
Class	Class represents fraud and valid transaction i.e., 0 for normal transaction and 1 for fraud transaction	Numerical	(0,1)

Table 2 Performance evaluation matrix

Performance matrix name	Explanation
True positive (TP)	Credit card fraud cases that model predicated as “fraud” $TP = \text{Count of positive } \gamma \rightarrow \text{positive } \hat{\gamma}$
False positive (FP)	Credit card non-fraud cases that model predicated as “fraud” $FP = \text{Count of negative } \gamma \rightarrow \text{positive } \hat{\gamma}$
False negative (FN)	Credit card fraud cases that model predicated as “non- fraud” $FN = \text{Count of positive } \gamma \rightarrow \text{negative } \hat{\gamma}$
True negative (TN)	Credit card non-fraud cases that model predicated as “non –fraud” $FP = \text{Count of negative } \gamma \rightarrow \text{negative } \hat{\gamma}$
Accuracy	Model accuracy which means our model must report positive cases are predicted as positive and negative cases are predicted as negative $Accuracy = \frac{TP+TN}{TP+FP+TN+FN}$
Precision	Precision is the propositions of predicted true positive cases are relevant among all true positive and false positive cases $Precision = \frac{TP}{TP+FP}$
Recall	Precision is the propositions of predicted relevant true positive cases are among all true positive and false negative cases $Recall = \frac{TP}{TP+FN}$
F1-score	F1 score describes about balance between the precision and recall $F1 - \text{Score} = \frac{2 \times \text{Precision} \times \text{Recall}}{\text{Precision} + \text{Recall}}$

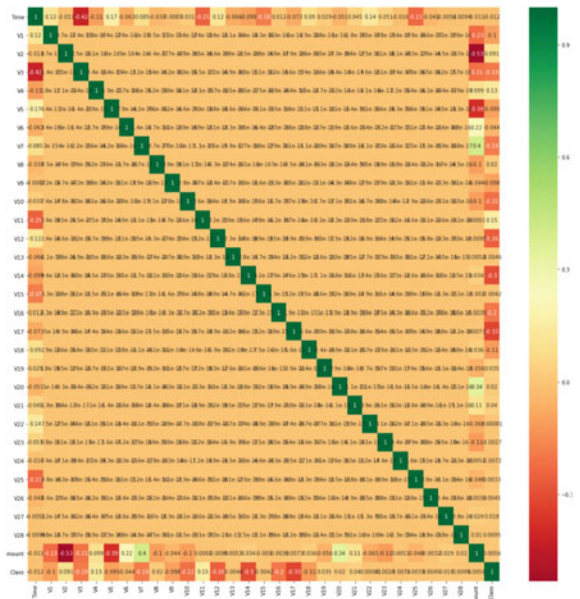
3.2 Model Performance Evaluation Matrix

Compared to other existing models, Table 2 displays the performance assessment matrix that we are using to show the performance of the proposed model.

3.3 Pre-processing

In Fig. 4 represents heatmap which means one variable that could be gently connected with another variable. It will be giving more effective outputs for investigations and displays more readily between factors. We can clearly understand the features V1–V28 are not connected each other so these features wouldn’t produce a good model. In feature selection process we skip or remove these features to get a good prediction model.

Fig. 4 Heat map for correlated features values in the dataset



3.4 Model Description

Here we focus on the fraud transaction recognition using the Isolation Forest Tree (IF) and Local Outlier Factor (LOF) model. Kaggle provides Kaggle notebook, a cloud-based machine learning platform that gives the advantages of reproducible and collaborative analysis. Kaggle provided dataset feed the ML models was trained on the two models.

(A) Isolation Forest Tree Model

Isolation Forest Tree (IF) machine learning algorithm is an anomaly detection method. IF algorithm can work either supervised neither unsupervised learning method. Isolation forest tree algorithm different from other type of distance or density-based method for outlier detection and algorithm tried tree to build extremely randomized decision tree for separating outlier. The equation for calculating outlier in Isolation forest trees as following:

$$s(x, n) = 2^{-\frac{E(h(x))}{c(n)}} \tag{1}$$

- $h(x)$ is analysis distance x .
- $c(n)$ is the average length of unsuccessful searches in the binary search tree.
- n is the number of nodes that are external.

(B) Local Outlier Factor for outlier detection

The Local Outlier Factor algorithm is an unsupervised outlier detection method which computes the local density deviation of a given data point with respect to its neighbors. It is considered as outlier samples which has substantially lower density than their neighbors.

4 Result and Discussion

In result and discussion section, we analyzed our proposed model performance and we also compared our proposed model with existing models showed in Table 3.

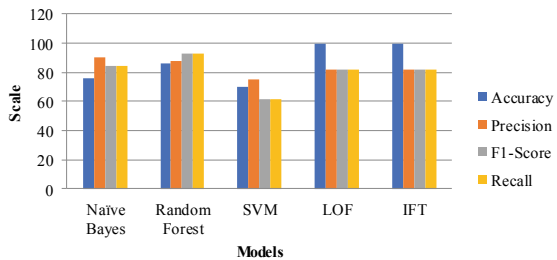
Isolation Forest tree algorithm detected 73 errors and its accuracy is about 99.74% which is greater than local outlier factor algorithm. Local Outline Factor (LOF) detected 97 error and its accuracy is around 99.65%. Using 10% of dataset for faster execution of learning and training model for predicting results. Figure 5 shows the graphical representation of comparison result, from that graph we can understand our two proposed models are far better than all the existing methods.

When we compare our model with existing models, we can easily say that our model’s prediction accuracy is far better than all the existing methods. When comparing the error precision and recall for Isolation Forest (IF) and Local Outlier Factor (LOF), the other models like Navie Bayes and Random Forest performed good because its dataset distribution of fraud and non-fraud transaction is almost equal. Overall performance of Isolation Forest (IF) is much better that Local Outlier

Table 3 Proposed model evaluations

Models	Accuracy	Precision	F1-score	Recall
Naïve bayes	75.8	90.5	84.5	84.5
Random forest	86.10	87.10	92.40	92.40
Support vector machine (SVM)	70.09	75.00	61.50	61.50
Local outlier factor	99.65	75.50	75.50	75.50
Isolation forest tree	99.74	81.50	81.50	81.50

Fig. 5 Graphical representation of proposed models comparison



Factor (LOF). Performance of model can be improved by using Deep learning or Neural Network however at the cost of computational expensive.

5 Conclusion

Credit card fraud detection involves the deep analysis of large group of credit card users in order to identify properly. According to federal law and issuer card network terms and policies, credit card owner doesn't have to pay cost of unauthorized purchases made with his cards. Financial institutions and merchants assumed responsible for the most of the money spent as product of fraud. Credit card fraud is happening when someone other than owner of credit card uses credit card or credit account to make transactions. In our proposed, we implemented two machine learning algorithms are Isolation Forest (IF) tree and Local Outlier Factor (LOF). Isolation Forest tree algorithm accuracy is about 99.74% which is greater than local outlier factor algorithm. Local Outlier Factor is around 99.65%. In both of these cases results are approximately same. When comparing the error precision and recall for Isolation Forest and Local Outlier Factor, the Isolation Forest Tree algorithm performed much better than the Local Outlier Factor. Overall performance of Isolation Forest (IF) is much better than Local Outlier Factor (LOF). Performance of model can be improved by using Deep learning or Neural Network however at the cost of computational expensive.

References

1. Krishnapur V, Thieves only need your credit card data, not your card to defraud you. *Economic Times*
2. Wong B, The 8 different types of card fraud. *Mastercard*
3. Bessette C, How serious a crime is credit card theft and fraud?. *Nerdwallet*
4. Setiawan N, Suharjito, Diana (2019) A comparison of prediction methods for credit default on peer to peer lending using machine learning. *Procedia Comput Sci* 157:38–45. <https://doi.org/10.1016/j.procs.2019.08.139>
5. Zheng L, Liu G, Yan C, Jiang C (2018) Transaction fraud detection based on total order relation and behavior diversity. *IEEE Trans Comput Soc Syst* 1–11. <https://doi.org/10.1109/tcss.2018.2856910>
6. Kalid SN, Ng K-H, Tong G-K, Khor K-C (2020) A multiple classifiers system for anomaly detection in credit card data with unbalanced and overlapped classes. *IEEE Access* 8:28210–28221. <https://doi.org/10.1109/access.2020.2972009>
7. Varmedja D, Karanovic M, Sladojevic S, Arsenovic M, Anderla A (2019) Credit card fraud detection—machine learning methods. In: 2019 18th international symposium INFOTEH-JAHORINA (INFOTEH). <https://doi.org/10.1109/infoteh.2019.8717766>
8. Awoyemi JO, Adetunmbi AO, Oluwadare SA (2017) Credit card fraud detection using machine learning techniques: a comparative analysis. In: 2017 international conference on computing networking and informatics (ICCNI). <https://doi.org/10.1109/iccni.2017.8123782>

9. Thennakoon A, Bhagyani C, Premadasa S, Mihiranga S, Kuruwitaarachchi N (2019) Real-time credit card fraud detection using machine learning. In: 2019 9th international conference on cloud computing, data science & engineering (Confluence). <https://doi.org/10.1109/confluence.2019.8776942>
10. Patil S, Nemade V, Soni PK (2018) Predictive modelling for credit card fraud detection using data analytics. *Procedia Comput Sci* 132:385–395. <https://doi.org/10.1016/j.procs.2018.05.199>
11. Makki S, Assaghir Z, Taher Y, Haque R, Hacid M-S, Zeineddine H (2019) An experimental study with imbalanced classification approaches for credit card fraud detection. *IEEE Access*, 1–1. <https://doi.org/10.1109/access.2019.2927266>
12. Taha AA, Malebary SJ (2020) An intelligent approach to credit card fraud detection using an optimized light gradient boosting machine. *IEEE Access* 1–1. <https://doi.org/10.1109/access.2020.2971354>
13. Itoo F, Meenakshi, Singh, S. (2020) Comparison and analysis of logistic regression, Naïve Bayes and KNN machine learning algorithms for credit card fraud detection. *Int J Inf Technol*. <https://doi.org/10.1007/s41870-020-00430-y>

Heat Transfer Characteristics of Spherical Finned Rectangular Microchannel



S. Venkata Sai Sudheer, C. H. Naveen Kumar, G. Mahesh,
and C. H. Bhanu Prakesh

Abstract In this study, a three-dimensional numerical model is developed to investigate the heat transfer characteristics of a rectangular microchannel with and without fins. The fins are in spherical shape placed at the inner bottom wall of the channel. A constant heat flux of 100 W/cm^2 is applied at the outer bottom wall. 3D conjugate heat transfer mechanism is considered and simulations are done at the Reynolds number of 300, 500 and 800. From the results, it is observed that placing the spherical fins on the inner bottom wall of the channel increases heat transfer from channel walls to bulk fluid. Hence, the wall superheat decreases. The spherical finned rectangular microchannel has high heat transfer coefficient as compared with rectangular microchannel without fins.

Keywords Microchannel · CFD analysis · Finned channels · Electronics cooling

1 Introduction

The immense technology growth in electronic industry leads to the miniature of electronic components such as semiconductors and chips. However, these electronic components dissipate more amount of heat in the order of 100 W/cm^2 . The reliability and safety of these electronic systems depend upon the operating temperature. So, the proper cooling mechanism is required. The improper cooling may lead to the decrease in the performance and sometimes failure also. There are various techniques available to remove the heat from these components. On those, microchannel is a lucrative option to remove heat from miniature electronic systems. The first authors introduced the microchannel concept in 1981 are Tuckerman and Peace [1]. They fabricated microchannel with silicon material with overall bottom surface area 1 cm^2 and water was working fluid. They varied channel height in between 287 and $376 \mu\text{m}$ and channel width of approximately $60 \mu\text{m}$. These channels successfully dissipated heat up to 790 W/cm^2 and the chip temperature below 110°C . This first study grab the

S. V. S. Sudheer (✉) · C. H. N. Kumar · G. Mahesh · C. H. B. Prakesh
Mechanical Engineering Department, Vishnu Institute of Technology, Bhimavaram, Andhra Pradesh, India

© The Author(s), under exclusive license to Springer Nature Singapore Pte Ltd. 2022
B. B. V. L. Deepak et al. (eds.), *Applications of Computational Methods in Manufacturing and Product Design*, Lecture Notes in Mechanical Engineering,
https://doi.org/10.1007/978-981-19-0296-3_43

attention of the scientific community to use microchannels in the electronic systems where the natural cooling is not sufficient to remove the heat. From their onwards, scientists focused on the enhancement of heat transfer in microchannels by varying geometrical and operating parameters. Some of the studies in the open literature discussed in the subsequent section.

Jang and Choi [2] numerically investigated the performance of rectangular microchannel heat sink with diamond nanofluid. In their experiments nanofluid having 1% volume fraction is used. The heat transfer increases to 10% for microchannel with nanofluid as working fluid as compared water as working fluid. Zolingen et al. [3] numerically studied the influence of temperature on Photo Voltaic cells efficiency. An empirical equation to estimate the efficiency that is a function of PV cell temperature is developed. The developed equation clearly showed a negative gradient between the temperature and the conversion efficiency.

Rahman and Gui [4] developed a numerical model to analyze the thermo-hydraulic behavior of a silicon-based microchannel heat sinks. In their model a simplified three-dimensional conjugate heat transfer model, i.e., 2D fluid flow and 3D heat transfer is incorporated. The thermo-physical properties are estimated as per the local working fluid temperature. They studied the influence of the geometric parameters and thermos-physical properties of the working fluid on thermo-hydraulic behavior microchannels. From their results, it is observed that the consideration of local thermo-physical properties significantly influences the performance of the microchannel heat sink.

Chen and Chen [5] numerically analyzed the effect of channel cross sectional shape on silicon microchannel performance. In their study trapezoidal, triangular and rectangular cross sectional shapes are considered. Water is used as a cooling medium and Reynolds number is varied from $Re = 50$ to 500. It is concluded from the results that the performance of triangular shaped channels is high compared to other channels (trapezoidal and rectangular) of the same hydraulic diameter. Similarly, Wang et al. [6] numerically analyzed the effect of channel cross section shapes such as triangular, rectangular, trapezoidal and hexagonal on the performance of microchannel. In this study, copper is used as microchannel material and water is used as a coolant. For the fixed hydraulic diameter, number of channels and the cross sectional area, rectangular cross sectional micro channels have lowest thermal resistance when compared other cross sectional channels.

From the literature [7–9] it is understood that rectangular microchannels (RMC) are widely used as a heat sink due to better stability, ease of fabrication and higher heat transfer performance. However, the rapid growth in science and technology increases the heat dissipation from the small electronic components. In this context increasing the performance of microchannels is a challenging task. From the open literature, it is observed that the performance of microchannels is strongly influenced by hydraulic diameter, channel cross section shape as well as fluid properties. A simple passive technique used to increase heat transfer for rectangular microchannel is by providing external surface (fins) [10]. So, in the present work spherical fins are provided at the inner bottom wall of the rectangular microchannel (SRMC). 3D conjugate heat transfer model used for the present study. Equal and same volume

flow rate is considered for both configurations (with and without spherical fins) for comparison.

2 Mathematical Modeling

A rectangular microchannel with a footprint area of $5\text{ cm} \times 5\text{ cm}$ is considered, due to the symmetry, a single microchannel cell is considered for the present numerical analysis. Figure 1 depicts the computational model of a single rectangular microchannel cell with spherical fins. The dimensions of the microchannels are given below in Table 1. Copper is used as the heat sink material and water is used as the coolant fluid. A 3D conjugate heat transfer approach is used in the present work. Constant heat flux (100 W/cm^2) boundary condition is imposed at the heat sink bottom wall. Simulations are done at the Reynolds number of 300, 500 and 800 respectively. The following assumptions are considered:

- (i) The fluid properties vary w.r.t bulk fluid temperature.
- (ii) The flow is laminar, steady, and incompressible.
- (iii) Heat loss to the ambient is negligible.

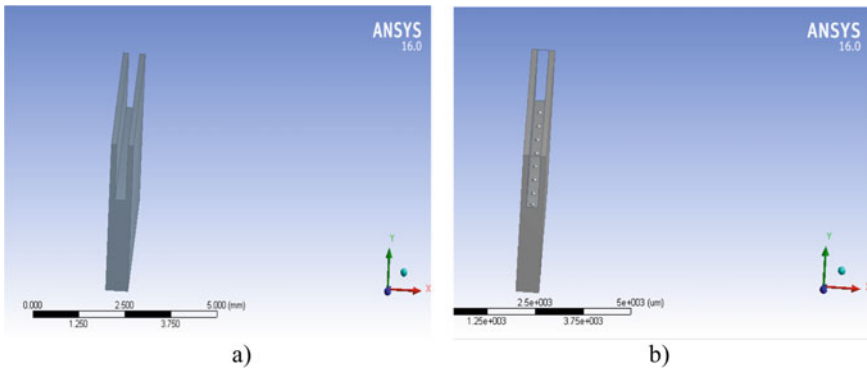


Fig. 1 a Rectangular microchannel b spherical finned rectangular microchannel

Table 1 Dimensions of the microchannel heat sink

S. No.	Name of the channel	Length of the channel (μm)	Width of the channel (μm)	Height of the channel (μm)	Depth of the channel (μm)	Fin radius and Height (μm)
1	Rectangular microchnnel	25,000	600	3200	1200	–
2	Spherical finned channel	25,000	600	3200	1200	50

(iv) No internal heat generation is considered here.

The continuity, momentum and energy equations for the fluid flow is given by.
Continuity equation:

$$\nabla \cdot (\rho \vec{v}) = 0 \quad (1)$$

Momentum equation

$$\nabla \cdot (\rho \vec{v} \vec{v}) = -\nabla P + \nabla \cdot (\mu \nabla \vec{v}) \quad (2)$$

Energy Equation

$$\nabla \cdot (\rho \vec{v} \vec{v}) = -\nabla P + \nabla \cdot (\mu \nabla \vec{v}) \quad (3)$$

Energy equation for solid zone is

$$\nabla \cdot (k \nabla T) = 0 \quad (4)$$

3 Data Reduction for Microchannel

1. Reynolds Number

$$Re = \frac{\rho U_{avg} D_{mc}}{\mu} \quad (5)$$

where

μ is dynamic viscosity of working fluid,

D_{mc} , U_{avg} and ρ are hydraulic diameter of microchannel, average fluid velocity and density of working fluid flowing through the microchannel, respectively.

2. Hydraulic diameter is calculated by

$$D_h = \frac{4 * W_{mc} * H_{mc}}{2(W_{mc} + H_{mc})} \quad (6)$$

where W_{mc} is width of single microchannel in m and H_{mc} is height of the microchannel in m .

3. Nusselts number is estimated by using

$$Nu = \frac{h D_h}{k} \quad (7)$$

where h and k represents convective heat transfer rate, thermal conductivity of working fluid, respectively.

4. The following equations are used to evaluate heat transfer coefficient and wall heat flux.

$$h = \frac{q_w''}{T_w - T_{avg}} \quad (8)$$

$$q_w'' = \frac{q'' * A_b}{N * A_s} \quad (9)$$

where

- T_w Channel wall temperature
- T_{avg} Average fluid temperature
- q'' Heat flux applied at the base of the channel.
- q_w'' Heat convected from inner bottom and side walls of channel.
- A_b Area of bottom wall
- A_s Sum of the surface areas of bottom and side walls of channel
- N Number of channels

5. Surface area of the hemisphere

$$A = 2\pi r^2 \quad (10)$$

where “ r ” is the radius of the sphere in μm .

4 Results and Discussion

4.1 Average Wall Temperature

Figure 2 depicts the variation of average local wall temperature across the length of the channel at the heat flux of 100 W/cm^2 . The local average wall temperature is increased across the channel length. It is observed that the average local wall temperature for the spherical finned RMC is less at every location as compared with RMC. This happened because, the spherical fins rapture the thermal boundary layer across the channel, and the redevelopment of thermal boundary offers better mixing. Which results in local wall temperature decreases. For a better understanding, wall temperatures contours are plotted for RMC and SRMC at Reynolds numbers of 500. The SRMC wall temperature contours exhibits linear uniform temperature distribution that can replicate in Fig. 3

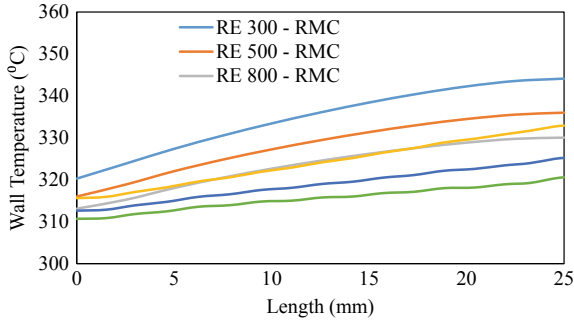


Fig. 2 Local average wall temperature profiles across the channel length

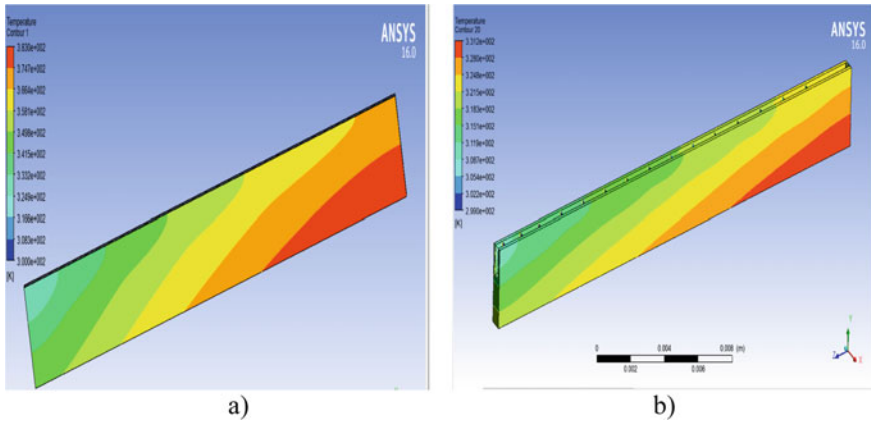


Fig. 3 Wall temperature distribution at Re-500 a RMC b SRMC

4.2 Wall Superheat

The relation between wall temperature and working fluid temperature is expressed in terms of wall superheat (the difference between wall temperature and working fluid temperature). Figure 4 depicts the influence of spherical fins on wall superheat. The wall temperature and bulk fluid temperature are considered at the fin and middle of two successive fins locations. It is observed that the wall superheat significantly differs for RMC and SRMC. In RMC wall superheat initially slightly decreases then after increases to a peak value and starts decreasing. The increased fluid temperature and decrement in wall temperature rise across the channel length cause such variation. Whereas in SRMC wall superheat exhibits oscillatory behavior observed. At the fin locations lower wall superheat and middle of the two fins higher wall superheat is obtained. The local bulk fluid temperature significantly differs at fin and middle of the fin locations. This is because, at fin location more area is available hence local bulk

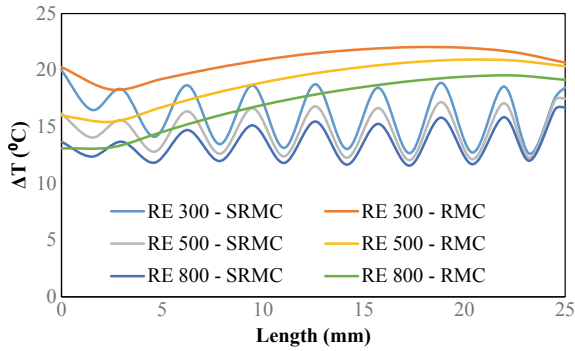


Fig. 4 Wall superheat across the channel length

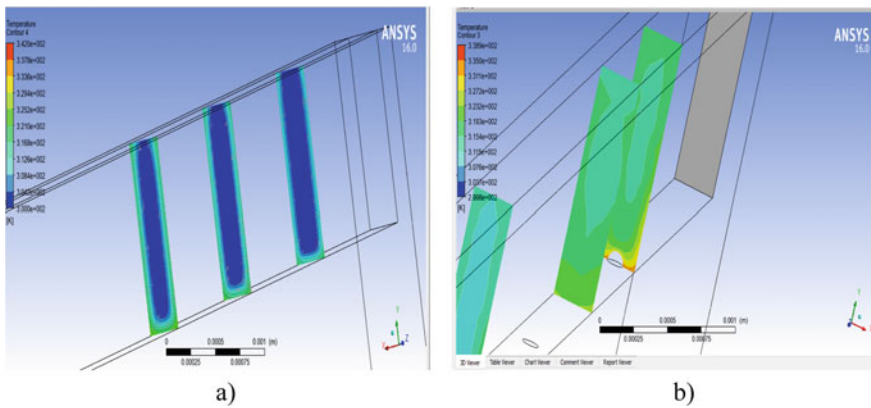


Fig. 5 Bulk fluid temperature at Re-500 for a) RMC b) SRMC

fluid temperature increases with the increased in heat transfer rate and decreases with wall superheat. The bulk fluid temperature contour plots (Fig. 5) clearly distinguish the influence of fin.

4.3 Heat Transfer Coefficient

Figure 6 depicts the local heat transfer coefficient (HTC) for RMC and SRMC across the channel length. HTC is a function of wall heat flux and wall superheat. For a fixed operating condition, i.e., heat flux input at bottom of the wall, working fluid inlet temperature and fixed mass flow rate, the HTC is a function of wall superheat. In RMC HTC decreases across the channel. This is because of the increase of wall superheat that was observed in Fig. 2. Whereas for SRMC similar to wall superheat

Fig. 6 Local heat transfer coefficient across the channel length

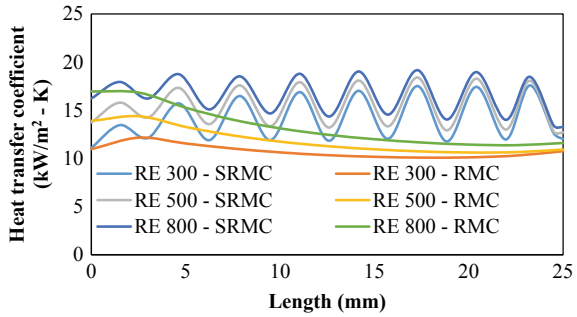
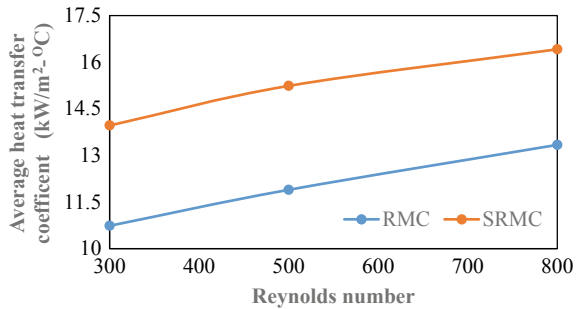


Fig. 7 Influence of Reynolds number on microchannel HTC



HTC also exhibits oscillatory behavior. It is observed that the local HTC is high at fin locations and low at the middle of the two successive fin locations. At the fins, more heat transfer took place hence the wall superheat decreases which results in increase in local HTC and vice versa.

4.4 Average Nusselt Number

Figure 7 shows the variation of the average HTC for different Reynolds number. The RMC and SRMC increase the HTC with the Reynolds number. Increase of Reynolds number increases the convection heat transfer that can lead to decrease in wall superheat (Fig. 4). Therefore, HTC increases. It is observed that SRMC has high HTC than the RMC. The average enhancement in HTC is 27.09%. The provision of fins on the bottom wall of the channel increases the heat transfer.

5 Conclusions

The major conclusions are drawn from the present numerical study as follows:

1. The average wall temperature decreases with the increase of the mass flow rate for RMC and SRMC channels.
2. For a particular mass flow rate the SRMC channel local wall temperature is always lesser than the RMC channel wall temperature.
3. The wall superheat for SRMC channel is oscillatory in behavior whereas for RMC channel it is almost linear variation. This is because, at the finned locations more amount of heat transfer took place.
4. Similar to wall superheat the local heat transfer coefficient also shown oscillatory behavior for SRMC. The maximum local heat transfer coefficient is obtained at fin location.
5. SRMC has high heat transfer coefficient at all the Reynolds numbers. The average increase in heat transfer coefficient over RMC is 27.09%.

References

1. Tuckerman DB, Pease RFW (1981) High-performance heat sinking for VLSI 126–9
2. Cho ES, Choi JW, Yoon JS, Kim MS (2010) Experimental study on microchannel heat sinks considering mass flow distribution with non-uniform heat flux conditions. *Int J Heat Mass Transf* 53:2159–2168. <https://doi.org/10.1016/j.ijheatmasstransfer.2009.12.026>
3. Van Helden WGJ, Van Zolingen RJC, Zondag HA (2004) PV Thermal systems: PV panels supplying renewable electricity and heat. *Prog Photovoltaics Res Appl* 12:415–426. <https://doi.org/10.1002/pip.559>
4. Rahman MM, Gui F (1993) Experimental measurements of fluid flow and heat transfer in microchannel cooling passages in a chip substrate. *ASME EEP* 4:685–692
5. Chen Y, Cheng P (2002) Heat transfer and pressure drop in fractal tree-like microchannel nets. *Int J Heat Mass Transf* 45:2643–2648. [https://doi.org/10.1016/S0017-9310\(02\)00013-3](https://doi.org/10.1016/S0017-9310(02)00013-3)
6. Wang H, Chen Z, Gao J (2016) Influence of geometric parameters on flow and heat transfer performance of micro-channel heat sinks. *Appl Therm Eng* 107:870–879. <https://doi.org/10.1016/j.applthermaleng.2016.07.039>
7. Ma H, Duan Z, Ning X, Su L (2019) Numerical investigation on heat transfer behavior of thermally developing flow inside rectangular microchannels. *Sci Total Environ* 0:1–30. <https://doi.org/10.1016/j.scite.2021.100856>
8. Mahesh P, Kumar KK, Balasubramanian K, Thejas (2019) Numerical modelling of nanofluid based microchannel heat sink. *Int J Adv Trends Comput Appl* 1:188–193
9. Su L, Duan Z, He B et al (2020) Heat transfer characteristics of thermally developing flow in rectangular microchannels with constant wall temperature. *Int J Therm Sci* 155:106412. <https://doi.org/10.1016/j.ijthermalsci.2020.106412>
10. Prajapati YK (2019) Influence of fin height on heat transfer and fluid flow characteristics of rectangular microchannel heat sink. *Int J Heat Mass Transf* 137:1041–1052. <https://doi.org/10.1016/j.ijheatmasstransfer.2019.04.012>

Design and Fabrication of Automatic Vehicle for Railway Track Monitoring by Using ESP8266 Module



L. Daloji, I. Ramu, Narasinga Rao, and P. Manikanta

Abstract The present work aims to detect the defects of the tracks by using Internet of Things Technology. From the recent study, it is observed that nearly 30% of the track length requires replacement due to various defects. This work deals with railway track monitoring using IR sensor, used to detect the defects on the tracks and to find exact location of the accident. The proposed system detects the crack on the railway track without any human interference i.e. automatically. The downloaded app is registered in the android device in which the message is sending by the ESP8266 module, connected through the Wi-Fi module to send alert messages. With the help of received message, can get the exact location of the defect which is opened in the Google map. IR sensor detects not only cracks but also the objects or any living beings which are across the track. Performed the prevention of train crash by detecting the cracks on the rail track using the Internet of Things Technology. The system accuracy is improved by inclusion of IR sensor and ESP8266 module at less cost and minimized time. Code has been developed to run the system.

Keywords ESP8266 module · Internet of Things · Railway track · IR Sensor · GPS system

1 Introduction

Railway is the lifeline or pulse of transportation in India, which is not only used for commercial purposes but also for transportation of goods and raw materials at cheaper cost. The main task of the system is to combine all the best and latest technologies by comparing different methods to achieve high accuracy at low cost [1]. In current scenario, humans are made to check and maintain the track, which

L. Daloji · I. Ramu (✉) · N. Rao
Faculty of Mechanical Engineering, Vishnu Institute of Technology, Bhimavaram,
Andhra Pradesh 534202, India

P. Manikanta
Student in Mechanical Engineering, Vishnu Institute of Technology, Bhimavaram,
Andhra Pradesh 534202, India

gives low accuracy when compared to automatic system. Maintenance of tracks are required in all seasons irrespective of climate conditions [2, 3]. Tracks in India are spread in 1, 15,000 km which seems highly impossible to check the cracks daily by human beings. Main objective of this work is to design the fully automatic crack detection system which is based on IR sensor technology. This proposed system is cost effective and takes less time to detect faults and send a message to receiver [4]. It also sends a specific fault details which ease out this task to inspect the whole track. Result of the fault along with co-ordinate is also displayed on the LCD mounted on the System [5]. To check what type of error is detected.

The developed power is used to drive the vehicle, the automated vehicle will detect the cracks [6]. Thentral et al. [7] studied the utilization of GPS system by using IR sensor and Arduino nano for transmitting and to get message when crack is identified. In this system, using GSM Module the fault data can be identified and send the message to railway management center. So, the location will be showed by GPS receiver [7]. Kuthe et al. proposed a smart robot for detection of cracks using assembled LED photodiode, by using this system accuracy obtained is 70% [8]. Image processing method is used by Rizvi et al. for inspecting the cracks automatically, this method uses a Video camera to take the images of the track in separate sections [9]. Jha et al. is used LDR sensor in solar system for automatic inspection of the tracks [10]. Automated vehicle is designed for crack inspection by Bhushan et al., field survey is conducted to gather the information about various errors. This inspection is done by using two different sensors which are incorporated in electronic setup [11]. Adarsh et al. examined and compared the performance of IR and Ultrasonic sensors which are used for distance measurement and done statistical analysis for distance measurement in both the tracks [12]. Railway Track Breakage Detection Method is done by Sharma et. al using Vibration Estimating Sensor, the system worked for automatic inspection of the cracks when compared with LED sensors and Imaging method [13]. Sandeep Kumar et. al developed an embedded system to check the error in rail track and at the same time message is sent to nearest station using ZIGBEE Technology [14]. The particular system is constructed with micro-controller and SPDT relays and driver IC. Prof. Navaraja introduced the concept of integration of ultrasonic and PIR sensors to detect the cracks in railway tracks [15]. The significance of GPS module and GSM module is explained in detail. From the various sources, the following case studies were identified where accidents were taken place due to various reasons. In the year of 2016, the accident taken place in Kanpur (GAISAL TRAIN) due to the reason called fracture and unevenness in the track. In the year of 2017, the accident taken place in MANIKPUR (VASCO DA GAMA EXPRESS) due to fracture in rail track. In the year of 2019, the accident taken place in Bihar (SEEMANCHAL express) because of missing of tracks was observed.

In recent times there is lot of train accidents taking place which cause economical as well loss of life [16]. The goal of project is to minimize accidents and also designed for effective checking of tracks and notify well before the accident. It can also be seen in various industrial applications, which is used for material handling in automobile, steel, coal, etc. Accidents of train are mostly caused due to track problems. From the

previous research, it is identified that the failure due to various reasons like fracture, misaligned, cracks or cuts, unevenness of track surface [17]. The aim of this study is to detect the cracks and obstacles automatically in the railway track by using IR Sensor and ESP8266 Module. Concept of GPS system is used to identify exact location of the train crash by detecting the cracks on the rail track by introducing IOT.

2 Design and Fabrication of Proposed System

A. Design of the model

The following design procedure is used in proposed model. Basically three major sensors are used for detection of faults namely, IR sensor. (R—right track and L—left Track), Vibration sensor. (V—Vibration) and Obstacle detection sensor. (A—Anti-collision). These sensors are connected to the programmed microcontroller by using jumper wire for flexibility purpose [1]. In the next step ESP Module and GPS kit along with Buzzer, Motor controller Module and Regulator are connected to the micro controller. To operate this particular system, a 6 V battery is used for power supply. The entire setup is attached to the acrylic plate and fixed on the frame. Now a 2 DC motors are of 12 V will be displayed below the frame, which is connected to the relay system. In the final step, GPS receiver is mounted on the top of the model. Thus the model is completed and represented in Fig. 1. And can be run on the track to detect the fault. And the circuit diagram is drawn for the system as shown in Fig. 2.

The major components like Buzzer, Motor driver, GPS and ESP module are represented in the circuit diagram (Fig. 2) and the input parameters are provided in the electrical setup to perform proper functioning of the vehicle.

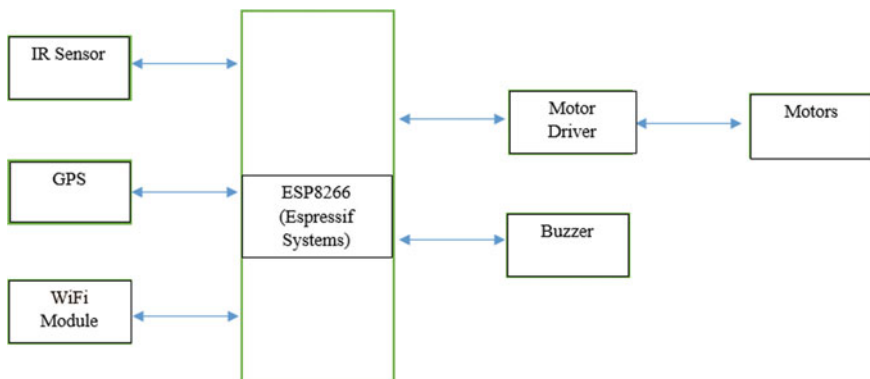


Fig. 1 Block diagram of the proposed system

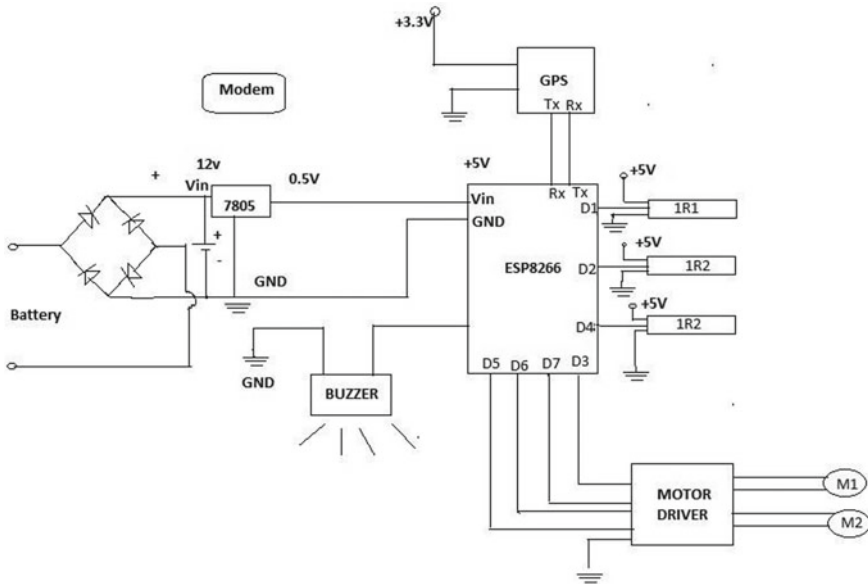
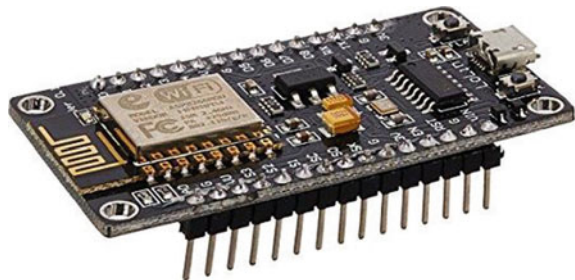


Fig. 2 Circuit diagram

B. Fabrication process

The automatic vehicle is designed and fabricated for identifying such kind of errors in an efficient way with high accuracy. The main components used in fabrication of proposed system like Frame or chassis, it is an important part of the system. Because all the loads of the equipment are handled by the frame. In fabrication of frame the material selected is mild steel because it offers great resistance against wear and tear. Similarly, Nut and bolt are used to fix all the components to the chassis. Another one which is used is Acrylic plate, this is to avoid any kind of shock or heating. Acrylic plate is used as it is a bad conductor of electricity. The designed system is working with ESP8266 Module as shown in the Fig. 3, it is an advanced micro controller and self-contained Wi-Fi networking solution [18]. This is capable of functioning

Fig. 3 ESP8266
(Electronics.com) [19]



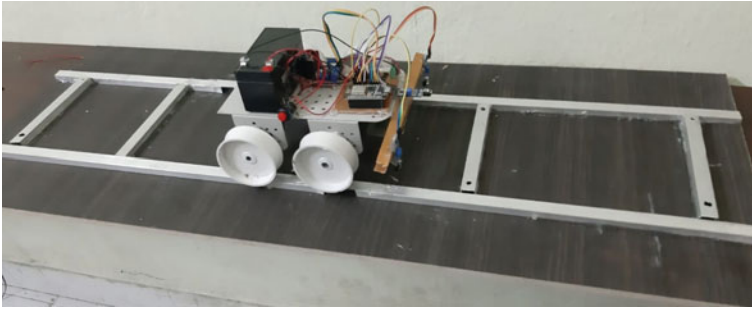


Fig. 4 Fabricated model of automated vehicle

consistently in various industry environments due to its wide operating range. It is very less cost.

In this process first Cutting of the acrylic plate has done according to dimensions. Fix all the components on acrylic plate by drilling with the help of nut and bolt. In the next step place the motor on the mainframe and fix all the components on the plate. Now combine the both steel frame and acrylic plate. Arrangement of sensor by using aluminum strip is done in the next step. The concept of soldering is used to connect all the components by using jumper wire. Finally provide electric connection to motor and check the condition of proposed system as illustrated in Fig. 4. Now place the GPS on top of the system.

2.1 Working of the System

After switching on the Power of automatic vehicle, it will move along the track. The condition of the track is going to monitor and inspected by IR sensor as represented in Fig. 5a and b. The vehicle will get stop there, when the crack is detected by Sensor and GPS receiver will analyze and receive the exact location of the vehicle position. GPS system will receive Latitude and longitude coordinates, which get converted into notification as shown in the Fig. 6a and b.

This is done by microcontroller. ESP8266 module sending the message to predefined application with the help of Wi-Fi which is inbuilt into the module. A message will be sent to the application, accordingly the vehicle will move forward depends up on type of crack occurred.

2.2 Experimental Results and Discussions

1. Constant Speed of the Vehicle is Calculated by Using Following Formula as Shown in Eq. (1)

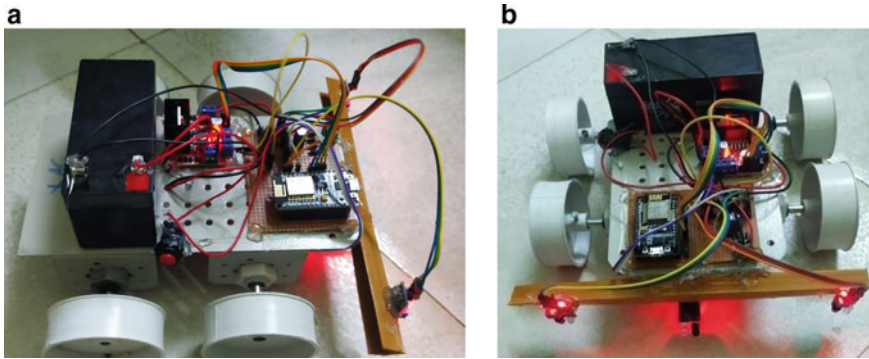


Fig. 5 **a** Side view representation of working model. **b** Front view representation of working model

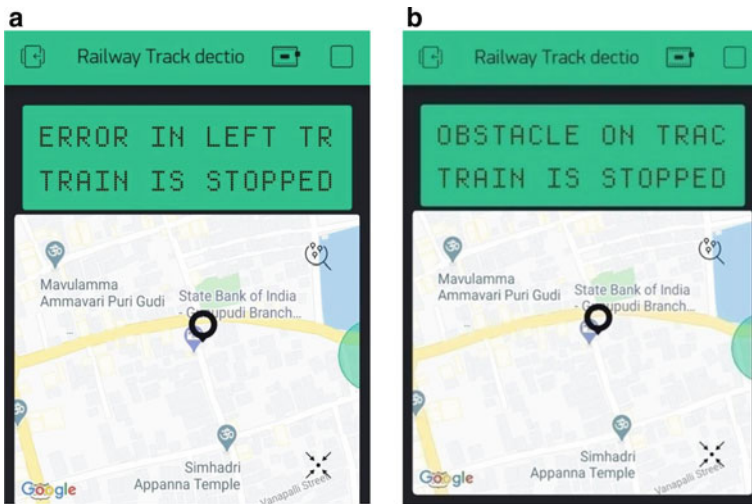


Fig. 6 **a** Error location in left track, **b** Obstacle location

$$\begin{aligned}
 \text{Constant speed} \left(\frac{\text{cm}}{\text{sec}} \right) &= \frac{\text{perimeter of the wheel}}{\text{time required for one revolution}} \\
 &= \frac{3.14 * 6}{7} = 2.75 \tag{1}
 \end{aligned}$$

From the Table 1, it is observed that at constant speed of the vehicle, crack detection time is very less in the proposed system. In all three cases irrespective of locations the time was calculated. Obstacle sensor detection was done by trial and error method (cm): 12 to 15 cm.

Program is written for error checking in left and right tracks and also for obstacle location. Representation of hardware program is also done for GPS system

Table 1 Crack calculation time

S. No.	Location of detected crack	Constant speed of vehicle (cm/sec)	Detection time	Actual distance of detected fault (cm)
1	R	2.75	8	22
2	L	2.75	15	41.25
3	A	2.75	21	57.75

messaging. Model test has been conducted to detect the crack on the track. In this work with the help of IOT, the message is sending by ESP8266 module which is connected through the Wi-Fi. Once receiving the message, can get the exact location of the error which is opened in the Google map.

3 Conclusion

The response of the system is very quick which takes less than 5 s to complete one cycle of detecting and sending message. The detection of cracks and obstacles was studied with the help of ESP8266 module with IOT concept. The accuracy of the system is improved when compared with other models according to reviewed literature, hence the system accuracy is up to 85%. Finding of the correct location of the crack was done with GPS system.

The future scope of this work is by adding a series of ultrasonic detectors and IR sensors, can improve the area of detection. Vibration sensor can also be used to detect moment in Left right, to and fro, and also up and down in X, Y and Z axis respectively. This will help to detect track surface in a wider area.

References

1. Ramavath Swetha WP, Prasad Reddy V (2016) Railway track crack detection autonomous vehicle (2016)
2. Naresh Kumar D, Uday M, Brahmini G, Mounika Reddy A, Sagar Kumar M (2017) Railway track crack detecting system. IJSDR 2(4), Apr 2017
3. Rakesh G, Durga Prasad B (2017) Automatic railway track crack detecting vehicle. JETIR (ISSN-2349-5162), 4(10), Oct 2017
4. Singh H, Singh J, Singh V, Pateriya R (2018) Railway accident protection. Int J Adv Res Sci Eng 7(6), June 2018
5. Addagatla P, Koteswar Rao G, A modern method for detecting cracks in railway tracks by the efficient utilization of LDR and LED system. Int J Eng Sci Invention
6. Madhu G, Yohan M (2019) Solar operated automatic crack detection system for railway track. Int J Mach Constr Eng 6(2) June 2019
7. Thamizh Thentral TM, Geetha A (2020) Railway track crack detection system. Int J Adv Sci Technol 29(10S):3164–3171

8. Kuthe SD, Amale SA, Barbuddhye VG (2015) Smart robot for railway track crack detection system using LED-photodiode assembly. *Adv Res Electr Electron Eng (AREEE)* 2(5), April–June
9. Rizvi AR (2017) Crack detection in railway tracks by image processing. *Int J Adv Res Ideas Innov Technol*
10. Jha CK, Singh SK, Sainath TT, Sumanth S (2017) Crack detection vehicle. *Int J Eng Sci Comput* April
11. Bhushan M, SujayTushar B, Chitra P, 4. Automated vehicle for railway track fault detection
12. Parrilla M, Nevado P, Ibanez A, Camacho J, Brizuela J, Fritsch C (2008) Ultrasonic imaging of solid railway wheels. *IEEE* 08:2008
13. Sharma K, Maheshwari S, Solanki R, Khanna V, (2014) Railway track breakage detection method using vibration estimating sensor network. *IEEE* (14)
14. Sandeep Kumar K, Srinivasa Reddy K, Dhanavath RK, Geetha Reddy E (2016) Railway security system for track fault detection using ZIGBEE communication. *Int J Adv Res Sci Eng Technol* 3(9) Sept 2016
15. Navaraja P (2014) Crack detection system for railway track by using ultrasonic and PIR sensor. *IJAICT* 1(1), May 2014
16. The Hindu Official Website (2012) Ultrasonic railway crack detection system
17. Shekhar RS, Shekhar P, Ganesan P (2015) Automatic detection of squats in railway track. In: *IEEE sponsored 2nd international conference on innovations in information embedded and communication systems*. 3(6), pp 413–413 Dec 2015
18. Ajith A, Aswathy KS, Binoy Kumar H, Davis D, Innovative railway track surveying with sensors and controlled by wireless communication. *IJREAT Int J Res Eng Adv Technol* 2(2), Apr-May 2014
19. Basic electronic components by Arther f. Seymer MSCC

Design and Evaluation of Manual Weeder for Dryland Crops



P. D. V. N. Krishna, V. Mahesh Chakravarthi, Mummina Vinod,
and Srinivas Pothala

Abstract This paper presents the work carried out to design a manual weeder used for dryland crops by using manual power. There are several types of such devices, but there is nowhere a proper way of designing this equipment. The designing of the weeder was carried out by calculating forces on tines and power developed by the operator. In this weeder, the power of the man can be utilized using these small devices and the output can be increased and these devices are very useful for lowland as well as upland conditions, dryland conditions, and for small farms because about 60% of the farms particularly in India are small farms. A prototype has been built and experiments performed which adequately indicates that the weeder gives good results when weeding operation was done within 15–20 days after sowing of seeds because the size of weeds was 2–5 cm.

Keywords Weeds · Design · Weeder · Manually operated weeder · Dryland

1 Introduction

The unwanted plant or other than required plant in crops is termed as weeds. Weeds are reducing the crop yield by up to 30–60%. Weeds always compete with the main crop and tend to dominate. The weeding operation in agriculture alone accounts for 25% of the total labor requirement (900–1200 man-h ha⁻¹) [1]. Weed management consists of several methods some of them are biological, chemical, cultural, and physical/mechanical control.

In biological weed control, pathogens and natural enemies are used to control the weeds.

Chemicals or herbicides are also used in weed management. For the last fifteen years, herbicides damage the environment and human health which leads to the development of new methods for non-chemical weed control [2, 3].

P. D. V. N. Krishna (✉) · V. M. Chakravarthi · M. Vinod · S. Pothala
Vishnu Institute of Technology, Bhimavaram 534202, India
e-mail: 16pa1a0377@vishnu.edu.in

The mechanical methods contain digging, hoeing, hand weeding, plowing, sickling, cutting, burning, flooding, mulching, etc. Hand weeding is removing unwanted plants by hand or using hand tools in crops. It is costly, time-consuming, and hard to organize. Weeds cannot be controlled alone by physical methods. They must be used in combination with other preventive and cultural methods [4].

There are different types of manual weeders are in existence. Some of them are Peg type weeder, Star weeder, Wheel hoe twin wheel type, Single row cono weeder, Wheel hoe single wheel type, etc. They are not used for large area crops, require manpower, are difficult to remove weeds close to crop plants, poor results when the soil is too dry or too wet. Based on the study conducted in the north of India about the injuries of farmhand tools [5], the hand tool causes major injuries (58%) in farming, among them female workers are highly injured (65%). An unsuitable handle dimensions decrease the essential force, demanding more impact velocities for cutting, loose grip, slippage, and wrong direction of applied force. Therefore, there is a need to develop a weeding machine that operates manually by considering the forces and comforts of the operator using designing techniques. This design includes applying engineering concepts to study the nature of forces and finding stresses on tines and field study for evaluating the model in terms of efficiency. While operating this manual weeder, the operator can discriminate the both crop and weed. so the operator can remove weed by using this manual weeder.

2 Design Procedure for Manually Operated Weeder

Design considerations are: Apex angle should be in the range of 35°–45°. Speed of operation is 30–50 strokes/min. The length of the stroke is 300–500 mm. The physiological cost should not exceed 110 beats min^{-1} in terms of cardiac cost or 0.71 min^{-1} in terms of consumption rate or 8 h work [7]. The speed and depth of operation are 1 km/hr and 5 cm, respectively. Unit draft of soil is 0.2 kg/cm^2 .

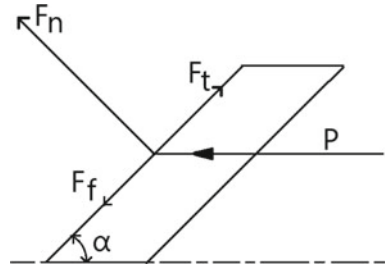
2.1 Force Analysis on Tines

This section represents the force on the tines of a manually operated weeder. The weed removal is mainly dependent upon the forces that are acting on the tines. Based on frictional force and cutting force the weed removal takes place. The representation of forces on tines is shown in Fig. 1. The following are the forces that are involved: Frictional Force (F_f), Tangential force (F_t), Normal Force (F_n), Pull or Push Force (P).

$$F_f = F_n \tan \psi \quad (1)$$

Normal Force (F_n) is the force that is normal to the surface of tines.

Fig. 1 Forces on tine



$$F_n = P \sin \alpha. \tag{2}$$

where α is apex angle = 35° , $P \sin \alpha$ is the component of P .

P = Pull or Push Force = 45 N for men and 36 N for females [6]. According to ergonomic considerations in the design of manual weeders, the weeding tool should be such that the operator does not have to exert more than 60 N push or 60 N pull [7].

$$F_n = 45 \times \sin 35^\circ = 25.81 \text{ N}$$

The value of angle of friction (Ψ) is selected as 30° (corresponding to soil & tool). From Eq. (1) & Eq. (2).

$$F_f = 25.81 \times \tan 30^\circ = 14.90 \text{ N}$$

Tangential force (F_t) is the force that acts in the direction of the tangent of a body.

$$F_t = P \cos \alpha. \tag{3}$$

$$= 45 \times \cos 35^\circ = 36.86 \text{ N}.$$

The root is cut through when the Tangential force (F_t), becomes higher than the Frictional force (F_f)

$$F_f < F_t. \tag{4}$$

From Eqs. (3) and (4)

$$F_n \tan \Psi < P \cos \alpha$$

$$14.90 < 36.86$$

Hence, the root is cut by the tines.

The angle of setting of the blade should be [7],

$$\alpha < (\pi/2 - \Psi)$$

$$35^\circ < \delta(\pi/2 - 30^\circ)$$

$$35^\circ < 70^\circ$$

Hence, the selected angles $\alpha = 35^\circ$ and $\Psi = 30^\circ$ satisfy the above condition.

2.2 Power Developed by the Operator

As per the ergonomic requirements, the power developed by the operator would be in the range of 0.10 hp [7].

$$\text{Power} = \text{Total Draft} \times \text{Speed}$$

$$0.1 \times 746 = D \times 1 \times (1000/3600) \tag{5}$$

$$D = 268.6 \text{ N.}$$

$$D = 27.37 \text{ kg.}$$

$$\text{Total Draft } (D) = 27.37 \text{ kg.}$$

2.3 Design of Tines

Tines play a major role in cutting of weeds. The diagrammatic representation of tines is shown in Fig. 2. The dimensions of tines are calculated below:

Width of furrow.

$$W = 2 a_{\max} + B_o \text{ [7]}$$

Consider, $a_{\max} = 5 \text{ cm}$, $B_o = 1 \text{ cm}$.

$$W = 2 \times 5 + 1.$$

$$W = 11 \text{ cm} = 110 \text{ mm.}$$

Fig. 2 Diagrammatic representation of tines

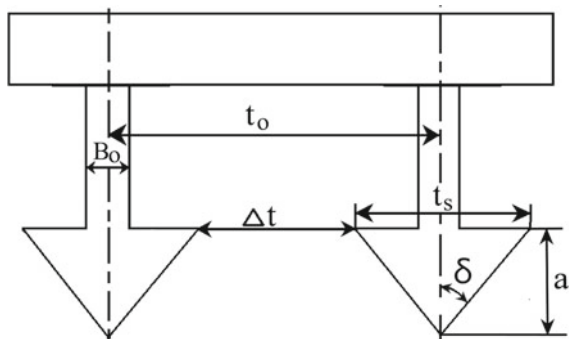
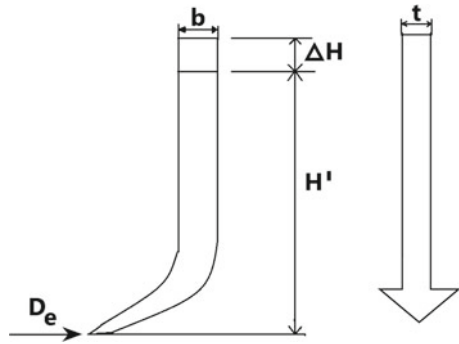


Fig. 3 Side view of a tine



Spacing between tines

$$t_o = 2a \tan \delta + B_o + \Delta t \quad [7] \tag{6}$$

Consider, Depth of furrow (a) = 5.5 cm, $\delta = 45^\circ$, Distance between tines (Δt) = 1 cm.

$$= 2 \times 5.5 \tan 45^\circ + 1 + 1 = 13 \text{ cm} = 130 \text{ mm.}$$

Draft on one tine (D_o) = Unit draft \times Cross-sectional area of the furrow.

Cross-sectional area of the furrow = (width of furrow \times depth of furrow) / 2.

$$= (12 \times 5) / 2 = 30 \text{ cm}^2.$$

Draft on one tine (D_o) = $0.2 \times 30 = 6 \text{ kg.}$

The side view of tine is shown in Fig. 3

$$\text{Actual Draft}(D_e) = D_o \times \text{FOS} \tag{7}$$

where, Draft on one tine (D_o) = 6 kg,

$$\begin{aligned} \text{Consider, Factor of safety (FOS)} &= 1.5 = 6 \times 1.5 \\ &= 9 \text{ kg} \end{aligned}$$

Number of tines [7] = Total draft/actual draft on one tine = $27.37 / 9 = 3.04$.

So, we take the number of tines as 3.

Moment on time,

Bending moment on tine(B_M) = Actual draft on one tine \times moment arm length

$$B_M = D_e \times H^1$$

Where, H^1 = moment arm length = 12 cm.

From Eq. (6)

$$B_M = 9 \times 12 = 108 \text{ kg} - \text{cm}$$

Bending stress,

$$\tau_b = \frac{BM \times Y}{I} \tag{8}$$

where, τ_b = Bending Stress, kg/cm².

Y = distance from the neutral axis to the point at which stress is calculated, cm.

I = polar moment of inertia of section, cm⁴

$$I = \frac{tb^3}{12}$$

The ratio between the thickness (*t*) and width (*b*) of the tine is generally assumed to be 1:4

Allowable stress of the material, i.e., for Mild Steel is 1050 kg/cm² [7]

$$1050 = \frac{108 \times \left(\frac{4t}{2}\right)}{\frac{64t^4}{12}}$$

$$t = 0.337 \text{ cm} = 3.4 \text{ mm} \tag{9}$$

But due to dimension stability, we generally take a minimum thickness of 5 mm. Therefore,

$$t = 5 \text{ mm and } b = 20 \text{ mm.}$$

2.4 Design of Handle

The specifications of the handle [7] are shown in Fig. 4 are: A standard lightweight M.S having 27.5 mm outside diameter conduit pipe is used for the handle of the tool carrier. The height of the handle is calculated based on the 5th percentile value of

Fig. 4 Specification of handle

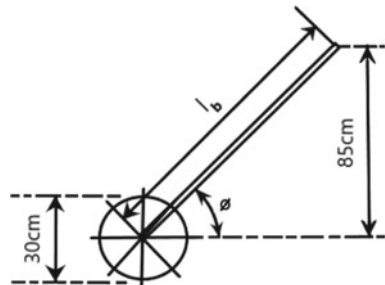


Table 1 Specifications

Components (mm)	Particular	Specifications
Overall dimensions	Length* width* Height	1650*400*1000
Weeding component	Thickness* Width	5*20
Whee	Diameter*Width	300*400
Handle	Length*Diameter	1500*27.5

the shoulder height of female operators (800–1020 mm). The distance between the wheel center to operating height is 850 mm. The diameter of the wheel is 30 cm. The angle of inclination (\varnothing) of the wheel hoe handle with horizontal is 35° .

Therefore,

The length of the handle is given by

$$l_b = \frac{85}{\sin 35^\circ}$$

$$l_b = 148.2 \text{ cm} = 1482 \text{ mm} \tag{10}$$

So, to accommodate 5–95% of operators, a 27.5 mm outer diameter conduit pipe having 1500 mm length is used for the handle. The material used for this is Mild Steel.

The specifications are shown in Table 1.

3 Designing of Manual Weeder

The design of the manual weeder is done by using AutoCAD 2015 software as shown in Fig. 5. This gives an idea about the weeder and also allows verification before fabrication. The model was designed based on the calculation done and the values that were obtained. The isometric and orthographic views were obtained to check the design model and modification was done.

Fig. 5 Isometric view of manually operated weeder



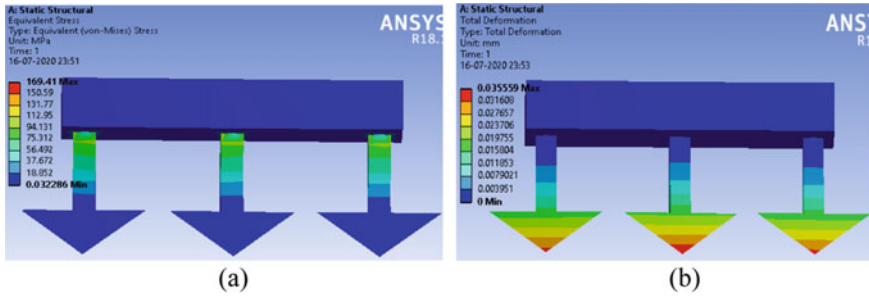


Fig. 6 Ansys model: a Equivalent (Von-Mises) Stress, b total deformation

4 Simulation

The Simulation performance of the system has been carried out in Ansys 18.1 software Fig. 6 diagram represents the model of tines. This model has been used to calculate the stress, strain, deformation in tines to ensure the model would be sustained in the field or not. The Actual draft (9.9 kg) was applied on the tines by fixing two faces on the support of a manually operated weeder.

The results of maximum equivalent stresses (a) are 169.41 MPa and total deformation (b) is 0.035 mm was obtained. The outcomes of static structural analysis done on tines showed that the stress values developed in the tines were within the limits of the yield stress of the material (250 MPa). The approximate yield strength of Mild Steel is 250 MPa [8]. Hence, the tines are chosen for the study can be accepted for the design of a weeder.

5 Results

The fabricated model is shown in Fig. 7 and it was made of Mild Steel material by using assembly techniques like welding, grinding, cutting, drilling, etc.

The following results were calculated based on experiments conducted on fields,



Fig. 7 Manually operated weeder

Weeding efficiency,

The weeding efficiency is calculated by using the formula. It is expressed in percentage.

$$\text{Weeding efficiency (\%)} = \frac{W_1 - W_2}{W_1} \times 100 \tag{11}$$

For the Maize crop,

W_1 = Number of weeds counted per 1 m² area before weeding operation = 33 weeds/m².

W_2 = Number of weeds counted in same 1 m² area after weeding operation = 9 weeds/m²

$$\begin{aligned} \text{Weeding efficiency (\%)} &= \frac{75 - 10}{75} \times 100 \\ &= 86.7\% \end{aligned}$$

Table 2 shows the weeding efficiencies of maize crop after the weeding operation is done. The weeds that are identified in the given crop are named in the table. W_1 is the average number of weeds per m² in the given crop before the weeding operation. W_2 is the average number of weeds per m² in the given crop after weeding.

Plant damage,

The plant damage is obtained by using the formula. It is expressed in percentage.

$$\text{Plantdamage(\%)} = \left(1 - \frac{q}{p}\right) \times 100 \tag{12}$$

For the Maize crop,

p = Number of plants in a 5 m row length of field before weeding = 25.

q = Number of plants in a 5 m row length of field after weeding = 24.

$$\begin{aligned} \text{Plantdamage(\%)} &= \left(1 - \frac{24}{25}\right) \times 100 \\ &= 4\%. \end{aligned}$$

Table 2 Weeding efficiencies for different crops

Crop	Weeds name	W_1 (weeds/m ²)	W_2 (weeds/m ²)	Weeding efficiency (%)
Maize	Cyanodondactylon,	60	12	80
	Chlorisbarbata,	66	24	78.8
	Acalyphaindica,	120	26	78.32
	Euphorbia prostrata	105	21	80
		75	10	86.66

Table 3 Comparison of different weeders

Item	Hand-push mechanical weeder (cone rotor blades)	Manual operated petrol engine powered weeder	Metallic wheel manually operated weeder
Width of cut	18 cm	38 cm	20
Depth of cut	0.2 cm	5 cm	5
Weeding efficiency	84.5%	71%	86.6%
Plant damage	8.33%	–	4%

Table 3 shows the comparison of Hand-push mechanical weeder (cone rotor blades) [9], Manual operated petrol Engine powered weeder [10], and manual weeder (Single wheel). The weeding efficiency for manual weeder is more compared to others because it was designed by considering all mechanical factors. Maintenance and environmental impact are less for manual weeder.

6 Conclusion

This paper presents a detailed design of a manually operated weeder. The design has been verified experimentally in fields. The design techniques and software like AutoCAD and Ansys help us to know the prototype model, stress concentration, and other parameters which lead us to optimum design. The machine was verified on the field to check efficiency and plant damage. The results were successful and the weeds were removed from the crop. This machine is economical and easily operated.

The above results show that weeding in dryland crops like maize was given good results and reduced the investment of farmers in weed removing process up to 60% compared to manual weeding. This weeder is affordable and does not cause any environmental damage like pollution.

References

1. Chethan CR Anantha Krishnan D (2017) Dynamic push-pull strength data generation for agricultural workers to develop manual dryland weeders 113(8):1601–1605, 25 Oct 2017
2. Harker KN, O'Donovan JT (2013) Recent weed control, weed management, and integrated weed management. *Weed Technol* 27:1–11
3. Panacci E, Tei F (2014) Effects of mechanical and chemical methods on weed control, weed seed rain and crop yield in maize, sunflower and soyabean. *Crop Prot* 64:51–59
4. Melander B et al. (2005) Integrating physical and cultural methods of weed control—Examples from European research. *Weed Sci* 53:369–381
5. Kumar A, Singh JK, Mohan D, Varghese M (2008) Farm hand tools injuries: A case study from northern India. *SafSci* 1; 46(1):54–65
6. Agrawal KN, Tiwari PS, Gite LP, Bhushanababu V (2010) Isometric push/pull strength of agricultural workers of Central India. *Agric Eng Int CIGR Ej Manuscript* 1342 XII:1

7. Farm Machinery by Prof. Tewari VK, IIT Kharagpur, NPTEL, Agriculture course, Lecture 33 & Lecture 36, <https://nptel.ac.in/courses/126/105/126105009/>
8. Material information about Mild Steel by Austen Knapman, <https://www.austenknappman.co.uk/blog/material-information/the-strength-of-mild-steel/>
9. Muhammad AI, Attanda ML (2012) Development of hand push mechanical weeder. Proc Niger Inst Agric Eng 33:89–98
10. Nkakini SO, Akor AJ, Ayotamuno MJ, Ikoromari A, Efenudu EO (2010) Field, performance evaluation of manual operated petrol engine powered weeder for the tropics. AMA, Agric Mechanization Asia, Africa Latin Am 41(4):68–73 ref.12

Computational Analysis of a Convergent Divergent Nozzle



Srinivas Pothala, M. V. Jagannadha Raju, B. Bangarraju,
and V. Lakshmi Narayana

Abstract Growth in demand for the fuel directed mankind to make best use of available technology to optimize the performance characteristics of the available devices i.e. nozzles which employed for higher velocity equipments where there is a desirability for supersonic flows. These devices (nozzles) now became integral parts of various applications such as efficient mixing, combustion of fuels, aircraft's thrust generation. However supersonic flow raises a few problems like the generation of shock waves in the flow domain which result in loss of thrust. This effect is a major concern in rocket applications. Since the atmospheric pressure changes with altitude the nozzle cannot always work at its design conditions. Hence during lift-off the rockets are generally over-expanded and shocks are present in the nozzle. These shocks can be influenced by introduction of swirling flows at the inlet. Swirling flows introduce an additional tangential velocity to the flow. Swirling flows are known to increase the central axial velocity in the nozzle and in turn improve the thrust obtained up to a certain extent. The given nozzle design is studied for non-swirling and swirling flows and their effect on the shock structure for over-expanded flows. The given design is studied for Nozzle pressure ratio (NPR) value of 1.52. Different swirling flows corresponding to different swirl numbers are simulated for the same NPR value. The different variables such as mach number, density, temperature variations across different swirl numbers are recorded.

Keywords Nozzle pressure ratio (NPR) · Combustion · Supersonic · Velocity

S. Pothala (✉) · B. Bangarraju
Faculty of Mechanical Engineering, Vishnu Institute of Technology-Bhimavaram, Kovvada,
Andhra Pradesh 534202, India

M. V. J. Raju
Department of Mechanical Engineering, Andhra University, Visakhapatnam, India

V. Lakshmi Narayana
Faculty of Mechanical Engineering, ShriVishnu Engineering College for Women-Bhimavaram,
Bhimavaram, Andhra Pradesh 534202, India

1 Introduction

The characteristics/directions of fluid flow can be altered by using a specially designed devices called as nozzles, which are usually tubes/pipes with varying cross sections used to control pressure, speed, flow rate, direction, shape etc. Nozzles are devices used to accelerate flow and generate thrust. The nozzles are usually employed for accelerating the pressurized and hot fluids to supersonic level in axial direct through transforming heat to kinetic energy [1]. Due to this feature these devices are used in supersonic jet engines. They have a wide range of application such as aeronautics, combustion applications also. Convergent-Divergent (CD) nozzles are usually operated at high supersonic speeds. From the throat to the diverging section the fluid expands supersonically and higher Mach numbers are attained at the outlet. This supersonic flow gives rise to shock waves. The above nozzle design has been used for this project. Swirling flow analysis of shock wave in this nozzle has been studied. The above nozzle design reference has been obtained from JC Dutton paper. This nozzle has been simulated for an NPR value of 1.52 for different swirl numbers and the change in performance has been studied. Consider the stream in a convergent divergent nozzle in the above figure. The upstream stagnation conditions are accepted steady; the weight in the leave plane of the divergent section is signified by nozzle releases to the back pressure, PB. With the valve at first shut, there is no move through the nozzle; the stagnation pressure is steady at P0. Opening the valve marginally delivers the weight circulation appeared by bend (I). Totally subsonic stream is perceived. At that point PB is brought down such that sonic condition is come to the throat (ii). The stream rate ends up most extreme for a given spout and the stagnation conditions. On advance diminishment of the back weight, the stream upstream of the throat does not react. Be that as it may, if the back weight is diminished further (cases (iii) and (iv)), the stream at first ends up supersonic in the separating area, however then acclimates to the back weight by methods for a typical stun remaining inside the spout. In that case, as the PB diminishes, location of stun proceeds to downstream. For the blend (iv) typical stun postures to comfortable leave plane. Stream in the whole unique segment up to the leave plane is currently supersonic. At the point when the back weight is lessened significantly further (v), there is no ordinary stun anyplace inside the spout, and the stream weight acclimates to PB by methods for sideways stun waves outside the leave plane. A meeting veering spout is for the most part proposed to create supersonic stream close to the leave plane. On the off chance that the back weight is placed along (vi), the stream would exist as reversible adiabatic all through spout, together with supersonic at spout's exit place. Spouts working at PB (comparing to bend (vi)) are said to be at configuration conditions. Rocket-moved vehicles utilize uniting wandering spouts to quicken the fume gases to the most extreme conceivable speed to create high push. Convergent-divergent nozzles find their application in areas where the velocity desired is greater than that of sound. Various studies have been conducted for estimating the performance of a CD nozzle which finds its applications in various domains such as aeronautics, combustion nozzles etc. [2]. The attenuations of jet noise, combustion chamber,

augmentation of heat transfer, pressure losses etc., were possible through swirl flows as they have higher mixing rate, entrainment and improvement of flame holder properties within combustion chamber [3–7]. Swirling flows were initially analysed in nozzles to study their effect on the flow-field, thrust as well as the mass flow generated by these devices. Performed experimental studies on swirl flows through the nozzles and recorded the experimental velocity and flow properties in form of graphs [8]. The investigations of flame stability and ignition of high-density polyethylene soil fuel with respect to inflowing swirl air through solid fuel ramjet (SFRJ) are done through numerically and experimentally as well [9]. From the investigation of R. T. Gilchrist and J. W. Naughton velocity profiles (qvortex, solid body type which are tangential in nature) with two levels of swirl numbers (0.25, 0.10), it found that the growth rates and swirl numbers are directly proportional in comparison with non-swirl jets [10]. Studies were conducted by Dutton [11] on supersonic nozzle flow both numerically and experimentally. His study concluded that whilst swirl has no significant effect on specific impulse efficiency, relatively large reductions in discharge co-efficient and vacuum thrust efficiency were observed at high swirl. Strong swirls have been utilized in supersonic gas separation processes to remove the condensable components from gas mixtures [12]. There has been limited numerical study on supersonic swirling flow in a convergent-divergent nozzle and its effect on the shock structure [13]. Most of the studies have been performed on combustion nozzles and mixing applications. Some studies incorporate the acoustic aspects of convergent-divergent nozzles whereas others emphasize on its performance enhancement. Also not many studies have been performed for evaluating the performance of convergent-divergent nozzles with different swirl number and swirl profiles along with its effect on the shock structure. There has been minimal research on the effect of swirl on the thrust obtained in the nozzle. The novelty of this work is to determine the contours of pressure and temperature with various swirl numbers and different shock waves to analyse strength of the CD nozzle.

2 Materials and Methods

Geometry is created using ANSYS mechanical modeller. The coordinates for the CD nozzle were taken from a reference paper. The points were imported and surfaces created with reference to these points. Three qualities of meshes were generated with half million nodes, 1 million nodes and 3 million nodes to perform a grid independent test. The mesh quality was greater than 0.8. The angle between the hexa elements was 90° which is considered to be of good quality. The boundaries were defined with inlet, outlet and wall being the outer surface of the CD nozzle. All simulations were performed for an NPR value. The reason for choosing this NPR value was to be able to validate the results with the reference paper. The mesh generated in the previous step was converted to an unstructured mesh and imported to ANSYS fluent for simulation. The orthogonality of the mesh was checked and found to be above 0.8. Select air as the working fluid (ideal gas). k-ε turbulence model with

RNG method was selected since it is reliable and converges fast and accurately. It is suitable for supersonic non-swirl flow simulations. The boundary conditions are taken from an existing paper. The inlet pressure is taken to be atmospheric pressure. Hybrid initialization was used for initializing the starting values. The simulation was set to run for 5000 iterations. The setup for capturing the shock was different. The flow was simulated for a total of 40 s. The k-epsilon RNG turbulence model was used since it is suitable for capturing shock in supersonic flows.

3 Results and Discussion

Geometry is created using ANSYS mechanical modeller. The coordinates for the Convergent-Divergent (CD) nozzle were taken from a reference [13]. The points were imported and surfaces created with reference to these points. The throat to exit area ratio is 2.5403 and inlet to throat area ratio is 1.497. The length of the CD nozzle is taken 3.1 m (Fig. 1).

The flow for CD nozzle was simulated for three mesh qualities, for half million nodes, 1 million nodes and 3 million nodes. The graph was plotted for pressure, velocity and mach number versus the position in flow direction. It was observed that the results had a slight deviation from $\frac{1}{2}$ million nodes to 1 million nodes whereas there was no significant difference between 1 million nodes and 3 million nodes. Hence to save computational time and get accurate results 1 million nodes of mesh quality was chosen for further analysis. Further increase in the swirl number to 0.3 still pushes the shock towards the outlet but with lesser effect. The pressure at the inlet for 0.3 swirl has further reduced as compared to 0.2 swirl. The outlet mach number for 0.3 swirl is lesser as compared to the 0.2 swirl and normal axial flow mach number.

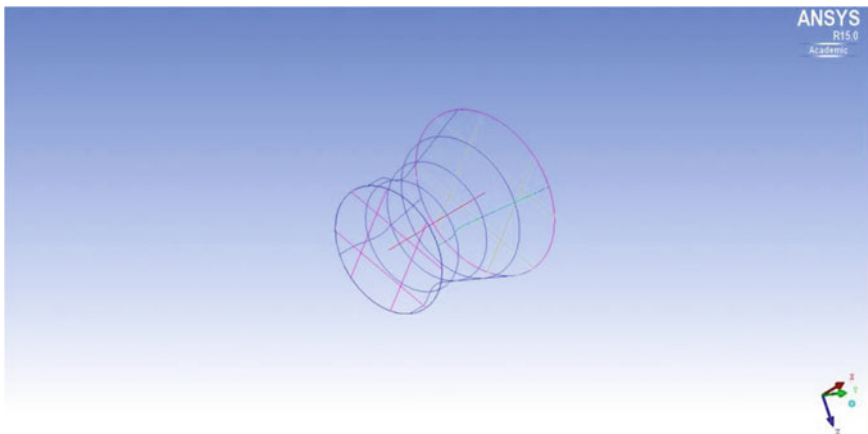


Fig. 1 Geometry of the nozzle created in Ansys ICEM

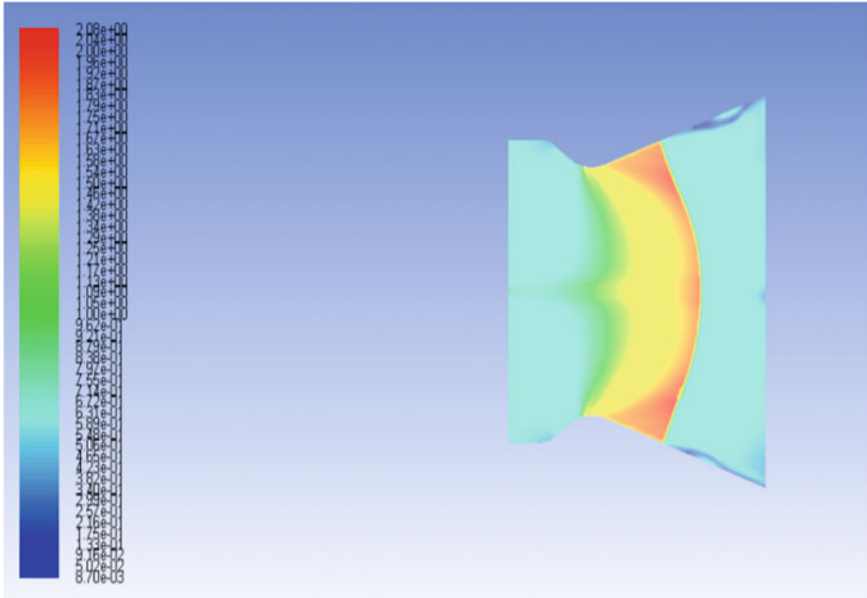


Fig. 2 Velocity contours of the nozzle obtained from Ansys

This can be attributed to the domination of tangential flow over axial flow which gives rise to vortex resulting in loss of pressure towards the throat. However, the inlet mach number is higher than both 0.2 swirl and normal axial flow mach number.

The simulation has been performed for a non-swirling flow in a CD nozzle. The velocity, temperature and pressure contours were plotted as shown in Figs. 2, 3 and 4. The results were validated from JC Dutton paper and an outlet mach number of 2.6 was recorded.

4 Conclusion

It is observed from the plots that for a complete expansion the introduction of swirl results in an increase in the mach number at the outlet. However, in case of over-expansion wherein a shock is developed within the flow domain introduction of swirl has resulted in increase of outlet mach number for low swirl number and reduction of mach number at the outlet at higher swirl numbers. The introduction of swirl also results in the reduction of flow separation as seen in the mach contours. This is an indication of weakened shocks in the flow regime. As the swirl number is increased the shock is pushed axially towards the outlet for the same BCs for a swirl number of up to 0.2. Further increase in swirl number results in the shock being pulled towards the throat since the tangential flow starts dominating the axial flow. These

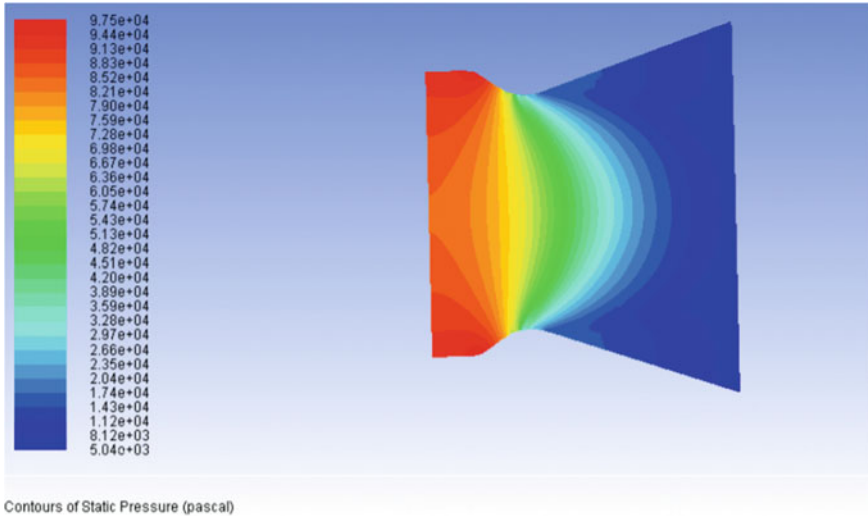


Fig. 3 Pressure contours of the nozzle obtained from Ansys

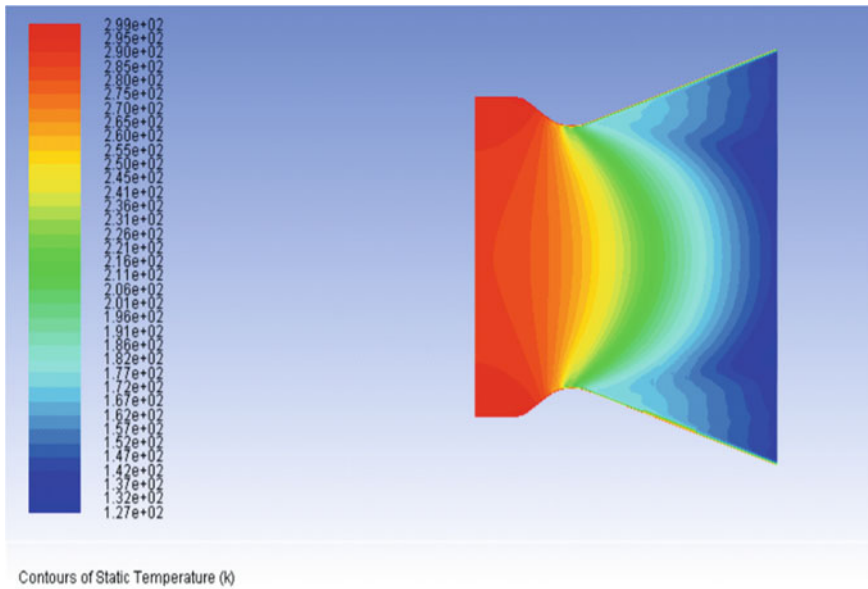


Fig. 4 Temperature contours of the nozzle obtained from Ansys

characteristics of a CD nozzle are important in rocket propulsion applications where during lift-off the nozzle is initially overexpanded and may develop shocks which result in loss in efficiency. However, as the rocket gains altitude, it reaches a point where the nozzle undergoes complete expansion i.e. it works at its design conditions and maximum efficiency. During this complete expansion it is observed that with increase in swirl number the outlet mach number constantly increases unlike the case during overexpansion with shocks. Hence the use of swirling flow can be optimized to full potential for initial overexpansion stage as well as during the complete expansion stage. Further increase in altitude results in under expansion which again develops shocks at the outlet of the nozzle.

References

1. Boyanapalli R, Vanukuri RSR, Gogineni P, Nookala J, Yarlagadda GK, Gada V (2013) Analysis of composite De-Laval nozzle suitable for rocket applications. *Int J Innovative Technol Exploring Eng* 2:336–344
2. Hoffman JD, Thompson HD, Marcum DL, Purdue Univ., West Lafayette. In: An analytical investigation of the effects of Swirler design on the performance of annular propulsive nozzles, AIAA-1984-0282
3. Rychkov D, Calculation of the swirling flow of an ideal gas in a de laval nozzle, UDC 533.6.011
4. Allé NK (2016) 2800 Kgs, CFD modelling of particle behaviour in supersonic flows with strong swirls for gas separation. In: Separation and purification technology, Science direct, Denmark vol 168, pp 68–73
5. Luca F (2006) A study on axially rotating pipe and swirling jet flows. Technical Reports from Royal Institute of Technology, Sweden
6. Gutti RR, Ramakanth US, Lakshman A (2013) Flow analysis in a convergent divergent nozzle using CFD. In: International journal of research in mechanical engineering, vol 1(2), Oct-Dec 2013, © IASTER 2013, pp 136–144
7. Liang H, Maxworthy T (2005) Department of aerospace and mechanical engineering, university of Southern California, CA 90089, USA, an experimental investigation of swirling jets. *J Fluid Mech* 525:115–159
8. Batson JL, Sforzini RH (1970) Swirling flow through a nozzle. *J Spacecr Rocket* 7(2):159–163
9. Dutton JC (1987) Swirling supersonic nozzle flow university of illinois at Urbana Champaign, Urbana, Illinois. *J Propul Power* 3:342–349
10. Gilchrist R, Naughton J (2003) An experimental study of swirling jets with different initial swirl profiles. In: 41st aerospace sciences meeting and exhibit
11. Örlü R, Alfredsson PH (2008) An experimental study of the near-field mixing characteristics of a swirling jet. *Flow, Turbul Combust* Apr 2008, 80(3):323
12. Balakrishnan P, Srinivasan K (2016) Department of mechanical engineering, IIT Madras, Chennai 600036, India Jet noise reduction using co-axial swirl flow with curved vanes. *J Vib Acoust* 138(6):061013 (Sep 09, 2016) (13 pages) Paper No: VIB-16–1146. <https://doi.org/10.1115/1.4034376>
13. Gilchrist T, Naughtony JW, University of Wyoming, Laramie, An experimental study of swirling jets with different initial swirl profiles R. In: 41st aerospace sciences meeting and exhibit, aerospace sciences meetings AIAA 2003–0639 WY 82071

Implementation of Autonomous Maintenance and Its Effect on MTBF, MTTR, and Reliability of a Critical Machine in a Beer Processing Plant



Aezeden Mohamed, Jacob Ben, and Kamalakanta Muduli

Abstract Research forms part of the beer production and plant trust improvement program. Research is a member of a drinking company. The filler/crowder with a glass bottle was 96.62 h of inactive time and quickly became a critical machine for a few months of machine failure collected. As a result of failures that affected the production and quality of the product, the availability of the critical machine was fully automated. Autonomous maintenance (AM) was introduced as part of total production maintenance on the bottle filler/crowner to minimize the maintenance pressure. The objective is to improve accessibility for machines so that professional service providers can focus their efforts on value-added and technological repairs through training and upgrading of shop floor operators. Averaging 1.15 h, shifts of 87% (12 h) and 76% throughout the day were average 87.42 h before the AM was filled (24 h). The MTTR was 113.27 h after two months of execution and the MTTR was 0.87 h with machine reliability rising by 90.0% and 81.0%. The results have shown that the independent maintenance of operators in their machinery is key in detecting equipment failures, cutbacks, reliability and improving machine performance.

Keywords Autonomous maintenance · Critical machine · Total productive maintenance

1 Introduction

The AM program in seven phases is [2]. The next phases are: (1) initial purification of and inspections (2) the elimination of pollution sources and the identification of areas that are difficult to clean; (3) the setting of standards for cleaning, inspection and graining; (4) overall wide range equipment controls; (5) independent

A. Mohamed (✉) · J. Ben · K. Muduli
Department of Mechanical Engineering, PNG University of Technology, Lae, Morobe Province,
Papua New Guinea
e-mail: Aezeden.Mohamed@pnuot.ac.pg

© The Author(s), under exclusive license to Springer Nature Singapore Pte Ltd. 2022
B. B. V. L. Deepak et al. (eds.), *Applications of Computational Methods in Manufacturing and Product Design*, Lecture Notes in Mechanical Engineering,
https://doi.org/10.1007/978-981-19-0296-3_47

511

equipment controls; these are under way to increase the know-how, involvement and responsibility of the operators for their equipment gradually.

The first step is to enhance basic knowledge about machine components and training providers to complete cleaning (TCO). While cleaning is usually considered to be an unqualified, low-status activity, it is considered a form of TPM inspection. The machinery and parts defects alongside pollution sources are identified, difficult to clean and inspect areas, and it plays an important role [1]. Inadequate cleaning, according to [2], may lead to component failure, quality deficiencies, and accelerated equipment deterioration. In addition, the accumulation of dust and dirt in equipment increases wear and frictional strength, causing loss of speed like inactivity and performance.

In steps two and three of the AM program, the abolition, reversing deterioration and retention of sources of dirt that cause accelerated deterioration and basic condition of the equipment are prioritized [3]. The key to such steps is not to perform detailed inspections during cleaning for the sake of purification. The reasons for pollution and reliable removal solutions can be identified here by the operators in the store. This transforms operators from reactive to proactive [4], achieving optimum conditions which prevent stops, and reduces component failures and machine failures.

The fourth to seven steps of autonomous maintenance address general and independent inspection, reviews and standards development and allow operators to manage their equipment independently. The operators will receive training in the areas of pneumatic machinery, electrical systems, hydraulics, lubrication systems, drives, bolts, nuts and safety standards [5]. This knowledge entitles them to understand, manage and improve their device and processes [6]. They are now fully aware of their machines. Operators can also visually inspect main parts and find and fix minor defects based on established standards. They can also inspect small parts. When machines are in operation, maintenance craftsmen cannot detect and cover all symptoms of a breakdown [7]. Operators can help detect abnormalities of equipment and prevent the symptoms of a catastrophic accident by gaining technical knowledge through the use of AM.

1.1 Reliability, MTBF and MTTR Critical Machinery

Machinery can be split into critical and non-critical machinery in any production plant. The longest downtimes and worst effects on the system are on a critical machine [8]. A machine's reliability is based on a probability that the machine performs or operates, under certain conditions, the necessary functions without fail for the specified operating time [9]. Lower reliability means more unforeseen stoppage and consequently less repairs and availability [10]. It means reduced trustworthiness. Reliability is measured in the intermediate times between failure (MTBF) and the intermediate times of repair (MTTR) for any particular equipment [11]. For any equipment, reliability is measured. For instance, for electrical equipment such as drive motors, MTTF is used for non-repairable components, while MTBF for repairable

components such as rotating shaft or rotating belt is used [12]. After a failure occurs, MTTR is the time to run a repair. In other words, it will take time for the maintenance of corrections [13]. MTBF and MTTR are two extremely important KPIs in terms of the system, facility, equipment, or process availability [14]. Equations (1), (2) and (3) shall contain both MTBF and MTTR as well as reliability formulas:

$$MTBF = \frac{\text{Operating Time}}{\text{Number of Failures}} \tag{1}$$

$$MTTR = \frac{\text{Downtime}}{\text{Number of Failures}} \tag{2}$$

$$R(t) = e^{(-\frac{t}{MTBF})} = e^{(-\lambda t)} \tag{3}$$

$$\text{Where } \lambda = \frac{1}{MTBF} = \text{failure rate} \tag{4}$$

The time of operation of a factory is the difference between time and unexpected downtimes [15]. The time comes for the system to operate and decide that it is necessary to inspect, clean, adjust, replace or replace the property.

2 Research Methodology

2.1 Machine Downtime Data

In a beer processing plant in a beverage production company, two months of history data for the top three critical machines were collected. Building on these data, 92 downtimes during this period led to the plant’s most critical bottle filler/crowner with

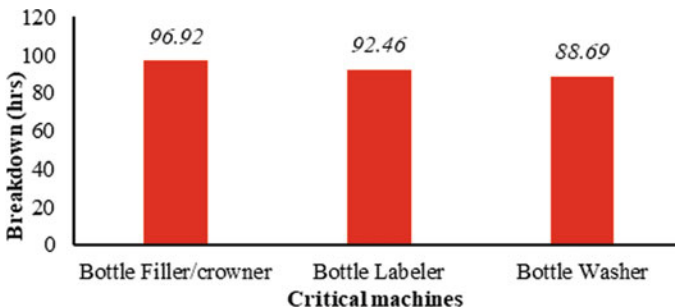


Fig. 1 Top 3 plant machines of critical importance



Fig. 2 The glass bottle is filled and crowned

96.92 h of downtime. The critical machines are shown in Fig. 1. The image on the main machine is shown in Fig. 2.

2.2 Autonomous Maintenance Implementation

The machinery managers had the task of monitoring their equipment continuously and of adjusting the glass filling/crowner machine in the essential working condition for minor adjustments and fundamental problems. This formed part of the creation of a program with the highest downtime on the most critical machine for independent maintenance (AM). As part of the reliability improvement program, this team was responsible for completing and manufacturing the seven AM steps in its machinery. The Fillers Bottle/Crowner Team was established in this business (fivefold core machine operators, onefold mechanical experts and onefold team supervisors).

Initially, key knowledge has been increased to a certain degree of cleaning and maintenance for machinery operators and machinery train operators. Parts of the machine with a detailed description of the individual training components were removed from the operating manual. The drivers could then conduct a careful cleaning and minor maintenance of the machine components as a result of their training. A maintainer was ready to deal with more challenging maintenance problems. In use, step 2 and step 3 to make minor changes to the preventive maintenance program have been devised for understanding and acceptance of the components of machinery (creation of standards of purification, inspection, lubrication and tightening). Machine and component anomalies and contamination sources have been identified, as well as areas which are difficult to purify and control. Lists with a clear idea of specific cleaning and control tasks to deal with pressure failures and to prevent machine efficiency. Temporary clean-up and control lists. Tags have been



Fig. 3 Dirt sources identified and removed in Step 2 of the AM

raised for damaged parts with a negative impact on the machine performance. They were then registered and sent to the PM team to be maintained in a tag registry. Steps 2 and 3 were easily achieved by providing the necessary information to the operators and technicians in stage one. Figure 3 shows the AM Step-2 Glass Filler/Crowner machine dirt source.

The establishment of standards for cleaning and routine maintenance in stage three of autonomous maintenance programs. Special actions to remove the root cause of defects and to routinely remove dusty components were identified in step II. Checklists showed a one-point (OPL), a cleaning inspection, lubricant and stressor (CILT) standard has been designed to prevent the equipment from deteriorating due to its correct operation and daily inspection. The aim was to lay down essential requirements for equipment maintenance and therefore improve machine reliability. Step 1 to Step 3 of the self-contained maintenance system allows operators to develop machine malfunctions, to understand bottle filler functions and components and to identify potential quality problems in the machine. Those skills were then employed for the identification and solution of product quality problems and chronic problems, for the detection and resolution of abnormality.

3 Results and Discussions

3.1 Detection of Machine Abnormalities

Detailed cleaning and inspection of filler/crowner machinery components was the starting point for error detection. In the machine oil leaks and beer spilling, glass fragments, dust particles and slims, etc., have been cleaned up and simultaneously monitored. All missing parts such as bolts, nozzles, screws and damaged items such as guides, transport systems, slides and cables were accurately tagged in the machines

and were fully identified clean-out (TCOs). Tags were raised for the deteriorated parts that have affected the performance of the machine. The components infeed, main engine and filler/crowner outfeed were machined in large plates in the layout and visible on the machine area for detailing parts and purposes. The machine’s layout identified all deficiencies and tags were recorded and forwarded to the PM team for maintenance plans. Each maintenance operation was more involved with independent maintenance by key operators on the ground as they were detecting errors in filler/crowner machines more closely in their daily functions. The lists

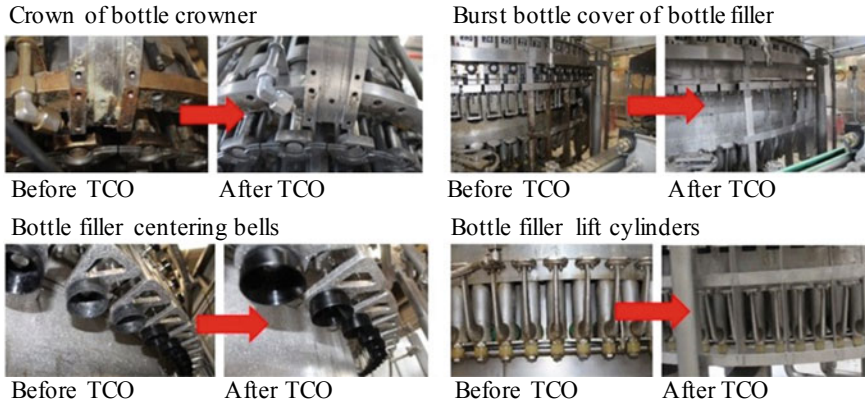


Fig. 4 Photos of filler/crowner components before and after TCO

BOTTLE FILLER CILT CHECKLIST-DAILY						
					Operator DS:	
Area	Activity	Specification/Standard	Equipment	Machine Status	Time	
1. Safety Door	Check the safety doors	Ensure paneling doors must Open & Close	Hand		1 min	
2. Filler/Crowner	Clean Crowner heads, neck guides, Central star, perspex glass+ Clean Filler lift cylinders, filling valves & ring bowl, format parts & machine surfaces	Must be free of slime,dirt, bottle fragments and crowns.	Spray gun, Scotching pad		15 mins	
	Remove crowns from crown track before hot water flushing. Also spray water on top of crown track, where dust usually builds up.	Crown track must be cleared	Cotton swab		10 mins	
	Inspect format parts, guides, wear strips and locking pins for wear and tear or defects.	No wear, tear, obstruction or loose bolts.	Hand, Spinner		1m in	
3. Filler/Crowner Hot water flushing	Do Hot water flushing with crowner. NB: Cover up all sensors, solenoids and valves with plastic before flushing.	Filler/Crowner must be sterilised	HMI		30 mins	
4. Running Inspection	Inspect filling for no overfoaming and underfills	Ensure filling tubes/Deflector/tulip cup not worn, broken, or missing.	Eye		1 min	
	b) Process Area - Check air, CO2 valves are open and no leaks along the line. Also inspect infeed sensor if it is operating according to standard.	Air ,CO2, H2O valves open and ensure air pressure is at 6 bar.	Eye		1 mh	

Fig. 5 Provisory CILT checklist for glass bottle filler/crowner under AM

were then clearly developed to determine how specific cleaning and inspection tasks address machine failures and small stops which affected the reliability of the machine. Figure 4 shows some pictures of the filler/crowner machine parts before and after TCO and Fig. 5 is the CILT checklist. Table 1 shows built to prevent deterioration of the component.

Table 1 Provisional CILT filler/crowner glass bottle checklist in AM step 3

Bottle filler CILT checklist daily						
#	Area	Activity	Specification	Equipment	Machine status	Times (mins)
1	Safety door	Check the safety doors	Ensure doors open and close	Hand	Stop	01
2	Crowner	Clean crowner heads, neck guides and machine surface	Must be free of slime, dirt, bottle fragments	Spray gun, scotching pad	Stop	15
		Remove crowns from crown track before hot water flushing	Crown track must be cleared	Cotton swab	Stop	10
		Inspect format parts, guides, wear strips and locking pins for wear and defects	No wear, tear, loose bolts	Hand, spinner	Stop	01
		Do hot water flushing with crowner	Filler must be sterilized	HMI	Stop	30
3	Crowner hot water flush	Inspect filling for no cover foaming	Ensure filling tubes	Eye	Reuse, Reduce, Recycle	01
4	Running inspection	Process area: check air, CO ₂ valves are open and no leaks		Eye	Reuse, Reduce, Recycle	01

3.2 Improvements in MTBF and MTTR of Critical Machines

Checklists created specifically to deal with component abnormalities contributed to the increase in machine accessibility and the intermediate time between failures (MTBF) and a significant reduction in the meantime to repair (MTTR). Furthermore, after two consecutive months of February to March 2020, the number of component breakdowns in the filler/crowner was reduced significantly. Figures 6 and 7 show that before and after autonomous maintenance, the bottle filler/crowner has MTBF and MTTR respectively. The results show that MTBF and MTTR are significantly increased after AM implementation.

Before AM, average MTBF:

$$MTBF (ave) = 87.42 \text{ h}$$

Average MTBF after AM:

$$MTBF = 113.27 \text{ h}$$

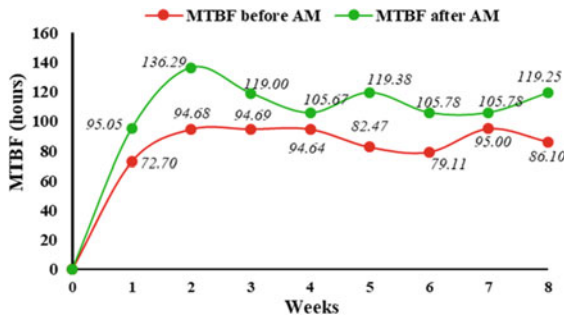


Fig. 6 Glass bottle MTBF before and after independent maintenance of the filler/crowner

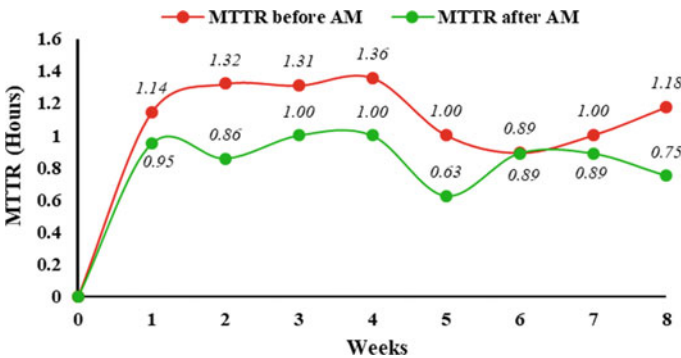


Fig. 7 Filling/crowner MTTR glass bottle prior to and after independent maintenance

Average MTTR before AM:

$$\begin{aligned}
 \text{MTTR (ave)} &= \frac{1.14 + 1.32 + 1.31 + 1.36 + 1.00 + 0.89 + 1.00 + 1.18}{8} \\
 &= 1.15 \text{ h}
 \end{aligned}
 \tag{5}$$

Average MTTR after AM:

$$\begin{aligned}
 \text{MTTR (ave)} &= \frac{0.95 + 0.86 + 1.00 + 1.00 + 0.63 + 0.89 + 0.89 + 0.75}{8} \\
 &= 0.87 \text{ h}
 \end{aligned}
 \tag{6}$$

3.3 Improved Critical Machine Reliability

The operators have kept their machines clean, well lubricated and safe with their new understanding of ownership of the independent maintenance system. You are constantly empowered to inspect, measure and diagnose reparations and adaptation problems and to take minor responsibility. Temporary cleaning and checklists have contributed to reducing chronic and minor stoppages in the reception and crowding parts. Reliability of equipment under the AM program has significantly increased. Figures 8 and 9 illustrate the reliability of the filler bottle/crowner in 12 and 24 h prior to and after independent maintenance respectively. The overall reliability of the machine was progressively improved.

Average $t = 12$ h pre-AM reliability:

$$R(12) = \frac{0.85 + 0.88 + 0.88 + 0.88 + 0.86 + 0.86 + 0.88 + 0.87}{8}$$

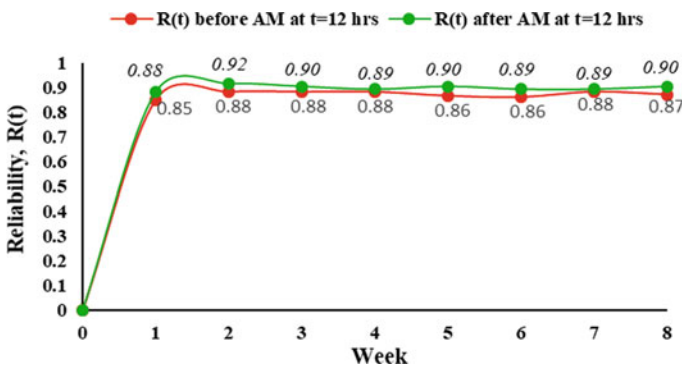


Fig. 8 Glass bottle filler reliability at $t = 12$ h prior and after AM

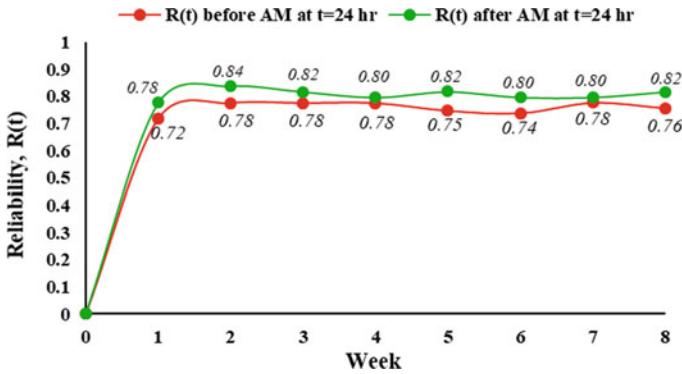


Fig. 9 Glass filler/crowner reliability at $t = 24$ h before and after AM

$$= 0.87 \tag{7}$$

Average $t = 12$ h after AM reliability:

$$R(12) = \frac{0.88 + 0.92 + 0.90 + 0.89 + 0.90 + 0.89 + 0.89 + 0.90}{8} = 0.90 \tag{8}$$

Average reliability $t = 24$ h prior to AM:

$$R(24) = \frac{0.72 + 0.78 + 0.78 + 0.78 + 0.75 + 0.74 + 0.78 + 0.76}{8} = 0.76 \tag{9}$$

Average $t = 24$ h after AM:

$$R(24) = \frac{0.78 + 0.84 + 0.82 + 0.80 + 0.82 + 0.80 + 0.80 + 0.82}{8} = 0.81 \tag{10}$$

4 Conclusions

The studies demonstrate the comprehensive program of autonomous maintenance that enables operators to learn, identify and optimize machine malfunctions, reduce downtime and reliability. With 96.92 h of downtime it was autonomously maintained and was the glass bottle filler/power machine, identified as the most critical in the plant. The average MTBF before AM implementation was 87.42 h, the mean MTTR

was 1.14 h, the shifts of the glass bottle (12 h) were 87 percent, with the total reliability of the full day (24 h), 76%. The machine reliability increased significantly to 113.27 h following AM implementation, the MTTR decreased to 0.87 h and machine reliability grew to 90% for 12 and 24-h operation and to 81% respectively. These results indicate that enabling operators to perform autonomous machinery maintenance is essential in detecting equipment failure, reducing downtime, increasing reliability and improving machine and plant performance.

References

1. Laquet A (2015) Maintenance optimization of centrifugal pumps in a European refinery: a case study. Master thesis, School of Industrial Engineering and Management, KTH Royal Institute of Technology
2. Nieminen H (2016) Improving maintenance in high-volume manufacturing. Case: ball beverage packaging Europe. Master's thesis, Lahti University of Applied Sciences
3. Habib Z, Wang K (2008) Implementation of total productive maintenance on Haldex assembly line. Master thesis, Department of Production Engineering, Royal Institute of Technology, Sweden
4. Shagluf A, Longstaff AP, Fletcher S (2014) Maintenance strategies to reduce downtime due to machine positional errors. In: International conference on maintenance performance measurement management. Huddersfield, United Kingdom, pp 111–118
5. Venkatesh J (2007) An introduction to total productive maintenance (TPM). Plant Maintenance Resource Center. Retrieved Aug 2020 from: http://www.plantmaintenance.com/articles/tpm_intro.shtml
6. Jasiulewicz-Kaczmarek M (2016) SWOT analysis for planned maintenance strategy—a case study. In: International federation of automatic control (IFAC)-papers online, vol. 49(12), pp 674–679
7. Fredriksson G, Larsson H (2012) An analysis of maintenance strategies and development of a model for strategy formulation—A case study. Master thesis, Department of Product and Production Development, Chalmers University of Technology
8. Ab-Samat, H, Jeikumar LN, Basri EI, Hrun NA, Kamaruddin S (2012) Effective preventive maintenance scheduling: a case study. In: International conference on industrial engineering and operations management. Istanbul, Turkey, 3–6 July
9. Ghodrati B (2005) Reliability and operating environment based spare parts planning. Doctoral thesis, Division of Operational and Maintenance Engineering, Luleå University of Technology
10. Tatis de Leon R (2012) Vibration measurement for rotatory machines—importance of maintenance practices. Bachelor's thesis, HAMK University of Applied Sciences, Finland
11. Deka D, Nath T (2015) Breakdown and reliability analysis in a process industry. *Int J Eng Trends Technol* 28(3):150–156
12. Fan Q, Fan H (2015) Reliability analysis and failure prediction of construction equipment with time series models. *J Adv Manage Sci* 3(3):203–210
13. Fridholm V (1992) Improve maintenance effectiveness and efficiency by using historical breakdown data from a CMMS: exploring the possibilities for CBM in the manufacturing industry. Degree Project, School of Innovation, Design and Engineering, Mälardalen University
14. Kiyak E (2011) The importance of preventive maintenance in terms of reliability in aviation sector. *ResGate Publ Eur*. Retrieved June 2020 from: <http://www.researchgate.net/publication/266492733>
15. Vijayakumar SR, Gajendran S (2014) Improvement of overall equipment effectiveness (OEE) in injection moulding process industry. *J Mech Civ Eng* 47–60

An Assessment on Bone Cancer Detection Using Various Techniques in Image Processing



Dama Anand, G. Arulselvi, and G. N. Balaji

Abstract Cancer cells are abnormal cells in the body that uncontrollably divide themselves and spreads over the body. Bone cancer, one kind of cancer, is a dreadful and threatening disease, usually caused due to the uncontrolled split up of bone cells. The cause for all other cancer types can be identified but this is not the case for bone cancer. It affects people in almost all age groups. The most challenging task is to detect bone cancer in the earlier stages. Hence for survival, the chances of detecting bone cancer in the earlier stages must be increased. Medical imaging like X-ray, MRI, or CT imaging in association with the techniques of image processing can provide remarkable results while detecting bone tumors. In this paper, existing works related to the detection of bone cancer are examined and further studied about bone cancer and their features for predicting its type. Several Image processing techniques are discussed for estimating X-Ray and MRI image interpretation.

Keywords Bone cancer · Medical imaging · X-ray · CT and MRI images · Image processing techniques

1 Introduction

Biomedical image processing is drastically developing nowadays and thus has attracted researchers of interdisciplinary fields like applied mathematics, statistics, computer science, engineering, medicine, biology, and physics. Due to the emerging trend of this high technology in the medical field, several challenges are faced in processing and analyzing numerous images such that vital disease information is diagnosed for treatment [1].

D. Anand (✉) · G. Arulselvi
Department of Computer Science and Engineering FEAT, Annamalai University, Chidambaram, India

G. N. Balaji
Department of IT, CVR COLLEGE of Engineering, Ibrahimpatnam, India

Generally, the articles examined classify the methods which are employed to process pixel and voxel data namely image segmentation, diagnosing applications, planning, and assisting in treatment. New magnetic resonance imaging (MRI) and CT device have scalable image resolution and reconstruction time and the entire body is scanned with this resolution reaching numerous Gigabytes (GB) of data load [2–4].

Cancer is a disease that may occur in any part of the body. It starts with the senseless cells and spreads to the neighboring cells. Every cell in the human body has certain functions to do [5]. The normal and abnormal bone cancer image is shown in Fig. 1.

Figure 2 shows the bone cancer estimation rate for both genders, male and female.

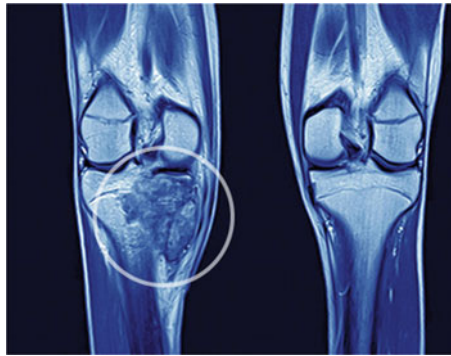


Fig. 1 Abnormal and normal bone cancer image

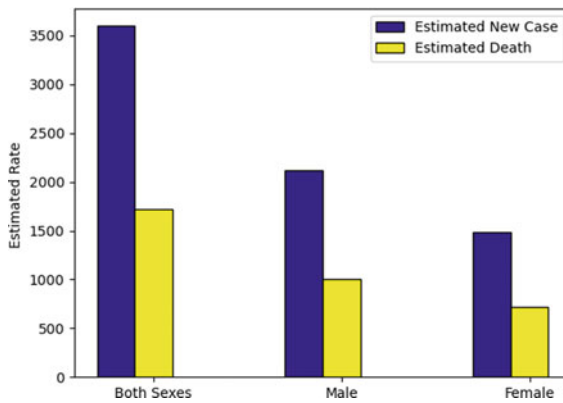


Fig. 2 Statistics data for bone cancer

2 Related Works

This section discusses the related works for the detection of bone cancer.

2.1 Preprocessing

Asuntha and Srinivasan [6] developed a method that utilized image processing method to detect tumors and classify cancer of patient's MR images using ANN (Artificial Neural Network) approach. Hambal et al. [7] discussed various linear and nonlinear filtering techniques for image noise reduction. Linear filters tend to blur image edges but it does not remove impulse noise. Singh and Aggarwal [8] described fuzzy filter as well as mean shift based fuzzy c-means method for image noise removal at preprocessing stage which required less computation time when compared to the traditional method. Sinthia and Sujatha [9] presented a bone cancer detection method for MRI images. For noise removal and to obtain smooth images, preprocessing methods like a bilateral and average filter were integrated. Binhssan [10] introduced a method for detecting enchondroma tumors in MR images. It was defined as a benign, solitary, and intramedullary cartilage tumor which was in the proximal humerus, distal femur, short tubular bones feet, hand, and other bones.

2.2 Segmentation

Shukla and Patel [11] examined bone cancer and its features for predicting the type of cancer and discusses various computer visions for discovering cancer in human organs. Tamgadge et al. [12] introduced an exceptional method to locate bone tumors for different modalities. This method gave structuring tumor recognition with less usage cost and computational time. Ramkumar and Malathi [13] classified bone disorders as normal, Osteoporosis, and Osteopenia for radiographic bone images. To predict accurate bone disorder classification, this method has three stages. Hossain and Rahaman [14] developed an object labeling method to segment bone tumors from MRI images and gave a comparison of existing methods.

2.3 Feature Extraction

Ikoma et al. [15] extracted reference region automatically by using the clustering method with three features based on anatomical and time course pattern data. From DCE-MRI images, two features related to the tie course shape were extracted from

the time course of every voxel. Boulehmi et al. [16] diagnosed sarcoma with a Generalized Gaussian Density (GGD) analysis approach. MRI bone image was partitioned into fixed-size sub-images and every sub-image was analyzed with GGD. From the original MRI, ROI was selected related to sub-images with the highest shape value. Xia and Chuli [17] utilized a support vector machine (SVM) to detect bone tumors with texture features of X-ray images. Due to the low incidence of bone tumors, it is hard to acquire datasets on a large scale. Baskaran et al. [18] proposed PET evaluation by using 18F-Fluoro-2-Deoxy-D-glucose (FDG) to assess historical responses of the affected bone sarcoma individuals when compared with standard MRI and volumetric variables.

2.4 Classification

Zhao et al. [19] proposed a GCTB (Giant cell tumor of bone) method for identifying from Mueller matrix polarization microscopic (MMPM) imaging and multi-parameters fusion network. Watanabe and Haruna [20] suggested ways to identify bone metastatic tumors from CT images. Primary cancer spreads to various organs and causes heavy problems. Zeelan Basha et al. [21] presented tumor detection using the machine learning method. An important goal was to find the bone tumor. Watanabe and Haruna [22] compared k-means against fuzzy C-Means (FCM) clustering procedure which helped to find pre-size accuracy of damages in the bone. In this research, at first, images go through segmentation and k-means and then applied the FCM method to find tumor regions in a bone. Ambalkar and Thorat [23] presented tumor detection by using the machine learning method. Especially in tumor detection, MRI resolved various difficulties. Fundamentally,

3 Comparative Study

Table 1 gives the summarization of existing works, the techniques used in them and their advantage, and its limitation. It also partitions the image into a distinct region. The partition of the image is the most significant and challenging issue in clinical diagnosis with computer-aided.

The accuracy of the MRI image in segmentation is the most important issue in clinical diagnosis [24]. Some tumor occurs along with the pleomorphic sarcoma which changes the properties of the nearby region. Manual segmentation is a very difficult process because it consumes more time [25].

Table1 Summarization of existing work with advantages and limitations

Sl. No.	Techniques used	Advantage	Limitation
1	IHS, PCA method integrated with retina inspired fusion models	Understand whole fusion process, select closer to real visual effect model triangular spectral model	Distinguishing exact edge from noise or trivial geometric features was difficult
2	Average filter and the bilateral filter, k-means algorithm	Focuses on the biggest development of picture capacity Image Margin was removed by estimating the centroid of every object	Hard to recognize precise edges from commotion or minor geometric elements
3	In canine bone cancer, diagnostic usage of thermographic imaging was determined	Detected canine bone cancer with the overall classification success rate Improved the classification rate	It was not enough for a reliable diagnosis
4	To optimize backpropagation NN, a heuristic search method was introduced	It was easy to segment images and tumors	Problems in trapping local minima and convergence rate were low with evolutionary learning approaches
5	Image quality assessment, Gabor filter with Gaussian rules	Features detected were accurate compared to pixels percentage with mask-labeling	Image pixel is low, has to increase cancer detection percentage
6	Sobel, Canny, Prewitt, Region Growing, k-means, edge, and region-based segmentation	Best segmentation approach suitable for gray scaled image	Pixel gradient was less compared to thresholds; the size of the kernel was low
7	Tumor detection using machine learning	The system was faster and more convenient	Did not find the exact location of affected tissues and tumor
8	Generalized Gaussian Density analysis (GGD)	Numerous bones MRI images were tested and perfectly detected tumors	Lacking in the ground truth prevented to accurately evaluate the segmentation rate of bone cancer

4 Analysis

From the literature, after investigating the techniques of segmentation, feature extraction, tumor detection, and classification, the common problems are observed and are mentioned which are as follows:

- When detection is not done at right time, complexity arises.

- Symptoms were overlooked and not examined at right time by the radiologist. Next, even after examining the signs, it was considered abnormal or not suspicious enough to examine further.
- Through ROI, image abnormality was identified which is not suspicious enough to recall.
- To classify the tumor density, Computer-aided diagnosis systems have been developed, having as a major challenge to define the features that represented images in a better way to classify.
- The study has to be done for the best feature extraction technique in tumor identification.
- The existing study in bone cancer has no grade and distant spread of the tumor.

5 Conclusion

A bone tumor is an anaplastic tissue growth in bone and it was categorized as primary tumors whose effect began in the bone or derived from cells and tissues. Tumors initiated in other locations and extend metastasis to the skeleton are secondary tumors. With this known factor, the prediction and identify the tumor stage is more important for therapists to treat effectively. To detect and identify the bone tumor, the normalized image was performed to get a defined standard image, and enhancements over the image were done by preprocessing stage. One major issue in medical history for disease diagnosis is that practitioners require supported data for detecting and predicting the stage of the disease. The early detection is not done with the optimal rate of accuracy in existing techniques. Future work for this review will be carried out in early symptom detection of the bone tumor with higher accuracy and provide the data about an affected area which would be useful for the practitioner in treating the disease with precautions.

References

1. Salem MAM, Atef A, Salah A, Shams M (2017) Recent survey on medical image segmentation. In: Handbook of research on machine learning innovations and trends. IGI Global, pp 424–464
2. Khoon LL, Chuin LS (2016) A survey of medical image processing tools. *Int J Softw Eng Comput Syst (IJSECS)* 2(1):10–27
3. Pradeep GGS, Kallam S, Kumari NV, Patan R (2020) Texture recognition and image smoothing for microcalcification and mass detection in abnormal region. In: 2020 international conference on computer science, engineering and applications (ICCSEA). IEEE, pp 1–6
4. Ghantasla GSP et al (2016) *Int J Res Eng IT Soc Sci* 06(09):50–54. Sept 2016. ISSN 2250-0588, Impact factor: 6.452
5. Avula M, Lakkakula NP, Raja MP (2014) Bone cancer detection from mri scan imagery using mean pixel intensity. In: 8th Asia modelling symposium IEEE, pp 41–146
6. Asuntha A, Srinivasan A (2018) Bone cancer detection using artificial neural network. *Indian J Sci Res* 17(2) (2018)

7. Hambal AM, Pei Z, Ishabailu FL (2017) Image noise reduction and filtering techniques. *Int J Sci Res (IJSR)* 6(3)
8. Singh B, Aggarwal P (2017) Detection of brain tumor using modified mean-shift based fuzzy c-mean segmentation from MRI Images. In: 8th IEEE annual information technology, electronics and mobile communication conference (IEMCON)
9. Sinthia P, Sujatha K (2016) A novel approach to detect bone cancer using k-means clustering algorithm and edge detection method. *Asian Res Publ Net ARPN J Eng Appl Sci* 11(13):8002–8007
10. Binhssan A (2015) Enchondroma tumor detection. *Int J Adv Res Comput Commun Eng* 4(6)
11. Shukla A, Patel A (2020) Bone cancer detection from X-ray and MRI images through image segmentation techniques. *Int J Recent Technol Eng (IJRTE)* 8(6):2277–3878
12. Tamgadge PB, Choudhari NK, Kate DM (2019) A review paper on detection of bone tumor using comparative analysis of segmentation technique
13. Ramkumar S, Malathi R (2018) An automatic bone disorder classification using hybrid texture feature extraction with bone mineral density. *Asian Pac J Cancer Prev APJCP* 19(12):3517–3524
14. Hossain E, Rahaman MA (2018) Comparative evaluation of segmentation algorithms for tumor cells detection from bone MR scan imagery. In: International conference on innovations in science, engineering and technology (ICISSET)
15. Ikoma Y, Kishimoto R, Tachibana Y, Omatsu T, Kasuya G, Makishima H, Higashi T, Obata T, Tsuji H (2020) Reference region extraction by clustering for the pharmacokinetic analysis of dynamic contrast-enhanced MRI in prostate cancer. *Magn Reson Imaging* 66:185–192
16. Boulehmi H, Mahersia H, Hamrouni K (2018) Bone cancer diagnosis using GGD analysis. In: 15th international multi-conference on systems, signals and devices (SSD), pp 246–251
17. Xia, Chuli (2018) SVM-based bone tumor detection by using the texture features of X-ray image. In: International conference on network infrastructure and digital content (IC-NIDC)
18. Baskaran K, Malathi R, Thirusakthimurugan P (2018) Feature fusion for FDG-PET and MRI for automated extra skeletal bone sarcoma classification. *Mater Today Proc* 5(1):1879–1889
19. Zhao Y et al (2020) Detecting giant cell tumor of bone lesions using mueller matrix polarization microscopic imaging and multi-parameters fusion network. *IEEE Sens J* 20(13):7208–7215
20. Basha CMAK, Padmaja M, Balaji GN (2018) Computer aided fracture detection system. *J Med Imaging Health Inform* 8(3):526–531
21. Zeelan Basha CMAK, Maruthi Padmaja T, Balaji GN (2018) Automatic X-ray image classification system. In: Smart innovation, systems and technologies, vol. 78. Springer Science and Business Media Deutschland GmbH, pp 43–52
22. Watanabe, Haruna (2019) Bone metastatic tumor detection based on AnoGAN using CT images. In: IEEE 1st global conference on life sciences and technologies (LifeTech)
23. Ambalkar SS, Thorat SS (2018) Bone tumor detection from MRI images using machine learning: a review. *Int Res J Eng Technol* 5(1)
24. Razia S, Narasingarao MR, Bojja P (2017) Development and analysis of support vector machine techniques for early prediction of breast cancer and thyroid. *J Adv Res Dyn Control Syst* 9(6):869–878
25. Rao AS, Srinivasu SVN, Gayatri P, Anand D (2020) Development of expert system for bone cancer detection. *Int J Adv Sci Technol* 29(7)

Small-Scale Hydropower Generation from the Otherwise-Wasted Kinetic Energy in MultiStory Building



Srikanth Allamsetty, Animesh Shukla, and Rishav Bhagat

Abstract The fuel required for hydropower generation is water, which is one of the renewable energy resources that is freely available in the nature. Generally, the hydropower plants would be constructed in hilly areas where there is an availability of head and discharge of the water. The power that can be generated would be highly dependent and proportional to these two quantities. The idea of this research work is to study the feasibility of employing a small/micro-scale hydropower generating unit in a multistory building to utilize the otherwise-wasted kinetic energy of water that is coming down from the overhead water tank. In this study, it is theoretically proved that the power generation is possible using the proposed method.

Keywords Micro-hydro · Novel designs · Energy generation · Hydro-energy · Pilot-scale model · Hydro-turbines

1 Introduction

Nowadays, industrialization, population growth, and modernization are leading to the increase in energy demand more than ever. Being conventional as well as renewable energy source, hydropower stations (HPSs) have been considered to be most suitable to reduce the dependency on thermal-based power plants. The power generation in HPS depends on the water availability. It is one of the renewable energy resources, for which the fuel is abundantly available in the nature. It is the general way that the site for the hydropower plants would be chosen based on the availability of head and discharge of the water. If the head and discharge are not naturally available, then they can be created by constructing a dam. As the power that can be generated would be highly dependent on these two quantities, they are treated as most important

S. Allamsetty (✉) · A. Shukla · R. Bhagat
School of Electrical Engineering, Kalinga Institute of Industrial Technology, Deemed to be
University, Bhubaneswar, Odisha, India
e-mail: srikanth.allamsettyfel@kiit.ac.in

© The Author(s), under exclusive license to Springer Nature Singapore Pte Ltd. 2022
B. B. V. L. Deepak et al. (eds.), *Applications of Computational Methods in Manufacturing
and Product Design*, Lecture Notes in Mechanical Engineering,
https://doi.org/10.1007/978-981-19-0296-3_49

531

factors while taking up construction of the HPS. In recent years, the small/micro-scale hydropower generation gained the interest, and plant personnel is in search of locations suitable, where head and discharge of the water are available.

The micro-hydro-technology was initially used by employing water wheels to cater the motive power to run devices such as grinders in Himalayan villages [1]. Hydropower production on either small or micro-scale would be one of the most cost-effective energy technologies that can be considered in less developed countries toward rural electrification [2]. The electrical energy can be generated from the force of moving water, which can be used to power a residential house to a small village [3].

The micro-HPS results from the natural hydro-logical cycle without any facility for impoundment of water, and its environmental impact is assumed to be negligible [4]. Large HPS has less attraction in the present world economy due to its large capital cost and environmental concerns [5]. Higher head would produce greater pressure regardless of the size of the stream and leads to higher output at the turbine [6].

The most suitable geographical areas for micro-hydropower generation can be found in hilly areas, where there are streams, steep rivers, creeks, or springs flowing year-round with high year-round rainfall [7]. An overview of micro-HPS technology and a brief description of its various components have been presented in [8]. Feasibility of electricity generation from micro-HPS at MGM Gandheli Campus, Aurangabad was analyzed and presented a detailed report in [9]. It was mentioned in [10] that even smaller turbines of 200–300 W might power a single home with a drop of only 1 m.

The head and discharge are the key parameters, which are if known, can be used to determine everything related to the HPS such as pipeline size, turbine type, specific speed, rotational speed, size of the generator, and also a rough estimate of cost [11]. It was mentioned in [12] that there are two accurate methods to design while measuring the head, which can be considered as accurate, i.e., direct height measurement and water pressure measurement.

The idea of this present research work is to study the feasibility of utilizing the water coming down from the overhead tank of a multistory building to generate electric power. Available head and discharge data have been collected from an apartment, and efforts are made to predict the power generation capability. In this present paper, theoretical study has been presented discussing the power that is being consumed for pumping the water to the overhead tank and power that can be generated by employing hydro-turbine-generator set at two different locations.

2 Materials and Methods

In case of multistory buildings, it can be noticed that the water would be utilized in large quantity, and the motors would be run to fill the tanks regularly, in some cases, continuously. If the boxes containing hydro-turbine-generator sets can be employed at appropriate places in the passage of water as shown in Fig. 1, the electric power

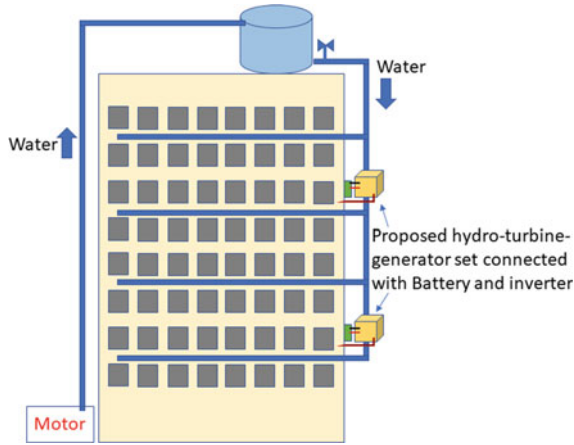


Fig. 1 Schematic diagram of the proposed design

can be generated from otherwise-wasted kinetic energy of water. The pictures of the apartment chosen and the water tanks can be seen in Fig. 2a and b, respectively. However, the proposed method can be applicable for multistory buildings having more number of floors than the chosen building.

First, the power consumed by the motor to pump the water to fill the tank has been estimated by collecting the data such as the rating of the motor and the duration of time for which the motor is switched ON in a day. Then, the height of the building is measured to find out the available head. Even though the proposed turbine-generator sets can be employed at multiple locations, one location at the first floor of the building has been chosen so that the head available would be maximum. Then, the second important parameter, i.e., the discharge has been calculated from the volume of the



(a)



(b)

Fig. 2 Pictures of a water tank b multistory building chosen for this study

overhead water tank. From these two parameters, the power that can be generated theoretically has been found using (1).

$$P_{th}(W) = \rho \times q \times g \times h \times \eta. \quad (1)$$

where,

- ρ Density (kg/m^3) ($\sim 1000 \text{ kg/m}^3$ for water).
- q Water flow (m^3/s).
- g Acceleration of gravity (9.81 m/s^2).
- h Falling height, head (m).
- η Efficiency of turbine-generator set.

The power generated by this method can be utilized to charge batteries and subsequently, can be converted from DC to AC using inverters to use it later as a standby supply. This method can be considered as an alternative for diesel generators and can help in reducing carbon emissions.

Obviously, the energy that can be generated by this method would not be greater than that of the energy delivered by the motor to fill the tank. So, a portion of the bills spent on electricity can only be recovered. Thus, a detailed study should be made whether it is feasible to employ the setup so as to understand how much time it takes to recover the capital cost.

3 Results and Discussion

The motor that has been employed for pumping the water is rated as 3 HP, i.e., approximately equivalent to 2.24 kW. It is observed that the motor has to be run for 50 min, i.e., 0.84 h, duration every day to fill the water tank. Thus, from this data, the number of units consumed for filling the water tank has been found as 1.87 kWh using (2).

$$\text{No. of units consumed} = \text{kW rating} \times \text{no. of running hours}. \quad (2)$$

The details of the water tank and the building that is chosen for this study have been mentioned in Table 1. As per the details of water tank, i.e., radius $r = 1.25 \text{ m}$ and length $l = 2.12 \text{ m}$, its volume (V) has been calculated as 10.4 m^3 using (3). Thus, the discharge has been taken as $10.4 \text{ m}^3/\text{sec}$.

$$V = \pi r^2 l. \quad (3)$$

If the proposed box is assumed to be employed at the first floor of the building, the available head would be 48 m. Assuming that the efficiency of turbine-generator

Table 1 Details of the water tank and the building

Component	Specification
Capacity of the tank	10,000 L
Radius of the tank	1.25 m
Height of the tank	2.12 m
Height of the apartment	60 m
No. of tanks in the apartment	4
No. of floors in the apartment	7

set is 90%, the power that can be produced using the setup has been calculated as 4407 kW using (1).

According to this estimated maximum amount of power that can be generated, the type and rating of the turbine have been decided from Fig. 3. From this figure, it can be said that the Francis turbine would be suitable for the proposed system as per the values of head, discharge, and power capacity.

The theoretical power that is shown as possible to be generated would be sufficient to serve an average residential load at a given instant of time. It can also be increased further by choosing a building with more height. However, the number of units those can be generated depends on the water consumption by the residents in the first floor of building. If the proposed box is placed at the top floor of the building, then

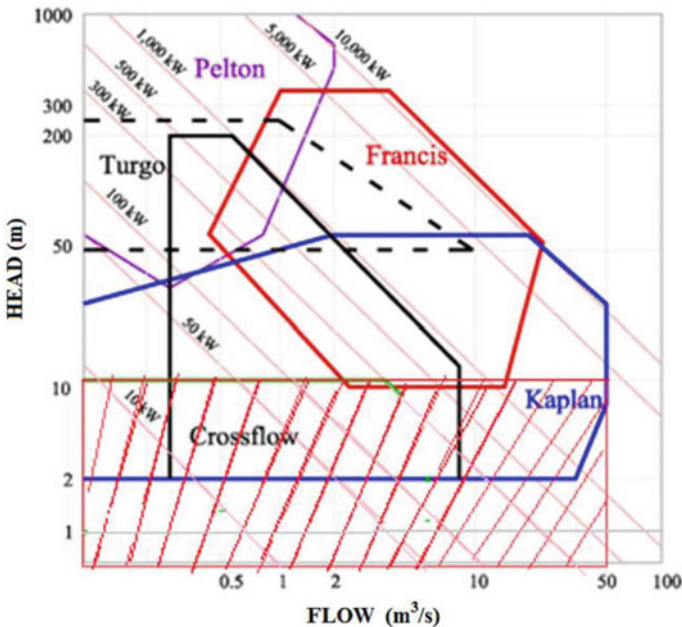


Fig. 3 Hydro-turbines characteristics in terms of water head and flow rate [13]

the water flow would be continuous as one if not the other would be utilizing the water during any time of the day. In this case, the available head would become less. It is observed that the head in this case is 8 m only. Thus, the power that can be produced using the setup has been found to be 734.5 kW. According to Fig. 3, the suitable turbine for this case would be Kaplan as the head is reduced to a value below 10 m. In this case also, how continuously the water flows to the downward direction and with what flow rate are little-known. Such details can be known only with the practical implementation of the method. The present work is to study the feasibility of employing the mentioned boxes with turbine-generator sets and theoretically prove that it is possible to generate the power in the proposed method. This study can be extended with a hardware setup and real-time implementation of the proposed method.

4 Conclusion

As per the availability of head and discharge of the water, the HPS would be constructed mostly in hilly areas. These are the two parameters which influence the power that can be generated by HPS. In this study, it is theoretically proved that the power generation is possible if a small/micro-scale hydropower generating unit is employed in a multistory building to utilize the otherwise-wasted kinetic energy of water that is coming down from the overhead water tank. However, the water utilization would be highly nonlinear. Thus, the generator associated with the hydro-turbine should work at variable speeds. Consequently, sophisticated power electronic devices-based charge controllers should be used to charge the battery. A provision should be made to access all these components on the outer wall. The design should be mechanically stable. These things would be studied in our future work through real-time implementation of the proposed method.

References

1. Bhat VI, Prakash R (2008) Life cycle analysis of run-of river small hydro power plants in India. *Open Renew Energy J* 1(1):11–16
2. Paish O (2002) Micro-hydropower: status and prospects. *Proc Inst Mech Eng Part A: J Power Energy* 216(1):31–40
3. Norman J, Got water, need power? technical report, ABS Alaskan, Inc, available online: <https://www.absak.com/pdf/books/ABSHydro.pdf>
4. Neil J, Jian K, Steve S, Abigail H, Papatya D (2011) Acoustic impact of an urban micro hydro scheme. *World Renew Energy Congr* 1448
5. Erinofiardi, Pritesh G, Abhijit D, Aliakbar A, Putra B, Ahmad FS, Afdhal KM, Agus N (2017) A review on micro hydropower in Indonesia. *Energy Procedia* 110:316–321
6. Agustín AI-R, José AC-R, Efraín O’N-C (2009) Achievable renewable energy targets for Puerto Rico’s renewable energy portfolio standard. *Micro Hydro energy resource*, Ch. 8, report, Universidad de Puerto Rico-Mayagüez

7. Micro-HydropowerSystems, A buyer's guide, natural resources Canada, available online at: <https://s1.solacity.com/docs/NRC/Micro-Hydropower%20Systems.pdf>
8. Anaza SO, Abdulazeez MS, Yisah YA, Yusuf YO, Salawu BU, Momoh SU (2017) Micro hydro-electric energy generation-An overview. *Am J Eng Res* 6(2):5–12
9. Arch M, Arch B (2019) Electricity generation from micro hydro power plant at MGM Gandheli Campus, Aurangabad. *Int J Appl Eng Res* 14(13):3048–3052
10. Zekâi Ş (2018) 4. 12 Hydropower conversion, *comprehensive energy systems* 4:545–572
11. Daniel AN, Guide to hydropower. canyon hydro inc. Available online at: <http://www.canyonhydro.com/guide/>
12. New D (2005) Intro to hydropower, Part 2: measuring head and flow. *Home power* 104
13. Hatata AY, El-Saadawi MM, Saad S (2019) A feasibility study of small hydro power for selected locations in Egypt. *Energ Strat Rev* 24:300–313

A Model for Identifying Fake News in Social Media



Ishita Singh, Joy Gupta, Ravikant Kumar, Srinivasan Sriramulu, A. Daniel, and N. Partheeban

Abstract Fake news and ruses are there even before the arrival of the web. The broadly recognized meaning of web fake or we can say wrong news is: spurious articles purposefully constructed to deceive readers. There is so much of spread of the fake news that has strong negative impact on the society and in person also. First of all, fake news is piece of work which is written and spread with wrong intentions. They deceive people to trust the auxiliary information just to meet the greed. Moreover, it is the most challenging part to take the normal people out of such misleading fake news, which is very large in number. The purpose of the work is to return up with an answer which will be used by users to detect and sieve sites comprising false and misleading information. We use simple and punctiliously designated features of the heading and post to precisely categorize fake posts. Throughout the paper we have shown the research related zones, open complications, and future directions for the research on fake news detection on social media. We wind up the report by elevate perception about examine and chance for businesses that are presently on the hunt to assist spontaneously detecting fake news by providing web services.

Keywords Machine learning · Python · TF-IDF vectorizer · Passive aggressive classifier

I. Singh · J. Gupta (✉) · R. Kumar · S. Sriramulu · A. Daniel · N. Partheeban
School of Computing Science and Engineering, Galgotias University, Greater Noida, Uttar Pradesh, India

S. Sriramulu
e-mail: s.srinivasan@galgotiasuniversity.edu.in

N. Partheeban
e-mail: n.partheeban@galgotiasuniversity.edu.in

© The Author(s), under exclusive license to Springer Nature Singapore Pte Ltd. 2022
B. B. V. L. Deepak et al. (eds.), *Applications of Computational Methods in Manufacturing and Product Design*, Lecture Notes in Mechanical Engineering,
https://doi.org/10.1007/978-981-19-0296-3_50

1 Introduction

The internet is chiefly obsessed by promotions, marketing, etc. Websites with astonishing captions are very fashionable, which result in advertising corporations capitalizing on the high traffic to the location [1]. The question remains how misinformation would then stimulate the general public. The scattering of misinformation can root misunderstanding and needless stress amongst the general public. We can term this as disinformation which is digital in nature [2]. So, fake news is generally created intentionally to harm and deceive the public. Propaganda has the potential to root issues, within actions, for many people [3]. Propaganda has been acknowledged to interrupt election procedures, generate disquiet, disagreements and hostility amongst the general public [4, 5].

These days, the internet has turned out to be a vigorous part of our day-to-day life. It was reported in 2017 that Facebook was the prime social media platform, hosting more than 1.9 million users world-wide [6, 7]. From all the social media platforms, the biggest impact in spreading the fake news is from Facebook alone, even it has the highest impact in spreading wrong information. It was reported that 44 percent of universal handlers get their bulletin from Facebook [8]. 23% of Facebook handlers have specified that they have shared wrong info or we can call it fake news, either intentionally or not. The roll out of false information is charged by platforms which are more social and it's occurring at distress speed.

2 Problem Formulation

The work cares with identifying an answer that would be able to spot and sieve articles comprising fake news for purposes of serving users to evade being deceived by click baits [9]. It is authoritative that such solutions are acknowledged as they're going to convince be useful to both readers and tech corporations intricate within the subject. Throughout the paper we have shown the research related zones, open complications, and future directions for the research on fake news detection on social media.

One of the most potent and exciting technologies which come in the real-world application is machine learning. Machine Learning techniques drastically change the computer application, and it simulates human-decision making using neural networks [10, 11].

Machine Learning is a domain of Artificial intelligence, where we bring AI into the equation by learning the input data. The process of making machines learn through the provided data is nothing but machine learning. Devices that are trained with a massive volume of data perform the task more accurately, and it can predict the result more precisely [12].

In general, an algorithm uses some mathematics and logic and takes some input to produce the output, but an AI algorithm takes a combination of both inputs and

outputs in order to learn and train the data and produce beneficial outputs [13, 14]. Algorithms in each group perform the same task of forecasting outputs on the given unknown inputs. However, here the data is the backbone when it comes to selecting the right and correct algorithm.

3 Implementation

The purpose of the work is to return up with an answer which will be used by users to spot and filter articles comprising false and deceptive info. We use modest and punctiliously selected features of the title and column to precisely recognize fake posts. Throughout the paper we have shown the research related zones, open complications, and future directions for the research on fake news detection on social media. We wind up the report by elevate perception about examine and chance for businesses that are presently on the hunt to assist spontaneously detecting fake news by providing web services.

It used various modules to get our model work better. We will be showing the implementation of all of some modules.

Python is the most significant language when it comes to modelling, data science or machine learning. Python being a data science tool gives us the ease to explore the basics of machine learning part. Whilst machine learning is more about probability, statistics, mathematical operations, etc. It is more powerful than any other language when it comes to visualization of data. Jupyter notebook is an open-sourced web-based interactive application that allows us to code, visualize, equate, and solve more easily. Data cleaning, data visualization, statistical modelling, machine learning are some common uses and the Python Package pip 20.2.3 used for implementations. Along with the above NumPy, pandas, matplotlib, seaborn, sklearn, nltk, wordcloud etc. are used.

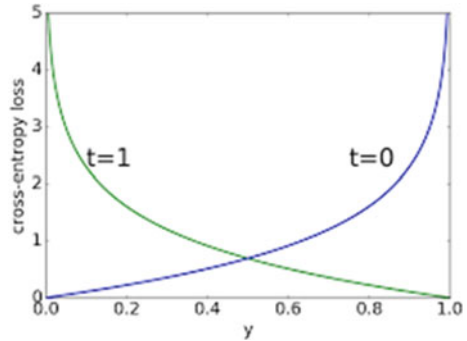
1. About the data: We have collected the data from Kaggle. It is very feasible to download the data in zip file from Kaggle. On downloading the dataset, we will get two csv files namely, true and fake. The “True.csv” dataset contains 21,418 rows whilst “Fake.csv” dataset contains 23,503 rows. The true dataset contains all the articles which are considered as “Real news”. The fake dataset contains all those articles which are considered as “Fake news”. We will merge both the dataset in the later part of our analysis.
2. Pandas: Pandas are the cost-free open source library used to perform data analysis various manipulation using data, built on of the Python programing language.
 1. Loading Dataset using pandas: we use.read_csv() method to load data in our notebook.
 2. Concatenating and Shuffling both the Dataset: using shuffle() and.concat() method.

3. Viewing the Dataset: `df.head()` method gives the first five rows of the dataset.
 4. Checking the shape, missing and duplicate values of the dataset:
 5. Dropping and Rechecking the duplicated values: by using `drop_duplicates()` method.
 6. Dropping attributes which we will not use in the analysis and converting all the text to lower case LetterCase letters.
 7. Other cleaning of the data: We will remove the punctuations and stopwords in the dataset. It makes the data noisy and later creates problems in the analysis. So better to get rid of them!
 8. Checking the final dataset: we can view the first five rows of the dataset by using `head()`
 9. Data visualization:
 - i. Divided the data on the basis of subject. Just like articles per subject. Here we are grouping data by subject and text.
 - ii. Then we have shown a bar graph for fake news versus true news. Here we are grouping data by target and text.
 - iii. We have also shown Word Cloud, which is the simplest technique to visualize the textual data and represent the bulk of words, used for representing text data in which the size of each word indicates its frequency or importance in the two respective articles.
 - IV. Checked which words are the most frequent words in the real and fake news respectively. We have again used the bar graph.
3. Sklearn: Scikit-learn is an open-source cost-free machine learning library based on Python. It comprises of many algorithms like support data modelling, numerical using python and scientific libraries.
 1. Modelling: using the function `plot_confusion_matrix()` to plot the confusion matrix of the models.
 2. Preparing the Data: Split the data to train and test the model, using `train_test_split()` method, and giving the `test_size`, `random_state` in the parameters.
 3. Logistic regression: Logistic Regression is used to classify data into categories like True or False, 1 or 0 etc. Extending Logistic Model to classify numerous classes of events such as whether the provided article is comprising of those words which are often used in Fake or Real News. It is used to define a relationship between one binary and one normal or more variables.

Logistic Regression habits a compound cost function as compared to Linear Regression. It is known as “Sigmoid Function”. The hypothesis of Logistic Regression makes sure that the limit of Sigmoid remains in between 0 and 1.

It is used to plot the forecasted outputs to the probability. Sigmoid Function converts all real value into the range of 0 to 1.

Fig. 1 Binary loss entropy



Hypothesis equation of Logistic Regression is little bit different from that of Linear Regression.

$$\sigma(Z) = \sigma(\beta_0 + \beta_1 X) \tag{1}$$

In Logistic Regression we use Binary Loss Entropy which varies as shown in Fig. 1.

Binary Loss Entropy makes sure that it would end up being a convex function and hence minimize the cost value.

Minimizing cost/loss with the help of cost function can be done using Gradient Descent. That derivative term is called “Descent”. It is responsible for global minima.

4. **Decision Tree Classifier:** It is an extrapolative modelling approach used in statistics, data mining and machine learning. Decision Trees are useful in Decision Analysis as it can be implemented to represent decision visually and explicitly and to inferred decision.

Decision Tree is the algorithm which is most commonly used in classification problems. However, it can also be used in regression problems as well. It is basically a tree like structure where nodes represent the features of a dataset and branches show the decision rule. The leaf node in decision tree shown in Fig. 2 is basically the outcome.

1. Begin the decision tree with the root node that holds complete dataset.
 2. Find out the best feature to split around using Attribute Selection Measure
 3. Now, divide the root node into possible values of best attribute
 4. Determine the best feature and create the decision tree node
 5. Repeat the same process again and again, until it is impossible for you to classify the node further.
5. **Random Forest Classifier:** It is based on ensemble tree-based learning algorithm. The Random Forest is made up of numerous dissimilar Decision Trees from a casually selected subset of the training set. It can handle many of provided

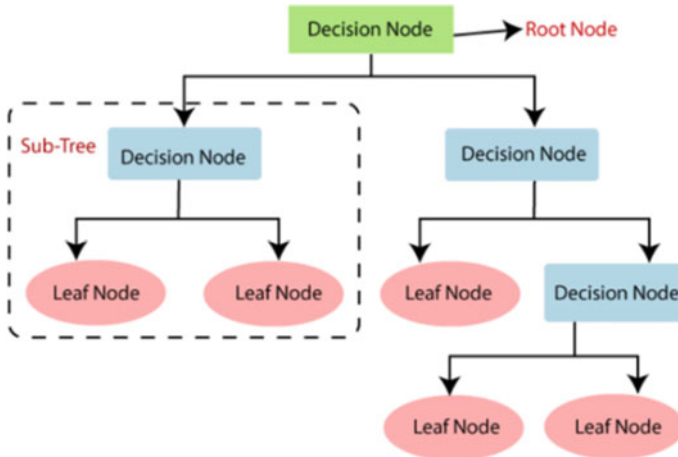


Fig. 2 Decision tree

variables without variable deletion. It obtains an extremely precise classifier. Thus, it is one of the most accurate learning algorithms available.

As its name suggest, it is collection of different Decision Trees. The difference is that the process of finding the root node and splitting around the best feature node will run automatically as represented in Fig. 3.

1. First step is to select “ K ” features out of “ m ” features where $k \ll m$

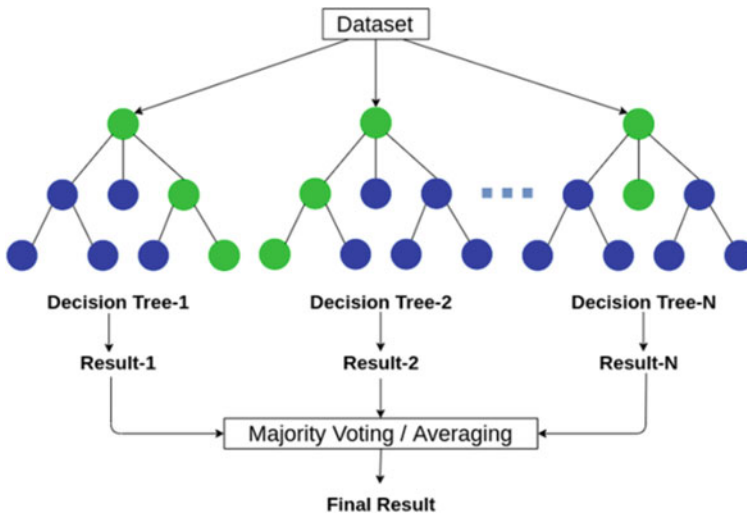


Fig. 3 Random forest

2. From K features, select best node d to split around
3. Split the node into children nodes using best split method
4. Now repeat first 3 steps up to a certain number of time.
5. Build different forest by repeating all four steps up to n number of times to create a random forest of n numbers of decision trees.

4 Experimental Output

Three algorithms are applied i.e. Logistic Regression, Decision Tree and Random Forest Classifier. We got best result from the Decision Tree as illustrated in Table 1. Logistic Regression (Fig. 4).

- First cell denotes that we have correctly classified 4609 fake news examples.
- Second cell denotes that we have mistakenly classified 67 fake news examples as real news.
- Third cell denotes that we have mistakenly classified 39 real news examples as fake news.
- Fourth cell denotes that we have correctly classified 4223 real news examples.

Random Forest Classifier (Fig. 5).

Table 1 Experimental results

Algorithm	Correct classifications	Accuracy (%)
Logistic regression	8832	98.81
Decision tree	8893	99.50
Random forest	8838	98.88

Fig. 4 Confusion matrix for logistic regression

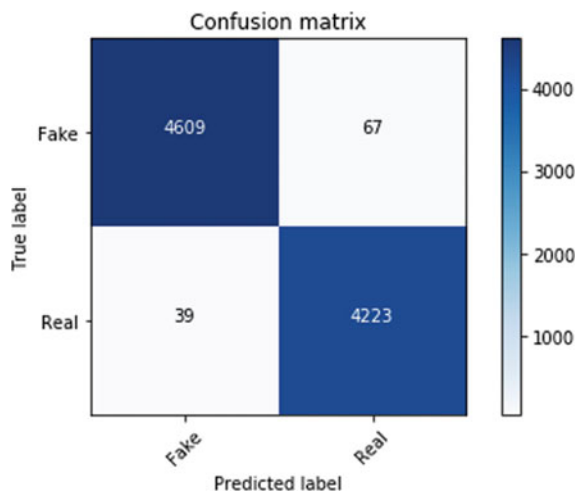
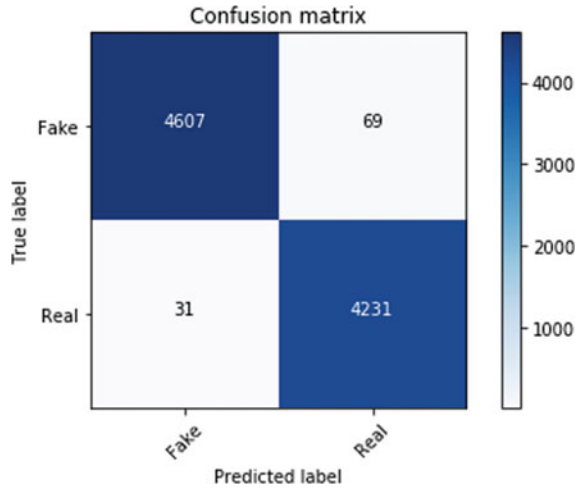


Fig. 5 Confusion matrix for random forest classifier



- First cell denotes that we have correctly classified 4607 fake news examples.
- Second cell denotes that we have mistakenly classified 69 fake news examples as real news.
- Third cell denotes that we have mistakenly classified 31 real news examples as fake news.
- Fourth cell denotes that we have correctly classified 4231 real news examples.

Decision Tree (Fig. 6).

- First cell denotes that we have correctly classified 4653 fake news examples.
- Second cell denotes that we have mistakenly classified 23 fake news examples as real news.

Fig. 6 Confusion matrix for decision tree

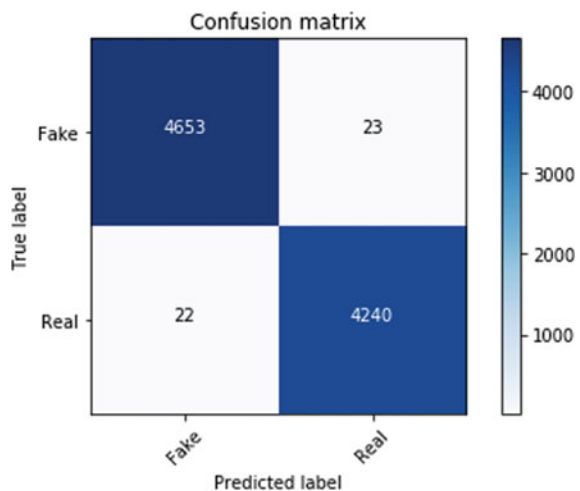


Fig. 7 Correct classification

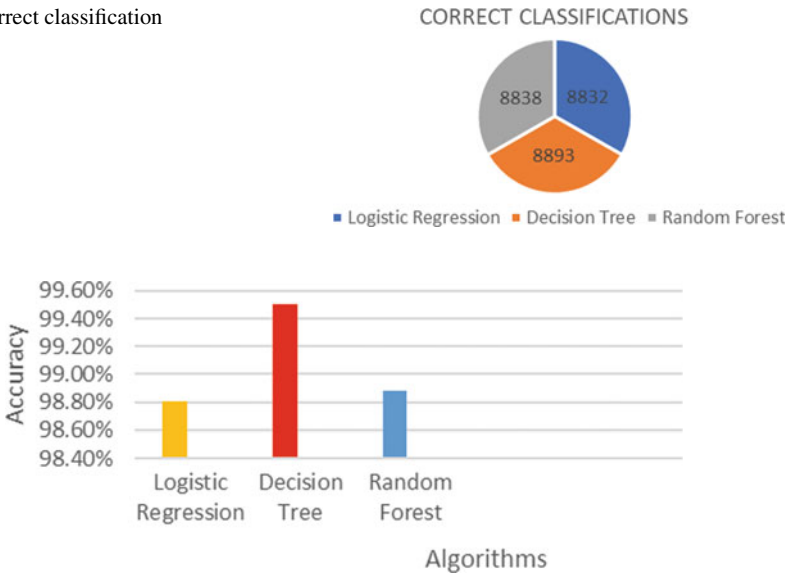


Fig. 8 Accuracy bar plot

- Third cell denotes that we have mistakenly classified 22 real news examples as fake news.
- Fourth cell denotes that we have correctly classified 4240 real news examples.

5 Experimental Results

Decision Tree has correctly classified maximum numbers of examples as illustrated in Fig. 7, followed by Random Forest and Logistic Regression. So, Decision Tree is suitable for fake news classification.

As it is evident from the Fig. 7 that Decision Tree is performing well over given dataset. This can also be seen from the Fig. 8.

6 Conclusion

In this paper, analyse about the need for “Fake News Detection” in the current era! How just a WhatsApp forward could lead to failure of the entire system. Along with some theoretical aspects, successfully built a machine learning model to classify whether the news is fake or genuine based on keywords present in it. It includes natural language processing and some of the machine learning algorithms are Logistic

Regression, Decision Tree, and Random Forest. We have checked which algorithm better suits to classify news.

Furthermore, we are looking forward to implementing the Recurrent Neural Network and see how it performs on the categorical data References.

References

1. García SA, García GG, Prieto MS, Guerrero AJM, Jiménez CR (2020) The impact of term fake news on the scientific community scientific performance and mapping in web of science. *Soc Sci* 9(5)
2. Hua J, Shaw R (2020) Corona virus (covid-19) “infodemic” and emerging issues through a data lens: the case of China. *Int J Environ Res Pub Health* 17(7):2309
3. Conroy NK, Rubin VL, Chen Y (2015) Automatic deception detection: methods for finding fake news. *Proc Assoc Inf Sci Technol* 52(1):1–4
4. Vosoughi S, Roy D, Aral S (2018) The spread of true and false news online. *Science* 359(6380):1146–1151
5. Wang WY (2017) Liar, liar pants on fire: A new benchmark dataset for fake news detection. Association for Computational Linguistics, Stroudsburg, PA, USA
6. Ruchansky N, Seo S, Liu Y (2017) Csi: a hybrid deep model for fake news detection. In: *Proceedings of the 2017 ACM on conference on information and knowledge management*. Singapore, pp 797–806
7. Bühlmann P (2012) Bagging, boosting and ensemble methods. In: *Handbook of computational statistics*. Springer, Berlin, pp 985–1022
8. Ahmed H, Traore I, Saad S (2018) Detecting opinion spams and fake news using text classification. *Secur Priv* 1(1) (2018)
9. Kaggle (2018) Fake news. Kaggle, San Francisco. <https://www.kaggle.com/c/fake-news>
10. Kaggle (2018) Fake news detection. Kaggle, San Francisco
11. Dos Santos EM, Sabourin R, Maupin P (2009) Overfitting cautious selection of classifier ensembles with genetic algorithms. *Inf Fusion* 10(2):150–162
12. Chen T, Guestrin C (2016) Xgboost: a scalable tree boosting system. In: *Proceedings of the 22nd ACM SIGKDD international conference on knowledge discovery and data mining*. San Francisco, pp 785–794
13. Hastie T, Rosset S, Zhu J, Zou H (2009) Multi-class adaboost. *Stat Interface* 2(3):349–360
14. Lam L, Suen SY (1997) Application of majority voting to pattern recognition: an analysis of its behavior and performance. *IEEE Trans Syst Man, Cybern—Part A: Syst Hum* 27(5):553–568

Driver Drowsiness Detection Using Machine Learning to Prevent Accidents



Srinivasan Sriramulu, A. Daniel, N. Partheeban, Vaibhav Singh, Asad Ali Khan, and Shivam Sharma

Abstract Drowsiness of driver is one of the major reasons for Accidents. Every year the number of such cases increases. In this paper, A drowsiness detector is presented that will reduce the number of such cases and hence increase the transportation safety. The system works on machine learning algorithm that locates the driver's face and eyes and closely monitors eye blink pattern of driver and alarms him in case of drowsiness.

Keywords Driver drowsiness · Transportation safety · Machine learning algorithm · Blink pattern

1 Introduction

With the splurge in the number of vehicles in recent years, the management of traffic has become quite a herculean ask. Cars have become necessary means of transportation in every family that can afford it. 2017 saw an increase of 0.3% in the total number of vehicles, with respect to 2016, summing to 97million vehicles around the globe [1]. In 2018, the total number of vehicles that were in use estimated to be more than 1 billion. The rapid increase owes to the utility of these vehicles, but every coin has two faces. Therefore, the increase in the number of vehicles is directly proportional to the increase in the number of road accidents [2, 3]. National Highway Traffic Safety Administration reported 7,277,000 traffic accidents in the United States in 2016, leading to 37,461 fatalities and 3,144,000 injuries [4]. In almost 20–30% of the total case, the reason for accidents was found to be fatigue. Thus, it could be said that fatigued driving contributes significantly to the cause of traffic accidents. It is a potential, yet latent danger that needs to be combatted [5].

S. Sriramulu (✉) · A. Daniel · N. Partheeban · V. Singh · A. A. Khan · S. Sharma
School of Computing Science and Engineering, Galgotias University, Greater Noida,
Uttar Pradesh, India
e-mail: s.srinivasan@galgotiasuniversity.edu.in

N. Partheeban
e-mail: n.partheeban@galgotiasuniversity.edu.in

© The Author(s), under exclusive license to Springer Nature Singapore Pte Ltd. 2022
B. B. V. L. Deepak et al. (eds.), *Applications of Computational Methods in Manufacturing and Product Design*, Lecture Notes in Mechanical Engineering,
https://doi.org/10.1007/978-981-19-0296-3_51

The need for a fatigued driving detection system stems from here, resulting in an increase in research for the development of such a system. Two types of detection methods are used- subjective detection method and objective detection method [6]. In the subjective detection method [7], a driver must participate in the evaluation, which is associated with the driver's subjective perceptions through steps such as self-questioning, evaluation and filling in questionnaires. This data is used to estimate the number of vehicles that are being driven by exhausted drivers and to assist them in planning their schedule accordingly. However, the objective detection method [8] does not take into account drivers' feedback. It monitors physiological state of the drivers and their driving-behavior characteristics in real time. The data collected by this method is used to evaluate level fatigue. The objective detection is further categorized into two types: contact method and non-contact method. The non-contact method is cheaper and more convenient because the system requires Computer is in technology or sophisticated camera that allow the use of the device in more cars. With this Python project, we will make a laziness identifying gadget. An incalculable number of individuals drive on the expressway day and night. Cabbies, transport drivers, transporters and individuals voyaging significant distance experience the ill effects of absence of rest. Because of which it turns out to be exceptionally risky to drive when feeling drowsy. Most of mishaps occur because of the tiredness of the driver. Thus, to forestall these mishaps we will fabricate a framework utilizing Python, OpenCV, SciPy, Playsound, Imultis and diLib which will caution the driver when he feels drowsy [9–11].

Humans have always invented machines and devised techniques to ease and protect their lives, for mundane activities like traveling to work, or for more interesting purposes like aircraft travel. With the advancement in technology, it has affected our lives in many ways. We can travel to place at a pace that even our ancestors would not have thought is possible. In modern times, almost everyone in this world uses some sort of transportation every day. However, there are a set of rules to be followed while driving, like staying alert and active while driving. We cannot neglect our duties toward safe traveling. It may look like an irrelevant thing to most people but following rules and regulations on the road is very important. It can be destructive and sometimes that carelessness can harm lives even of the people on the road. One kind of carelessness is not admitting when we are too tired to drive. In order to monitor and prevent a destructive outcome from such negligence, many researchers have written research papers on driver drowsiness detection systems. But at times, some of the points and observations made by the system are not accurate enough. Hence, to provide data and another perspective on the problem at hand, in order to improve their implementations and to further optimize the solution, this project has been done.

Our present measurements uncover that simply in 2017 India alone, 148,707 individuals passed on because of vehicle related mishaps. Of these, at any rate 21 percent were caused because of weariness making drivers commit errors. This can be a generally more modest even number, as among the various causes that can lead to a mishap, the inclusion of weariness as a reason is by and large horribly thought little of. Weariness joined with terrible framework in agricultural nations

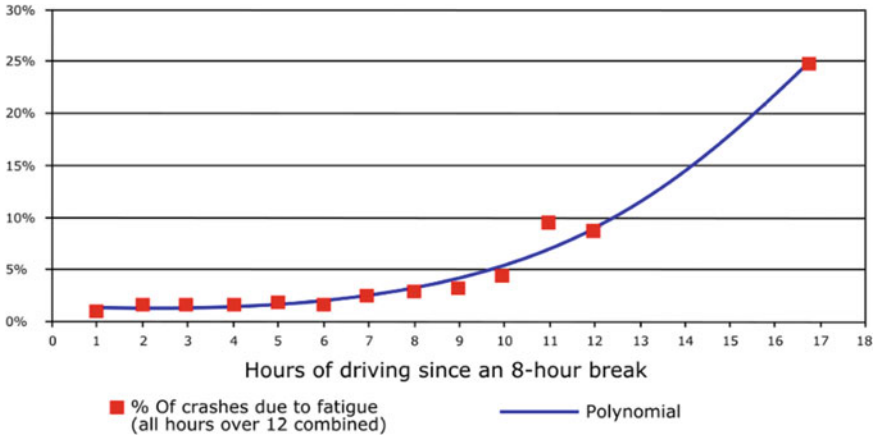


Fig. 1 Percentages of crashes due to fatigue

like India is a catastrophe waiting to happen. Exhaustion, by and large, is extremely hard to quantify or notice dissimilar to liquor and medications, which have clear key pointers and tests that are accessible without any problem. Likely, the best answers for this issue are mindfulness about exhaustion related mishaps and elevating drivers to concede weariness when required. The previous is hard and substantially more costly to accomplish, and the last is not conceivable without the previous as driving for extended periods is exceptionally rewarding. When there is an expanded requirement for a work, the wages related with it expands prompting an ever-increasing number of individuals receiving it. Such is the situation for driving vehicle vehicles around evening time. Cash propels drivers to make imprudent choices like driving all night even with weariness. Figure 1 shows the variation of crashes due to fatigue.

2 Implementation

This is for the most part since the drivers are not themselves mindful of the enormous danger related with driving when exhausted. Figure 2 shows the crashes due to drowsy drivers. A few nations have forced limitations on the quantity of hours a driver can drive at a stretch, yet it is as yet not enough to tackle this issue as its usage is troublesome and expensive.

The following things are to be used for processing to the experiment.

- Python: Python is the basis of the program that we wrote. It utilizes many of the python libraries.
- Numpy: Pre-requisite for Dlib.
- Scipy: Used for calculating Euclidean distance between the eyelids.
- Playsound: Used for sounding the alarm.

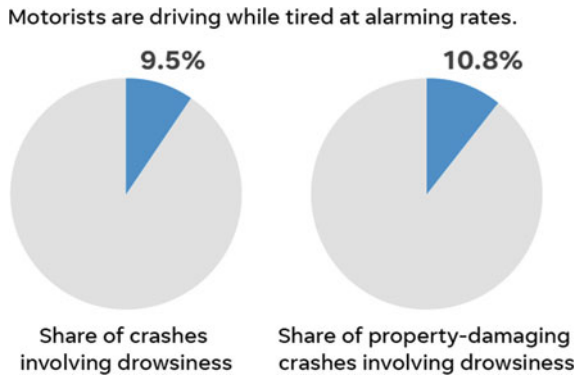


Fig. 2 Crashes involving drowsy drivers

- Dlib: This program is used to find the frontal human face and estimate its pose using 68 face landmarks.
- Imutils: Convenient functions written for Opencv.
- Opencv: Used to get the video stream from the webcam, etc.
- OS: Program is tested on Windows 10 build 1903 and Pop OS 19.04.
- Laptop: Used to run our code.
- Webcam: Used to get the video feed.

Our system will be trained as illustrated in Table 1, in such a way that after getting following results; it will reach to the corresponding decision.

The model will be implemented on a web application using HTML and CSS. User will show its face through webcam attached with Laptop as in Fig. 3. The webcam will scan the face of person and determine whether the driver is sleepy or not depending upon the Euclidean distance of eyelids.

Table 1 System behavior result

Test ID	Test case title	Test condition	System behaviour	Expected result
T01	NGSY	Straight face, good light, with glasses	Non drowsy	Non drowsy
T02	YTGN	Tilted face, good light, no glasses	Drowsy	Drowsy
T03	YTGy	Tilted face, good light, with glasses	Drowsy	Drowsy



Fig. 3 Sample testing for decision making

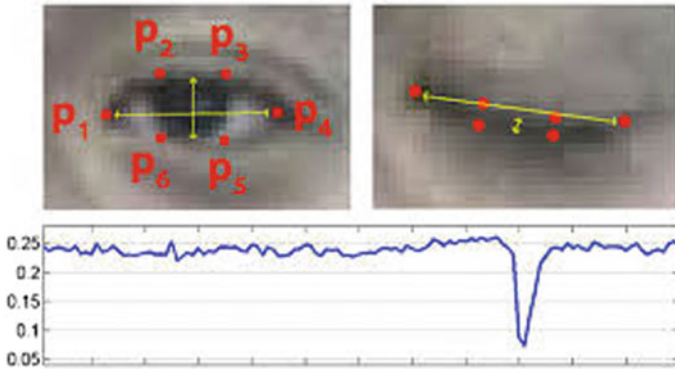


Fig. 4 Distinct vertical distances measuring

3 Experimental Result

In our program we used Dlib, a pre-trained program trained on the HELEN dataset to detect human faces using the pre-defined 68 landmarks. The video will be passed through Dlib frame by frame, so that we can detect left eye and right eye features of the face. Now, we drew points and mark the shape and size of eye using OpenCV. Using SciPy’s Euclidean function, we calculated sum of both eyes’ aspect ratio which is the sum of 2 distinct vertical distances between the eyelids divided by its horizontal distance as represented in Fig. 4.

4 Algorithms

There will be 6 reference points on eyelid:

- (p1, p2, p3, p4, p5, p6)

$$EAR = \frac{\|p2 - p6\| + \|p3 - p5\|}{2\|p1 - p4\|}$$

Example

- `from scipy.spatial import distance`
- $\|p2 - p6\| = \text{distance.euclidean}(p2, p6)$
- $\|p3 - p5\| = \text{distance.euclidean}(p3, p5)$
- $\|p1 - p4\| = \text{distance.euclidean}(p1, p4)$

Above images in Fig. 5 show how our result is dependent on number of frames and so it creates a difference in a blink and drowsiness reorganized human faces and their eyes, and by using SciPy we measured the distance between the points marked on eyes accurately, in order to find out whether the driver is drowsy or not, by comparing our result with the threshold value, i.e., 0.25(0.25 was chosen as a base case after some tests). Finally our model depicts perfectly whether the person is drowsy or not, though there is a room for improvement and that always exists, so we can modify it by adding more parameters in future.

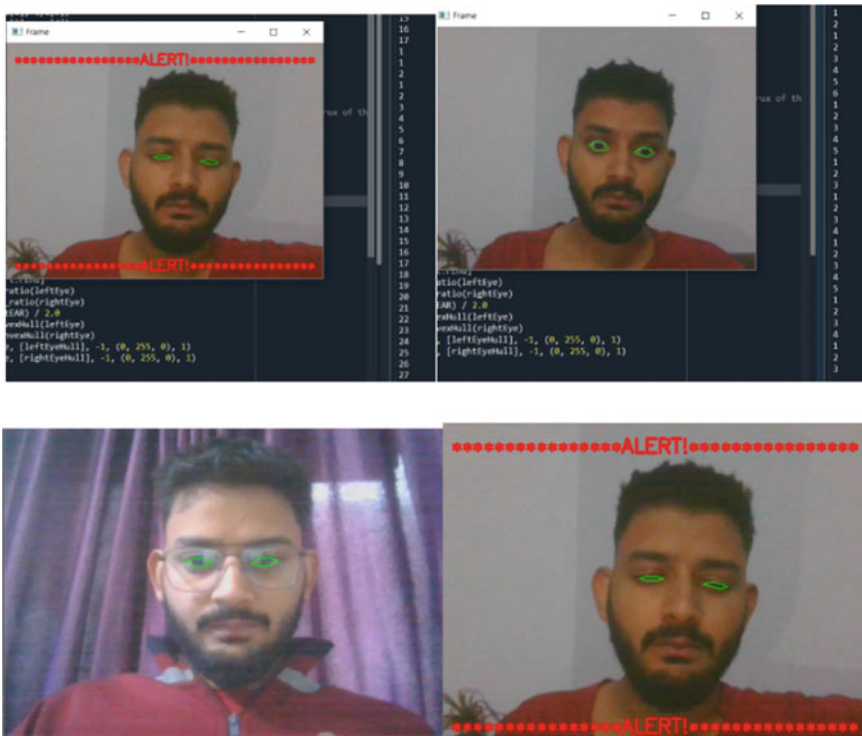


Fig. 5 Driver drowsiness reorganization

5 Conclusion

It completely meets the objectives and requirements of the system. The framework has achieved an unfaltering state where all the bugs have been disposed of. The framework cognizant clients who are familiar with the framework and comprehend its focal points and the fact that it takes care of the issue of stressing out for individuals having fatigue-related issues to inform them about the drowsiness level while driving. To make our model more accurate we can add several parameters such as blink rate and yawning as further steps, if these things implemented correctly accidents will reduce. This model can be used for various other uses like streaming services such as Amazon Prime and Netflix can detect when the user is asleep and stop the video accordingly. This will also be used in applications that require user attention.

References

1. Romdhani S, Torr P, Scholkopf B, Blake A (2001) Computationally efficient face detection. In: Proceedings Eighth IEEE international conference on computer vision. ICCV 2001, 7–14 July 2001, 7024346. <https://doi.org/10.1109/ICCV.2001.937694>, Vancouver, BC, Canada.
2. Boser BE, Guyon IM, Vapnik VN (1992) A training algorithm for optimal margin classifiers. In: Proceedings of the 5th ACM workshop on computational learning theory, pp 144–152
3. Burges CJC (1996) Simplified support vector decision rules. In: 13th International conference on machine learning, pp 71–77
4. Osuna E, Freund R, Girosi F (1997) Training support vector machines: an application to face detection. CVPR, pp 130–136
5. Platt J (1999) Fast training of support vector machines using sequential minimal optimization. In: Advances in kernel methods-support vector learning. MIT Press, Cambridge pp 185–208
6. Rowley H, Baluja S, Kanade T (1998) Neural network-based face detection. PAMI 20:23–38
7. Schneiderman H, Kanade T (2000) A statistical method for 3d object detection applied to face and cars. In: CVPR, pp 746–751
8. Scholkopf B, Burges CJC, Smola AJ (1999) Advances in Kernel methods—support vector learning. MIT Press, Cambridge
9. Scholkopf B, Mika S, Burges C, Knirsch P, Müller KR, Rätsch G et al (1999) Input space vs. feature space in kernel-based methods. IEEE Trans Neural Netw 10(5):1000–1017
10. Sung KK, Poggio T (1994) Example-based learning for view-based human face detection. In: Proceedings from Image Understanding Workshop, Nov 1994
11. Vapnik V (1995) The nature of statistical learning theory. Springer, New York

Comparative Study of Various Authentication Schemes in Tele Medical Information System



Charul Dewan, T. Ganesh Kumar, and Sunil Gupta

Abstract Use of Technology and gadgets makes us smart. Globalization has made the world easy to access and the world is centered across IT. Use of IT services, smart gadgets have improved our life, but it is at the cost of security. Authentication schemes and protocols are required to secure the system against cryptographic attacks. Authentication scheme given and proposed by various authors in a multi-server environment will be compared in this paper to provide the solution to the security flaws. Cryptographic techniques have been used to authenticate the protocols against security attacks. The computational cost and the energy were calculated throughout the survey and we tried to find out the suitable scenario for secure telemedical healthcare services.

Keywords Mutual authentication · User anonymity · Malicious attacks · Telemedical information system

1 Introduction

Traditional client–server architecture and computing environment has been replaced by modern devices and gadgets like smartphones, smart home monitoring system, smart health, and many more. Yet, the ease of use and easy accessibility of data has led to data thefts, leakage, and forging. The more human race has switched to wireless media, data communication devices, more we are vulnerable to data loss and leakage.

C. Dewan (✉)

Dr. Akhilesh Das Gupta Institute of Technology and Management, Shastri Park, New Delhi, India

T. Ganesh Kumar

School of Computing Science and Engineering, Galgotias University, Uttar Pradesh, Greater Noida, India

S. Gupta

University of Petroleum and Energy Studies, Dehradun, India

Thus, preventive and countermeasures are required to secure the data from leakage. TMIS refers to Telecare medicine Information system in which healthcare facilities are provided to the patients, especially older and disabled people. TMIS will be beneficial when disease can be contracted by another person who will come in close vicinity of the infected person. This can be easily cited through the current global scenario where people are suffering from Covid-19 and others are contracting by coming in contact with the diseased patient. In such cases, telecare medicine information system will help to isolate the patient while providing treatment by just sitting at home. This can be supported with the help of technology. IoT devices are the interconnected devices like wearable's, smart devices, smart homes, gadgets, etc. which have the capability to connect and communicate to other devices throughout the world. Though devices will share and transmit the information but security will be an issue always.

Moreover, data and information which is being shared is classified into homogeneous and heterogeneous data. Here, we are dealing with heterogeneous data, so we require a standard platform as the devices and data are growing at a tremendous rate [1]. TMIS involves the use of various IoT devices and this information is transmitted over the cloud. Cloud server stores the information and processes it accordingly. Services provided by cloud can be classified into Software as a Service (SaaS), Platform as a Service (PaaS), and Infrastructure as a Service (IaaS). Public cloud platforms are accessible to all customers and organizations on pay-as-you-need basis whereas private cloud platforms are not accessible without authorization. With the rapid advancement of internet services, data is being stored online and, thus, cloud security is an important issue.

Information is vulnerable to various attacks and when the confidential data is being transferred from multiple IoT devices to the cloud servers, then it can be stolen or attacked by malicious users. Though each cloud data source protects its data and applies various security mechanisms, still, security threats may occur. Some of the security threats have been listed.

- **Insider Attack:** It is a malicious attack committed by a person with authorized system access. The person is an insider and is aware of internal network architecture. This insider threat is more harmful as an organization always makes policies for external attacks [2].
- **Identity and that information are used to make transactions.** It refers to stealing personal or financial information of another person. For example- Social Security Number (SSN), ATM Cards, Passport.
- **Password Guessing:** A brute force attack in which the malicious person guesses the password by trying every possible code or combination to unlock websites and web servers. It helps the intruder to gain access to a system by trying different combinations of usernames and passwords.
- **Denial of Service: DoS** is a malicious attack to tie down an online service or website, thereby, making it inaccessible to users. Their motive is to introduce more traffic on the server than it can handle so as to make it inoperable. Hackers

can attack the online services from any location, thus, making it difficult to track them.

- **Impersonation Attack:** It is an attack where the attacker pretends himself as a trusted or legitimate party to dupe an employee. Employee gets duped by transferring money into a fraudulent account or he reveals login credentials or shares sensitive information. It is a form of cyber-attack which results in great financial loss.

2 Literature Survey

To get secure access to confidential information from any private cloud server of the distributed system, this article compares pros and cons of various protocols defined by researchers in their articles. It will analyze features like user anonymity and how security attacks can be prevented in a much better way. “Mutual authentication proof has been done using BAN logic and the protocol simulation using AVSIPA results in ensuring security safety of the protocol. The performance study of our protocol is better than other works in terms of computation, storage, and communication cost” [3].

In 2018, Amin [4], in this research paper author discusses the various challenges faced while implementing Telemedicine in healthcare applications. As per the author, the health practitioner can obtain real-time information from the server about patient’s medical history, thereby, helping the patient to seek medical treatment anytime and anywhere. Health care data is one important element in patient data that they do not want to share with others. The medical system architecture which has been proposed by the authors work in different phases, i.e., setup, medical server registration, physician server registration, patient registration, login, authentication and session key, negotiation, new physician server addition, password renewal, and biometric renewal. First one is Setup Phase where Medical Registration Server (MRS) selects a key and it is shared among all medical servers. Second phase is Medical Server Registration Phase and as the name suggests medical server needs to register with MRS. Next, we have Physician server Registration phase and, in this phase, author proposed a session key between patient and a physician server. Fourth phase is Patient Registration Phase and patient has to register himself with the medical server so as to access physician server. Fifth phase is Login and Authentication phase, where a patient can access the medical data from a physician server and this is done through smartcard. Mutual authentication and session execution are being performed in session key agreement phase. In order to achieve scalability and Reliability, physician servers are being added and the phase is new physician server addition phase. Password and biometric information is being updated in the last two phases, i.e., password update phase and biometric renewal phase, respectively. The author conveyed that the protocol will be evaluated on various parameters like computation cost, security properties, communication cost, and storage cost and revealed that protocol holds good for user anonymity and user intractability.

In 2018, Amin has developed have developed Light Weight Authentication Protocol for IoT-enabled Devices in Distributed Cloud Computing Environment [3]. They have developed a protocol using AVISPA and BAN logic which is resistant to many attacks like offline password guessing, user impersonation, user anonymity, session key disclosure, and privileged insider at the server end. As per the authors of this paper, the protocol which has been designed by them is basically used to retrieve the information from cloud architecture-based environment and confidential information is being stored in private cloud server. In order to access the information from distributed cloud environment, the process has been divided into six phases namely cloud server registration phase followed by user registration phase. Then, third phase is login phase followed by authentication phase and password change phase. At last, identity update phase is being executed. In the first phase, i.e., the server sends identity to the control server and, in return, the server stores secret parameter. During second phase, user chooses identity and password to pass it to the server securely, thereby, generating some random number to resist insider attack. In third phase, the card reader calculates various values to authenticate the smart card punch followed by authentication phase which is necessary for mutual authentication and key agreement among user, server, and control server. During fifth phase, an existing user can change the password by providing relevant information, and smartcard authentication information will be provided by the user. Last phase suggests that it is necessary to update the identity of the user. All the phases have been implemented by the authors using the AVISPA software along with various operations like hash operation, X-OR operation, and concatenation operation. As per the author, few schemes do not hold mutual authentication.

In 2017, Ali [5], provided the security aspect of smart card-based user authentication scheme using BAN logic and AVISPA tool. They have proposed three factor-based authentication protocols which according to them can withstand network attacks as compared to earlier proposed two factor-based authentication protocols. For this, they have proposed threat model where an attacker can attack the system's data maliciously and steal the sensitive information. In order to secure the data, authors have proposed six phases, i.e., initialization phase, server registration phase, user registration phase, login phase, authentication and key agreement phase, and password change phase, respectively. Their protocol is based on Elliptic curve cryptography (ECC) which is an encryption technique based on algebraic structure of elliptic curves. First phase is initialization phase, where secret and public parameters are being selected. The second phase, i.e., server registration phase calculates some hash values and sends them to server. Third phase is user registration phase in which user registers it to get access to server services. Fourth phase is login phase where login process is being performed using a smartcard reader. Fifth phase is authentication and key agreement phase where user is authenticated by the server on the basis of login and reply messages. Last phase is password change phase where after authenticating his identity a user can change the password.

In 2017, Li [6] proposed a secure authentication and data encryption scheme for the IoT-based medical care system, which addresses user anonymity and prevents the security threats of many attacks, out of which, most common is replay attack.

Moreover, according to the authors, to reduce the redundancy in protocol design, they have modified the authentication process, and the proposed scheme is more efficient in performance. “Their scheme consists of five phases, including: setup phase, registration phase, login phase, verification phase, and access control and encryption phase. Their scheme tried to overcome the issues faced in Liu–Chung’s authentication scheme which was vulnerable to many attacks like password disclosure, offline password guessing, sensed data disclosure, sensed data forgery, replay, and the stolen smart card problem [7]”. The enhanced scheme proposed by the authors indicates that it is able to prevent attacks mentioned above and satisfies all user security issues, such as user anonymity, mutual authentication, session key security, and an efficient verification mechanism.

In 2017, Mohit et al.’s [8] proposed a scheme that was secure against patient anonymity and mobile device stolen attacks. In their scheme, five entities were there viz. patient, Doctor, Cloud, Healthcare Center, and Body Sensor. They also proposed an architecture that defines the process of medical treatment. At the start, the patient registers himself as he visits the healthcare center for medical examination. where hospital maintains the report of patients. After the health checkup, the health care department prepares the report and then uploads it onto the cloud. IoT devices and body sensors will collect the patient’s health data this data will be uploaded too onto the cloud server and report can be generated. The patient’s report from the cloud server will be forwarded to the respected doctor. Based on the report generated, the doctor will prescribe the treatment and medicines to the patient and generate a new document. He, then, uploads this document with the digital signature to the cloud server. The final report will be sent to the patient which contains the treatment of the patient. Their protocol consists of four phases: (1) Healthcare center upload phase, (2) Patient data upload phase, (3) Treatment phase, and (4) Checkup phase. Though they have proposed a scheme that will secure and mutually authenticate the data but failed to do so.

In 2015, Quan et al. proposed an authentication protocol based on identity–based cryptography to solve issues common to wireless sensor networks. WSNs have sensor nodes that are susceptible to various attacks as they are deployed in open environments, thereby, leading to user authentication issues. Zhou et al. [9] designed a secure protocol for WSN environment (Fig. 1).

3 Comparative Analysis

A protocol is to be developed which will provide mutual authentication. In this given Fig. 2, a TMIS has been shown where we have a doctor and a patient. The patient data is being stored in cloud server. So, we have to provide mutual authentication among the patient and the data stored over the cloud server and from cloud server to the data being stored in IoT devices at patient’s end. Secondly, this patient data will be accessed by doctor. Thus, that process needs to be authenticated too. It means the data is stored at doctor’s end to the cloud server and vice versa. Now, after storing

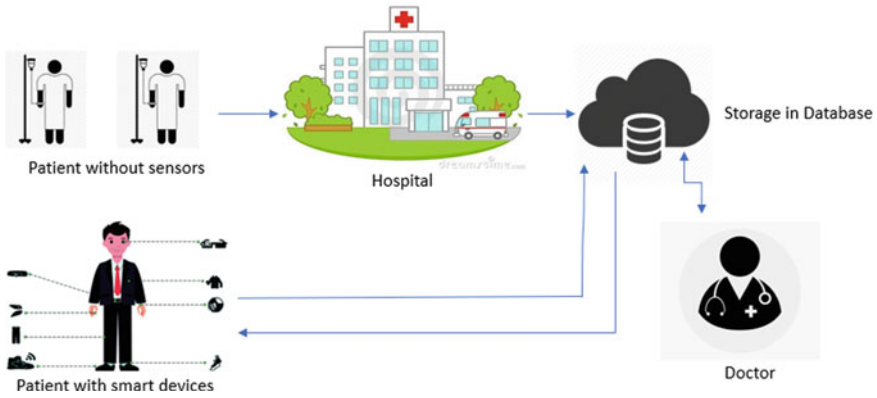


Fig. 1 Patient tracking in two different environments

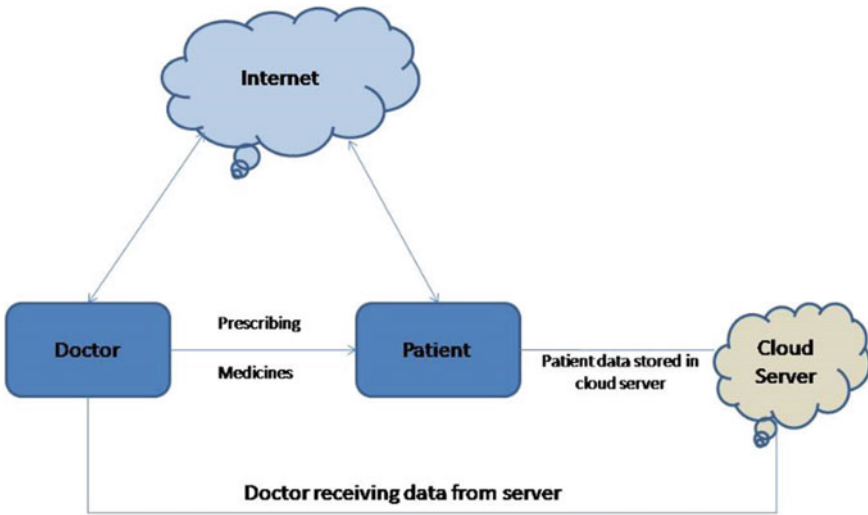


Fig. 2 Medical data storage in a cloud environment

the data at both the ends, i.e., doctor’s end and patient’s end, thirdly, we require authentication among patient and doctor too. Doctor will prescribe medicines to the patient and patient will follow the doctor’s advice. In Fig. 3, it has been depicted that IoT network which will gather the patient data consists of Information Technology (IT), Operational Technology (OT), and smart objects.

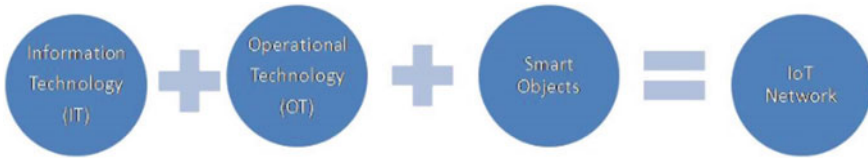


Fig. 3 IoT network

4 Comparative Results

The papers and their work have been compared in this paper which basically involves the proposed authentication schemes and resistance to various security attacks. Though each one has tried overcoming security flaws but was unable to achieve it fully. We also did the analysis of previous work and showed it in Table 1.

Table 1 Analysis of previous work

S. No.	References	Tools used	Attacks resisted	Computation cost
1	Amin et al. [4]	Used AVISPA and Scyther Used hash function and cryptography for security analysis	Focused on patient anonymity and intraceability	$5T_h$
2	Amin et al. [3]	Used BAN Logic for mutual authentication and AVISPA tool for protocol simulation	Resists user anonymity	$22T_h$
3	Ali et al. [5]	Used Oracle Random model and BAN logic to check the security validation	Prevent password guessing attack, user impersonation attack, insider and user anonymity attack	$4T_h$
4	Li [6]	Used IoT-based wireless sensor networks Based on one-way hash function and elliptic curve discrete logarithm problem	Prevent security threats like replay attacks and password data disclosure attacks	$4T_h$
5	Liu [7]	Used wireless sensor technology	Resist impersonation attack, stolen verifier attack	$3T_h$
6	Mohit [8]	Used AVISPA tool and proposed a session key agreement scheme	More secure	$35T_h$

5 Conclusion

We have outlined authentication schemes from various authors designed for a TMIS. We have discussed the weakness of all schemes and found that the schemes presented by various authors are not resistant to attacks like patient anonymity, mobile device stolen, insider, replay and they are not able to secure the mutual authentication [10]. We have then analyzed a new user authentication scheme, which can fix the aforementioned security weaknesses and will be able to provide mutual authentication at patient end as well as doctor's end. In addition, we showed that schemes should be developed which will be more secure as compared to previously existing schemes.

References

1. Zaslavsky AB, Perera C, Georgakopoulos D (2012) Sensing as a service and big data. In: International conference on advances in cloud computing, ACC, 2012, Bangalore, India, July 2012, p 219
2. Malviya DK, Lilhore UK (2018) Int J Trend Sci Res Dev. 3(1). ISSN No: 2456|Nov-Dec 2018
3. Amin R, Kumara N, Biswas GP, Iqbal R, Chang V (2018) A light weight authentication protocol for IoT-enabled devices in distributed cloud computing environment. *Fut Gener Comput Syst* 78:1005–1019
4. Amin R, Hafizul Islam SK, Gope P, Choo K-KR (2018) Anonymity preserving and lightweight multi-medical server authentication protocol for telecare medical information system. *IEEE J Biomed Health Inform*
5. Ali R, Pal AK (2017) Efficient three factor-based authentication scheme in multiserver environment using ECC. Wiley. <https://doi.org/10.1002/dac.3484>
6. Li C-T, Tsu-Yang W, Chen C-L, Lee C-C, Chen C-M (2017) An efficient user authentication and user anonymity scheme with provably security for IoT-based medical care system MDPI. *Sensors* 17:1482. <https://doi.org/10.3390/s17071482>
7. Liu CH, Chung YF (2016) Secure user authentication scheme for wireless healthcare sensor networks. *Comput Electr Eng* 59:250–261
8. Mohit P, Amin R, Karati A, Biswas GP, Khan MK (2017) A standard mutual authentication protocol for cloud computing based health care system. *J Med Syst* 41:50. <https://doi.org/10.1007/s10916-017-0699-2>
9. Quan Z, Chunming T, Xianghan Z, Chunming R (2015) A secure user authentication protocol for sensor network in data capturing. *J Cloud Comput Adv Syst Appl* 4:6. <https://doi.org/10.1186/s13677-015-0030-z>
10. Somasundaram R, Thirugnanam M (2020) Review of security challenges in healthcare internet of things. In: *Wireless networks*. Business Media, LLC, part of Springer Nature 2020

Analysis of Load Balancing Detection Methods Using Hidden Markov Model for Secured Cloud Computing Environment



M. Arvindhan and D. Rajesh Kumar

Abstract Cloud computing is rapidly growing nowadays and stands a creative computing paradigm which provides Internet facilities to meet users' storage needs. Various interconnected technologies exist in Cloud. Each one has some weaknesses which raise many concerns about privacy and security. One among Cloud computing's main security issues is to safeguard against network encroachments affecting the security, availability, and legitimacy of Cloud services and resources provided. Hidden Markov model is a state-based transition model by which the transition of states is been used to estimate using the distributions of probabilities from another state to previous and next another state. This model can also be used here on this paper for both the identification and prevention of intrusion. Except in the cloud setting where security issues and confidentiality are main concerns, identification and prevention of attack is done. Compared to some other current intrusion detection methodology the recommended methodology applied here is successful. This model also increases the real positive rate of intrusion detection systems and reduces the false positive rate.

Keywords Cloud computing · Challenges in cloud computing · Virtual machine · Hidden Markov Model

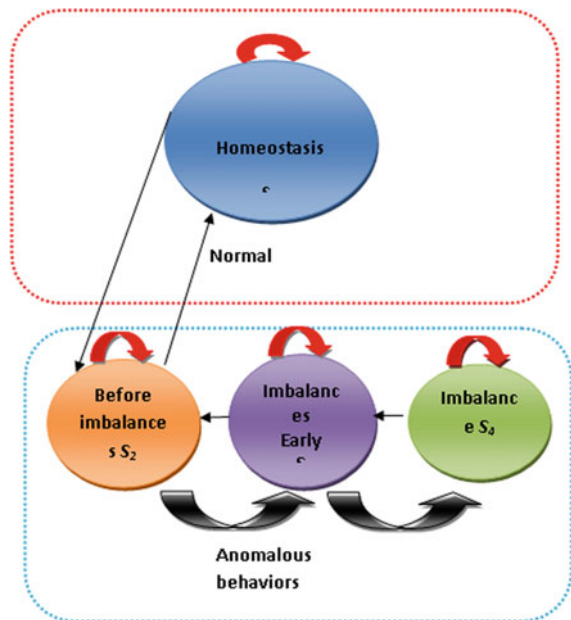
1 Introduction

Cloud computing defines a concept emanates from pay-per-use approach for on demand contact to pooled services. An incessant review of the operational state for the system is necessary which identifies performance deprivations and malfunctioning resources as fast as possible in order to control the resources effectively. Any change in the load, computer state, or software code may change the device status from normal to irregular, which causes deterioration of service efficiency and quality. Such shifts or anomalies range from a basic incremental load raise to flash

M. Arvindhan (✉) · D. Rajesh Kumar
Galgotias University, Greater Noida, India

gatherings, faults in equipment, glitches in software, etc. Such new featured cloud services primarily illustrate the necessitate for intricate and reliable health management systems that reduce the necessitate for human interference [1–3]. A key aim for CSPs is to perceive innovative procedure to leverage resources to maximize resource efficiency and to assure the quality of service (QoS) for clients encounter. Breaching of such Service Level Agreements (SLA) will cost suppliers fines for SLA interruptions or loss of credibility. Conversely, given the complex scenery of cloud systems, hardware condition change, workload, or software could amend the position of the entire system from usual to that can improve performance and QoS. This can be a very imperative statement, particularly in support of wide-scale web application environments wherever the relationship between users and web-servers can amend constantly, disturbing workload patterns and the specifications of resources. For example, web applications are shown to be vulnerable to several of the stability issues that involve CPU and memory capacity. An automated framework for detecting anomalies must be capable to evaluate the performance data obtained from cloud services and create models that can distinguish variance points wherever the device is heading to anomaly state (Fig. 1). During metrics selection, templates building and warnings activating there are still a few obstacles that must always be addressed in the process of gathering measurements, creating models including triggering warnings [4–6].

Fig. 1 Introduction behavioral of anomalous state diagram



1.1 Model Anomaly Scalability

High optimization anomaly detection: An anomaly detection device can also be scaled if this can handle a considerable number of queries. In cloud computing environments such information is very relevant. The main key advantages of cloud-dependent requests become scalability that enables device components to be extent-up to hundreds even maximum of virtual machines (VMs). In this kind of dynamic environment, the distributed procedure to analysis of anomalies becomes an issue particularly if we would like to represent the condition of the entire system in a single form [7–9].

1.2 Significant Decrease of Output Data

A significant amount with monitoring data is obtained through Cloud service. For illustration, Amazon’s Cloud Watch supplies users over 250 monitoring measurements per instance involving CPU usage, disk read bytes with network performance. The huge proportion of performance measures calculated in cloud systems makes the concept of anomaly monitoring highly intricate and can sustain significant transparency for the managed infrastructure. The presence of needless measurements also adds more measuring noise, which will reduce rather than enhance the precision of the analysis.

1.3 Unsupervised Learning

Several current techniques for detecting anomalies depend on labeled data sets for model training. But in actuality cloud computing systems, the labeled data are not always available. The application working within the cloud can sometimes appear to the cloud service administrator as a black box, making it difficult to obtain comprehensive application details or discern typical cloud behaviors and anomalies in progress. Besides, novel phenomena will be viewed as common activities despite not being classified in the data sets of the training [10–12].

1.4 Recurrent Model Tanning Parameters

Because of the heterogeneous existence of cloud web applications, the standard state of the system will modify dramatically, regardless of the number of desires submitted to the system. In such a case, finding phenomena for a typical setting which was previously overlooked is another obstacle we must believe. Almost all

of the current algorithms involve regulation and specification of parameters before upgrading the models. This technique annexes additional transparency to the system specifically for constantly evolving environments. The recommended approach to anomaly detection is simple, requiring no modification based on the workload and any expensive processing of the data [13–15].

1.5 Serial Denial

A serial Denial of Service Attack is one among the most common networks of attacks, whereby one victim machine can obtain far more than the ability and other beginning-user requests could not be supported by the server, and also in the cloud virtual environment, this form of assault dismiss becomes more dangerous than untroubled environment due to neighboring VMs and resource sharing in the cloud technology environment (Fig. 2).

1.6 SYN Flooding

A SN Flood can indeed a DoS attack that would be vulnerable to any TCP / IP application. In every half-open TCP link through to a computer basis the ‘tcpd’ server to attach with a testimony to the information building structure that holds information documenting every correspondence that has been pending. This data structure has infinite in size and can be overflowed with simply creating so many partly open connections. This data structure has half-open connections on the fatality server list will gradually plugin and the device cannot be able to recognize several incoming new connections until the table is filled [16–18].

1.7 Anomaly Detection

Identification of abnormalities: Identification of abnormalities (or behaviours) is disturbed with detecting events which tend to be anomalous as per standard machine behavior. A broad range of techniques together with data mining, mathematical modeling, and hidden Markov models have prospected as dissimilar ways to tackle anomaly identification. The anomaly-based technique entails gathering data corresponding to the actions of lawful customers over several years, and then applying statistical tests to the actions detected, which decide whether or not that performance is lawful. This has the benefit of identifying threats that were not previously discovered. The key component to effectively use this technique is to create rules in

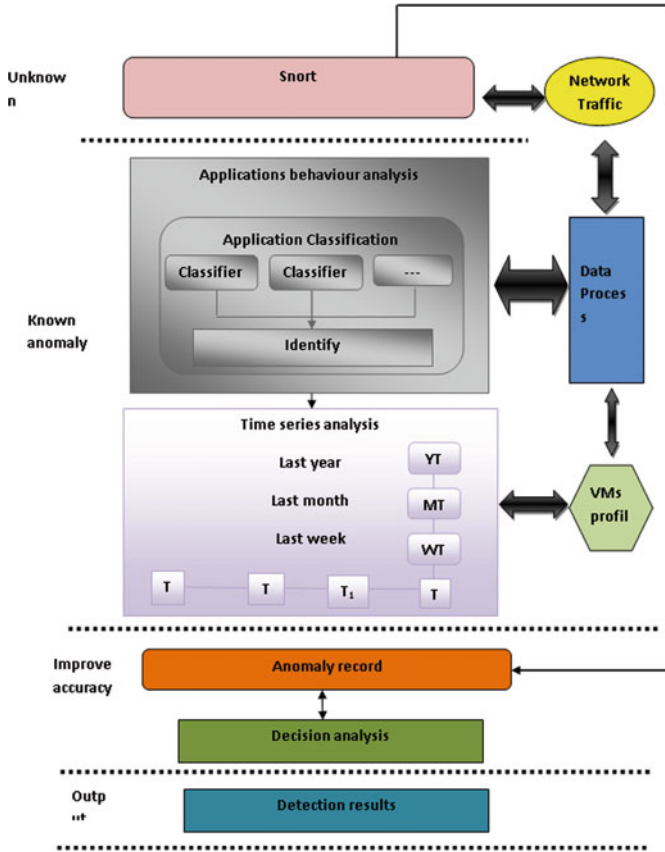


Fig. 2 High level anomaly time series and application behavioral

such a way that it might lower the false positive rate for unidentified and also established attacks given outlier-based elucidation to avoid interruption into the real-time network, that examines procedure-based attack and multidimensional traffic [19, 20].

2 Motivation and Related Work

In general speaking, the great best part of technology facility on anomaly detection, and anomaly-based IDSs, recommend a new intrusion prevention strategy and then contrast it with a limited collection of specific algorithms operating on a distinct dataset. In particular, important examples are cited in this article [21]. This framework is very useful when it comes to introducing a novel algorithm and demonstrating how it works in comparison with any existing one. But the experimental correlation of the

goal algorithm against revolutionary algorithms is mostly inadequate to evidence-of-concept experiments or only some objective datasets. A problem that is frequently left unanswered whether an algorithm is known to be successful in support of a particular deposition or database has a comparable behavior when useful to another-albeit similar-setting, or when measured using a special metric. We assume a thorough review of algorithms will be useful by considering various types of attacks, with target structures (datasets), and scoring metrics. Have been conscious that with reference to ‘silver bullet’ algorithm, or perhaps an algorithm that often plays improved than in others, we believe that a deep comparison between anomaly discovery algorithms for intrusion prevention is important to consider the algorithm (family of) has suggested when production with a definite discussion of attacks and systems [22].

2.1 Algorithm Selection

While our survey operation many unsupervised algorithms of detection of anomalies were found. A few unsupervised algorithms listed in have been preferred that meet the subsequent criterion: algorithms need not implement (semi) a supervised learning strategy that will not be suitable for adaptive systems and zero-day threats. There by we restrict our research to implement with algorithms that are not supervised Fig. 3.

- The set of protocols will cover the key background of unsupervised algorithms for completeness: clustering, angle-based, mathematical, adjacent, density-based, distinction-based.
- Intrusion mitigation algorithms would already have been implemented.

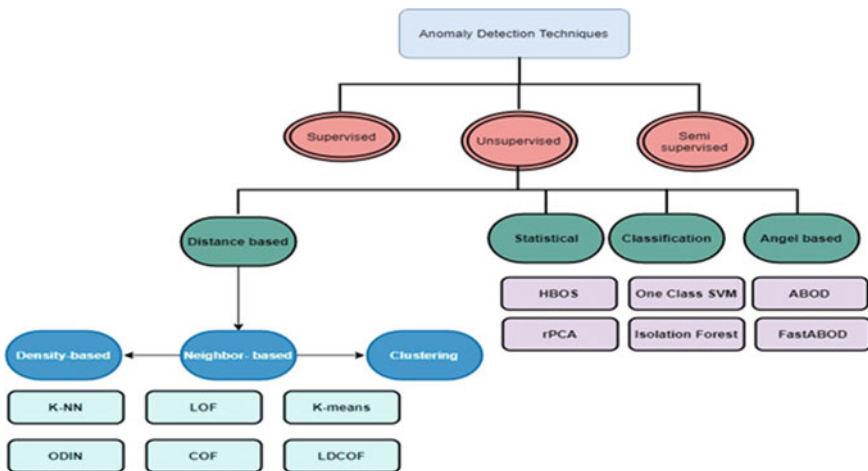


Fig. 3 Classification of anomaly detection algorithms with unsupervised families

3 Materials and Methods

In Clustering K-means Clustering (K-Means) algorithm type is a common clustering variable algorithm which classifies explanatory variables into k clusters through various functionality values. Initially, the k cluster centroids with a configured erratically. Then, every data register is allocated to the nearby centroid cluster, and the changed cluster centroids are certainly-calculated. This phase stops once the centroids no longer alter. Data points are positioned in the same constellation according to a given distance function when they have similar character value. Results of every data point within a cluster are ultimately determined as the range to its centroid. Data arguments distant from the center of their clusters are called anomalous [23, 24].

Local Density Cluster-based Outlier Factor (LDCOF) estimates their cluster concentration induce and uses the clustering algorithm K-means. For each constellation, the ordinary distance to the centroid of all of its data sets is determined, normalized by the standard depth of this cluster’s data points to its centroid, and be used an anomaly score. Hence, predicted a data points contribute to have smaller ratings, i.e. close to 1.0, Table 1 since their densities are as high as their array neighbors’ densities. Alternatively, anomalies will lead to higher scores as their densities are lower than their nodes in the neighborhood ‘high density’.

Accordingly, two key sections of the IFAD system are defined as data planning frameworks for every VM to evaluate the unique characteristics of the time-dependent datasets like inclination/seasonal variation, and the anomaly identification

Table 1 Different specified data sets parallel with size and attack

Dataset	size	Attacks	%	Attacks
KDD Cup 99 (KC)	311,027	223,298	71.79	41
NSL-KDD (NK)	22,542	12,850	47.05	40
ISCX2012 (IX)	571,698	66,813	12	16
ADFA-LD (AL)	2,132,075	243,601	12	2
UNSW-NB15 (UN)	180,114	120,401	67.06	45

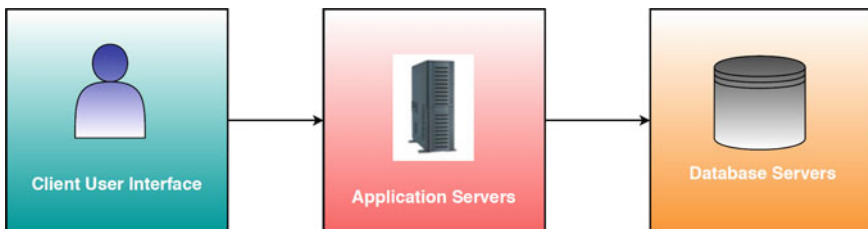


Fig. 4 Sample layers used by clients

modules (Fig. 4). Our model targets three-layer cloud-based applications, a common architecture followed by several web applications [25–28].

- **Presentation Layer:** User interacting interface to access the application layer.
- **Application Layer:** For application layer the main components are representing application/business logic area unit enforced during this layer.
- **Data Layer:** The continued information which will be calculated by the application layer is managed by more than one or a lot of information servers during this layer

The performance efficiency of the application which runs in the server is monitored by the VM device. Through VM periodically tracks its performance data and forward back with the Anomaly Detection system. The per-Virtual Machine monitoring strategy helps with the program to easily segregate the cause of the problem into the target Virtual Machine and concentrate for finding the machine’s fundamental purpose. System-wide solutions which track the correlation coefficients of performance indicators in the structure may overlook this type of issue. We obtain a statics either machine related, such as CPU, free disk, or unique metrics including SQL database, for memory or operation [29–31].

4 Anomaly Detecting and System Design

The HMM working in connection with DAC-Hmm creates two premises. First, the actual condition of virtual size image in the cloud environment depends merely on the preceding condition, which forms into Complex structure in the cloud environment. Secondly, the measurement of the efficiency (i.e. efficiency metrics) at time t depends on the virtual resource which will be hidden on the cloud environment. It needs to be noted that the validity of this statement is incredibly low.

The monitoring information is continuously collected throughout the Cloud activity. The three main performance measurements for anomaly detection are CPU usage, memory access, and input/output (I/O) disk (Table 2). Graphical representation of performance measurements for anomaly detection as follows:

- Use of CPU: Based on the available utility of CPU percentage the CPU is calculated and it’s used in this case. This metric defines the computing power a chosen instance needs to run an application.

Table 2 CPU operation range for workload level

Workload level	CPU operation (%)
Low	5–55
Medium	56–75
High	76–100

- (ii) Memory available: this amount covers all the available memory on the Virtual Machine and it is automatically accessible for applications to utilize. Free memory reflects potential capability for additional instances of applications [32–34].
- (iii) Disk I/O: total number of I/O operations on a disk per second.

$$CTH_x = TH_x * CPER_x \tag{1}$$

S_x is a Three-dimensional vector. It represents observed current state of Virtual Machine.

Where,

‘0’—Normal level.

‘1’—Abnormal level.

If the predefined $CTH_x >$ monitored metric value, the value for metric x for $S(x)$ will be set to 1 or 0.

When the value of a monitored metric exceeds the predefined CTH_x , the corresponding value of metric x in $S(x)$ will be set to 1 (otherwise, 0) (Fig. 5).

At which a control node routinely collects a fixed awaiting interval for the local state information. Given its efficiency, this context-blind quarterly sampling limits the provision of cost-effective state security solutions and can result in significant unnecessary overheads [35–37].

One interesting finding is that the height of the use of performance indicators causing anomalous condition does not arrive in a rapid [38, 39]. Before it attains, the proportions of resource usage rise slowly toward the risky point, and the potential for anomaly rises. A simple simulation scheme to change the sampling distances dynamically dependent on the degree of risk is introduced. If we denote the as the can be defined as follows (Fig. 6):

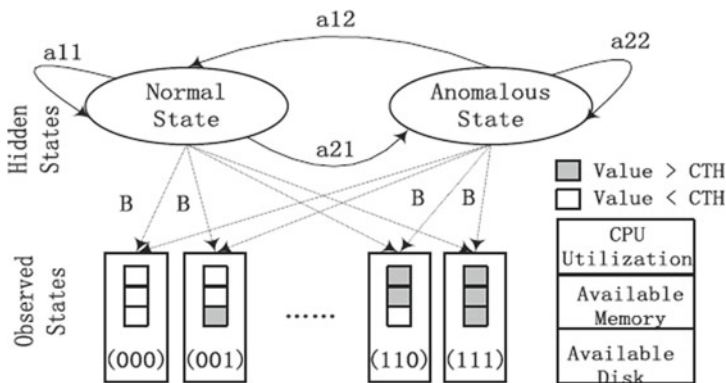


Fig. 5 Anomaly detection for HMM

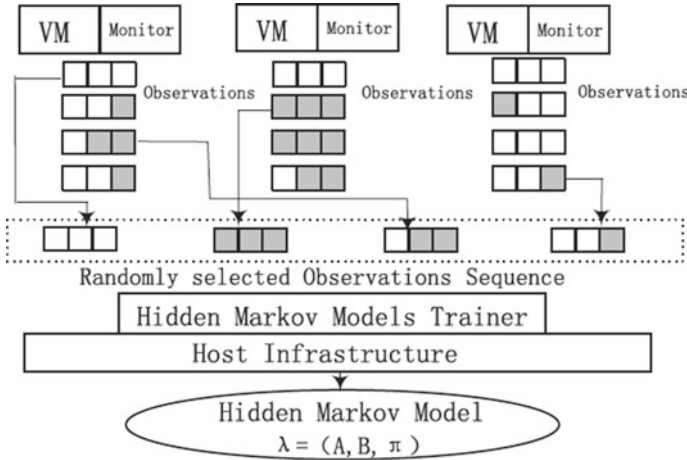


Fig. 6 Training model for testing and updating on HMM

$$R_t = \frac{V_x}{TH_x} * 100\% \tag{2}$$

$$R_t = 100 \times (V_x/TH_x).$$

where,

R_t —level of risk.

TH_x —user-defined threshold for metric x .

$V_x(t)$ —runtime value of metric x at time t .

Anomaly Detecting

Inputs: HMM Parameters $\lambda = (A, B, \pi)$.

Experiential Sequence (from $t - T$ to t).

Outputs: System Anomaly Alert.

Step1: initializing the count = 0 from $CL = 0$.

Step 2: looping statement starts for $t = 1$ to T .

Step 3: Time t starts with algorithm.

Step 4: Second looping if $S_i = \text{Anomaly}$ indicates.

Step 5: increasing the value of count++

Step 6: Finally end if.

Step 7: if $45\% < P(S_i = \text{Anomaly reports}) < 50\%$

Step 8: $cl(i) = 1$.

Step 9: end if.

Step 10: end for.

5 Experimental Results

The initial chance of transition between state one $Q1$ to second state $Q2$ in a given instance of time $t + 1$ varies by the state of time t as per the Markov hypothesis [38–41]

I.e.

$$a_{ij} = p(qt + 1 = Sj|qt = si)$$

The transfer probability of the states is irrespective of the real time when the shift occurs according to the stationary hypothesis.

I.e.

$$p(qt + 1 = sj|qt1 = si) = p(qt2 + 1 = sj|qt2 = si)$$

Observation, probability of state transition can be computed using some algorithm.

1. The probability of general pocket would be computed after each step Q of the transition to be
2. The avg. Probability could be calculated using

$$\delta_{avg} = (\sum k = 1 T \delta k(i)) / T$$

3. The intrusion is detected in the packet when the average probability is less than the threshold value

$$\delta_{avg} < (\text{first threshold value})$$

4. For example, in this value there might be a database source that contains a various values of properties such as source, destination, port, database error rate or time and that certain rules are established based on regression coefficient values but these guidelines are used for intrusion prevention (Table 3). Thus the result analysis of detecting the intrusions for accurate system has been analyzed with various comparison values (Figs. 7, 8 and 9).

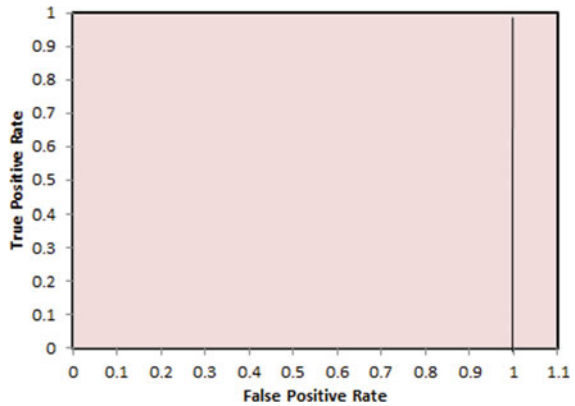
6 Result Analysis

AUC Chart: This chart shows that detection of intrusion by the accurate system.

Table 3 Comparison of proposed method with existing technique

T_P	T_N	F_P	F_N	F_P -Rate	T_P -rate	AUC	Accuracy rate	Threshold rate
0	9	0	92	0	0	0	0.099	27,770.67
0	9	0	94	0	0	0	0.099	27,809.67
0	9	0	95	0	0	0	0.099	27,848.67
0	9	0	96	0	0	0	0.099	27,868.67
0	9	1	93	0.1	0	0	0.099	27,866.67
0	8	2	92	0.2	0	0	0.089	3483.633
0	7	3	92	0.3	0	0	0.078	2005.867
0	5	5	92	0.5	0	0	0.056	1553.33
0	4	6	92	0.6	0	0	0.045	1076.767
0	3	7	92	0.7	0	0	0.033	833.33
0	2	8	91	0.8	0	0	0.025	733.33
0	1	9	91	0.9	0	0	0.015	390
0	0	10	91	1	0	0	0	245.6
90	0	10	0	1	1	0	0.99	0

Fig. 7 AUC chart: this chart shows that detection of intrusion by the accurate system



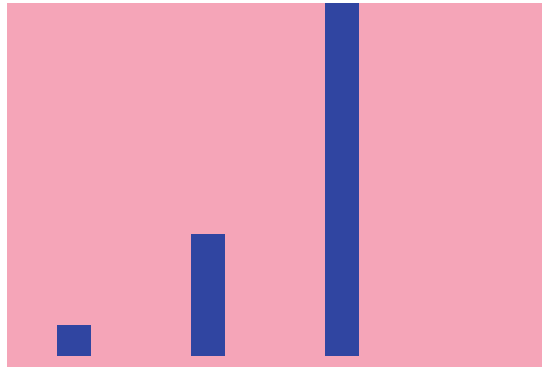
7 Conclusion

The present work suggests that data security are the key problems that need to be tackled, efforts are being made to build more effective solutions which can provide user-level protection and privacy and protect the user’s trust and intellectual property rights. It is planned to develop a protected framework for computation, using a simple Hidden Markov model. Cloud computing model works with the new inclination when it comes to mobile computing, it can support both the endeavor and the consumer by fulfilling the requirements, Thereby company needs to construct definite and reliable methods to secure consumer data. In future, the direction of our work would be to



Fig. 8 AUC chart based on throughput

Fig. 9 Intrusion detection rate



study sample weights and optimizing virtual machine parameters of the algorithm which will be stated. A mixed approach of a deep learning algorithm and genetic algorithms will be reliable to improve the accuracy of the model.

Although the methodology used here to detect and preventing interruption carried out in the cloud environment leveraging Hidden Markov Model is proficient when it comes of discovery and preventing rate as well as cost-effective, other improvements can be made in forms of bandwidth and energy consumption. We can also add a few more methods for detecting interruption attempts and preventing them as shown by device requirement.

References

1. Ismail MN, Aborujilah A, Musa S, Shahzad A (2013) Detecting flooding based DoS attack in cloud computing environment using covariance matrix approach
2. John EK, Thaseen S (2012) Efficient defense system for IP spoofing in networks. *Comput Sci In Technol (CS & IT)*, pp 185–193
3. Wang Q, Wang C, Ren K, Lou W, Li J (2011) Enabling public auditability and data dynamics for storage security in cloud computing. *IEEE Trans Parallel Distrib Syst* 22(5):847–859
4. Khosronejad M, Sharififar E, Torshizi HA, Jalali M (2013) Developing a hybrid method of Hidden Markov Models and C5.0 as a Intrusion Detection System. *Int J Database Theory Appl*. <https://doi.org/10.14257/ijdta.2013.6.5.15>. Corpus ID: 32936020
5. Sultana A, Hamou-Lhadj A, Couture M (2012) An improved Hidden Markov Model for anomaly detection using frequent common patterns. In: 2012 IEEE international conference on communications (ICC). <https://doi.org/10.1109/ICC.2012.6364527>
6. Barsoum A, Hasan A (2012) Enabling dynamic data and indirect mutual trust for cloud computing storage systems. <https://doi.org/10.1109/TPDS.2012.337>. 1045-9219/12/\$31.00 © 2012 IEEE
7. Ali S, Siegel HJ, Maheswaran M, Hensgen D, Ali S (2000) Representing task and machine heterogeneities for heterogeneous computing systems. *Tamkang J Sci Eng* 3(3):195–207
8. Azimzadeh F, Biabani F (2017) Multi-objective job scheduling algorithm in cloud computing based on reliability and time. In: 2017 third international conference on web research (ICWR). IEEE, pp 96–101
9. Luo, L, Li H, Qiu X, Tang Y (2016) A resource optimization algorithm of cloud data center based on correlated model of reliability, performance and energy. In: 2016 IEEE international conference on software quality, reliability and security companion (QRS-C), Vienna, pp 416–417
10. Madni SHH, Shafie ALM, Abdulhamid SM (2017) Optimal resource scheduling for IaaS cloud computing using Cuckoo search algorithm. *Sains Humanika* 9(1–3)
11. Mastelic T, Oleksiak A, Claussen H, Brandic I, Pierson J-M, Vasilakos AV (2015) Cloud computing: survey on energy efficiency. *ACM Comput Surv* 47(2):33
12. Shuja J, Gani A, Shamshirband S, Ahmad RW, Bilal K (2016) Sustainable cloud datacenters: a survey of enabling techniques and technologies. *Renew Sustain Energy Rev* 62:195–214
13. Singh S, Chana I (2016) A survey on resource scheduling in cloud computing: issues and challenges. *J. Grid Comput* 14(2):217–264
14. Youn C-H, Chen M, Dazzi P (2017) Cloud broker and cloudlet for workflow scheduling. KAIST Research Series book series. KAISTRS Springer, pp 2214–2541
15. Zhang S, Chatha KS (2007) Approximation algorithm for the temperature aware scheduling problem. In: Proceedings of international conference on computer aided design, pp 281–288
16. Zhou A, Wang S, Zheng Z, Hsu CH, Lyu MR, Yang F (2016) On cloud service reliability enhancement with optimal resource usage. *IEEE Trans Cloud Comput* 4(4):452–466
17. Zhang Y, Hong B, Zhang M et al (2013) ECAD: cloud anomalies detection from an evolutionary view. *International Conference on Cloud computing and Big Data (CloudCom-asia)*. IEEE, pp 328–334
18. Boutros T, Liang M (2011) Detection and diagnosis of bearing and cutting tool faults using hidden Markov models. *Mech Syst Signal Process* 25(6):2102–2124
19. Lopes Dalmazo B, Vilela JP, Curado M (2013) Predicting traffic in the Cloud: a statistical approach. 2013 Third international conference on cloud and green computing (CGC). IEEE, pp 121–126
20. Tan Y, Nguyen H, Shen Z et al (2012) Prepare: detective performance anomaly prevention for virtualized Cloud systems. In: 2012 IEEE 32nd international conference on distributed computing systems (ICDCS). IEEE, 285–294
21. Koch R, Golling M, Rodosek GD (2014) Behavior based intrusion detection in encrypted environments. *Commun Mag* 52(7):124–131

22. Zhao D, Traore I, Sayed B, Lu W, Saad S, Ghorbani A, Garant D (2013) Botnet detection based on traffic behavior analysis and flow intervals. *Comput Secur* 39:2–16
23. Zheng X, Martin P, Brohman K, Xu LD (2014) CLOUDQUAL: a quality model for cloud services. *IEEE Trans Ind Informat* 10(2):15271536
24. Shi Y, Larson M, Hanjalic A (2014) Collaborative filtering beyond the user-item matrix: a survey of the state of the art and future challenges. *ACM Comput Surv* 47(1):3
25. Xing T, Huang D, Xu L, Chung CJ, Khatkar P (2013) Snortflow: a openflow-based intrusion prevention system in cloud environment. In: *Research and Educational Experiment Workshop (GREE)*, 2013 Second GENI, 2013, pp 89–92
26. Oktay U, Sahingoz OK (2013) Attack types and intrusion detection systems in cloud computing. In: *2013 6th International information security & cryptology conference*, pp 71–76
27. Zhang X, Meng F, Chen P, Xu J (2016) Taskinsight: a fine-grained performance anomaly detection and problem locating system. In: *Proceedings of the 2016 IEEE 9th international conference on cloud computing (CLOUD)*. San Francisco, CA
28. Matsuki T, Matsuoka N (2016) A resource contention analysis framework for diagnosis of application performance anomalies in consolidated cloud environments. In: *Proceedings of the 7th ACM/SPEC on international conference on performance engineering (ICPE)*, Delft, The Netherlands
29. Calheiros RN, Ramamohanarao K, Buyya R, Leckie C, Versteeg S (2017) On the effectiveness of isolation-based anomaly detection in cloud data centers. *Concurrency Computat Pract Exper* 29(18):e4169
30. Tan Y, Nguyen H, Shen Z, Gu X, Venkatramani C, Rajan D (2012) Prepare: predictive performance anomaly prevention for virtualized cloud systems. In: *Proceedings of the 32nd IEEE international conference on distributed computing systems*, Macau, China
31. Cetinski K, Juric MB (2015) AME-WPC: advanced model for efficient workload prediction in the cloud. *J Netw Comput Appl* 55:191–201
32. Ibidunmoye O, Hernández-Rodríguez F, Elmroth E (2015) Performance anomaly detection and bottleneck identification. *ACM Comput Surv* 48(1):4:1–4:35
33. Sharma B, Jayachandran P, Verma A, Das CR (2013) CloudPD: Problem determination and diagnosis in shared dynamic clouds. In: *Proceedings of the 43rd Annual IEEE/IFIP International Conference on Dependable Systems and Networks (DSN'13)*. IEEE, pp 1–12
34. Smith D, Guan Q, Fu S (2010) An anomaly detection framework for autonomic management of compute cloud systems. In: *Proceedings of the IEEE 34th annual computer software and applications conference workshops (COMPSACW'10)*. IEEE, pp 376–381
35. Tan Y, Adviser-Gu XH (2012) Online performance anomaly prediction and prevention for complex distributed systems. North Carolina State University
36. Wang T, Zhang W, Wei J, Zhong H (2012) Workload-aware online anomaly detection in enterprise applications with local outlier factor. In: *Proceedings of the IEEE 36th annual computer software and applications conference (COMPSAC'12)*. IEEE, pp 25–34
37. Kumar DR, Krishna TA, Wahi A (2018) Health monitoring framework for in time recognition of pulmonary embolism using Internet of Things. *J Comput Theor Nanosci* 15(5):1598–1602. <https://doi.org/10.1166/jctn.2018.7347>
38. Krishnasamy L, Dhanaraj RK, Ganesh Gopal D, Reddy Gadekallu T, Aboudaif MK, Abouel Nasr E (2020) A Heuristic angular clustering framework for secured statistical data aggregation in sensor networks. *Sensors* 20(17), 4937. <https://doi.org/10.3390/s20174937>
39. Dhiviya S, Malathy S, Kumar DR (2018) Internet of Things (IoT) elements, trends and applications. *J Comput Theor Nanosci* 15(5):1639–1643. <https://doi.org/10.1166/jctn.2018.7354>
40. Rajesh Kumar D, Shanmugam A (2017) A hyper heuristic localization based cloned node detection technique using GSA based simulated annealing in sensor networks. In: *Cognitive computing for big data systems over IoT*, pp 307–335. Springer International Publishing. https://doi.org/10.1007/978-3-319-70688-7_13
41. Prasanth T, Gunasekaran M, Kumar DR (2018) Big data Applications on Health Care. 2018 4th International conference on computing communication and automation (ICCCA). 2018 4th

International conference on computing communication and automation (ICCCA), Dec 2018.
<https://doi.org/10.1109/cca.2018.8777586>

42. Lin YD, Lu CN, Lai YC, Peng WH, Lin PC (2019) Application classification using packet size distribution and port association. *Journal of Network and Computer Applications* 32(5):1023–1030

Banking Management System—The Web Application Way



Prathmesh Rai, Aryan Singh, Tushar Sharma, and N. M. Sreenarayanan

Abstract In the current times, time is equivalent to money. Nobody wishes to spend their half a day at banks for transactions such as enquiring balance, transferring funds etc. Entire banking system which here is made on java aim's complete resolution to bank related deeds and one may do their crucial bank rituals from the safety of their house. The idea behind the creation of this application is efficient management of client's bank account. We in this project have tried to provide all the basic functionalities of the banks that the user might require. The aim was to provide an application that enables users to perform all the banking chores in a well-built environment. Besides we have also laid emphasis on the security that we give to the clients through our work so that only the legitimate users are able to access their bank account. This project on Banking Management System that has been crafted here has involved in it use of technologies solely based on relevance. The ultimate goal of the work being done here is to create software that allows users to deal with their bank related work with greater ease. It is a common understanding that things that are done manually can be done with much more efficiency if performed by means of some technology.

Keywords Bank management · Digital banking · Service quality · Virtual transactions

1 Introduction

Banks are corporations that accept deposit, pay benefit at descent value, take care of check, allow people to take money and at times intervene in a transaction. There are many other works that a bank does for its users. This project looks into various bank deeds with an aim to ultimately allow the profits made by its user be maximum. These deeds being managing of assets, liabilities, capitals and what is popularly called liquidity benefits [1]. If we backtrack the establishment of banks it turns out that they began to be established in ancient Romanian civilizations. The scalability

P. Rai (✉) · A. Singh · T. Sharma · N. M. Sreenarayanan
School of Computing Science and Engineering, Galgotias University, Greater Noida, Uttar Pradesh, India

© The Author(s), under exclusive license to Springer Nature Singapore Pte Ltd. 2022
B. B. V. L. Deepak et al. (eds.), *Applications of Computational Methods in Manufacturing and Product Design*, Lecture Notes in Mechanical Engineering,
https://doi.org/10.1007/978-981-19-0296-3_54

581

of those ancient banks was much smaller compared to modern day banks that serve much larger audience.

Banks now a days try to follow the rules made by the governing body of the State. The power of the state has a vital role in the bank functioning. Banking Management System now becomes even more important to guarantee that all that the users and the government need is delivered to them in good time [2].

2 Literature Survey

The ICT (Information and communication technology) has led a rigorous competition globally. According to global history many nations are highly immense rise in advanced because of having a clear view of usage of high sum of money in the country's development [3]. There is an involvement of SOA architecture mainly to ensure scalability and reliability of the services hence a detailed study has been carried out to learn the usage of Service Oriented Architecture for convenient implementation there is also a reference taken on the case study of Schavadian and a Swiss bank. These banks have been engaged in the usage of various aspects of Service Oriented Architecture for providing the service for the client. It lends potent of larger organization-based agility (and thus competitiveness). While the second case discusses problems faced during bank transactions [4]. It also discusses how to fix the issue of transaction failure. We read about how Italian companies were big defaulters to banks who had big losses in the past. It has been seen that due to lack of proper legal enforcement into these banks such losses are witnessed. Improper enforcement hence may bring about a system-based problem in handling transaction it may motivate bank clients to default large sum after their relationship with the bank becomes questionable. When someone talks about banks the prime concern happens to be security only then will someone bother to invest [5]. We in work have emphasized on customer security more than anything else whereby client will be asked multiple security questions for the sake of their protection. Existing System: Talking of the current system every transaction is carried out in hand. It is a tiring procedure and involves plenty of paper work. Besides, threat control is a major issue as well [6].

3 Proposed Method

Banking software system allows its clients to reach their account and other info about bank's services from the comfort of their computer. This targets to secure bank systems that will be accessible to any authenticated user with valid user id and password. Through this software, client can use their account from any location.

Modules

- Login Module

- Open Account
- Balance Enquiry
- Account History
- Admin Module
- Loan Module
- Money Transfer.

Module Description

1. Login Module

This module is coded to generate the interface that allows clients to login into their respective bank accounts with their credentials.

2. Open account

Open account module deals with new users for account creation purposes they will be needed to fill-out a form online at the end of which they get their credentials to verify themselves.

3. Balance Enquiry

As the name suggests this module allows users to enquire their balance.

4. Account History

This module allows users to check their account history. These include information of the account, last few transactions carried out etc. The module will easily handle relatively small transactions such as small withdrawals etc.

5. Admin Module

This module dedicated to the admin as he will have complete control over all activities happening inside the bank.

6. Loan Module

Client can use this module to opt loans from the bank. Various loans offered by the bank like education, home, personal loans etc. are included. The user need to provide required documents for getting the loan from the bank. This module further helps them to know whether they are credible as per the bank norms for getting loans.

7. Money Transfer

Indicative of its name this module is referenced by the clients when they want to transfer money from one account to the other.

Software Requirements

Operating System:	Windows XP or higher or Linux or MAC
Server:	Tomcat 5.1

User Interface: HTML, APPLET
Database: Oracle
Programming Language: JAVA.

Hardware Requirements

RAM: 256 MB or more
Processor: Pentium IV or higher
Hard disk: Minimum 10 GB.

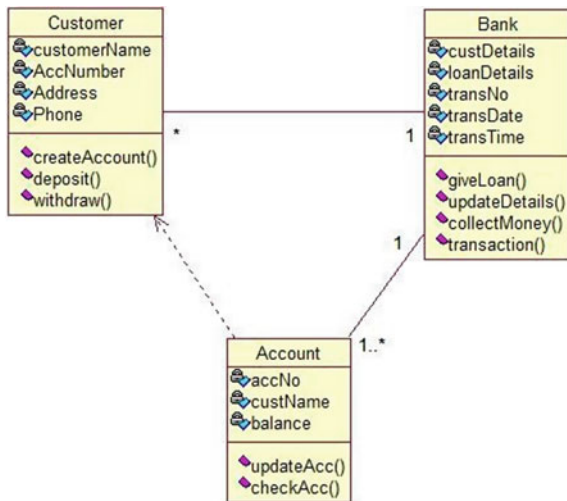
4 UML Diagrams

Class Diagram

Figure 1: The above is a class diagram for banking management system. It shows 3 classes basically the customer class that describes the characteristics of the bank clients, account class that describes the attributes of a typical bank account and the bank class that shows various functionalities that users can retrieve

Talking of softwares, a **class diagram** is a type of UML or the Unified Modelling Language diagram is one of the static structures which is used to describe the build of the system by involving use of system classes, operations and functions, and finally relationship between object(s) [7]. These diagrams are one of the main build-ups of object-based models. The main use is general concept-based model creation for the app, besides it is needed to write programs that represent various model(s). This diagram may help to model data as well. Class here shows communication between modules of the app and modules that will be coded [8].

Fig. 1 Bank management class diagram



In these structures, class is shown in a box which has 3 parts in it:

First part shows the class name. The name is written in bold font with opening letter in caps.

The mid part shows attribute related to class. Alignment is set as left and opening letter is small.

The last part has the operation that class will run. Alignment set is left and opening letter is small.

Use Case Diagram

Figure 2 illustrates the use case diagram wherein customer, manager, loan officer and clerk are 4 use cases which point toward their respective modules with which they interact for example the clerk has the responsibility to clear cheques and open bank account and likewise explanation for others [9].

In use-case-diagram we try to highlight software needs for a software that is in the development phase. The case here implies to response to be expected it does not focus on how it will be achieved. These schematic pictures can be either presented in the form of text or visuals. One of the features of these structures is that they allow one to think from the client perspective. It turns out that these diagrammatic representations are very productive to visualize software from client’s view [10].

Use-Case-Diagrams are simplistic. They do not reveal insights of their cases:

- They highlight certain relations among use-case-actor and the software.
- The procedure followed to achieve the needs of each use case remains hidden.

Fig. 2 Use case diagram for bank system

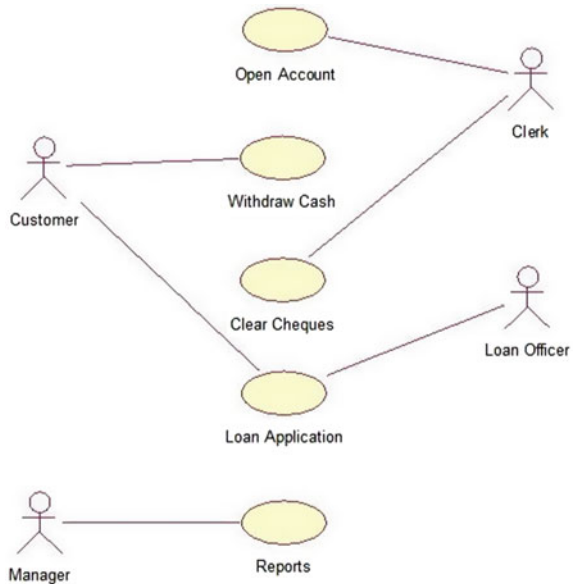
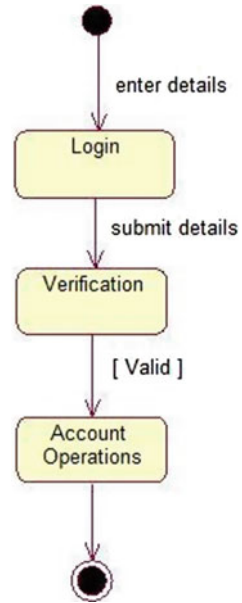


Fig. 3 State chart diagram for Bank system



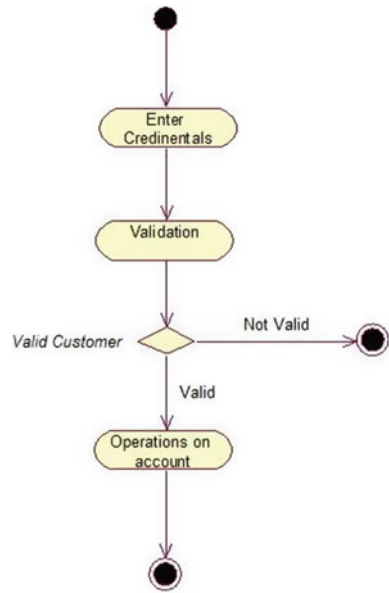
- Use case diagrams must be simplistic. More than a certain number of use cases and the structure must be re-evaluated.

State Chart Diagram

Figure 3 represents how the software system authenticates the user once they provide valid credentials they finally are able to perform the account operations.

The purpose and other necessary usage about the diagram is indicative of its name. The different states of a software system are described here. It should be clear that 'state' corresponds to a particular component of the system [11]. It is equivalent to a state automaton. It is defined as a machine which defines different states of an object and speaking precisely the 'state' of a component here is controlled by both inner as well as outer happenings. Statechart diagram is one of the five UML diagrams used to model the dynamic nature of a system. They define different states of an object during its lifetime and these states are changed by events. Statechart diagrams are useful to model the reactive systems. Reactive systems can be defined as a system that responds to external or internal events. Statechart diagram describes the flow of control from one state to another state. States are defined as a condition in which an object exists and it changes when some event is triggered [12]. The most important purpose of Statechart diagram is to model lifetime of an object from creation to termination. Statechart diagrams are also used for forward and reverse engineering of a system. However, the main purpose is to model the reactive system.

Fig. 4 Activity diagram for bank system



Activity Diagram

Figure 4 illustrates how the user is verified by the software system if a valid user tries to access his account he ends up landing in a state where he can perform bank chores otherwise enters in a state where is restricted from performing bank chores.

Demonstration of flow control in a software is done using what is called an Activity Diagram. One models both stepwise as well as simultaneous flowing activities using these diagrams [13]. It may even be attributed as graphic representation of the workflow. The main concentration is put upon how conditional statements monitor flow control by means of these UML structures. The reason for the happening of an event is shown using Activity Diagrams. UML diagrams are concerned at depicting three types of diagrams structures, interactions and behaviors. Activity diagrams are concerned at showing behaviors [14]. From the start till the end entire control flow is showcased, all the paths were decisions taken through the activity are also highlighted. As mentioned earlier both simultaneous as well as one at a time processes can be showcased. Activity diagrams show the dynamic behaviors of business models for which they are primarily used [15].

ER Diagram

Figure 5 is a System ER Diagram shows the various entity sets and relationships between them and also the attributes of various entities involved in the banking management system.

ER diagrams show relations between entity sets. By definition entity sets are basically collection of entities and they have characteristic values called attributes [16]. DBMS defines an entity as a real-world object that is distinguishable from

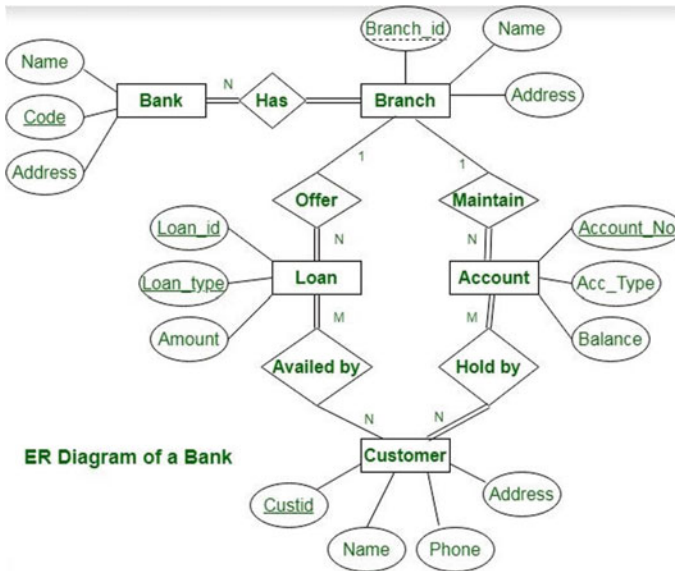


Fig. 5 System ER Diagram for Bank system

other objects of similar kind, so ER diagram focuses mainly on showing relationship between various entity sets, thereby representing the database at the logical level [17].

5 Conclusion

The vision behind the creation of this project is to look after the requirements of the clients pertaining to bank related chores. This domain looks a promising prospect toward great futuristic development. Other than cheque write-ups and deposits which would appear anyone as a conventional way of moving money in and out of an active bank account, most recent advancement now allows usage of ATMs and debit cards for either withdrawing or depositing money. There are rules now in existence that define after what time intervals can one access their deposits, the count of debit card and ATM card withdrawals that one can make in 24 h time. There is also a feature that now allows the organizations to cease the access over accounts by individuals for unforeseen circumstances. Various internet-based facilities are provided by banks to draw customers' attention. A detailed study has revealed that much of the internet account holders are youngsters and self-employed people. This innovation of online banking system is becoming compulsorily important with every passing day. Such an online system is a boon for banks to make reasonable profits in the market of growing competition. Banks should strive at further making their

websites easier to use by many other users so they may benefit with the power of this technology. Hence the project of Bank Management System has been completed successfully.

6 Future Works

The project on Banking Management System is a very valuable idea. We are privileged enough to get a chance to work in this area. The thing that should not be forgotten is that this project has undergone hours of painstaking work. On the grounds of the research, successful creation of an online portal has been possible. If one wishes to look at the futuristic goals of an online banking system, we must look at the current system at first. An online bank would make one think of having a computer setup a long process involving authentication of users which finally opens the door for them to access their accounts and perform operations of their wish and will. The most valuable future looks are following below:

- As the time passes by and bank becomes international more and more ATM machines will be put up and it will also need a regulation in the online system so that scalability can be increased.
- Proper online help desks need to be setup so that customer issues can be dealt with ease and in a way such that customer queries get resolved and he ends up with a positive impression of the online bank.

Creating a handset compatible application which helps facilitate clients with bank chores so that need not traverse the bank all they need to do is sign up in the mobile app only once and then login every time with his unique username and password once done with this the entire facilities provided by the bank are accessible to him at one click.

References

1. Baldonado M, Chang C-CK, Gravano L, Paepcke A (1997) The Stanford digital library metadata architecture. *Int J Digit Libr* 1:108–121
2. Communication Management in Electronic Banking (2014) Better communication for better relationship. In: *Procedia—social and behavioral sciences* [online], vol 124, pp 361–370. Available at: <https://www.sciencedirect.com/science/article/pii/S187704281402045X>
3. Emerald Insight (2013) A case study on knowledge management implementation in the banking sector | Emerald Insight. VINE [online]. Available at: <https://www.emerald.com/insight/content/>; <https://doi.org/10.1108/03055720610683013/full/html>
4. Altinok D (2018) An ontology-based dialogue management system for banking and finance dialogue systems [online]. arXiv.org. Available at: <https://arxiv.org/abs/1804.04838>
5. Samuel O, Mokaya, Kipyegon M (2014) Determinants of employee engagement in the Banking Industry in Kenya; Case of Cooperative Bank [online], vol 2, no 2, pp2333–6404. Available at: http://jhrmls.com/journals/jhrmls/Vol_2_No_2_June_2014/12.pdf

6. Raut R, Cheikhrouhou N, Kharat M (2017) Sustainability in The Banking Industry: a strategic multi-criterion analysis. *Bus Strat Environ* [online] 26(4):550–568. Available at: <https://online.library.wiley.com>; <https://doi.org/10.1002/bse.1946>
7. Fedyshyn MF, Abramova AS, Zhavoronok AV, Marych MG (2019) Management of competitiveness of the banking services. *Finan Credit Act Probl Theor Pract* [online] 1(28):64–74. Available at: <http://fkd.org.ua/article/view/163340>
8. Biswas M (2011) Sustainable green banking approach: the need of the hour [online], vol 1. Available at: http://admin.iaasouthbengalbranch.org/journal/1_Article5.pdf
9. Fama EF (1980) Banking in the theory of finance. *J Monetary Econ* [online] 6(1):39–57. Available at: <https://www.sciencedirect.com/science/article/abs/pii/0304393280900173>
10. Emerald Insight (2013) Corporate social responsibility in Nigerian banking system | Emerald Insight. *Soc Bus Rev* [online]. Available at: <https://www.emerald.com/insight/content>; <https://doi.org/10.1108/17465680810852748/full/html>
11. Hackethal A (2021) German banks and banking structure. *Econstor.eu* [online]. Available at: <https://www.econstor.eu/handle/10419/76961>
12. Luarn P, Lin H-H (2005) Toward an understanding of the behavioral intention to use mobile banking. *Comput Hum Behav* [online] 21(6):873–891. Available at: <https://www.sciencedirect.com/science/article/abs/pii/S0747563204000470>
13. Hamidi H, Safareeyeh M (2019). A model to analyze the effect of mobile banking adoption on customer interaction and satisfaction: a case study of m-banking in Iran. *Telematics Inform* [online] 38:166–181. Available at: <https://www.sciencedirect.com/science/article/abs/pii/S0736585318306464>
14. Kamath KV, Kohli SS, Shenoy PS, Kumar R, Nayak RM, Kuppuswamy PT, Ravichandran N (2003) Indian Banking Sector: challenges and opportunities. *Vikalpa: J Decis Makers* [online] 28(3):83–100. Available at: <https://journals.sagepub.com>; <https://doi.org/10.1177/0256090920030308>
15. Shandy Utama A (2019) History and development of Islamic Banking Regulations in the National Legal System of Indonesia. *AL-'ADALAH* [online] 15(1):37. Available at: <http://103.88.229.8/index.php/adalah/article/view/2446>
16. Emerald Insight (2013) Consumer attitudes, system's characteristics and internet banking adoption in Malaysia | Emerald Insight. *Management Research News* [online]. Available at: <https://www.emerald.com/insight/content>; <https://doi.org/10.1108/01409170610645411/full/html>
17. The Performance, Banking risks and their regulation. *Procedia Econ Financ* [online]. 20:35–43. Available at: <https://www.sciencedirect.com/science/article/pii/S2212567115000441>

A Novel of Survey: In Healthcare System for Wireless Body-Area Network



C. Rameshkumar and T. Ganeshkumar

Abstract WBAN is a type of wireless sensor network designed for the human body to be wearable or implanted. A modern invention targeted at medical care is the WBAN. WBAN has taken excellent care of health, medical, entertainment, and various apps. The fundamental outline behind WBAN innovation is to place them around sensor nodes located inside the patient's body or around the patient's body within the medical system. It does not just offer more comfort to patients, but the patient may monitor the health care staff remotely. It is very helpful for the elderly or people with disabilities to obtain or have emergency medical equipment. In recent years, WBAN has been an enormous field for researchers. In this paper, we discussed a number of WBAN approaches presented and further opportunities for exploration in this field. The literature study shows that current systems are also updated further to provide WBAN systems with more reliable solutions.

Keywords Wireless body-area network · WSN · Security · Privacy · Threats · Attacks · Healthcare systems · Healthcare applications

1 Introduction

As the world's population is rapidly expanding the cost of health care, the health of patients must be monitored either inside or outside the hospital. In mobile electronics, wireless communication, portable batteries, and sensors, the advancement of research and technology has led to the progress of the wireless body-area networks (WBANs). The WBAN is an automated control network that can independently connect and interact between various medical devices and sensors within or external to the human body. In addition to reducing costs and flexibility, WBAN applications have incredible advantages in medical care, for example, tolerant versatility as compact screens and sensors, and WBAN utilizes area apparatuses that do not have

C. Rameshkumar (✉) · T. Ganeshkumar
School of Computing Science and Engineering, Galgotias University, Greater Noida, Uttar Pradesh, India
e-mail: c.ramesh@galgotiasuniversity.edu.in

present day electronic WBAN can likewise associate with the Internet and information move it to a distant data set or worker and stretch out the WBAN application to military and sports instruction territories also since the fighter or contender [1].

Noticed a critical expansion in the quantity of registering items utilized by people, work stations, PCs, tablets, cell phones, and an individual regularly utilizes extra items laying on a typical premise. Different items are planted in people to control the body's different capacities and conditions and the climate [2]. WBAN is an applied strategy to distantly screen patients and gather related data from inserted sensors. It includes a little distant framework that contains a couple of little contraptions, for example, sensor center points and actuators. The sensors are put clearly on the body or under the skin of a man to figure persuaded boundaries regarding the body, for instance, an electrocardiogram (ECG), electroencephalogram (EEG), development of internal heat level, circulatory strain, glucose, Plasmon biosensor, pulse, respiratory rates [3]. These sensors are planned implied for explicit purposes to get together end-client prerequisites. For instance, an EEG sensor was intended to screen cerebrum electrical movement. One more occurrence is the ECG sensor intended to screen cardiovascular capacity. IEEE 802.15.6 proposes a scientific categorization for WBAN hubs, contingent upon how it is applied to the body with their duty in the framework [4]. In view of the hubs it is conceivable to group how they are applied to the accompanying:

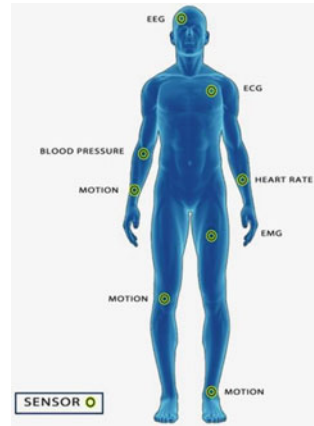
- Implant hub: This sort of hub is fixed inside the skin or body tissue.
- The surface of the body: To be found on the outside of 2 cm as of the human body.
- External hub: Does not touch the individual's body alongside a couple of centimeters from the human body up to 5 m.

There are three kinds of nodes in a WBAN that match their network roles. Coordinator: This node works because it is opposite the WBAN, confidence, or access coordinator, a gateway to the call. A WBAN coordinator where all other nodes may interact could be the PDA. Recent Notes: This type of host is limited to running the built-in program, but cannot forward messages to other hosts. Relays: Such nodes are intermediate relay nodes. The contact node is made up of message-transmitting parent and child nodes. If a node is on foot, all information sent must be transmitted by each node before it can enter the PDA. Moreover, data from other nodes is experienced by these nodes.

By following the prescribed instructions, the operators act upon the sensor information. The shoot is designed with a built-in tank and to measure glucose levels, it uses sufficient hypoglycemic doses. Diabetics, for starters. Figure 1 demonstrates the situation with sensors through WBAN [5]. In many other fields and services, it is also used, such as environmental monitoring, physiological and medical monitoring, interaction between people and machines, education, and entertainment.

The Smartphone has far off admittance to data that detects sensors or computerized individual aide (PDA) among doctor and patient, medical attendants, drug stores who settle on reasonable choices and activities dependent on data from sensors acquired from them [7]. These basic arrangements and well-being data ought to be ensured against unapproved access, which might be risky to the patient's life and now and

Fig. 1 WBAN sensors [4]



then lead to death [8], for example, adjust the portion of the medication or treatment systems when it falls into hands [9] thus adaptable and hearty security components are required and incorporate safe driving gatherings, protection, privacy, honesty, permitting, and validation. Remote application for well-being administrations and numerous advantages and difficulties for medical services.

These advantages give an agreeable climate that can screen the patient’s everyday life and clinical status whenever, anyplace and without constraint [10, 11]. On the other offer, one of the predominantly huge difficulties confronting new advances is well-being and security in the well-being area, which makes the privacy of patients more defenseless [12, 13]. The physiological essential indications of the patient are exceptionally touchy, particularly when the patient is upset from horrendous disease. A particularly patient may be mortified with the smallest or even a mental issue if the sickness or low quality (QoS) data was unintentionally revealed. Now and again, data on the infection may prompt occupation deficiencies. Once in a while, data makes it outlandish for a patient to implement security. Medical sensors see the state of the body of the patient and send communications while delivering these messages to the specialist or the clinic worker and sensors may be beaten. For example, alongside changing the results, an opponent can collect information from remote channels [14, 15]. He should promote the knowledge to the committed or the worker that is being undermined. This can jeopardize the lives of patients. Given the weakness of patient protection, because of the use of creativity in the medical care framework [16], well-being should be paramount when flashy snares are used.

Exceedingly significant patient data is put away, utilized and sharpened, yet it very well may be, particularly for individuals with socially unsatisfactory diseases. The disappointment of well-being data for this kind of patient may prompt embarrassment, bungle, and association issues or even work misfortune [14, 15]. Well-being data, which is viewed as negative, may likewise hold up via the person’s ability to get health care coverage inclusion. It is hence essential to guarantee that the safety and classification of these data are safely put away and communicated.

The remainder of the text is arranged as follows. The WBAN architecture is depicted in Segment 2. Area 3 presents the security of WBAN as well as security specifications and security hazards of WBAN. Area 4 presents the latest initiatives in terms of protection. WBAN follows evaluations of protection and information assurance and then follows the dialogue in Chap. 5. In Chap. 6, the primary investigations and possible exploration zones can be found. The end is indicated in the section.

2 WBAN Architecture

In order to comprehend the kind of security system that can be utilized in WBAN, we should initially comprehend the construction of correspondence inside each organization and their correspondence with the rest of the world and other WBANs. Consequently, the widespread underlying model of the WBAN network has three levels: Intra-WBAN, Inter-WBAN, and Out-WBAN (Fig. 2).

Level 1: Level 1 WBAN communication demonstrates network interaction between nodes and the corresponding transmission ranges (2 m) in and around the human body. WBAN communication between WBAN and WBAN and multiple levels. Tier-1 uses various sensors to transmit body signals to the Tier-1 personal server (PS). The processed physiological data are then transmitted to a Tier-2 access point [2].

Level 2: Inter-WBAN communication at this level is between PS and one or more access points. APs can be regarded as part of the infrastructure or are strategically located in a dynamic environment for emergency management.

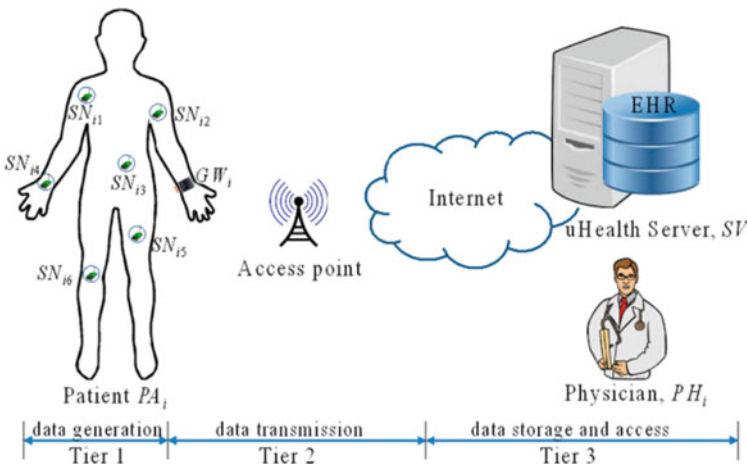


Fig. 2 WBAN-based healthcare monitoring architecture

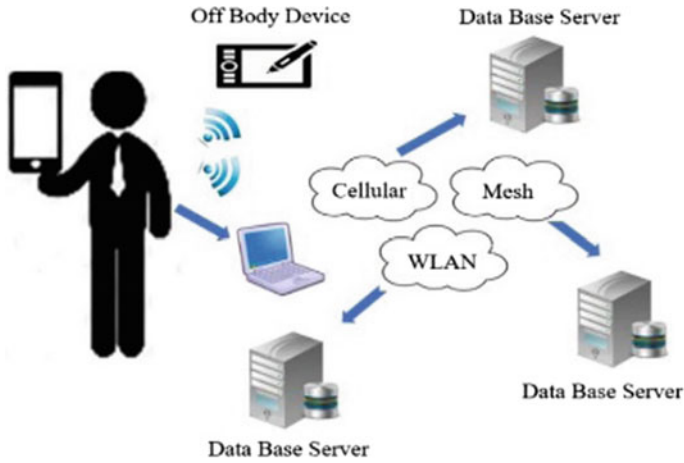


Fig. 3 Inter-WBAN communication: infrastructure-based architecture

Level 3 communications are to connect WBAN to the various networks that are easy to access in everyday life and in mobile networks and the Internet. The more technology that WBAN supports, the easier it is to integrate into applications. WBAN communication paradigms are divided into two subcategories [14, 15].

2.1 Infrastructure-Based Architecture

Most of WBAN applications, as it facilitates active operation in a partial area, such as a hospital, and provides centralized managing along with security controls. AP can operate as a database server associated with its application as shown in Fig. 3 [8].

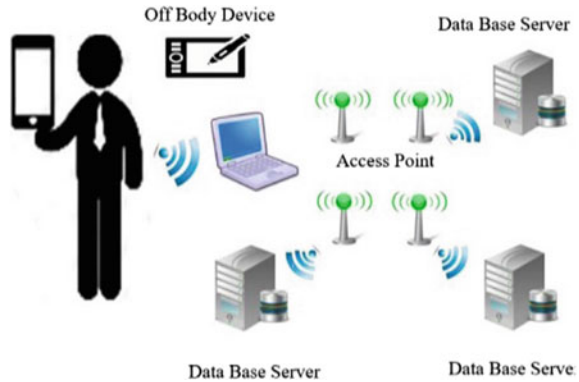
2.2 Ad-Hoc-Based Architecture

In this architecture, more APs transmit information to medical centers as shown. APIs in this architecture create a network structure that enables flexible and fast deployment, enabling easier network expansion, providing multiple wireless coverage thanks to multi-hop distribution and facilitating patient mobility as shown in Fig. 4.

The configuration of this configuration is much larger than the infrastructure-based architecture, and thus facilitates traffic around larger areas. In fact, this relationship extends the WBAN range from 2 to 100 m, which is both short and long-term [6].

Level 3: Beyond-WBAN correspondence: The correspondence layer can be utilized in metropolitan regions. The port can be utilized as a PDA to defeat the connection

Fig. 4 Inter-WBAN communication: ad hoc-based architecture



between Tier-2 and Layout; fundamentally from the Internet to the clinical worker (MS) in an application. Be that as it may, the Tier-3 correspondence arrangement is application-explicit. Basically, in a medical care climate, the data set is one of the most part focal segments of Tier-3, as it incorporates a clinical history and client profile. Thusly, the well-being place in any case patients can be educated regarding a crisis circumstance by means of the web or through short instant messages (SMS). Likewise, Tier-3 permits the recuperation of all important patient data for treatment. Contingent upon the application, be that as it may, PS can utilize the GPRS/3G/4G card in the Tier-1 rather than the AP [9].

3 WBAN Applications

The ability to install a limited number of wireless antenna nodes during the human body suggests that many applications can be applied in many areas as shown in Table 1.

3.1 Health

At first glance, this is generally a talented area of application for WBAN. Many pointless sensors in or on the human body allow patients and physicians to continuously transmit biopsy signals over a long and long period of time. Rapid events such as heart attacks and epileptic seizures can be detected and predicted by constant monitoring of heart and brain activity [17]. The use of WBAN is commonly used to expand health care systems to better treat and detect disease and respond to crises, not just recovery [18].

Table 1 WBAN application

WBAN application	Medical	Wearable WBAN	Assessing soldier fatigue and battle readiness
			Aiding professional and amature Sport training
			Sleep staging
			Asthma
			Wearable health monitoring
		Implant WBAN	Cardiovascular diseases
			Cancer detection
		Remote Control of Medical Devices	Ambient assisted living
			Patient monitoring
			Telemedicine systems
Non-medical	Real-time streaming		
	Entertainment application		
	Emergency (non-medical)		

3.2 Sports and Entertainment

Real-time parameters, same as blood pressure, heart rate; asymmetry and posture of the blood can improve shape and sport. This allows users to gather information about their sports and use them to prevent injuries and plan future workouts to improve their performance. WBAN better understands the entertainment experience of users. Motion recording techniques allow the position of different parts of the body to be tracked through a gyroscope and accelerometer that are wirelessly connected to a central node and carried by the user. Real-time traffic information allows the user to use their body as a video game controller. In addition, film making creates realistic digital films in which actors play non-human themes through motion capture and post-production.

3.3 Military and Defenses

Network Activation Capability (NEC) is the name of a long-term program designed to achieve the enhanced impact of hostilities through information systems. The capabilities added by WBAN improve the performance of soldiers involved in military operations, at the individual and group levels. On a personal level, a set of sensors can monitor basic parameters and provide environmental information to avoid hazards and team level information allows the commander to improve organize the actions

and tasks of the team. Different WBAN (WBAN Communication) spatial localization and communication techniques [18].

3.4 *WBAN for Animals*

Wireless banking systems are very useful tools. It's able to be used designed for the health and diagnosis of both human and animal infectious diseases. It is very important that if we want to improve human health and control the disease, we must first improve animal health and monitor human illnesses, milk, meetings, eggs, etc. One of the major important motives of this motif is that man and animals are mutually dependent. There is a symbiotic relationship [19].

4 Literature Review

Khalilian et al. [20], Effective Method for Improving Security in WBAN. This article introduces another strategy that increases security issues with WBAN. The purpose of this article is to reduce the required multilateral control package memory to control the superstructure and control the current damage through high-speed information exchange nodes. This article improves security, AES-256 plan.

Tiwari et al. [21]. Security and Data Protection, Control Health and WBAN are largely keyed to people who are suffering from diseases such as heart disease, rational violence patients, pregnant women, etc. This requires continuous detection are related to these tasks, require greater security. So this book presents security and safety issues.

Sahnadu et al. [22], BEC: Modern Balanced Powerless Networks Routing Protocol. From the point of view of their participation in a range of health checks along with non-medical applications, wireless body-area networks (WBANs) are expanding. These WBAN applications remain utilitarian, requiring vitality for a longer period of time. We propose another WBAN BEC (Balanced Power Consumption Management) agreement in this paper. Within the glow of cost capacity, polling stations are chosen in BEC, centers may send their information to their nearest node to hit the sink. The data can be expressly given by nodes nearer to the sink. Furthermore, if the life force is not an accurately specified cap, the centers just submit basic details. As the ultimate aim is a more even distribution of stacks, each turn is turned by distribution centers, taking the cost of capacity keenly on the version. Reenactment reveals that BEC has achieved a lifetime percent longer than the OINL estimate (to increase network lifecycle).

Ha et al. [23], "Technology and Scientific Trends in Wireless Personal Network Health: Systematic Literary Overview" This article demonstrates that WBAN has environmental features that are not the same as existing WSNs. Existing WSNs related to developments have not associated WBAN on the basis that remote sensors

BAN may refer to the dissimilar parts of the person's body and have a completely different system environment as opposed to current remote sensing systems.

Lee et al. [24] is a two-channel printed metal aerial for WBAN applications that work in 2.5 and 5.8 GHz industrial, scientific, and health (ISM) groups. Analyze the performance of the proposed antenna test on a physical body-loving disc.

Thamilarasu et al. [25] proposed an independent mobile negotiator based on base-based intrusion detection plan for wireless network security. This paper recognizes WBAN penetration through mobile agent migration and collaboration performance. Some nodes in WBAN behave like a computation node. In this article, a multi-mobile penetration discovery scheme has been developed, so learning and solution solutions are distributed over completely different nodes on the network.

Froehle et al. [26]. It provides a WBAN analysis plan for an area that secures the future exploration space craft in exploration, having good health, and technology. In the cosmic bomb health monitoring system, the Bluetooth component along with sensors must be applied to the under-pressure interior to gain an effective live signal and protect the tools from the worst environment and connect the antenna to Bluetooth. In the simulation, the Perfect Electric Controller (PEC) was used, as the plane of the ground, which improves the transmitter productivity with an air gap, has the disadvantage of pressure to reduce this gap.

Kim et al. [27]. Kim has presented a multi-component WBAN design theme with 3 actions: (1) setting topologies in clusters, (2) mobility support, and (3) improving transfer efficiency. Existing circuits work on a 1-inch star network, which is only useful for short-wave networks on the backside.

He et al. [28], the body model of the body topology was mostly based resting on the spatial distribution of medical sensors. This model was used by two AODV and DSDV Adhoc routing protocols. Both AODV protocols are more suitable for transferring knowledge in the form of installation.

An algorithmic synchronization rule without time is suggested by Ramlall et al. [29]. In this algorithm, after messages are transmitted to the central communication node, sensors can adjust. The central communication node knows that the time node compensation of the sensor often needs time accuracy, and the central node communicates with the sensor node if the shifted time exceeds the need for time accuracy at that point.

Dual-core, magnetic-electric dipole antennas were proposed by Yan et al. [30]. The recommended antennas are designed for end-users, so the antennas under the binding conditions will be checked for body efficiency. The evaluation is carried out by simulating the antenna mounted on top of a vacuum tube with a different radius. This auxiliary antenna provides reliable output in a broad, working wavelength range for gain, radius, and radiation.

Al Rasyid et al. [31], This demonstrates the effectiveness of WBAN for monitoring body temperature, heart rate, and oxygen saturation. The sensor element detection data for the server receiver was analyzed at a different distance.

5 WBANs Network Design Issues

In any WBAN that collects significant data from various parts of the human body, data portability and latency are very critical. The WBAN's reliability and latency primarily rely on the central access level's material inventory. The MAC layer helps to define network efficiency and network problems that mostly decide a WBAN network's normal and operating costs. The design of the MAC layer also assists in determining the usage of WBAN electricity, which is a significant project. The physical level also defines the WBAN's accuracy.

5.1 Energy Efficiency

In any respect, energy management is always an important operational issue, especially in WBAN. Using PHY (physical) and MAC will optimize WBAN power management (average access control). A much higher degree of energy savings is introduced by the MAC layer since it uses a variety of strategies, such as software packages and methods that arrive on a channel that displays smart signaling techniques and optimum packet structure. The PHY level can increase the probability of successful mapping by choosing the correct modulation and coding techniques. Completion Package Delays and Budget Output WBAN blocks can be concentrated by increasing the probability of packages.

WBAN's reliability is directly related to delays in the transmission of packets and the probability of loss of packets. The MAC bit rate (BIR) and the channel transmission protocol influence the likelihood of packet loss. The actual frequency of transmission errors at the WBAN PHY level can be reduced by adaptive modulation and coding techniques which satisfy the conditions of the channel where the transmission takes place. Using the error correction technique, the real rate of inaccuracy can be centered (EFR). Using this approach allows additional extra bits to be transmitted, which may increase the WBAN node's power consumption by transmitting additional bits. Network status can also influence what can influence a WBAN's reliability and performance. For efficient packet transmission, the node must have very high transmission power if the network interface and noise level are high.

5.2 Scalability

For a patient monitoring system like WBAN, scalability is very important, as it is often necessary to change the number of nodes and collect different physiological data from the body of the patient. Physicians can easily add or delete a few nodes when scaling the WBAN without impacting the WBAN's overall operation. Since the scalability of the WBAN is highly dependent on the MAC level, since PHY layers

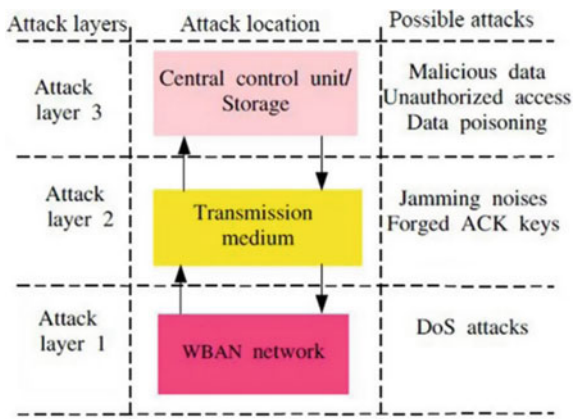
are set, this MAC level plays a vital role in maintaining reliability under changing transmission conditions, and the MAC level also helps maintain service quality.

6 Security Protocols of WBAN

WBAN frameworks require certain safe strategies to ensure the security of classification, information honesty, and patient well-being records. The WBAN uphold foundation should perform explicit security tasks that give these highlights [32]. The two primary highlights of each WBAN system are the well-being and classification of patient details. Security hopes that in the event that they are securely moved, collected, handled, and put away, information is ensured by unapproved customers. Information protection assumes the management of the social affair on the previous offer as well as the use of individual information. For example, a patient can request that their information not be exchanged with insurance companies that use this information to limit inclusion.

Specifically, the basic information inside the WBAN conspire is entirely helpless, so in the event that it comes to unapproved faculty, there might be numerous ramifications for the patient, for example, loss of work, public embarrassment, and mental shakiness. Another model is the place where culprits truly record the hub and change the data with admittance to data; in this way bogus data is sent to the specialist, which may show the technique toward the passing of the patient. Somebody may utilize the person’s clinical records to look for individual discussion with the patient. Accordingly, more noteworthy consideration and consideration ought to be paid to unapproved access, use and change of this touchy and basic data [33]. Figure 5 shows a safe information logging instrument and different organization focuses, including the last one, where information must be decoded by approved faculty and individual distinguishing proof apparatuses.

Fig. 5 Security and privacy preservation in healthcare system



The main requirements for WBAN security and widespread consumer recognition in terms of data security and protection are:

Data Security. The preservation of personal data from exposure, which is considered essential in the WBAN, is data protection. Since WBANs in applied health contexts can rely on sensitive and personal information and rely on patient well-being, the data must be shielded from unauthorized access, which can be life-threatening to the patient. During transmission, these critical transmissions are often “heard,” which can affect the patient or the device itself. By providing a common key secure communication channel between safe WBANs and coordinators, it encrypts this sensitive data even further.

Information Uprightness. Data unwavering quality alludes to measures for the security, precision of the dependability of message content. This applies to both single-message and message streams [34]. Information insurance, nonetheless, does not shield information from outside adjustments for data that might be unlawful if the information is sent to risky WBAN as a rival who can undoubtedly realize the patient’s information prior to reaching the organization organizer. In particular, changes should essentially be possible by coordinating a couple of pieces, control the information in a group, and sending the bundle to the PS. This snooping alongside adjustment can prompt grave well-being inconvenience, even passings in outrageous cases. Thusly, it is basic that the data is inaccessible and potential rivals are adjusted by utilizing validation conventions.

Information Freshness. The method of the newness of information successfully guarantees that the uprightness and classification of information are secured by the chronicle and playback of the old guilty party information and disturbed by organizer WBAN. This guarantees that the old information is not streaming and the casing is right. Two sorts of newness information are as of now utilized: Strong newness guarantees, delays in the connection justification of staff; shortcoming and newness, which is just an obligatory casing however does not give any ensure scope. Solid newness is required for synchronization if the transducer is conveyed by a WBAN organizer and the low newness WBAN utilized hubs with low cycle lifetime [35].

Accessibility of the Organization. The specialist’s instinct has viable admittance to tolerant data. As this framework conveys significant, profoundly touchy and possibly life-saving data, it is absolutely critical that the organization is consistently accessible for patients if there should be an occurrence of a crisis [32]. For this reason, it is critical to move the tasks to another WBAN in case of a deficiency of accessibility.

Information Validation. Medical and non-clinical applications may require confirmation of information. Along these lines, WBAN hubs should have the option to watch that the data is sent from a realized trust community and not constrained. Consequently, the arrange hub of the organization and all information ascertains the message confirmation code (MAC) by partitioning an unrecognized key. The precise MAC code calculation gives the organization organizer a dependable hub [35].

Secure Administration. To guarantee the WBAN key conveyance, disentangling and encryption require secure coordination from the facilitator. The job of the organizer is the free from any and all harm inclusion of WBAN hubs when joining and detaching hubs.

Dependability. The framework is solid and solid. Stopping the right information is simply WBAN as it could be hazardous for the patient [36]. Adjustment methods can be utilized to address this issue.

Safe Restriction. For most WBAN applications, an appropriate evaluation of the patient's area is required. The absence of following techniques may permit the aggressor to pass erroneous subtleties, for instance, by reacting to a bogus patient with a spot marker [24]. The creators [12] examine confinement frameworks and their assaults.

Responsibility: Healthcare suppliers need to keep the well-being data of the patients in the clinical field. On the off chance that your specialist co-op neglects to give this data or, more awful, mishandles their duty, the person is liable for forestalling further abuse. The creator examined the subject of responsibility and recommended a procedure that ensures him against it.

Adaptability. The patient ought to be adaptable in deciding the AP control of clinical records in WBAN. For instance, if there should arise an occurrence of a crisis, consent to decipher tolerant information might be submitted to another doctor on solicitation, not really recorded in the approval list [37]. In another model, if the patient is changed by the emergency clinic or the doctor, it is important to permit access control to be communicated.

Information Protection and Compliance Requirements. The need to give private well-being data is a worldwide issue. Quite possibly the main individual information insurance measures is the meaning of arrangements/approaches that patients need to get to secret information to secure the classification of patients [38]. The Health Regulations contain various guidelines and acts. There are presently different security approaches around the planet. HIPAA contains rules for specialists, medical services suppliers, and clinics and is planned to guarantee the insurance of individual well-being and clinical records. HIPAA depicts the itemized safeguards to be taken to utilize quiet information for managerial or correspondence purposes. The law incorporates both common and criminal results, including a \$250,000 fine and/or detainment for a very long time if the supplier unveils individual data about the money gains.

7 WBAN Security Threats

WBANs will be helpless against extraordinary assaults and dangers. WBANs are regularly open to numerous outside dangers and gatecrashers that can infiltrate

through the organization, as demonstrated in the Fig. 6. Thusly, security and information insurance issues should be dealt with quite well, assaulting WBAN as deactivation of a hub or a hub, which at times brings about death toll for the patient [37]. For instance, a rival can catch or separate the EEG sensor and do not uncover it to the doctor. This can prompt a hazardous, perilous circumstance, or demise.

The adversary can likewise utilize quiet or impedance. Contamination (radio recurrence obstruction) can be utilized by the foe on numerous hubs to impede the whole organization [39]. This strategy cannot obstruct huge organizations, yet since WBANs are for the most part little organizations, odds of hindering organizations are very high, however they likewise lead to parcel misfortune. Indeed, the foe once in a while gives actual impulse to WBAN. An aggressor can electronically upset, harm, or supplant WBAN to get the patient’s very own well-being information. You can likewise utilize flood mass strategies to deplete your memory by over and over sending extra superfluous bundles that the framework cannot deal with. This keeps legitimate organization clients from getting to administrations or assets [40]. This should be possible by a (DoS) assault planned not exclusively to demolish, subvert and devastate the organization yet to diminish the capacity of the organization to give the vital crisis administrations. Table 2 ordinarily presents security dangers and conceivable security arrangements that can be utilized in WBAN.

WBAN security is significant and ought not to be neglected. This is touchy clinical data that is delicate and which is regardless ensured and kept up by unapproved people who may utilize information that might be hurtful to the person. WBAN suggests various security arrangements, and these are the accompanying.

TinySec is an answer that permits association layer encryption and confirmation of information in biomedical sensor organizations. This strategy is WSN interface layer insurance design and is authoritatively important for the TinyOS discharge. In this

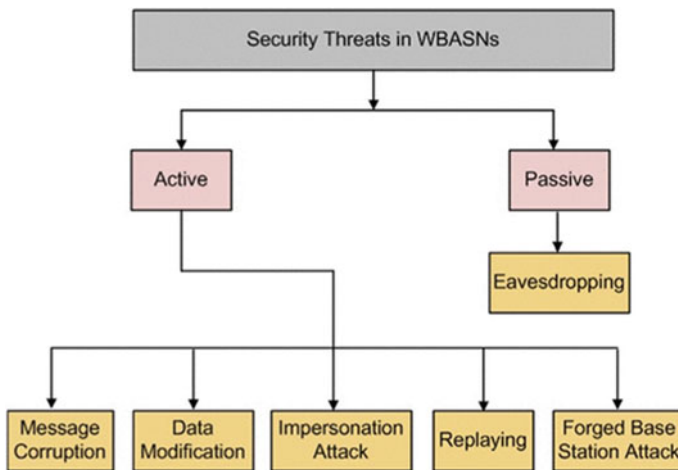


Fig. 6 Classification of security threats in WBANs

Table 2 Security threats and possible security solutions in WBAN

Security threats	Security requirements	Possible security solutions
Unauthorized access	Key establishment and a trust set up	Random key distribution and public key cryptography
Message disclosure	Confidentiality and privacy	Link/network-layer encryption and access control
Message modification	Integrity and authenticity	The keyed secure hash function and digital signature
Denial of service (DOS)	Availability	Intrusion detection systems and redundancy
Compromised node	Resilience to node compromise	Inconsistency detection and node revocation and Tamper—proofing
Routing attacks	Secure routing	Secure routing protocols
Intrusions and malicious activities	Secure group management, Intrusion detection systems and secure data aggregation	Secure group communication Intrusion detection systems

framework, a bunch key is utilized for the sensor hubs, ensured encoded parcels, and MAC for the whole bundle. It depends on a solitary default key that is physically customized in the sensor hubs. This guarantees a base degree of security and cannot be ensured against actual hubs as it is shared [3].

Biometrics. This strategy is broadly used to guarantee the correspondence of biometric information in a biomedical sensor organization. The strategy recommends utilizing self-assessment as a method of dealing with cryptographic sensor keys joined to the client’s body. In the event that the estimation esteem is EEG indistinguishable from the two distinctive body sensors, it creates a key that safely disseminates the symmetric key or encodes or decodes [41].

IEEE 802.15.4 and IEEE 802.15.6 Security Conventions. The security parts are revised within this system in compliance with IEEE 802.15.4. Two key modes are split into protection kits: secured and unprotected. A mode that is not supported means no protection packages are selected. There are 8 new security secrets specified in the standard. The Null Suite, which does not have protection, is the first and the others are distinguished by different security levels. A fine-grained representation of this norm will be found for you. Likewise, the best IEEE 802.15.6 format was approved in 2012. In and around the human body, this best-in-class standard worldwide guarantees low unshakable consistency, remote instant compliance. Depending on specifications, it supports large data transfer from narrowband (75.9 Kbps) to super wideband (15.6 Mbps) [42].

ZigBee Security Administrations. ZigBee has assembled another importance for the super low power remote correspondence as an aggregate of industry players. ZigBee Network Layer (NWK) characterizes extra security highlights, including

IEEE802.15.4, key verification and trading measures. The ZigBee standard recognizes a believed focus that is important for the organizer's duty to permit hubs to associate with the arrange and convey keys [43].

Conventions for Bluetooth Protection. Contains different conventions such as Baseband, Connection Manager Protocol (LMP) and Control and Adaptation of Logic Links (L2CAP). Bluetooth modules and commercial information can be linked through the main bar. Security problems such as encryption, authentication, and encryption keys are the responsibility of the LMP. L2CAP encourages the multiplexing and interconnection of major levels that can lead to the essence of administrative adequacy [44].

Agreements for Remote Security. In order to have a remote organization, numerous protection agreements have been set up, such as WEP, Wi-Fi Protected Access (WPA), and Wi-Fi Protected Access 2 (WPA-2). For a remote entity, the special encryption rules are WEP. There were a lot of security concerns, so it was superseded by WPA and WPA-2. WPA encrypts information using the Pre-Shared Key (PSK) and the Short Respect Information Key (TKIP). The improved WPA-2 uses the more stable and efficient Encryption Advanced Encryption Standard (AES) innovation.

Encryption Hardware. Hardware encryption is carried out using a viable ChipCon 2420 ZigBee radio transmitter instead of programming-based encryption, such as TinySec. With AES encryption with 128-digit keys, the CC2420 will perform IEEE 802.15.4 security behavior. Tasks use a counter using modes such as CTR, decryption, and encryption.

Elliptical Bending Cryptography. This method is definitely a good choice for WBAN public key cryptography. The main application of circular bending cryptography (ECC) is a centralized computer, small and conservative. Although energy demand remains high, other current frameworks may opt for significant security [45].

Encryption Procedures. BAN can provide vital security by encrypting an organization with various keys. It offers a significant degree of security with three unique tools, currently available strong encryption, symmetric key, traditional public key and face encryption.

8 Conclusion and Future Scope

We study existing studies on the body's wireless health care system in this survey. WBAN is a highly useful breakthrough that through continuous monitoring and early detection of infections, has a range of benefits for clinical applications, patients and society. The use of the WBAN clinical care system will enhance their appearance and help minimize development rates. WBAN offers quality service, low power consumption, ongoing monitoring of well-being, and portability. In addition to the various

security modules, we considered various instruments depending on the MAC standard, the actual level and the level of transport. WBAN has many applications, and different instruments are collected to promote the exhibition, depending on the application. In obvious circumstances and assumptions, each of the suggested systems works well, but each has its limitations. In this regard, it can be concluded that in all cases, no instrument is extremely successful, but in specific circumstances, it is excellent. We hope that this analysis will inspire potential scientists to accept more generous protection characteristics for continuing health care. The impressive design will allow you to explore an enhanced leadership conspiracy using a character-based aggregation signal as a future job. It was proposed to provide WBSN with full anonymous protection for message verification to this end.

References

1. Khan RA, Pathan A-SK (2018) The state-of-the-art wireless body area sensor networks: a survey. *Int J Distrib Sens Netw* 14(4):1550147718768994
2. Albahri OS, Albahri AS, Mohammed KI, Zaidan AA, Zaidan BB, Hashim M, Salman OH (2018) Systematic review of real-time remote health monitoring system in triage and priority-based sensor technology: taxonomy, open challenges, motivation, and recommendations. *J Med Syst* 42(5):80
3. Sawaneh IA, Sankoh I, Koroma DK (2017) A survey on security issues and wearable sensors in wireless body area network for the healthcare system. In: 2017 14th international computer conference on wavelet active media technology and information processing (ICCWAMTIP), pp 304–308. IEEE
4. Zuhra FT, Abu Bakar KB, Arain AA, Tunio MA (2017) Routing protocols in wireless body sensor networks: a comprehensive survey. *J Netw Comput Appl* 99:73–97
5. Jiang W, Wang Z, Feng M, Miao T (2017) A survey of thermal-aware routing protocols in wireless body area networks. In: 2017 IEEE international conference on Computational science and engineering (CSE) and embedded and ubiquitous computing (EUC), vol 2, pp 17–21. IEEE
6. Bhanumathi V, Sangeetha CP (2017) A guide for the selection of routing protocols in WBAN for healthcare applications. *HCIS* 7(1):24
7. Kompara M, Hölbl M (2018) Survey on security in intra-body area network communication. *Ad Hoc Netw* 70:23–43
8. Wang J, Zhang Z, Xu K, Yin Y, Guo P (2013) A research on security and privacy issues for patient-related data in medical organization system. *Int J Security Appl* 7(4):287–298
9. Crosby GV, Ghosh T, Murimi R, Chin CA (2012) Wireless body area networks for healthcare: a survey. *Int J Ad Hoc Sens Ubiquitous Comput* 3(3):1–26
10. Siddiqui MA, Kamal MB, Moinuddin H (2013) Towards the development of cross-layer approach for energy efficiency and mobile wireless body area networks. *Int J Comput Inform Technol* 542–547
11. Rocker C, Ziefle M (2011) E-health, assistive technologies and applications for assisted living: challenges and solutions. *Med Inform Sci Ref* 392. ISBN13:9781609604691
12. Rehman OU, Javaid N, Bibi A, Khan ZA. Performance study of localization techniques in wireless body area sensor networks. In: 11th IEEE international conference on trust, security, and privacy in computing and communications, pp 1968–1975
13. Pathania S, Bilandi N (2014) Security issues in wireless body area network. *Int J Comput Sci Mobile Comput* 3(4):1171–1178
14. Li M, Lou W, Ren K (2010) Data security and privacy in wireless body area networks. *IEEE Wirel Commun* 17(1):51–8

15. Al Ameen M, Liu J, Kwak K (2012) Security and privacy issues in wireless sensor networks for healthcare applications. *J Med Syst* 36:93–101
16. Tachtatzis C, Di Franco F, Tracey DC, Timmons NF, Morrison J (2011) An energy analysis of IEEE 802.15. 6 scheduled access modes for medical applications. In: International conference on ad hoc networks. Springer, Berlin Heidelberg, pp 209–22
17. Cavallari R, Martelli F, Rosini R, Buratti C, Verdone R (2014) A survey on wireless body area networks: technologies and design challenges. *IEEE Commun Surv Tutor* 16(3):1635–1657
18. Movassaghi S, Abolhasan M, Lipman J, Smith D (2014) Wireless body area networks: a survey. *IEEE Commun Surv Tutor* 16(3):1–28
19. Maulin P, Wang FJ (2010) Applications, challenges and prospective in emerging body area networking technologies. *IEEE Wirel Commun* 1284–1536
20. Khaliliam R, Rezai A, Abedini E (2016) An efficient method to improve WBAN security 64:43–46
21. Tiwari A, Verma P (2016) Security and privacy in E-healthcare monitoring with WBAN. *Int J Comput Appl* 136:37–42
22. Sahnadu MM, Javaid N, Imran M, Guizani M, Ali Khan Z, Qasim U (2015) BEC: a novel routing protocol for balanced energy consumption in wireless body area networks. In: IEEE, pp 653–657
23. Ha I (2015) Technologies and research trends in wireless body area networks for healthcare: a systematic literature review. *Int J Distrib Sens Netw* 14
24. Lee W, Choi J (2015) A dual-band printed antenna with metal back-cover for WBAN applications. In: 2015 IEEE international symposium on antennas and propagation & USNC/URSI national radio science meeting, pp 936–937. IEEE
25. Thamilarasu G, Ma Z (2015) Autonomous mobile agent-based intrusion detection framework in wireless body area networks. In: 2015 IEEE 16th international symposium on world of wireless, mobile and multimedia networks (WoWMoM), pp 1–3
26. Froehle P, Przybylski T, McDonald C, Mirzaee M, Noghianian S, Fazel-Rezai R (2015) Flexible antenna for wireless body area network. In: 2015 IEEE international symposium on antennas and propagation & USNC/URSI national radio science meeting, pp 1214–1215. IEEE
27. Kim T-Y, Youm S, Jung J-J, Kim E-J (2015) Multi-hop WBAN construction for healthcare IoT systems. In: 2015 international conference on platform technology and service (PlatCon), pp 27–28. IEEE
28. He P, Li X, Yan L, Yang S, Zhang B (2015) Performance analysis of WBAN based on AODV and DSDV routing protocols. In: 2015 2nd international symposium on future information and communication technologies for ubiquitous healthcare (Ubi-HealthTech), pp 1–4. IEEE
29. Ramlall R (2015) Timestamp-free synchronization for wireless body area networks. In: Consumer communications and networking conference (CCNC), 2015 12th annual IEEE, pp 166–167. IEEE
30. Yan S, Soh PJ, Vandenbosch GAE (2015) Wearable dual-band magneto-electric dipole antenna for WBAN/WLAN applications. *IEEE Trans Anten Propag* 63(9):4165–4169
31. Al Rasyid H, Udin M, Lee B-H, Sudarsono A (2015) Wireless body area network for monitoring body temperature, heartbeat and oxygen in the blood. In: 2015 international seminar on intelligent technology and its applications (ISITIA), pp 95–98
32. Kumar R, Mukesh R (2013) State of the art: security in wireless body area networks. *Int J Comput Sci Eng Technol (IJCSET)* 4(5):622–630
33. Kargar MJ, Ghasemi S, Rahimi O (2013) Wireless body area network: from electronic health security perspective. *Int J Reliab Qual E-Healthc (IJRQEH)* 2(4):38–47
34. Al Ameen M, Liu J, Kwak K (2012) Security and privacy issues in wireless sensor networks for healthcare applications. *J Med Syst* 36(1):93–101
35. Kavitha T, Sridharan D (2010) Security vulnerabilities in wireless sensor networks: a survey. *J Inf Assurance Sec* 5(1):31–44
36. Somasundaram M, Sivakumar R. Security in wireless body area networks: a survey. In: International conference on advancements in information technology ICBMG, IPCSIT, Singapore, p 20

37. Fatema N, Brad R (2014) Security requirements, counterattacks and projects in healthcare applications using WSNs—a review. *Int J Comput Network Commun (IJCNC)* 2(2)
38. Medical Privacy (2015) National standards of protect the privacy of personal-health-information. <http://www.hhs.gov/ocr/privacy/hipaa/administrative/privacyrule/index.html>. Accessed 20 Dec 2015
39. Ullah S, Higgins H, Braem B, Latre B, Blondia C, Moerman I, Saleem S, Rahman Kwak KS (2012) A comprehensive survey of wireless body area networks. *J Med Syst* 36(3):1065–1094
40. Latif R, Abbas H, Assar S (2014) Distributed denial of service (DDoS) attack in cloud assisted wireless body area networks: a systematic literature review. *J Med Syst* 38(11):1
41. Ramli SN, Ahmad R, Abdollah MF, Dutkiewicz E. A biometric-based security for data authentication in wireless body area network (wban). In: In the 15th international conference on advanced communication technology (ICACT), pp 998–1001
42. Saleem S, Ullah S, Kwak KS (2011) A study of IEEE 802.15.4 security framework for wireless body area networks. *Sensors* 11(2):1383–1395
43. Mistic J (2008) Enforcing patient privacy in healthcare WSNs using ECC implemented on 802.15.4 beacon enabled clusters. In: 2008 sixth annual IEEE international conference on pervasive computing and communications (PerCom), Hong Kong, pp 686–691
44. Ahmadi A, Shojafar M, Hajeforosh SF, Dehghan M, Singhal M (2014) An efficient routing algorithm to preserve k-coverage in wireless sensor networks. *J Supercomput* 68(2):599–623
45. Zhao Z (2014) An efficient anonymous authentication scheme for wireless body area networks using elliptic curve cryptosystem. *J Med Syst* 38(2):1–7

Facial Expression Recognition System and Play Customized Ad



Shivalik Sharma, Arnav Ajey, Nishant Singh, and N. M. Sreenarayanan

Abstract According to a recent study, almost 70% of smartphone users experience random app pop-ups that interrupt what they are doing on their phone and they are hard to close out (Samadiani et al., *Sensors* 19(8):1863 (2019) [1]). Most of the time it is an ad for a game and other times it is an ad for insurance. Some pop-ups make noise and some do not. It is irritating for a person when he/she is listening to music on YouTube and it totally stops the song altogether and after that, the ad just stays on and it does not resume the music. This is a very serious and a grave problem faced by many users. Our project idea aims to soothe the experience and make it less of an annoying and a bad experience for all users. The motivation behind choosing this topic specifically lies in the huge investments large corporations do in feedback and surveys but fail to get an equitable response on their investments. Emotion and Facial Detection is a technology that is designed/worked upon to better services and product performance by inspecting and analyzing user behaviour (Li, *IEEE Trans Affec Comput* (2020) [2]). Support Vector machines or more commonly known as SVMs are used to plot the training vectors in high-dimensional spaces, and also as a means to label each vector with its class.

Keywords Keras · CNN · CVV · Tensorflow · Image classification · Algorithms

1 Introduction

One of the foremost common kinds of non-verbal communication from which someone understands one's mood/attitude is facial expressions. Facial expression recognition is one of the most interesting and challenging fields of machine learning and computer vision. Facial expressions can be categorized as (Happy, Angry, Sad,

S. Sharma (✉) · A. Ajey · N. Singh · N. M. Sreenarayanan
School of Computing Science and Engineering, Galgotias University, Plot No. 2, Yamuna Expressway, Opposite Buddha International Circuit, Sector 17A, Greater Noida, Uttar Pradesh, India

A. Ajey
e-mail: arnav1298@gmail.com

© The Author(s), under exclusive license to Springer Nature Singapore Pte Ltd. 2022
B. B. V. L. Deepak et al. (eds.), *Applications of Computational Methods in Manufacturing and Product Design*, Lecture Notes in Mechanical Engineering,
https://doi.org/10.1007/978-981-19-0296-3_56

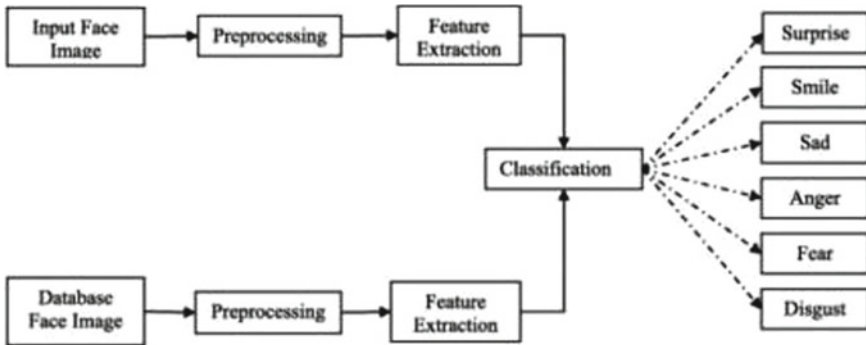


Fig. 1 Facial expression recognition steps

Fear, Surprise). In the field of computer vision, facial expression systems are not only limited to understanding Psychological analysis but also they can be used in other fields such as a lie detector, movie recommendation according to someone mood, fatigue detection of drivers, music recommendation as per mood, etc. Facial expression recognition has four steps, shown in Fig. 1.

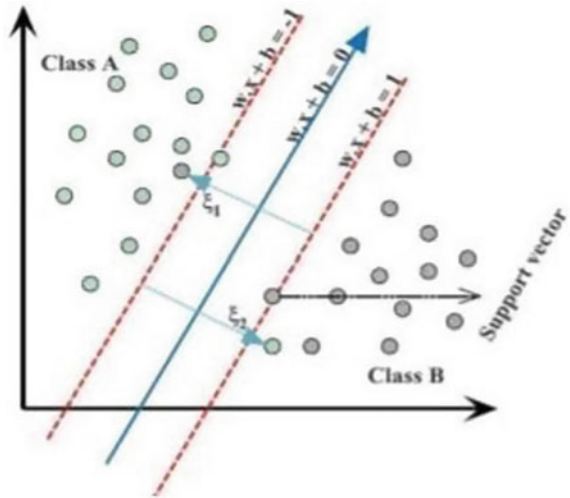
1.1 Motivation

The main motivation behind choosing this project as our final year project is that many MNCs invest millions and billions to get the feedback of their product for more sales and profit but somewhat they are not getting the favorable result as expected. Facial expression recognition system is a project that aims to enhance the product and service performance by extracting the mood of their customers after getting or using the product.

1.2 Examples

- Disney is using it to find the feedback of its customers.
- Kellogg's uses the software Affective to find the audience mood for its cereal.
- Unilever uses Hire Vue's for recruitment purposes to get better employees for its company.

Fig. 2 Support vector machine analysis



2 Literature Review

Support Vector machines or more commonly known as SVMs are used to plot the training vectors in high-dimensional feature space, and also a means for each vector to be labeled with its class. Figure 2 shows SVM Analysis. A hyperplane is constructed between the different training vectors that in turn maximize the distance between the different available classes. The hyperplane is determined with the help of a kernel function, which is provided as input for the classification software [3, 4]

For the deepest level of abstraction of an image, we use Preprocessing. Preprocessing steps are:

- I. Reducing the noise or error
- II. Converting the Image or photo into Grayscale
- III. Transformation of Pixel Brightness
- IV. Transformation in terms of Geometry.

3 Problem Formulation

Imagine on a good day, a person walks through a store or browses through an online e-commerce website. What if that person is not bothered by ads or shown ads that may further brighten up his/her day, OR, what if a person is annoyed or stressed out and that person is greeted with annoying ads that have no relevance to the person's requirements, then that person would further get irritated and take irrational decisions. Our project aims to solve this issue by using facial expression technology to deliver better and more appropriate ads to soothe the overall experience of the user.

3.1 Dataset Description

The dataset which we have used for training our model is taken from Kaggle. It consists of photos of 48×48 pixel grayscale. Our model's task is to categorize the images based upon the five categories (0 for "Angry", 1 for "Happy", 2 for "Sad", 3 for "Surprise", 4 for "Neutral").

3.2 Data Preprocessing

- I. The Harcasscade .xml consists of three columns namely emotion, pixels, and purpose.
- II. The column in pixel first of all is stored in a list format.
- III. Since computational complexity is high for computing pixel values in the range of (0–255), the data in pixel field is normalized to values between [0 – 1].
- IV. The face objects stored are reshaped and resized to the mentioned size of 48×48 (Fig. 3).

4 Tools Used

- PYTHON = the programming language commonly used in AI/ML
- TENSOR FLOW = the core open-source library that helps you develop and train ML models
- KERAS = an API that supports core ML functions
- NUMPY = a package for scientific computations in Python
- SK-IMAGE = a collection of algorithms for image processing.

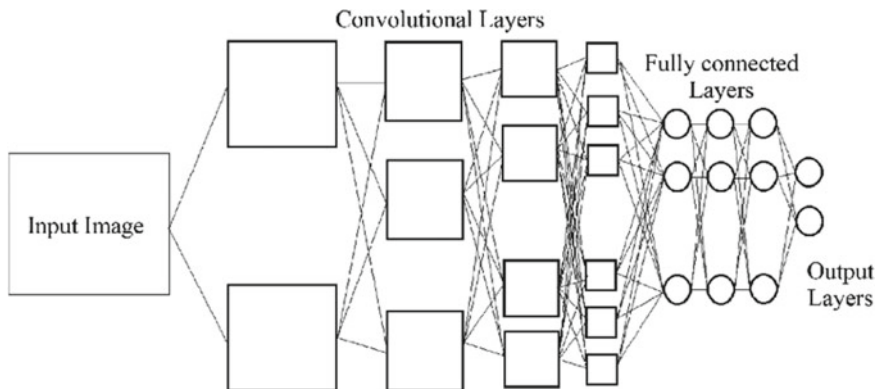


Fig. 3 Convolutional neural network for facial expression recognition

5 Merits of Proposed System

If you are familiar with Tom Cruise’s movie “Minority Report”, in the scene where Tom Cruise walks into a Gap clothing store. A retinal scanner scans his eyes, and displays a redid promotion suited for him. We do not need to bother about retinal scanners, as we have technologies like Artificial Intelligence (AI) and Machine Learning (ML). With the use of Deep Learning to perform facial/expression acknowledgment we can afterward utilize a Neural Network Text to Speech (TTS) motor to display a more appropriate commercial much more suited under the circumstances Envision at best, an individual strolls through a store or peruses an online internet business site. What if that person is not bothered by ads or shown ads that may further brighten up his/her day, OR, what if a person is annoyed or stressed out and that person is greeted with annoying ads that have no relevance to the person’s requirements, then that person would further get irritated and take irrational decisions. Our project aims to solve this issue by using facial expression technology to deliver better and more appropriate ads to soothe the overall experience of the user.

6 Implementation and Description of Project Module

CNN: A CNN is a type of Neural Network (NN) every now and again utilized for picture arrangement undertakings, for example, face acknowledgment, and for whatever other issue where the information has a matrix-like geography [5]. In CNNs, few out of every odd hub is associated with all hubs of the following layer; as such, they are not completely associated with NNs. This forestalls overfitting issues that surface in completely associated NNs, also extra-moderate intermingling that results from an excessive number of associations in a NN. Train a CNN model:

```
cnn = ConvolutionalModel(dataSet) cnn.train(n_epochs = 50) cnn.evaluate().
```

So, face detection—time to dive into some code. Here is a Python class that implements our face detector:

```
from PIL import Image
from matplotlib import pyplot
from mtcnm import MTCNN
from numpy import asarray
from skimage import io
from util import constant
class MTCnnDetector:

    def __init__(self, image_path):
        self.detector = MTCNN()
        self.image = io.imread(image_path)
```

The name of our class is *MTCnnDetector* because the predefined detector we will use is MTCNN (Multi-Task-Convolutional-Neural-Network). This is a type of CNN that follows the principle of Multi-Task learning. It is able to learn multiple tasks at the same time, thus supporting simultaneous detection of multiple faces. Using the MTCNN algorithm, we identify the bounding boxes of countenances in a picture, alongside 5-point facial tourist spots for each face (the easiest model, which distinguishes the edges of the eyes and the lower part of the nose). The identification results are improved dynamically by going the contributions through a CNN, which returns competitor jumping boxes alongside their likelihood scores. This is the main method of the class:

```
def process_image(self, plot=False):
    faces = self._detect_face();
    resized_face_list = []
    for f in faces:
        extracted_face = self.__extract_face(f)
        resized_face = self._resize_img_to_face(extracted_face)
        resized_face_list.append(resized_face)
    if plot:
        self._plot_face(resized_face)
    return resized_face_list
```

The technique is basic: it calls the `detect_face()` strategy to get all faces from the picture (whose way was contributed before through the class constructor), extricates the faces and resizes them, and returns a rundown of resized pictures. Also, it plots the detected faces if `plot` is true. It utilizes the accompanying private strategies as assistants:

```
def _detect_face(self):
    return self.detector.detect_faces(self.image)

def _extract_face(self, face):
    x1, y1, width, height = face['box']
    x2, y2 = x1 + width, y1 + height
    return self.image[y1:y2, x1:x2]

def _resize_img_to_face(self, face):
    image = Image.fromarray(face)
    image = image.resize((constant.DETECTOR_FACE_DIM,
    constant.DETECTOR_FACE_DIM))
    return asarray(image)

def _plot_face(self, face):
    pyplot.imshow(face)
    pyplot.show()
```

So the `detect_face()` strategy detects faces utilizing the `self.detector.detect_faces()` technique. The `extract_face()` strategy separates from the picture the part relating to the jumping box returned before. At last, the `resize_img_to_face()` technique inputs the recently acquired bit of the picture and resizes it to predefined measurements. The `plot_face()` technique plots the subsequent face.

Keras: The most compelling reasons to use Keras arise mainly from its core values. Keras Python library offers simple model structure and simplicity in learning, Keras also offers the added merits of expansive reception, and with a very high scope of working along with other back-end motors like TensorFlow, CNTK, MXNet, PlaidML, etc. and also comprehensive help for multiple GPUs. To top it off, Keras is well-supported by major tech giants like Google, Microsoft, Amazon, Apple, Nvidia, Uber, etc.

6.1 Output

Figure 4 shows various facial expressions identified by the system. The first person's expression is that of angry person, second and third are happy and the last one is neutral. Our model was 68.4% accurate.

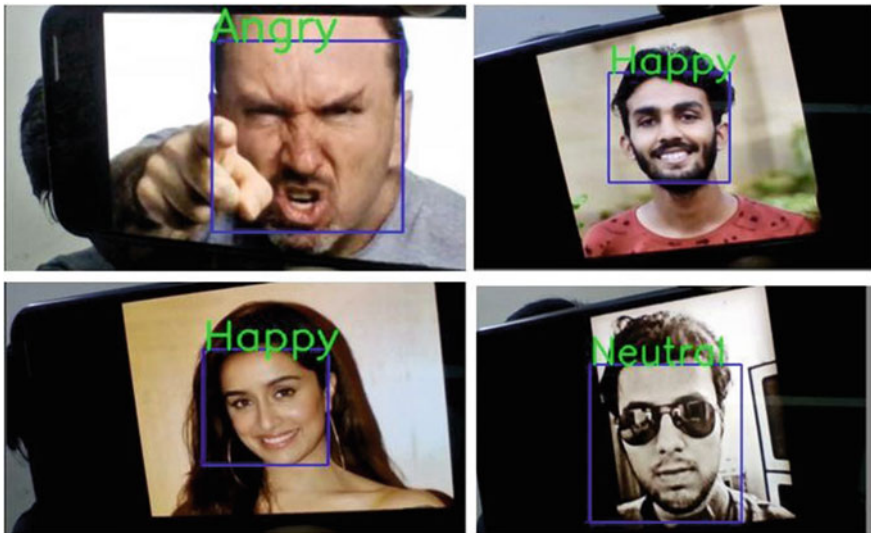


Fig. 4 Different facial expressions

7 Feasibility Analysis

As the code is now ready, we can now train our CNN. This is done by initiating the “Convolutional Model” class on the dataset and subsequently “evaluate” method is called. The training period is run for 50 epochs, the CNN models deliver an accuracy of almost 65% on the test images. This implies that our CNN model would now be able to recognize each one of the emotions mentioned in our project with an accuracy of 65%. The CNN model learns the representation features of images from the training images. We note that our model starts to overfit around 10 epochs, at which validation accuracy reaches its plateau. Therefore, we take the validation accuracy to be 65–66%. The validation accuracy as high as 65–66% is satisfactory as while predicting one of the many emotions the probability is the inverse of the number of emotions. While detecting an emotion, when the true label is equal to the class with highest probability, we mark it with black color, else if the label is wrong then it is marked with blue color. Some of the pictures are even completely misclassified, for example, a few objects are labeled as happy but wrongly classified by our neural network as angry with approximately 100% certainty. The picture of an angry human can easily be perceived by humans. Therefore, we can also conclude that facial expressions are very difficult to classify because of complicated muscle movements on the face of a human, but it still deliver a 65% accuracy in total.

8 Limitations and Future Scope

The worldwide facial expression detection and acknowledgment market size are suspected to grow from a whopping USD 21.6 billion industry in 2019 to a whopping USD 56.0 billion industry by 2024, with a Compound Annual Growth Rate of 21.0% during the given time frame. Factors like the rising requirement for socially wise counterfeit specialists, expanding request for speech-based biometric frameworks to empower multifaceted validation, mechanical headways worldwide, and developing requirements for greater operational greatness are going to enter the market sooner or later [6].

Outward appearances are a combination of a person’s intellectual state, goal, character, furthermore, brain research and are very often used to impart messages in relational relationships. Facial articulations are likewise signals that are amazingly useful in reacting to a specific discourse. Facial acknowledgment programming is a fundamental piece of the feeling location and acknowledgment framework as it empowers the distinguishing proof of feelings or reactions from outward appearances and produces continuous outcomes [7].

9 Conclusion

All in all, with advancements in the field of Facial and Emotion detection systems, its applications will also get favored. As we see the potential growth in the field (as mentioned in the above points) we can be sure that this technology is supposed to last and is going to go a long way in making user experiences much better for all users. This would help the customer to choose the product efficiently and it would increase the sale of the firms [8]. Both the customer and the company will get the advantage of using this system. And, it would reduce the shopping time if the customers start using this system and adapt to it efficiently.

References

1. Samadiani N et al (2019) A review on automatic facial expression recognition systems assisted by multimodal sensor data. *Sensors* 19(8):1863
2. Li S, Deng W (2020) Deep facial expression recognition: a survey. *IEEE Trans Affect Comput*
3. Kar NB et al (2019) Face expression recognition system based on ripplelet transform type II and least square SVM. *Multimed Tools Appl* 78(4):4789–4812
4. Gangopadhyay I, Chatterjee A, Das I (2019) Face detection and expression recognition using Haar cascade classifier and Fisherface algorithm. In: *Recent trends in signal and image processing*. Springer, Singapore, pp 1–11
5. Fan Y, Lam JCK, Li VOK (2018) Multi-region ensemble convolutional neural network for facial expression recognition. In: *International conference on artificial neural networks*. Springer, Cham
6. Kuo C-M, Lai S-H, Sarkis M (2018) A compact deep learning model for robust facial expression recognition. In: *Proceedings of the IEEE conference on computer vision and pattern recognition workshops*
7. Chen J, Konrad J, Ishwar P (2018) Vgan-based image representation learning for privacy-preserving facial expression recognition. In: *Proceedings of the IEEE conference on computer vision and pattern recognition workshops*
8. Revina IM, Sam Emmanuel WR (2018) A survey on human face expression recognition techniques. *J King Saud Univ Comput Inform Sci*
9. <http://www.paulvangent.com/2016/04/01/emotion-recognition-with-python-opencv-and-a-face-dataset/>
10. <https://heartbeat.fritz.ai/building-a-motivation-bot-with-tensorflow-js-face-detection-and-emotion-classification-7b80a38eb9c3>
11. <https://algorithmia.com/blog/introduction-to-emotion-recognition>
12. https://www.researchgate.net/publication/333618311_Facial_Expression_Recognition_using_Convolutional_Neural_Network_with_Data_Augmentation
13. <https://www.freecodecamp.org/news/facial-emotion-recognition-develop-a-c-n-n-and-break-into-kaggle-top-10-f618c024faa7/>
14. <https://scholarworks.rit.edu/cgi/viewcontent.cgi?article=11364&context=theses>

Application of Taguchi Technique to Study the Influence of Process Parameters of Ultrasonicator-Assisted Stir Casting on Tensile Strength of Al6061/Nano Rice Husk Ash Composites



Subrahmanyam Vasamsetti, Lingaraju Dumpala, and V. V. Subbarao

Abstract Nano rice husk ash particles were prepared from completely combusted rice husk by ball milling. These particles were successfully reinforced in Al6061 metal matrix through ultrasonicator-assisted stir casting process in different proportions such as 1, 2, 3, 4, and 5 in weight percentage. In order to produce the composites, different parameters were selected such as melting temperature, stirring time, and stirring speed. The influence of the percentage weight of the reinforcement and the different casting process parameters on the tensile strength of the developed composite had been analyzed in detail. The aluminum alloy was melted at selected temperatures about 700 °C, 750 °C, and 800 °C, and stirring was carried out at different selected speeds 400 rpm, 500 rpm, and 600 rpm for 60 s, 90 s, and 120 s. Finally, the improvement in tensile strength is observed with the increase in the percentage of the NRHA composition up to 2 weight percent and then deteriorated. But these tensile strength values are much better than bare material. The optimum process parameters were found to be 800 °C melting temperature at 600 rpm of stirring speed for 120 s.

Keywords Rice husk ash · Nano rice husk ash · Taguchi method of optimization · Nanocomposites

1 Introduction

Nowadays, researchers are searching for naturally available reinforcements and industrial or agro wastes to decrease the cost of materials and to generate wealth from waste. Rice husk (RH) is the agro waste left after extracting rice from paddy.

S. Vasamsetti (✉) · L. Dumpala · V. V. Subbarao
JNTUK, Kakinada, Andhra Pradesh, India

S. Vasamsetti
Godavari Institute of Engineering and Technology, Rajahmundry, Andhra Pradesh 533296, India

Rice husk is rich in oxygen and carbon, and its combustion is an exothermic reaction. Hence, it had been used as fuel in small-scale industries such as power plants, sugar, and paper industries. Rice husk ash (RHA) is the industrial waste and has least applications. Completely combusted RHA is in white color and consists of very high percentage of silicon. The silicon is present in the form of oxide, i.e., silica (SiO_2).

1.1 Literature Review

Several researchers successfully fabricated metal matrix composites in liquid metallurgy route.

Prasad et al. successfully reinforced RHA and SiC particulates to aluminum alloy using stir casting method and claimed increase in tensile and yield strengths due to increase in dislocation density [1–5]. The increase in corrosion and wear resistance was identified by Bodurin et al., with the reinforcement of RHA and SiC to Al–Mg–Si matrix [6–8]. The increase in tensile, compressive, and hardness properties with the reinforcement of RHA to AlSi10Mg is presented by Saravanan and Kumar [9]. So far, the reinforcement of RHA in micro-size was present in the available literature and in nano-size was not found. The present investigation is focused on reduction of RHA into nano-size, fabrication of Al6061 matrix-based composites by reinforcing with NHRA and establishing the influence of casting parameters on the tensile strength of the fabricated composites.

2 Materials and Methodology

RH is the industrial waste and was collected from a local rice mill [10, 11]. It was cleaned, dried, and combusted in muffle furnace under controlled environment. The complete combusted RHA is free from carbon and is in shiny white color. The RHA was milled in planetary ball mill with 10:1 ball to powder ratio, until the average particle size was reduced lesser than 100 nm [12]. The average particle size was measured in dynamic light scattering (DLS) device.

Al6061 alloy was chosen as matrix material which is widely used for automobile and aeronautical applications. Agglomeration and clustering are the major challenges with nanomaterials. Several researchers successfully reinforced nanomaterials into aluminum metal matrixes through ultrasonicator-assisted stir casting technique (UST) [13–15] which is shown in Fig. 1. NRHA particles were successfully reinforced in Al6061 metal matrix through UST.

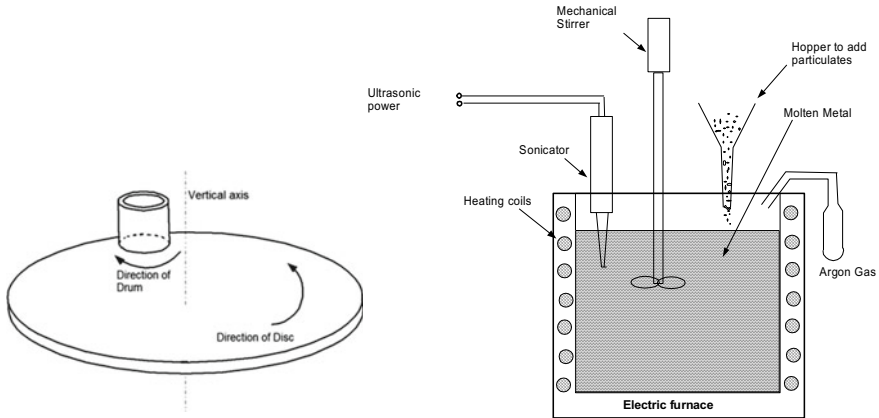


Fig. 1 Planetary ball mill and stirrer furnace with ultrasonicator

2.1 Design of Experimentation

An experiment was designed with six different weight proportions of NRHA, i.e., 0 (bare material), 1, 2, 3, 4, and 5 Wt%, three levels of melting temperatures 700 °C, 750 °C, and 800 °C, three levels of stirring speed 400 rpm, 500 rpm, and 600 rpm, and was carried out for different stirring times 60 s, 90 s, and 120 s. Mixed-level design of experiments L18 ($1^6, 3^3$) orthogonal array was chosen and is presented in Table 1. The process parameters and their levels are presented in Table 2. The interactions in the casting parameters may also play constructive role in deciding the tensile strength of the composite.

The first column 'A' was assigned to weight percent of the reinforcement NRHA, second column 'B' melting temperature, third column 'C' stirring speed, and the fourth column 'D' stirring time. The response to be studied is the tensile strength with the objective 'as greater as possible' is the best. The outcomes include signal-to-noise ratio (S/N ratio) to determine the optimum process parameters.

3 Results

After frequent intervals of ball milling of the RHA, the particle size was tested in the DLS machine and found that 43.8 nm after 85 h of ball milling and is as shown in Fig. 2. The micrograph of 4 Wt% NRHA-reinforced Al6061 composite sample is shown in Fig. 3, which reveals that no clustering happened; i.e., NRHA is uniformly distributed. The microstructure revealed that the nanoparticles were distributed uniformly due to the non-presence of clusters.

Table 1 Design of experiments L18 orthogonal array matrix ($6^1, 3^3$)

Ex. No.	A	B	C	D
1	1	1	1	1
2	1	2	2	2
3	1	3	3	3
4	2	1	1	2
5	2	2	2	3
6	2	3	3	1
7	3	1	2	1
8	3	2	3	2
9	3	3	1	3
10	4	1	3	3
11	4	2	1	1
12	4	3	2	2
13	5	1	2	3
14	5	2	3	1
15	5	3	1	2
16	6	1	3	2
17	6	2	1	3
18	6	3	2	1

Table 2 Process parameters and levels

Parameters	Wt% weight percentage of reinforcement	T: melting temperature (°C)	S: stirring speed (rpm)	Time: stirring time (s)
Level 1	0	700	400	60
Level 2	1	750	500	90
Level 3	2	800	600	120
Level 4	3	–	–	–
Level 5	4	–	–	–
Level 6	5	–	–	–

The tensile strength responses, corresponding S/N ratios, and their mean values of all L18 experiments are presented in Table 3 and were analyzed with Minitab 17 software.

The influence of different levels of parameters such as Wt% of the NRHA reinforcement, melting temperature, stirring speed, and stirring time was analyzed, and the rank of each parameter is presented with the support of S/N ratio in Table 4.

After the analysis, the optimum conditions were drawn using S/N ratio in the diagram.

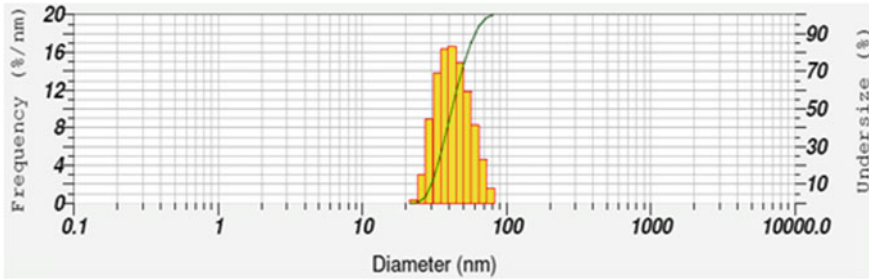
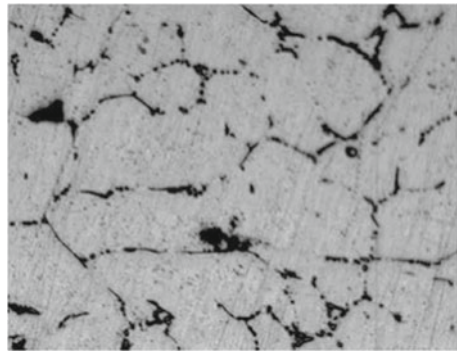


Fig. 2 NRHA particle size using dynamic light scattering device

Fig. 3 Microstructure of 4 Wt% NRHA-reinforced Al6061 composite



The predicted value can be found using the formulae given in the Eqs. (1–6)

$$Y_p = Y_E + (Y_A - Y_E) + (Y_B - Y_E) + (Y_C - Y_E) + (Y_D - Y_E) \tag{1}$$

where

Y_p : predicted value,

$$Y_E : \text{experimental value} = \text{average of all responses} \\ = \left[\frac{\sum(\text{Tensile strength Responses})}{18} \right] \tag{2}$$

$$Y_A : \text{average responses of A at optimum level (L3)} \\ = \left[\frac{\sum(\text{Responses corresponding to Level 3 of Wt\%})}{3} \right] \tag{3}$$

$$Y_B : \text{average responses of B at optimum level (L3)} \\ = \left[\frac{\sum(\text{Responses corresponding to Level 3 of Temperature})}{6} \right] \tag{4}$$

Table 3 Tensile strength responses, S/N ratios, and their mean values

Ex. No.	Wt	T	S	Time	Tensile strength	SNRA1	MEAN1
1	0	700	400	60	120.65	41.63055	120.65
2	0	750	500	90	122.16	41.73858	122.16
3	0	800	600	120	122.21	41.74213	122.21
4	1	700	400	90	124.37	41.89431	124.37
5	1	750	500	120	127.23	42.09179	127.23
6	1	800	600	60	129.47	42.24338	129.47
7	2	700	500	60	134.71	42.58800	134.71
8	2	750	600	90	138.39	42.82209	138.39
9	2	800	400	120	140.96	42.98192	140.96
10	3	700	600	120	132.25	42.42791	132.25
11	3	750	400	60	134.17	42.55311	134.17
12	3	800	500	90	136.24	42.68609	136.24
13	4	700	500	120	129.96	42.27619	129.96
14	4	750	600	60	130.92	42.34012	130.92
15	4	800	400	90	131.14	42.35470	131.14
16	5	700	600	90	125.57	41.97772	125.57
17	5	750	400	120	126.12	42.01568	126.12
18	5	800	500	60	127.81	42.13130	127.81

Table 4 Response table for S/N

Level	Wt	T	S	Time
1	41.70	42.13	42.24	42.25
2	42.08	42.26	42.25	42.25
3	42.80	42.36	42.26	42.26
4	42.56	–	–	–
5	42.32	–	–	–
6	42.04	–	–	–
Delta	1.09	0.22	0.02	0.01
Rank	1	2	3	4
Optimum levels	L3	L3	L3	L3

$$\begin{aligned}
 Y_C &: \text{average responses of } C \text{ at optimum level (L3)} \\
 &= \left[\frac{\sum(\text{Responses corresponding to Level 3 of stirring speed})}{6} \right] \quad (5)
 \end{aligned}$$

Y_D : average responses of D at optimum level (L3)

Table 5 Confirmation test result

Predicted value	Practical value		Error
	Experimental values of 2 Wt%, 800 °C, 600 rpm and 120 s	Average	
139.86	138.34	138.80	0.7%
	139.27		

$$= \left[\frac{\sum (\text{Responses corresponding to Level 3 of stirring time})}{6} \right] \tag{6}$$

Therefore, the predicted value, $Y_P = Y_A + Y_B + Y_C + Y_D - 3Y_E = 139.86$ MPa at (3 3 3 3) Levels i.e., at 2 Wt% of reinforcement, 800 °C of melting, 600 rpm of stirring speed, and about 120 s of stirring.

3.1 Confirmation Test

A confirmation test was conducted by taking the optimum levels of the predicted value, i.e., at 2 Wt% of reinforcement, 800 °C of melting temperature, 600 rpm of stirring speed, and about 120 s of stirring. The results were presented in Table 5 and are found satisfactory.

The main effects plots for means and S/N ratios are shown in Figs. 4 and 5. The tensile strength was increased with the increase in Wt% of NHRA up to 2 Wt%. The increased surface area of the NHRA particles provides more resisting area against tensile loading which leads to enhanced tensile strength. Beyond 2 Wt% of NHRA, inclusion results in clusters formation, and reduction in tensile strength was observed. The melting temperature was another parameter and has considerable effect on tensile strength of the composite. The increase in melt temperature enhances the ability to disperse NHRA particles uniformly in the matrix material results in improvement in the strength. The stirring speed and time have negligible effect on the composite tensile strength.

3.2 Analysis of Variance for Tensile Strength

Analysis of variance (ANOVA) on the tensile strength for the reinforcement of NRHA on Al6061 metal matrix is done to find the exact contribution percentage of individual parameters on the tensile strength of the composite prepared and is presented in Table 6 and Fig. 6. The ANOVA is conducted at 5% significance level up to 95% confidence level. The fourth column in the table indicates percentage of contribution of the parameters chosen. From Table 6, it can be found that the Wt% of reinforcement

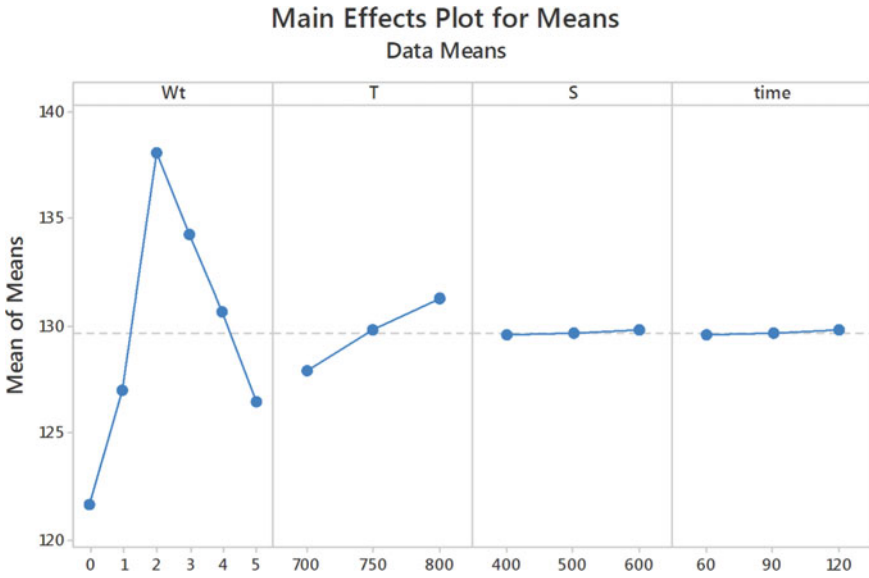
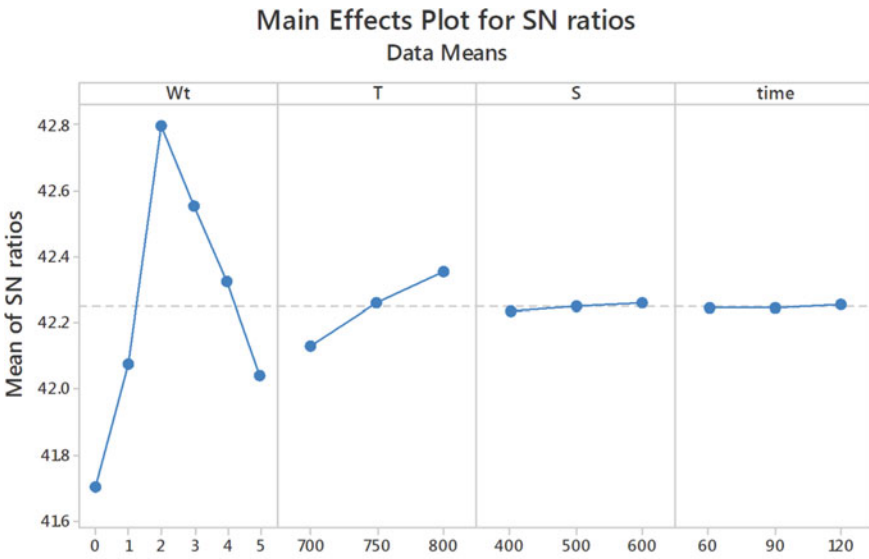


Fig. 4 Main effects plot for means



Signal-to-noise: Larger is better

Fig. 5 Main effects plot for S/N ratios

Table 6 One-way ANOVA: SNRA1 versus Wt%, T, S, and time

Source	DF	Seq SS	Contribution	Adj SS	Adj MS	F-value	P-value
Wt	5	2.3112	92.13%	2.3112	0.46224	28.09	0.000
T	2	0.1517	6.05%	0.1517	0.07585	0.48	0.626
S	2	0.00131	0.05%	0.00131	0.000654	0.00	0.996
Time	2	0.00036	0.01%	0.00036	0.000179	0.00	0.999

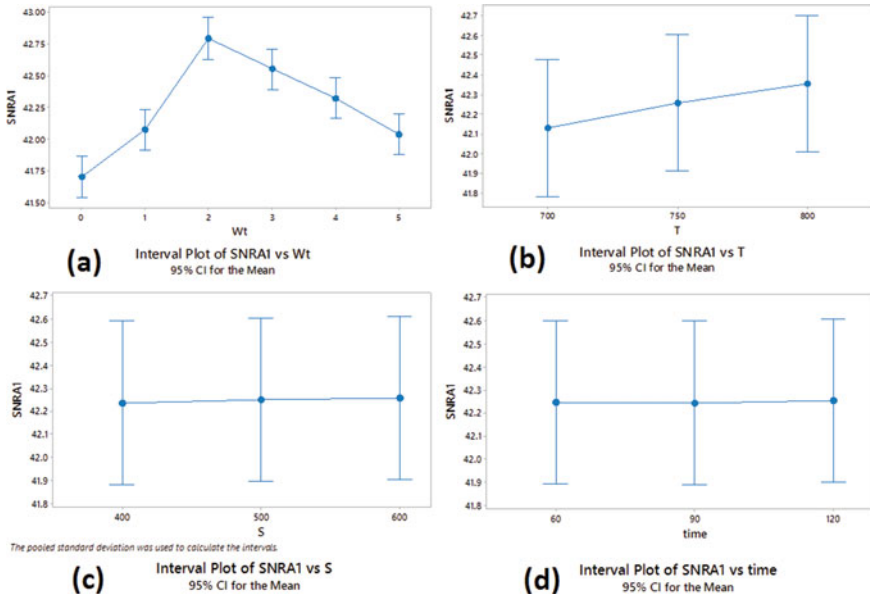


Fig. 6 Interval plots of **a** SNRA1 versus Wt%, **b** SNRA1 versus temperature of melting, **c** SNRA1 versus stirring speed, and **d** SNRA1 versus stirring time

is playing a greater contribution in the tensile strength of resultant composite. The melting temperature of furnace is playing greater contribution in process parameters. Stirring speed and stirring times are contributing next to temperature. But, it does not indicate that the influence of the other parameters is negligible, because the levels of these parameters were chosen based on the literature available [13–15]. So the range of parameters is closure to optimum values and not shown much effect with the change in values.

3.3 General Linear Model: Tensile Strength Versus Wt, T, S, Time

General linear regression equation was developed using Minitab 17. This developed model gives the relationship between predicted values and response variables by fitting a linear Eq. (7) to the measured data.

Regression equation:

$$\begin{aligned}
 \text{Tensile strength} = & 129.685 - 8.012 \text{ Wt}\%0 - 2.662 \text{ Wt}\%1 \\
 & + 8.335 \text{ Wt}\%2 + 4.535 \text{ Wt}\%3 \\
 & + 0.988 \text{ Wt}\%4 - 3.185 \text{ Wt}\%5 - 1.767 T_{700} \\
 & + 0.147 T_{750} + 1.620 T_{800} \\
 & - 0.117 S_{400} + 0.000 S_{500} \\
 & + 0.117 S_{600} - 0.063 \text{ time}_{60} \\
 & - 0.040 \text{ time}_{90} + 0.103 \text{ time}_{120}
 \end{aligned} \tag{7}$$

The normal plot of residuals as shown in Fig. 7 revealed that the experimental values are closely following straight line and are more accurate.

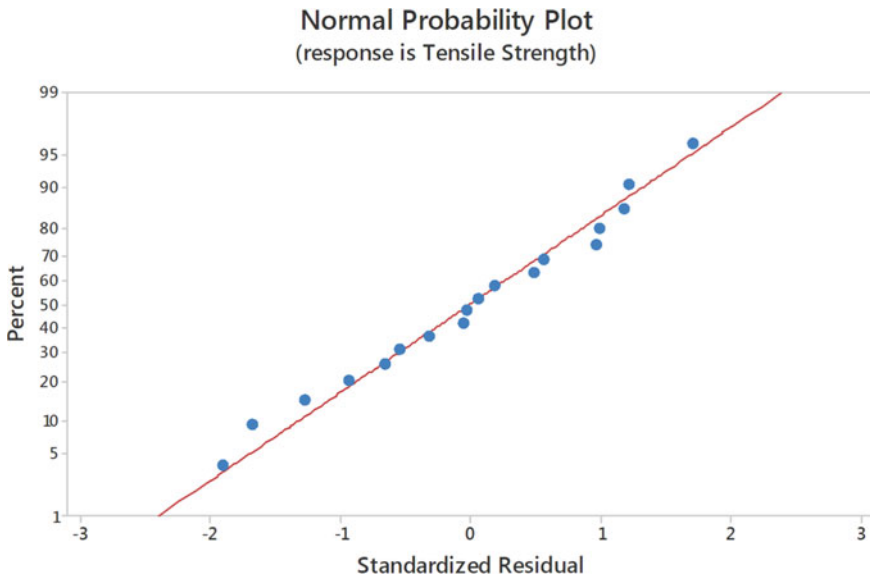


Fig. 7 Normal plot of residuals for tensile strength

4 Conclusions

1. NRHA-reinforced Al6061 composites were successfully fabricated using ultrasonicator-assisted stir casting. The microstructure revealed uniform distribution of reinforcement particles.
2. It is found that the Wt% of reinforcement is playing a major role in the strength of resultant composite. In the other parameters, the melting temperature is more influential within the given ranges.
3. The confirmation test was conducted at optimum levels of all the factors, and the result is found satisfactory.
4. The influence of the other parameters, viz. melting temperature, stirring speed, and stirring time, was analyzed using ANOVA and found that the increase in all these parameters improved the tensile strength. This is due to proper mixing of metal and reinforcement and avoidance of clusters.
5. The normal plot of residuals revealed that the experimental values are closely following straight line and were more accurate.
6. When compared with the present available literature, better tensile strength values were obtained with the addition of less weight percentage of RHA in nano-size than micro-size. This is due to the increase in the surface area of nanoparticles provided more resisting area against tensile loading which leads to enhanced tensile strength. The ultrasonication and stirring methods distributed the particles uniformly and avoided clustering and thereby improved the tensile strengths of composites developed.

References

1. Prasad DS, Shoba C, Ramanaiah N (2014) Investigations on mechanical properties of aluminum hybrid composites. *J Mater Res Technol* 3(1):79–85
2. Shoba C, Ramanaiah N, Rao DN (2015) Optimizing the machining parameters for minimum surface roughness in turning Al/6% SiC/6% RHA hybrid composites
3. Prasad DS, Shoba C (2014) Hybrid composites—a better choice for high wear resistant materials. *J Mater Res Technol* 3(2):172–178
4. Prasad DS, Shoba C (2016) Experimental evaluation onto the damping behavior of Al/SiC/RHA hybrid composites. *J Mater Res Technol* 5(2):123–130
5. Shoba C, Ramanaiah N, Rao DN (2015) Influence of dislocation density on the residual stresses induced while machining Al/SiC/RHA hybrid composites. *J Mater Res Technol* 4(3):273–277
6. Alaname KK, Adewale TM, Olubambi PA (2015) Corrosion and wear behavior of Al-Mg-Si alloy matrix hybrid composites reinforced with RHA and SiC. *J Mater Res Technol* 3(1):9–16
7. Alaname KK, Olubambi PA (2013) Corrosion and wear behavior of RHA—alumina reinforced Al-Mg-Si alloy matrix hybrid composites. *J Mater Res Technol* 2(2):188–194
8. Bodurin MO, Alaname KK, Chown LH (2015) Aluminum matrix hybrid composites: a review of reinforcement philosophies; mechanical, corrosion and tribological characteristics. *J Mater Res Technol* 4(4):434–445
9. Saravanan SD, Kumar MS (2013) Effect of mechanical properties on RHA reinforced AlSi10Mg matrix composites. *Proc Eng* 64:1505–1513

10. Subrahmanyam V, Lingaraju D, Subbarao VV (2015) Synthesis and Raman scattering characterization of NRHA for nanocomposite applications. *Mater Today Proc* 2:4317–4322
11. Subrahmanyam V, Lingaraju D, Subbarao VV (2018) Synthesis, characterization and hardness studies of NRHA reinforced Al6061 nanocomposites. *J Eng Sci Technol* 13:2916–2929
12. Subrahmanyam V, Lingaraju D, Subbarao VV (2018) Optimization of milling parameters of planetary ball mill for synthesizing nano particles. *Int J Mech Eng Technol* 9:1579–1589
13. Yang Y, Lan J, Li X (2004) Study on bulk aluminum matrix nano-composite fabricated by ultrasonic dispersion of nano-sized SiC particles in molten aluminum alloy. *Mater Sci Eng* 380:378–386
14. Jia S, Zhang D, Nastac L (2013) Experimental and numerical analysis of the 6061-based nanocomposites fabricated via ultrasonic processing. *J Mater Eng Perform* 24(6):2225–2233
15. Kumar VMV, Shirur S, Nampoorhiri J, Ravi KR, Siddhalingeswar IG (2018) Synthesis, characterization and mechanical properties of AA7075 based MMCs reinforced with TiB₂ particles processed through ultrasonic assisted in-situ casting technique. *Trans Indian Inst Met* 71(4):841–848

Effects of UAV Flight Parameters Over Droplet Distribution in Pesticide Spraying



Umamaheswara Rao Mogili, B. B. V. L. Deepak, P. Syam Sundar, and Ramu Eswam

Abstract The development of UAV vehicles in India has many benefits; the main one is in the field of agriculture. There has been a lot of ground machinery uses in the agricultural field. However, until now, there are still many deficiencies in practice. The aspect that is considered quite influential in this case is the droplet deposition over the crop. The distribution of the droplets and the characteristics of the downward swirling flow field in the unmanned plant protection machine under precise operating parameters (speed, height) are discussed. The research results can be used for low altitude and volume unmanned plant protection technology research and the establishment of machines for low altitude and volume applications. The present study is to observe the influences of the flight parameters over droplet distributions. The spray test was carried out by changing the operating heights 2 m, 3 m, and 4 m of the quadcopter at a speed of 4 m/s. The sampling droplet collectors are set in three layers along with the height of the crop, and water-sensitive papers are used as droplet collectors. The result shows, a flying height of 2 m, the total amount of droplets deposited in three layers of the crop is high. The deposition of droplets on the top layer of the crop is higher than the deposition on the middle and bottom layers. The deposition effect and the effect of coefficient of variation of the distribution uniformity of the droplets on the top, middle, and bottom layers of the crop plant are different. Results of the present study prove that UAV aerial spraying is the most reliable solution for pesticide spraying applications.

Keywords UAV · Quadcopter · Water-sensitive paper · Nozzles · Droplet deposition

1 Introduction

Agriculture is the foundation of people's livelihood and is strong in the country. India is a country with the highest wide area. Especially, crop diseases pose a major threat,

U. R. Mogili (✉) · B. B. V. L. Deepak · P. Syam Sundar · R. Eswam
Industrial Design Department, National Institute of Technology, Rourkela, India

© The Author(s), under exclusive license to Springer Nature Singapore Pte Ltd. 2022
B. B. V. L. Deepak et al. (eds.), *Applications of Computational Methods in Manufacturing and Product Design*, Lecture Notes in Mechanical Engineering,
https://doi.org/10.1007/978-981-19-0296-3_58

633

affecting food production safety, and restricting agricultural production. There are many types of crop diseases and insect pests in India, and the amount is heavy. This is an important factor that decides the improvement of product quality and agriculture production in any country. Presently, ground machinery is using to control these diseases in agriculture fields, and recently, unmanned aerial vehicles (UAVs) are introduced for these purposes. These are also called drones. UAVs are non-pilot vehicles to fly wireless or automatic adjustment without boarding. These aircraft includes vertical takeoffs, horizontal takeoffs, tilt rotors, duct fan, and helicopter, and they can be divided by the distance [1, 2].

UAVs have been applied to a variety of precision agriculture applications like vegetation monitoring; investigation of the substance content, soil content estimation, and pesticide spraying. Coming to the pesticide spraying applications, pesticides are a major agricultural material that is indispensable in agriculture. These pesticides increase crop productivity by 45% [3]. Pesticide spraying is more popular in the present trend of UAV practices. UAV pesticide spraying is harmful while spraying the pesticides over the crops comparing with manual spraying. The implementation of these technologies will change traditional Indian mechanization. The method of applying pesticides in the agriculture fields makes the realization of high stalk crop plant protection mechanization as possible. Currently, with the application of agriculture unmanned helicopters, the spray quality of agriculture drone spraying device and the prevention of field pests conducted some explorations by national and international research scholars [4–6]. The research in the development of the plant protection operations of different types of crops has some achievements. A UAV is developed for plant protection operation; the droplet particle size and spray flow rate were studied [7]. A study was made using a WPH642 unmanned helicopter which influences machine spraying parameters on the distribution of droplet deposition on rice crop [8]. A Z3 type plant protection drone with a flying height of 5 m and flying when the operating speed is 3 m/s and the crosswind speed is 3 m/s, the result shows that 90% of the droplet drift under this condition is within 8 m [9].

Due to the influence of aerial operation conditions and airflow, plant protection drones are relatively on the ground; pesticide drift is more likely to occur during aviation operations [10, 11]. Droplet floating migration is divided into ground spray drift and airborne spray drift. The test method of ground spray drift is mainly used droplet collectors such as water-sensitive papers (WSPs), mylar cards, and polyester cards for receiving the airborne droplets [12–14]. An indoor UAV simulation platform was constructed to conduct the test for droplet deposition over the water-sensitive paper to analyze the droplet deposition characteristics under different conditions [15]. A field trial was conducted by using a UAV with a height of 2 m above the rice crop and a flying speed of 2 m/s, 4 m/s, 6 m/s. For droplets, the collection used a water-sensitive paper and statically analyzed the deposition on the rice plant [16].

The above-limited technical research on pesticide spraying was conducted in different conditions with different parameters. At the same time, the above research aimed for large-scale area crop fields but not for the small-scale area crop fields. The present study focuses on the small-scale crop fields and deposition of droplets over the crop plants. The characteristics of droplet drift distribution using drones were

analyzed with different parameters. Wind speeds, specific environmental parameters, and flight parameters have explained the law of droplet drift with the ground-drifting test. Conditions like operating height and flight speed influence the amount of drift on the ground and in the air. At the same time, the study focuses on small-scale area crop fields with low-volume pesticide spraying rates. The study evaluates the spray deposition uniformity by using a quadcopter UAV with a height of 2 m, 3 m, 4 m above the rice crop and a constant flying speed of 4 m/s.

2 Materials and Methods

2.1 Parameters of UAV

The quadcopter UAV spray equipment, which was used in this study, was built in the industrial design department, National Institute of Technology, Rourkela, India. The quadcopter UAV pesticide spraying system is shown in Fig. 1. The quadcopter was built with four brushless motors, a flight controller, four ESCs, 2 clockwise carbon propellers, 2 anticlockwise carbon propellers, GPS, and a 4S LIPO battery.

The equipped pesticide tank capacity is 1 L, and the amount of liquid applied is 0.75 L; spray width is 1.5 m; operating speed is 4 m/s; there is two twin jet nozzle; each nozzle has a flow rate of 250 mL/min. All technical parameters are shown in Table 1. The quadcopter has controlled with manual mode and automatic mode also. The working height and speed can be controlled according to the job requirement.



Fig. 1 Quadcopter ready to fly in departmental lawn

Table 1 Technical parameters of quadcopter spraying system

Parameters	Value	Remark
Flying height (m)	2, 3, 4	Autonomous set
Flying speed (m/s)	4	Autonomous set
Spraying width (m)	1.5	–
Altitude (m)	0–20	Autonomous set
Control distance (m)	500	Flysky i6 remote control
Rotor diameter (inch)	10 * 4.7	APC SF Carbon fiber
Motor speed (Kv)	920	DJI
Battery (v)	16.8	LIPO
Spraying nozzles	2	–
Nozzle type	Flat fan	Twin jet
Nozzle pressure (mPa)	0.2	–
Spray flow rate (mL/min)	250	–

2.2 Experimental Method

The experiment was carried out in departmental lawns of the National Institute of Technology, Rourkela, India. The departmental lawns have planted with the Iresine plant, which bears extremely beautiful foliage in different shades of red and green. Moreover, this plant height is equal to the healthy rice plant of 1–1.4 m. The author doing this experiment using Iresine plants, because of preventing the damage in the healthy rice plants resides in original crop field. The lifting capacities of the quadcopter were measured to test the constraints of lifting a pesticide sprinkling UAV device [17].

Instead of using harmful chemicals, water was used as a liquid volume pesticide. The pesticide tank is filled with 1 L of water and is equipped with a quadcopter system. Water-sensitive papers with the size of 0.075 m × 0.025 m are using as droplet collectors for collecting droplets while spraying the pesticide. In the experimental site, the droplet collectors were placed on the Iresine plant in the top, middle, and bottom layers shown in Fig. 2. The bottom layer is positioned at the height of 0.4 m from the soil surface, the middle layer positioned at the height of 0.8 m, and the top layer positioned at the height of 1.2 m. The water-sensitive papers were attached with clips because papers have not trembled while increasing the propeller's throttle at various speeds.

During the test, the quadcopter controller obtains real-time information through the onboard GPS speed, and altitude information is used to control the flight altitude of the quadcopter. The remote control quadcopter took off 10 m from the test site and accelerated as per the test schedule. Set the speed, open the spray system, maintain a constant speed, and follow the predetermined height and pass through the droplet collators at a fixed point in the horizontal position are shown in Fig. 3. After Continues fly for 8 m turn off the spray system, bypass machine from test site and return

Fig. 2 Deployment of droplet collectors

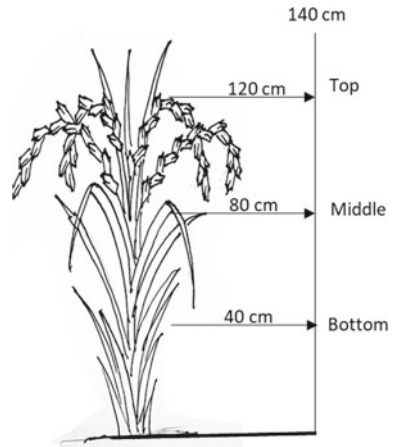


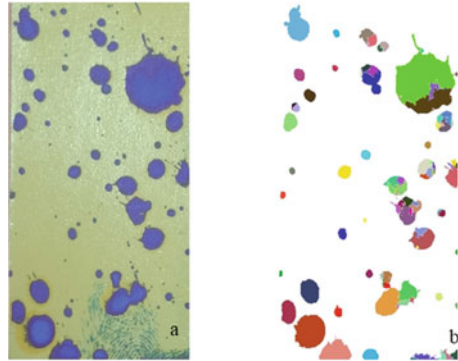
Fig. 3 Quadcopter spraying pesticide over the plants



it to starting point using RTL (Return To Launch) command. During the test, the quadcopter takes off three times with the flight height of 2 m, 3 m, 4 m, and a constant speed of 4 m/s. Positioning data are obtained from the momentum of the quadcopter takes off.

After completing the three test flights, water-sensitive papers were collected immediately from the plant and gathered into ziplock covers. Mark, it to be ready to test after the deposited water drops have dried. The collected WSP was classified according to each test and scanned using a public mobile application DropLeaf

Fig. 4 **a** Collected WSP from the test site, **b** analyzed droplet distribution on dots per cm^2



[18] to analyze digitally. The analyzed and sample water-sensitive paper is shown in Fig. 4a and b.

3 Results and Discussion

3.1 Droplet Deposition Density

Spray uniformity was tested at different flying heights with a constant flying speed. The droplet dots placed on WSP were sum up to decide the number of droplets per cm^2 which provides information on the uniformity shown in Table 2. However, the key issue in aerial spraying applications depends on parameters such as accuracy, mobility, efficiency, and drift of the pesticides reached the target plants. Any spraying test is decided by the speeds of rotors, which influences the droplet deposition on test plants that could be appropriate to apply the same scenario for aerial spraying applications over rice plants [19].

The droplet deposition densities on the top, middle, and bottom layers were decreasing when the flight height is increasing shown in Table 2. The droplet densities were smallest with 6.41, 4.23, and 2.01 droplets per cm^2 under the flight height of 4 m and flight speed of 4 m/s. The same, droplet deposition density was highest

Table 2 Droplet deposition at different heights

Quadcopter height (m)	Quadcopter speed (m/s)	Number of drops	Coverage area (%)	Droplet density (drop/ cm^2)		
				Top layer	Middle layer	Bottom layer
2	4	146	38.09	10.25	8.21	5.26
3	4	111	16.05	7.58	5.92	2.56
4	4	79	10.56	6.41	4.23	2.01

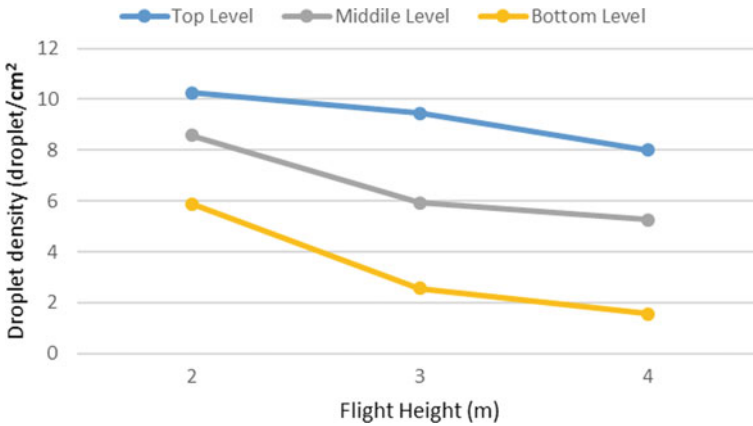


Fig. 5 Statics of droplet densities in different layers at various heights

with 10.25, 8.21, and 5.26 droplet/cm² under the flight height of 2 m and flight speed of 4 m/s. The droplet deposition density was smallest in the top layer and largest in the bottom layer.

Figure 5 shows the percentage of droplet densities of each layer of the crop plant at different heights. Due to the flight parameters, droplet densities of each layer are increased from the bottom layer to the top layer. Droplet density happened during the quadcopter spraying with the flying height of 2 m shows the highest density at three layers as 10.25, 9.45, and 8.01 followed by the flying height of 3 m/s and 4 m/s, respectively, with a constant flying speed of 4 m/s.

3.2 Spray Uniformity

The spray uniformity of the droplet spatial deposition is defined by calculating the coefficient of variation (CV) of droplet deposition. The spraying uniformity of different height at various layers is shown in Table 3. The following Eq. (1) calculated the CV of droplet deposition density.

Table 3 Spraying uniformity at various heights

Quadcopter height (m)	Droplet density (drop/cm ²)			Std.	CV (%)
	Top layer	Middle layer	Bottom layer		
2	10.25	8.59	5.89	2.84	34.43
3	9.45	5.92	2.56	4.91	82.19
4	8.01	5.26	1.56	4.34	87.73

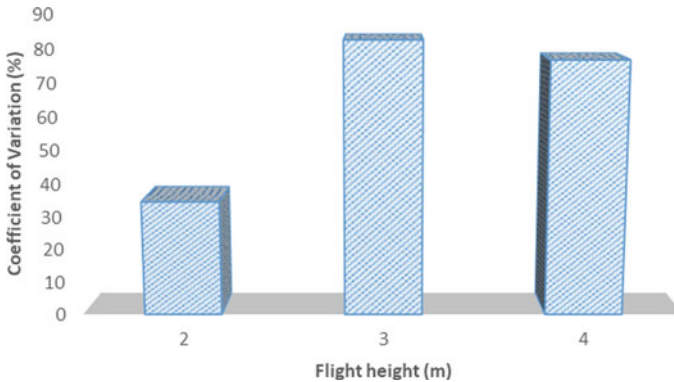


Fig. 6 Spraying uniformity of different flight heights

$$CV(\%) = \frac{S}{\bar{V}} \times 100 \quad (1)$$

where S is the standard deviation, and \bar{V} is the number of droplets per unit area at each sampling collector.

$$S = \sqrt{\frac{\sum_{i=1}^n (V_i - \bar{V})^2}{(n - 1)}} \quad (2)$$

where V_i is the droplet deposition value of each sampling point, and n is the total number of sampling points. The CV of the droplet densities is shown in Table 3.

Spray uniformity of the droplet deposition on the crop plants is set out by the coefficient of variation. If the coefficient of variation value is smaller, then the spray uniformity of the droplet deposition is good, and the coefficient of variation value is high; then, the spray uniformity of the droplet deposition is not that good. Figure 6 shows the spraying uniformity of different flight heights. The CV value 34.43% at flight height 2 m shows the smallest value compare to other flight height. Hence, the coefficient of variation value of droplet deposition densities formed during the flight height 2 m at quadcopter flying speed 4 m/s shows the best uniformity. Therefore, the flight parameters influence the spray deposition over the crop plants.

4 Conclusion

Agriculture is the primary source in India and the largest producer of wheat and rice product in the world. However, the non-availability of laborers and the increasing cost of agriculture planting are the main drawbacks in the Indian agriculture field.

The new mechatronic equipment's (UAVs) efficiency is higher compared to manual mechanization. At the same time, it reduces the labor and agriculture planting costs. This study aimed at the behavior of the quadcopter spraying system under different operating heights with a constant flying speed. At different flight heights and flying speeds, they can affect the size and droplet distribution. Because of this study, the operating height is decreased; the droplet deposition rate is increased at variable flying speed. The top layer had a max droplet density of 10.25 compared to the other two layers with 7.51 and 6.41; this occurred in almost all treatments. In three treatments flying speed of multi-rotor machine is 4 m/s at flying heights of 2 m, 3 m, and 4 m. As a result, flight height 2 m and flying speed 4 m/s suitable for spraying in small are crops. The research would help to provide a technical assistant to improve the efficiency and effectiveness of the quadcopter aerial spraying system for wheat and rice cultivation.

Acknowledgements The work is sponsored by Science and Engineering Research Board, Government of India with a sanction order number ECR/2017/000140 granted on July 5, 2017.

References

1. Zhang C, Kovacs JM (2012) The application of small unmanned aerial systems for precision agriculture: a review. *Precision Agric* 13(6):693–712
2. Mogili UR, Deepak BBVL (2018) Review on application of drone systems in precision agriculture. *Proc comput Sci* 133:502–509
3. Oerke EC (2006) Crop losses to pests. *J Agric Sci* 144(1):31–43
4. Giles DK, Billing RC (2015) Deployment and performance of a UAV for crop spraying. *Chem Eng Trans* 44:307–322
5. Huang Y, Hoffmann WC, Lan Y, Wu W, Fritz BK (2009) Development of a spray system for an unmanned aerial vehicle platform. *Appl Eng Agric* 25(6):803–809
6. Mogili UR, Deepak BBVL (2020) An intelligent drone for agriculture applications with the aid of the mavlink protocol. In: *Innovative product design and intelligent manufacturing systems*, pp 195–205. Springer, Singapore
7. Huang Y, Hoffmann WC, Lan Y et al (2009) Development of a spray system for an unmanned aerial vehicle platform. *Appl Eng Agric* 25(6):803–809
8. Jing Z, Xiongui H, Jianli S et al (2012) Influence of spraying parameters of unmanned aircraft on droplets deposition. *Trans Chin Soc Agric Mach* 43(12):94–96
9. Xinyu X, Kang T, Weicai Q et al (2014) Drift and deposition of ultra-low altitude and low volume application in paddy field. *Int J Agric Biol* 7(4):23–28
10. Antuniassi UR, Motta AAB, Chechetto RG et al (2014) Spray drift from aerial application. *Asp Appl Biol* 122:279–284
11. Thomson SJ, Womac AR, Mulrooney JE (2013) Reducing pesticide drift by considering propeller rotation effects from aerial application near buffer zones. *Sustain Agric Res* 2(3):41
12. Qin W, Xue X, Zhang S, Gu W, Wang B (2018) Droplet deposition and efficiency of fungicides sprayed with small UAV against wheat powdery mildew. *Int J Agric Biol Eng* 11(2):27–32
13. Tang Y, Hou CJ, Luo SM, Lin JT, Yang Z, Huang WF (2018) Effects of operation height and tree shape on droplet deposition in citrus trees using an unmanned aerial vehicle. *Comput Electron Agric* 148:1–7
14. Zhou Q, Xue X, Qin W, Chen C, Cai C (2020) Analysis of pesticide use efficiency of a UAV sprayer at different growth stages of rice. *Int J Precis Agric Aviat* 3(1)

15. Lv M, Xiao S, Yu T, He Y (2019) Influence of UAV flight speed on droplet deposition characteristics with the application of infrared thermal imaging. *Int J Agric Biol Eng* 12(3):10–17
16. Kharim MNA, Wayayok A, Shariff ARM, Abdullah AF, Husin EM (2019) Droplet deposition density of organic liquid fertilizer at low altitude UAV aerial spraying in rice cultivation. *Comput Electron Agric* 167:105045
17. Mogili UR, Deepak BBVL (2020) Study of takeoff constraints for lifting an agriculture pesticide sprinkling multi-rotor system. In: *Advances in materials and manufacturing engineering*, pp 203–210. Springer, Singapore
18. Brandoli B, Spadon G, Esau T, Hennessy P, Carvalho A, Rodrigues Jr J, Amer-Yahia S (2020) DropLeaf: a precision farming smartphone application for measuring pesticide spraying methods. *J Comput Electron Agric*
19. Mogili UR, Deepak BBVL (2020) Influence of drone rotors over droplet distribution in precision agriculture. In: *Advanced manufacturing systems and innovative product design: select proceedings of IPDIMS 2020*, p 401

A Review of Human Activity Recognition (HAV) Techniques



T Venkateswara Rao and Dhananjay Singh Bisht

Abstract Human–computer interaction (HCI) has become a very common phenomenon in the present day as many human activities including learning are increasingly becoming digital. Smart personal computing devices like smartphones and tablets, laptops and personal computers are increasingly becoming ubiquitous. To enable HCI, human activity can be recognized by the use of different interactive devices. Some recent important research in this field have been discussed in this paper. Human action recognition-based (HAV) technology and research approaches and their applications have also been discussed.

Keywords Human–computer interaction (HCI) · Human action recognition (HAV) · Natural user interface (NUI)

1 Introduction

Human–machine interaction (HMI) is a term which has largely been substituted by the term human–computer interaction (HCI) [1]. The communication process between user and computer or machine is called as HCI/HMI [2]. Today, the term machine typically refers to some smart device like a mobile phone, tablet, laptop, personal computer, or even an IoT-based product with which a human user frequently interacts with [3]. Many are involved in developing some interactive technology that can be helpful for everyday problems in human life. Human action recognition (HAR) is finding important applications in the fields of gaming, health care, architecture, etc., leading to the design and development of various interactive interfaces between users and computing devices [4].

T Venkateswara Rao (✉) · D. S. Bisht
National Institute of Technology, Rourkela, Odisha 769008, India

© The Author(s), under exclusive license to Springer Nature Singapore Pte Ltd. 2022
B. B. V. L. Deepak et al. (eds.), *Applications of Computational Methods in Manufacturing and Product Design*, Lecture Notes in Mechanical Engineering,
https://doi.org/10.1007/978-981-19-0296-3_59

2 Human-Computer Interaction

The goal of HCI is described as “to improve or develop usability, effectiveness, efficiency, safety, and utility of systems that include computer” [5]. Figure 1 shows the HCI interaction loop which consists of a “human layer” based on the vocal or human motor system for defining the task and performing it as an input to the subsequent “computation layer” [6]. From the computation layer, one receives the output through human senses. Sensors are used in the computation layer for receiving the input from human layer. The computer system will process the input and show its current state while generating its response using outputs such as audio speakers, visual display monitors, and head-mounted displays [6].

HCI is a field of research in multidisciplinary areas dealing with both software and hardware aspects for development of an end application device [7]. During the interaction between human and computer, comfort and usability are generally two important considerations [8].

2.1 User Interfaces

The interface between a computing system and a user is represented as user interface (UI). Design of user interfaces is an important activity in HCI. The early UIs for HCI were operable using devices such as keyboard and mouse [9].

Natural user interface (NUI) is a special kind of UI. Today, monitoring and recognition of user’s eye, face, hand, body motion, motion tracking, gesture, or pose can be done with help of different NUIs. NUI is further characterized into vision user interfaces (VUIs), audio user interface (AUI), touch user interface (TUI), etc. Shown in Table 1 are different devices based on NUIs along with their corresponding applications in the real world [10]. Also, Table 2 lists a few popular sensors used in different NUI devices, along with their applications and brief operational descriptions.

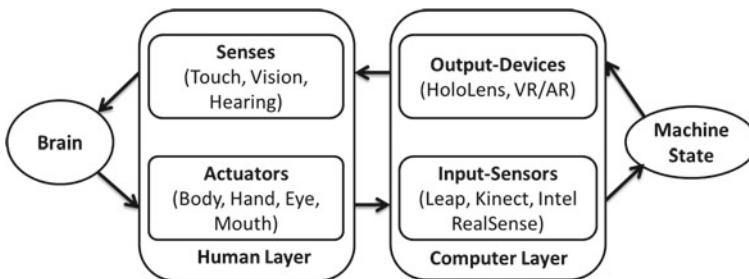


Fig. 1 HCI working loop

Table 1 Different NUIs with device and application

S. No.	Type of NUI	Examples of devices	Applications
1	Vision user interface (VUI)	Tobii EyeX [1]	Gaming
2	Tactile user interface (TUI)	Touch X [2], Phantom Omni [3]	Smart phones, tablets, personal computer, game consoles, ATM, patient mobility, drawing, etc.
3	Audio user interface (AUI)	Apple Siri, Amazon Alexa, Microsoft Windows (Cortana), Google Assistant [4]	Automobile interiors, home appliances, speech-to-text, etc.
4	Motion tracking	Wii remote, play station move, Kinect [5], leap motion [6], Xtion,	Gaming, surveillance, rehabilitation, education

Table 2 Activity recognition sensors

S. No.	Type of sensor	Applications	Description
1	Motion sensor [7]	Security, gaming	Motion detection and tracking, counting of users could be done
2	Proximity sensor [8]	Gesture recognition	Detect objects nearby, also without having physical contact
3	Accelerometer [9]	Tracking, fall detection, activities of daily living, posture recognition	Calculate rate of change of motion, useful to detect and track movements
4	Magnetometer [10]	Posture recognition	By measuring changes in magnetic field, changes in position can be monitored

3 Categories of Human Activity Recognitions (HAV)

Today, HAR seems to be an attractive research area for researchers in the applied areas of health, gaming, security, remote monitor and intelligent environments. Activity recognition is expressed as the capability for detecting/recognizing a physical activity on the basis of data received from various sensors. Using such technology, users can capture their daily activities like cooking, watching TV, sleeping, and eating [11]. Different sensors are utilized for capturing daily life human activities [12]. Vision-based activity recognition approaches are at the forefront of such applications where a camera captures human activity information. Computer vision-based technology is easy to customize and provides good results, but issues such as violation of human privacy exist [13].

Activity recognition involves recognition of physical activities for an individual human being or a group of people. Some of the activities are performed by a single

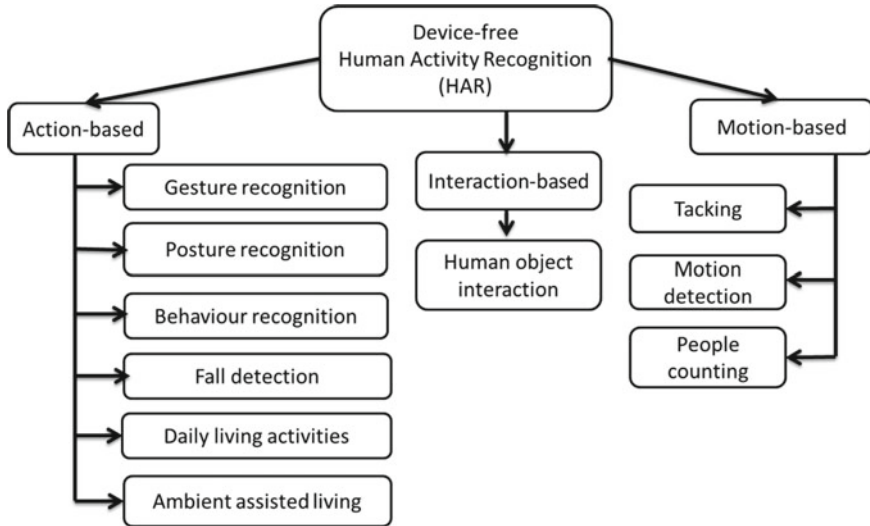


Fig. 2 Schematic classification of different categories of HAR [14]

person using whole body like walking, sitting, jumping, dancing, and running. Some activities are performed by specific body parts such as using hands for waving and performing different gestures. HAR could be understood in three sub-categories: (1) action-based activities, (2) interaction-based activities, and (3) motion-based activities depicted as in Fig. 2 [11].

3.1 Action-Based Activities

Such activities are performed by the action of a human body involving either a specific body part or the entire body. In the following, sub-sections are presented different categories of human activities relevant for action recognition also depicted in Table 3 [11].

3.1.1 Gesture Recognition

Gesture recognition is one of the most prominent kind of action recognition. Gestures have enormous potential to deliver intuitive, creative, and natural methods for communicating with computers. The interaction process involves three main phases, i.e., tacking, detecting, and recognition. Interactive technologies for recognition of hand gesture are of two main kinds—vision based and contact based [31].

Table 3 Technologies used in action-based recognition and applications

S. No.	Action-based recognition	Approach	Technology	Sensor used	Application	Refs.
1	Gesture recognition	Vision based	Surveillance camera	Leap motion, Kinect, Intel RealSense, RGB camera	Remote monitoring, gaming, sign language, smart screen interaction	[15] [16] [17] [18]
		Object tagged	Accelerometer, microphone			
		Wearable devices	Smartwatch, gloves, bracelet			
2	Posture recognition	Vision based	Camera	Intel RealSense,	Care centers, smart homes, hospitals, smart offices	[19] [20] [21] [22]
		Device free	Wi-Fi			
		Wearable devices	Gyroscope, smartphone, accelerometer			
3	Behavior recognition	Vision based	Camera	Intel RealSense, Kinect, leap motion	Care centers, shopping centers, security and surveillance	[23] [24] [25] [26]
		Device free	Wi-Fi			
4	Fall detection recognition	Device free	Wi-Fi	Asus Xtion, RGB camera, Motion sensor	Industrial workplace, care centers, hospitals	[27] [25] [28] [29]
		Wearable devices	Accelerometer, smartphone, magnetometer			
5	Daily living activities recognition	Vision based	Camera	Intel RealSense, Kinect, Leap motion	Care centers, security and surveillance, smart homes,	[26] [30] [25] [31]
		Device free	Motion sensor, temperature sensor			
		Wearable devices	Gyroscope, accelerometer, temperature sensor			
6	Ambient-assisted living recognition	Vision based	Camera	RGB camera, Wii remote	Exercise management, care center	[32] [33]
		Wearable devices	Infrared sensor, inertial sensors			

3.1.2 Posture Recognition

Many activities of daily living involve frequent changes to human posture such as walking, jumping, playing, and cooking food. Here, recognition of posture is achieved using different vision-based and wearable devices, as well as through

device-free means. Sensors like cameras, accelerometers, and gyroscopes are frequently used for this purpose [34].

3.1.3 Behavior Recognition

Behavior recognition is often more relevant in contexts such as classrooms, elderly care centers, and shopping malls. Human behavior data can be captured through various means such as proximity and depth sensors, vision-based devices and through device-free approaches [35].

3.1.4 Fall Detection

Fall involves sudden positioning of the human body from a standing/sitting state to that of lying down without any control [32]. Falls may lead to major or minor injuries. Today, many researchers are conducting research in the field of fall detection. Fall detection is typically performed using wearable devices as well as device-free approaches. Some of the applications of fall detection research are within the contexts of hospitals, industrial work places, and elder care centers [30].

3.1.5 Daily Living Activities

Research involving recognition of daily living activities is typically made indoors in the contexts of eating, sitting, cooking, bathing, sleeping, dressing, etc. Recognition of such types of activities is important in smart homes, care centers, hospitals, etc. Some of the technologies (e.g., motion sensors, camera, accelerometer, temperature sensors) and approaches (e.g., vision based, wearable devices, device free) find applications in various settings of daily living activities, e.g., security, care centers, smart environments, etc. [4].

3.1.6 Ambient-Assisted Living

Aged people may need someone's help in certain situations where ambient-assisted living tools could be useful. Different approaches (e.g., vision based, wearable devices) and technology (e.g. inertial sensors, camera) are used for ambient assisting living typically in the contexts of elderly care centers, exercise management, medical management, and independent living [36].

4 Discussion and Conclusion

In the context of education, and especially to improve teaching and learning for academicians and learners, there exists an enormous potential in using different human action recognition-specific interactive devices today [37]. Also, educational systems are increasingly becoming digital and online where principles of digital, interactive, and instructional learning, many times based on immersive environment experiences find relevance [38]. As described in this paper, HCIs that find popularity among interactive devices today include recognition of gestures, facial features, human voice, eye movements, and touch and multi-touch [39].

A popular research theme in the scientific domains like computer vision, HCI, and machine learning (ML) is HAR since it plays a vital role in applications like development of NUIs and visual surveillance [40]. Within action-based recognition systems, gestures find important application in contexts such as sign languages, learning, entertainment, human–robot interaction (HRI), and increasingly for interaction and play in virtual environment using 2- or 3-dimensional images. For these purposes, depth-based cameras like Intel RealSense, Astra Pro, and Kinect are popularly used for capturing images in real world [33]. Various sensors popularly integrated with HAR-based interactive devices include wearable camera, hybrid sensor, gyroscope, magnetometer, and accelerometer [41].

HCI interfaces are increasingly becoming more accessible and easier to use in the daily living context due to easy and cost-effective availability of hardware such as cameras and sensors and related software development kits (SDK). Some of the popular applications of such devices are within the contexts of smart phones, smart homes, driverless cars, HRI, etc. The information offered in this review paper could be helpful for exploring research potential in many fields including digital learning, entertainment, health care, and elderly care.

References

1. Ke Q, Liu J, Bennamoun M, An S, Sohel F, Boussaid F (2018) Computer vision for human-machine interaction. Elsevier Ltd.
2. Bauer Z, Dominguez A, Cruz E, Gomez-Donoso F, Orts-Escolano S, Cazorla M (2020) Enhancing perception for the visually impaired with deep learning techniques and low-cost wearable sensors. *Pattern Recogn Lett* 37:27–36. <https://doi.org/10.1016/j.patrec.2019.03.008>
3. Papanastasiou G, Drigas A, Skianis C, Lytras M, Papanastasiou E (2018) Patient-centric ICTs based healthcare for students with learning, physical and/or sensory disabilities. *Telemat Inform* 35(4):654–664. <https://doi.org/10.1016/j.tele.2017.09.002>
4. Pazhoumand-Dar H (2018) Fuzzy association rule mining for recognising daily activities using Kinect sensors and a single power meter. *J Ambient Intell Humanized Comput* 9(5):1497–1515. <https://doi.org/10.1007/s12652-017-0571-8>
5. Ahmed F, Bari ASMH, Gavrilova ML (2020) Emotion recognition from body movement. *IEEE Access* 8:11761–11781. <https://doi.org/10.1109/ACCESS.2019.2963113>

6. Alonso DG, Teyseyre A, Soria A, Berdun L (2020) Hand gesture recognition in real world scenarios using approximate string matching. *Multimed Tools Appl* 79(29–30):20773–20794. <https://doi.org/10.1007/s11042-020-08913-7>
7. Shanthakumar VA, Peng C, Hansberger J, Cao L, Meacham S, Blakely V (2020) Design and evaluation of a hand gesture recognition approach for real-time interactions. *Multimed Tools Appl* 79(25–26):17707–17730. <https://doi.org/10.1007/s11042-019-08520-1>
8. Shao L, Cai Z, Liu L, Lu K (2017) Performance evaluation of deep feature learning for RGB-D image/video classification. *Inf Sci* 385–386:266–283. <https://doi.org/10.1016/j.ins.2017.01.013>
9. Chang Y (2019) Research on de-motion blur image processing based on deep learning. *J Vis Commun Image Represent* 60:371–379. <https://doi.org/10.1016/j.jvcir.2019.02.030>
10. Rashid FAN, Suriani NS, Nazari A (2018) Kinect-based physiotherapy and assessment: a comprehensive review. *Indonesian J Electr Eng Comput Sci* 11(3):1176–1187. <https://doi.org/10.11591/ijeecs.v11.i3.pp1176-1187>
11. Briz-Ponce L, Pereira A, Carvalho L, Juanes-Méndez JA, García-Peñalvo FJ (2017) Learning with mobile technologies—students’ behaviour. *Comput Human Behav* 72:612–620. <https://doi.org/10.1016/j.chb.2016.05.027>
12. Staddon JER (1983) Adaptive behavior and learning
13. Rodrigues H, Almeida F, Figueiredo V, Lopes SL (2019) Tracking e-learning through published papers: a systematic review. *Comput Educ* 136:87–98. <https://doi.org/10.1016/j.compedu.2019.03.007>
14. Hussain Z, Sheng QZ, Zhang WE (2020) A review and categorization of techniques on device-free human activity recognition. *J Netw Comput Appl* 167:102738. <https://doi.org/10.1016/j.jnca.2020.102738>
15. Rahim MA, Shin J, Islam MR (2020) Gestural flick input-based non-touch interface for character input. *Vis Comput* 36(8):1559–1572. <https://doi.org/10.1007/s00371-019-01758-8>
16. Lan YJ, Fang WC, Hsiao IYT, Chen NS (2018) Real body versus 3D avatar: the effects of different embodied learning types on EFL listening comprehension. *Educ Technol Res Dev* 66(3):709–731. <https://doi.org/10.1007/s11423-018-9569-y>
17. Pavlovic VI et al (2019) Touch gesture performed by children under 3 years old when drawing and coloring on a tablet. *Multimed Tools Appl* 11(2):1–13. <https://doi.org/10.1007/s10462-012-9356-9>
18. Li G, Wu H, Jiang G, Xu S, Liu H (2019) Dynamic gesture recognition in the internet of things. *IEEE Access* 7:23713–23724. <https://doi.org/10.1109/ACCESS.2018.2887223>
19. Ren W, Ma O, Ji H, Liu X (2020) Human posture recognition using a hybrid of fuzzy logic and machine learning approaches. *IEEE Access* 8:135628–135639. <https://doi.org/10.1109/ACCESS.2020.3011697>
20. Wang J, Payandeh S (2017) Hand motion and posture recognition in a network of calibrated cameras. *Adv Multimed* 2017. <https://doi.org/10.1155/2017/2162078>
21. Gochoo M et al (2019) Novel IoT-based privacy-preserving yoga posture recognition system using low-resolution infrared sensors and deep learning. *IEEE Internet Things J* 6(4):7192–7200. <https://doi.org/10.1109/JIOT.2019.2915095>
22. Shum HPH, Ho ESL, Jiang Y, Takagi S (2013) Real-time posture reconstruction for Microsoft Kinect. *IEEE Trans Cybern*. <https://doi.org/10.1109/TCYB.2013.2275945>
23. Han J et al (2016) CBID: a customer behavior identification system using passive tags. *IEEE/ACM Trans Netw* 24(5):2885–2898. <https://doi.org/10.1109/TNET.2015.2501103>
24. Zeng Y, Pathak PH, Mohapatra P (2015) Analyzing shopper’s behavior through Wi-Fi signals. In: *WPA 2015—Proceedings of the 2nd workshop on physical analytics*, pp 13–18. <https://doi.org/10.1145/2753497.2753508>
25. Shi Y, Du J, Ahn CR, Ragan E (2019) Impact assessment of reinforced learning methods on construction workers’ fall risk behavior using virtual reality. *Autom Constr* 104:197–214. <https://doi.org/10.1016/j.autcon.2019.04.015>
26. Adame T, Bel A, Carreras A, Melià-Seguí J, Oliver M, Pous R (2018) CUIDATS: an RFID–WSN hybrid monitoring system for smart health care environments. *Futur Gener Comput Syst* 78:602–615. <https://doi.org/10.1016/j.future.2016.12.023>

27. Parada R, Melià-Seguí J, Morenza-Cinos M, Carreras A, Pous R (2015) Using RFID to detect interactions in ambient assisted living environments. *IEEE Intell Syst* 30(4):16–22. <https://doi.org/10.1109/MIS.2015.43>
28. Shojaei-Hashemi A, Nasiopoulos P, Little JJ, Pourazad MT (2018) Video-based human fall detection in smart homes using deep learning. In: *Proceedings—IEEE International Symposium on Circuits and Systems*, vol 2018, pp 0–4. <https://doi.org/10.1109/ISCAS.2018.8351648>
29. Sung YT, Chang KE, Liu TC (2016) The effects of integrating mobile devices with teaching and learning on students' learning performance: a meta-analysis and research synthesis. *Comput Educ* 94:252–275. <https://doi.org/10.1016/j.compedu.2015.11.008>
30. Zhu C, Sheng W (2011) Wearable sensor-based hand gesture and daily activity recognition for robot-assisted living. *IEEE Trans Syst Man Cybern Part A Syst Humans* 41(3):569–573. <https://doi.org/10.1109/TSMCA.2010.2093883>
31. Alzahrani MS, Jarraya SK, Ben-Abdallah H, Ali MS (2019) Comprehensive evaluation of skeleton features-based fall detection from Microsoft Kinect v2. *Signal Image Video Process* 13(7):1431–1439. <https://doi.org/10.1007/s11760-019-01490-9>
32. Chernbumroong S, Cang S, Atkins A, Yu H (2013) Elderly activities recognition and classification for applications in assisted living. *Expert Syst Appl* 40(5):1662–1674. <https://doi.org/10.1016/j.eswa.2012.09.004>
33. Yang L, Zhang L, Dong H, Alelaiwi A, El Saddik A (2015) Evaluating and improving the depth accuracy of Kinect for Windows v2. *IEEE Sens J* 15(8):4275–4285. <https://doi.org/10.1109/JSEN.2015.2416651>
34. Webster D, Celik O (2014) Systematic review of Kinect applications in elderly care and stroke rehabilitation. *J Neuroeng Rehabil* 11(1):1–24. <https://doi.org/10.1186/1743-0003-11-108>
35. Chuang TY, Kuo MS, Fan PL, Hsu YW (2017) A Kinect-based motion-sensing game therapy to foster the learning of children with sensory integration dysfunction. *Educ Technol Res Dev* 65(3):699–717. <https://doi.org/10.1007/s11423-016-9505-y>
36. Bhuiyan M, Picking R (2011) A gesture controlled user interface for inclusive design and evaluative study of its usability. *J Softw Eng Appl* 04(09):513–521. <https://doi.org/10.4236/jsea.2011.49059>
37. Lai NK, Ang TF, Por LY, Liew CS (2018) Learning through intuitive interface: a case study on preschool learning. *Comput Educ* 126:443–458. <https://doi.org/10.1016/j.compedu.2018.08.015>
38. Al Mamun MA, Lawrie G, Wright T (2018) Instructional design of scaffolded online learning modules for self-directed and inquiry-based learning environments. *Comput Educ* 144:103695. <https://doi.org/10.1016/j.compedu.2019.103695>
39. Rautaray SS, Agrawal A (2012) Vision based hand gesture recognition for human computer interaction: a survey. *Artif Intell Rev* 43(1):1–54. <https://doi.org/10.1007/s10462-012-9356-9>
40. Saini R, Kumar P, Roy PP, Dogra DP (2018) A novel framework of continuous human-activity recognition using Kinect. *Neurocomputing* 311:99–111. <https://doi.org/10.1016/j.neucom.2018.05.042>
41. Guzsvinecz T, Szucs V, Sik-Lanyi C (2019) Suitability of the Kinect sensor and leap motion controller—a literature review. *Sensors* 19(5). <https://doi.org/10.3390/s19051072>
42. Franco A, Magnani A, Maio D (2020) A multimodal approach for human activity recognition based on skeleton and RGB data. *Pattern Recognit Lett* 131:293–299. <https://doi.org/10.1016/j.patrec.2020.01.010>
43. Lu H et al (2017) Depth map reconstruction for underwater Kinect camera using in painting and local image mode filtering. *IEEE Access* 5:7115–7122. <https://doi.org/10.1109/ACCESS.2017.2690455>
44. Oguntala GA et al (2019) SmartWall: novel RFID-enabled ambient human activity recognition using machine learning for unobtrusive health monitoring. *IEEE Access* 7:68022–68033. <https://doi.org/10.1109/ACCESS.2019.2917125>

Pothole Detection on Roads Using Canny Edge Detection Algorithm



Gunji Bala Murali, V. Santosh Kumar, Dibya Narayan Behera,
Kapil Kumar Mohanta, Omkar Tulankar, and Sanketh S. Salimath

Abstract Asphalt-surfaced pavements are subjected to broad traffic levels, from two-lane rural routes to multi-lane interstate highways. They age and deteriorate; thus, they require corrective measures to restore safety and ride-ability. The most common forms of distress on asphalt-surface pavements are potholes. In this paper, pothole detection is done with the help of machine vision, and canny edge algorithm is implemented for image segmentation and clustering, and recognized potholes are highlighted by outlining the detected potholes. Canny edge detection algorithm is used in combination of computer vision, and the model is developed using Python platform. A brief review of existing pothole recognition method is done, and based on the combination of based possible method, this model is developed, and conclusions are drawn in this paper.

Keywords Pothole detection · OpenCV · Canny edge algorithm

1 Introduction

Since the dawn of automobile industry, a number of automobiles driving on the road are increasing exponentially. Many measures are taken to improvise the driving scenario and to enhance the safety of the vehicle. Among the many factors taken into

G. B. Murali (✉) · O. Tulankar · S. S. Salimath
Vellore Institute of Technology, Vellore, Tamil Nadu 632014, India
e-mail: balamurali.g@vit.ac.in

O. Tulankar
e-mail: omkar.patil2018@vitstudent.ac.in

S. S. Salimath
e-mail: sankeths.salimath2019@vitstudent.ac.in

V. Santosh Kumar
Durga Bhavani Pracetech, Hyderabad 500033, India

D. N. Behera · K. K. Mohanta
Modern Engineering and Management Studies, Balasore 756056, India

consideration, road safety is one of the main concerns. Smooth roads without any obstructions are expected for safe driving [1]. But, due to many factors, the road safety has been reduced; one reason of this is generation of potholes on the road. There are three approaches for pothole detection which are based on 3D reconstruction [2], vibration and vision-based analysis, and vibration-based methods. Vibration method makes use of application of GPS data and accelerometer [3]. In vision-based methods, three processes are adopted, image segmentation, spectral clustering, texture matching. LASER and stereo vision are used in 3D reconstruction. One of the main concerns while developing a vision-based detection method is differentiation of the potholes with the other objects present in the frame [5]. To come up with the algorithm that effectively rectifies this problem is the concern of this paper. We have modeled the entire algorithm in Python as the programming language using OpenCV.

2 Literature Survey

The previous work done in the area of pothole detection is majorly in the areas of image segmentation, accelerometer-based data, texture mapping, and neural networks. From the literature surveyed, the usage of methods can be classified as shown in Fig. 1.

Most of the methods used comprise of image segmentation [4] methods for the reason that segmentation is much faster in terms of computation as compared to texture matching or neural networks. Koch and Brilakis [5] devised a method that uses image segmentation using histogram shape-based thresholding approximated utilizing morphological thinning and elliptic regression and later a texture comparison for detection.

The work carried by Ryu et al. [6] in image-based pothole detection system for ITS Service and Road management System uses segmentation methods that use the histogram of an input image by histogram shape-based thresholding (HST).

Fig. 1 Methods used in pothole detection survey

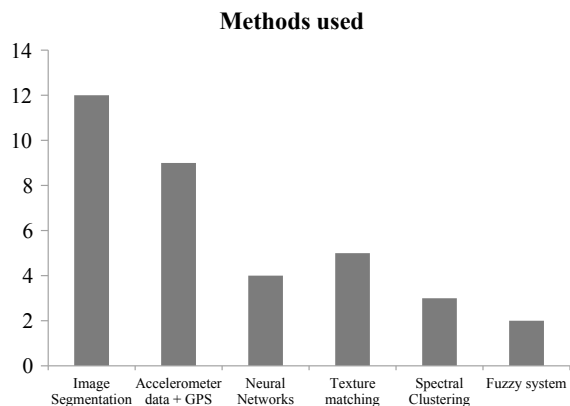
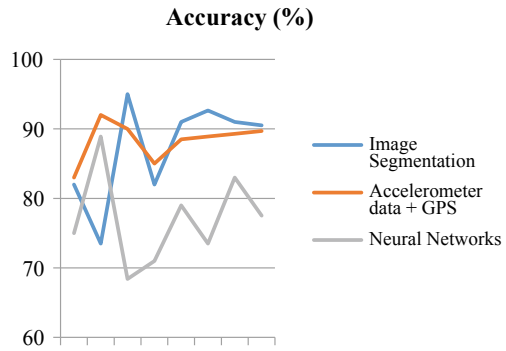


Fig. 2 Accuracies of methods



Segmentation methods used in the above literature yield a good level of accuracy as compared to other methods. The accuracies of the methods are shown in Fig. 2.

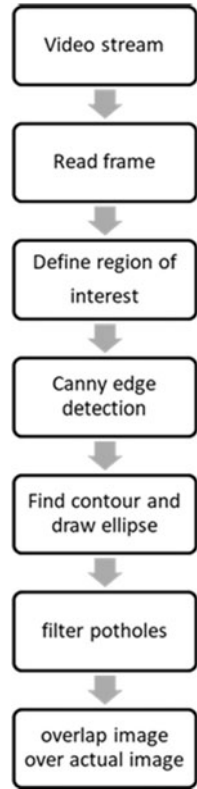
Development of pothole detection for autonomous vehicle using LIDAR-based method is developed by Suggang [7]. Automatic detection and notification of potholes and humps on roads to aid drivers with the help of vision-based approach are developed by author Madli et al. [8]. In this research article, a simple method using MATLAB to identify the path holes on the road has been proposed using canny edge detection method, which doesn't require any sort of training the algorithms like in ANN or CNN to identify the path holes.

3 Proposed Methodology

In the proposed methodology, video stream is converted in to read frame mode/image mode. Later, in that image, region of interest has been decided instead of whole image to save processing time. Apply canny edge detection method to find the edges of the potholes on the road. Draw ellipse shape for the detected edges of the potholes on the road and filter the potholes. Finally, overlap the image on the original image to match with the existed potholes on the road. The proposed methodology of detecting the potholes is shown in Fig. 3.

As described in Fig. 3, for the development of the model, following steps were adopted: Video is fed to the system live or manually. The frames are detected from the video for image segmentation. Region of interest is defined in the frame to reduce the noise. Canny edge detection algorithm is employed for edge detection of the frame. Based on the algorithm, contours are detected, and ellipse is drawn around the detected pothole surfaces. Potholes are filtered for further feature extraction from the frames. Overlap the image with the original image to highlight the detected potholes.

Fig. 3 Proposed methodology



4 Results and Discussions

The video source is first captured by the camera and read by OpenCV frame by frame, and each of the operations is done while iterating through a loop for each frame. The region of interest is an area in which the image operations are carried out so that the background is unaffected by the operations as shown in Fig. 4. In the case of our work, we define the region of interest in which the detection of potholes is carried out. We have defined it in the form of a six-sided polygon that matches the shape of the road. The region of interest is marked in terms of the frame width and height as parameters so that the algorithm can be generalized for all sizes of frames.

For creation of the region of interest, a copy of the current frame is made with all pixels having its value of 0. A polygon is defined in terms of its coordinates which is a function of the frame width and height. A bitwise addition is done between the copy and the original frame using an AND operator so that all pixels lying inside the region of interest are only added, and the rest are discarded. The region of interest copy and the original frame is then superimposed on each other, but the further operations are only carried out inside the region of interest. The region of interest creation also causes an increase in the computation speed.



Fig. 4 Region of interest in the frame

4.1 Contour Formation and Pothole Detection

The canny edge detection algorithm is a multi-stage algorithm with noise reduction, finding intensity grading of the image, non-max suppression, and thresholding as shown in Fig. 5. The noise is removed by a 5×5 Gaussian filter to remove the noise and further filtered to compute gradient using any of the gradient operators (Roberts, Sobel, Prewitt, etc.). We have used a Sobel kernel which finds the edge gradients and direction for each pixel as follows:

$$\text{Edge Gradient } (G) = \sqrt{(G_x^2 + G_y^2)} \tag{1}$$

where G_x and G_y are the derivatives in the x and y directions, respectively. The angle can also be found out by finding the slope of the derivatives.

Further, non-maxima pixels in the edges in obtained above have to be suppressed to thin the edge ridges. To do so, check to see whether each non-zero is greater than its two neighbors along the gradient direction. If so, keep unchanged, otherwise, set it to 0. A full image scan is done to remove any pixels that do not constitute to form an edge, which is decided if the gradient is perpendicular to the edge direction.

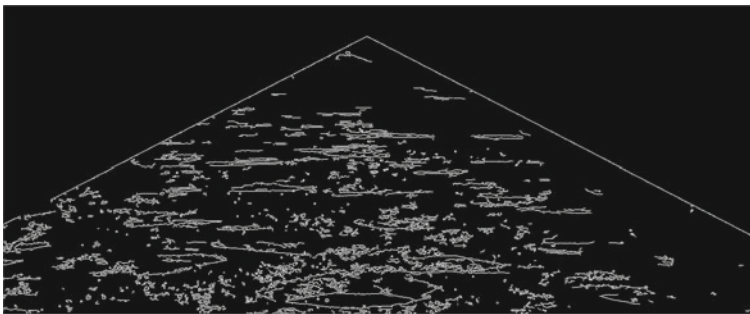


Fig. 5 Canny edge detection



Fig. 6 Pothole detection

Thresholding is done with minimum and maximum values, and the pixels which do not fall in this range are discarded.

Contours are obtained where points obtained for edges are closed to each other. The chain approximation method is not used to store the information of the contour since we need the entire information of the boundary of the contour.

For each contour, a bounding box is drawn, and an ellipse is fit into it by the least squares method from a set of 2D points [9]. Ellipses are used for the very reason that extracting information of ellipses is much simpler and easy to interpret in terms of its coordinates, as well as most potholes when looked from an egocentric view look like an ellipse.

The generated ellipses are overlapped on the original frame. This process is done for all frames of a video stream for detection of potholes.

The ellipses obtained depict the potholes in Fig. 6. It is easy to extract the data of the potholes as a measure of their coordinates in the frame.

4.2 Filtering of Pothole Detections

During detection, the algorithm detects potholes of all sizes, many being too small and insignificant to make any impact on a real-time driving scenario. Therefore, few parameters have been defined, and thresholds have been applied for filtering the potholes:

Pothole area: The pothole area is in terms of the area of an ellipse which can be defined as:

$$\text{Pothole image area} = \frac{\pi}{4} (\text{width}) * (\text{height}) \quad (2)$$

Based on a trial method, we have fixed the thresholds between 400 and 1000 units that are sufficient enough to accurately detect potholes that can cause damage.

Ellipse angle: The ellipse angle is an output from the angle of the bounding box generated and is kept 110 and 80 degrees as the normal to the surface of the potholes approximately perpendicular to the surface of the road.

Aspect ratio: The aspect ratio is defined as the ratio of the minimum dimension to the maximum dimension. Since it is difficult to determine which side of the ellipse is the height or width, we use a maximum or a minimum operator to calculate this:

$$\text{Aspect ratio} = \frac{\min(\text{width}, \text{height})}{\max(\text{width}, \text{height})} \quad (3)$$

Based on the parameters, the pothole detection can be tuned to suit the different environments. But, however, the most influencing parameters are the canny edge detection gradient thresholds G_x and G_y which have to be tuned properly so that the detection is accurate. This is discussed in the calibration section.

4.3 Calibration of the Algorithm

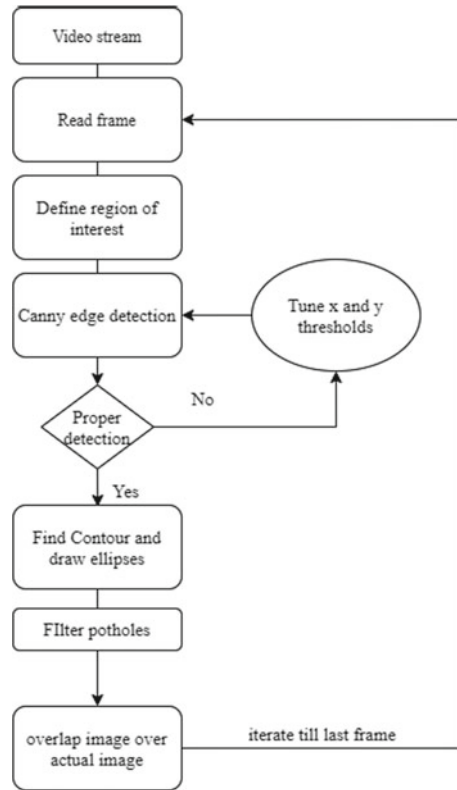
Firstly, the region of interest has to be properly defined for different cameras since their field of view may differ. Also, due to variation in the resolution, environments can be seen at different pixel intensities for different cameras. Therefore, there is a need to properly tune the parameters for different cameras. Once the parameters are tuned, it can be used without any further change. The parameters G_x and G_y are varied based on a trial and error approach to get the correct predictions. Our program uses a graphical user interface involving a slider bar for each of the parameters so that it can tune manually. The flowchart of the proposed algorithm is shown in Fig. 7

The pothole detection model designed in this paper shows a good accuracy of around 75–95% accuracy depending on the proper extent of calibration and environmental factors. The image segmentation-based method which uses canny edge detection is a much faster method compared to others that are listed with a good level of accuracy. This method is majorly designed keeping in mind the Indian road conditions and are calibrated according to them. Although image segmentation provides a considerably good result, there is always scope to improve the accuracy of the model by combining it with other conventional methods.

5 Conclusion

The pothole detection algorithm using image segmentation provides a good level of accuracy as compared to other methods. It can also be used on relatively low computational power systems. Using these detections along with vehicle controls,

Fig. 7 Flowchart for calibrating the algorithm



accidents could be prevented early, and the information about the road can be used to maintain them periodically.

References

1. Wilson TP, Romine AR (1999) Materials and procedures for repair of potholes in asphalt-surfaced pavements, Report No. FHWA-RD-99-168
2. Jog GM, Koch C, Golparvar-Fard M, Brilakis I (2012) Pothole properties measurement through visual 2D recognition and 3D reconstruction. *Comput Civ Eng* 553–560
3. Koch C, Brilakis I (2011) Pothole detection in asphalt pavement image. *Adv Eng Inform* 25(3):507–515
4. Karuppuswamy J, Selvaraj V, Ganesh MM, Hall EL (2000) Detection and avoidance of simulated potholes in autonomous vehicle navigation in an unstructured environment. *Intell Robots Comput Vis XIX Algorithms Tech Active Vis* 4197:70–80
5. Koch C, Brilakis I (2011) Pothole detection in asphalt pavement images. *Adv Eng Inform* 25(3):507–515
6. Ryu S-K, Kim T, Kim Y-R (2015) Image-based pothole detection system for ITS service and road management system. *Math Prob Eng* 2015

7. Sugang NJ, Ramos Jr M, Arriola NA (2017) Road surface obstacle detection using vision and LIDAR for autonomous vehicle. In: Proceedings of the international multicongference of engineers computer scientists (IMECS), Hongkong, China
8. Madli R et al (2015) Automatic detection and notification of potholes and humps on roads to aid drivers. *IEEE Sens J* 15(8):4313–4318
9. Fitzgibbon AW, Fisher RB (1995) A buyer's guide to conic fitting. In: Proceedings of the 6th British conference on machine vision, vol 2, pp 513–522. BMVA Press

Survey on Optimization of Resource Scheduling in Cloud Platforms



Bhaskararao Kasireddi and Raju Anitha

Abstract Task scheduling plays major role in cloud computing research fields as it deals with the appropriate allocation of resources to perform tasks in cloud environments. Task scheduling has number of possible solutions while allocating resources since task scheduling is an np-hard problem. A lot of research work has been devoted in order to obtain optimal solutions for task scheduling. However, no single technique is globally accepted because of the desires of the cloud environments. This current study addresses the detailed developments in the last two decades toward the achievement of optimal solutions to obtain the resource allocation plans to execute the tasks.

Keywords Virtual machines · Cloud computing · Task scheduling · Artificial intelligence · Optimization

1 Introduction

Cloud computing is an internet-based application to provide service. In the last two decades, a bulk amount of research work has been performed in cloud computing. From Fig. 1 it is noticed a gradual increase in the number of publications with respect to the timeline.

1.1 Cloud Types in Cloud Computing

In general cloud computing is modeled in two categories:

1. *Deployment Models*—Refers to the location and management of the clouds structure

B. Kasireddi (✉) · R. Anitha
Department of Computer Science and Engineering, Koneru Lakshmaiah Education Foundation,
Guntur, Andhra Pradesh, India

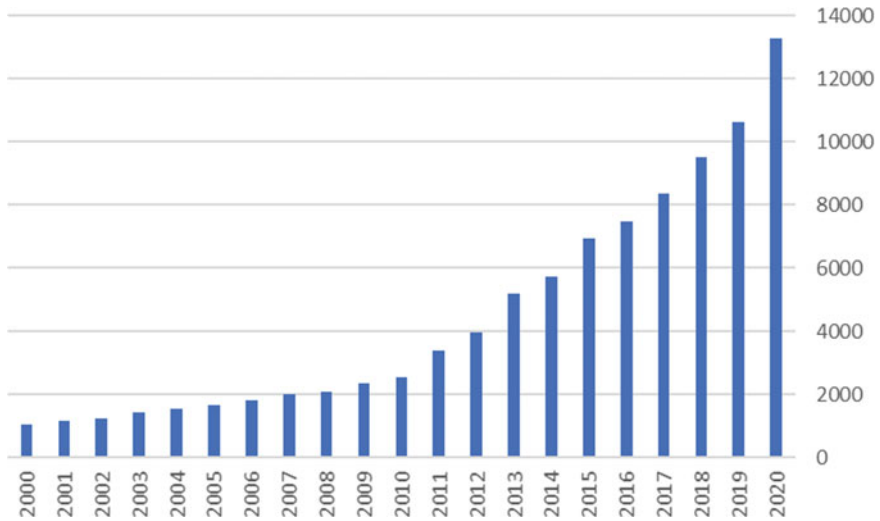


Fig. 1 Research output number with respect to time line of last two decades

2. *Service Models*—This is particular type of service that can access on cloud computing platforms

1.1.1 Deployment Models

A deployment model defines the purpose of the cloud and the nature of how the cloud is located. There are four deployment models as below:

1. *Public cloud*: This infrastructure is available for public use alternatively for a large industry group.
2. *Private cloud*: This infrastructure is operated for the exclusive use of an organization. These clouds may be either on-or-off-premises.
3. *Hybrid cloud*: This infrastructure combines multiple clouds where they can retain their unique identities but are bound together as a unit.
4. *Community cloud*: In this, cloud has been organized to serve a common function or purpose. This cloud can be managed by constituent organization or by a third party.

1.1.2 Service Models

In cloud computing, different vendors offer clouds that have different services associated with them. The following three service types have been universally accepted:

1. *Infrastructure as a Service (IaaS)*: In this, client has provision to access virtual infrastructures.

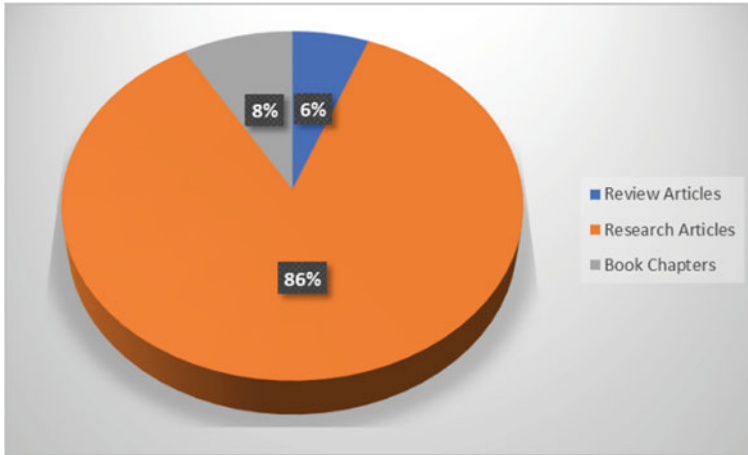


Fig. 2 Categorization of outcomes with cloud computing (through SCOPUS database)

2. *Platform as a Service (PaaS)*: In this, several control structures are incorporated to provide the service.
3. *Software as a Service (SaaS)*: In this, applications of operating system and their management through user interface is provided.

Although a good amount of works devoted in cloud computing areas, among the published works major contributions are from the research articles as shown in Fig. 2

1.2 Why Optimization of Task Scheduling

Task scheduling optimization in a distributed heterogeneous computing environment is an np-hard problem that plays a major role in optimizing cloud utilization and QoS. As cloud task scheduling is an np-hard problem we should increase the efficient use of the shared resources to achieve optimal task scheduling. To attain optimal task scheduling, so many meta-heuristic algorithms have been developed.

2 Task Scheduling Classification

The current study analyses the various optimal task scheduling plans as per the classifications illustrated in Fig. 3.

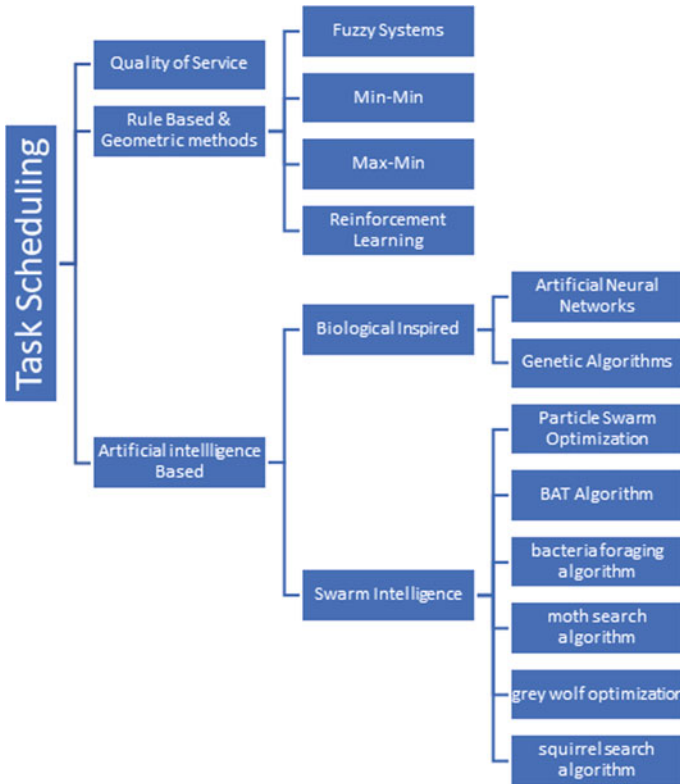


Fig. 3 Techniques used for task scheduling

2.1 Quality of Service (QoS) in Task Scheduling

The cloud earner should assure the QoS (quality of service) to its users with best way of resources allocation while executing tasks [1]. To implement QoS [2] in cloud computing, task scheduling algorithm is used by Service Level Agreement Violation [3]. Multi-objective task scheduling is considered for processing time suitable for cloud environments with Service Level Agreement [4, 5]. Grouped task scheduling-based QoS is solved in [6] and cost performance of task scheduling is addressed in [7, 8]. Authors in [9] emphasize how to deliver cloud services with QoS requirements.

Further, QoS guarantees the robust scheduling when cloud is integrated into cyber-physical systems [10]. QoS-aware architecture for fog services has been introduced in [11, 12].

2.2 Rule-Based and Geometric Methods in Task Scheduling

In rule-based techniques, certain rules are formed for proper allocation of resources to the virtual machines. In min-min algorithm [13] the task with minimum execution time (i.e., min) is selected among all the tasks. That task is allocated to the resource which has minimum completion time (min). The process continues until all the tasks are executed. As this algorithm completes small tasks first there will be a greater delay of larger tasks.

In fuzzy systems, certain number of rules are to be identified by the user to plan the optimal task scheduling [14, 15]. An optimal service load balancing based task scheduling is done with the aid of Fuzzy-TOPSIS [16] in cloud environment. In addition, dynamic scheduling in virtualized data centers is predicted with the help of fuzzy inference systems [17].

One of the famous geometric approaches of machine learning strategy is Reinforcement Learning [18]. Q-learning is a technique of reinforcement learning which can be implemented for task scheduling schemes in cloud environments [19]. Further, Q-Learning-based dynamic task scheduling strategy is proposed in [20] for energy-efficient cloud computing.

2.3 Artificial Intelligence for Task Scheduling

To attain optimal task scheduling, so many meta-heuristic algorithms have been developed. From the past studies, it is identified biological inspired and swarm intelligence-based have been implemented to solve task scheduling in cloud environments.

2.3.1 Biologically Inspired Methods for Task Scheduling

Topic of Swarm intelligence and bio-inspired algorithms is emerging trends toward the developments of new algorithms enthused by nature [21]. Biologically inspired methods are the techniques inspired by cells, bodies, and societies.

(A) Genetic Algorithm (GA)

One of the famous bio-inspired artificial intelligence is genetic algorithm which is inspired by the replicate way of forming biological organisms and sub-organism entities [22]. An improved genetic-based task scheduling [23] is proposed for scientific workflows in cloud environments [24]. An adaptive genetic theory [25] is introduced to minimize the energy consumption in data centers. It is noticed that the genetic algorithm performs better when it is hybridized with some other artificial intelligence techniques as compared to the sole implementation of genetic algorithm [26, 27].

(B) *Artificial Neural Networks (ANN)*

ANN is a fundamental bio-inspired AI technique that mimics the nature of connection of neurons with brain to pass data for necessary processing. ANN-based energy-efficient task scheduling strategies have been implemented in cloud infrastructures [28, 29]. Task scheduling can be achieved by considering it as multi-objective optimization criterion with the aid of ANN [30]. For better performance, Mobile augmented reality networks cloud environment is introduced [31]. ANN has been implemented successfully for security-aware scheduling in computational distributed environments [32].

2.3.2 Swarm Intelligence for Task Scheduling

The concept of a swarm suggests multiplicity, stochasticity, randomness, and messiness, and the concept of intelligence suggests that the problem-solving method is successful [33].

(A) *Particle swarm optimization for task scheduling*

Past studies represent Particle Swarm Optimization (PSO) has been widely used for solving task scheduling [34–37]. PSO-based load balancing strategy has been implanted for cloud computing platforms in [34]. Task scheduling can be achieved by considering it as multi-objective optimization criterion with the aid of nested PSO framework [35, 36]. It is noticed that the PSO gives better results when it is hybridized with some other artificial intelligence techniques as compared to the sole implementation of PSO [37].

(B) *Symbiotic organisms search*

Next to PSO, symbiotic organisms search (SOS) plays vital role in solving task scheduling in cloud computing platforms [38–40].

(C) *Other Swarm Intelligence techniques*

Apart from the afore mentioned swarm-based task scheduling plans, other several techniques have been implemented to solve task scheduling in cloud platforms. Past studies represent various swarm intelligence techniques such as Bacteria foraging algorithm [40], BAT algorithm [41], squirrel search algorithm [42], gray wolf optimization [43], moth search algorithm [44], artificial bee colony [45], firefly approach [46] have been implemented to solve task scheduling in cloud environments.

2.4 Heuristics Methods for Task Scheduling

Besides the addressed artificial intelligence techniques, several researchers implemented heuristic methods to achieve optimal task scheduling plans. A heuristic algorithm for workflow scheduling [47] and multisite computation offloading [48] is

implemented in cloud environments. Heuristics-based task scheduling for power efficiency-based scheduling [49], energy efficiency-based scheduling [50], and cost optimization-based scheduling [51] have been implemented in cloud platforms. To schedule a bag of tasks in cloud platforms, meta-heuristics have been implemented [52, 53]. For better performance of task scheduling plans in cloud computing, hybrid heuristics have also been implemented [54, 55].

3 Review Analysis

Figure 4 represents the number of research outcomes during the last two decades with keyword search “task scheduling, artificial intelligence and cloud computing” in scopus database.

Figure 5 represents the type outcomes of artificial intelligence-based task scheduling. Among the total works, major contributions are toward the research articles.

Figure 6 represents the methods to solve the task scheduling in various cloud platforms. Among the total works, most of the past researchers are contributed the task scheduling with swarm intelligence approaches. Later preference is given to the biologically inspired techniques for task scheduling in cloud computing.

Figure 7 illustrates the detailed research outcomes toward the task scheduling with the help of several artificial intelligence techniques. Among which particle swarm optimization has been implemented by major of the cited works to solve task scheduling.

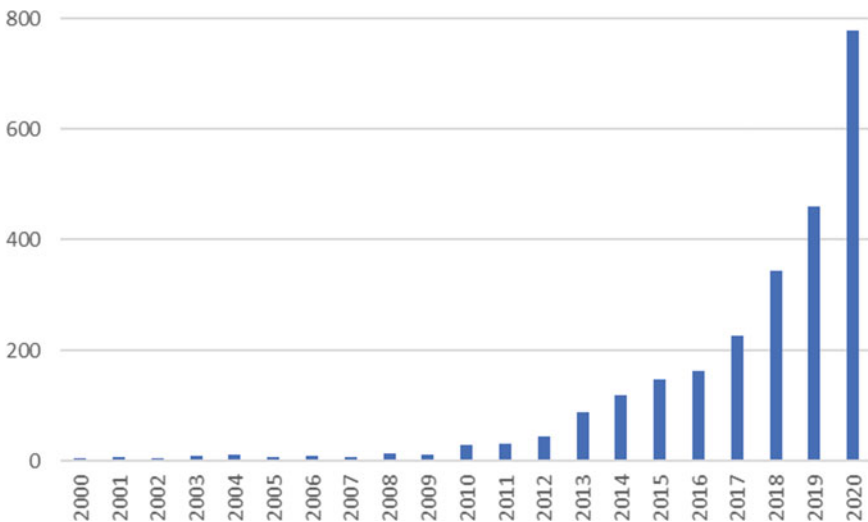


Fig. 4 Timeline viz research outcomes of artificial intelligence-based task scheduling

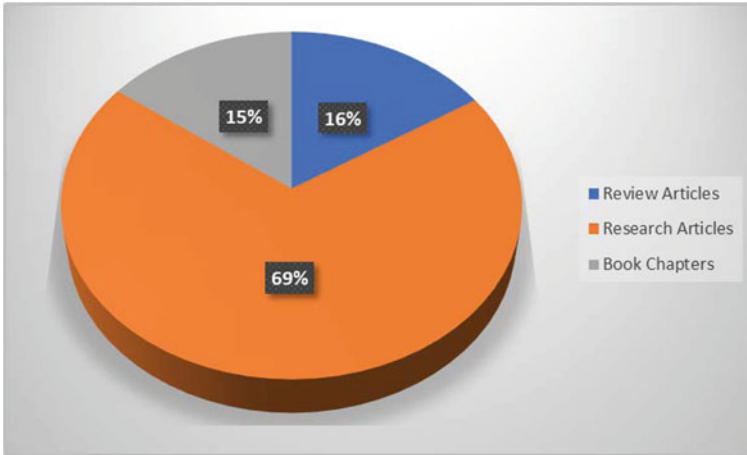


Fig. 5 Type outcomes of artificial intelligence-based task scheduling

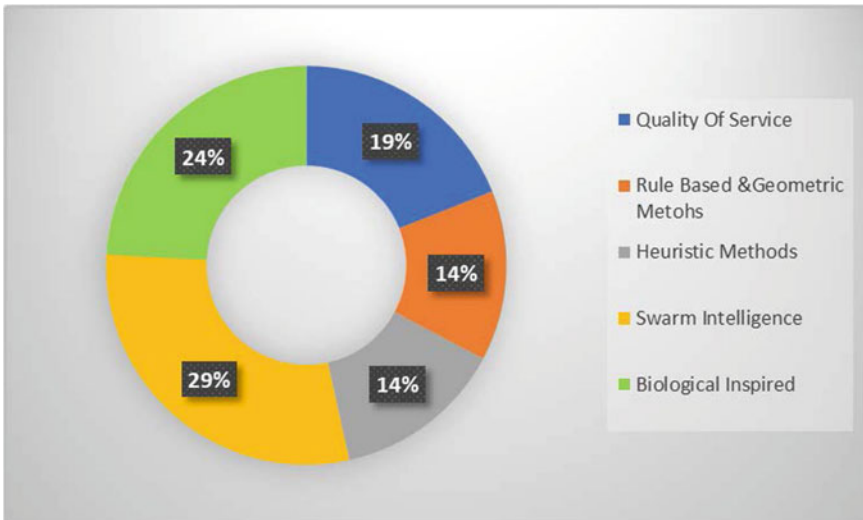


Fig. 6 Methods to solve the task scheduling

4 Conclusion

An elaborative study has been presented on implementation of artificial intelligence techniques for solving task schedules presented in this review article. From the study, it is found that most of the works dealt with the genetic algorithm, particle swarm optimization, and ant colony optimization. However, a few research works have been devoted to implementation of hybrid techniques for task scheduling.

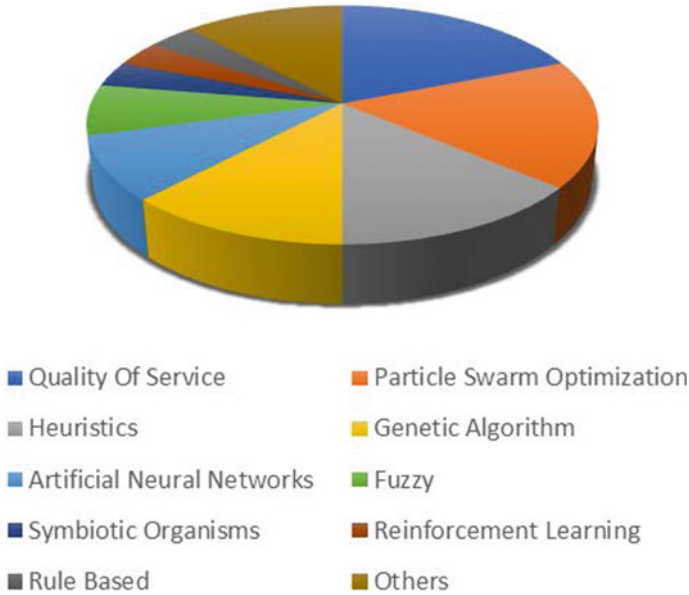


Fig. 7 Details QoS and AI-based studies for task scheduling

From the review analysis, it is observed that a suitable algorithm is to be implemented which has less number of tuning parameters so as to obtain the solution without the mathematical complexity.

4.1 Research Gaps

From the review analysis, it is observed that a researcher aims toward the generation of optimal task scheduler for allocating the resources in the cloud environments with the following research scopes:

Research gap—1: To frame appropriate objective functions to solve the task scheduling problem. The task schedulers may consider one or combination of any of the objective criteria with processing cost, execution time, and throughput.

Research gap—2: To find the suitable soft computing techniques which can solve the task scheduling problem with less mathematical complexity and obtain the solution within a less search space.

Research gap—3: To develop artificial intelligence-based strategies for optimal resource allocation in cloud environments while satisfying minimum processing time, cost and maximizing throughput.

References

1. Wu X, Deng M, Zhang R, Zeng B, Zhou S (2013) A task scheduling algorithm based on QoS-driven in cloud computing. *Proc Comput Sci* 17:1162–1169
2. Nasr AA, El-Bahnasawy NA, Attiya G, El-Sayed A (2018) A new online scheduling approach for enhancing QOS in cloud. *Futur Comput Inform J* 3(2):424–435
3. Lu YC, Lin CK, Lai KC, Tsai MH, Wu YJ, Chang HY, Huang KC (2019) Service deployment and scheduling for improving performance of composite cloud services. *Comput Electr Eng* 74:616–634
4. Yakubu IZ, Musa ZA, Muhammed L, Ja'afaru B, Shittu F, Matinja ZI (2020) Service level agreement violation preventive task scheduling for quality of service delivery in cloud computing environment. *Proc Comput Sci* 178:375–385
5. Lavanya M, Shanthi B, Saravanan S (2020) Multi objective task scheduling algorithm based on SLA and processing time suitable for cloud environment. *Comput Commun* 151:183–195
6. Ali HGEDH, Saroit IA, Kotb AM (2017) Grouped tasks scheduling algorithm based on QoS in cloud computing network. *Egypt Inform J* 18(1):11–19
7. Bansal N, Maurya A, Kumar T, Singh M, Bansal S (2015) Cost performance of QoS driven task scheduling in cloud computing. *Proc Comput Sci* 57:126–130
8. Stavrinides GL, Karatza HD (2019) An energy-efficient, QoS-aware and cost-effective scheduling approach for real-time workflow applications in cloud computing systems utilizing DVFS and approximate computations. *Futur Gener Comput Syst* 96:216–226
9. Quarati A, Clematis A, D'Agostino D (2016) Delivering cloud services with QoS requirements: business opportunities, architectural solutions and energy-saving aspects. *Futur Gener Comput Syst* 55:403–427
10. Chejerla BK, Madria SK (2017) QoS guaranteeing robust scheduling in attack resilient cloud integrated cyber physical system. *Futur Gener Comput Syst* 75:145–157
11. Badidi E, Ragmani A (2020) An architecture for QoS-aware fog service provisioning. *Proc Comput Sci* 170:411–418
12. Murtaza F, Akhunzada A, Ul Islam S, Boudjadar J, Buyya R (2020) QoS-aware service provisioning in fog computing. *J Netw Comput Appl* 165:102674
13. Patel G, Mehta R, Bhoi U (2015) Enhanced load balanced min-min algorithm for static meta task scheduling in cloud computing. *Proc Comput Sci* 57:545–553
14. Mansouri N, Zade BMH, Javidi MM (2019) Hybrid task scheduling strategy for cloud computing by modified particle swarm optimization and fuzzy theory. *Comput Ind Eng* 130:597–633
15. Chakravarthi KK, Shyamala L (2020) TOPSIS inspired budget and deadline aware multi-workflow scheduling for cloud computing. *J Syst Architect* 101916
16. Samriya JK, Kumar N (2020) An optimal SLA based task scheduling aid of hybrid fuzzy TOPSIS-PSO algorithm in cloud environment. *Mater Today Proc*
17. Kong X, Lin C, Jiang Y, Yan W, Chu X (2011) Efficient dynamic task scheduling in virtualized data centers with fuzzy prediction. *J Netw Comput Appl* 34(4):1068–1077
18. Sutton RS, Barto AG (2018) Reinforcement learning: an introduction. MIT press
19. Tong Z, Chen H, Deng X, Li K, Li K (2020) A scheduling scheme in the cloud computing environment using deep Q-learning. *Inf Sci* 512:1170–1191
20. Ding D, Fan X, Zhao Y, Kang K, Yin Q, Zeng J (2020) Q-learning based dynamic task scheduling for energy-efficient cloud computing. *Futur Gener Comput Syst* 108:361–371
21. Fister Jr I, Yang XS, Fister I, Brest J, Fister D (2013) A brief review of nature-inspired algorithms for optimization. arXiv preprint [arXiv:1307.4186](https://arxiv.org/abs/1307.4186)
22. Kar AK (2016) Bio inspired computing—a review of algorithms and scope of applications. *Expert Syst Appl* 59:20–32
23. Keshanchi B, Soury A, Navimipour NJ (2017) An improved genetic algorithm for task scheduling in the cloud environments using the priority queues: formal verification, simulation, and statistical testing. *J Syst Softw* 124:1–21

24. Casas I, Taheri J, Ranjan R, Wang L, Zomaya AY (2018) GA-ETI: an enhanced genetic algorithm for the scheduling of scientific workflows in cloud environments. *J Comput Sci* 26:318–331
25. Ibrahim H, Aburukba RO, El-Fakih K (2018) An integer linear programming model and adaptive genetic algorithm approach to minimize energy consumption of cloud computing data centers. *Comput Electr Eng* 67:551–565
26. Velliangiri S, Karthikeyan P, Xavier VA, Baswaraj D (2020) Hybrid electro search with genetic algorithm for task scheduling in cloud computing. *Ain Shams Eng J*
27. Sharma M, Garg R (2020) HIGA: harmony-inspired genetic algorithm for rack-aware energy-efficient task scheduling in cloud data centers. *Eng Sci Technol Int J* 23(1):211–224
28. Sharma M, Garg R (2020) An artificial neural network based approach for energy efficient task scheduling in cloud data centers. *Sustain Comput Inform Syst* 26:100373
29. Rawat PS, Gupta P, Dimri P, Saroha GP (2020) Power efficient resource provisioning for cloud infrastructure using bio-inspired artificial neural network model. *Sustain Comput Inform Syst* 28:100431
30. Ismayilov G, Topcuoglu HR (2020) Neural network based multi-objective evolutionary algorithm for dynamic workflow scheduling in cloud computing. *Futur Gener Comput Syst* 102:307–322
31. Sharma V, Jayakody DNK, Qaraqe M (2020) Osmotic computing-based service migration and resource scheduling in mobile augmented reality networks (MARN). *Futur Gener Comput Syst* 102:723–737
32. Grzonka D, Kołodziej J, Tao J, Khan SU (2015) Artificial neural network support to monitoring of the evolutionary driven security aware scheduling in computational distributed environments. *Futur Gener Comput Syst* 51:72–86
33. Kennedy J (2006) Swarm intelligence. In: *Handbook of nature-inspired and innovative computing*, pp 187–219. Springer, Boston, MA
34. He X, Ren Z, Shi C, Fang J (2016) A novel load balancing strategy of software-defined cloud/fog networking in the internet of vehicles. *China Commun* 13(Supplement2):140–149
35. Jena RK (2015) Multi objective task scheduling in cloud environment using nested PSO framework. *Proc Comput Sci* 57:1219–1227
36. Adhikari M, Srirama SN (2019) Multi-objective accelerated particle swarm optimization with a container-based scheduling for internet-of-things in cloud environment. *J Netw Comput Appl* 137:35–61
37. Devaraj AFS, Elhoseny M, Dhanasekaran S, Lydia EL, Shankar K (2020) Hybridization of firefly and improved multi-objective particle swarm optimization algorithm for energy efficient load balancing in cloud computing environments. *J Parallel Distrib Comput* 142:36–45
38. Abdullahi M, Ngadi MA, Dishing SI, Ahmad BIE (2019) An efficient symbiotic organisms search algorithm with chaotic optimization strategy for multi-objective task scheduling problems in cloud computing environment. *J Netw Comput Appl* 133:60–74
39. Abdullahi M, Ngadi MA (2016) Symbiotic organism search optimization based task scheduling in cloud computing environment. *Futur Gener Comput Syst* 56:640–650
40. Srichandan S, Kumar TA, Bibhudatta S (2018) Task scheduling for cloud computing using multi-objective hybrid bacteria foraging algorithm. *Futur Comput Inform J* 3(2):210–230
41. Kaur N, Singh S (2016) A budget-constrained time and reliability optimization bat algorithm for scheduling workflow applications in clouds. *Proc Comput Sci* 98:199–204
42. Sanaj MS, Prathap PJ (2020) Nature inspired chaotic squirrel search algorithm (CSSA) for multi objective task scheduling in an IAAS cloud computing atmosphere. *Eng Sci Technol Int J* 23(4):891–902
43. Natesan G, Chokkalingam A (2019) Task scheduling in heterogeneous cloud environment using mean grey wolf optimization algorithm. *ICT Express* 5(2):110–114
44. Abd Elaziz M, Xiong S, Jayasena KPN, Li L (2019) Task scheduling in cloud computing based on hybrid moth search algorithm and differential evolution. *Knowl-Based Syst* 169:39–52
45. Dhinesh Babu LD, Krishna PV (2013) Honey bee behavior inspired load balancing of tasks in cloud computing environments. *Appl Soft Comput* 13(5):2292–2303

46. Adhikari M, Amgoth T, Srirama SN (2020) Multi-objective scheduling strategy for scientific workflows in cloud environment: a firefly-based approach. *Appl Soft Comput* 93:106411
47. Abazari F, Analoui M, Takabi H, Fu S (2019) MOWS: multi-objective workflow scheduling in cloud computing based on heuristic algorithm. *Simul Model Pract Theory* 93:119–132
48. Enzai NIM, Tang M (2016) A heuristic algorithm for multi-site computation offloading in mobile cloud computing. *Proc Comput Sci* 80:1232–1241
49. Lin W, Wang W, Wu W, Pang X, Liu B, Zhang Y (2018) A heuristic task scheduling algorithm based on server power efficiency model in cloud environments. *Sustain Comput Inform Syst* 20:56–65
50. Hosseinioun P, Kheirabadi M, Tabbakh SRK, Ghaemi R (2020) A new energy-aware tasks scheduling approach in fog computing using hybrid meta-heuristic algorithm. *J Parallel Distrib Comput* 143:88–96
51. Alkhanak EN, Lee SP (2018) A hyper-heuristic cost optimisation approach for scientific workflow scheduling in cloud computing. *Futur Gener Comput Syst* 86:480–506
52. Moschakis IA, Karatza HD (2015) A meta-heuristic optimization approach to the scheduling of bag-of-tasks applications on heterogeneous clouds with multi-level arrivals and critical jobs. *Simul Model Pract Theory* 57:1–25
53. Gutierrez-Garcia JO, Sim KM (2013) A family of heuristics for agent-based elastic cloud bag-of-tasks concurrent scheduling. *Futur Gener Comput Syst* 29(7):1682–1699
54. Rashidi S, Sharifian S (2017) A hybrid heuristic queue based algorithm for task assignment in mobile cloud. *Futur Gener Comput Syst* 68:331–345
55. Jena UK, Das PK, Kabat MR (2020) Hybridization of meta-heuristic algorithm for load balancing in cloud computing environment. *J King Saud Univ Computer and Information Sciences*.